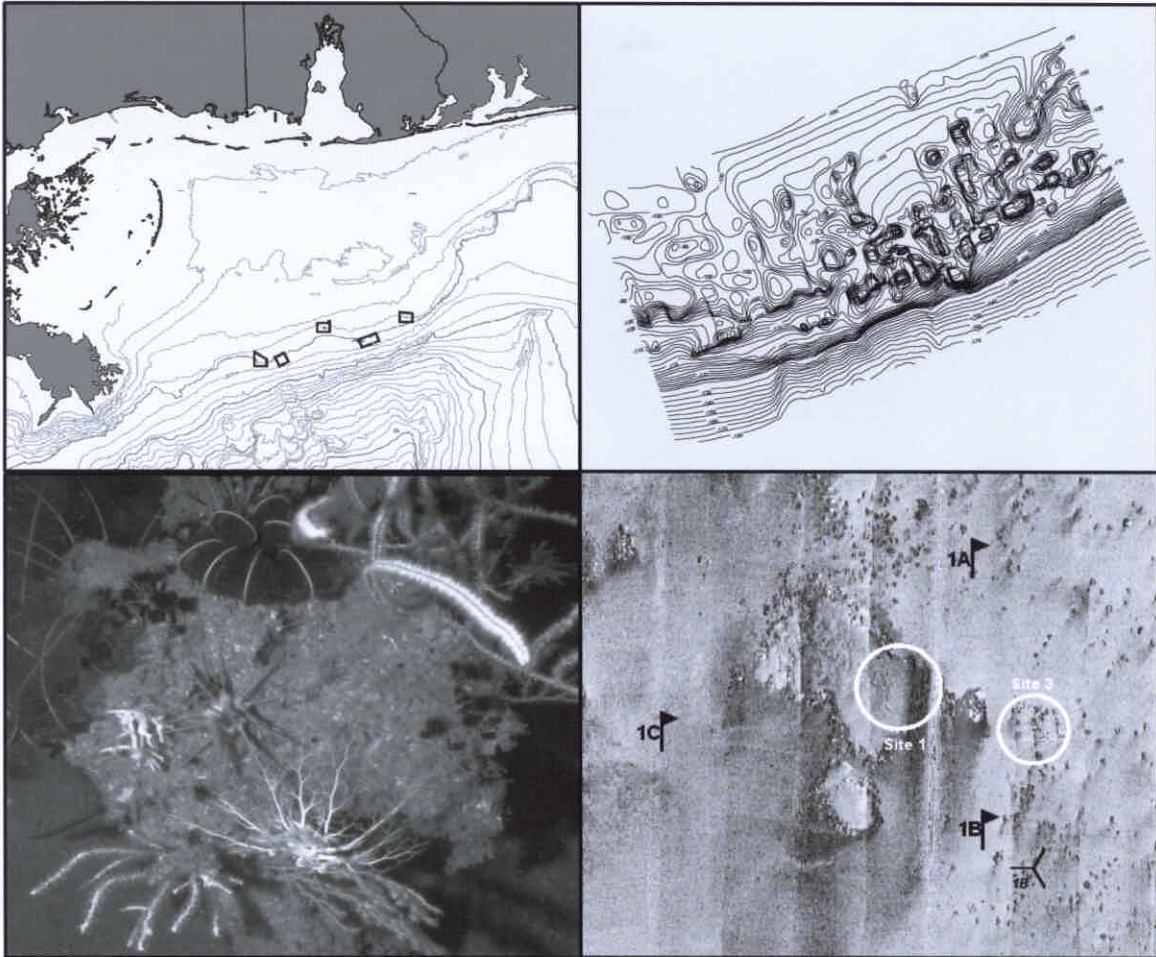


**Biological Sciences Report
USGS BSR 2001-0007
OCS Study MMS 2001-080**



**Mississippi/Alabama Pinnacle Trend Ecosystem Monitoring,
Final Synthesis Report**



Biological Sciences Report
USGS BSR 2001-0007
OCS Study MMS 2001-080

Mississippi/Alabama Pinnacle Trend Ecosystem Monitoring, Final Synthesis Report

October 2001

Prepared under USGS contract
1445-CT09-96-0006
by
Continental Shelf Associates, Inc.
759 Parkway Street
Jupiter, Florida 33477
and
Texas A&M University, Geochemical and
Environmental Research Group
833 Graham Road
College Station, Texas 77845

in cooperation with the

MMS U.S. Department of the Interior
Minerals Management Service
Gulf of Mexico OCS Region

PROJECT COOPERATION

This study was procured to meet information needs identified by the Minerals Management Service (MMS) in concert with the U.S. Geological Survey, Biological Resources Division (BRD).

DISCLAIMER

This report was prepared under contract between the U.S. Geological Survey, Biological Resources Division (BRD) and Continental Shelf Associates, Inc. This report has been technically reviewed by the BRD and the MMS, and has been approved for publication. Approval does not signify that the contents necessarily reflect the views and policies of the BRD or MMS, nor does mention of trade names or commercial products constitute endorsement or recommendation for use. It is, however, exempt from review and compliance with the MMS editorial standards.

REPORT AVAILABILITY

Extra copies of this report may be obtained from the following address:

U.S. Department of the Interior
Minerals Management Service
Gulf of Mexico OCS Region
Public Information Office (MS 5034)
1201 Elmwood Park Boulevard
New Orleans, LA 70123-2394

Telephone: (504) 736-2519 or
1-800-200-GULF

SUGGESTED CITATION

Continental Shelf Associates, Inc. and Texas A&M University, Geochemical and Environmental Research Group. 2001. Mississippi/Alabama Pinnacle Trend Ecosystem Monitoring, Final Synthesis Report. U.S. Department of the Interior, Geological Survey, Biological Resources Division, USGS BSR 2001-0007 and Minerals Management Service, Gulf of Mexico OCS Region, New Orleans, LA, OCS Study MMS 2001-080. 415 pp. + apps.

Contributors

Program Management

Program Manager	David A. Gettleson ¹
Deputy Program Manager	Mahlon C. Kennicutt II ²
Field Logistics Coordinator.....	Frederick B. Ayer II ¹
Data Manager.....	Alan D. Hart ¹
Deputy Data Manager.....	Gary A. Wolff ²

Principal Investigators and Authors

Geological Characterization.....	William W. Sager ² William W. Schroeder ⁶
Geochemistry	Mahlon C. Kennicutt II ²
Sediment Dynamics.....	Ian D. Walsh ⁵
Physical Oceanography/Hydrography.....	F.J. Kelly ² Norman L. Guinasso, Jr. ² Les C. Bender ²
Hard Bottom Communities.....	Dane D. Hardin ³ Keith D. Spring ¹ Stephen T. Viada ¹ Alan D. Hart ¹ Bruce D. Graham ¹ Michael B. Peccini ²
Fish Communities.....	David B. Snyder ¹
GIS and Microhabitat Studies.....	Ian R. MacDonald ² Michael B. Peccini ²
Epibiont Recruitment.....	Tara J. Holmberg ⁴ Paul A. Montagna ⁴
Synthesis.....	Neal W. Phillips ¹ David A. Gettleson ¹

Report Production

Report Editor.....	Neal W. Phillips ¹
Document Production Coordinator.....	Deborah V. Raffel ¹
Technical Editor.....	Melody B. Powell ¹
Administrative Assistant.....	Debbie Paul ²
Graphics.....	Suzanne R. Short ¹
Clerical.....	Deborah M. Cannon ¹ Karen I. Stokesbury ¹

Affiliations:

¹Continental Shelf Associates, Inc.

²Texas A&M University

³Applied Marine Sciences

⁴University of Texas at Austin

⁵Oregon State University

⁶Independent consultant

Contents

	Page
Figures.....	xi
Tables.....	xxiii
Acronyms and Abbreviations	xxxii
Executive Summary	ES-1
Chapter 1: Introduction	1
Background.....	1
Objectives	4
Phases.....	5
Components	5
Report Contents and Organization.....	8
Chapter 2: General Methods	9
Experimental Design.....	9
Site Selection	10
Site Descriptions	10
Overview of Sampling Program	18
Chapter 3: Geologic Characterization	23
Introduction.....	23
Methods.....	25
High-Resolution Geophysical Baseline Cruise (1A)	25
Other Cruises (1C, M2, M3, M4)	25
TAMU ² Sonar Data Interpretation	26
Subbottom Profile Interpretation	27
High-Resolution Bathymetry	27
Sediment Grain Size Analysis	27
ROV Video and Photo Classification	27
Results.....	29
Megasite Bathymetry and Mosaics.....	29
Monitoring Site Descriptions.....	45
Mound Morphology and Characteristics	73
Subbottom Profiles	82
Grain Size Data	86
Discussion.....	89
Chapter 4: Geochemistry	95
Introduction.....	95
Methods.....	96
Collection.....	96
Total Inorganic and Organic Carbon	96
Hydrocarbon Analyses.....	96

Contents (continued)

	Page
Trace Metal Analyses	97
Results and Discussion	98
Chapter 5: Sediment Dynamics	105
Introduction.....	105
Field and Laboratory Methods.....	106
CTD/DO/Transmissometer/OBS Data Sets.....	106
Sediment Traps	109
Results and Discussion	113
Water Column.....	113
Sediment Traps	117
Conclusions.....	124
Chapter 6: Physical Oceanography/Hydrography	127
Introduction.....	127
Methods.....	128
Overview.....	128
Equipment	132
Collateral Data	142
Results.....	144
Time-Series Data	144
Vertical Profiles	151
Unique Weather Events	151
Discussion.....	161
Flow at 16 mab.....	161
Flow at 4 mab.....	162
Vertical and Horizontal Flow Comparisons	162
Flow Structure over Generalized Mounds	167
Waves.....	179
September 1998 Events.....	181
Freshwater Input	187
In Situ Measurements of Water Properties	188
Vertical Profiles	189
Conclusions.....	203
Chapter 7: Hard Bottom Communities	209
Introduction.....	209
Field Methods	210
Equipment.....	211
Quality Assurance.....	212
Navigation.....	212
Site Definitions	212

Contents (continued)

	Page
Random Quadrats.....	213
Fixed Quadrats.....	213
Video Records.....	215
Voucher Specimens	215
Laboratory Methods.....	216
Random Quadrats.....	216
Fixed Quadrats	217
Taxonomy	217
Statistical Analyses	218
Results.....	223
General Observations.....	223
Random Quadrats.....	229
Fixed Quadrats	259
Discussion.....	261
Chapter 8: Fish Communities.....	269
Introduction.....	269
Methods.....	269
Field Methods	269
Laboratory Analysis.....	270
Data Analysis	272
Results.....	275
Descriptive Statistics and ANOVAs.....	275
Detrended Correspondence Analysis.....	284
Canonical Correspondence Analysis	284
Fish-Habitat Associations	288
Trophic Composition	292
Discussion.....	294
Chapter 9: GIS and Microhabitat Studies	299
Introduction.....	299
Methods.....	301
Geographic Information System.....	301
Measurement of Gorgonian Orientation	302
Statistical Methods.....	302
Current Meter Analysis.....	303
Selection of Microhabitat and Classification of Substrata.....	303
Results and Discussion	308
Orientation of Gorgonian Colonies and Predominant Water Transport	308
Gorgonian Distribution and Microhabitat Factors.....	317

Contents (continued)

	Page
Chapter 10: Epibiont Recruitment	327
Introduction.....	327
Methods.....	328
Experimental Design.....	328
Settlement Plates and Mooring Design.....	329
Determination of Process Effects.....	334
Laboratory Analysis.....	339
Statistical Analysis.....	340
Results.....	341
Taxa and Categories.....	341
Temporal Study.....	343
Elevated Spatial Study.....	351
Bottom Spatial Study.....	363
Discussion.....	371
Bottom Temporal Study.....	371
Bottom Spatial Study.....	372
Elevated Spatial Study.....	373
Conclusions.....	379
Chapter 11: Synthesis	381
Hard Bottom Communities and Environmental Conditions.....	381
Sediment Flux and Related Variables.....	381
Substrate and Microhabitat.....	390
Currents.....	393
Epibiont Recruitment.....	396
Management Implications.....	396
Oil and Gas Activities.....	396
Fishing.....	400
Evaluation of Program Objectives.....	400
Chapter 12: Literature Cited	403
Appendices	415
Appendix A: Cruise Summaries	A-1
Appendix B: Data Management	B-1
Appendix C: Grab and Box Core Locations and Sediment Grain Size Data	C-1
Appendix D: Synopses of Hydrographic and Collateral Data for Cruises	D-1

Figures

	Page
1.1 Study area.....	2
1.2 Locations of selected previous hard bottom studies in the northeastern Gulf of Mexico.....	3
2.1 Geographic locations of megasites surveyed during Cruise 1A	11
2.2 Locations of final monitoring sites	12
2.3 Side-scan sonar mosaic showing the setting of Sites 1 and 3	15
2.4 Side-scan sonar mosaic showing the setting of Site 2	15
2.5 Side-scan sonar mosaic showing the setting of Site 4	16
2.6 Side-scan sonar mosaic showing the setting of Sites 5 and 6	16
2.7 Side-scan sonar mosaic showing the setting of Site 7	17
2.8 Side-scan sonar mosaic showing the setting of Sites 8 and 9	17
2.9 Sampling schedule	19
3.1 Locations of MAMES, MASPTHMS, USGS study, and Megasites 1-5.....	24
3.2 Bathymetry of Megasite 1, derived from <i>TAMU</i> ² sonar data	31
3.3 <i>TAMU</i> ² side-scan sonar mosaic of Megasite 1, showing monitoring Sites 1–3.....	32
3.4 Megasite 1 sonar mosaic interpretation showing mounds and high-backscatter areas.....	33
3.5 Example of high-backscatter “tail” southwest of a mound in Megasite 1 and associated erosional gully	34
3.6 Bathymetry of Megasite 2, derived from <i>TAMU</i> ² sonar data.....	36
3.7 <i>TAMU</i> ² side-scan sonar mosaic of Megasite 2, showing monitoring Site 4	37
3.8 Megasite 2 sonar mosaic interpretation showing mounds and high-backscatter areas.....	38
3.9 Bathymetry of Megasite 3, derived from <i>TAMU</i> ² sonar data.....	39
3.10 <i>TAMU</i> ² side-scan sonar mosaic of Megasite 3, showing monitoring Sites 4 and 6.....	40

Figures
(continued)

	Page
3.11 Megasite 3 sonar mosaic interpretation showing mounds and high-backscatter areas	41
3.12 Bathymetry of Megasite 4, derived from <i>TAMU</i> ² sonar data.....	43
3.13 <i>TAMU</i> ² side-scan sonar mosaic of Megasite 4.....	44
3.14 Bathymetry of Megasite 5, derived from <i>TAMU</i> ² sonar data.....	46
3.15 <i>TAMU</i> ² side-scan sonar mosaic of Megasite 5, showing monitoring Sites 7-9	47
3.16 Megasite 5 sonar mosaic interpretation showing mounds and high-backscatter areas	48
3.17 Bathymetry of Monitoring Site 1	49
3.18 Side-scan sonar image of Monitoring Site 1	49
3.19 Bottom type map for Site 1 derived from ROV photo and video observations	51
3.20 Bathymetry of Monitoring Site 2.....	52
3.21 Side-scan sonar image of Monitoring Site 2.....	52
3.22 Bottom type map for Site 2 derived from ROV photo and video observations	53
3.23 Bathymetry of Monitoring Site 3	55
3.24 Side-scan sonar image of Monitoring Site 3	55
3.25 Bottom type map for Site 3 derived from ROV photo and video observations	56
3.26 Bathymetry of Monitoring Site 4.....	57
3.27 Side-scan sonar image of Monitoring Site 4.....	57
3.28 Bottom type map for Site 4 derived from ROV photo and video observations	59
3.29 Bathymetry of Monitoring Site 5.....	60
3.30 Side-scan sonar image of Monitoring Site 5.....	60

Figures (continued)

	Page
3.31 Bottom type map for Site 5 derived from ROV photo and video observations	61
3.32 Bathymetry of Monitoring Site 6.....	63
3.33 Side-scan sonar image of Monitoring Site 6.....	63
3.34 Bottom type map for Site 6 derived from ROV photo and video observations	64
3.35 Bathymetry of Monitoring Site 7.....	65
3.36 Side-scan sonar image of Monitoring Site 7.....	65
3.37 Bottom type map for Site 7 derived from ROV photo and video observations	66
3.38 Bathymetry of Monitoring Site 8.....	68
3.39 Side-scan sonar image of Monitoring Site 8.....	68
3.40 Bottom type map for Site 8 derived from ROV photo and video observations	70
3.41 Bathymetry of Monitoring Site 9.....	71
3.42 Side-scan sonar image of Monitoring Site 9.....	71
3.43 Bottom type map for Site 9 derived from ROV photo and video observations	72
3.44 Histograms of aspect ratios from carbonate mounds in Megasites 1-3 and 5.....	74
3.45 Number of mounds versus mound area for Megasites 1-3 and 5	75
3.46 Side-scan sonar images showing individual “unit” mounds and a composite mound.....	76
3.47 Side-scan sonar images showing complex, irregular mounds from Megasite 2.....	78
3.48 Side-scan sonar images showing smooth-top mounds.....	79
3.49 Chirp sonar profile over broad, carbonate hard bottom type mound in Megasite 2.....	80

Figures (continued)

		Page
3.50	Chirp sonar subbottom profile from Megasite 1 showing rough mound flank and typical sediment layering in the shallow subbottom.....	83
3.51	Histogram of mean grain sizes for the 229 grab samples from all cruises	87
3.52	Ternary diagrams showing size classifications of 229 grab samples from all cruises	88
3.53	Comparison of grain size data with side-scan sonar backscatter near Site 7	90
3.54	Mound distribution on the Mississippi-Alabama outer continental shelf and megasite locations	91
4.1	Comparison of total polycyclic aromatic hydrocarbon (PAH) and lead (Pb) concentrations in sediments at sites sampled during this study and at sites sampled near and far from platforms in the western Gulf of Mexico during GOOMEX PHASE 1 (Kennicutt 1995).....	102
4.2	Comparison of cadmium (Cd) and barium (Ba) concentrations in sediments at sites sampled near and far from platforms in the western Gulf of Mexico during GOOMEX PHASE 1 (Kennicutt 1995).....	103
5.1	Calibration plot of Niskin bottle particle concentration against the particle beam attenuation data from the transmissometer for the same depths and cast by cruise for four mooring servicing cruises	107
5.2	Calibration plot of data from Fig. 5.1 treated as a single data set.....	108
5.3	Particle beam attenuation (c_p) plotted against the LSS (Seatech Light Scattering Sensor) data from a representative cast showing the correlation between the two data sets.....	110
5.4	Profiles of density, salinity, potential temperature, and particle concentration from the calibrated beam attenuation data from two casts at the Site 1 mooring taken during the January 1998 mooring service cruise (S2)	114
5.5	Plot of particle beam attenuation (c_p) versus potential temperature for selected casts taken during the January 1998 mooring servicing cruise (S2).....	115
5.6	Mean particle profiles compiled from all available transmissometer casts at each site	116
5.7	Mean particle profiles from Fig. 5.6 presented on a common height above bottom scale (a) and the variance for that data presented as the standard deviation divided by the mean (b)	118

Figures (continued)

		Page
5.8	Bulk fluxes recorded during the study at Sites 1, 4, 5, and 9.....	119
5.9	Total organic carbon (TOC) concentrations and TOC fluxes presented for each sample period at each site.....	121
5.10	Comparison of bulk fluxes measured during the first year of the program at three moorings at Site 1	122
5.11	Comparison of (a) total organic carbon (TOC) concentrations and (b) TOC fluxes measured during the second year of the program at Site 5	123
5.12	Barium concentrations measured at the four sediment trap sampling sites during the program.....	125
6.1	Schematic drawing of the instrument mooring.....	129
6.2	Current meter mooring locations at Site 1 (indicated by flags).....	130
6.3	Current meter mooring location at Site 4 (indicated by flag).....	131
6.4	Current meter mooring locations at Site 5 (indicated by flags).....	131
6.5	Current meter mooring location at Site 9 (indicated by flag).....	145
6.6	Freshwater flow onto the Mississippi-Alabama shelf.....	145
6.7	Example of a Summary Page (C1A7) for a current velocity time series.....	146
6.8	Example of a monthly time-series plot (C1A7) for data recorded by a current meter	148
6.9	Example of a plot of data (O1A8) collected by the YSI 6000 Monitor.....	149
6.10	Derived center-plane streamline (top) and surface shear-stress patterns (bottom) for a Froude number (U/Nh) $F=0.2$ (From: Hunt and Snyder 1980)	170
6.11	Derived center-plane streamline (top) and surface shear-stress patterns (bottom) for a Froude number (U/Nh) $F=0.4$ (From: Hunt and Snyder 1980)	172
6.12	Derived center-plane streamline (top) and surface shear-stress patterns (bottom) for a Froude number (U/Nh) $F=1.0$ (From: Hunt and Snyder 1980)	173

Figures (continued)

		Page
6.13	Derived center-plane streamline (top) and surface shear-stress patterns (bottom) for a Froude number (U/Nh) $F=1.7$ (From: Hunt and Snyder 1980).....	174
6.14	Derived center-plane streamline (top) and surface shear-stress patterns (bottom) for a Froude number (U/Nh) $F=\infty$ (infinity) (From: Hunt and Snyder 1980).....	175
6.15	Selected examples of smoothed vertical profiles of buoyancy frequency	177
6.16	Froude number (U) plotted as a function of buoyancy frequency (N) and current speed; (a) for a hill height of 15 m; (b) for a hill height of 5 m	178
6.17	Map showing the path of Hurricane Earl.....	182
6.18	Map showing the path of Hurricane Georges	183
6.19	September 1998 stick vector plot of currents recorded at 16 meters above the bottom (mab) at Sites 1, 4, 5, and 9	184
6.20	September 1998 current speeds recorded at 4 meters above the bottom (mab) at Sites 1, 4, 5, and 9.....	185
6.21	Turbidity (NTU) recorded at Sites 5A and 5B at 2.3 meters above the bottom during 20 July through 14 October 1998.....	186
6.22	Temperature-salinity (T-S) relationships for the nine cruises thus far in the program	190
6.23	Comparison of dissolved oxygen concentrations for the combined cruises during this study versus the Levitus 94 climatology for the one-degree square encompassing the study region.....	195
6.24	Comparison of corrected dissolved oxygen concentration for the cruises during this study versus the Levitus climatology by season.....	196
6.25	Comparison of salinity for the combined cruises during this study versus the Levitus 94 climatology for the one-degree square encompassing the study region.....	197
6.26	Comparison of salinity for the cruises during this study versus the Levitus climatology by season.....	198
6.27	Comparison of temperature for the combined cruises during this study versus the Levitus 94 climatology for the one-degree square encompassing the study region.....	199

Figures (continued)

		Page
6.28	Comparison of temperature for the cruises during this study versus the Levitus climatology by season.....	201
6.29	Vertical profiles at Site 9 during Cruise S1 that shows the intrusion of the Loop Current with its signature of salinity greater than 36.5	202
6.30	Salinity profile at Site 1 showing the range of temporal variations that can occur.....	204
6.31	Density profiles at Site 5 showing small spatial variations	205
6.32	A typical summer profile of temperature, salinity, and density collected at Site 1 during Cruise S3	206
7.1	(a) Example of random point allocation within eight sectors of a site. A quantitative photograph was to be taken at each random point. (b) Actual ROV track and photograph locations at Site 7 on Cruise M2.....	214
7.2	Cumulative percentage of mean total cover contributed by the 40 most abundant hard bottom taxa.....	233
7.3	Distribution of solitary Scleractinia and <i>Rhizopsammia manuelensis</i> according to location on hard bottom features.....	246
7.4	Distribution of <i>Ulosa</i> sp., unidentified Rhodophyta, orange amorphous Porifera, amorphous indistinct Porifera, Crinoidea, Corallinaceae, and unidentified Bryozoa according to location on hard bottom features.....	248
7.5	Distribution of total cover according to location on hard bottom features	249
7.6	Distribution of coralline algae (Corallinaceae) according to bearing from the center of hard bottom features	249
7.7	Distribution of Hydroida according to bearing from the center of hard bottom features.....	250
7.8	Distribution of solitary Scleractinia and <i>Rhizopsammia manuelensis</i> according to bearing from the center of hard bottom features.....	250
7.9	Distribution of <i>Madracis/Oculina</i> sp., Crinoidea, and total antipatharians according to bearing from the center of hard bottom features.....	251
7.10	Comparison of the percentages of currents, kinetic energy in currents, and food flux provided by currents that flow toward different directions.....	251
7.11	Distribution of sites along canonical correspondence axes on Cruise M2	255

Figures (continued)

		Page
7.12	(a) Distribution of 40 dominant hard bottom taxa along canonical correspondence axes 1 and 2 and (b) magnification of the region near the origin.....	256
7.13	(a) Distribution of 40 dominant hard bottom taxa along canonical correspondence axes 3 and 4 and (b) magnification of the region near the origin.....	257
7.14	Relationship between 40 dominant hard bottom taxa and environmental variables along four canonical correspondence analysis axes	258
7.15	Percent of fixed quadrats observed that included sediment deposition, sediment erosion, organism growth or recruitment, and organism damage or mortality.....	264
8.1	Total fish taxa observed on video transects at Sites 1 through 9 for four monitoring cruises.....	283
8.2	(a) Sample scores from detrended correspondence analysis of taxa-by-samples matrix based on video transects plotted on Axes 1 and 2. (b) Species scores from the same analysis.....	285
8.3	(a) Sample scores from canonical correspondence analysis of taxa-by-samples matrix based on video transect. (b) Species scores for the same CCA analysis	286
8.4	Ordination of (a) large scale habitat classes (sites) and (b) species in large scale habitat classes by correspondence analysis.....	290
8.5	Ordination of (a) meso-scale habitat classes and (b) species in meso-scale habitat classes by correspondence analysis.....	291
8.6	Ordination of (a) small scale habitat classes and (b) species in small scale habitat classes by correspondence analysis.....	293
9.1	Substrate classifications. A. Vertical outcrop, thick, silty veneer and large-scale perforation with medium surface roughness. B. Mounded outcrop, moderate silty veneer and no sand-fill.....	304
9.2	Substrate classifications. A. Fine sediment as thick, silty veneer on outcropped surface. B. Coarse sediment as sandy fill with near-complete burial of outcropped surface	305
9.3	Substrate classifications. A. Combination of fine, coarse, and rubble sediment on area of no outcropping. B. Outcropping with high surface roughness and moderate silty veneer	306

**Figures
(continued)**

	Page
9.4 Overview of study sites discussed in this chapter.....	309
9.5 Gorgonian orientations and mean directional water flow at Site 1.....	310
9.6 Gorgonian orientations and mean directional water flow at Site 3.....	311
9.7 Gorgonian orientations and mean directional water flow at Site 5.....	312
9.8 Gorgonian orientations and mean directional water flow at Site 7.....	313
9.9 Gorgonian orientations and mean directional water flow at Site 9.....	314
9.10 Microhabitat utilization by gorgonians and antipatharians at Site 1.....	322
9.11 Microhabitat utilization by gorgonians and antipatharians at Site 3.....	323
9.12 Microhabitat utilization by gorgonians and antipatharians at Site 5.....	324
9.13 Microhabitat utilization by gorgonians and antipatharians at Site 7.....	325
10.1 Location of study sites	330
10.2 Experimental settling plate manipulations.....	333
10.3 TAMU ² side-scan sonar mosaic of Site 1	335
10.4 TAMU ² side-scan sonar mosaic of Site 4.....	335
10.5 TAMU ² side-scan sonar mosaic of Site 5.....	336
10.6 TAMU ² side-scan sonar mosaic of Site 9.....	336
10.7 Biomoooring with three replicate triads at two heights above bottom	337
10.8 Percent cover results for exposure period from temporal study by taxa with >10% total coverage	344
10.9 Percent cover results for exposure period from temporal study by taxa and categories with <10% total coverage	344
10.10 Artistic interpretation of average epibenthic community structure at 0 m above bottom based on percent cover and abundance means after 5-month settling plate exposure period	345

Figures (continued)

	Page
10.11 Artistic interpretation of average epibenthic community structure at 0 m above bottom based on percent cover and abundance means after 15-month settling plate exposure period.....	346
10.12 Artistic interpretation of average epibenthic community structure at 0 m above bottom based on percent cover and abundance means after 27-month settling plate exposure period.....	347
10.13 Abundance of solitary taxa for exposure periods during the temporal study.....	350
10.14 Interaction for abundance ($\ln n + 1$) between exposure periods and experimental manipulations for <i>Ostreoida</i>	350
10.15 Percent cover for taxa and categories site by sites from the elevated spatial study.....	353
10.16 Percent cover for taxa and categories for height (meters) above bottom (mab) from the elevated spatial study.....	354
10.17 Percent cover results for taxa and categories for experimental manipulations from the elevated spatial study.....	356
10.18 Percent cover for orientation from the elevated spatial study by taxa and category.....	357
10.19 Abundance ($\ln n + 1$) of solitary taxa for sites from the elevated spatial study.....	361
10.20 Abundance ($\ln n + 1$) for solitary taxa by height (meters) above bottom (mab) during the elevated spatial study.....	361
10.21 Abundance ($\ln n + 1$) of solitary taxa by experimental manipulation during the elevated spatial study.....	362
10.22 Abundance ($\ln n + 1$) of solitary taxa by plate orientation during the elevated spatial study.....	362
10.23 Principal components analysis results of percent cover from the elevated spatial study for all taxa and categories.....	365
10.24 Principal components analysis results of abundance from the elevated spatial study for all solitary taxa.....	365
10.25 Principal components analysis loading scores for abundances by site from the elevated spatial study.....	366

Figures (continued)

	Page
10.26 Principal components analysis loading scores for abundance by height (meters) above bottom (mab) from the elevated spatial study.....	366
10.27 Percent cover for taxa and categories by site during the bottom spatial study.....	367
10.28 Percent cover for taxa and categories by experimental manipulation during the bottom spatial study.....	367
10.29 Abundance ($\ln n + 1$) of solitary taxa by site during the bottom spatial study.....	371
10.30 Abundance of solitary taxa ($\ln n + 1$) by experimental manipulation during the bottom spatial study.....	371
10.31 Artistic interpretation of average epibenthic community structure at 0 m above bottom based on average percent cover and abundance after 15-month settling plate exposure period.....	374
10.32 Artistic interpretation of average epibenthic community structure at 3 m above bottom based on average percent cover and abundance after 19-month settling plate exposure period.....	375
10.33 Artistic interpretation of average epibenthic community structure at 13 m above bottom based on average percent cover and abundance after 19-month settling plate exposure period.....	376
11.1 Vertical relief (range of photographic station depths) at each site.....	383
11.2 Mean particle profiles presented on a common height above bottom scale (From Walsh, Chapter 5).....	384
11.3 Sediment flux (mean over all non-hurricane periods) vs. (a) water depth and (b) distance from Mississippi River mouth.....	386
11.4 Overall relationships between hard bottom communities and substrate vertical relief: (a) biotic cover; (b) number of epibiotal taxa; and (c) number of fish taxa.....	387
11.5 Overall relationships between hard bottom communities and sediment flux: (a) biotic cover; and (b) number of epibiotal taxa at each site.....	389
11.6 Overall relationships between numbers of taxa at each site and total area of mounds in each megasite: (a) number of epibiotal taxa and (b) number of fish taxa.....	391

Figures
(continued)

	Page
11.7 Percentage of substrate types making up each of the nine monitoring sites.....	392
11.8 Overall relationships between hard bottom communities and areal percentage of hard bottom within sites (including continuous hard bottom, mound, and monolith substrate types): (a) biotic cover; (b) number of epifaunal taxa; and (c) number of fish taxa	394
11.9 Locations of oil and gas platforms near the five megasites	397
11.10 Snapper grouper landing trends for NMFS statistical grid 10, which includes the study area, for 1977 to 1998	401

Tables

	Page
1.1 Program components	6
2.1 Monitoring site locations	13
2.2 Summary of activities conducted on each monitoring cruise and mooring service cruise.....	20
3.1 Seafloor geologic descriptors used for ROV photo and video classification	28
4.1 Summary of average sediment characteristics at the study sites during Cruise 1C	99
4.2 Summary of the average total organic (TOC) and inorganic (TIC) carbon content (%) of sediments at the study sites during Cruises 1C, M2, M3, and M4	100
5.1 Matrix of recovered sediment trap samples	111
5.2 Matrix of deployment (D) and recovery (R) dates for each sediment trap during the time series	112
6.1 Cruise dates, designations, and CTD cast information	132
6.2 Locations, dates, and times of deployment of the instrument moorings	133
6.3 Summary of the time-series data return, sorted by deployment period and instrument locations	136
6.4 Dates of NEGOM cruises relevant to this study	143
6.5 Data summary for mooring C1A, 16 mab, all good periods: C1A1, C1A3, C1A4, C1A5, C1A6, C1A7, and C1A8	150
6.6 Data summary for mooring C1A, 4 mab, all good periods: C1A1, C1A2, C1A3, C1A5, and C1A8	150
6.7 Data summary for mooring C1A, 16 mab, for periods in common with 4 mab: C1A1, C1A3, C1A5, and C1A8.....	152
6.8 Data summary for mooring C1A, 4 mab, for periods in common with 16 mab: C1A1, C1A3, C1A5, and C1A8.....	152
6.9 Data summary for mooring 4A, 16 mab, all good periods: C4A1, C4A3, C4A6, C4A7, and C4A8	153

Tables (continued)

		Page
6.10	Data summary for mooring 4A, 4 mab, all good periods: C4A3, C4A4, C4A7, and C4A8.....	153
6.11	Data summary for mooring 4A, 16 mab, for periods in common with 4 mab: C4A3, C4A7 (through 11-30-98), and C4A8	154
6.12	Data summary for mooring 4A, 4 mab, for periods in common with 16 mab: C4A3, C4A7 (through 11-30-98), and C4A8	154
6.13	Data summary for mooring 5A, 16 mab, all good periods: C5A1, C5A2, C5A3, C5A6, C5A7, and C5A8.....	155
6.14	Data summary for mooring 5A, 4 mab, all good periods: C5A1, C5A2, C5A3, C5A4, C5A6, C5A7, and C5A8	155
6.15	Data summary for mooring 5A, 16 mab, for periods in common with 4 mab: C5A1, C5A2, and C5A3 (to 11/30/99).....	156
6.16	Data summary for mooring 5A, 4 mab, for periods in common with 16 mab: C5A1, C5A2, and C5A3 (to 11/30/99).....	156
6.17	Data summary for mooring 9A, 16 mab, all good periods: C9A1, C9A2 (to 10/3/97), C9A3, C9A4 (to 4/24/98), C9A5 (to 5/24/98), C9A6, C9A7, and C9A8	157
6.18	Data summary for mooring 9A, 4 mab, all good periods: C9A1, C9A3, C9A4 (to 3/11/98), C9A5 (to 5/29/98), C9A6, C9A7 (to 12/21/98), and C9A8.....	157
6.19	Data summary for mooring 9A, 16 mab, for periods in common with 4 mab: C9A1, C9A3, C9A4 (to 3/11/98), C9A5 (to 5/24/98), C9A6, C9A7 (to 12/21/98), and C9A8	158
6.20	Data summary for mooring 9A, 4 mab, for periods in common with 16 mab: C9A1, C9A3, C9A4 (to 3/11/98), C9A5 (to 5/24/98), C9A6, C9A7 (to 12/21/98), and C9A8.....	158
6.21	Summary of principal axes analysis	159
6.22	Data summary for mooring 1B, 16 mab, for periods in common with 4 mab: C1B1, C1B2, and C1B3 (to 12/31/97).....	164

Tables (continued)

	Page
6.23 Data summary for mooring 1B, 4 mab, for periods in common with 16 mab: C1B1, C1B2, and C1B3 (to 12/31/97).....	164
6.24 Data summary for mooring 1C, 16 mab, for the period in common with 4 mab, which is just deployment C1C4	165
6.25 Data summary for mooring 1C, 4 mab, for the period in common with 16 mab, which is just deployment C1C4	165
6.26 Data summary for mooring 1A, 16 mab, for just deployment C1A4 (for comparison with Tables 6.24 and 6.25)	166
6.27 Data summary for mooring 5C, 16 mab, for the period in common with 4 mab, which is just deployment C5C8	168
6.28 Data summary for mooring 5C, 4 mab, for the period in common with 16 mab, which is just deployment C5C8	168
6.29 Froude number for Sites 1, 4, 5, and 9 computed from mound height (13 m, 10 m, 10 m, and 3 m, respectively), an assumed N of 0.01 rad/s, and the upper limit of each speed range in the joint frequency distribution (JFD) tables of speed vs. direction.....	179
6.30 Minimum wave period for a wave to influence the bottom and top of each site	180
6.31 Distribution of wave period observed at NDBC Buoy 42040 during 1 January 1997 through 31 December 1999	180
6.32 Combined freshwater flow data averaged over the 30 days preceding the start of each cruise.....	188
6.33 Summary of oceanographic results and observations from each cruise together with contemporaneous collateral data from other sources.....	192
7.1 Schedule of cruises for sampling hard bottom communities	210
7.2 Types and purposes of samples collected	211
7.3 Physical characteristics for each hard bottom site	220

Tables (continued)

		Page
7.4	Mean percent areal cover of the 40 most abundant hard bottom taxa, as indicated by mean percent cover at nine sites in the northeastern Gulf of Mexico	231
7.5	ANOVA results for differences among categories of habitat relief, region and cruise for the percent cover of 40 hard bottom taxa, the aggregate cover for five taxon groups, and the total aggregate cover for all hard bottom taxa.....	235
7.6	Habitat and region preferences of taxa based upon ANOVA results for the effects of relief and region (see Table 7.4)	238
7.7	General linear models results for the effects of eight variables on the percent cover of 40 hard bottom taxa, the aggregate cover for five groups, and the total aggregate cover for all hard bottom taxa at all sites listed according to taxa preferences for habitat relief and region.....	239
7.8	Results of general linear models for effects of 11 variables on the percent cover of hard bottom taxa and taxon groups that have highest abundances at medium and high relief sites listed according to region preference.....	242
7.9	Number and percentage of the medium-high relief hard bottom taxa for which 11 environmental variables were significant in two models (see Table 7.7 and Table 7.8) tested for effects of the variables on taxa abundances.....	243
7.10	Results of general linear models for the effects of eight variables on the percent cover of hard bottom taxa and taxon groups that have highest abundances at low relief sites listed according to region preference	244
7.11	Number and percentage of low relief hard bottom taxa for which eight environmental variables were significant in two models (see Table 7.7 and Table 7.10) tested for effects of the variables on taxa abundances.....	245
7.12	Results of linear regressions to determine the relationships between taxa abundances on each side of features (i.e., at different bearings from the center, the dependent variable) and the currents, current kinetic energy, and food flux flowing toward those sides of the features (independent variables).....	252
7.13	Depth intervals used for pooling data to define samples in canonical correspondence analysis.....	252

Tables (continued)

		Page
7.14	Correlation coefficients between environmental variables and canonical correspondence analysis ordination axes	253
7.15	Results of the canonical correspondence analysis using nine environmental variables	253
7.16	Number of observations of fixed quadrats that were repeatable from the previous cruise	259
7.17	Representative observations from fixed quadrats at three sites	260
7.18	Number of observations of sediment deposition, sediment erosion, organism growth or recruitment, and organism damage or mortality in fixed quadrats.....	262
7.19	Results of chi-square tests for differences between observed and expected frequencies of sediment deposition and sediment erosion in fixed quadrats over all times and from before and after Hurricanes Earl and Georges.....	263
7.20	Results of chi-square tests for differences between observed and expected frequencies of epifaunal growth or recruitment and damage or mortality in fixed quadrats over all times and from before and after Hurricanes Earl and Georges	263
8.1	Environmental variables used in analyses of fish communities	273
8.2	Fish taxa observed (●) in still photographs and videotapes from each site during Cruises 1C, M2, M3, and M4	276
8.3	Top 20 fish taxa observed in video transects at all nine sites combined during Cruises 1C, M2, M3, and M4 ranked by frequency of occurrence	280
8.4	Top 20 fish taxa observed in video transects during Cruises 1C, M2, M3, and M4 combined at Sites 1 through 9, ranked by frequency of occurrence.....	281
8.5	Species and species codes used in ordination plots	282
8.6	Canonical coefficients and inter-set correlations for the first four axes of canonical correspondence analysis of fish assemblages and five environmental variables	287

Tables (continued)

		Page
8.7	Frequency of fishes observed by habitat category for large, meso-, and small scale analyses	289
9.1	Layers of the geographic information system (GIS) database	301
9.2	Taxonomic designations for gorgonians and antipatharians used in microhabitat investigations	302
9.3	Circular statistics for gorgonian orientations at selected study sites	308
9.4	Circular statistics for current flux measured at current meter moorings.....	315
9.5	Partial analysis of variance for influence of microhabitat factors upon abundance of gorgonian and antipatharian colonies at Site 1	318
9.6	Partial analysis of variance for influence of microhabitat factors upon abundance of gorgonian and antipatharian colonies at Site 3	319
9.7	Partial analysis of variance for influence of microhabitat factors upon abundance of gorgonian and antipatharian colonies at Site 5	320
9.8	Partial analysis of variance for influence of microhabitat factors upon abundance of gorgonian and antipatharian colonies at Site 7	321
10.1	Temporal study time line and sampling schedule for biomooring deployments and retrievals at Site 4	331
10.2	Spatial study time line and sampling schedule for biomooring deployments and retrievals	331
10.3	Taxa found in the study area by site	342
10.4	Rates of change in taxa coverage (cm ²) averaged over 27 months of exposure caused by ecological process in the temporal study	348
10.5	Percent of variance for sources of variation from temporal study by taxa and category	348
10.6	Rates of change in abundance (ln <i>n</i> + 1 individuals) averaged over 27 months of exposure caused by ecological processes in temporal study	351
10.7	Percent of variance for taxa and categories in temporal study calculated for abundance (ln <i>n</i> + 1) by variance component analysis	351

Tables (continued)

	Page
10.8	Significance values for percent cover calculated by a 4-way ANOVA from elevated spatial study by taxa and category352
10.9	Rates of change in coverage (cm ²) caused by ecological process in the elevated spatial study over 19 months of exposure.....355
10.10	Percent of variance for each source of variation in the elevated spatial study, calculated for percent cover in a variance component analysis359
10.11	Summary of 4-way ANOVA results for abundance (ln $n + 1$) by taxa and category for the elevated spatial study360
10.12	Rates of change in abundance (ln $n + 1$ individuals) caused by ecological processes during the elevated, spatial study over 19 months of exposure360
10.13	Percent of variance from each component of the elevated spatial study364
10.14	Results from 2-way ANOVA of percent cover by taxa and category for bottom spatial study368
10.15	Rate of change in coverage (cm ²) over 15 months of exposure caused by ecological processes during the bottom spatial study368
10.16	Results from 2-way ANOVA on taxa abundance (ln $n + 1$) during the bottom spatial study369
10.17	Rate of change in abundance (ln $n + 1$) over 15 months of exposure caused by ecological process in bottom spatial study.....369

Acronyms and Abbreviations

ADCP	acoustic doppler current profiler
ANOVA	analysis of variance
AVHRR	advanced very high resolution radiometer
BLM	Bureau of Land Management
BP	before present
CA	correspondence analysis
CCA	canonical correspondence analysis
CTD	conductivity/temperature/depth
CVAAS	cold vapor atomic absorption spectrophotometry
DCA	detrended correspondence analysis
DO	dissolved oxygen
EOM	extractable organic matter
EPA	Environmental Protection Agency
FAAS	flame atomic absorption spectrophotometry
GC/FID	gas chromatography/flame ionization detection
GC/MS	gas chromatography/mass spectrometry
GERG	Geochemical and Environmental Research Group
GFAAS	graphite furnace or flameless atomic absorption spectrophotometry
GIS	geographic information system
GPS	global positioning system
INAA	instrumental neutron activation analysis
JFD	joint frequency distribution
LATEX	Texas-Louisiana Shelf Circulation and Transport Process Program
LSS	light scattering sensor
mab	meters above bottom
MAFLA	Mississippi-Alabama-Florida
MAMES	Mississippi-Alabama Marine Ecosystems Study
MASPTHMS	Mississippi-Alabama Shelf Pinnacle Trend Habitat Mapping Study
MDL	method detection limit
MMS	Minerals Management Service
MSD	minimum significant difference
NEGOM	Northeastern Gulf of Mexico (Physical Oceanography Program)
NDBC	National Data Buoy Center
NOAA	National Oceanic and Atmospheric Administration
NODC	National Oceanographic Data Center
NTU	nephelometric turbidity unit
OBS	optical backscatter
OCS	outer continental shelf
OEI	Oregon Environmental, Inc.
PAH	polycyclic aromatic hydrocarbon
PAR	photosynthetically active radiation
PCA	principal component analysis
QA/QC	quality assurance/quality control
RLM	reef-like mound
ROV	remotely operated vehicle

Acronyms and Abbreviations **(continued)**

SIM	selected ion monitoring
SOP	standard operating procedure
SST	sea surface temperature
TAMU	Texas A&M University
TIC	total inorganic carbon
TOC	total organic carbon
TPH	total petroleum hydrocarbons
UCM	unresolved complex mixture
USGS	U.S. Geological Survey
UTC	coordinated universal time

Executive Summary

This Final Synthesis Report summarizes a four-year program to characterize and monitor carbonate mounds on the Mississippi/Alabama outer continental shelf (OCS). The study area is shown in **Fig. ES.1**. The study was conducted by Continental Shelf Associates, Inc. and the Geochemical and Environmental Research Group (GERG) of Texas A&M University (TAMU), for the U.S. Geological Survey (USGS), Biological Resources Division.

Based on previous studies and new geophysical reconnaissance, nine sites in the Mississippi/Alabama "pinnacle trend" area were selected for monitoring (**Fig. ES.1**). Hard bottom community structure and dynamics were monitored because the potential sensitivity of these communities to OCS oil and gas industry activities is of interest to the Minerals Management Service (MMS), the client agency for which the USGS administered this program. Geological and oceanographic processes were studied to help to understand environmental factors that control or influence hard bottom communities. These included substrate characteristics such as relief, microtopography, sedimentology, and contaminant levels; near-bottom current patterns; and the presence, extent, and dynamics of nepheloid layers. In addition, two "companion studies" provided information on epibiont recruitment and the distribution and orientation of sea fans in relation to currents and microtopography.

Objectives

Overall program goal:

- To characterize and monitor biological communities and environmental conditions at carbonate mounds along the Mississippi/Alabama OCS.

Specific objectives:

- To describe and monitor seasonal and interannual changes in community structure and zonation and relate these to changes in environmental conditions (i.e., dissolved oxygen, turbidity, temperature, salinity, etc.); and
- To characterize the geological, chemical, and physical environment of the mounds as an aid in understanding their origin, evolution, present-day dynamics, and long-term fate.

Phases and Cruise Scheduling

The program consisted of four phases, each lasting approximately 12 months. These are summarized briefly below.

- Phase 1 included two reconnaissance cruises (Cruise 1A, November 1996; and Cruise 1B, March 1997) followed by final site selection (April 1997) and the beginning of monitoring and companion studies on Cruise 1C (May 1997).
- Phase 2 included two monitoring cruises, M2 (October 1997) and M3 (April-May and August 1998). In addition, mooring service cruises were conducted in July 1997 (S1), January 1998 (S2), and July 1998 (S3).

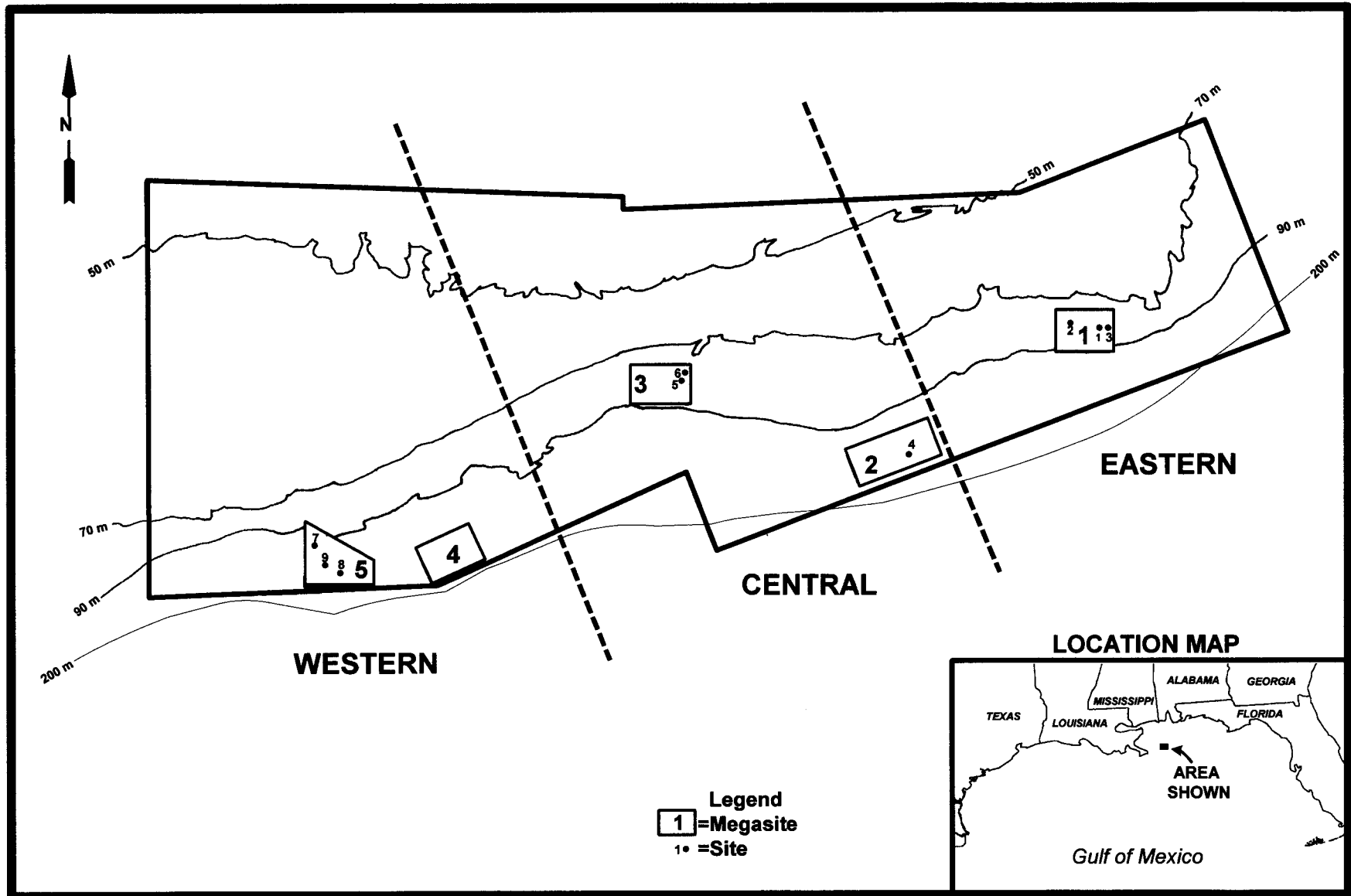


Fig. ES.1. Locations of final monitoring sites.

- Phase 3 concluded the field sampling program with two additional mooring service cruises (S4, October 1998; and S5, January-February 1999) and one final monitoring cruise (M4, April and July-August 1999).
- Phase 4 did not include any new field work. During this phase, investigators analyzed and synthesized data from the entire program. Preliminary results have been discussed in three previous Annual Interim Reports.

Site Selection

The contract specified that nine sites be selected, including high (>10 m), medium (5 to 10 m), and low (<5 m) relief sites in the eastern, central, and western parts of the study area. Other factors considered in site selection were representativeness, availability of existing video and photographic data, and previous oil and gas industry activities. Site selection during Phase 1 involved the following steps:

- *Megasite Selection.* Prior to Cruise 1A, five large areas (“megasites”) were selected for geophysical reconnaissance (**Fig. ES.1**). The selection of the five megasites was based on geophysical data collected during previous MMS-sponsored studies in the area. The megasites were selected because they were known to contain numerous features of varying relief (candidate sites) and could be surveyed within the time and financial constraints of the contract.
- *Geophysical Reconnaissance and Preliminary Site Selection.* During Cruise 1A (November 1996), the five megasites were surveyed using swath bathymetry, high-resolution side-scan sonar, and subbottom profiler to produce detailed maps. After the initial survey of all five megasites, small subsets were chosen for higher resolution mapping. After the cruise, a list of candidate high, medium, and low relief features within the megasites was prepared and the historical video and photographic data were tabulated. At this point, three high relief and two medium relief sites were tentatively selected.
- *Visual Reconnaissance.* Three low relief sites and one medium relief site with little or no previous video or photographic data were identified as needing visual reconnaissance. During Cruise 1B (March 1997), these features were briefly surveyed using a remotely operated vehicle (ROV) to determine whether a hard bottom community was present. All sites visited during Cruise 1B were ultimately chosen as final sites.
- *Final Site Selection.* After the completion of Cruises 1A and 1B, the program managers and key principal investigators developed a final site list in consultation with the USGS, the MMS, and a Scientific Review Board.

Site Descriptions

The nine monitoring sites ultimately selected are shown in **Fig. ES.1**, and characteristics are summarized in **Table ES.1**. Each site was defined as a circular area of a certain diameter. Diameters of the nine sites were determined through an analysis of the bathymetric data collected during Cruise 1A. Resulting site diameters ranged from 100 to 200 m. Physical oceanographic moorings and epibiont recruitment arrays (biomoorings) were placed on areas of flat bottom near certain sites. **Fig. ES.2** shows an example of a side-scan image of Sites 1 and 3 with adjacent moorings.

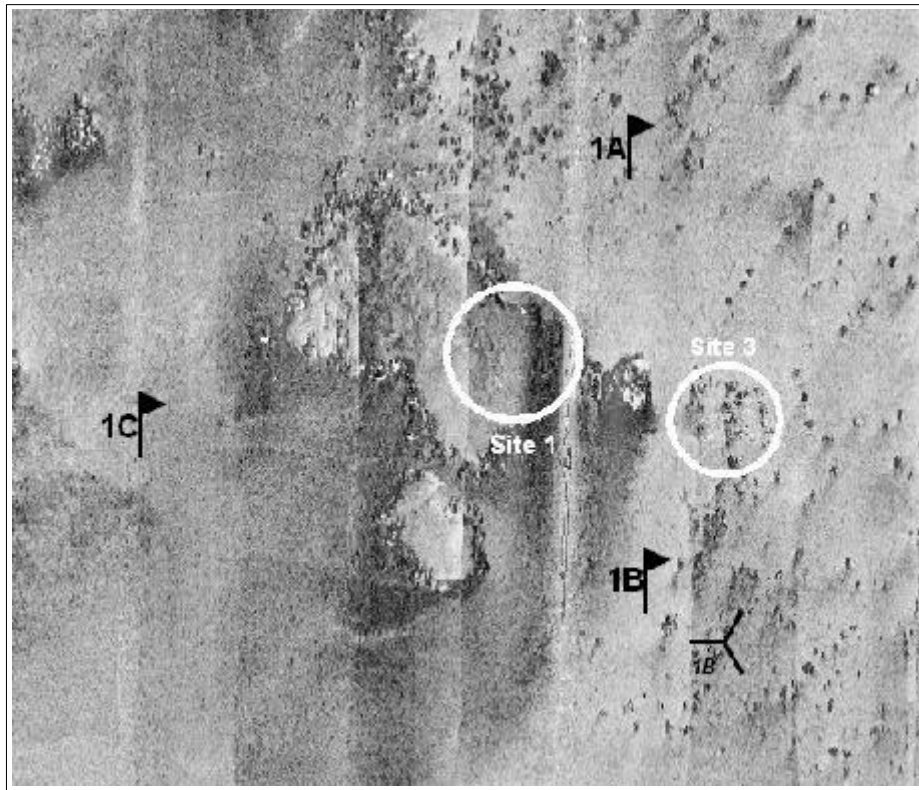


Fig. ES.2. Side-scan sonar mosaic showing the setting of Sites 1 and 3. Site diameters are 200 m for Site 1 and 150 m for Site 3. Current meter mooring locations are indicated by flags and the biomoooring location is indicated by a triad.

Table ES.1. Monitoring site locations.

Site	Megasite	Geographic Category	Relief Category	Water Depth (m) ^a			Site Diameter (m)	Lat/Long	Lease Block
				Min	Max	Mean			
1	1	Eastern	High	60.4	78.2	66.0	200	29°26'19.131"N 87°34'27.273"W	Destin Dome 533
2	1	Eastern	Medium	70.3	82.3	77.6	120	29°26'41.053"N 87°36'26.512"W	Destin Dome 532
3	1	Eastern	Low	74.5	83.2	79.9	150	29°26'15.901"N 87°34'15.266"W	Destin Dome 533
4	2	Central	Medium	96.5	108.7	102.2	140	29°19'39.041"N 87°46'07.849"W	Destin Dome 661
5	3	Central	High	61.8	77.6	68.2	160	29°23'35.930"N 87°58'51.055"W	Main Pass 223
6	3	Central	Low	68.2	75.7	72.8	150	29°23'52.887"N 87°58'42.610"W	Main Pass 249
7	5	Western	High	69.0	88.0	77.7	200	29°15'24.844"N 88°20'21.455"W	Main Pass 286
8	5	Western	Medium	87.0	97.0	92.2	100	29°13'53.857"N 88°19'01.565"W	Main Pass 285
9	5	Western	Low	86.9	95.5	92.3	150	29°14'19.499"N 88°19'36.859"W	Main Pass 286

^a Minimum, maximum, and mean water depths recorded at photographic stations within the site.

Overview of Sampling Program

Fig. ES.3 shows the general schedule of field sampling activities. A brief summary is presented below.

During Cruise 1C (May 1997), subbottom profiling was conducted to geophysically characterize each site in more detail than was possible with the broad-scale geophysical reconnaissance (Cruise 1A). Grab samples were collected for geological and geochemical analyses. Hydrographic profiling was also conducted at each station. Hard bottom and fish community monitoring was conducted at each site using the ROV. Monitoring included random video/photographic transects and stations and fixed video/photoquadrats. Voucher specimens also were collected at some sites to help identify certain species.

The overall program consisted of repeating the Cruise 1C sampling (except for subbottom profiling) on three subsequent monitoring cruises. These were Cruise M2 (October 1997), Cruise M3 (April-May and August 1998), and Cruise M4 (April and July-August 1999).

Six physical oceanographic/sediment dynamics moorings were installed during Cruise 1C. Three moorings were installed at Site 1, and one each at Sites 4, 5, and 9. Each of these sites had at least one oceanographic mooring in place throughout the study. After about a year (Cruise M3), two of the three moorings initially placed at Site 1 were redeployed at Site 5 for the remainder of the program. Each mooring included current meters at 4 and 16 m above bottom (mab), sediment traps at 2, 7, and 15 mab, and an instrument that measured temperature, conductivity, dissolved oxygen, and turbidity.

Eleven “biomoorings” (arrays containing sets of settling plates) were also deployed during Cruise 1C as part of the epibiont recruitment study. Eight were deployed at Site 4 as a “time-series” experiment, with plates retrieved after different intervals of exposure. Single biomoorings were deployed at Sites 1, 5, and 9 and left in place for the same length of time to investigate spatial differences among sites.

Report Organization and Chapter Summaries

The Final Synthesis Report discusses all program components. Chapter 1 (Introduction) discusses the rationale and background for the program and summarizes program objectives, phases, components, and report contents and organization. Chapter 2 describes Site Selection and General Methods. The geological components are discussed in Chapter 3 (Geological Characterization), Chapter 4 (Geochemistry), and Chapter 5 (Sediment Dynamics). Chapter 6 discusses Physical Oceanography and Hydrography. Chapters 7 and 8 discuss Hard Bottom Communities and Fish Communities, respectively. Chapters 9 and 10 discuss the two companion studies (GIS and Microhabitat Studies, and Epibiont Recruitment, respectively). Each subject chapter includes an introduction, methods, results, and discussion. Chapter 11 (Synthesis) draws together information from all study components. One-page summaries are presented on the following pages.

Geologic Characterization (Chapter 3)

Investigators W. Sager and W. Schroeder	
Objectives <ul style="list-style-type: none"> • Characterize the geology and morphology of carbonate mounds • Characterize monitoring sites (bathymetry, topography, sediment texture, etc.) 	Methods <ul style="list-style-type: none"> • Geophysical surveys (high-resolution side-scan sonar, swath bathymetry, subbottom profiler) • Grain size analysis of grab samples • Visual analysis of substrates seen in photographs and videotapes
Results and Discussion <p>Four megasites (1, 2, 3, and 5) contained recognizable carbonate mounds. The size, number, and morphology of mounds varied significantly. For purposes of discussion, the mounds were classified into several different forms: small, "unit" mounds; composite mounds; irregular mounds; smooth-top mounds; and carbonate hard bottoms.</p> <p>From prior MMS-funded surveys in the study area, it was known that carbonate mounds are often clustered with sizes ranging from several meters on a side to hundreds of meters wide and 10 to 18 m high. It was also known that areas of high acoustic backscatter are associated with many mounds and that in some cases these areas are located to the southwest of the mounds. The present study emphasizes and broadens these findings. In addition, the study improved our understanding of the relationship of backscatter to the mounds and the sediment characteristics.</p> <p>Although it was known that many of the carbonate mounds are subcircular in plan view, new side-scan sonar data show the details of mound flanks and co-occurrences with far greater resolution. The data also show that the shelf-edge, irregular "pinnacle" mounds are unlike the shallower mounds in that the pinnacle mounds are often irregular or linear in plan view whereas the shallower mounds are usually subcircular in plan view and often made up of clusters of smaller subcircular "unit" mounds. The data also imply a third class of mounds: low, wide, carbonate hard bottoms hundreds of meters in diameter but only a few meters in height. These mounds often have tops with features a few meters or less in height that make them appear to be made up of many smaller "mini-mounds" and in this sense they are similar to many of the other, shallower subcircular mounds.</p> <p>Morphologic differences among mounds suggest differences in development. The low, wide carbonate hard bottoms imply slow upward growth over a large area, perhaps indicating stable sea level or slow sea level rise. It was previously speculated that such mounds grew at the shelf-edge during the slow sea level rise after the last ice age, but now they are known to be even more widespread. The tall, steep-sided "pinnacle" mounds suggest rapid growth during faster sea level rise. The widely-dispersed, shallower mounds, which are highly variable in size and height, may represent a short period of sea level stabilization in the middle of the deglaciation.</p> <p>The data also give insights about the location of mound formation. Prior data implied the mounds formed atop erosional unconformities on the two deltas in the study area. The new data support this observation. The data also imply that in some places, larger mound groups formed on bathymetric scarps or atop carbonate hard bottoms, suggesting that the mounds formed where suitable substrates were available.</p> <p>Subbottom profiles over the mounds frequently show asymmetric profiles, another clue to mound formation. Often large mounds have a peak at the seaward edge and have sediments dammed up on their landward sides. These characteristics suggest that mound growth was most intense on the side facing the sea, where perhaps nutrients are highest and sediments least. This is similar to the formation of coral reefs and lends credence to the hypothesis that mounds were formed by biological action in shallow water.</p> <p>Sediments at the monitoring sites are mainly sand, with a small and variable amount of clay. The sand-silt-clay ternary diagram implies two end-members, sand and clay, that are intermixed. Since the sediments currently being deposited in the region are fine clays, this could occur due to resuspension events that mix clay with sand in sediments. A third component consists of gravel-sized fragments, usually shell fragments or other biogenic debris. Gravel content is usually highest near mounds, indicating them as a source or suggesting mound proximity as an important factor controlling the presence of organisms. While normal sedimentation is not very active, evidently there are high-current events that cause significant reworking of the sediments. Evidence comes from both the grain size data and from scour marks seen in the side-scan sonar mosaics and the chirp sonar profiles that imply sediment redeposition during storms.</p>	

Geochemistry (Chapter 4)

Investigator	
M. C. Kennicutt II	
Objectives	Methods
<ul style="list-style-type: none">• Document the degree of hydrocarbon and trace metal contamination in the benthic environment at each site• Characterize the geochemical environment at each site to aid in determining the origins of sediment and to define the relationship between sediment texture and biological patterns	<ul style="list-style-type: none">• Analysis of hydrocarbons (total petroleum hydrocarbons [TPH], extractable organic matter [EOM], polycyclic aromatic hydrocarbons [PAHs]), and selected trace metals in grab samples (Cruise 1C only)• Analysis of total organic carbon (TOC) and total inorganic carbon (TIC) in grab samples from all four monitoring cruises• Trace metal and TOC/TIC analysis of sediment trap samples
Results and Discussion	
<p>Measures of sediment hydrocarbons at the sites were low and relatively uniform. Little or no evidence of petroleum related hydrocarbons was observed at any of the nine study sites. PAHs were at or below the method detection limits and appear to be derived from low-level, background contamination from atmospheric deposition that is seen Gulf-wide. The levels detected are several orders of magnitude below concentration levels that are thought to invoke biological responses. PAH concentrations at the study sites are equal to or lower than concentrations that have been detected at undisturbed sites in the western Gulf of Mexico far from platforms. There was a slight increase in EOM and PAHs toward the west, which is most likely due to finer sediments in that area (i.e., silts and clays tend to have higher concentrations of these contaminants).</p> <p>Trace metals indicative of contamination were at or near background levels at all sites as well. Barium, a tracer of drilling mud discharges, was observed to be at background levels with only a very few samples that might be interpreted as slightly elevated. Sediment metal concentrations in the study area are similar to those that have been observed far from platforms in the western Gulf of Mexico. These comparisons suggest that the study sites have been exposed to little or no contamination and that the concentrations observed are well below levels known to induce biological responses. There was a slight increase in a few metals (barium, chromium, iron, and zinc) toward the west, which is most likely due to finer sediments in that area (i.e., silts and clays tend to have higher concentrations of these metals).</p> <p>TOC in sediments at the study sites was low and relatively uniform. In most instances, TOC was less than 0.5%, occasionally reaching 1.0% or more. Sedimentary carbon was primarily in the form of carbonate. TIC ranged from ~3.5% to more than 8% (pure calcium carbonate would be 12% carbon). Carbonate content decreased from east to west by nearly a factor of two, reflecting proximity to riverine inputs of particulate matter.</p>	

Sediment Dynamics (Chapter 5)

Investigator	
I. Walsh	
<p>Objectives</p> <ul style="list-style-type: none"> • Make quantitative and qualitative measurements of extent and occurrence of the nepheloid layer • Determine sedimentation and resuspension rates • Determine how topographic highs affect present-day sedimentation • Relate short-term sediment dynamics to long-term sediment accumulation 	<p>Methods</p> <ul style="list-style-type: none"> • Vertically separated sediment traps (2 m, 7 m, and 15 m above bottom [mab]) • CTD/transmissometer/OBS profiles on each cruise • OBS instruments on current meter arrays • Trace metal, grain size and TOC/TIC analysis of sediment trap samples • ROV observations
<p>Results and Discussion</p> <p>The study area exhibits high spatial and temporal variability in particle flux. However, a benthic nepheloid layer (BNL) was present at all sites in all casts, though its intensity as measured by the beam attenuation and the vertical gradient in attenuation was variable. The BNL increased as bottom water temperatures decreased. The surface layer was characterized by low salinity and a local maximum in the particle concentration reflecting biological activity during both Cruise M2 (October 1997) and Cruise S2 (January 1998), with lower salinity and higher particle concentrations encountered in a westward direction.</p> <p>Particles in the nepheloid layer are inferred to have had similar size distributions and adsorption properties throughout the study period. This argues strongly for a local origin for the nepheloid layer particles, and against significant wide-scale advection of sediments through these sites. Rather, the local surface sediments probably have a rapid cycling between the water column following resuspension events and the surface sediments following deposition.</p> <p>Sediment trap results reflect the influence of resuspension at the study sites, with fluxes increasing toward the bottom for all moorings and time periods. Average vertical fluxes during non-hurricane periods ranged from 1.5 to 6 g m⁻² d⁻¹ in the traps 15 mab and from 6.7 to 29.3 g m⁻² d⁻¹ in the 2.5 mab traps. A persistent and energetic nepheloid layer at Site 5 resulted in the highest average bulk fluxes and lowest TOC concentrations in the settling material. Sites 1 and 4 had the lowest rates of resuspension and the lowest fluxes, though Site 1 had the highest sediment trap TOC concentrations. Site 9 had a robust and persistent nepheloid layer, with a peak mean concentration twice that found at Sites 1 and 4, though half of the peak mean was found at Site 5. Similarly, Site 9 fluxes fell between the low fluxes measured at Sites 1 and 4 and the high fluxes measured at Site 5. There was no consistent geographic trend in the sediment trap data set at any given depth level, suggesting that mesoscale variability was more important than local effects averaged over a mesoscale time period (i.e., the trapping period).</p> <p>No seasonal trends are apparent over the study period, which may reflect the dominance of storm and event-driven resuspension. The dominant temporal signal in the data set is the extremely high fluxes recorded during period 6 (21 July to 13 October 1998). During this period, Hurricane Georges passed near the mooring sites and energetic currents were recorded. Fluxes during this period were the highest recorded for each site and depth during the study, and ranged from 4 to 70 times the average fluxes exclusive of period 6.</p>	

Physical Oceanography/Hydrography (Chapter 6)

Investigators	
F. Kelly, N. Guinasso, Jr., and L. Bender	
Objectives <ul style="list-style-type: none"> • Characterize regional and local current dynamics • Determine the dynamics of important environmental parameters including temperature, salinity, dissolved oxygen, and turbidity • Define the relationship of current dynamics and environmental parameters to the geological and biological processes of the mounds 	Methods <ul style="list-style-type: none"> • Moored instrument arrays (currents, conductivity, temperature, dissolved oxygen, turbidity, sediment traps) • CTD/DO/transmissivity/PAR/OBS profiles • Collateral data (satellite imagery, meteorological observations, etc.)
Results and Discussion <p>Current meters at 16 meters above bottom (mab) measured the mesoscale flow just above the mounds. Across the entire study region there was substantial similarity in the observed flow fields. The most frequent direction octant and the direction of the vector mean current were east at Sites 1 and 9. At Site 4, located farther from shore in deeper water, there was a slight southwesterly bias as compared with the other sites. At all sites, the most frequent speed range was 5 to 10 cm/s, reflecting the normal tidal influence. Strong currents, i.e., greater than 40 cm/s, were most frequently directed to the southwest or west, particularly during Hurricane Georges (maximum of 97 cm/s at Site 1, 92 cm/s at Site 9, and 66 cm/s at Site 4).</p> <p>The near-bottom (4 mab) flow was more site specific. Bottom friction and the local topography influenced flow, particularly at Site 1. Compared to the other three sites, the 4 mab currents at mooring Site 1A (located about one "mound diameter" northeast of Site 1) had (a) a lower mean speed, (b) a greater percentage of near stagnant conditions, and (c) a much larger counter-clockwise rotation of the principal axis. These observed characteristics are consistent with the downstream flow disruption observed in published reports of laboratory experiments of stratified non-rotating flow over small hills.</p> <p>September 1998 was the most unusual month because of several events. Hurricane Earl crossed the eastern side of the study area on 3 September and the eye of Hurricane Georges passed over Site 5 on 29 September. Currents were strongest during Hurricane Georges. At 16 mab, speed reached 97 cm/s at Site 1. The direction of hurricane driven currents was mainly southwest at Sites 1 and 4, and shifted between southwest and northwest at Sites 5 and 9. Hurricane Earl, which moved more quickly across the shelf, forced a response of about half the intensity forced by Hurricane Georges. In the near-bottom currents (4 mab), the response to Hurricane Earl was strongest at Site 1, reaching about 50 cm/s, and was almost nonexistent at Site 4. During Hurricane Georges, the near-bottom response was strongest at Site 4, reaching 60 cm/s. Only during the hurricanes did turbidity values exceed normal background ranges. Between the two hurricanes, an oceanic circulation feature may have intruded onto the shelf. The intrusion event between the hurricanes was most evident at Site 4, where current speed at 4 mab exceeded 20 cm/s for 8 days.</p> <p>Based on a review of the temperature, salinity, and density profiles for each of the cruises, the density of the water in the upper part of the water column is controlled mainly by salinity. This suggests water properties determined by coastal processes. In the lower half of the water column, density is mainly controlled by the temperature, which suggests water properties determined by the presence of Gulf waters. Bottom salinity always ranged from 36.0 to 36.5 regardless of site depth, site location, season, or year. Water with this salinity is indicative of common Gulf water. Furthermore, salinity was generally uniform in the bottom half of the water column. Temporal variations in density, which were frequently seen, are the result of temperature variations. Intrusion of Loop Current water was seen only during the summer (July 1997) Cruise S1, occurring across the study region. The presence of Mississippi River plume water in the surface layer was seen in every summer cruise at every site. During the spring cruises, plume water was seen sporadically at the western sites. Plume water was not seen during the autumn and winter cruises.</p>	

Hard Bottom Communities (Chapter 7)

Investigators D. Hardin, K. Spring, S. Viada, A. Hart, B. Graham, and M. Peccini	
Objectives <ul style="list-style-type: none"> • Describe hard bottom community structure and seasonal dynamics at each site • Identify differences in hard bottom community structure among sites differing in relief and location • Understand relationships between community structure and environmental parameters 	Methods <ul style="list-style-type: none"> • Random video/photographic transects and stations • Fixed video/photoquadrats • Collection of voucher specimens
Results and Discussion <p>A total of 2,997 random photographs were analyzed from four monitoring cruises. With a few exceptions where the water was too turbid to obtain clear images, at least 85 random photographs were analyzed from each site on each cruise.</p> <p>The 40 taxa with the highest overall cover represented 14 taxon groups. Octocorals were the most diverse group (10 taxa), followed by sponges (6), ahermatypic corals (4), antipatharians (4), and ectoprocts (4). Ahermatypic corals were the most abundant group, due to the dominance of <i>Rhizopsammia manuelensis</i>. Cover varied substantially among sites but not much between cruises. Mean biotic cover (combined over all taxa and cruises) ranged from 13.5% at Site 3 to 30.6% at Site 4. Cover of <i>Rhizopsammia manuelensis</i> averaged 6.0% (over all sites and cruises).</p> <p>Statistical analysis showed that most of the 40 dominant taxa varied with respect to both relief category and region, as well as related environmental variables. Most of the taxa preferred medium-high relief habitat. Many taxa were found in higher abundances toward the east (i.e., farther from the Mississippi River), but some taxa increased toward the west. The generally low amount of variation accounted for by the linear models suggests that stochastic or unexamined processes contribute substantially to distribution patterns of hard bottom communities. Very patchy occurrences of dominant taxa within sites, such as <i>Madrepora carolina</i> and <i>Rhizopsammia manuelensis</i> at Site 3, exemplify this situation.</p> <p>Both linear models analysis and canonical correspondence analysis (CCA) indicated an important effect of sediment veneer, especially for medium-high relief taxa. CCA results indicated that 25% of the 40 dominant taxa were negatively related to the presence of a sediment veneer.</p> <p>The highest overall abundance was observed at high relief sites, with organisms distributed primarily on the sides and tops of features. These observations substantiate previous findings of high organism abundances on features elevated above the surrounding seafloor. This pattern may reflect reduced sedimentation and flux of suspended sediments, as well as increased food flux associated with current acceleration. Multiple regression using sediment trap data indicates there is a strong combined influence of proximity to the Mississippi River and height above the bottom on normal fluxes of suspended sediments, which could be influencing hard bottom communities.</p> <p>Observations from the fixed quadrats reveal a dynamic near-bottom environment. Numerous instances of sediment deposition, and occasional instances of erosion and organism growth and damage or mortality were noted. Over all sites and all fixed quadrat observations, the observed frequency of sediment deposition exceeded that of sediment erosion. Frequencies of damage/mortality and growth/recruitment were about equal.</p>	

Fish Communities (Chapter 8)

Investigator D. Snyder	
<p>Objectives</p> <ul style="list-style-type: none"> • Describe fish community composition and temporal dynamics at each site • Identify differences in fish community composition among sites differing in relief and location • Understand relationships between fish communities and environmental parameters • Identify trophic relationships among fishes, as well as between fishes and the epibenthic community 	<p>Methods</p> <ul style="list-style-type: none"> • Analysis of video and photographs from hard bottom community monitoring • Literature review of trophic relationships
<p>Results and Discussion</p> <p>Analysis of videotapes and still photographs yielded 76 fish taxa in 33 families. Mean numbers of fish taxa per cruise (combined over all sites) varied from 15 to 28. There were no significant differences in numbers of taxa among cruises, sites, relief categories, or location categories. Total numbers of taxa were not strongly correlated with any environmental variables.</p> <p>The most speciose families were sea basses (Serranidae), squirrelfishes (Holocentridae), morays (Muraenidae), lizardfishes (Synodontidae), jacks (Carangidae), wrasses (Labridae), and butterflyfishes (Chaetodontidae). The most frequently occurring taxa were rougtongue bass (<i>Pronotogrammus martinicensis</i>), short bigeye (<i>Pristigenys alta</i>), bank butterflyfish (<i>Chaetodon aya</i>), red barbier (<i>Hemanthias vivanus</i>), scorpionfish (<i>Scorpaena</i> sp.), and tattler (<i>Serranus phoebe</i>). Streamer basses (e.g., rougtongue bass and red barbier) probably numerically dominate the mounds. These species hover above the substrate, picking plankton from the water column. Streamer basses provide forage for a number of piscivorous species (e.g., amberjacks, groupers, sharks, and mackerels). The ichthyofauna consists primarily of reef fishes, although pelagic species (e.g., sharks, jacks, bluefish, and king mackerel) and demersal fishes (flounders) also were observed. Commonly seen species represent the deep reef fish assemblage reported for water depths of 50 to 100 m in the western Atlantic. The total number of taxa represents about half of the fish fauna known from the hard banks and reefs of the northern Gulf of Mexico.</p> <p>The influence of environmental variables on fish assemblage composition was examined by canonical correspondence analysis. Variables included relief, location, water depth, substrate classification, sediment flux, and distance from the Mississippi River mouth. Overall, there were no strong, consistent relationships. Site 1 had the most distinct species composition and supported the highest richness of reef species. Site 1 is in the high relief category, is the farthest from the Mississippi River mouth, and more importantly, is the shallowest of the study sites. Many fishes observed here, but not at other sites, commonly occur in shallow waters. The different species composition at Site 1 may be due to shallow water depth or other unmeasured correlates of water depth rather than relief category or distance from the Mississippi River.</p> <p>Frequency of occurrence of 17 common taxa was analyzed in relation to habitat characteristics at three scales: large (tens of kilometers to hundreds of meters), meso (tens of meters to 1 m), and small (1 m to centimeters). There were no strong patterns at the large scale. Meso-scale observations showed that some species regularly used portions (tops, sides, bases) of larger features, generally reflecting their feeding behavior. A fundamental pattern observed in meso- and small scale analyses was the separation of sedimentary and hard bottom habitats. Most smaller species remain near features for shelter from larger groupers, amberjacks, and sharks that patrol the structures. There was considerable overlap in use of the small scale habitats. Crevices, ledges, and holes were especially important to some species such as short bigeye (<i>Pristigenys alta</i>) and spinycheek soldierfish (<i>Corniger spinosa</i>).</p>	

GIS and Microhabitat Studies (Chapter 9)

Investigators	
I. MacDonald and M. Peccini	
<p>Objectives</p> <ul style="list-style-type: none"> • Integrate physical measurements with biological observations on a microhabitat scale within study sites • Provide uniform mapping products and geographic tools in support of the overall program 	<p>Methods</p> <ul style="list-style-type: none"> • Geographic information system (GIS) techniques were used to integrate and display data. Base maps of each site were prepared. Layers included bathymetry, side-scan sonar imagery, photograph and video transect locations, grab sample and mooring locations, substrate classifications, and gorgonian orientations.
<p>Results and Discussion</p> <p>Orientations of gorgonian colonies were measured from videotapes recorded at Sites 1, 3, 5, 7, and 9. The angle perpendicular to the major axis of the fans was used for the analysis. Colony numbers were plotted as a circular histograms. Circular statistics were used to test for relationships between mean current direction and gorgonian orientation.</p> <p>At every site, gorgonian orientations were non-random, with a distinct and unimodal central tendency. Gorgonian orientations at Sites 3, 5, and 7 generally agreed with the mean vectors of water flow recorded by the nearby current meters. Colony orientations at Site 9 were rotated counterclockwise from the mean flow, which is consistent with an Eckman effect upon the near-bottom flow. Gorgonian orientations at Site 1 were rotated by about 15° counterclockwise from the mean vector of the water flow; it is not clear whether all of the observed rotation is due to an Eckman effect. The results suggest that mean orientations of gorgonians are strongly influenced by mean directional water flow. Deviations from the current meter readings probably indicate local topographic steering that is not captured by moorings located well away from features.</p> <p>A detailed substrate classification scheme was applied to photographs taken at Sites 1, 3, 5, and 7. Six habitat categories were selected for further analysis. These were morphology, location on feature, silt veneer, small-scale roughness, medium-scale roughness, and slope. Abundances of gorgonian and antipatharian colonies in random photographs were then compared against habitat factors, following a set of standardized routines. Partial ANOVA tests were completed for the pooled abundance of all taxonomic groups (total colonies) and for the most abundant groups.</p> <p>In all cases, substrate characteristics were significant factors in determining the abundance of gorgonian or antipatharian colonies. Morphology, which distinguished among types of attachment substrata, was nearly always a significant factor in determining colony abundance. Although colonies did occur at photo-stations where there was no visible hard substratum, most were associated with a hard structure on the seafloor. Comparison of the types of structures used at different sites and by different taxonomic groups provides an indication of habitat preferences.</p> <p>Location on the feature was also a significant factor for the total abundance of all groups. Consistent with previous findings, the top edges and sides of features were preferred locations. Individual groups occupied a wider range of locations. The <i>Bebryce</i> and <i>Ctenocella</i> (<i>Ellisella</i>) groups, for example, were frequently found on the interior of the hard bottom features.</p> <p>Other important factors included silt veneer, which was a significant influence primarily at Site 3, a low-relief feature. This is consistent with a regime in which partial burial of hard bottom was common. Silt veneer was also significant at Site 7, where the sediment flats beyond the edges of the mound occupied a substantial portion of the study area.</p>	

Epibiont Recruitment (Chapter 10)

Investigators T. Holmberg and P. Montagna	
<p>Objectives</p> <ul style="list-style-type: none"> • Document the process of larval settlement, growth, and community development of hard bottom epibiota • Test hypotheses about the effects of location, height above bottom, duration of deployment, surface texture, predation, and water flow on recruitment 	<p>Methods</p> <p>Settling plates were attached to “biomoorings.” Major elements of the settling plate experiment studies were</p> <ol style="list-style-type: none"> 1. Spatial study at Sites 1, 4, 5, and 9 to last for 1 year; 2. Replication of the spatial study during the second year; 3. Uncaged, caged, and partially-caged treatments; 4. Three heights above bottom (0 m, 3 m, and 13 m), and; 5. Time series study at one station (Site 4), retrieval after 1 year and 2 years.
<p>Results and Discussion</p> <p>Nine phyla were found in the recruitment studies: Rhizopoda, Porifera, Cnidaria, Ectoprocta, Entoprocta, Mollusca, Annelida, Arthropoda, and Chordata. All except Porifera were present at every study site. Sponges were found on only a handful of samples from 3 and 13 meters above bottom (mab) at Sites 1 and 4.</p> <p><u>Bottom Temporal Study</u> – There were significant temporal changes for most taxa and categories at near-bottom depths. The <i>r</i>-selected, opportunistic epifauna were the earliest colonizers of new substrate patches in the study area. Diversity was low after 5 and 15 months but increased by 27 months of exposure. Specialized, <i>K</i>-selected species settled and grew in greater numbers throughout time. Community composition within phyla changed over time as well. For example, there was a shift in bryozoan communities from predominantly soft-bodied Ctenostomata to calcareous Cheilostomata and Cyclostomata. Overall, there was succession on the settling plates. The surrounding hard bottom communities were the likely source of recruits.</p> <p><u>Bottom Spatial Study</u> – There were significant differences in community structure and development among sites on near-bottom (0 mab) substrates. Settlement plates in the bottom spatial study were deployed and retrieved over a 15- or 27-month period. Site 4 was a polychaete-dominated community after 15 and 27 months exposure. Both Sites 1 and 9 were dominated by bivalves, but Site 1 had almost as many polychaetes as bivalves. Community differences among Sites 1, 4, and 9 at 0 mab were not reflected at 3 and 13 mab. It is unclear if there was sufficient difference in physical variation among Sites 1, 4, and 9 to cause the differences in community structure and development.</p> <p><u>Elevated Spatial Study</u> – There were no consistent trends among sites for percent cover, abundance, or community structure. Height of plates above bottom had the greatest spatial effect on community abundance and structure. Percent cover and abundance were greatest at 3 mab compared to 0 and 13 mab when differences existed. There were no significant patterns for effects of disturbance and small-scale turbulence on community structure. Plate orientation was a significant factor; vertical plates were covered by significantly greater abundances of stoloniferous organisms, including bryozoans, while solitary or slow-growing colonial animals were less abundant on the sides when compared to the bottom-oriented, or often top-oriented, plates. Results suggest that substrate relief and microhabitat characteristics (e.g., orientation of substrata to mean flow) have the strongest effects on community structure and development. Variations in larval supply due to flow field variance and sediment flux may explain the site-to-site and height above bottom differences.</p> <p>Just the earliest successional stages of community development were found on settling plates, and community structure was quite different from the surrounding, mature, hard bottom communities. Therefore, if disturbed, deepwater hard bottom communities could require decades to recover.</p>	

Synthesis (Chapter 11)

Investigators N. Phillips and D. Gettleton	
<p>Objectives</p> <ul style="list-style-type: none"> • Highlight relationships between hard bottom communities and environmental conditions, including temporal changes • Discuss implications of study findings for resource management • Evaluate program objectives 	<p>Methods</p> <ul style="list-style-type: none"> • Review and interpretation of previous chapter findings • Review of relevant published literature
<p>Results and Discussion</p> <p>Hard bottom community development is generally greater on higher relief features, and this result is likely due in part to the negative effects of resuspended sediments on hard bottom epibiota. Even though our sites were east of the 70 km “Mississippi Threshold” hypothesized by previous authors, there are some east-west patterns in hard bottom communities in the study area. Whether these reflect a direct or indirect influence of the Mississippi River or some other factor is not known. Other factors, including substrate variables and stochastic or unexamined processes, contribute substantially to distribution patterns of hard bottom communities.</p> <p>Substrate characteristics exert a profound influence on the distribution and abundance of hard bottom epibiota. At the regional scale, the mounds are “islands” of hard bottom in a surrounding “sea” of soft bottom sediments. Among sites, there is generally a positive relationship between percentage of emergent hard bottom and biological variables including biotic cover and numbers of epibiotal and fish taxa. At a finer scale, relationships between microhabitat factors and hard bottom taxa were documented, including effects of feature morphology, small- and medium-scale roughness, slope, location on feature, and sediment veneer. Habitat use by fishes within sites was documented, including certain species making use of features such as crevices, holes of different sizes, and epibiota such as sponges, crinoids, and soft corals.</p> <p>The current meter data indicate a regional flow regime with local variations dependent on topography, rather than a strong east-west or onshore-offshore gradient. Current direction is an important influence on the orientation of filter-feeding sea fans. The distribution of other epifauna on hard bottom features may also be affected by current directions. Existing knowledge of flow over bottom features suggests that different mounds, and different areas within a mound or mound complex, could experience local flow regimes that could affect the exposure of epibiota to sedimentation, erosion, and food flux. Also, effects of storm currents on sediment distribution around mounds is evident in the geological data, though effects on hard bottom community distribution have not been investigated.</p> <p>Information from this program may be used by the MMS to aid in leasing decisions. The existing lease stipulation focuses on avoiding mechanical damage (from placement of rigs, platforms, and pipelines) rather than avoiding exposure to drilling discharges. The emphasis on mechanical damage rather than sedimentation seems appropriate because the communities are exposed to significant natural sedimentation. However, relationships among community development, relief, and sediment flux suggest that it would be more detrimental to discharge drilling effluents on top of large, flat top mounds than to discharge them in low relief areas. Because the stipulation avoids features during rig and platform placement, drilling discharges are unlikely to occur on or near large, high relief mounds. This study does not suggest any simple classification scheme for mound communities for management purposes. Data collected during this program suggest that recovery of hard bottom communities following a disturbance would be slow.</p>	

Chapter 1: Introduction

Neal W. Phillips and David A. Gettleston

This report summarizes a four-year program to characterize and monitor carbonate mounds on the Mississippi/Alabama outer continental shelf (OCS). The study area is shown in **Fig. 1.1**. The “Northeastern Gulf of Mexico Coastal and Marine Ecosystems Program: Ecosystem Monitoring, Mississippi/Alabama Shelf” was conducted by Continental Shelf Associates, Inc. and the Geochemical and Environmental Research Group (GERG) of Texas A&M University (TAMU), for the U.S. Geological Survey (USGS), Biological Resources Division.

Based on previous studies and new geophysical reconnaissance, nine sites in the Mississippi/Alabama “pinnacle trend” area were selected for monitoring. Hard bottom community structure and dynamics were monitored because the potential sensitivity of these communities to OCS oil and gas industry activities is of interest to the Minerals Management Service (MMS), the client agency for whom the USGS administered this program. Geological and oceanographic processes were studied to help to understand environmental factors that control or influence hard bottom communities. These included substrate characteristics such as relief, microtopography, sedimentology, and contaminant levels; near-bottom current patterns; and the presence, extent, and dynamics of nepheloid layers. In addition, two “companion studies” provided information on epibiont recruitment and the distribution and orientation of sea fans in relation to currents and microtopography.

Background

The Mississippi-Alabama OCS is an important multiple use area for human commerce, fisheries harvest, recreation, and other activities, including oil and gas exploration and development (Brooks 1991). Adjacent states have placed heavy demands on its natural resources for marine transportation, dredge dumping, and commercial and recreational fishing. Because of the petroleum industry’s interest in the area and the potential for environmental impacts, an understanding of hard bottom communities and environmental processes that influence them is critical.

Fig. 1.2 shows locations of selected previous studies in the region. Hard bottom features on the outer shelf were first reported by Ludwick and Walton (1957), who documented a 1.6-km-wide band of shelf-edge features in water depths ranging from 68 to 101 m. These “pinnacles¹” typically had vertical relief of about 9 m, with some exceeding 15 m. Subsequent observations were reported during oil and gas lease block surveys by Woodward-Clyde Consultants (1979) and Continental Shelf Associates, Inc. (1985). Two major mapping and characterization studies were subsequently funded by the MMS: the Mississippi-Alabama Marine Ecosystems Study (MAMES) (Brooks 1991) and the

¹ Hence the term “pinnacle trend.” A more general term for hard bottom features in the study area is “carbonate mounds.” The pinnacles described by Ludwick and Walton (1957) are a subset of this category (see Chapter 3).

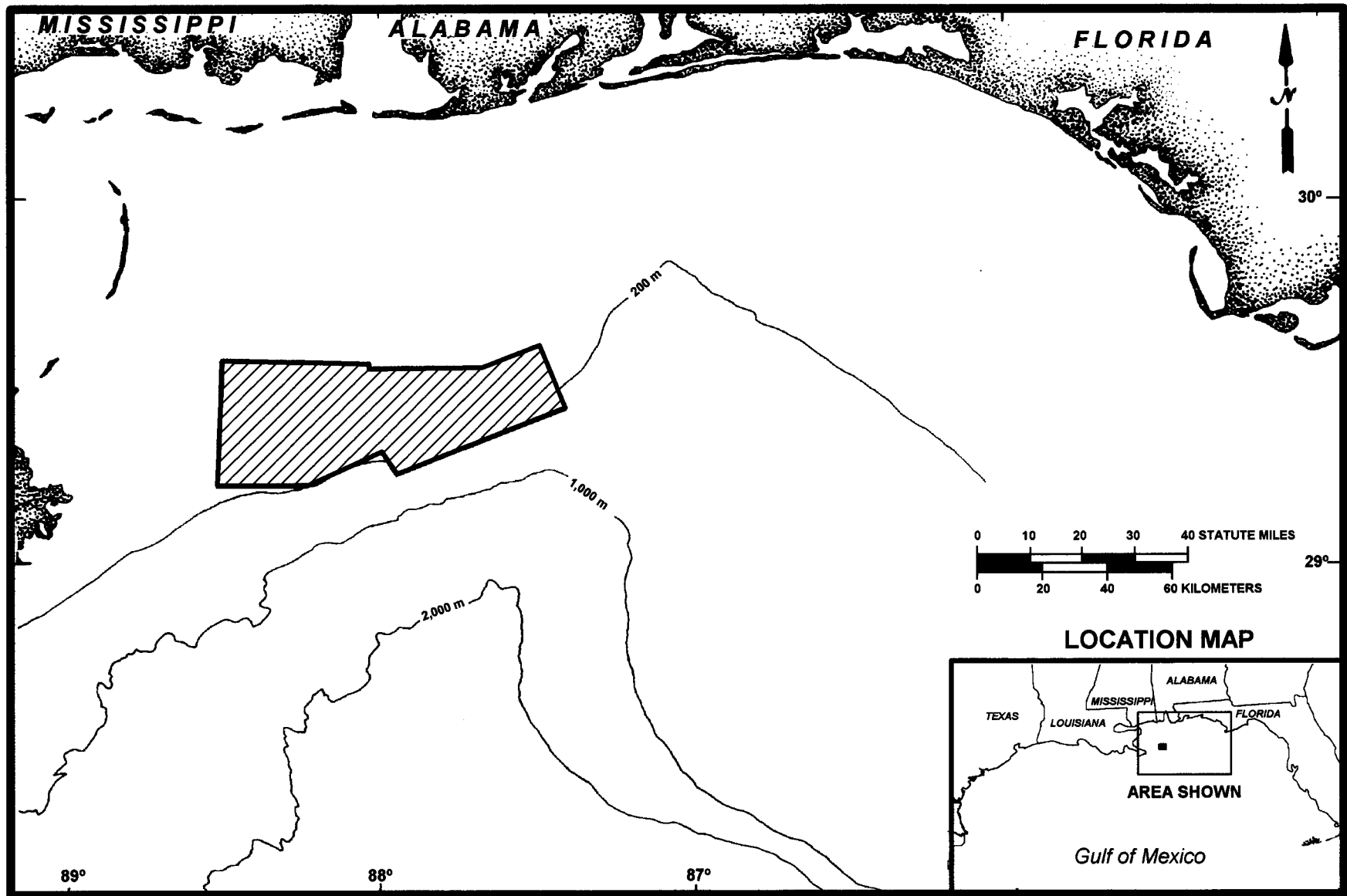


Fig. 1.1. Study area.

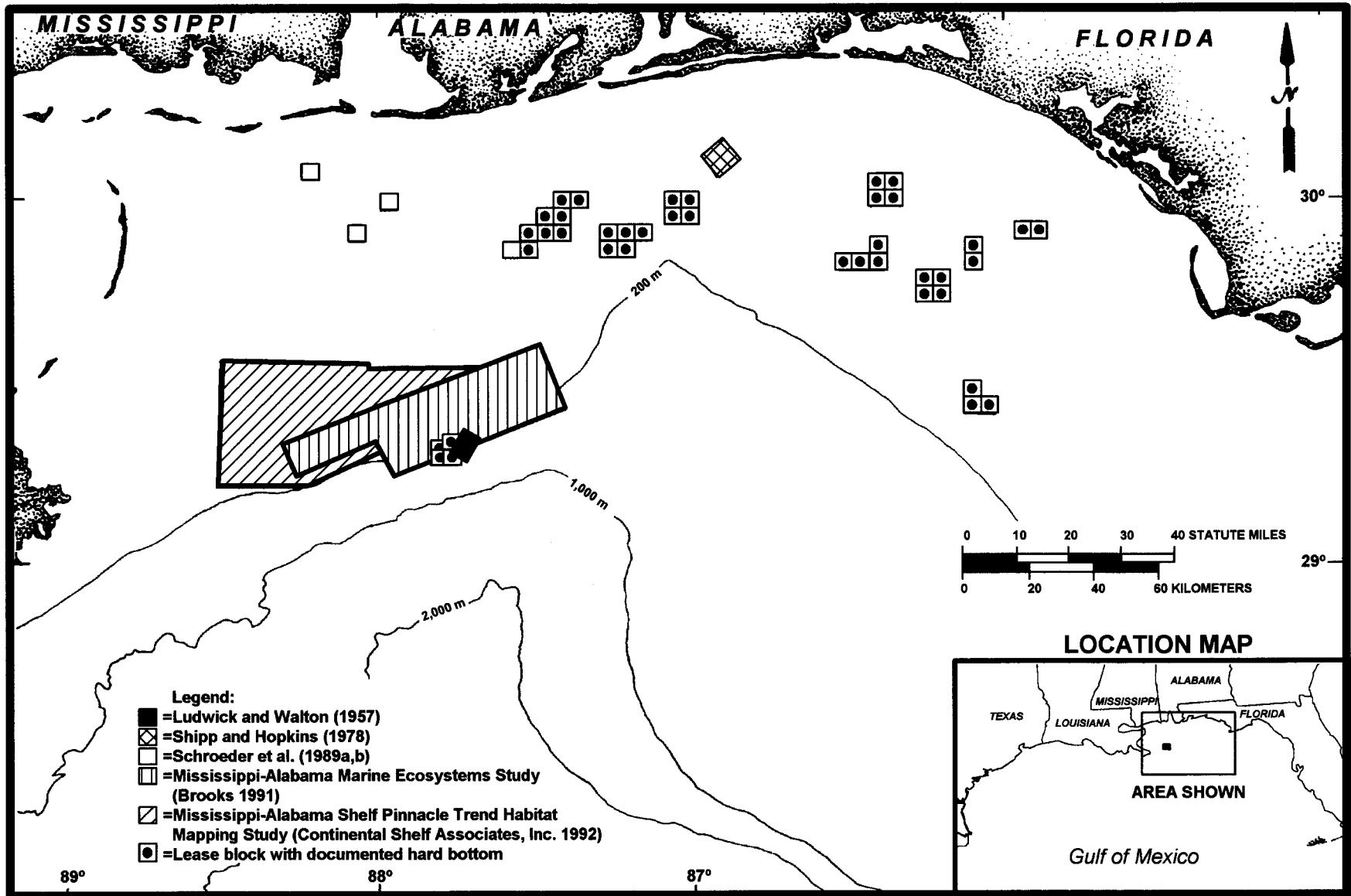


Fig. 1.2. Locations of selected previous hard bottom studies in the northeastern Gulf of Mexico.

Mississippi-Alabama Shelf Pinnacle Trend Habitat Mapping Study (MASPTHMS) (Continental Shelf Associates, Inc. 1992). MAMES included new field studies and provided a detailed synthesis of existing regional information about water masses and circulation, sediment characteristics and contaminants, water column biota, and soft bottom benthic communities including demersal fishes.

Information collected during MAMES, MASPTHMS, and earlier reconnaissance efforts consisted mainly of descriptive observations. These studies characterized major habitat types and identified some representative species. In addition, they provided some initial indications that epibiota vary with proximity to the Mississippi River, vertical relief of hard bottom, and position on hard bottom features, possibly due to current exposure and near-bottom fluxes of suspended sediments (Gittings et al. 1991, 1992). However, several data needs were identified (Continental Shelf Associates, Inc. 1992). These included investigations to determine the origin, current state, and probable future of carbonate mounds, both biologically and geologically; studies of turbidity and nepheloid layers on the Mississippi-Alabama shelf; and studies of species tolerance to turbidity and other factors. The present study was conducted to gather more detailed information about the distribution of carbonate mounds in the study area, to document the characteristics of hard bottom communities at greater resolution and in greater detail than was previously possible, to study relationships between epibiota and environmental variables, and to monitor the dynamics of biological and physical variables over time.

Ultimately, the information from this program may be used to aid in OCS leasing decisions and to evaluate potential lease stipulations to protect pinnacle communities during petroleum exploration and development. A series of studies during the 1970's and 1980's resulted in a biological community-based classification scheme for the Flower Garden Banks and northern Gulf hard banks (Rezak et al. 1985). These studies also documented the extent and importance of the nepheloid layer in controlling the composition of hard bottom communities. Biological, geological, and oceanographic data from these studies were used to develop lease stipulations, including shunting requirements and no-discharge zones near certain banks, which have been used successfully for many years in the northern Gulf of Mexico.

Objectives

The overall goal of this program was to characterize and monitor biological communities and environmental conditions at carbonate mounds along the Mississippi-Alabama OCS. Specific objectives were as follows:

- To describe and monitor seasonal and interannual changes in community structure and zonation and relate these to changes in environmental conditions (i.e., dissolved oxygen, turbidity, temperature, salinity, etc.); and

- To characterize the geological, chemical, and physical environment of the mounds as an aid in understanding their origin, evolution, present-day dynamics, and long-term fate.

Phases

The program consisted of four phases, each lasting approximately 12 months. These are summarized briefly below, and details are provided in Chapter 2.

- Phase 1 included two reconnaissance cruises (Cruise 1A, November 1996; and Cruise 1B, March 1997) followed by final site selection (April 1997) and the initiation of monitoring and companion studies on Cruise 1C (May 1997).
- Phase 2 included two monitoring cruises, M2 (October 1997) and M3 (April-May and August 1998). In addition, mooring service cruises were conducted in July 1997 (S1), January 1998 (S2), and July 1998 (S3).
- Phase 3 concluded the field sampling program with two additional mooring service cruises (S4, October 1998; and S5, January-February 1999) and one final monitoring cruise (M4, April and July-August 1999).
- Phase 4 did not include any new field work. During this phase, investigators analyzed and synthesized data from the entire program. Preliminary results have been discussed in three previous Annual Interim Reports (Continental Shelf Associates, Inc. and Texas A&M University, Geochemical and Environmental Research Group 1998a,b, 1999).

Components

Table 1.1 summarizes program components, including objectives, methods, and principal investigators. Four components formed the core of the program. These are geology, physical oceanography/hydrography, hard bottom communities, and fish communities.

The geology component included three subtasks: geologic characterization, geochemistry, and sediment dynamics. The geologic characterization attempted to derive as detailed a physical picture of the mounds as can be done with conventional geophysical and geologic data. Target areas were mapped using high-resolution side-scan sonar images, high-frequency subbottom profiles, grab samples, and video observations. The geochemistry subtask included a combination of hydrocarbon, metal, grain size, total organic carbon, and total inorganic carbon measurements in sediments and sediment trap materials. The sediment dynamics subtask included monitoring of nepheloid layer dynamics using sediment traps, transmissometer and optical backscatter profiles, and optical backscatter instruments on moored arrays.

Table 1.1. Program components.

Component	Objectives	Methods	Principal Investigators
Geology			
<i>Geological Characterization</i> (Chapter 3)	<ul style="list-style-type: none"> Derive as detailed a physical picture of the mounds as can be done with conventional geophysical and geologic data Document spatial and temporal variations in sediment texture (grain size) Characterize substrates according to morphology, roughness, and sediment cover 	<ul style="list-style-type: none"> High-resolution side-scan sonar High-frequency subbottom profiles Grain size analysis of grab samples Visual analysis of videotapes 	W. Sager W. Schroeder
<i>Geochemistry</i> (Chapter 4)	<ul style="list-style-type: none"> Document the degree of hydrocarbon and trace metal contamination in sediments at each site Determine concentrations of total organic carbon and total inorganic carbon in sediments and sediment trap materials 	<ul style="list-style-type: none"> Hydrocarbon and trace metal analysis of grab samples (Phase 1) TOC/TIC analysis of grab samples and sediment trap samples 	M. Kennicutt
<i>Sediment Dynamics</i> (Chapter 5)	<ul style="list-style-type: none"> Determine sedimentation and resuspension rates Describe the extent and dynamics of nepheloid layers Determine how topographic highs affect present-day sedimentation Relate short-term sediment dynamics to long-term sediment accumulation 	<ul style="list-style-type: none"> Vertically separated sediment traps CTD/transmissometer/OBS profiles Optical instruments on moored arrays Trace metal and grain size analysis of sediment trap samples 	I. Walsh
Physical Oceanography/ Hydrography (Chapter 6)	<ul style="list-style-type: none"> Characterize regional and local current dynamics Determine the dynamics of temperature, salinity, dissolved oxygen, and turbidity Define the relationship of current dynamics and environmental parameters to the geological and biological processes of the mounds 	<ul style="list-style-type: none"> Moored instrument arrays (currents, suspended sediments, conductivity, temperature, and dissolved oxygen, sediment traps) CTD/DO/transmissivity/OBS profiles Meteorological observations Collateral data (satellite imagery, etc.) 	F. Kelly N. Guinasso L. Bender

Table 1.1. (continued).

Component	Objectives	Methods	Principal Investigators
Hard Bottom Communities <i>(Chapter 7)</i>	<ul style="list-style-type: none"> Describe hard bottom community structure and seasonal dynamics at each site Describe differences in hard bottom community structure among sites differing in relief (high/med/low) and location (east/central/west) Describe relationships between community structure and environmental parameters such as small-scale habitat variability, rock type, sediment cover, turbidity, and other geologic and oceanographic variables 	<ul style="list-style-type: none"> Random video/photographic transects and stations (ROV) Fixed video/photoquadrats (ROV) Collection of voucher specimens (ROV) 	D. Hardin K. Spring S. Viada A. Hart B. Graham M. Peccini
Fish Communities <i>(Chapter 8)</i>	<ul style="list-style-type: none"> Describe fish community composition and temporal dynamics at each monitoring site Identify differences in fish community composition among sites differing in relief and location Identify relationships between fish communities and environmental parameters such as small-scale habitat variability, rock type, sediment cover, etc. Identify trophic relationships among fishes, as well as between fishes and the epibenthic community 	<ul style="list-style-type: none"> Analysis of video and photographs from hard bottom community monitoring (ROV) Literature review of trophic relationships 	D. Snyder
GIS and Microhabitat Studies <i>(Chapter 9)</i>	<ul style="list-style-type: none"> Determine whether sea fan orientation corresponds to predominant current direction Determine relationships between sea fan distribution and substrate/microhabitat types 	<ul style="list-style-type: none"> Analysis of photographs and videotapes from hard bottom community component Development of GIS as illustrative and analytical tool 	I. MacDonald M. Peccini
Epibiont Recruitment <i>(Chapter 10)</i>	<ul style="list-style-type: none"> Document process of larval settlement, growth, and community development of hard bottom epibiota Test hypotheses about effects of time and space, height above bottom, orientation of settling surface, disturbance, and flow disruption 	<ul style="list-style-type: none"> Settling plates on moored arrays ("biomoorings") 	T. Holmberg P. Montagna

Abbreviations: CTD = conductivity/temperature/depth; DO = dissolved oxygen; GIS = geographic information system; OBS = optical backscatter; ROV = remotely operated vehicle; TIC = total inorganic carbon; TOC = total organic carbon.

Physical oceanographic and hydrographic data were collected to help understand the geological and biological processes of the carbonate mounds. Data from moored instrument arrays, hydrographic profiles, and collateral sources provided a basis for characterizing regional and local current dynamics and understanding the dynamics of environmental parameters such as temperature, salinity, dissolved oxygen, and turbidity.

Hard bottom and fish community monitoring consisted mainly of video and photographic sampling at each site. These included both random photography and video transects, as well as repetitive photography of fixed stations. Random photographs were used to estimate the abundances of sessile and motile epibiota, whereas video images were used to quantify larger and more widely dispersed organisms and to broadly characterize substrates and species composition. Fixed video/photoquadrats were used to study temporal changes related to growth, recruitment, competition, and mortality.

In addition, two “companion studies” were designed to provide information on key ecological processes. The first, Microhabitat Studies, focused on sea fan orientation in relation to currents, and sea fan distribution in relation to microtopography. The microhabitat studies also included development of a geographic information system (GIS) that proved useful in other parts of the program. The second companion study, Epibiont Recruitment, used settlement plates deployed on moored arrays to document the process of larval settlement, growth, and community development. It tested hypotheses about variations with time and space, height above bottom, and orientation of settling surface, as well as effects of disturbance and small-scale turbulence.

Report Contents and Organization

This report presents the rationale and methods for all field work and discusses results from all program components. Following this introduction, Chapter 2 describes Site Selection and General Methods. The geological components are discussed in Chapter 3 (Geological Characterization), Chapter 4 (Geochemistry), and Chapter 5 (Sediment Dynamics). Chapter 6 discusses Physical Oceanography and Hydrography. Chapters 7 and 8 discuss Hard Bottom Communities and Fish Communities, respectively. Chapters 9 and 10 discuss the two companion studies (GIS and Microhabitat Studies, and Epibiont Recruitment, respectively). Each subject chapter includes an introduction, methods, results, and discussion. Chapter 11 (Synthesis) draws together information from all study components.

Chapter 2: General Methods

Neal W. Phillips

Detailed methods for each program component are included in the individual chapters. This chapter discusses site selection and presents an overview of the sampling program.

Experimental Design

This program is not, strictly speaking, a monitoring program. Monitoring studies are conducted to detect whether a change occurs in the existing or baseline condition, usually due to human activities (Green 1979). Although there has been some oil and gas drilling activity in the study area, sediment sampling indicates contaminant concentrations are not elevated (see Chapter 4). Moreover, the purpose is not to detect changes due to human activities. Therefore, this program might be more appropriately termed a “baseline study” in which spatial and temporal variations in the baseline condition are included.

The program design was specified in the contract issued by the USGS. The contract specified that a total of nine sites be selected, including high (>10 m), medium (5 to 10 m), and low (<5 m) relief sites in the eastern, central, and western portions of the study area. These were to be “monitored” on four surveys. This design was intended to facilitate a factorial analysis with three main categorical variables (relief, location, and survey). The four surveys provided some information about temporal variability, though sampling was not frequent enough to detect seasonal changes.

Stratification of sites by relief and longitude was considered reasonable based on previous studies. Studies of hard bottom communities in the Gulf of Mexico, South Atlantic Bight, and off Southern California have shown that community structure varies greatly with substrate relief (Marine Resources Research Institute 1984; Rezak et al. 1985; Continental Shelf Associates, Inc. 1987a; Phillips et al. 1990; Hardin et al. 1994). Observations with a remotely operated vehicle (ROV) during MAMES showed that the composition of hard bottom communities varied with relief and proximity to the Mississippi River plume. It was hypothesized that the river plume influences long-term water quality, resulting in diminished community development on hard bottom features close to the Mississippi River delta (Gittings et al. 1992).

In practice, the designation of sites as high, medium, or low relief proved simplistic due to the size of sites in relation to the mounds. For example, high relief sites were generally located on top of large mounds where there were extensive areas of relatively flat hard bottom. At other sites, the presence of multiple smaller mounds created a variety of hard bottom relief and orientation that was not captured by the single relief designation of a whole site. These issues are revisited in the Hard Bottom Communities chapter (Chapter 7) and the Synthesis chapter (Chapter 11). However, the designations for relief and geographic location are maintained throughout this report for completeness.

Site Selection

As noted above, the contract specified that nine sites be selected, including high (>10 m), medium (5 to 10 m), and low (<5 m) relief sites in the eastern, central, and western parts of the study area. Other factors considered in site selection were representativeness, availability of existing video and photographic data, and previous oil and gas industry activities. Site selection during Phase 1 involved the following steps:

- *Megasite Selection.* Prior to Cruise 1A, five large areas (“megasites”) were selected for geophysical reconnaissance (**Fig. 2.1**). The selection of the five megasites was based on geophysical data collected during MAMES (Brooks 1991) and MASPTHMS (Continental Shelf Associates, Inc. 1992). The megasites were selected because they were known to contain numerous features of varying relief (candidate sites) and could be surveyed within the time and financial constraints of the contract.
- *Geophysical Reconnaissance and Preliminary Site Selection.* During Cruise 1A (November 1996), the five megasites were surveyed using swath bathymetry, high-resolution side-scan sonar, and subbottom profiler to produce detailed maps (see Chapter 3). After the initial survey of all five megasites, small subsets were chosen for higher resolution mapping. After the cruise, a list of candidate high, medium, and low relief features within the megasites was prepared and the historical video and photographic data were tabulated. At this point, three high relief and two medium relief sites were tentatively selected.
- *Visual Reconnaissance.* Three low relief sites and one medium relief site with little or no previous video or photographic data were identified as needing visual reconnaissance. During Cruise 1B (March 1997), these features were briefly surveyed using an ROV to determine whether a hard bottom community was present. All sites visited during Cruise 1B were ultimately chosen as final sites.
- *Final Site Selection.* After the completion of Cruises 1A and 1B, the program managers and key principal investigators prepared a final site list. Site selection was discussed and approved during a teleconference with the USGS Contracting Officer's Technical Representative, the Scientific Review Board, and the program principal investigators.

Site Descriptions

The nine monitoring sites ultimately selected are shown in **Fig. 2.2**, and characteristics are summarized in **Table 2.1**. Brief monitoring site descriptions are presented below. Detailed descriptions of bathymetry and substrate characteristics are given in Chapter 3.

Each site was defined as a circular area of a certain diameter. Diameters of the nine sites were determined through an analysis of the bathymetric data collected during Cruise 1A. In this analysis, the standard deviation of the slope magnitude, slope direction, and depth were iteratively calculated for progressively larger areas of each feature, starting at the

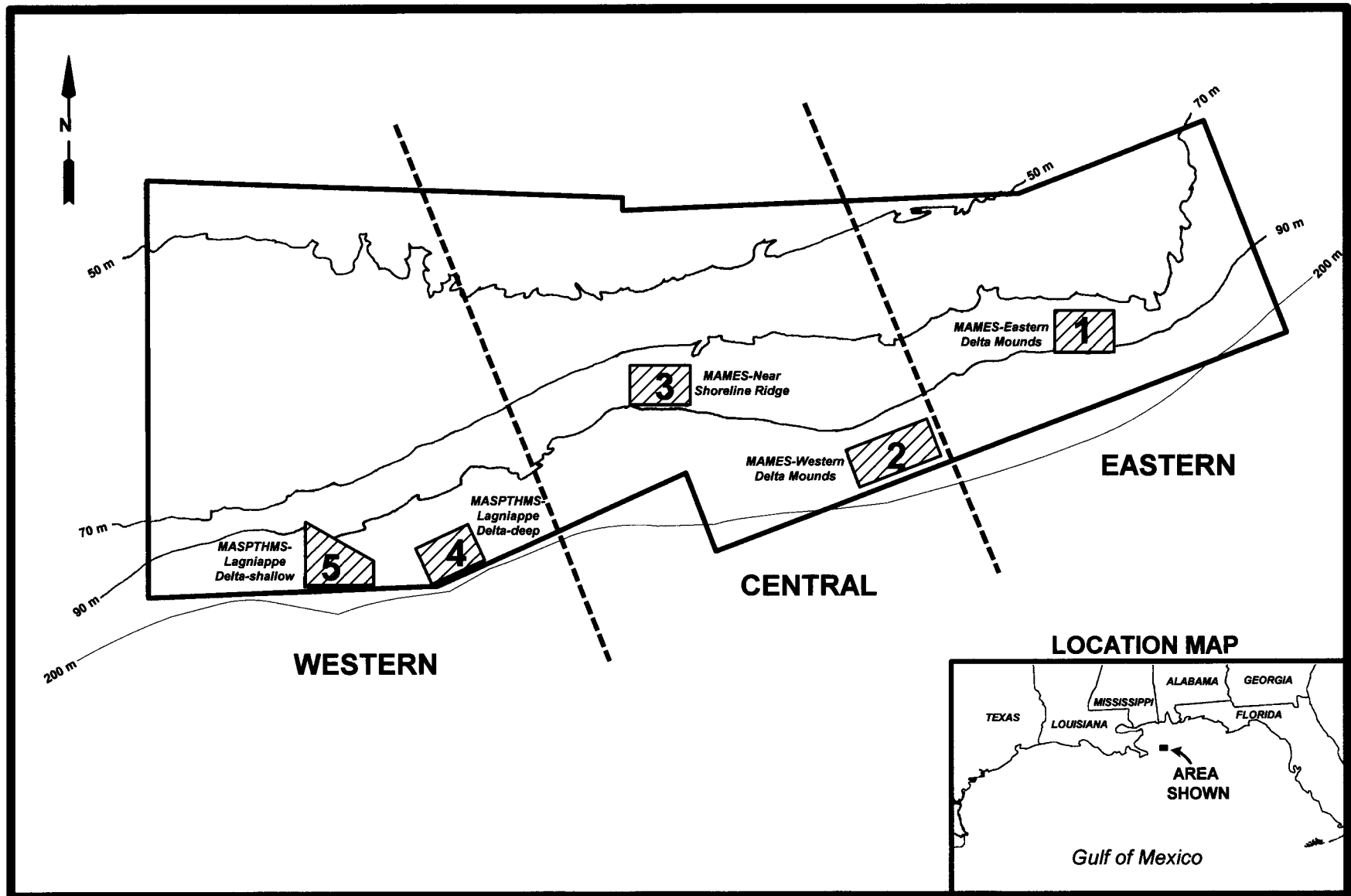


Fig. 2.1. Geographic locations of megasites surveyed during Cruise 1A.

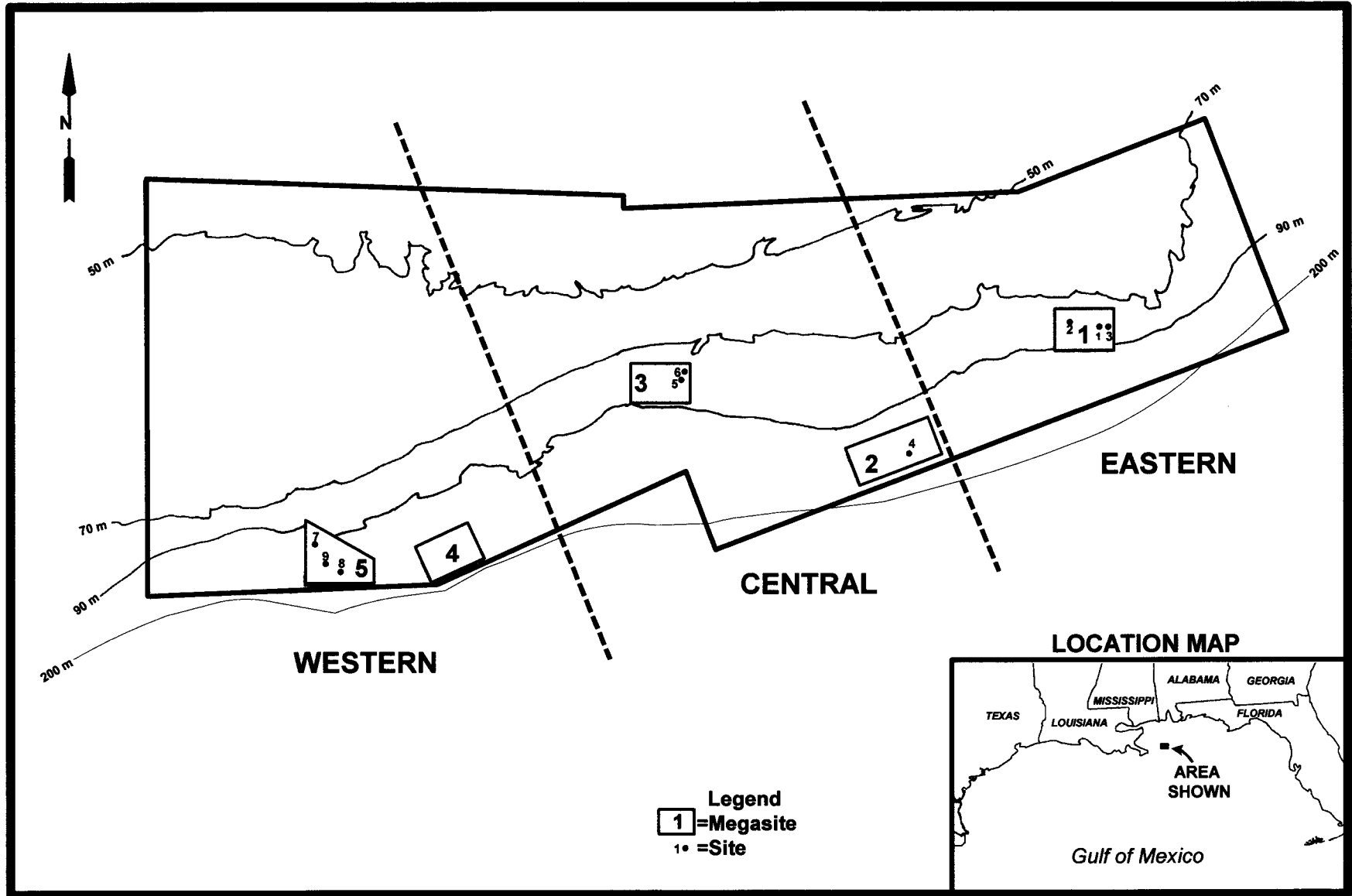


Fig. 2.2. Locations of final monitoring sites.

Table 2.1. Monitoring site locations.

Site	Megasite	Geographic Category	Relief Category	Water Depth (m) ^a			Site Diameter (m)	Lat/Long	Lease Block
				Min	Max	Mean			
1	1	Eastern	High	60.4	78.2	66.0	200	29°26'19.131"N 87°34'27.273"W	Destin Dome 533
2	1	Eastern	Medium	70.3	82.3	77.6	120	29°26'41.053"N 87°36'26.512"W	Destin Dome 532
3	1	Eastern	Low	74.5	83.2	79.9	150	29°26'15.901"N 87°34'15.266"W	Destin Dome 533
4	2	Central	Medium	96.5	108.7	102.2	140	29°19'39.041"N 87°46'07.849"W	Destin Dome 661
5	3	Central	High	61.8	77.6	68.2	160	29°23'35.930"N 87°58'51.055"W	Main Pass 223
6	3	Central	Low	68.2	75.7	72.8	150	29°23'52.887"N 87°58'42.610"W	Main Pass 249
7	5	Western	High	69.0	88.0	77.7	200	29°15'24.844"N 88°20'21.455"W	Main Pass 286
8	5	Western	Medium	87.0	97.0	92.2	100	29°13'53.857"N 88°19'01.565"W	Main Pass 285
9	5	Western	Low	86.9	95.5	92.3	150	29°14'19.499"N 88°19'36.859"W	Main Pass 286

^a Minimum, maximum, and mean water depths recorded at photographic stations within the site. For more general bathymetry of each site including surrounding areas, see Chapter 3.

center of the study site. Plots of these calculated standard deviations versus area were examined to ascertain the areas around the site center over which the standard deviations stabilized. This insured that the variability in elevation that the feature added to the surrounding background elevation was appropriately considered. Resulting site diameters ranged from 100 to 200 m. Physical oceanographic moorings and epibiont recruitment arrays (biomoorings) were placed on areas of flat bottom near certain sites, as discussed later.

- **Site 1.** This site is located on a large, flat-top mound known as 40 Fathom Fishing Grounds. The site extends across the top of the mound and down the steep northeastern flank toward a flat seafloor (**Fig. 2.3**). This was the shallowest site, and most photographic stations were on top of the mound (mean depth of 66 m); however, photographic station depths ranged from 60 to 78 m.
- **Site 2.** Bathymetry data show a mainly flat seafloor at a depth of about 78 to 80 m with a medium-sized mound about 50 m in diameter along the southern edge of the site (**Fig. 2.4**). The mound is about 9 to 10 m in height. Photographic station depths ranged from 70 to 82 m.
- **Site 3.** This low relief site is located to the east-southeast of the large mound where Site 1 is located (**Fig. 2.3**). It consists of patchy low relief mounds with diameters ranging from 1 to 10 m and relief of a few meters. Photographic station depths ranged from 74 to 83 m.
- **Site 4.** This medium relief site is located among large “pinnacle” mounds near the shelf edge. The site is located on a mound at least 10 m in height with a northwest trending ridge on its northwest side and a relatively flat top (**Fig. 2.5**). On top, the substrate is hard bottom with a thin sand veneer and low relief rock outcrops (0.5 to 2 m). This was the deepest site, with photographic station depths ranging from 96 to 109 m.
- **Site 5.** This high relief site has a tall, flat-top mound near its center and a lower mound at its southwestern edge (**Fig. 2.6**). Smaller outcrops occur along the edges of the mound. Photographic station depths ranged from 62 to 78 m.
- **Site 6.** This low relief site covers part of a large, carbonate hardground (**Fig. 2.6**). It consists of extensive areas of low-relief rock features ranging up to about 1 m in height on a relatively flat seafloor and covered with a thin layer of fine sediments. Photographic station depths ranged from 68 to 76 m.
- **Site 7.** This high relief site is located on a large, flat top mound known as 36 Fathom Ridge, which is elongated north-south (**Fig. 2.7**). The mound has more irregular edges than the two other flat top mounds (Sites 1 and 5). Photographic station depths ranged from 69 to 88 m.

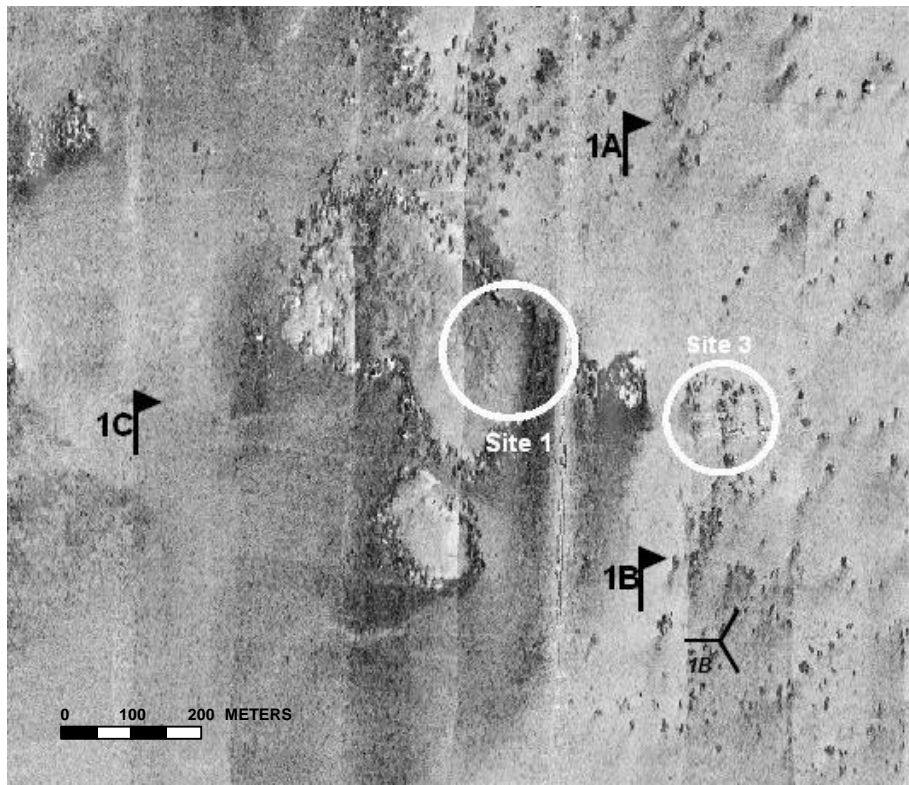


Fig. 2.3. Side-scan sonar mosaic showing the setting of Sites 1 and 3. Site diameters are 200 m for Site 1 and 150 m for Site 3. Current meter mooring locations are indicated by flags and the biomoooring location is indicated by a triad.



Fig. 2.4. Side-scan sonar mosaic showing the setting of Site 2. Site diameter is 120 m. There were no current meters or biomoorings located near this site.

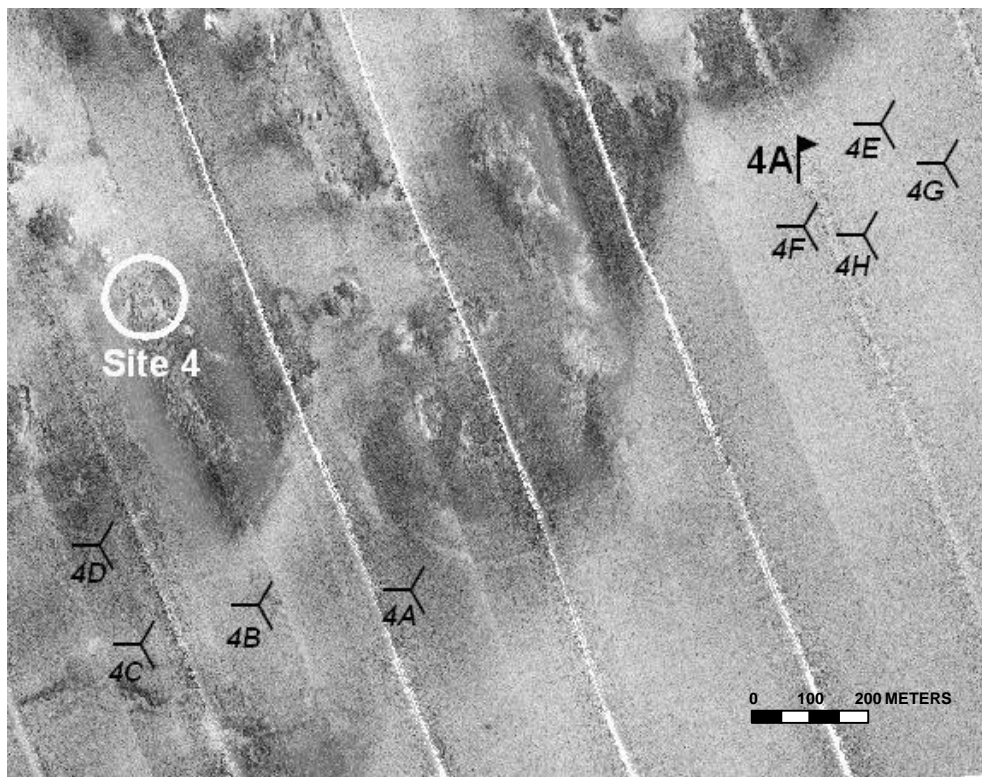


Fig. 2.5. Side-scan sonar mosaic showing the setting of Site 4. Site diameter is 140 m. Current meter mooring location is indicated by a flag and biomoooring locations are indicated by triads.

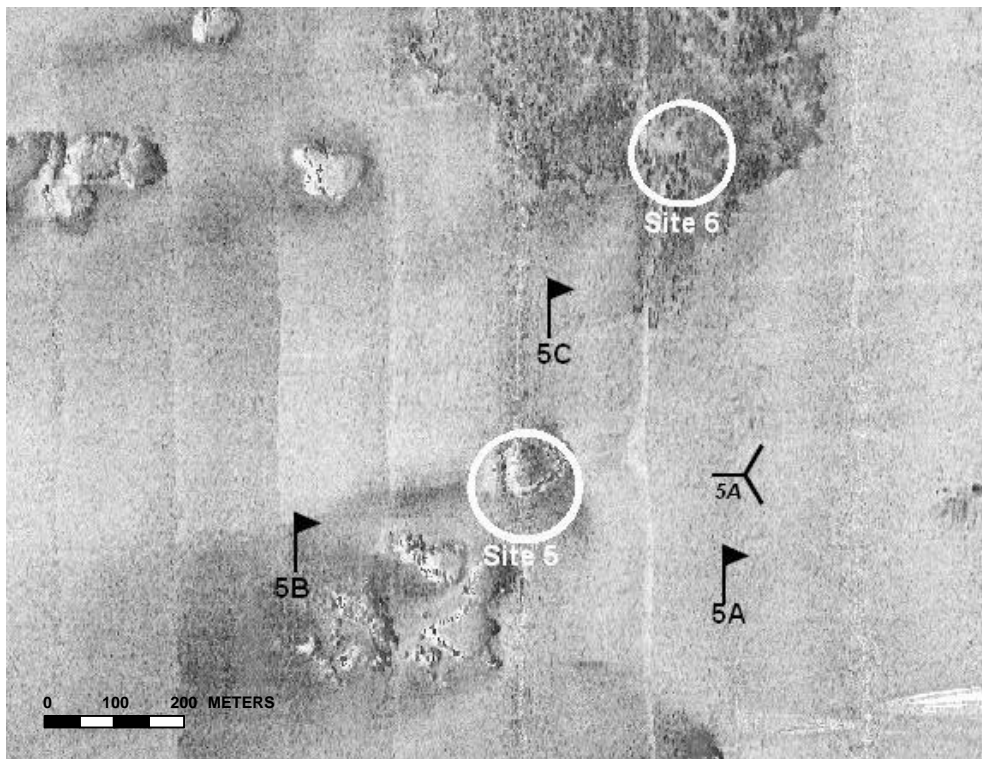


Fig. 2.6. Side-scan sonar mosaic showing the setting of Sites 5 and 6. Site diameters are 160 m for Site 5 and 150 m for Site 6. Current meter mooring locations are indicated by flags and the biomoooring location is indicated by a triad.

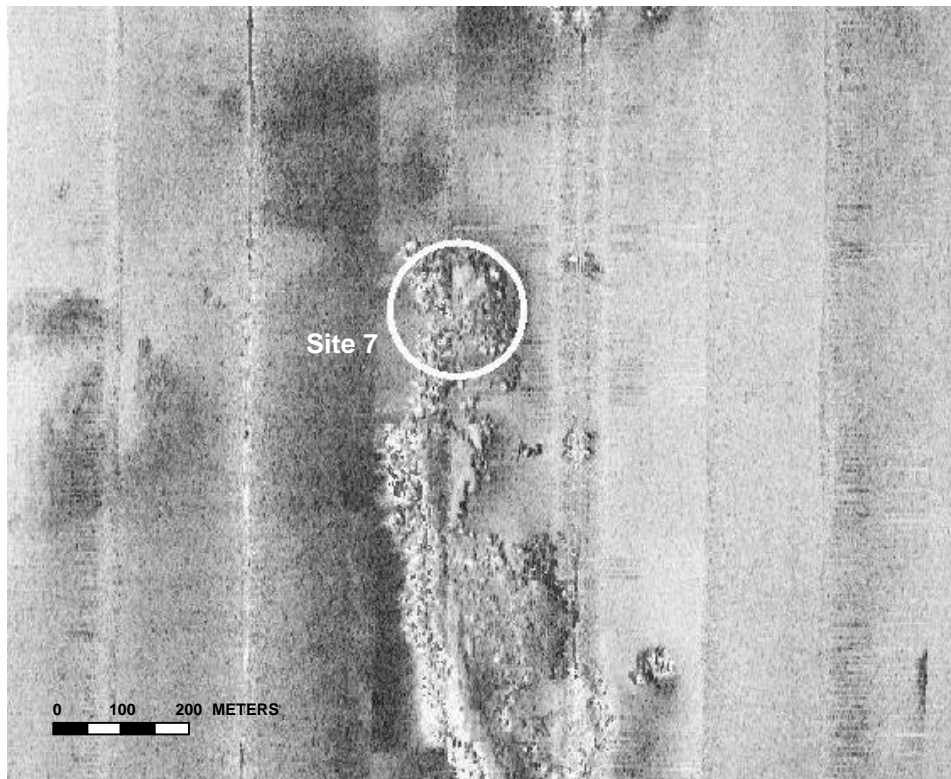


Fig. 2.7. Side-scan sonar mosaic showing the setting of Site 7. Site diameter is 200 m. There were no current meters or biomoorings located near this site.



Fig. 2.8. Side-scan sonar mosaic showing the setting of Sites 8 and 9. Site diameters are 100 m for Site 8 and 150 m for Site 9. Current meter mooring location is indicated by a flag and the biomoring location is indicated by a triad.

- **Site 8.** This medium relief site has a rugged mound near its center with numerous crevices and overhangs. The mound is slightly-elongated, approximately 40 m in north-south extent and 15 m in east-west extent with a smaller mound located nearby to the east (**Fig. 2.8**). Relief is 7 to 8 m above the surrounding seafloor. Photographic station depths ranged from 87 to 97 m.
- **Site 9.** This low relief site consists of low subcircular mounds, generally 0.5 to 2 m in height with diameters of 5 to 20 m (**Fig. 2.8**). There are a few features with up to 5 m relief with ledges, overhangs, and crevices. Photographic station depths ranged from 87 to 96 m.

Overview of Sampling Program

Fig. 2.9 shows the general schedule of field sampling activities. **Table 2.2** provides more detailed information about the specific sampling activities conducted at each site on each cruise. Cruise summaries are presented in **Appendix A**.

During Cruise 1C (May 1997), subbottom profiling was conducted to geophysically characterize each site in more detail than was possible with the broad-scale geophysical reconnaissance (Cruise 1A). Grab samples were collected for geological and geochemical analyses (see Chapters 3 and 4). Hydrographic profiling was also conducted at each station, including conductivity/temperature/depth (CTD), dissolved oxygen (DO), photosynthetically available radiation (PAR), transmissivity, and optical backscatter (OBS) (see Chapter 6). Hard bottom and fish community monitoring was conducted at each site using the ROV (see Chapters 7 and 8). Monitoring included random video/photo-graphic transects and stations and establishment of fixed video/photoquadrats. Voucher specimens also were collected at some sites to aid in species identification.

The overall program consisted of repeating the Cruise 1C sampling (except for subbottom profiling) on three subsequent monitoring cruises. These were Cruise M2 (October 1997), Cruise M3 (April and August 1998), and Cruise M4 (April and July-August 1999).

Six physical oceanographic/sediment dynamics moorings were installed during Cruise 1C (see Chapter 6). Three moorings were installed at Site 1, and one each at Sites 4, 5, and 9. Each of these sites had at least one oceanographic mooring in place throughout the study. After about a year (Cruise M3), two of the three moorings initially placed at Site 1 were redeployed at Site 5 for the remainder of the program. Each mooring included current meters at 4 and 16 m above bottom (mab), sediment traps at 2, 7, and 15 mab, and an instrument that measured temperature, conductivity, DO, and turbidity.

Eleven “biomoorings” (arrays containing sets of settling plates) were also deployed during Cruise 1C as part of the epibiont recruitment study (see Chapter 10). Eight were deployed at Site 4 and one each at Sites 1, 5, and 9. The biomoorings at Sites 1 and 9 were retrieved during the second leg of Cruise M3 (August 1998); turbidity prevented

Table 2.2. Summary of activities conducted on each monitoring cruise and mooring service cruise.

Site	Cruise and Date(s)										
	1C	S1	M2	S2	M3		S3	S4	S5	M4	
	(May 1997)	(Jul 1997)	(Oct 1997)	(Jan 1998)	(Apr-May 1998)	(Aug 1998)	(Jul 1998)	(Oct 1998)	(Jan-Feb 1999)	Apr 1999	July-Aug 1999
1	PHGV D(3) d(1)	HS(3)	HGV S(3)	HS(3) d(1)	HGV S(1) R(2)	r(1)	HS(1)	HS(1)	HS(1)	HR(1)	HGV r(1)
2	PHGV	--	HGV	--	HG	V	--	--	--	--	HGV
3	PHGV	--	HGV	--	HG	V	--	--	--	--	HGV
4	PHGV D(1) d(8)	HS(1)	HGV S(1) r(1)	HS(1) d(1)	HG S(1)	V r(3) ^a	HS(1)	HS(1)	HS(1)	HR(1)	HGV r(4)
5	PHGV D(1) d(1)	HS(1)	HGV S(1)	HS(1) d(1)	H S(1) D(2)	G	HS(3)	HS(3)	HS(2) D(1) ^b	HR(3)	HGV r(2) ^c
6	PHGV	--	HGV	--	H	G	--	--	--	--	HGV
7	PHGV	--	HGV	--	H	GV	--	--	--	--	HGV
8	PHGV	--	HGV	--	H	GV	--	--	--	--	HGV
9	PHGV D(1) d(1)	HS(1)	HGV S(1)	HS(1) d(1)	HS(1)	GV r(1)	HS(1)	HS(1)	HS(1)	HR(1)	HGV r(1)

Abbreviations: P = subbottom profiling D(#) = deploy oceanographic mooring(s) d(#) = deploy biomoorings(s)
H = hydrographic profiling S(#) = service oceanographic mooring(s) r(#) = retrieve biomoorings(s)
G = grab sampling R(#) = remove oceanographic mooring(s) V = video and photography

^a A fourth biomoorings was not recovered because it was visibly damaged (no plates remaining).

^b Array not recoverable, replacement deployed. Top current meter subsequently found by a fishing boat; data recovered.

^c Includes one biomoorings that could not be retrieved on Cruise M3 due to turbidity.

retrieval of the Site 5 biomoooring. Another set of biomoorings was deployed at the same sites on Cruise S2 (January 1998) and was recovered on the second leg of Cruise M4 (July-August 1999). The eight biomoorings at Site 4 are a “time-series” experiment; the original plan was to retrieve one on each subsequent service cruise and monitoring cruise until all eight were retrieved. However, this was changed so that all biomoorings could be retrieved on monitoring cruises when the ROV was present to cut the anchor line. One Site 4 mooring was retrieved on Cruise M2 (October 1997) and redeployed on Cruise S2 (January 1998). On the second leg of Cruise M3 (August 1998), three of the original Site 4 moorings were recovered and one was found to be damaged (no plates remaining); the remaining four were recovered on the second leg of Cruise M4 (July-August 1999).

Chapter 3: Geologic Characterization

William W. Sager and William W. Schroeder

Introduction

The purpose of the geologic characterization segment of this program was to investigate the geology and morphology of carbonate mounds and surrounding sediments on the Mississippi-Alabama outer continental shelf (OCS). These mounds formed in an unknown manner at lower sea level stands of the Pleistocene-Holocene transgression (Ludwick and Walton 1957; Sager et al. 1992) and they have become a substrate upon which a diverse marine ecosystem has evolved (Gittings et al. 1992).

Much of our current geological knowledge of the Mississippi-Alabama carbonate mounds and their environs comes from two prior MMS-funded studies: Mississippi-Alabama Marine Ecosystems Study (MAMES; Brooks 1991) and Mississippi-Alabama Shelf Pinnacle Trend Habitat Mapping Study (MASPTHMS; Continental Shelf Associates, Inc. 1992), both of which mapped the occurrence of carbonate mounds and the distribution of surficial sediments. Thousands of carbonate mounds ranging from less than a few meters in diameter to nearly a kilometer were found arrayed mostly in two isobath-parallel bands (Sager et al. 1992). Isobath-parallel ridges also were mapped in the shallower of these two depth zones. Both features are thought to be related to sea level stillstands during the last deglaciation. Surficial sediments are largely related to three late Pleistocene deltas, the Lagniappe Delta (Kindinger 1988, 1989) in the western part of the present study area (**Fig. 3.1**) and the "eastern" and "western" deltas in the original MAMES study area (Sager et al. 1999). These delta sediments were deposited during sea level lowstands, or in the case of the "eastern delta," during the early part of the last deglaciation (Sager et al. 1999). Atop these sediments is a thin, variable-thickness layer, consisting mostly of sand, that is thought to have been deposited by reworking of shelf sediments near sea level as it rose across the shelf during the last deglacial transgression (Sager et al. 1999).

The goal of the geologic characterization subtask has been to derive as detailed a physical picture of the mounds as can be done with conventional geophysical and geologic data, in effect, to bridge the gap between prior broad-scale surveys and seafloor observations made in other elements of this program. The MAMES and MASPTHMS surveys were reconnaissance in nature, defining the broad distribution and setting of the Mississippi-Alabama OCS mounds. This project has sought to provide greater detail in the characterization of the mounds and their geologic environment. Target areas were mapped using four different data types: (1) high-resolution side-scan sonar images; (2) high-frequency subbottom profiles; (3) grab samples; and (4) remotely operated vehicle (ROV) videos. High-resolution side-scan sonar mapping was used to construct acoustic images of the seafloor, which yield large-scale physical characteristics, such as shape, location, and large-scale roughness. Swath bathymetry data were derived from the side-scan and also give a rough measure of morphology. High-resolution subbottom profiler records and grab samples have been used to examine surrounding sediments and long term sedimentation. ROV videos were used to provide geologic characteristics at an even smaller scale (down to centimeters).

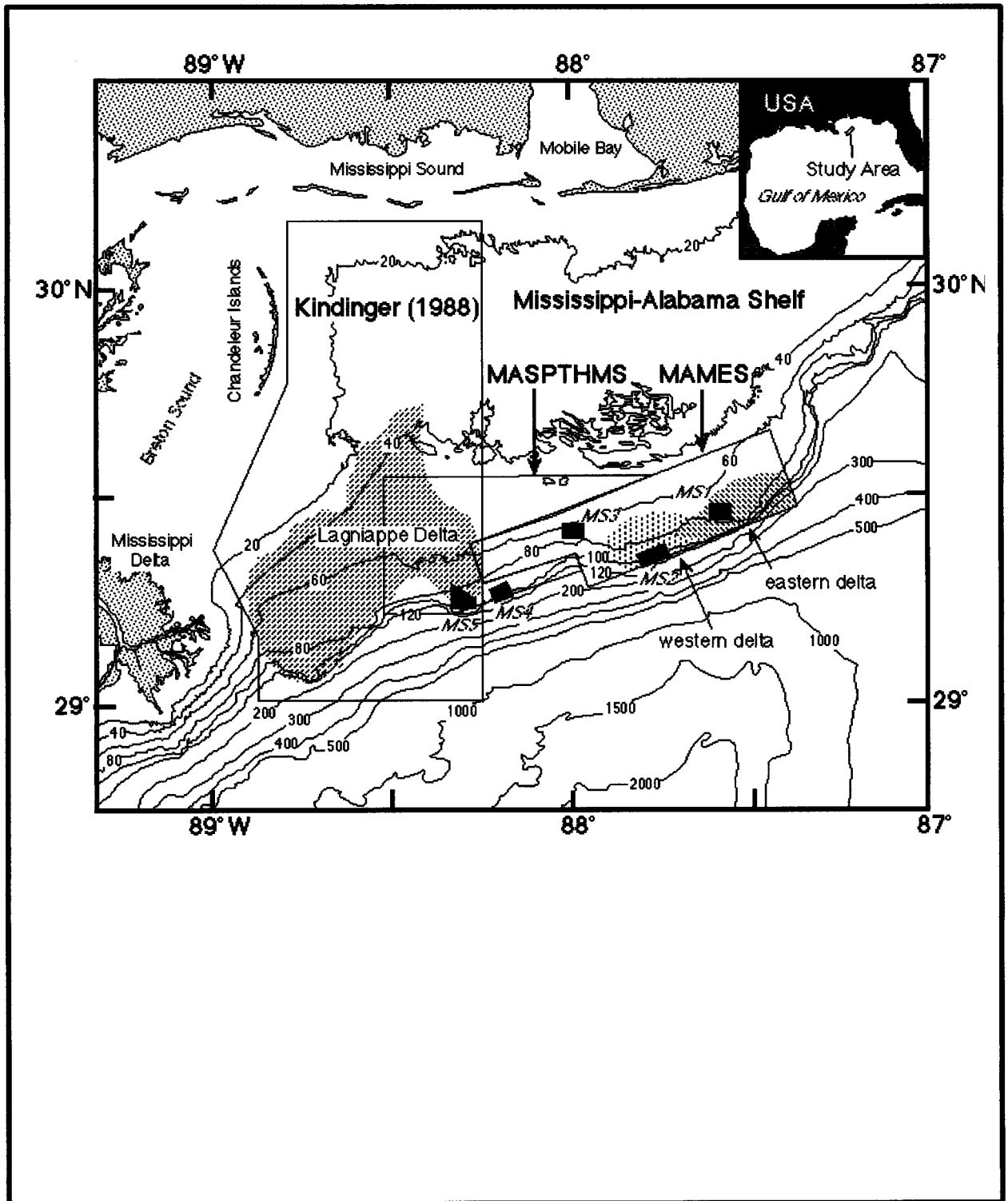


Fig. 3.1. Locations of MAMES, MASPTHMS, USGS study, and Megasites 1-5. Boxes show areas surveyed by MMS-funded MAMES and MASPTHMS studies along with area encompassed by USGS survey (Kindinger 1988; 1989). Small, numbered black boxes show megasite survey areas from this study. Hachured areas show locations of shelf-edge fluvial deltas mapped with high-resolution seismic reflection data (Kindinger 1988; 1989; Sager et al. 1999). Isobaths at 20-m intervals to 120 m and at 100-m intervals for deeper depths are shown for reference.

Methods

High-Resolution Geophysical Baseline Cruise (1A)

The purpose of the high-resolution geophysical baseline cruise was to gather large-scale geophysical images of the five megasites (**Fig. 3.1**). Two geophysical tools, a digital 72 kHz *TAMU²* side-scan sonar and an X-Star 2-12 kHz chirp sonar profiler were employed to produce three different data types: (1) sonar seafloor images; (2) swath bathymetry; and (3) subbottom acoustic reflection profiles.

One hundred eighty track lines, totaling 797 km in length and covering an area of 144.5 km² with side-scan sonar swaths, were collected at the five megasites with the side-scan sonar and chirp sonar. Ship's tracks were spaced 175 m apart and the ship's speed was approximately 5.5 knots with a sonar layback of about 85 m continuously measured with an ultra-short baseline acoustic tracking system. Navigation was done using a *Skyfix* differential global positioning system (GPS), with an accuracy of better than 5 m. On these tracks, which were either oriented at a heading of 0° or 30°, an image swath of 400 m was used to provide ~228% coverage of the seafloor. This allowed features directly beneath the sonar on one ship track to be imaged by adjacent tracks. This duplication was important because features have different appearances depending on the incidence angle of the acoustic waves and because the *TAMU²* sonar has a “blind spot” directly beneath the track. Because the sonar bathymetry swath is limited to 3.4 times water depth, the bathymetry swaths overlapped by 25% to 50% in these surveys.

The sonar digitization rate was typically 1,650 pixels per ping at a ping rate of 2.5 per second. This configuration implies that each pixel is representative of an area of seafloor 1.25 m by 0.24 m. In addition to these data, slightly higher resolution data were also collected during Cruise 1A on tracks oriented perpendicular to the main survey tracks over areas of particular interest. These “detailed” surveys typically had track spacings of 150 m, sonar swath widths of 200 m, and were digitized with 3,300 pixels per ping, and at up to 5 pings per second. The goal was to provide higher resolution images of likely sites for more detailed study. In all, 34.7 km of data were collected on these “detailed survey” lines covering an area of 5.6 km² with side-scan swaths.

Other Cruises (1C, M2, M3, M4)

Grab samples were collected for geologic analysis on the ROV baseline cruise (1C) and subsequent monitoring cruises (M2, M3, and M4). In total, 94 grabs were collected at the nine monitoring sites on Cruise 1C and five grab stations at each site were re-collected on subsequent cruises for a total of 45 samples for each cruise (**Appendix C**).

Additional chirp sonar data were collected on Cruise 1C. A grid of perpendicular lines was acquired between the lines collected over the “detailed” survey sites from Cruise 1A. Because the original grid had tracks with an east-west spacing of 175 m and north-south spacing of 150 m, the Cruise 1C data filled in the grids at spacings of 87.5 and 75 m.

Cruise 1C subbottom lines were positioned by differential GPS with an accuracy of about 5 m. The total length of subbottom data collected on Cruise 1C was 199.8 km.

TAMU² Sonar Data Interpretation

Sonar backscatter mosaics were produced by C&C Technologies, Inc. using proprietary image manipulation software. Images for each track were imported, georeferenced, and adjusted for sonar layback. The entire mosaic was built up of images for each of the component lines. Data gaps at the sonar nadir were filled with data from adjacent tracks. Owing to limitations of the proprietary image manipulation software, typical pixel sizes are about 1 m x 3-5 m. Subsequent analysis of the sonar mosaics has been carried out using ERMapper, a geographic information system (GIS) analysis software package. Analysis showed that the “detailed” surveys produced images with a resolution only marginally better than the standard surveys. Moreover, the detailed survey swaths contained data gaps between lines owing to the lesser swath widths. As a consequence, most of the sonar image analysis was done on the standard survey lines, with the “detailed” survey lines used for comparison where appropriate.

Bathymetry grids also were produced by C&C Technologies, Inc. Using proprietary software, sonar acoustic raypath takeoff angles were computed from phase angles measured at the sonar acoustic arrays. Takeoff angles and acoustic wave round-trip travel times were used to compute a depth profile perpendicular to the sonar track for each sonar ping. Depth locations and raypaths were corrected for variations in sound speed determined from periodic conductivity/temperature/depth (CTD) casts made during the survey. Depth values were binned and plotted using the public domain Generic Mapping Tools (GMT) software package (Wessel and Smith 1995). Megasite bathymetry grids were binned at 15-m intervals whereas detailed survey bathymetry data were binned at 1-m intervals.

The analysis of *TAMU²* images and mosaics is similar to geologic interpretation of aerial photographs. These images give a high-detail acoustic picture of sea bottom morphology and surface texture. The sonar builds an image based on the amplitude of acoustic return (“backscatter”) from the seafloor and this is related to morphology, roughness, and volume scattering within near-surface sediments (Johnson and Helferty 1990). Other data, such as swath bathymetry, subbottom profiles, and seafloor grabs, give different characteristics or ground-truth data (the grabs) that have been used to understand and interpret the images collected by the sonar. Using megasite sonar mosaics, we classified and characterized backscatter patterns and used these to make interpretation maps of geologic features. Sonar images were also used to describe mound morphology in a variety of ways: classifying mound shapes, calculating mound size distributions, and calculating mound aspect ratio variations.

TAMU² bathymetry data were used to make large and small-scale contour maps of each megasite and each monitoring site. These have been used to examine seafloor topography and mound morphology, orientation, and large scale roughness.

Subbottom Profile Interpretation

Data from the chirp echo sounder have been used to examine thickness and character variations of shallow sediments in the study areas. The profiles have been analyzed using standard seismic stratigraphic techniques (e.g., Mitchum and Vail 1977). This involves (1) recognition and correlation of acoustic reflectors by their characteristics, and (2) mapping and interpretation of seismic facies. The latter step assumes that sediments of different sedimentary facies give a common, recognizable acoustic response. In addition, the subbottom records have been an invaluable tool for interpreting the side-scan sonar mosaics because they show seafloor topography and sediment layers that can be compared with the sonar images.

High-Resolution Bathymetry

Because of the limited resolution of the TAMU² bathymetry (see next section), additional bathymetry data were collected at each of the monitoring sites using a high-frequency echo sounder during the monitoring cruises. These data were gridded to produce higher resolution bathymetry maps of the monitoring sites.

Sediment Grain Size Analysis

Grain size measurements were made on grab samples using standard techniques (Folk 1974). Samples were homogenized, treated with bleach to oxidize organic matter, and washed with distilled water to remove soluble salts. Sodium hexametaphosphate was added to deflocculate each sample before wet-sieving with a 62.5 micron (4ϕ) sieve to separate the sand and gravel from the mud fraction. The sand and gravel fraction was dried, weighed, and sieved at $1/2\phi$ intervals from -1.5ϕ to 4.0ϕ . Each fraction was examined for aggregates and those found were disaggregated. Sample fractions were weighed to three significant figures. The mud fraction was analyzed for particle size by the pipette settling method at intervals of 4.5ϕ , 5.0ϕ , 5.5ϕ , 6.0ϕ , 7.0ϕ , 8.0ϕ , 9.0ϕ , and 10.0ϕ .

ROV Video and Photo Classification

ROV videotapes and still photographs were collected during the baseline and three monitoring cruises. These data provide valuable geologic information concerning seafloor features, hard bottom types, and texture. Tapes and photos from Cruise 1C were viewed and characterized for all sites using the descriptors in **Table 3.1**. As a first cut, we attempted to characterize only the random photo stations, thinking that they constituted the most uniform data set since all photos were taken at the same distance from the sea bottom (0.7 m). However, it became apparent that the geologic context was difficult to assess solely from the photos owing to the small area covered by each (approximately 0.75 m x 0.75 m). Consequently, transects between photo stations were analyzed to determine the broader geologic setting.

The set of descriptor terms (**Table 3.1**) was selected to describe the morphology, roughness, and sediment cover of the sea bottom viewed by the ROV. These terms are an

attempt to assess qualitative features that might be significant to biologic populations for comparison with biologic data collected in other aspects of this program. Because rock outcrop is often covered by a veneer of sediments, the presence or absence of outcrop was determined by seafloor relief or lack thereof. Flat areas were mainly described by their surroundings: open, channel, and terrace. Outcrop areas were characterized in a number of ways. Relief was described as near-vertical, moderate, or near-horizontal. Outcrops were classified by size: small outcrops (~meter size) were termed mounds, large isolated rocks were termed monoliths, whereas extensive hard substrates were termed hard bottoms. In this context, the top of a large mound would be described as a hard bottom. Where a station was on an outcrop that rose above an area of flat sediments, the height was estimated. Sediment cover was described on outcrop areas in two ways. At many sites, fine-grain sediments tend to make a veneer whereas coarse sediments and shell hash often fill depressions. In such situations, the descriptors thin, moderate, and thick were applied to the veneer of fine-grain sediments. For coarse sediments, the degree of burial was estimated (none, partial, near complete). The surfaces of outcrops often show small-scale texture or pitting, probably owing to dissolution or bioerosion. When present, we classified this texture as small (tens of cm) or medium (~50-100 cm). Using a GIS program (ArcView), the photo stations and video transects were plotted and continuous boundaries between morphological regions were approximated.

Table 3.1. Seafloor geologic descriptors used for ROV photo and video classification.

General	Morphology (large scale)	Relief (scale m)	Texture (scale cm)	Sediment Texture (Fine)	Sediment Texture (Coarse)
Relief present (outcrop)	Mound Monolith Hard Bottom	Vertical Moderate Near- Horizontal	Small (10s cm) Medium (50-100 cm)	Thin Moderate Thick	None Part burial Near-complete burial
Flat area (no outcrop)	Open Channel Terrace	Not desc.	Not desc.	Not desc.	Not desc.

Results

Megasite Bathymetry and Mosaics

The bathymetry data produced from the *TAMU²* sonar far exceed previous similar data sets for accuracy and coverage. Nevertheless, several limitations of this sonar are obvious in bathymetry maps produced for this project. To obtain greater depth precision, adjacent data values were averaged, so mounds have rounded shapes in comparison to their shapes seen in the sonar backscatter images. Furthermore, small mounds do not appear in the data because the averaging process causes smoothing, which attenuates them. Overlapping data from adjacent tracks are frequently offset by 10 to 15 m (and sometimes more), owing to navigation uncertainties, so a small mound on one track can be averaged with a flat patch of seafloor on an adjacent track. Furthermore, smaller mounds are usually averaged with adjacent flat seafloor when their size is much smaller than the depth value bin size. As a result of this smoothing, the megasite bathymetry maps typically show only those mounds greater than about 25 m in diameter. In the detailed survey bathymetry, features with diameters greater than about half that size are preserved.

Two additional artifacts are noted by their along-track trends. First, the data occasionally display offsets of ~1 m from data collected on one track to those adjacent. In some instances this may be a “roll bias” in which the values on one side of the cross-track depth profile are slightly too great or too small. It is most obvious when we examine the data in extreme detail in small areas around the monitoring sites. The second artifact may be related. It appears as a crenulation of the contours in a track-parallel direction caused by the cross-track depth profile being bowed upwards in the center. This is probably a result of imperfect corrections for the refractive effects of sound-velocity variations in the water column because it is worse at some sites (e.g., Megasites 1, 2, and 5) than at others (e.g., Megasites 3 and 4). To understand this effect, recall that depths near the track lines are calculated from acoustic waves that travel nearly vertically through the water column and are therefore less affected by refraction. In contrast, depth soundings near the edge of the sonar swath leave the sonar at shallow angles, so their paths are affected by refraction to a greater degree. Consequently, a small error in determining water velocity versus depth profiles can translate to a greater error in determining depth at the edges of the sonar swath. At Megasite 1, for example, the crenulations typically appear as variations of about ± 150 m in the lateral position of a particular contour in “flat” areas. The regional slope is about 0.17° , so this suggests an error of about ± 0.45 m in depth, which is in turn 0.6% of the water depth in Megasite 1. Thus, the bathymetry data are better than “hydrographic” precision (<1% of water depth), yet because the slope is very shallow, the bathymetry contours appear irregular. For presentation purposes, the large scale bathymetry maps in the following sections were hand-smoothed and redigitized.

Mosaics made from *TAMU²* side-scan sonar data contain images constructed from the merging of backscatter image strips from individual ship’s tracks. The side-scan sonar sends out a fan-shaped acoustic pulse that is narrow and parallel to the ship’s track and wide in the orthogonal direction. The sonar then plots a “scan” depicting the amplitude

of the backscattered signal for that particular pulse. By sequentially plotting many scans from subsequent pulses, an image is constructed. Typically the image is transformed to appear as if made by an "aerial photograph" illuminated from the ship's track, i.e., "light" areas face the sonar and shadows are on the opposite sides. Usually little of the returned acoustic energy comes from reflection because the incidence angle is such that most such energy continues to propagate away from the sonar. Most of the returned energy is "backscattered," a process that includes diffraction from microtopography and scattering of energy from particles in the uppermost sediments (so called "volume scattering") (Johnson and Helferty 1990). In the images, strong echoes are plotted dark whereas weak returns and shadows are light. Much of the returned acoustic signal appears to be related to mound topography and roughness (i.e., shadows, strong returns from faces that are directed towards the sonar, and diffraction from rough areas) and backscatter variations caused by sediment textural variations.

Megasite 1

Megasite 1 (Figs. 3.2, 3.3, and 3.4) shows two large mound clusters near the shelf edge in water depths of 68 to 90 m. The western cluster is subcircular, approximately 600 m in diameter, and contains several smaller, steep-sided mounds. The other cluster is a crescentic band, approximately 800 m wide and 3,000 m long, located in the northeast part of the megasite. It contains two large flat-top mounds, approximately 300 to 400 m in diameter, and about a dozen smaller mounds. The large features are part of the "40-Fathom Fishing Ground" mound cluster that has been studied in prior MMS projects. One of these is the location of Site 1 (Fig. 3.3). The seafloor around the mounds is nearly flat, with a shallow slope to the south. Contours suggest that there is a 3 to 5 m depth difference from north to south across the crescentic mound band. This is in part owing to sediments tending to pile up on the north sides of these features.

Prominent in the Megasite 1 mosaic are numerous groups of medium to large mounds, principally located in the northern, central, and western parts of the survey area (Figs. 3.3 and 3.4). In contrast, much of the seafloor in the southern part of the survey area is mostly featureless. The large mound group in the north-central part of the megasite contains several large, flat-top mounds greater than 100 m in diameter. Numerous smaller mounds are associated with these larger mounds. Another large mound group appears at the western edge of the survey. Associated with all of the mounds are areas of high backscatter, which appear dark in these mosaics. These high-backscatter features usually are located on the southwest sides of the large mounds and mound groups. In subbottom profiler records, these areas show some erosion of the surficial sediments, so they are probably a textural difference caused by current winnowing (see discussion of sediment texture below). Many small to medium mounds show high-backscatter "tails" extending to the southwest (Fig. 3.5). These appear as shallow gullies in the subbottom profiler records, implying erosion by bottom currents (Fig. 3.5; see discussion of current scour marks below). In the northeast part of Megasite 1 are three linear to sub-linear high-backscatter features that appear to be small buried ridges in the subbottom profiler records. The most linear is about 25 m wide by 300 m long. These may be related to the shoreline ridges noted in the original MAMES survey (Sager et al. 1992).

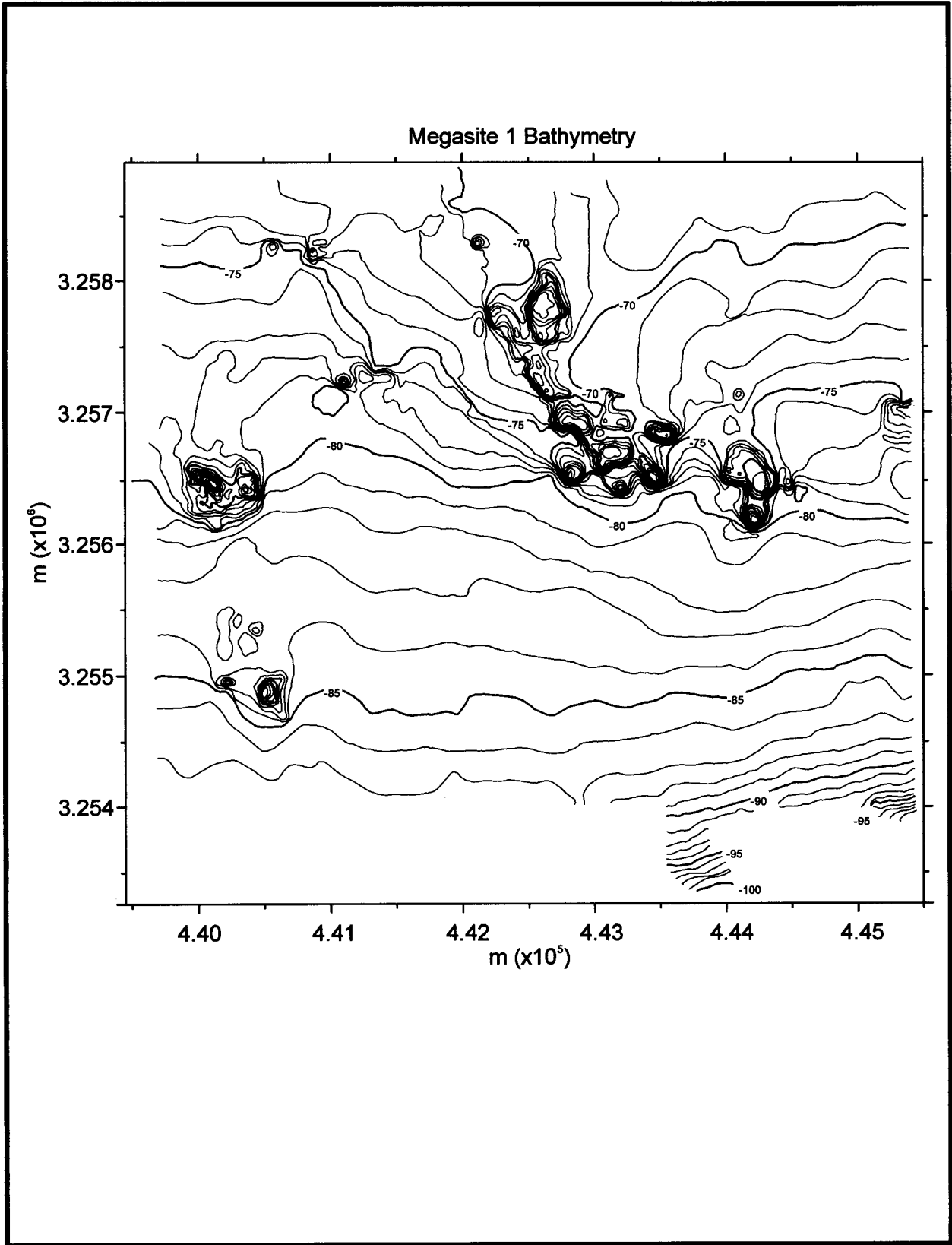


Fig. 3.2. Bathymetry of Megasite 1, derived from TAMU² sonar data. Contours shown at 1-m intervals with 5-m contours bold. UTM plot with axes labeled in meters.

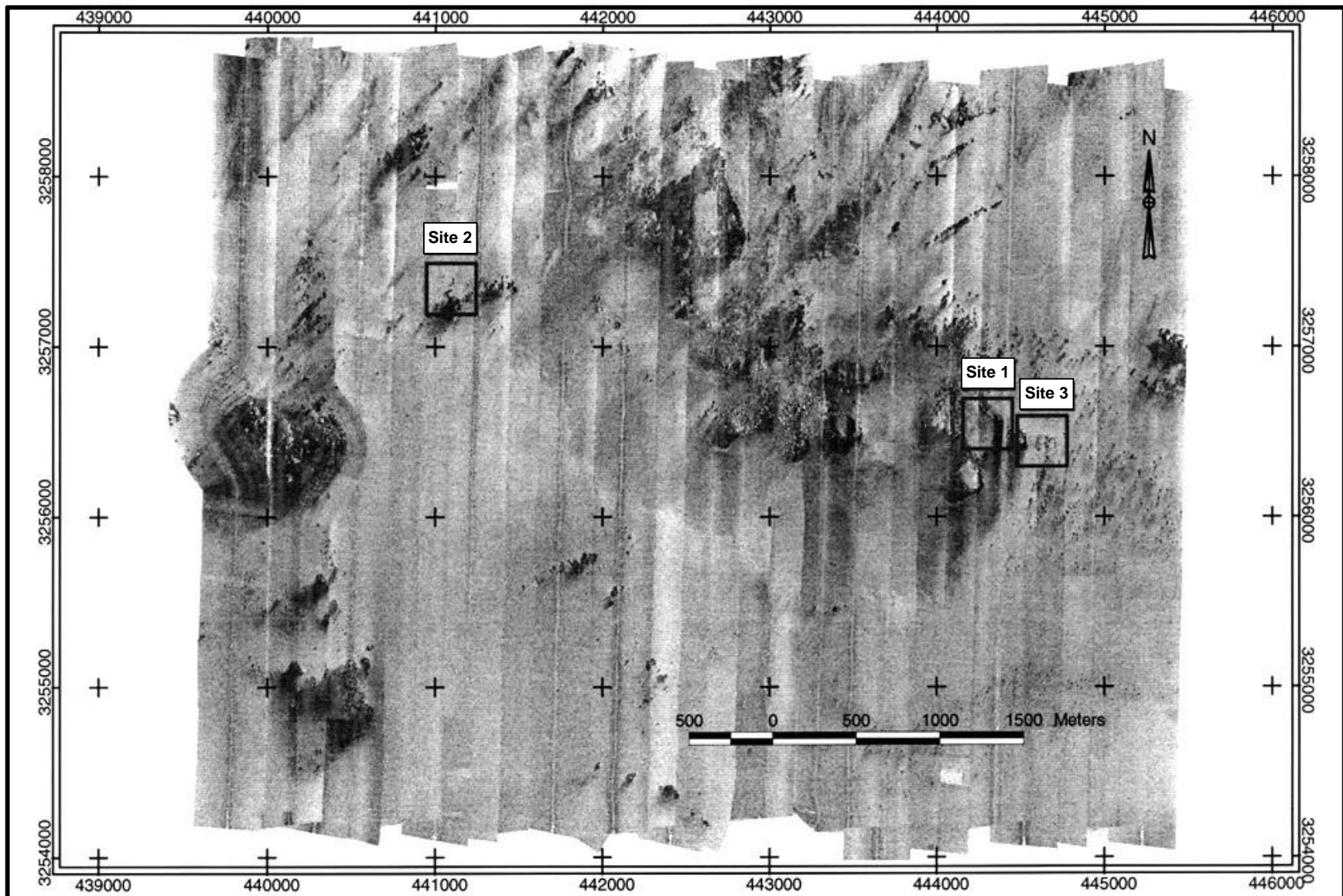


Fig. 3.3. TAMU² side-scan sonar mosaic of Megasite 1, showing monitoring Sites 1-3 (small boxes). Vertical stripes are individual trackline side-scan sonar records pieced together to make the mosaic. Dark areas are high acoustic return (backscatter), whereas light areas are low backscatter. UTM plot with axes labeled in meters.

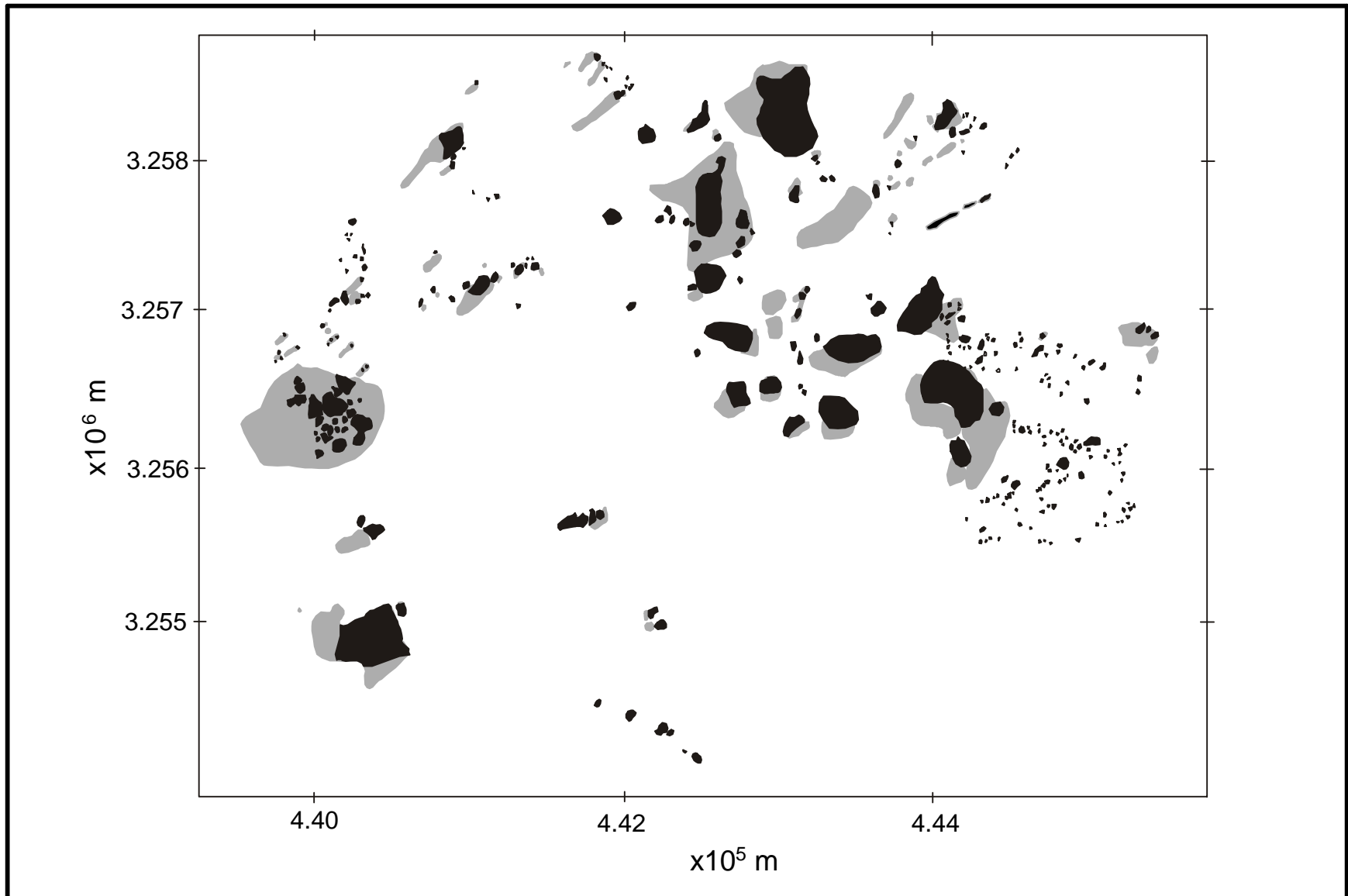


Fig. 3.4. Megasite 1 sonar mosaic interpretation showing mounds (black) and high-backscatter areas (gray). Plot is in UTM coordinates.

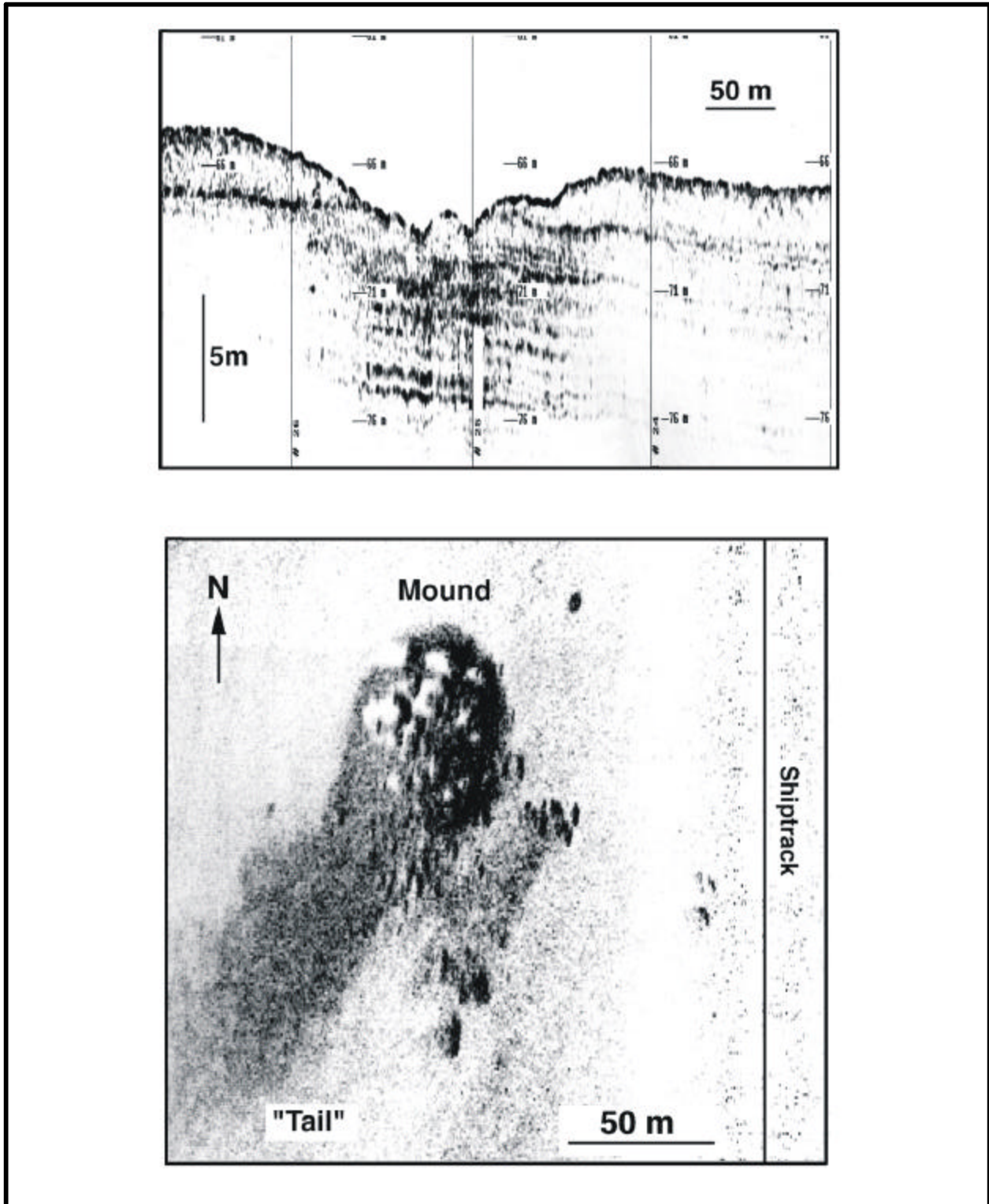


Fig. 3.5. Example of high-backscatter "tail" southwest of a mound in Megasite 1 and associated erosional gully. (Top) Chirp sonar subbottom profile showing gully approximately 3-m deep and 150 m across. (Bottom) High-backscatter "tail" to southwest of mound. Dark areas indicate high backscatter and light represents low backscatter. Acoustic illumination is directed away from shiptrack (vertical line at right). Note: The two examples are from different locations because the subbottom profiler must pass directly over the tail feature to image it, but the side-scan sonar does not image well directly beneath the sonar.

Megasite 2

Depths in Megasite 2 range from 93 to 200 m and show numerous mounds at the shelf edge (**Figs. 3.6, 3.7, and 3.8**). Seafloor north of the mounds is flat and is at about 100 to 103 m depth. To the south, the shelf edge, at about 115 m depth, separates the mounds from the steeper upper slope to the south. The mounds are subcircular to linear in plan view and seem to have two distinct morphologies. One type occurs as broad, low, round, flat-topped topographic features several hundred meters in diameter. The others appear as taller, steeper, less-rounded features. The latter are the “pinnacles” described by Ludwick and Walton (1957), whereas the low features appear to be carbonate platforms. The bathymetry shows that these low platforms are typically flush with the seafloor on their north sides, whereas the south sides usually have a drop of 3 to 5 m. The bathymetric map shows that the steepest and tallest mounds are clustered in the central and eastern part of the megasite, whereas those mounds in the western part tend to be dominantly the low, hard bottom type.

The Megasite 2 mosaic shows numerous mound clusters in a broad band that trends southwest to northeast across the survey area (**Figs. 3.7 and 3.8**). In the western part of the survey area, areas of medium backscatter define broad, low hard bottoms typically several hundreds of meters across. Detailed examination of the sonar records shows that small mounds, typically less than 10 to 15 m across, are associated with these features. These large features appear to be carbonate hard bottoms, which may consist of many smaller mounds. In the central and east-central part of the survey area, taller mounds are evidenced by acoustic shadows. These are often irregular in shape and associated with subcircular regions of high backscatter. In the far-eastern part of the survey, small mound clusters are associated with subcircular areas of high backscatter. Subbottom profiler records suggest these small mounds are the outcropping parts of larger buried mounds. There is also a suggestion that some of the tall irregular mounds are associated with broad carbonate bases, as if they grew atop hard bottoms similar to those farther west. Unlike high-backscatter features in other megasites, those in Megasite 2 are not linear and rarely appear to have a preferred direction or location relative to the mounds. Near the southern edge of the mosaic, a faint, curvilinear higher-backscatter feature is the scar of a slump mapped by prior MMS surveys (Laswell et al. 1992).

Megasite 3

Megasite 3 shows a gently sloping area of the outer shelf with depths of 64 to 86 m (**Figs. 3.9, 3.10, and 3.11**). The main feature is a bulge in the contours that represents a broad, thin dome of sediments surrounding several groups of mounds. One mound group, in the western part of the megasite, is linear with a south-southeast trend. This linear feature is asymmetric, with a shallow slope on its north side and a steeper slope on its south side. To the north and southeast of this linear feature, two other smaller mounds have similar trends, implying some relationship. In the eastern half of the megasite, about a dozen medium mounds appear in several clusters. These are associated with a broad, low mound, similar to those in Megasite 2. This broad mound is about 400 x 800 m in dimension, and like its cousins in Megasite 2, it shows a 2 to 3 m drop off its south edge, whereas its northern edge is flush with surrounding seafloor. The side-scan

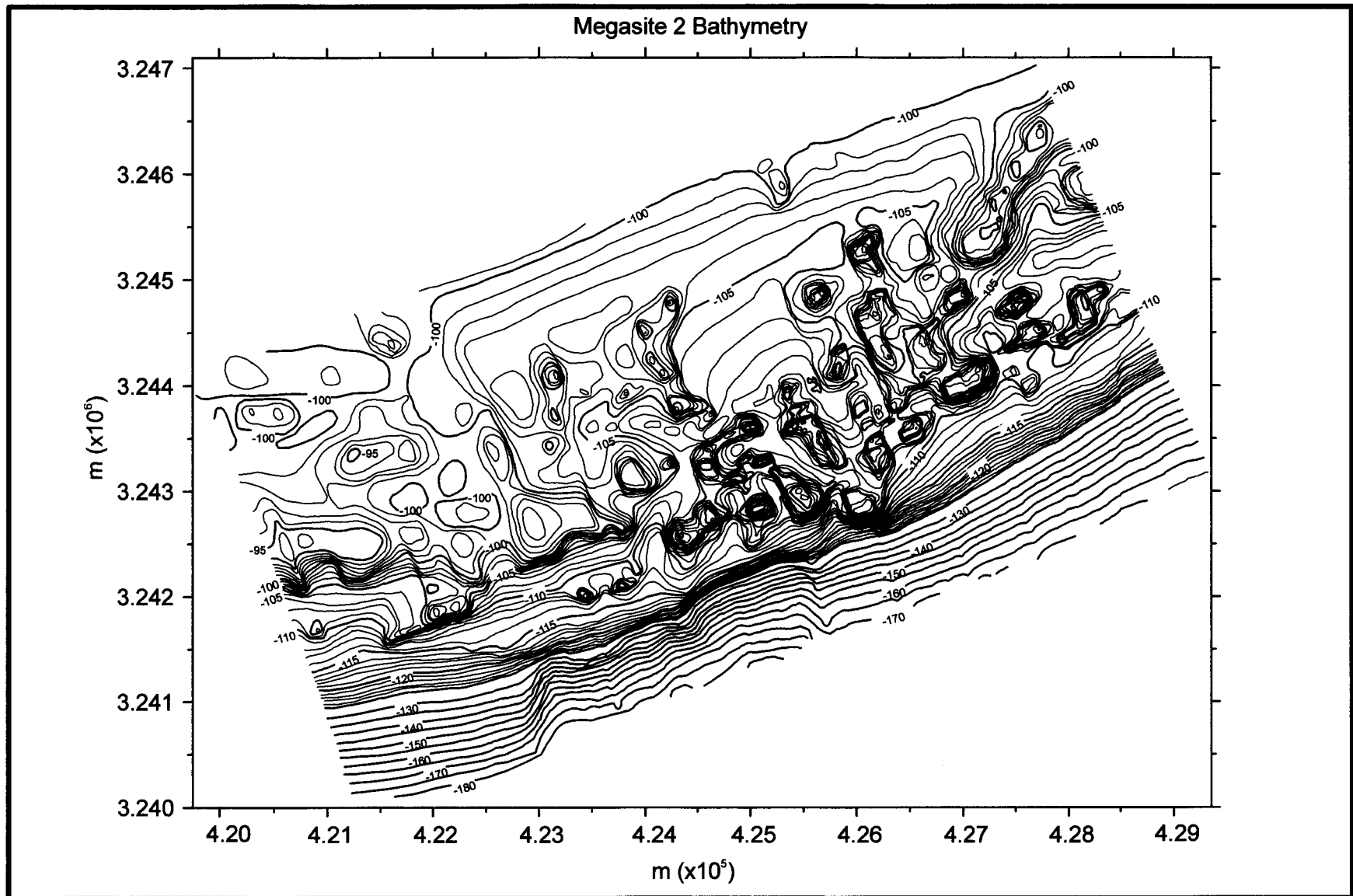


Fig. 3.6. Bathymetry of Megasite 2, derived from *TAMU²* sonar data. Conventions as in Fig. 3.2.

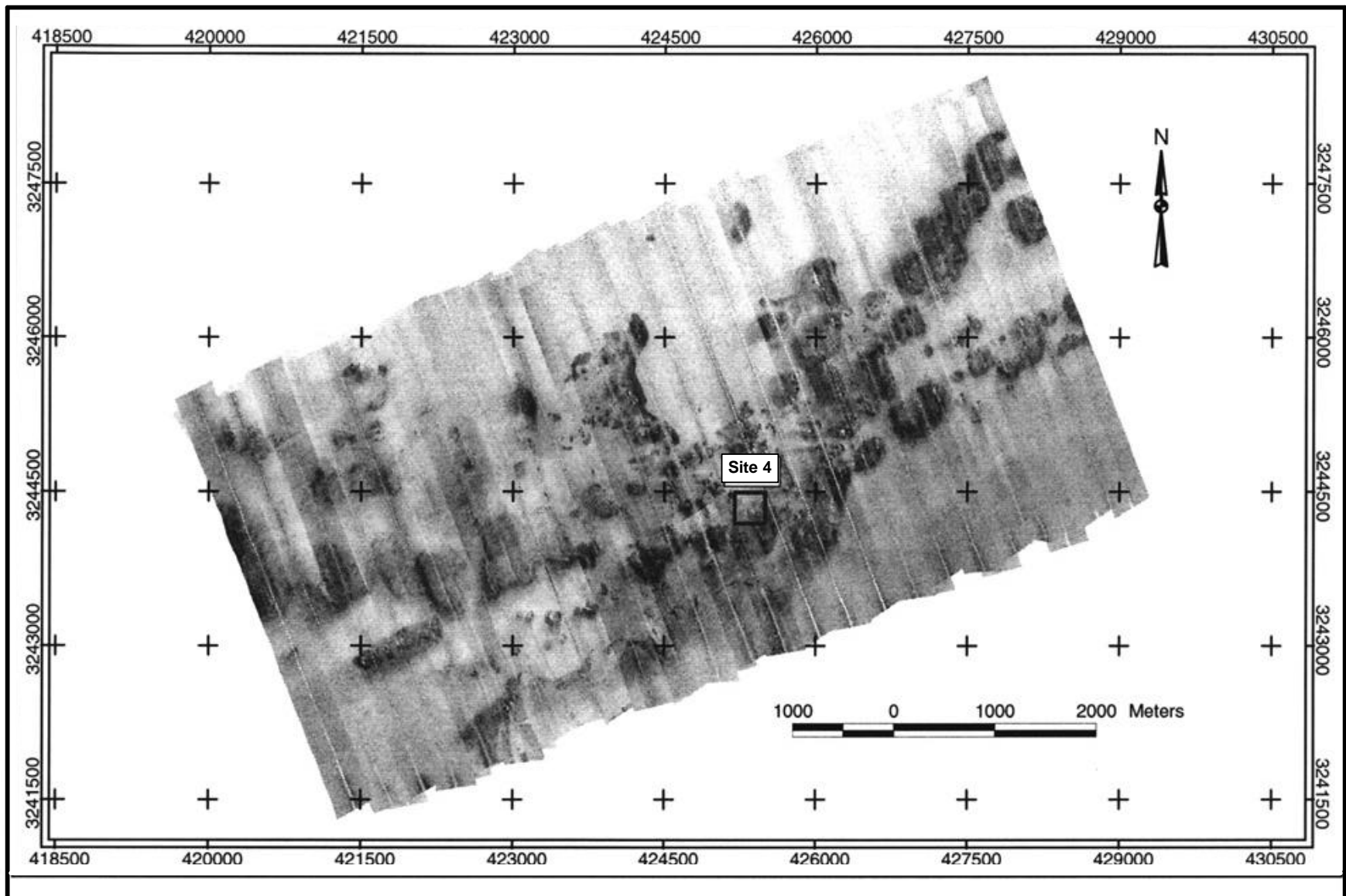


Fig. 3.7. *TAMU²* side-scan sonar mosaic of Megasite 2, showing monitoring Site 4 (small box). Conventions as in Fig. 3.3.

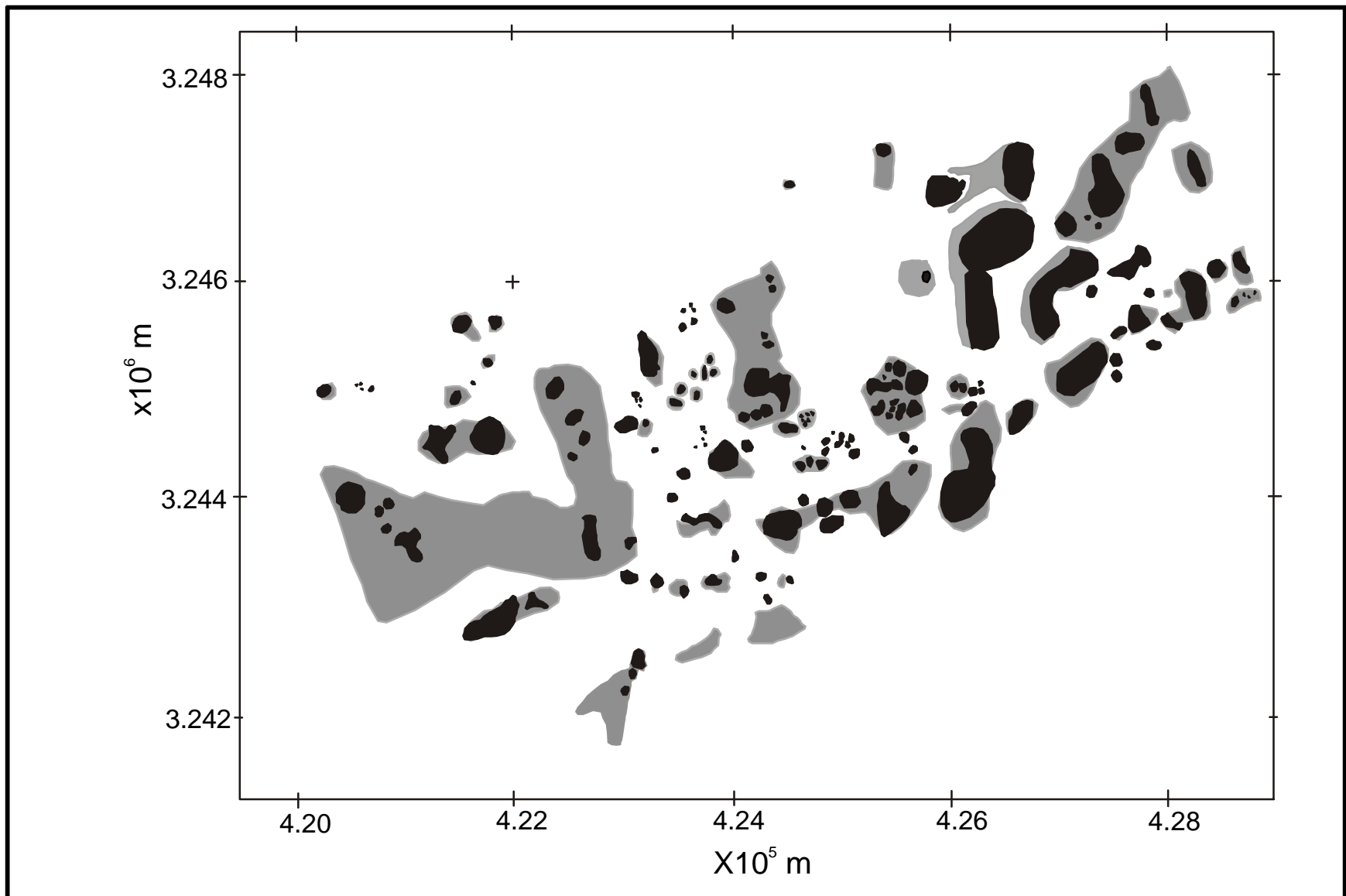


Fig. 3.8. Megasite 2 sonar mosaic interpretation showing mounds (black) and high-backscatter areas (gray). Plot is in UTM coordinates.

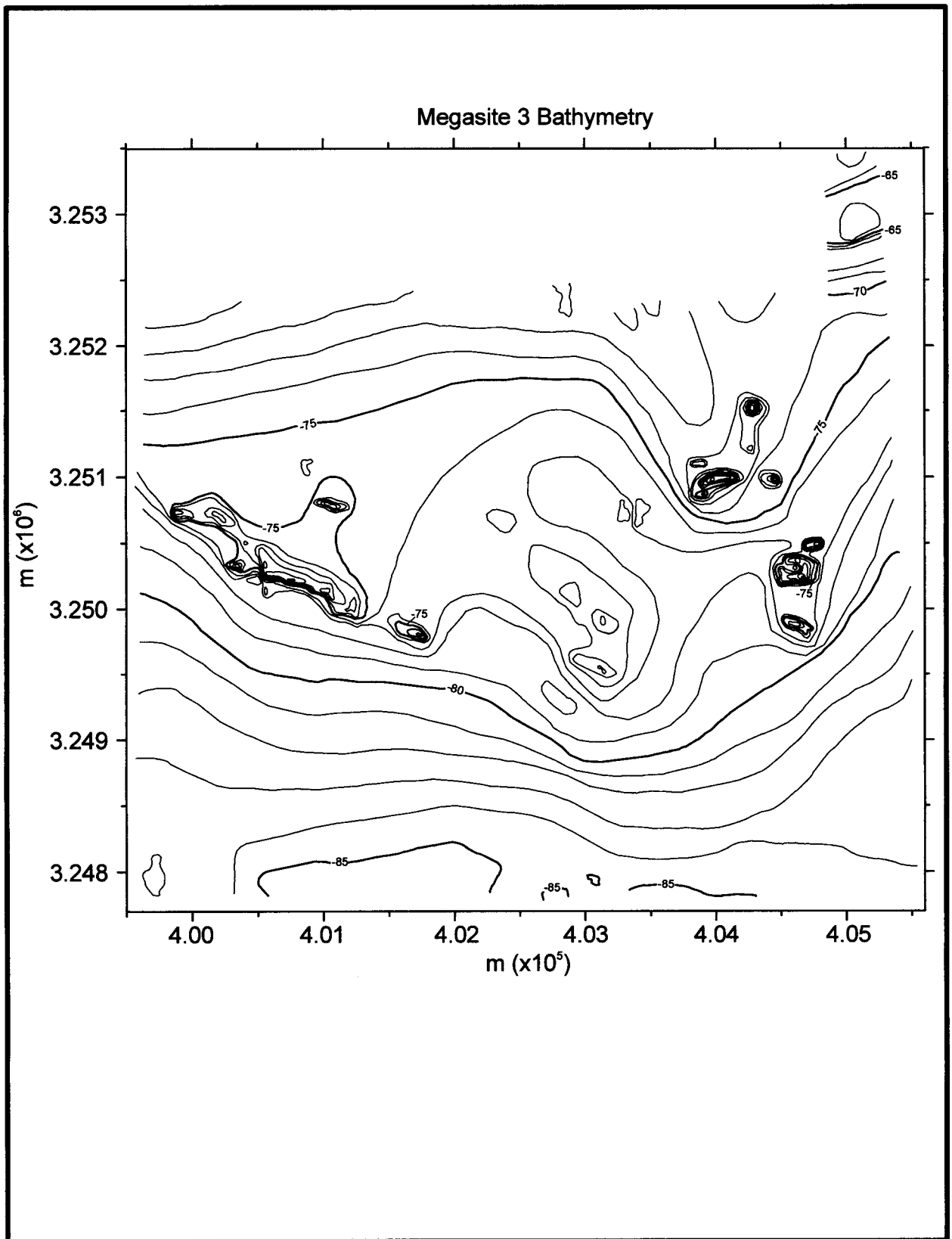


Fig. 3.9. Bathymetry of Megasite 3, derived from *TAMU²* sonar data. Conventions as in Fig. 3.2.

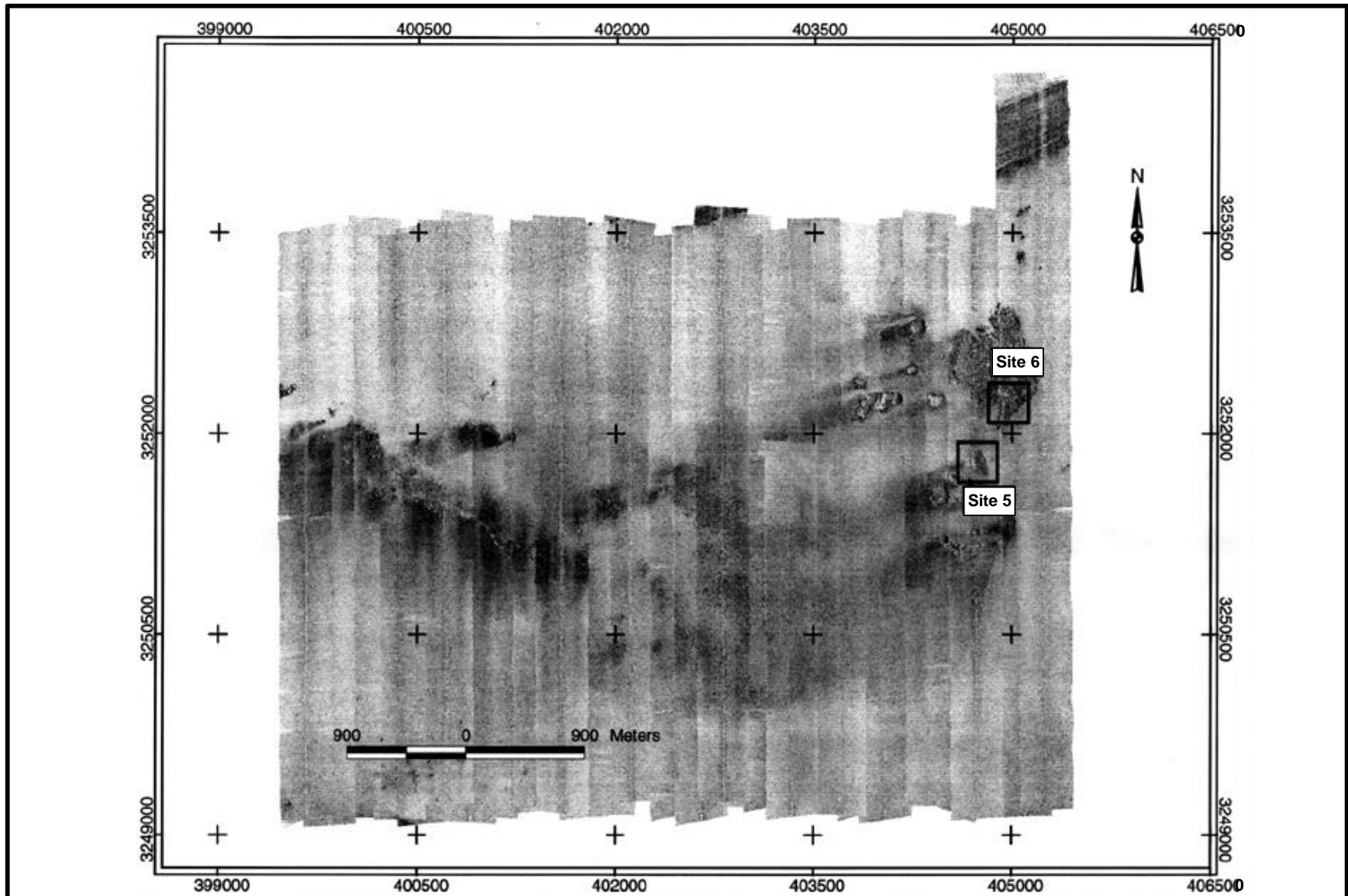


Fig. 3.10. TAMU² side-scan sonar mosaic of Megasite 3, showing monitoring Sites 4 and 6 (small boxes). Conventions as in Fig. 3.3.

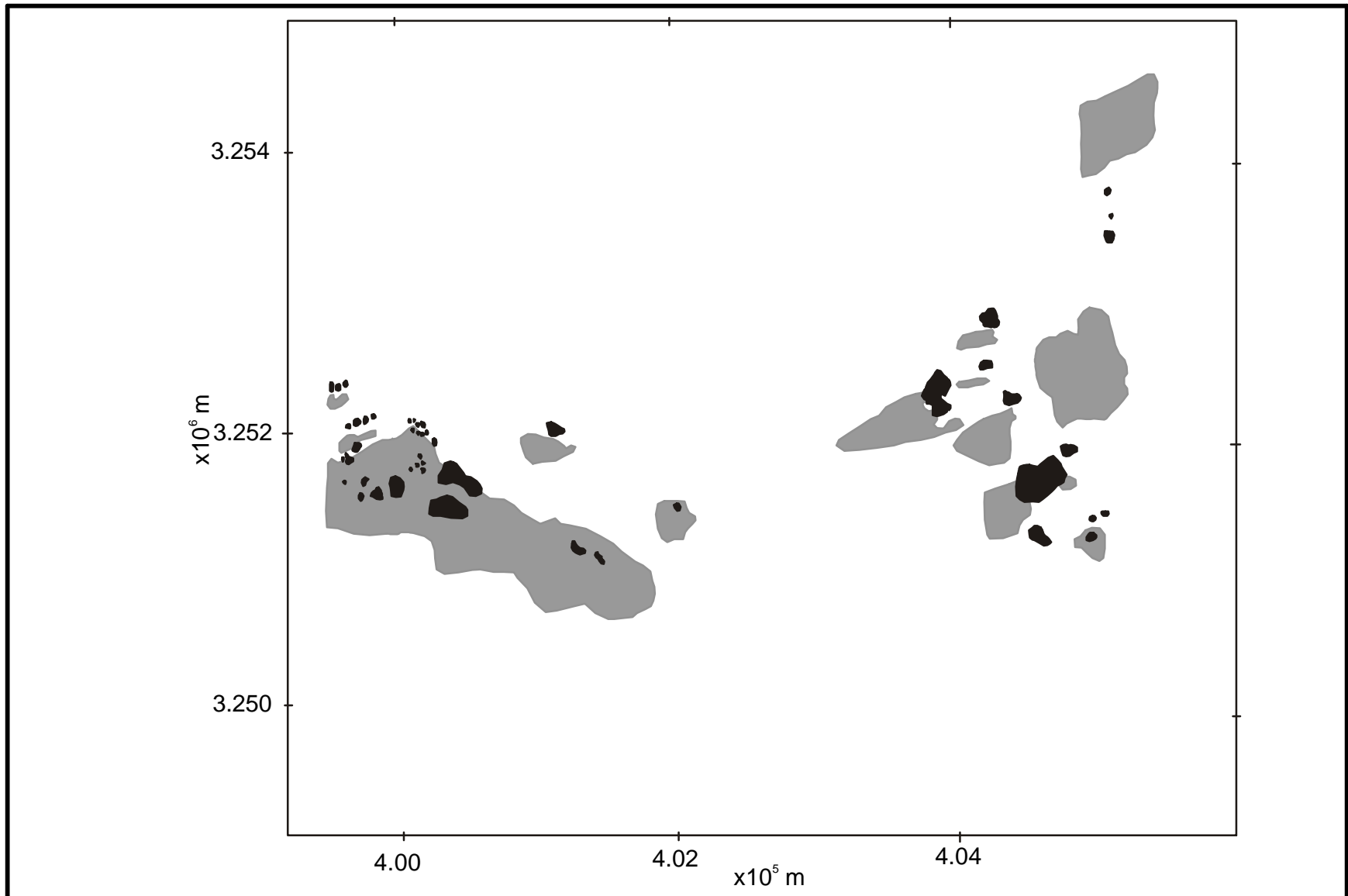


Fig. 3.11. Megasite 3 sonar mosaic interpretation showing mounds (black) and high-backscatter areas (gray). Plot is in UTM coordinates.

sonar mosaics also show a larger, but less obvious low hard bottom in the central region of Megasite 3. This is seen in the bathymetry contours by slightly steeper slopes on its south edge, in the south-central part of the megasite.

The Megasite 3 mosaic shows four main features: mounds, low carbonate hard bottoms, high-backscatter areas, and a shoreline ridge (**Fig. 3.10**). Large mounds are seen clustered in two main areas on the east and west sides of the site (**Fig. 3.11**). The eastern mounds are mainly subcircular features 50 to 100 m in diameter and many have flat tops. Site 5 is located in the cluster in the eastern central part of the megasite (**Fig. 3.10**). On the west side of the megasite, large and small mounds are clustered into a linear group that trends to the southeast. Two smaller groups appear to its north and northeast. Two areas of broad carbonate hard bottoms appear in the megasite, one in the center of the survey and another in the northeast corner. These low hard bottoms are similar in appearance to those noted in Megasite 2. Both of these hard bottoms have higher backscatter than the surrounding seafloor, although the northeastern one shows more backscatter contrast. In detail, each hard bottom appears to have many smaller mounds, less than 10 to 15 m across, making up much of its surface. This is also similar in appearance to the Megasite 2 hard bottoms. As at other sites, areas of higher backscatter are associated with the mounds, often on the southwest sides of the topographic features. Also like other sites, many of these high-backscatter areas are linear, or have linear edges, with a west-southwest trend. The linear, shoreline ridge feature appears mainly in an extension on the northeast corner of the survey. This extension was added because the ridge was known to be there from previous MMS surveys. The ridge shows high backscatter and is patterned with streaks parallel to its trend. This part of the ridge connects with a larger ridge that extends for over 10 km to the east (Sager et al. 1992).

Megasite 4

Depths in Megasite 4 range from 93 to 189 m (**Figs. 3.12** and **3.13**). This site is similar to Megasite 2 in its shelf-edge position. Slopes in Megasite 4 are somewhat steeper than the others, being about 0.7° landward of the 120 m isobath. The main bathymetric features are curvilinear areas of steeper slope that appear to be the edges of fluvial deltas. The most prominent such feature runs from west to east across the southern part of the megasite at depths of 112 to 133 m. Another obvious feature of the bathymetry in Megasite 4 is the lack of large mounds. This implies that all of the mounds are too small to be seen in the 15-m bathymetry grid.

The appearance of the Megasite 4 mosaic is unique among all of the sites that were surveyed (**Fig. 3.13**). Unlike any other site, there are no large mounds. Mounds in this mosaic, if they exist, are seen only as small, subcircular, high-backscatter features typically less than 20 m in diameter. Few show any evidence of acoustic shadow, indicating they are also low in height. The most obvious mosaic features are mottled backscatter seafloor in the north and northwest parts of the megasite, and a curvilinear feature that runs from west to east across the southern part of the megasite. The curvilinear feature coincides with an area of slightly greater slope in the bathymetry (**Fig. 3.12**) and probably indicates the edge of a delta sediment wedge. The patchy backscatter areas in the northern parts of the survey do not match up with features in the

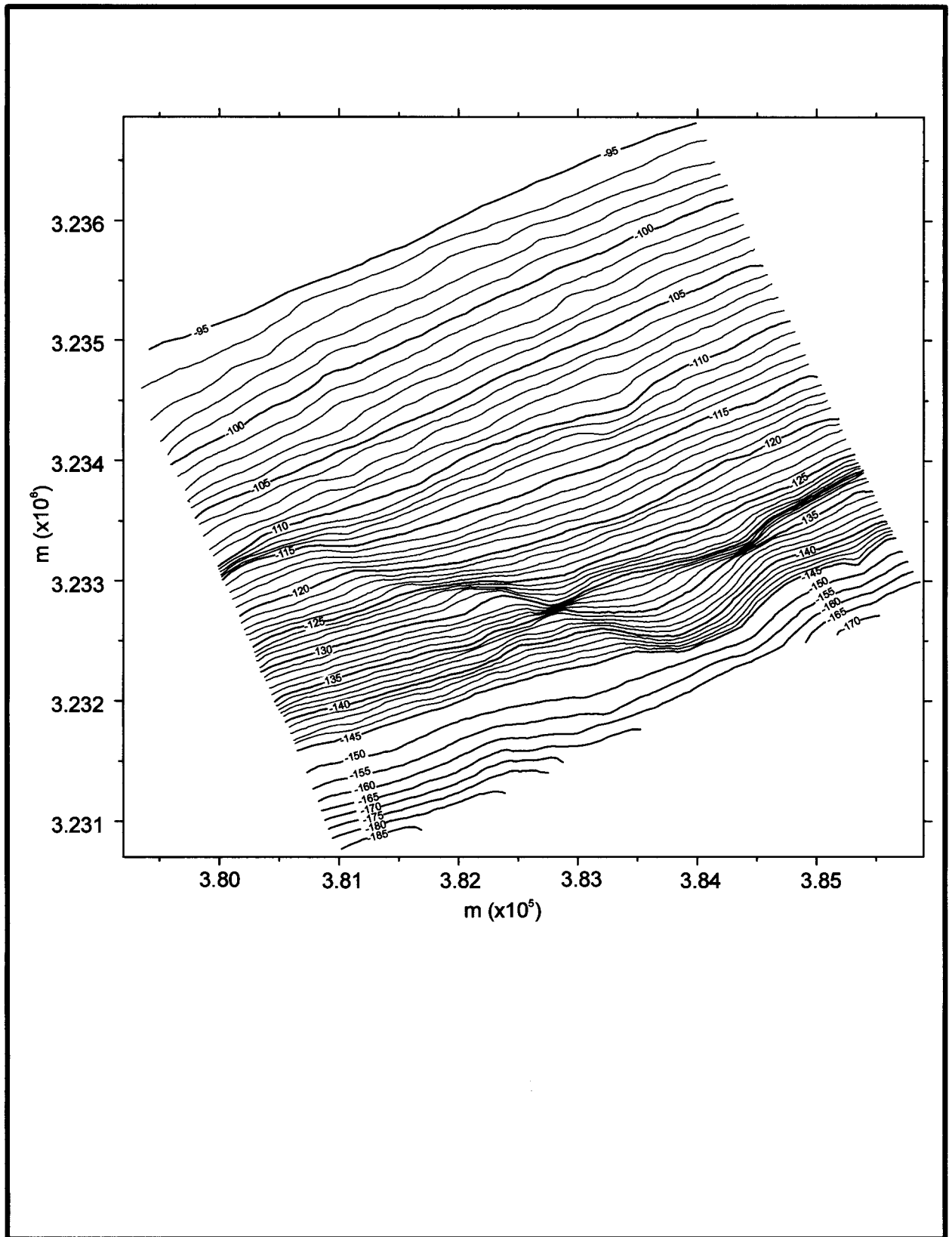


Fig. 3.12. Bathymetry of Megasite 4, derived from *TAMU*² sonar data. Conventions as in Fig. 3.2.

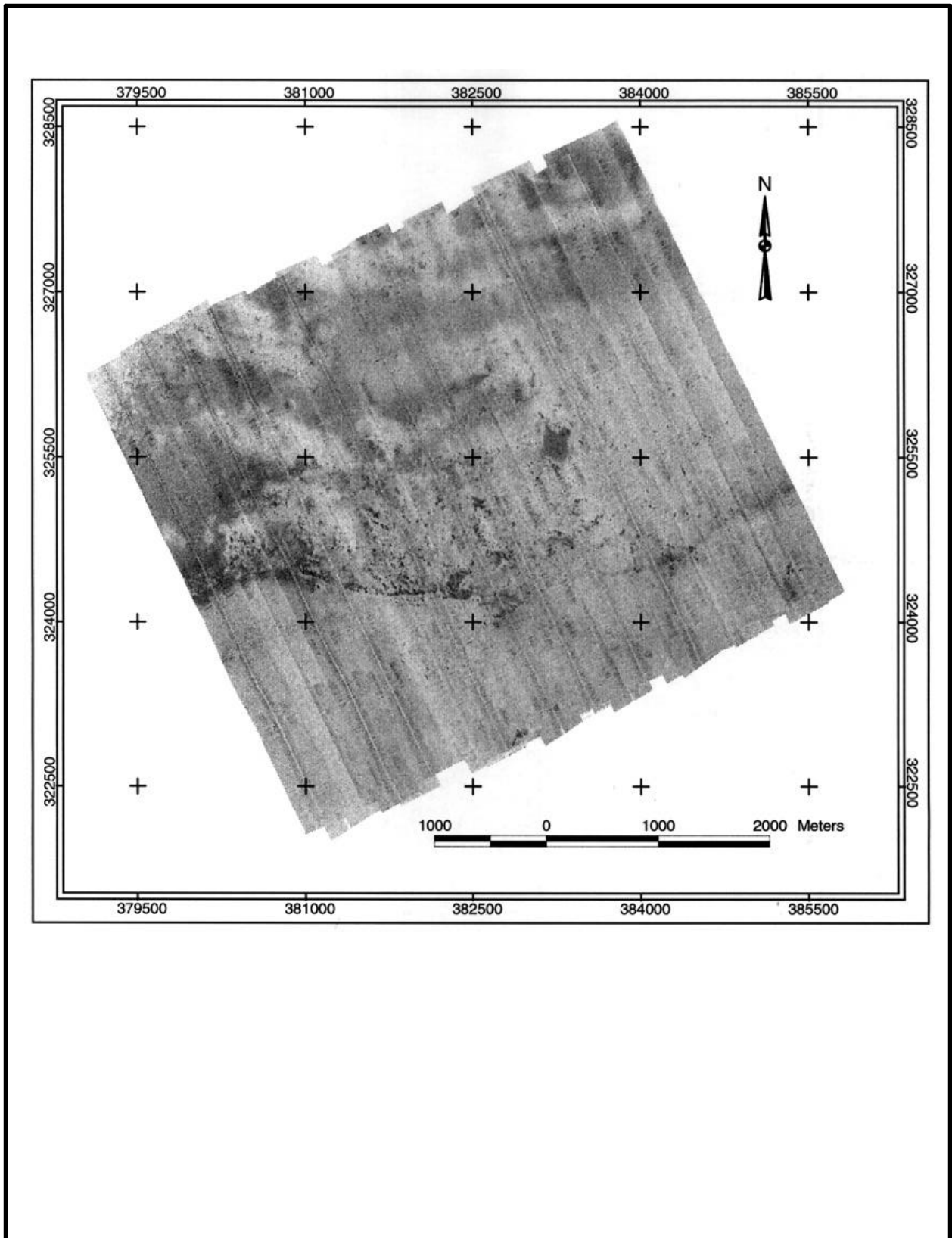


Fig. 3.13. TAMU² side-scan sonar mosaic of Megasite 4. Conventions as in Fig. 3.3.

subbottom profiler or bathymetry data. These are probably areas of slightly different sediment texture.

Megasite 5

The shelf edge is also a prominent feature in the Megasite 5 bathymetry map, which shows depths ranging from 69 to 161 m (**Figs. 3.14, 3.15, and 3.16**). Most of the northern two-thirds of the megasite is relatively flat seafloor of the outer shelf. Superimposed is a curvilinear mound group that stretches from northwest to southeast across almost the entire megasite. The bathymetry shows several large mounds and numerous smaller mounds and mound groups. An extraordinary feature is the tall, linear mound at the northwest end of the mound group, which is the location of Site 7 (**Fig. 3.15**). Across the curvilinear mound group, the contours often show a depth offset of about 2 to 4 m. Seaward of the mound lineation is a flat bench at a depth of about 95 m, adjacent to the shelf edge.

In the Megasite 5 mosaic, a curvilinear group of hundreds of large to small mounds is the most obvious feature (**Fig. 3.15**). This group contains most of the mounds in the megasite. At its northwest end is a large, rough, linear mound (named “36-Fathom Ridge”) whose north-south trend deviates from the overall northwest-southeast trend of the mound group. This mound is about 1,000 m long by about 150 to 300 m wide. Site 7 is at the northeast end of this mound. In the center of the curvilinear mound group are several large mounds, approximately 50 to 100 m across, including two that appear to have flat tops. The number of mounds decreases to the southeast, except for one moderately large group. As at other megasites, high-backscatter areas are associated with the mounds. Usually these areas are on the southwest sides of mounds and mound groups and often they are linear with a southwest-northeast trend. A unique feature of Megasite 5 is a curvilinear, high-backscatter band that appears seaward of the mound group. This feature is not associated with any mounds nor is it evident in the bathymetry. It appears to be the upper edge of certain sediment layers exposed at the shelf edge.

Monitoring Site Descriptions

Site 1

Monitoring Site 1 bathymetry shows the northeast flank of the large flat-topped mound in eastern Megasite 1 (**Fig. 3.17**). The data show a large flat-topped feature with a top depth of about 66 m, a steep flank, and flat seafloor to the northeast at depths of about 75 to 80 m. Depth variation on the flat top of the mound appears to be generally less than 1 m. The regional seafloor depth increases from about 76 m on the north side of the mound to 82 m on the southeast side. This increase is a result of greater burial of the mound by sediments on the north side.

In the side-scan sonar mosaic (**Fig. 3.18**), sediments to the northeast of the mound display low backscatter, whereas the top of the mound shows high backscatter. This difference is likely a result of the difference in texture: the flat seafloor is mantled by fine-grain sediments that cause little backscatter, but the mound top has much centimeter-to-meter-

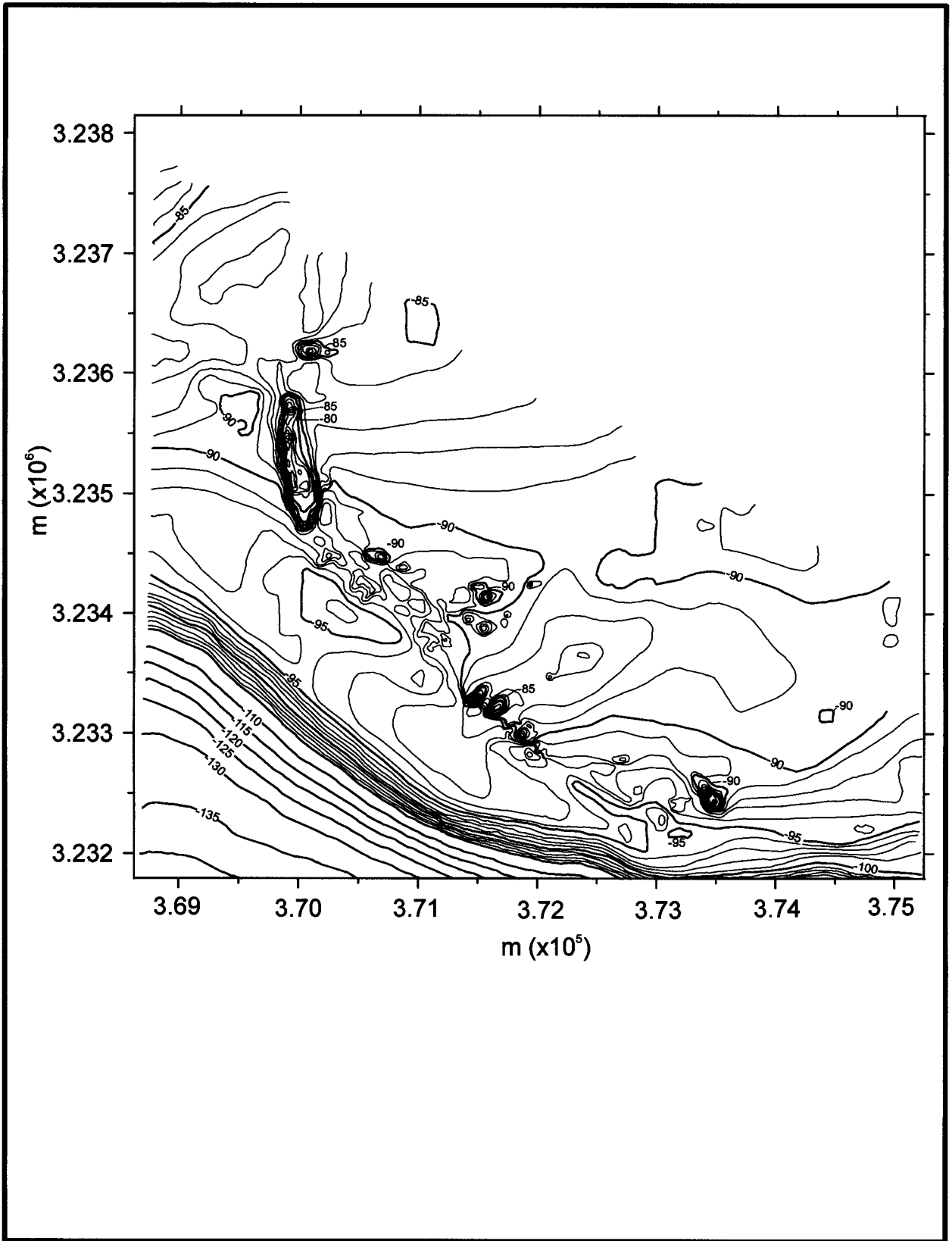


Fig. 3.14. Bathymetry of Megasite 5, derived from TAMU² sonar data. Conventions as in Fig. 3.2.

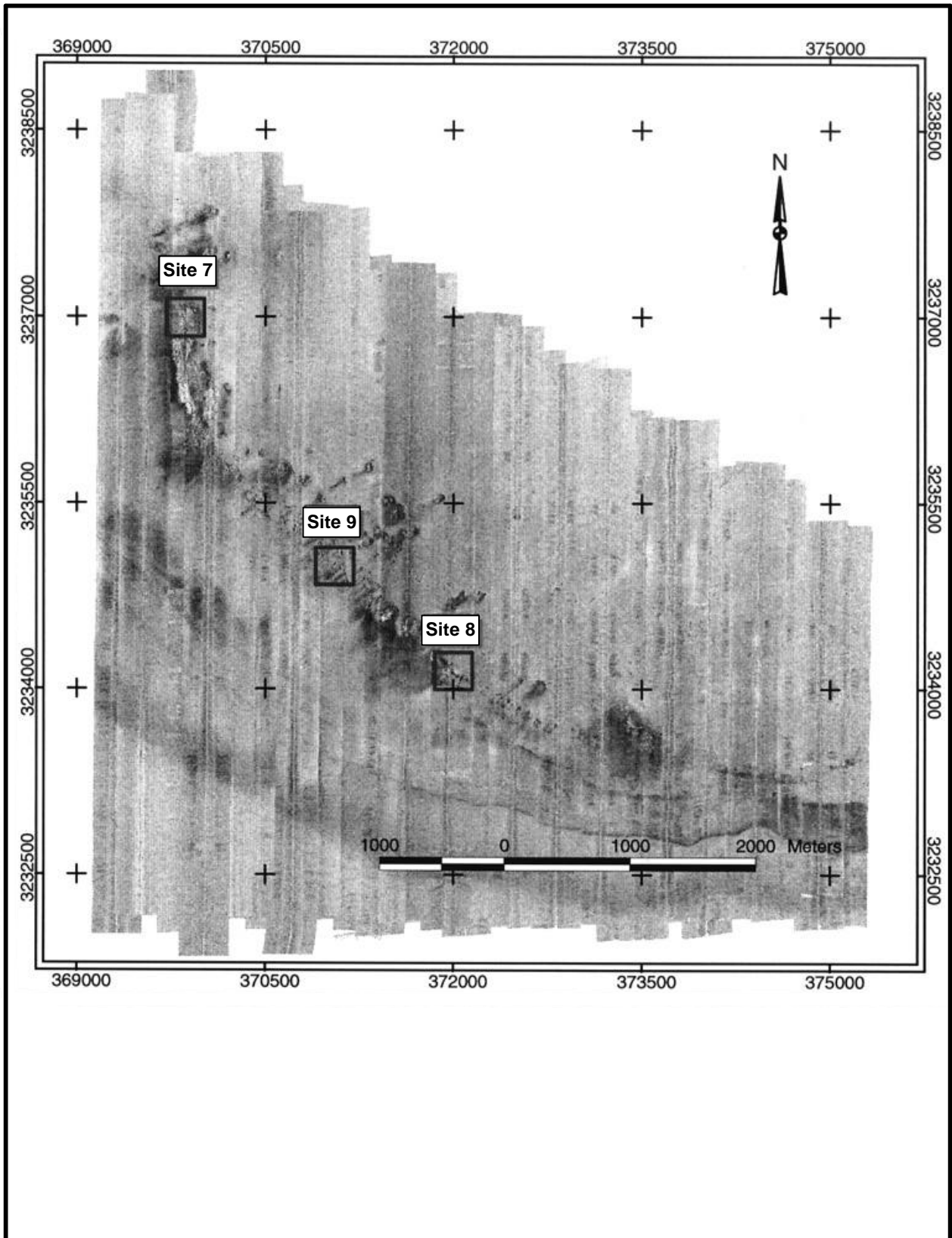


Fig. 3.15. TAMU² side-scan sonar mosaic of Megasite 5, showing monitoring Sites 7-9 (small boxes). Conventions as in Fig. 3.3.

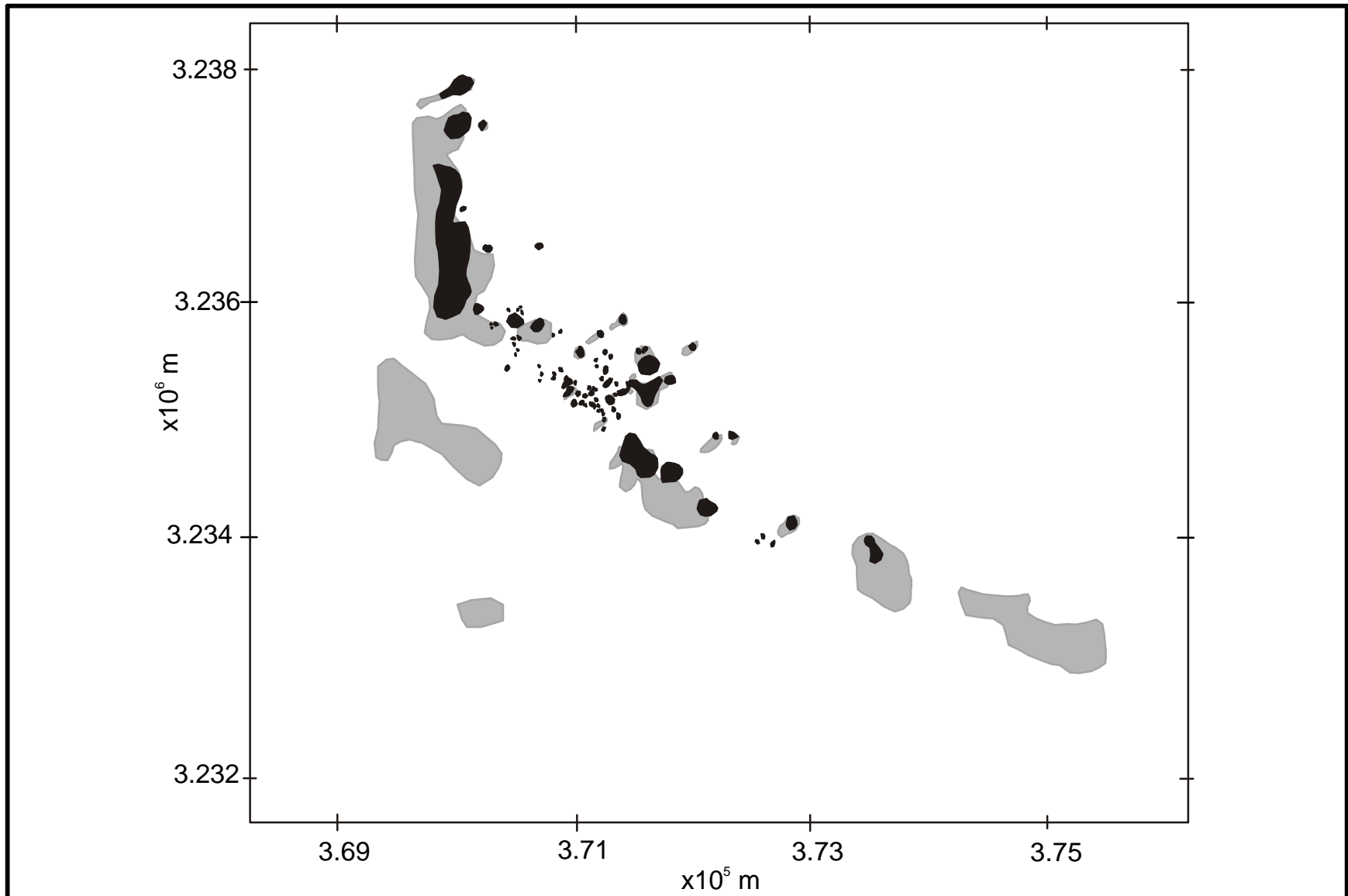


Fig. 3.16. Megasite 5 sonar mosaic interpretation showing mounds (black) and high-backscatter areas (gray). Plot is in UTM coordinates.

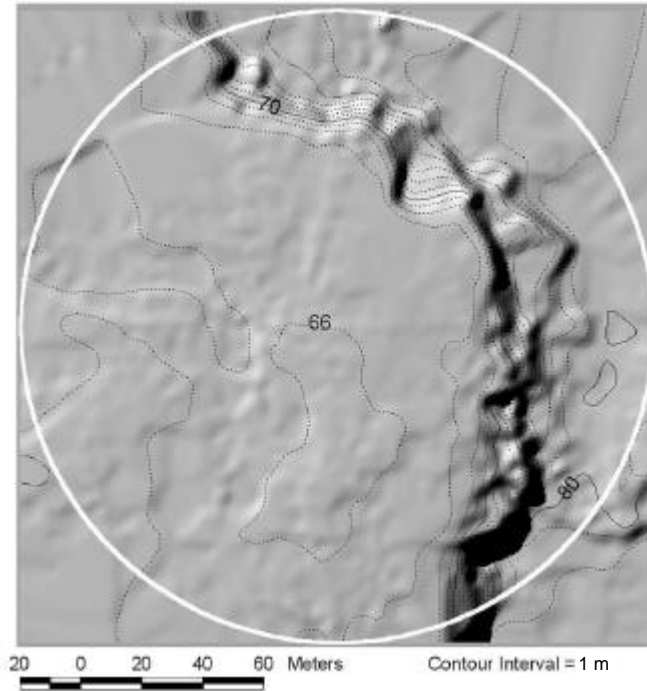


Fig. 3.17. Bathymetry of Monitoring Site 1. Contours shown at 1-m intervals. Circle indicates the boundary of ROV seafloor observations.

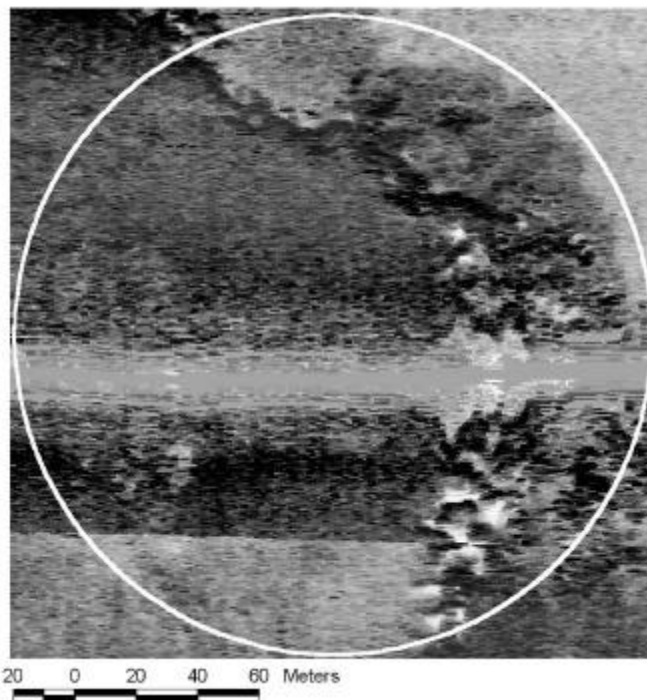


Fig. 3.18. Side-scan sonar image of Monitoring Site 1. Circle indicates the boundary of ROV seafloor observations.

scale roughness that causes higher acoustic backscatter. The mound flanks and an apron at the base of the flank give high backscatter. Dark/light zones show large monolithic rocks that occur at the edge and their acoustic shadows (white areas). The apron probably displays strong backscatter because it is composed of coarse debris from the mound.

Most photo stations from Site 1 are on the top of the mound, so most geologic observations apply to this environment. Although sediment cover is partial or complete at most stations, outcropping carbonate rock is also common, so the area is characterized as continuous hard bottom (**Fig. 3.19**). Nevertheless, meter-scale relief is typically low and the small-scale roughness is low to medium. Sediments are typically coarse and shell hash is common, implying a significant biogenic component. Monolithic outcroppings describe the flanks of the mound with its large boulders and rubble, whereas flat bottom mantled with sediment is typical of the seafloor to the northeast (**Fig. 3.19**). Unlike many other monitoring sites, the three zones are large and contiguous with sharp boundaries between them. There is also a significant depth difference (11-14 m) from the plateau atop the mound and the surrounding seafloor.

Site 2

Monitoring Site 2 encompasses a medium-size mound located in the western part of Megasite 1 (**Fig. 3.3**). Bathymetry data from this site show a subcircular, medium-size mound approximately 30 m (top) to 60 m (base) in diameter sitting on flat seafloor at a depth of about 78 to 80 m (**Fig. 3.20**). Contours indicate the mound is approximately 9-10 m in height and reaches a depth of approximately 70 m. Smaller closed contours around the base of the mound suggest smaller mounds.

The side-scan sonar image shows a mound consisting of a collection of subcircular bumps, each 8-10 m in diameter (**Fig. 3.21**). On the image, these bumps show high backscatter (dark) on the side facing the sonar and shadow on the opposite side (light). This mound, and many others like it, suggest that some mounds are composite features amalgamating many smaller mounds. High backscatter is also seen on the south and east sides of the mound. The highest backscatter area is lobate and follows the slightly elevated bathymetry of several smaller mounds on the east side of the larger mound. From its highly variable texture in the sonar image, this high-backscatter area looks like it may be a zone of coarse rubble. The high-backscatter region to the south and southwest of the larger mounds is one of the dark, linear backscatter "tails" seen to emanate from many mounds in this megasite (see **Fig. 3.3**).

Analysis of seafloor photographs and videos showed only two bottom types, monolithic outcroppings and flat, sediment mantled seafloor (**Fig. 3.22**). The largest monolith zone corresponds to the area around the main mound. Located atop the medium-size mound, approximately half of the photo stations show rock outcrop and these are preferentially on the northeast side of the mound. Such a configuration is consistent with current flow from the northeast, which would account for the southwestward trending high-backscatter "tail" emanating from this mound group, causing sediments to be eroded off the northeast side of the mound and deposited on the southwest side. Most stations, however, show

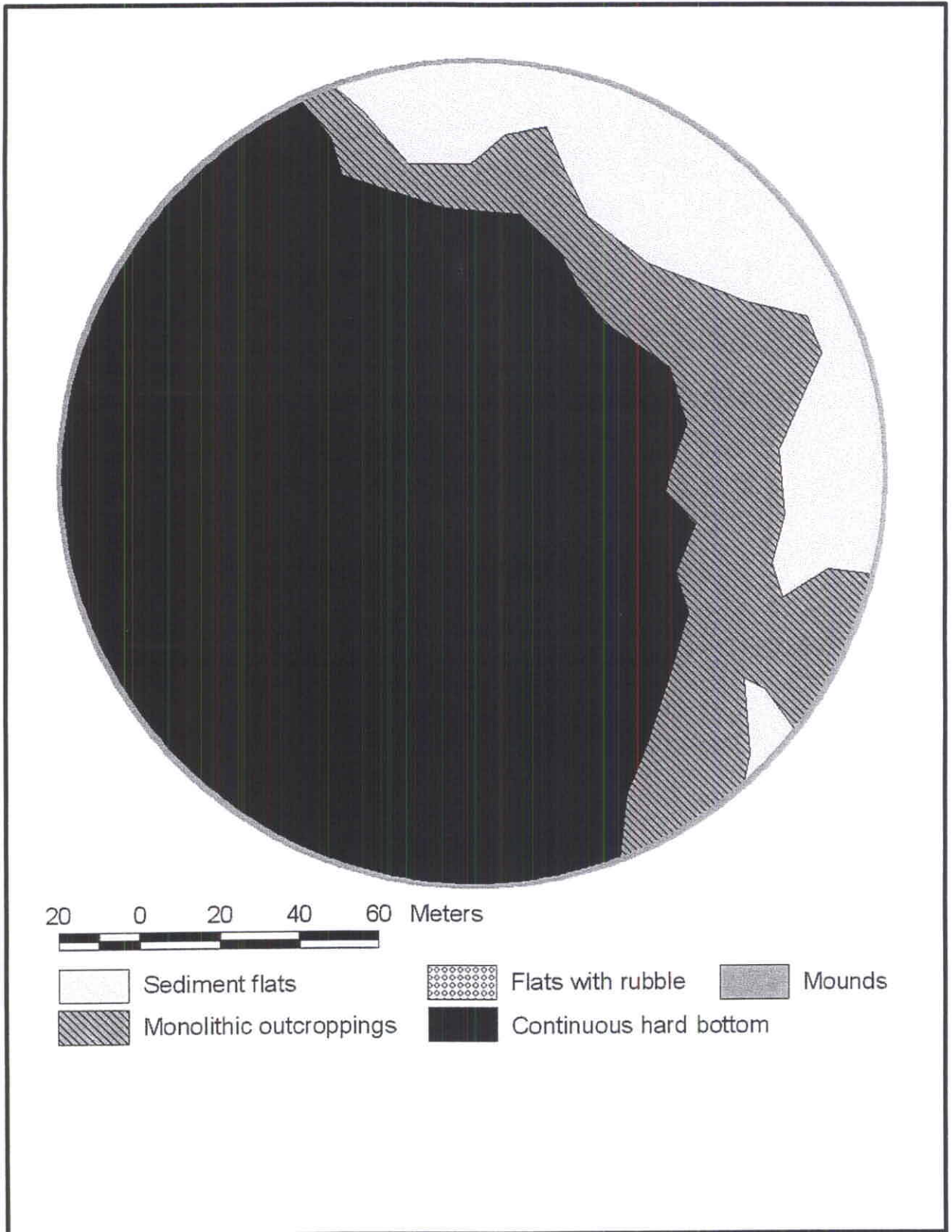


Fig. 3.19. Bottom type map for Site 1 derived from ROV photo and video observations. Circle boundary corresponds to circles in Figs. 3.17 and 3.18.

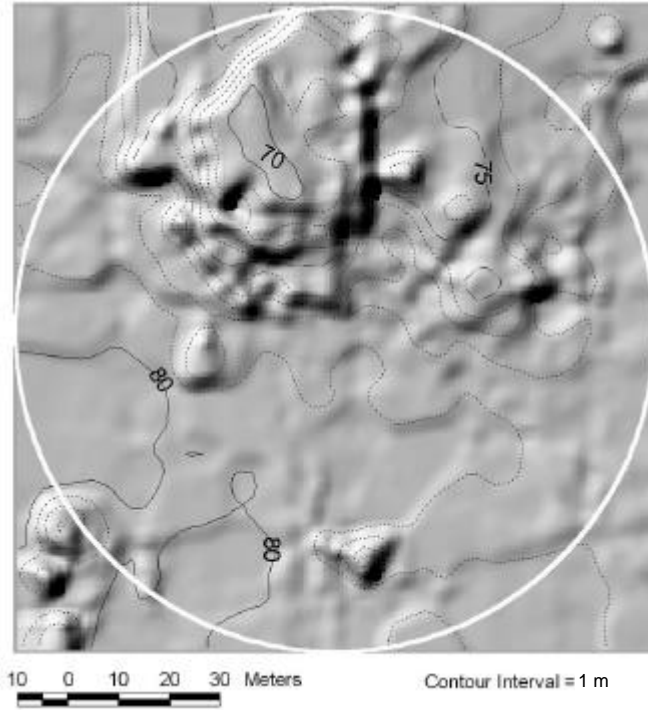


Fig. 3.20. Bathymetry of Monitoring Site 2. Contours shown at 1-m intervals. Circle indicates the boundary of ROV seafloor observations.

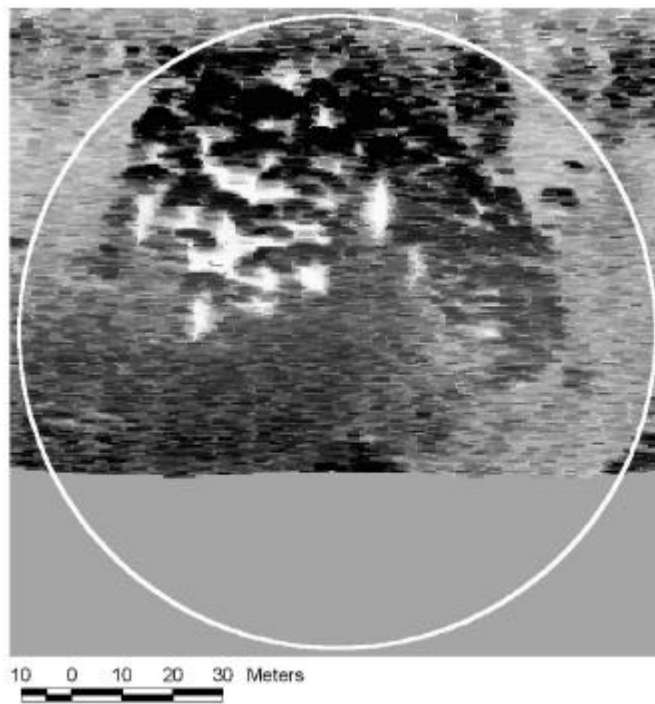


Fig. 3.21. Side-scan sonar image of Monitoring Site 2. Circle indicates the boundary of ROV seafloor observations.

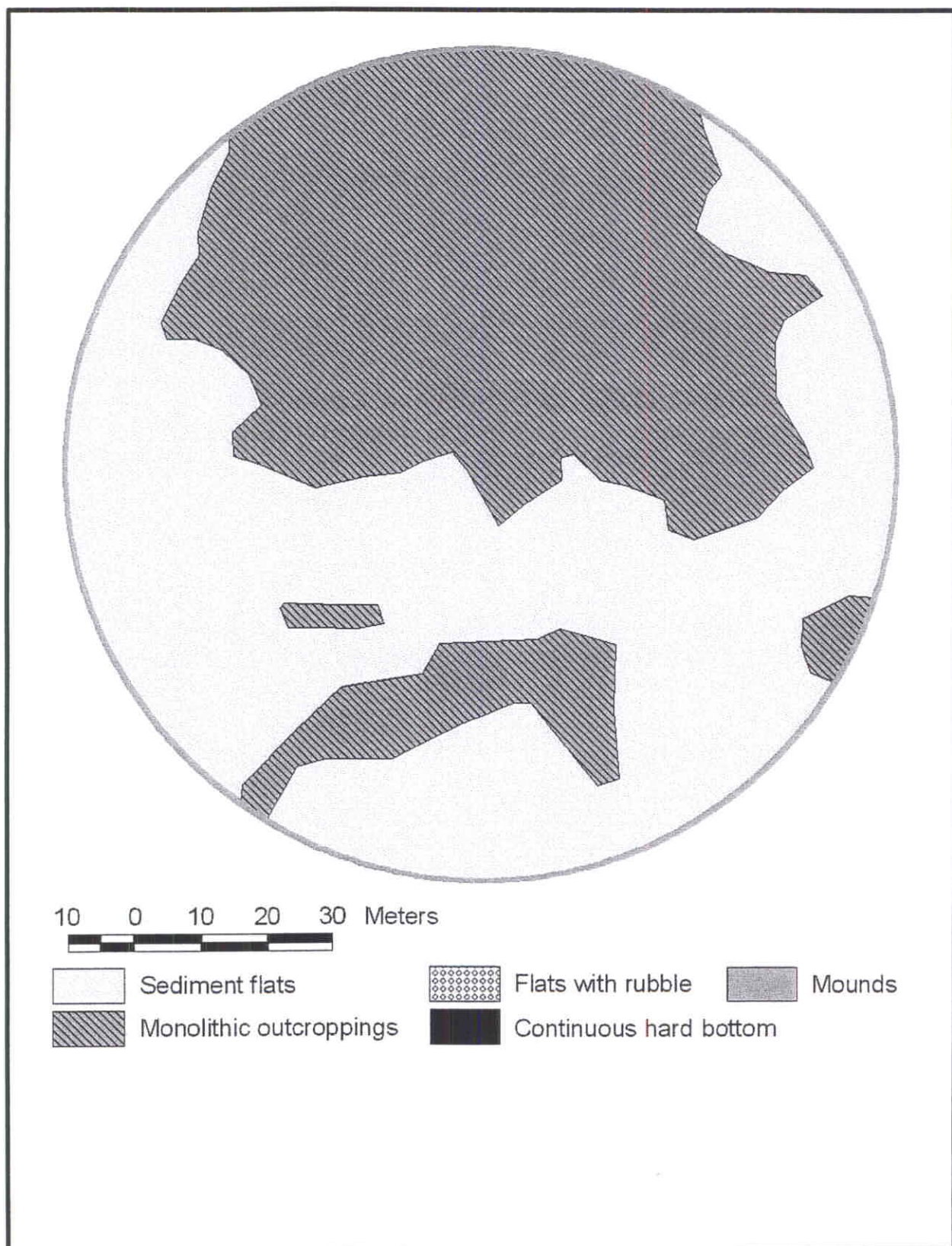


Fig. 3.22. Bottom type map for Site 2 derived from ROV photo and video observations. Circle boundary corresponds to circles in Figs. 3.20 and 3.21.

partial sediment cover and the sediments are generally fine, so any currents are not so energetic as to sweep the mound bare of sediments. Both meter-scale relief and centimeter-scale roughness vary from small to large, and aside from a cluster of stations that show flat seafloor on the southwest side of the mound, these parameters are intermixed. This suggests that the character of the mound varies significantly on a lateral scale of meters.

Site 3

Monitoring Site 3 examined small mounds in eastern Megasite 1 (**Fig. 3.3**). Bathymetry contours are few and meandering, denoting nearly flat seafloor (**Fig. 3.23**). Depths change by only about 2 m across the monitoring area (from 81 to 83 m). Furthermore, the data show little evidence of the small mounds in the area. The 81 and 82 m contours on the north side of the site are close and follow one another, trending west-northwest. This suggests a slightly greater slope probably caused by a sediment pile on the north side of the site.

The side-scan sonar image shows many small, high-backscatter features that appear to be small mounds 3-5 m across (**Fig. 3.24**). Many of these small mounds appear to cluster together in groups that range from subcircular to linear. Only a few of these mounds display shadows and presumably these are the largest. Much of the seafloor gives low backscatter, suggesting that the mounds are located on otherwise flat, sediment-covered seafloor.

Site 3 contains three seafloor bottom types (**Fig. 3.25**). Mounds and monolithic outcropping areas appear as smaller patches surrounded by flat, sediment-covered seafloor. Interestingly, the areas characterized as “mounds” appear to correspond to amorphous, moderate-backscatter areas, whereas the zones of monolithic outcrops are associated with the smaller, more obvious mounds. This difference may have to do with low roughness and greater sediment cover on the mounds. Despite the fact that the sonar mosaic for Site 3 shows a loose cluster of low mounds on an expanse of apparently flat seafloor, many of the photo stations showed outcropping rock and many of these were classified as monoliths, meaning mounds larger than the typical ROV-video view. Roughness and relief both vary from low to high, but low to medium values are more common. Sediment texture is mainly fine and sediment cover is usually partial. These observations make a picture of an environment of flat seafloor with many low mounds from boulder to house-size or larger, surrounded by fine sediments.

Site 4

Monitoring Site 4 is located among large “pinnacle” mounds near the shelf edge in central Megasite 2 (**Fig. 3.7**). Bathymetry data show a broad mound consisting of a northwest trending ridge (**Fig. 3.26**). Although the mound does not appear tall, the mound flank shows a continuous slope of 14° to the southwest. Thus, we do not see the entire height of this mound within the study site. The contours imply the mound is at least 10 m high, with a nearly flat top at about 100 m depth.

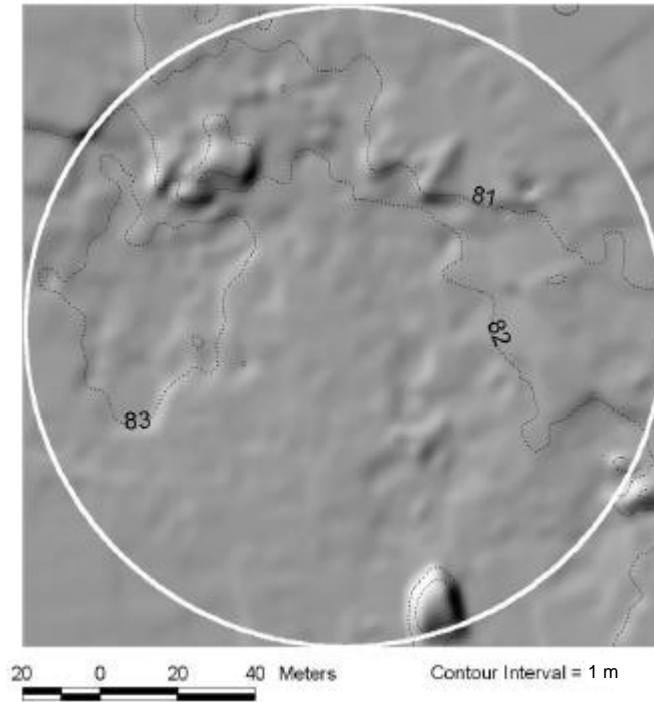


Fig. 3.23. Bathymetry of Monitoring Site 3. Contours shown at 1-m intervals. Circle indicates the boundary of ROV seafloor observations.

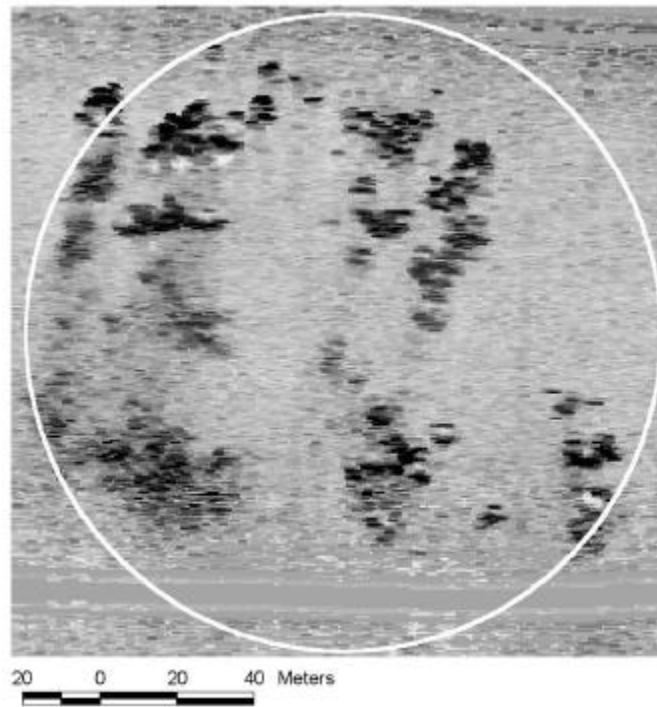


Fig. 3.24. Side-scan sonar image of Monitoring Site 3. Circle indicates the boundary of ROV seafloor observations.

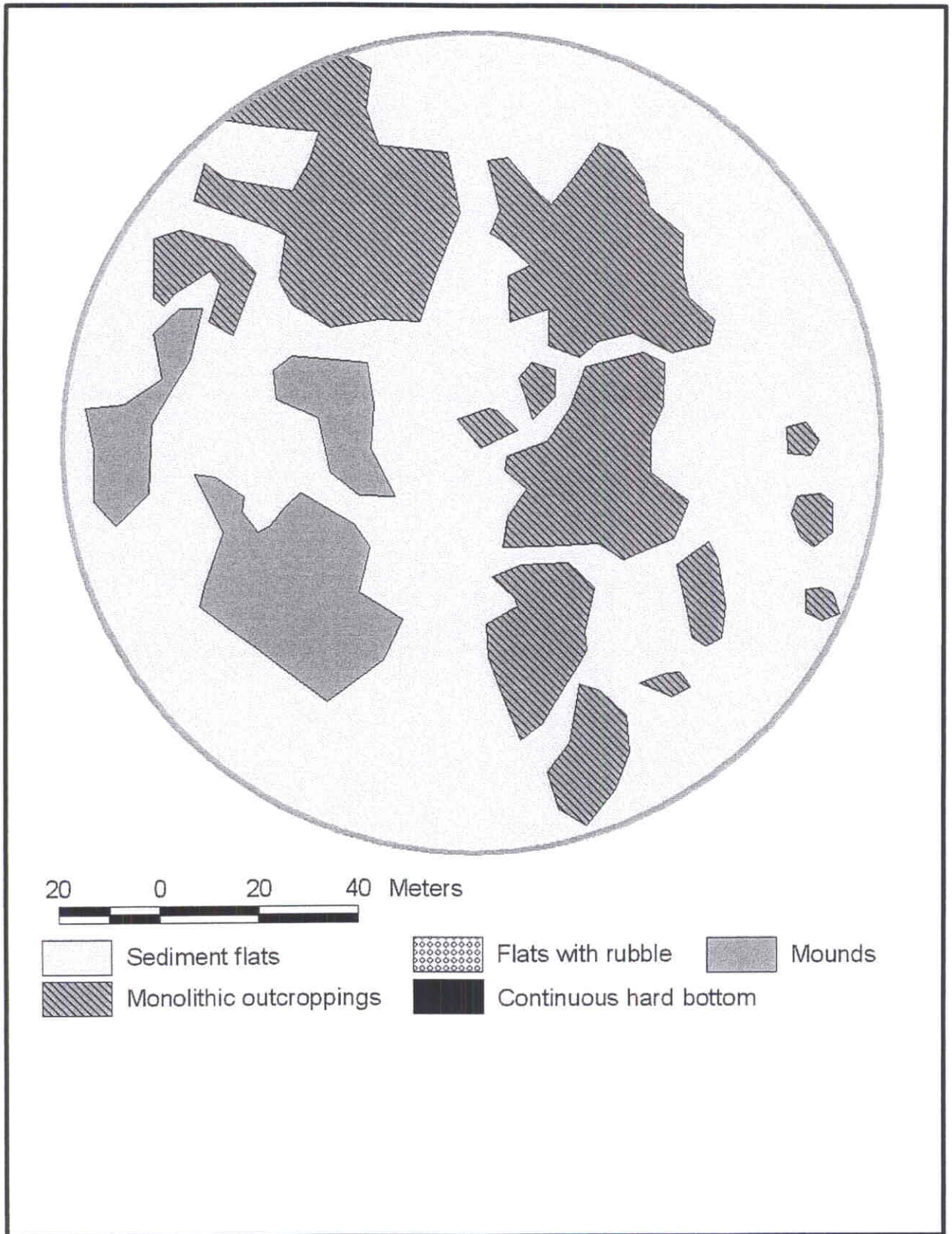


Fig. 3.25. Bottom type map for Site 3 derived from ROV photo and video observations. Circle boundary corresponds to circles in Figs. 3.23 and 3.24.

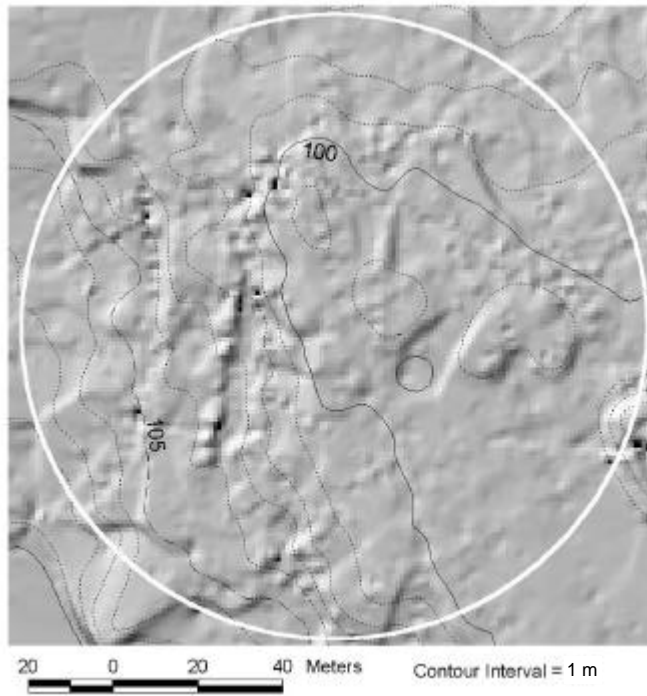


Fig. 3.26. Bathymetry of Monitoring Site 4. Contours shown at 1-m intervals. Circle indicates the boundary of ROV seafloor observations.

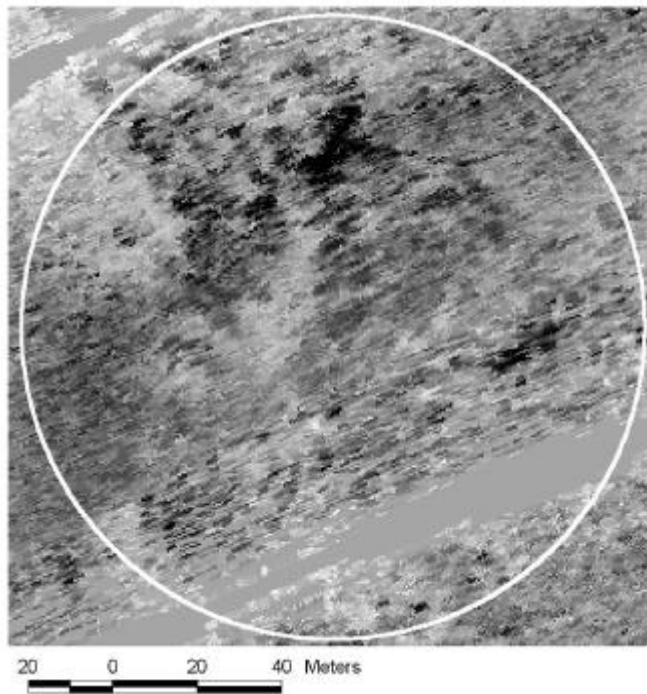


Fig. 3.27. Side-scan sonar image of Monitoring Site 4. Circle indicates the boundary of ROV seafloor observations.

The side-scan image of Site 4 shows few of what one might recognize as mound-like features. In general, dark, high-backscatter streaks and patches appear against a moderate-backscatter background (**Fig. 3.27**). The lack of obvious shadows suggests that these features are not tall and steep, but are more likely variations in seafloor roughness. Many mounds in Megasite 2 are almost entirely mantled with sediment, showing only features at their summits, and this may be the reason for the appearance of Site 4.

Comparison of the bottom-type interpretation (**Fig. 3.28**) with the sonar mosaic suggests a reason for the apparent uniformity of the sonar image. Most of the area is typified by low mounds, which accounts for the widespread moderate, mottled backscatter appearance. Several patches of monolithic outcroppings are within the site and some of these obviously correlate to the high-backscatter patches, undoubtedly because the monoliths are strong acoustic reflectors. Photo station observations display considerable lateral variability. Stations at which outcrop is visible or not are about evenly divided and sediment types range from fine to coarse with several stations showing shell hash. Roughness ranges from low to high and relief ranges from flat to medium. Although many stations near the center of the site were classified as monoliths, most others on the periphery were classified as mounds. These observations indicate that geological conditions are laterally highly variable at this site.

Site 5

Monitoring Site 5 examines a tall, small-diameter, flat-topped mound located in eastern Megasite 3 (**Fig. 3.10**). Bathymetry data show a tall, subcircular mound, approximately 100 m in diameter, surrounded by flat seafloor (**Fig. 3.29**). The mound has a nearly flat top, with depths of 68-69 m, and steep, rough, sides. The rough sides appear to show many individual blocks, small ridges, and indentations. In many ways, this mound is similar to the large flat-topped mound at Site 1 in Megasite 1. Seafloor surrounding the mound is at a depth of about 80 m, indicating the mound is approximately 12 m in height.

The side-scan sonar image of Site 5 shows the flat-topped mound with a halo of moderate backscatter from sediments surrounding its west, south, and east sides (**Fig. 3.30**). Notably, this halo does not appear to affect the contours, indicating it has no discernable bathymetric expression. The top of the mound shows a nearly uniform, moderate backscatter, similar to the mound at Site 1. Also like the Site 1 mound, the mound sides show strong backscatter and shadows from the large blocks.

Bottom type-zones at Site 5 are nearly concentric around the tall mound (**Fig. 3.31**). Photo stations on top of the mound all showed outcropping carbonate and were classified as continuous hard bottom. Meter-scale relief atop the mound is low to medium, consistent with the flat top observed in the side-scan images. The mound sides contained large, individual blocks and are classified as monolithic outcroppings. Surrounding the northwest and south sides of the mound are flat areas with debris that seem to correspond with much of the moderate-backscatter halo that flanks the mound. The featureless area to the south of the mound consists of flat, sediment-covered seafloor. Photo stations near the center of the site all showed outcrop and are surrounded by stations at which no rock is visible.

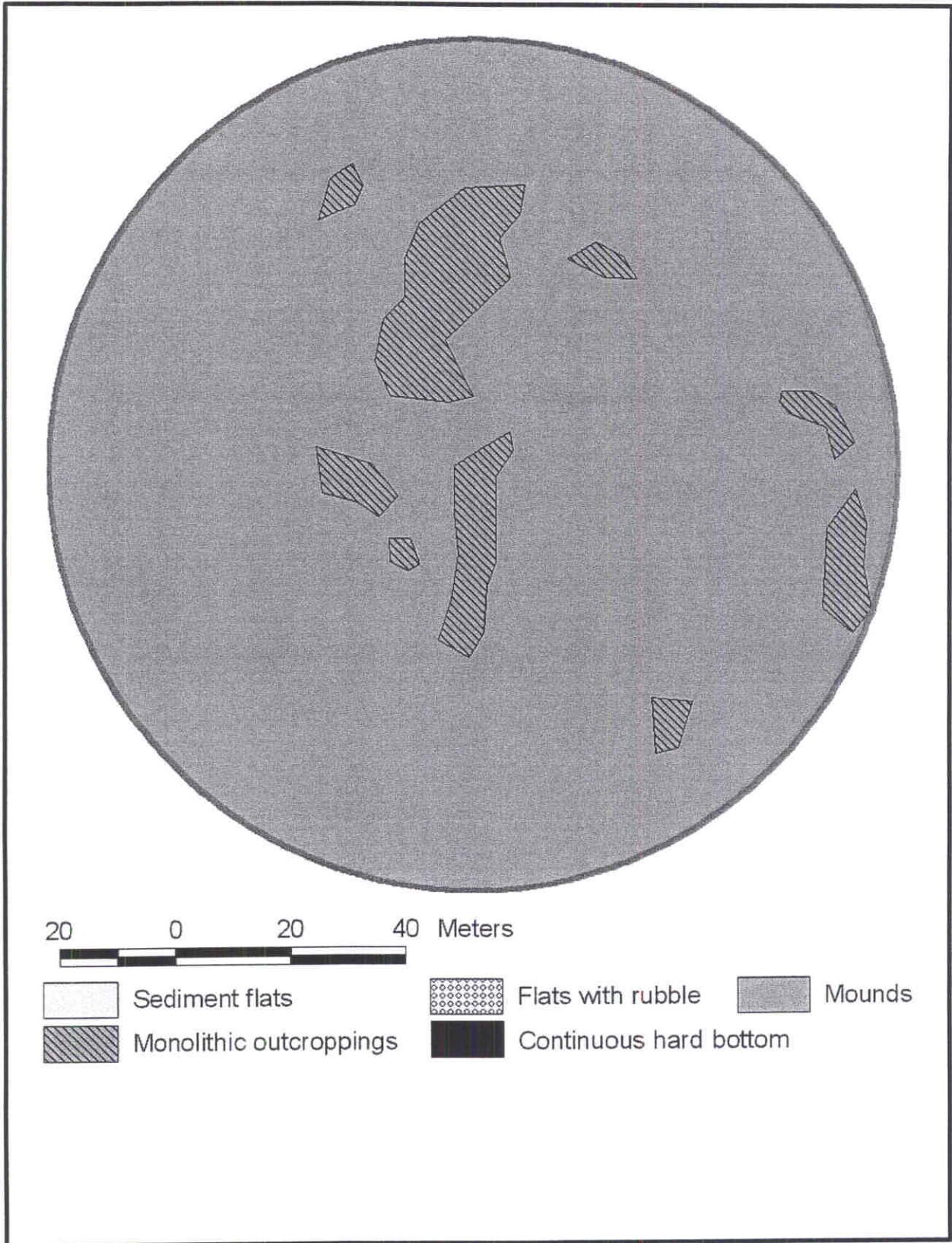


Fig. 3.28. Bottom type map for Site 4 derived from ROV photo and video observations. Circle boundary corresponds to circles in Figs. 3.26 and 3.27.

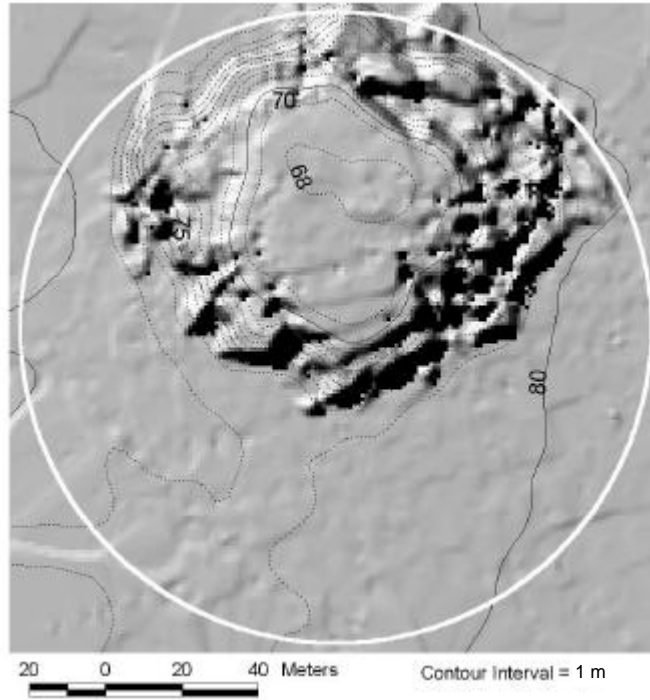


Fig. 3.29. Bathymetry of Monitoring Site 5. Contours shown at 1-m intervals. Circle indicates the boundary of ROV seafloor observations.

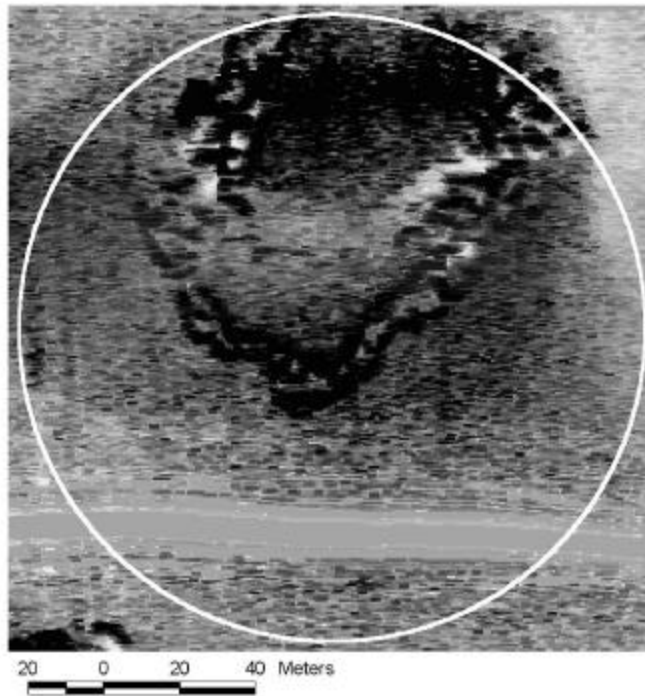


Fig. 3.30. Side-scan sonar image of Monitoring Site 5. Circle indicates the boundary of ROV seafloor observations.

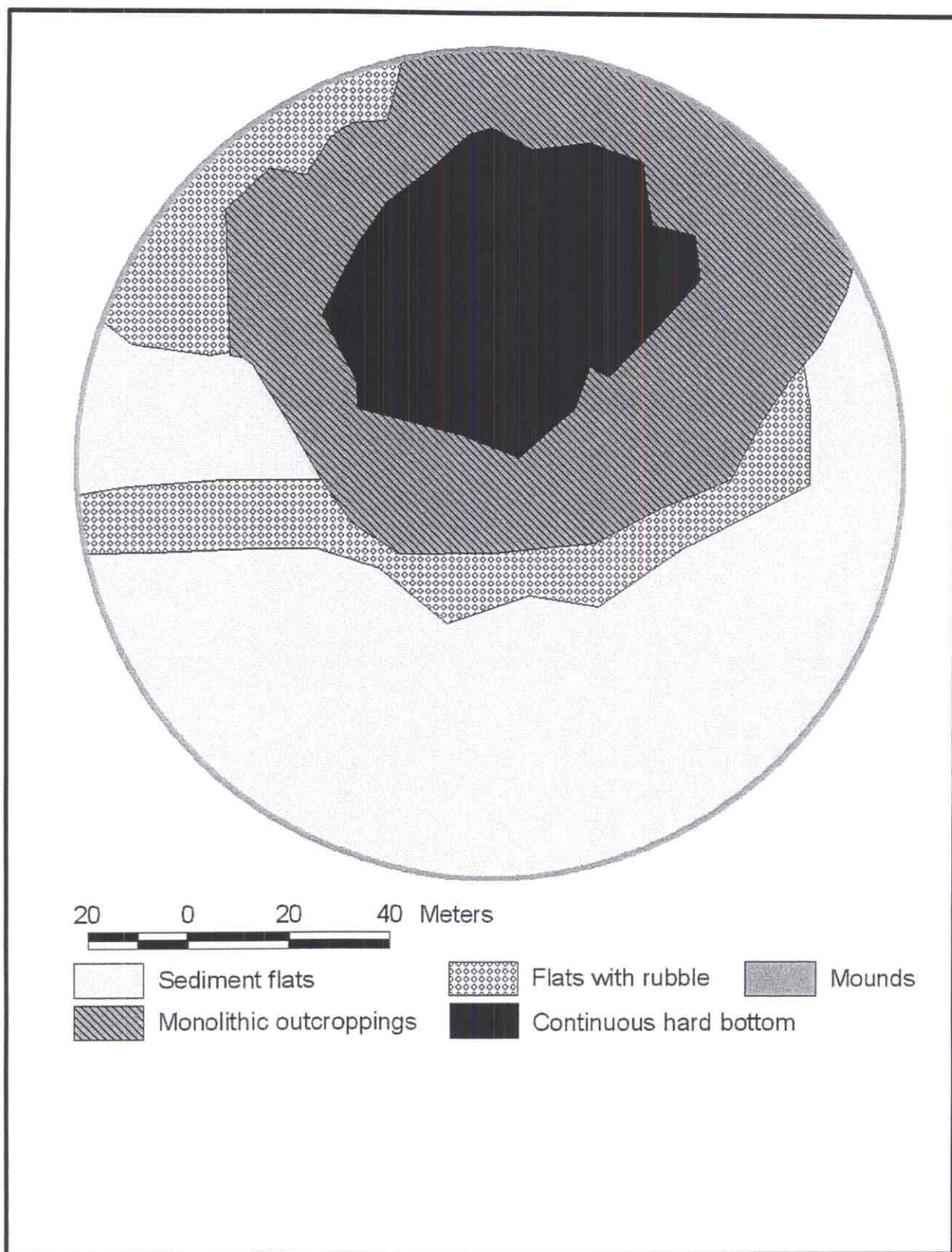


Fig. 3.31. Bottom type map for Site 5 derived from ROV photo and video observations. Circle boundary corresponds to circles in Figs. 3.29 and 3.30.

Site 6

Monitoring Site 6 is a low relief site covering part of a large, carbonate hardground in eastern Megasite 3 (**Fig. 3.10**). Because of the low relief, the bathymetry shows only a few meandering contours (**Fig. 3.32**). The seafloor depth deviates little from 77-78 m. At the south edge of the site, some deeper contours are seen, corresponding to the south edge of the large hard bottom area on which Site 6 is located.

The side-scan sonar mosaic shows many subcircular, high-backscatter features that appear to be low mounds 10-15 m in diameter (**Fig. 3.33**). Interspersed within the mounds and mound clusters are lighter areas that represent sediment pockets.

ROV videos from Site 6 show an area that appears blanketed by a cover of fine sediments. Stations with large outcrops were mostly clustered in the northwest and southeast quadrants. Although many stations are mantled by fine sediments, coarse sediments are common. Relief and roughness are often medium. These observations are consistent with the side-scan images that suggest the site is a low, wide carbonate hard bottom with a rough upper surface. The fine sediment cover is partial and often limited to sediment pockets within the hard bottom, consistent with subbottom profiler records. Virtually the entire site has been classified as a zone of low mounds (**Fig. 3.34**). Sediment flats characterize two areas on the west side of the site and there are several small areas with monolithic outcrops.

Site 7

Monitoring Site 7 is located on the northernmost part of the large, linear mound in northwest Megasite 5 (**Fig. 3.15**). The bathymetry contours show a large, flat-topped mound with a summit depth of about 72 m (**Fig. 3.35**). The mound is about 100 m across at its summit but several hundred meters in length. A narrow ridge connects this mound to a larger edifice farther south. Although it has an overall north-south trend that mirrors the elongation of the entire mound, the Site 7 mound is irregular in shape with rough topography on its flanks. The mound rises from a flat seafloor at a depth of 86 m, making its height 14 m.

Side-scan sonar data from Site 7 show many subcircular bumps with dark, high-backscatter returns on the side facing the sonar and white shadows on the opposite side (**Fig. 3.36**). The bumps appear to be 15-20 m in diameter and correspond to the flanks of the tall mound. Comparison of the side-scan data with the bathymetry implies that the mound flanks probably contain many large, monolithic blocks that are not well-represented by the gridded bathymetry data. The flat summit shows moderate and variable backscatter and the seafloor on the outer edges of the site shows moderate but more homogeneous backscatter, as would be expected of flat, sediment-mantled seafloor.

The seafloor bottom-type map (**Fig. 3.37**) shows zones concentric with the mound. The center, representing the mound top, is characterized as continuous hard bottom, whereas the mound flanks are characterized by monolithic outcroppings. Surrounding the mound

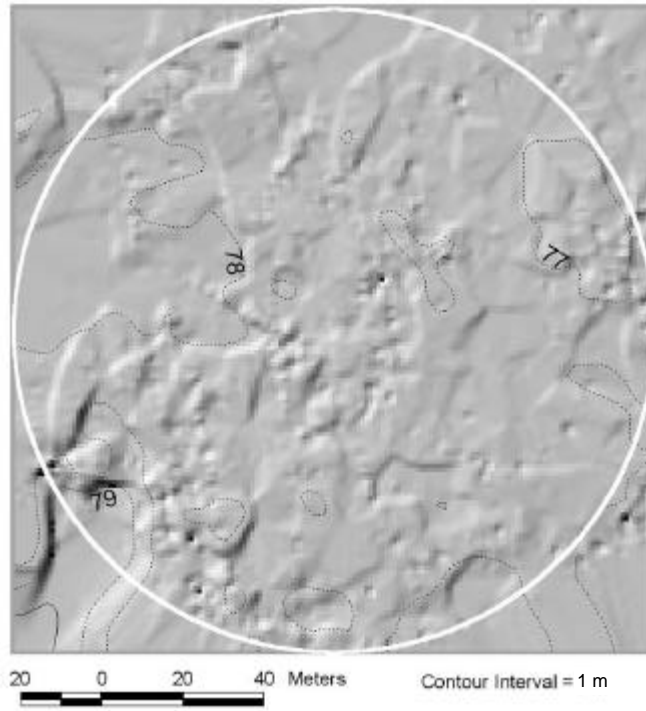


Fig. 3.32. Bathymetry of Monitoring Site 6. Contours shown at 1-m intervals. Circle indicates the boundary of ROV seafloor observations.

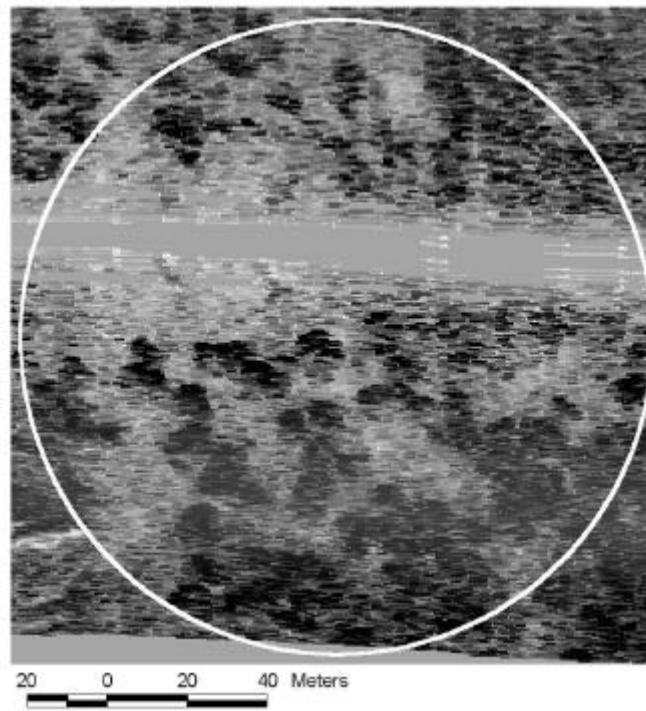


Fig. 3.33. Side-scan sonar image of Monitoring Site 6. Circle indicates the boundary of ROV seafloor observations.

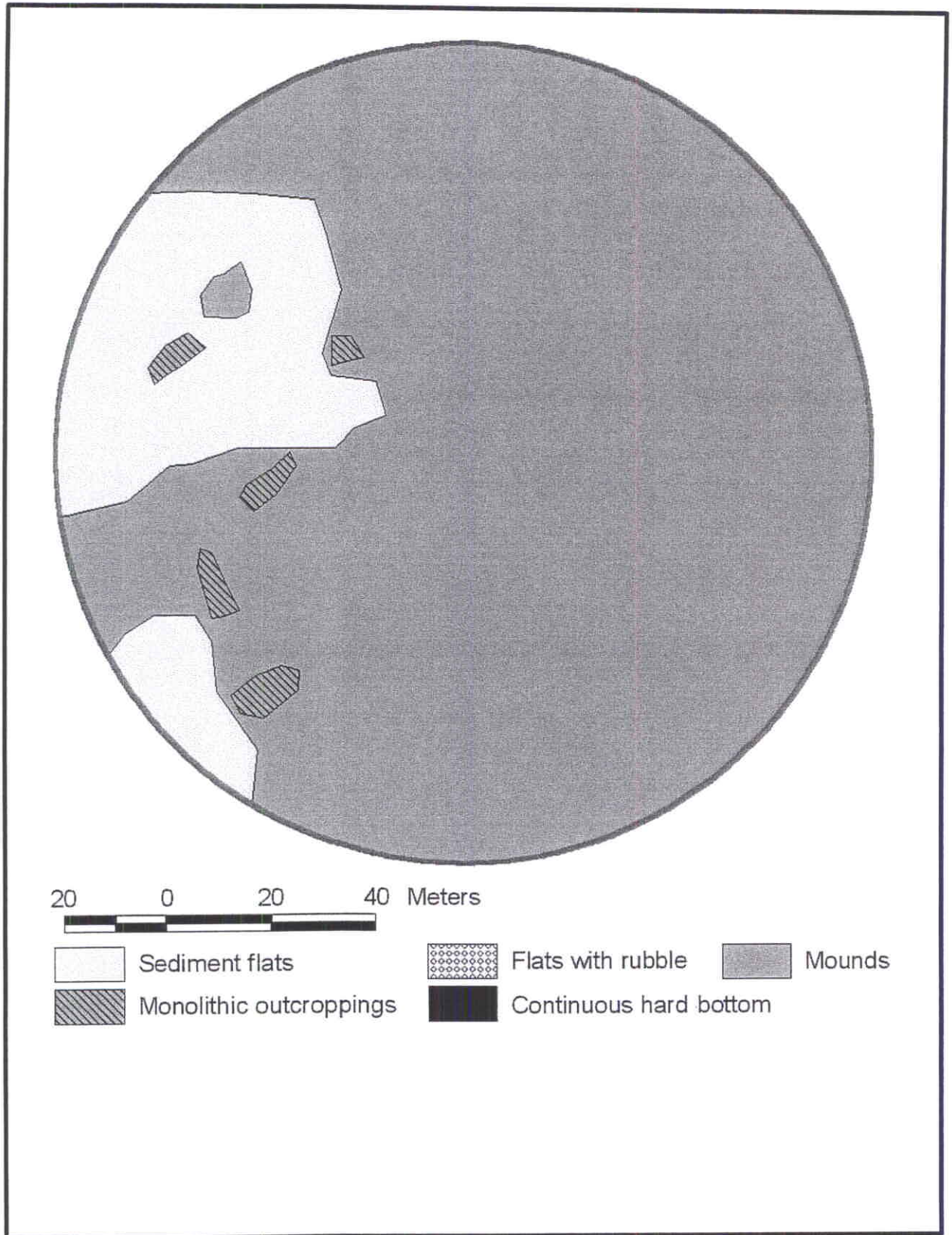


Fig. 3.34. Bottom type map for Site 6 derived from ROV photo and video observations. Circle boundary corresponds to circles in Figs. 3.32 and 3.33.

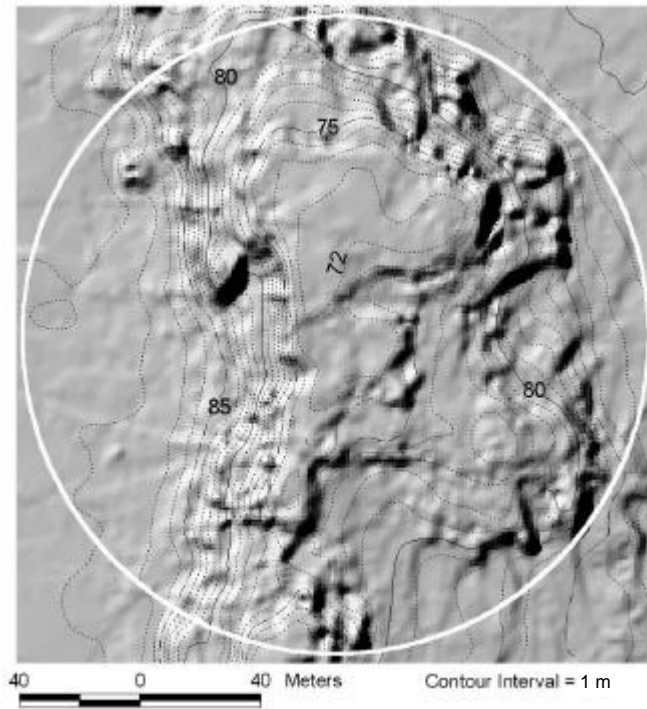


Fig. 3.35. Bathymetry of Monitoring Site 7. Contours shown at 1-m intervals. Circle indicates the boundary of ROV seafloor observations.

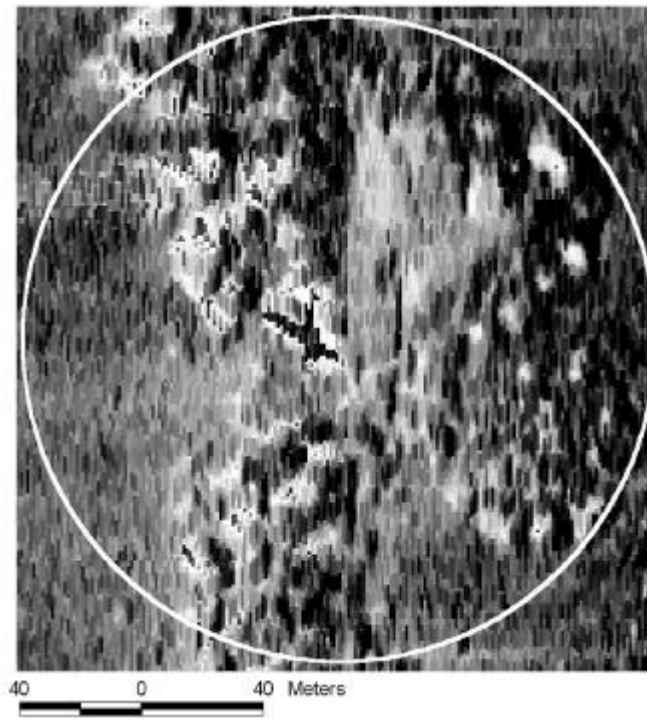


Fig. 3.36. Side-scan sonar image of Monitoring Site 7. Circle indicates the boundary of ROV seafloor observations.

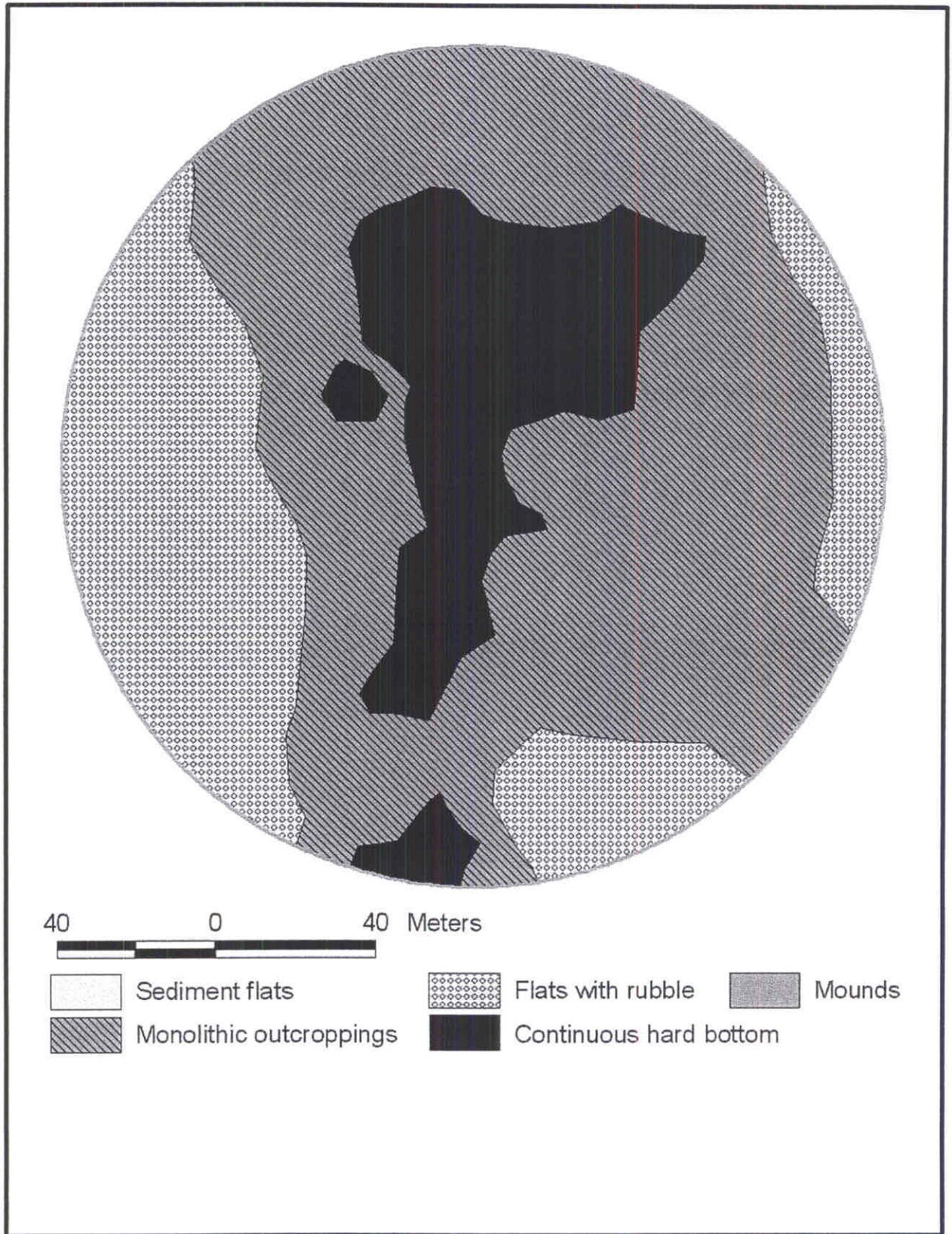


Fig. 3.37. Bottom type map for Site 7 derived from ROV photo and video observations. Circle boundary corresponds to circles in Figs. 3.35 and 3.36.

is a zone of flat seafloor containing abundant debris probably shed from the large mound. The debris on the seafloor around the mound probably explains why the sonar backscatter from the seafloor is moderate, rather than low as is usual for flat sedimented areas.

Site 7 ROV photo stations are described mostly as outcrop, with many stations classified as medium to high relief, and the roughness is often medium. Nevertheless, a number of stations, particularly on top of the mound, are characterized by low roughness, consistent with the relatively flat summit seen in the bathymetry map. The surface of this area is blanketed by a layer of silty to sandy sediment ranging from a thin veneer to near complete burial. Although often obscured by sediment cover, the surface texture exhibits small pits and depressions, but lacks large-scale roughness seen in other areas.

At the edge of the flat summit, the carbonate surface begins to break up, often in steep, meter scale faces. This transition grades outward into an area dominated by high relief monoliths (large, isolated rocks) several meters in relief and extent. These features often have broad bases and slope steeply upward to one or several peaks. The peaks may or may not be flat-topped and some have undercut edges. The surfaces of the monoliths are often mantled by a thin veneer of fine sediment and biogenic material. The monoliths tend to be separated by channels or valleys with sediment flats at their bottoms. General observations suggest the monoliths are more deeply eroded with distance from the center of the mound. The relief and size of these features seems to decrease with distance from the mound center, whereas sediment cover seems to increase.

The region of monoliths changes into a surrounding region in which sediment cover is complete and little or no evidence of outcrop is seen. These areas show a mixture of fine and coarse sediments with loose rocks and shells scattered on the surface. This area appears to begin at roughly equivalent depths on the north, east, and west sides. However, the sediment flats to the south occur at a shallower depth and lack some of the surface rubble seen on other sides. Eleven stations on the west side of the site show flat seafloor or depression with shell hash or rubble. These stations are on the seafloor adjacent to and on the west side of the mound that shows high backscatter. These characteristics imply significant input of biogenic material from the mound and the depression suggests erosion.

Site 8

Monitoring Site 8 contains a medium-size mound located in central Megasite 5 (**Fig. 3.15**). Bathymetry data show a slightly-elongated mound, approximately 40 m in north-south extent and 15 m in east-west extent with a smaller mound located nearby to the east (**Fig. 3.38**). The mound appears to rise about 7-8 m above the surrounding seafloor to a rounded summit at a depth of 91 m. Notably, there is a northeast-southwest bathymetric gradient across the site with depths becoming greater to the southwest by about 5 m from 94 to 99 m. This gradient probably represents thinning sediments since the mound lineament in Megasite 5 often appears in the chirp sonar profiles to be a boundary between thicker and thinner sediments.

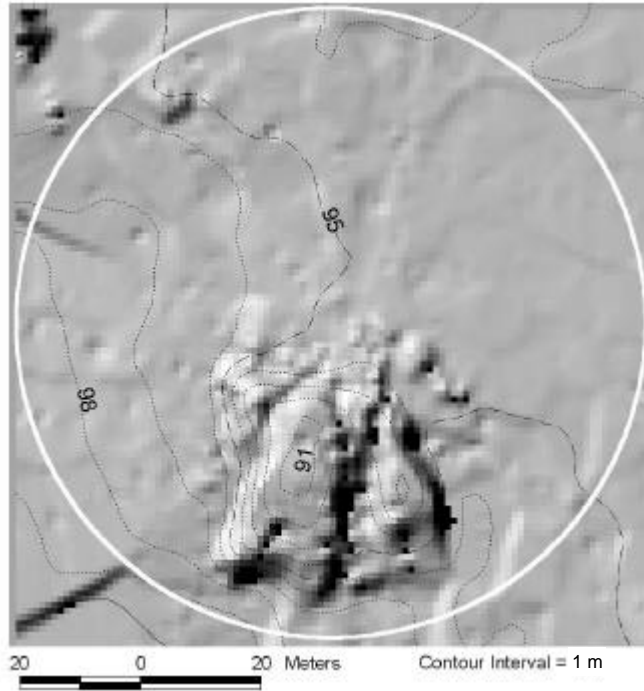


Fig. 3.38. Bathymetry of Monitoring Site 8. Contours shown at 1-m intervals. Circle indicates the boundary of ROV seafloor observations.

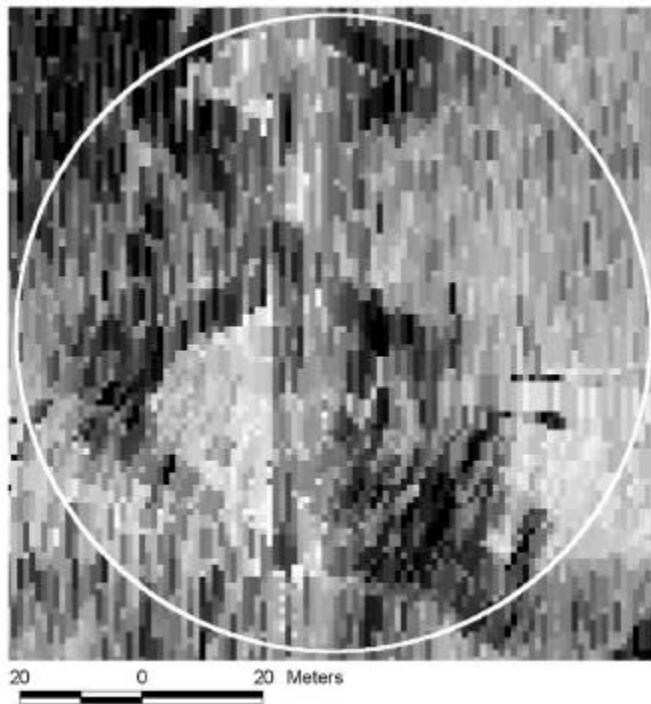


Fig. 3.39. Side-scan sonar image of Monitoring Site 8. Circle indicates the boundary of ROV seafloor observations.

The mound in Site 8 is difficult to discern in the side-scan sonar image (**Fig. 3.39**) because it is small, so the pixels appear large, and because it occurs at the join between two adjacent sonar tracks, so it changes appearance at the join. The two mounds seen in the bathymetry are within a larger area of irregular seafloor that appears as a dark, high-backscatter ring in the southern part of the site. High backscatter extends to the northwest, following the trend of the larger mound lineament (see **Fig. 3.15**). The high backscatter probably results from carbonate debris shed from the mounds along the lineament.

Seafloor bottom types (**Fig. 3.40**) show an area of monolithic outcroppings that corresponds to the ring-shaped high-backscatter zone in the side-scan sonar mosaic. Other areas, characterized as having low mounds, correspond to other areas of high backscatter in the sonar image. The northeastern half of the site is typified by flat, sediment-mantled seafloor.

Site 9

Relief at Site 9, located at a site with low mounds along the Megasite 5 mound lineament (**Fig. 3.15**), is low, so the contours mostly wander at depths of about 90-94 m (**Fig. 3.41**). As at Site 8, there is a slight bathymetric gradient with depths becoming a few meters deeper from northeast to southwest, reflecting the change across the lineament. A few closed contours show low mounds at the site.

The side-scan sonar image shows a loose cluster of subcircular mounds, 5-20 m in diameter (**Fig. 3.42**). The mounds display dark, high backscatter on the sides facing the sonar and white shadow on the opposite sides. Surrounding seafloor appears gray, indicating low backscatter. Across the bottom part of the site, the sonar image shows two linear, high-backscatter “tails” trending southwest from one of the larger mounds in the site and another just outside the image. In the bathymetry, these tails can be seen as slight depressions (**Fig. 3.41**).

Sea bottom types are patchy in the site indicating high lateral variability (**Fig. 3.43**). The background appears to be flat, sedimented seafloor with patches of monolithic outcroppings corresponding to the mound locations. In the center of the site is a linear patch of seafloor characterized as having many low mounds. Farther south, the two high-backscatter tails are characterized by linear zones with carbonate debris on the seafloor.

Consistent with its location on low mounds in the center of Megasite 5, Site 9 photo stations are characterized by fine sediments, flat to low relief, low roughness, and fine sediments. One station shows shell hash, one shows medium roughness, and several show medium relief, suggesting scattered small mounds.

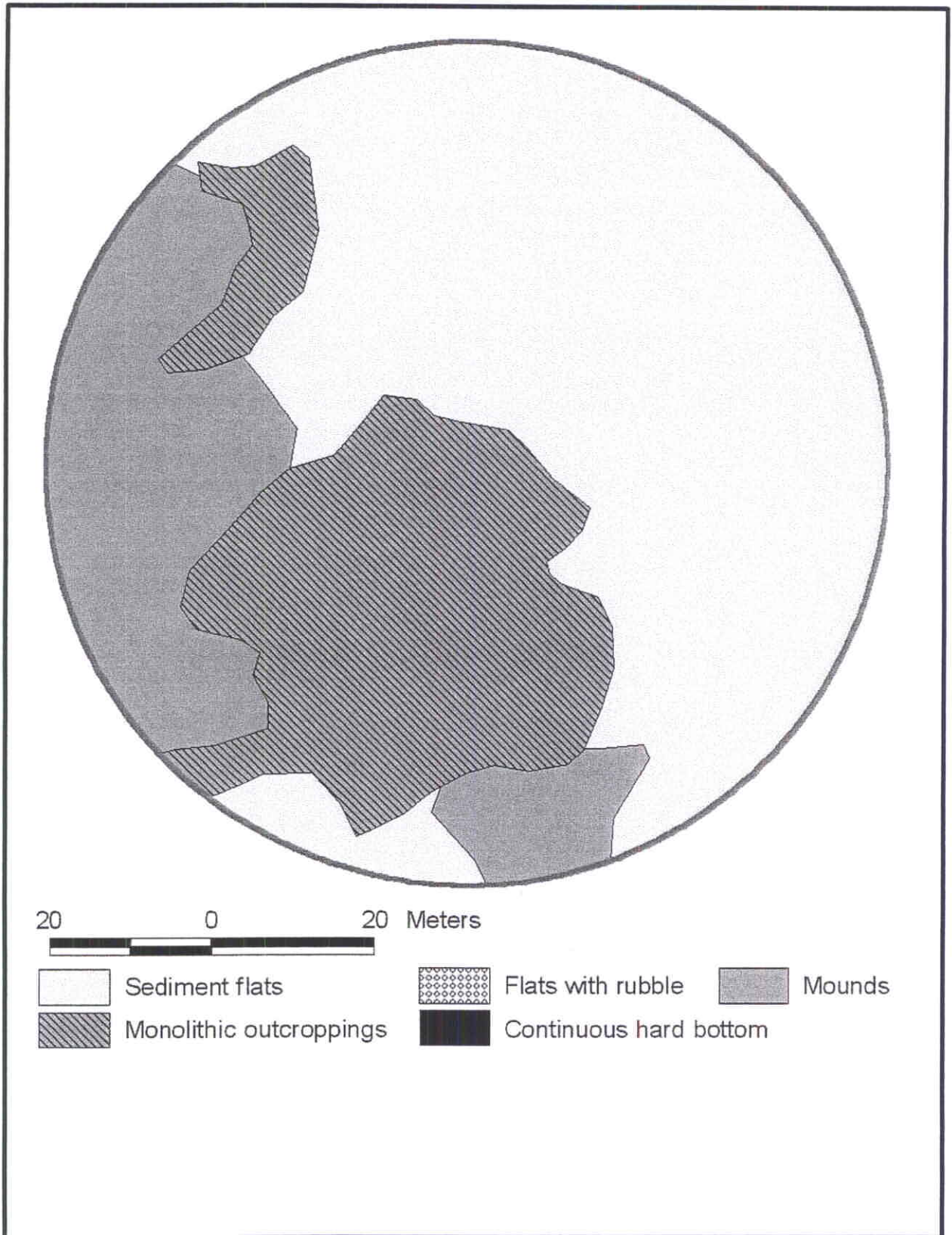


Fig. 3.40. Bottom type map for Site 8 derived from ROV photo and video observations. Circle boundary corresponds to circles in Figs. 3.38 and 3.39.

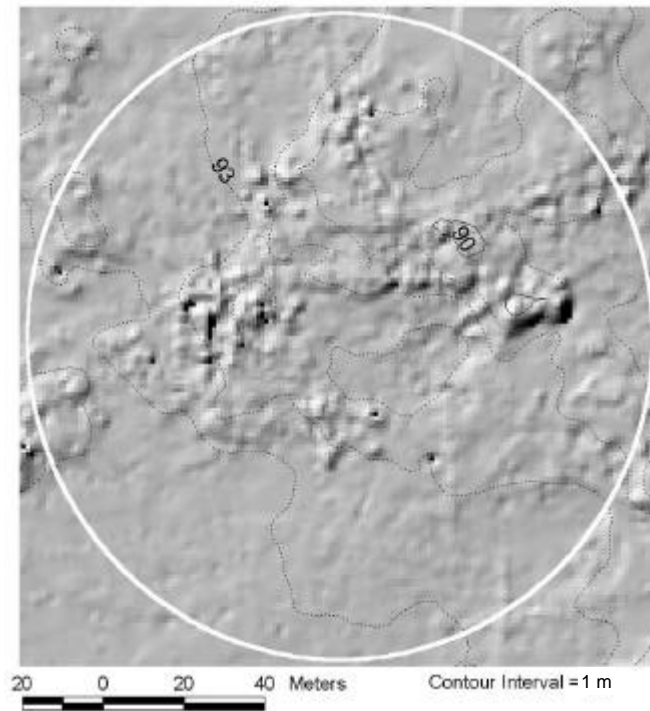


Fig. 3.41. Bathymetry of Monitoring Site 9. Contours shown at 1-m intervals. Circle indicates the boundary of ROV seafloor observations.

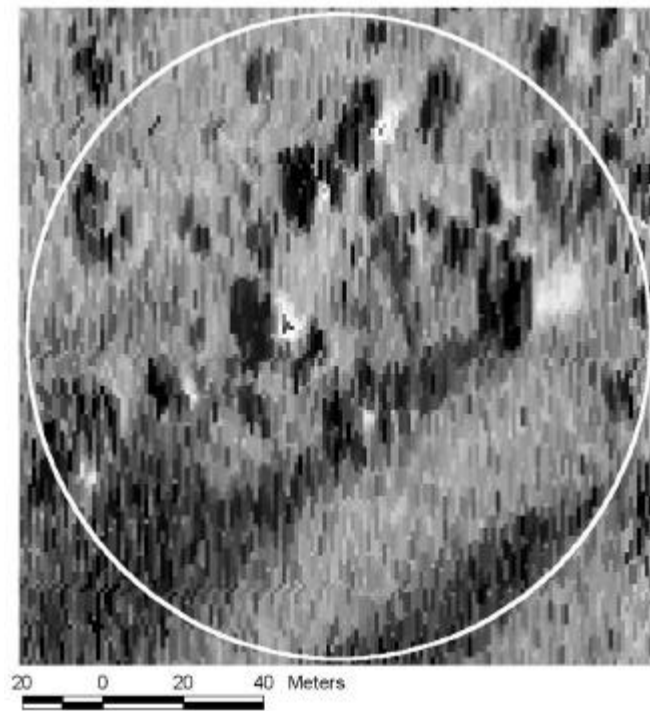


Fig. 3.42. Side-scan sonar image of Monitoring Site 9. Circle indicates the boundary of ROV seafloor observations.

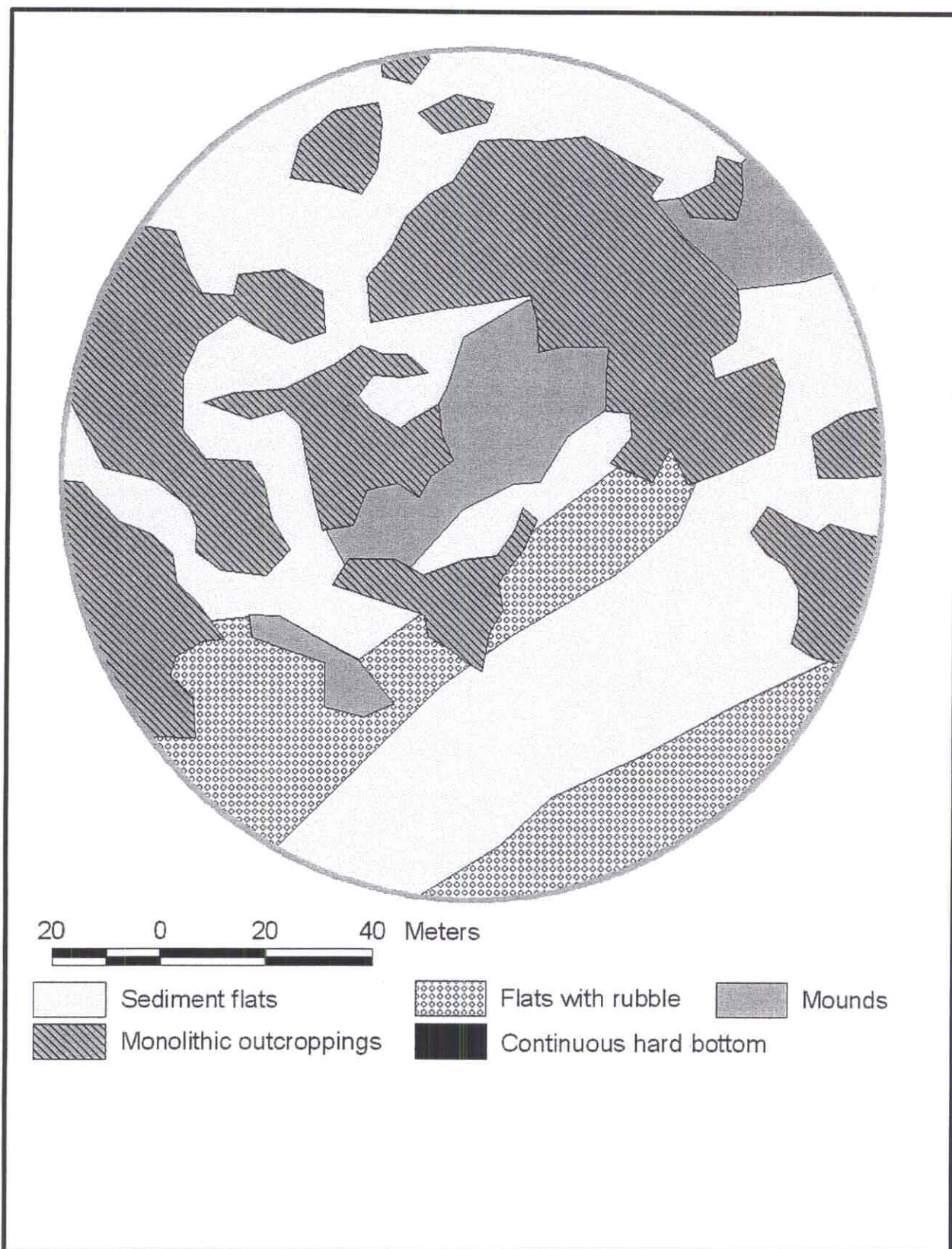


Fig. 3.43. Bottom type map for Site 9 derived from ROV photo and video observations. Circle boundary corresponds to circles in Figs. 3.41 and 3.42.

Mound Morphology and Characteristics

General Observations

Of the five megasites, four of them (1, 2, 3, and 5) contain recognizable carbonate mounds. The size, number, and morphology of mounds at each site vary significantly (**Figs. 3.4, 3.8, 3.11, and 3.16**). Diameters range from 1-2 m to >1 km. Numbers of mounds in each megasite vary by about two orders of magnitude. At Megasite 1 there are over 1,000 mounds, whereas Megasite 5 contains only about 120. The mounds are generally subcircular in shape with the majority having an aspect ratio of about 1:1 (**Fig. 3.44**). (Note: the aspect ratio is the ratio of the major and minor axes of the ellipse that best fits the mound outline.) However, some are elongated with aspect ratios as high as 8:1. Heights are not as well measured by our data as shape and diameter, but it appears the largest mounds in the present study are about 13-23 m tall, and the shortest are less than 1 m. The largest and tallest mounds are few in number, whereas smaller mounds occur in greater numbers. A logarithmic-axis plot of the number of mounds versus mound area is linear, within a given megasite, with correlation factors >85%-95% (**Fig. 3.45**). This indicates that the number of mounds goes up exponentially with decreasing area. This is a common attribute of natural systems, like tree branches, streams, and earthquakes, that can be described by fractal geometry.

In general, we can classify the mounds into several different forms: (1) small, “unit” mounds; (2) composite mounds; (3) irregular mounds; (4) smooth-top mounds; and (5) carbonate hard bottoms. These groups are not distinct, i.e., there are no clear boundaries between different groups, but these classifications are useful for the purpose of discussion.

Unit mounds. The smallest mounds are subcircular and appear to be about 1-15 m in diameter and <1-3 m in height. Because they are typically one, subcircular feature, we call them “unit” mounds. They may be isolated or occur in clusters of various tightness, although they are commonly found in fields of tens to hundreds in number (**Fig. 3.46**). Unit mounds occur in all megasites, probably including Megasite 4, in which the complex sea bottom backscatter patterns make it difficult to recognize mounds unequivocally.

Composite mounds. Composite mounds are usually several tens of meters in diameter and appear to consist of several to several tens of unit mounds, tightly clustered with sides touching (**Fig. 3.46**). Mounds in Site 6 (Megasite 3) and Site 9 (Megasite 5) are examples of unit mounds (**Figs. 3.33 and 3.42**). Heights of smaller composite mounds are generally only several meters, but large, smooth-top mounds may also be composite features (see below). Based on appearance, we believe composite mounds may result from the coalescence of unit mounds. Composite mounds are found in Megasites 1-3 and 5. Site 2, in Megasite 1, has the appearance of a composite mound made up of about 20 smaller unit mounds (**Fig. 3.21**).

Irregular mounds. Irregular mounds are different from composite mounds in that they have jagged, irregular outlines and rough surfaces. In addition, irregular mounds often

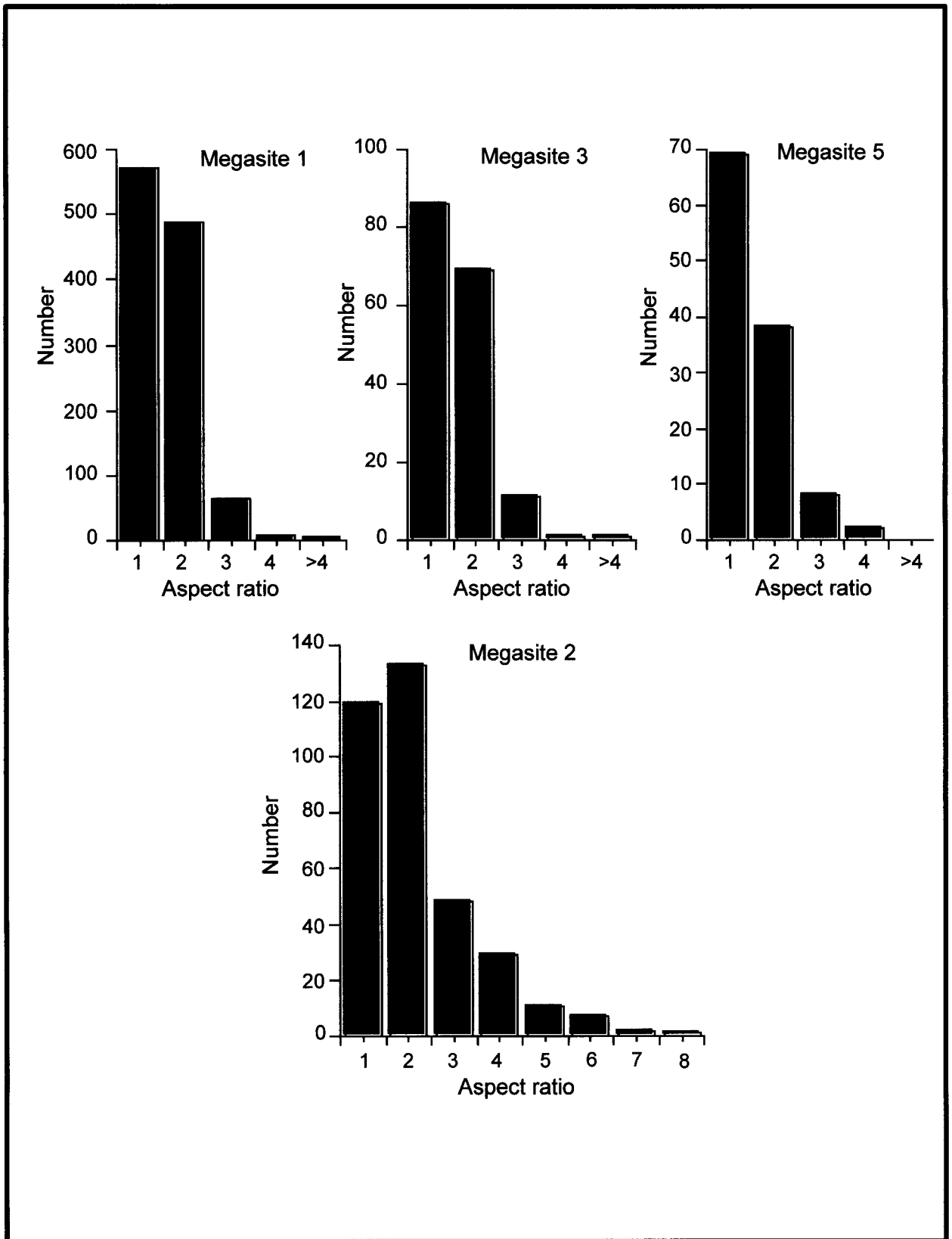


Fig. 3.44. Histograms of aspect ratios from carbonate mounds in Megasites 1-3 and 5. The aspect ratio is the ratio of the maximum and minimum axes of the ellipse that best fits the mound shape.

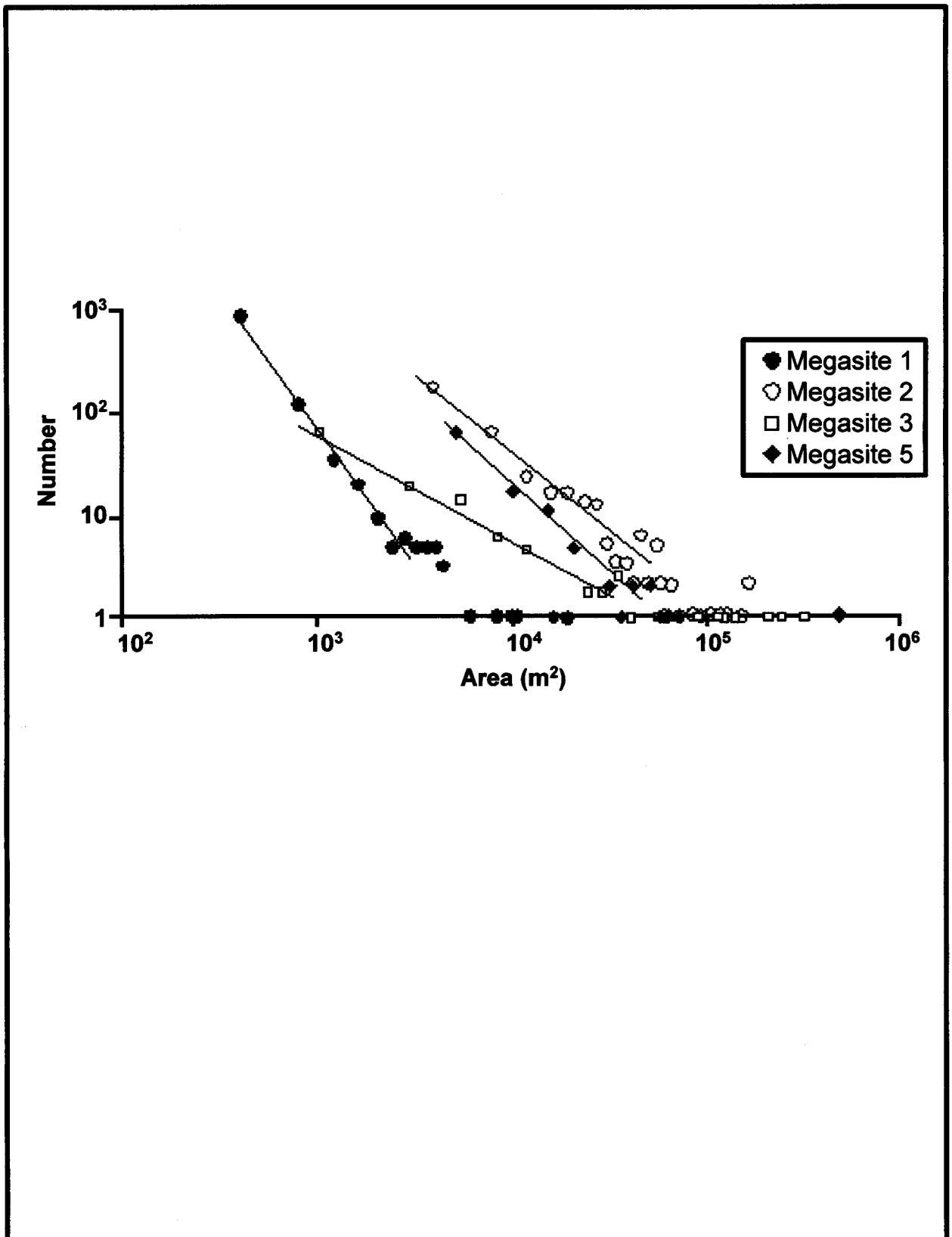


Fig. 3.45. Number of mounds versus mound area for Megasites 1-3 and 5. Both axes are logarithmic. Lines show best linear fit to data points from each megasite.

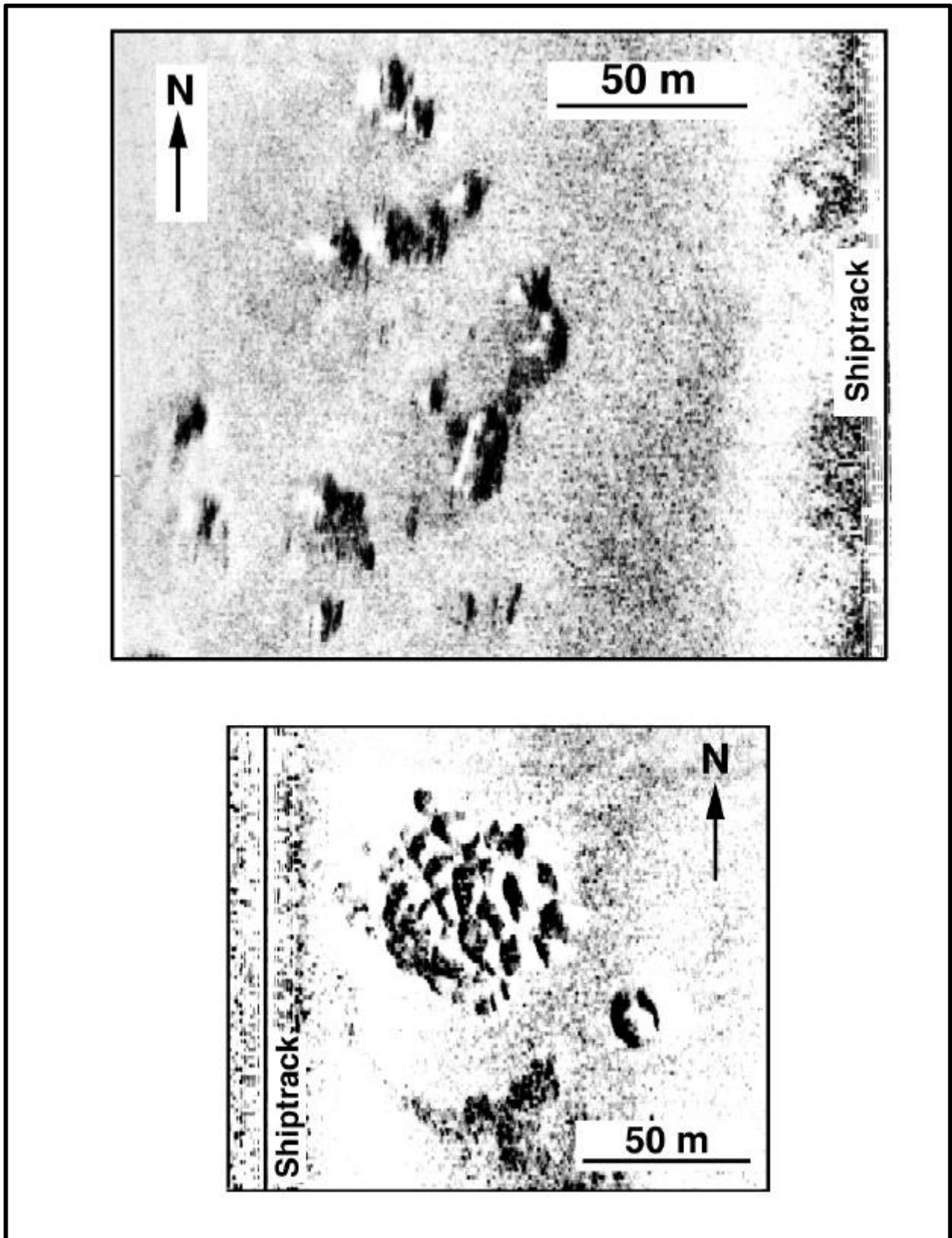


Fig. 3.46. Side-scan sonar images showing individual "unit" mounds (Top) and a composite mound (Bottom). Dark areas represent high backscatter and light areas are low backscatter. Acoustic illumination is from the shiptrack (vertical line).

have large aspect ratios, but the unit and composite mounds are frequently nearly equidimensional. Whereas composite mounds seem to be made up of bumps of similar size and subcircular shape, irregular mounds have surface roughness across a broader size range and with irregular spacing and outline (**Fig. 3.47**). Irregular mounds occur rarely in Megasites 1, 3, and 5, but are common in Megasite 2.

Smooth-top mounds. Many of the largest mounds have smooth tops. Some have flat tops, all at the same level, suggesting sea level control (Sager et al. 1992). However, others are more rounded and not all at the same level. Typically flat and smooth-top mounds are over 10 m in height. Their sides are typically steep and contain large blocks or monoliths (**Fig. 3.48**). Smooth-top mounds exhibit edges that range from nearly vertical with few or no blocks to those that contain hundreds of blocks (**Fig. 3.48**). The blockiness is reminiscent of rubble developed on the edges of carbonate hard bottoms on the U.S. east coast owing to bioerosion of the hard bottom (Riggs et al. 1996). Although bioerosion may be a factor in producing the blocks at the edges of some smooth-top mounds, the blocks rarely form uniform rings around the mounds, as might be expected if bioerosion were occurring on all edges over a long period of time. Furthermore, the blocks sometimes have the appearance of mound clusters and grade from composite mounds into smooth-top mounds. Therefore, we think the blocky edges of most of the smooth-top mounds are not solely a result of bioerosion. The largest mounds, >500 m in diameter, are smooth-top mounds. At the smallest, these mounds are 40-50 m across. Smooth-top mounds occur in Megasites 1, 3, and 5. Interestingly, the smooth-top mounds tend to be in the shallower sites but not at the deep shelf-edge sites (Megasites 2 and 4). A possible explanation is that the flat summits formed because of upward growth limitation caused by sea level during a period of sea level still-stand (Sager et al. 1992).

Carbonate hard bottoms. Carbonate hard bottoms are large, tabular carbonate features typically greater than a few hundred meters across (**Fig. 3.49**). Many of these features appear as a well-defined mound, but others have irregular outlines and seem to consist of tens to thousands of small unit mounds that form their surface. Often these features are buried on their upslope ends with a small drop of a few meters on their seaward ends; this is probably a result of the features being partly buried by sediments that thicken landward. In Megasite 2, these features are numerous and come in a wide range of heights, some reaching more than 10 m from top to bottom, but most showing only a few meters of relief. Many of these are partly buried so that only their tops can be seen on the side-scan sonar records (**Fig. 3.47**). In Megasite 2, irregular or unit mounds often form lineaments that follow the edges of the carbonate hard bottom (**Fig. 3.47**). What is more, most of the tall, irregular "pinnacle" mounds of Ludwick and Walton (1957) rest upon such bases. Sager et al. (1992) hypothesized that the low hard bottoms formed during a time when sea level was stable near the shelf edge, whereas the irregular pinnacles formed later during rapid sea level rise. Carbonate hard bottoms also occur in Megasites 1 and 3, but are less numerous. Megasite 3 contains two extensive hard bottoms with hundreds of unit mounds. Megasite 1 contains a hard bottom upon which some of the large smooth-top mounds are built.

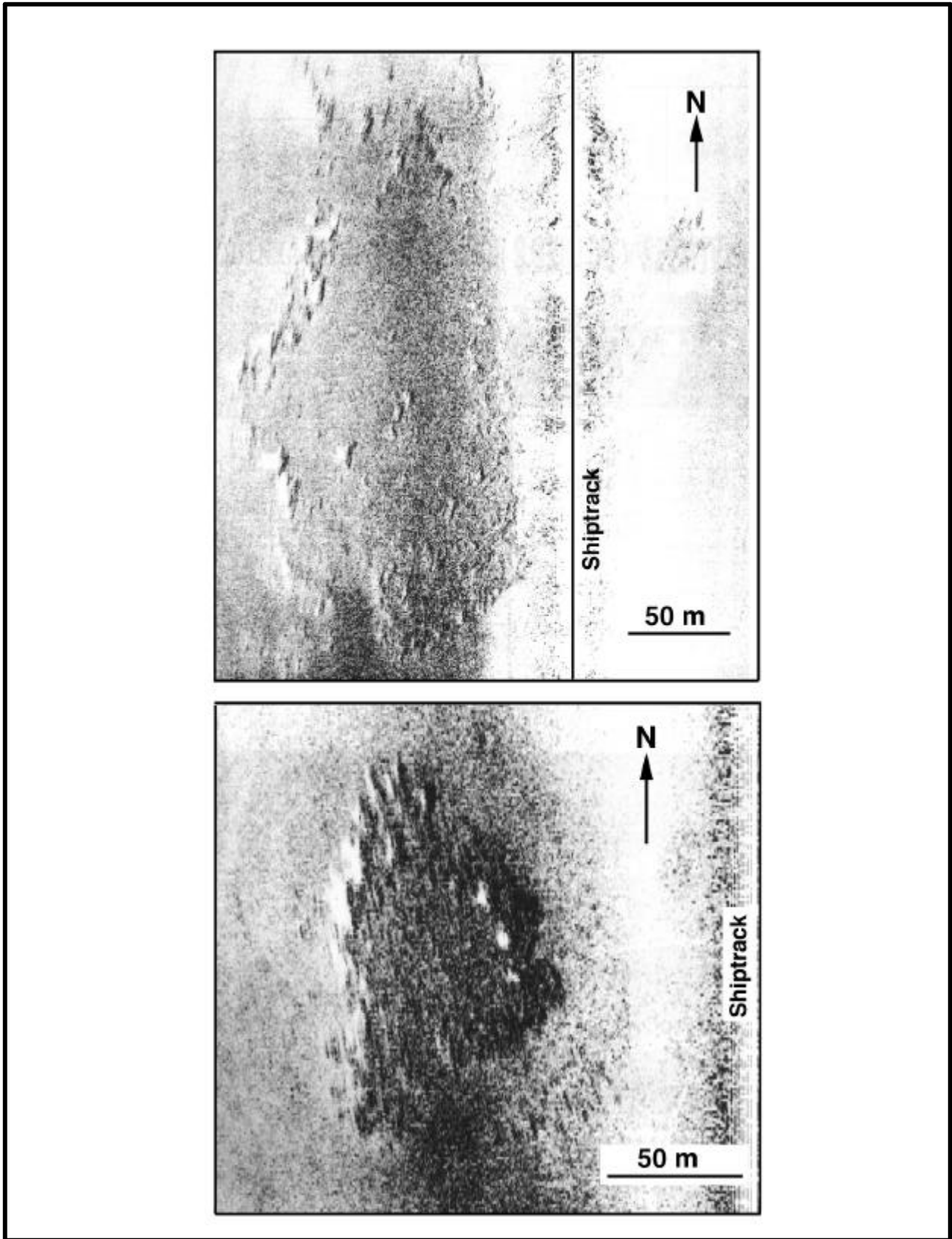


Fig. 3.47. Side-scan sonar images showing complex, irregular mounds from Megasite 2. Conventions as in Fig. 3.46.

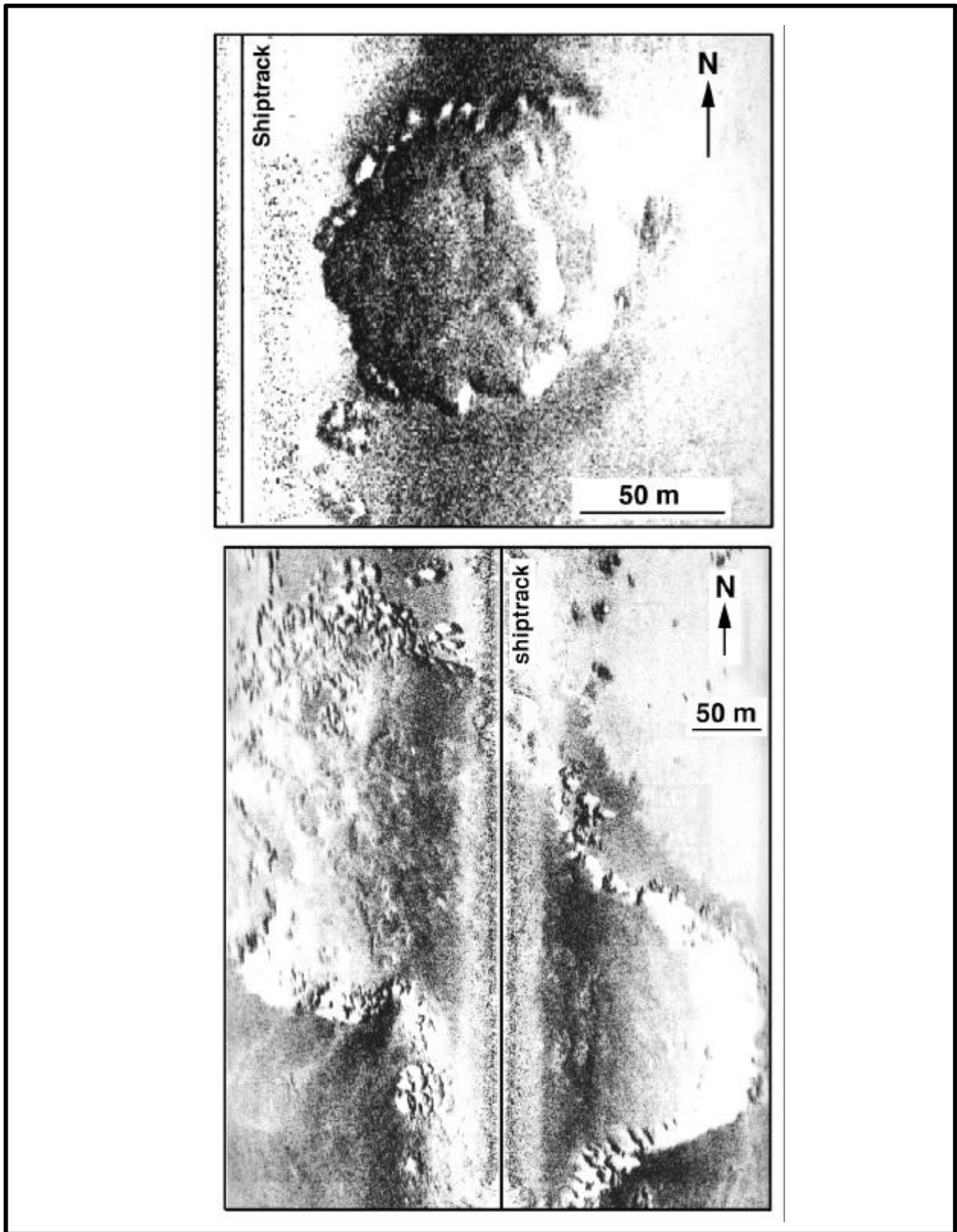


Fig. 3.48. Side-scan sonar images showing smooth-top mounds. (Top) Example from Megasite 3. Note the smooth top shows two levels. (Bottom) Large, flat-topped mound from Megasite 1. Monitoring Site 1 is located on the northeast edge of the top. Conventions as in Fig. 3.46.

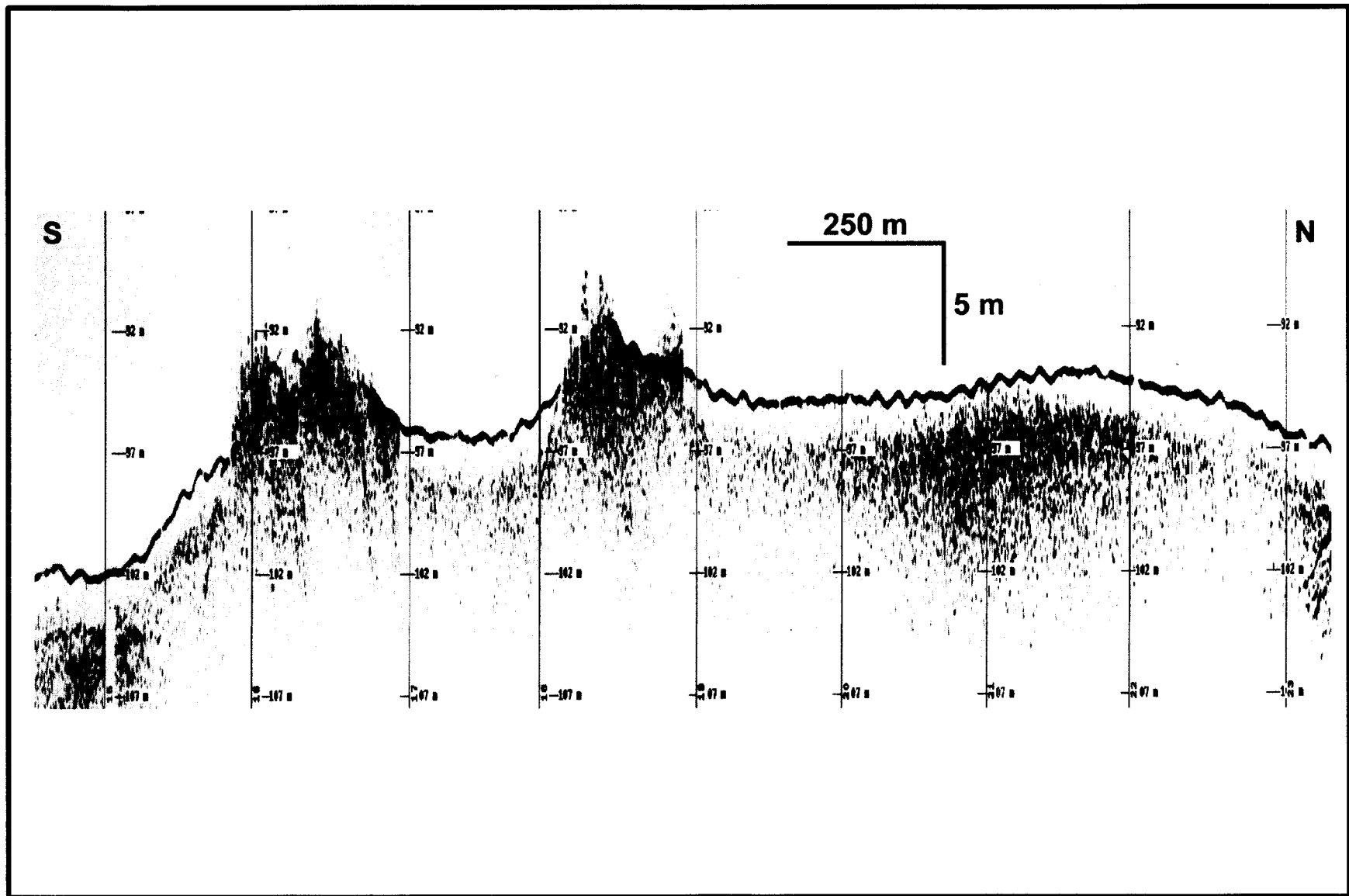


Fig. 3.49. Chirp sonar profile over broad, carbonate hard bottom type mound in Megasite 2. Mound is 1.8 km across and mostly about 5 m in height, however, two "pinnacle" mounds extend upward from its summit by an additional 5-9 m. Note that the northern end sits higher than the southern end and the bathymetric drop is greater on the south side.

Megasite 1 contains the greatest number of mounds (>1,000). They are dominantly subcircular in shape and the smaller mounds (<10 m) tend to be the most nearly circular. Within Megasite 1, 53% of the mounds have an aspect ratio near 1:1 and 43% have an aspect ratio near 2:1 (**Fig. 3.44**). The number of mounds with higher aspect ratios falls off dramatically and only 0.05% fall into the 3:1 category or greater.

The majority of small mounds in our surveys are found in Megasite 1, especially in the western half. These mounds have both smooth and jagged outlines, with sizes ranging from 2-15 m across. Most are isolated, but some form small clusters. In the southwest corner of the site there is a large raised hard bottom that is marked by an area of very high backscatter and is covered with small mounds. Toward the north and east, medium to large mounds become the dominant features (**Fig. 3.3**). The larger mounds are typically smooth-topped and have irregular outlines; although, some seem to be lower composite mounds. Additionally, in the northeast part of Megasite 1 there are two low hard bottoms that have highly irregular outlines. The first (or more northern) one is the foundation for large mounds that are >50 m across. The second (or more eastern one) is a raised hard bottom characterized by an area of high sonar backscatter and that appears to contain many small mounds.

Unlike other megasites, in which mounds of different sizes cluster in different places, there appears to be little sorting of mounds in Megasite 2, because all sizes of mounds are scattered fairly evenly across the site (**Fig. 3.7**). This site contains the greatest range of shapes with aspect ratios varying from 1:1 up to 8:1, whereas the other sites only range from 1:1 up to 4:1. The majority of the mounds, however, still fall in the 1:1 and 2:1 categories (34% and 38%, respectively), but unlike other sites, the 2:1 category mounds are more numerous. Mounds at this site are typically elongated and trend in the north-south direction. More so than any other site, many of the mounds in Megasite 2 appear to be composites of smaller ones. Even where true composites are not seen, there are often close clusters of small mounds, which may be antecedents of composite mounds. This gives the edges of many mounds a jagged appearance and causes their surface to appear rough. Another interesting feature of these small mounds is that most appear to be roughly the same size, a few tens of meters across.

Megasite 3 is similar to Megasite 1, in that 51% of the mounds have aspect ratios near 1:1 and 41% are near 2:1 (**Figs. 3.44**). The majority of the mounds lie in the western half of the site and most fall in a northwest-southeast trending linear array that is composed of small, individual mounds and what appear to be composites of small mounds that have grown together. About a dozen flat-top mounds, measuring ~ 60 m across, occur in the eastern part of the megasite (**Fig. 3.10**). As well as the smaller mounds, two broad, low-relief hard bottoms are present and are characterized by regions of moderate to high backscatter (**Fig. 3.10**). Both seem to contain many smaller mounds; however, we cannot discern whether the hard bottoms are composites of small mounds or the foundations for a later generation of small mounds.

A notable feature in Megasite 5 is the curvilinear, nearly isobath-parallel group of hundreds of large to small mounds that contains the majority of the mounds at this site

(Fig. 3.14). At the northwest edge of the group there is a large, rough, linear mound that is approximately 1 km in length, 150 to 300 m wide, and 18-24 m tall. It is by far the largest and tallest mound in the entire study area. In general, the mounds at this site have the following aspect ratio distribution: 59% near 1:1, 32% near 2:1 and 9% at 3:1 or 4:1 (Fig. 3.44). Once again, the dominant shape is subcircular. The large mound, mentioned above, has the characteristics of a composite mound, which is evidenced by its jagged edges that seem to be made up of small mounds. On the subbottom records, the top surface of the large mound has flat areas at its highest extent, but rough areas of peaks and valleys in between these plateaus. Surrounding this large mound are other small to medium-size composite mounds as well as a number of singular small mounds that, as with those in Site 1, have a very circular appearance. To the south and east, other composite mounds of various sizes can be identified; however, the number of mounds falls off rapidly toward the eastern edge of the site.

Subbottom Profiles

Subbottom profiler records acquired with the X-STAR 2-12 kHz chirp sonar show the seafloor and internal acoustic interfaces within the uppermost sub-seafloor sediments. These records were acquired for two purposes: (1) to provide auxiliary data for the interpretation of side-scan sonar records, and (2) to examine the distribution of recent sediments.

In general, most profiles show a thin, relatively transparent layer a few meters thick overlying a deeper horizon (Fig. 3.50). In places, this upper drape layer appears to contain more than one unit. The deeper horizon often appears as an angular unconformity where underlying delta foreset beds are truncated. In most of the survey areas, this horizon may represent erosion that occurred during the last glacial lowstand (Kindinger 1989; Sager et al. 1999). However, in Megasite 1, which sits atop the "eastern delta" of the MAMES study, this horizon may be younger (Sager et al. 1999). Thus, the age of the unconformity at a particular site cannot be determined without additional age information.

One goal of the study was to create isopach maps of sediments overlying the erosional unconformity at all sites to better understand the long-term influence of the mounds on sediment distribution. However, there were two impediments to attaining this goal. First, most records show the upper transparent layer as a relatively uniform layer, i.e., isopach maps show little of interest. Second, it is difficult to discern this horizon or it is difficult to determine reflector continuity in many places. In some spots, it is evident that the sediments overlying the erosional unconformity constitute more than one layer, of which the upper transparent layer is only the latest. Much of the problem is that acoustic penetration was inadequate to consistently define sediment layer thickness. In part, this may result from unusually impervious seafloor because the X-STAR records show penetration of 15 m or more in Megasite 4, but not in the other areas.

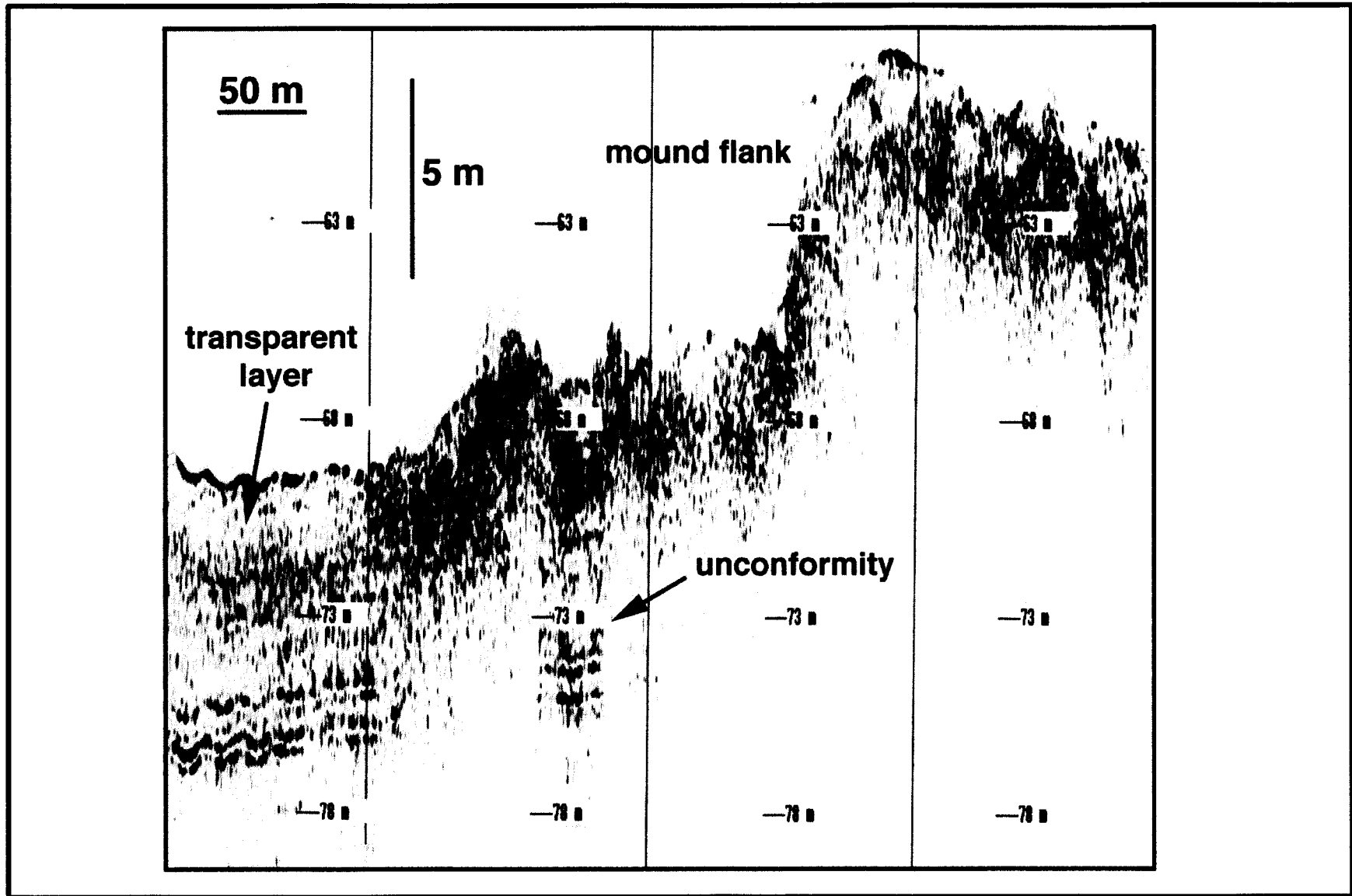


Fig. 3.50. Chirp sonar subbottom profile from Megasite 1 showing rough mound flank and typical sediment layering in the shallow subbottom.

Megasite 1

In Megasite 1, the bottom of the transparent layer was relatively easy to follow. The upper transparent layer is relatively uniform at 1.0 to 2.5 msec (0.8 to 1.9 m; assuming 1,500 m/sec sound velocity) in thickness, but reaches 5.0 msec (4.0 m) at one location. At this megasite there is a notable correlation between areas where this uppermost layer has been eroded and dark (high-backscatter) areas in the side-scan sonar mosaic (Fig. 3.5). The high-backscatter areas are preferentially located on the southwest sides of the mounds, so most profiles over larger mounds show an erosional hole on the southwest side. Near the largest mounds, erosion occurs over a broad area several hundred meters across to a depth of 1 to 2 m. Behind one mound at the eastern edge of the megasite, the erosional hole has reached the underlying unconformity, but in most places some of the transparent layer remains. On several profiles, linear high-backscatter "tails" trailing southwest from small to medium mounds have been matched with gullies, typically 20 to 200 m wide and 1 to 2 m in depth. The cause of the relationship between erosion and high backscatter is not yet clear. It probably represents a current winnowing effect that coarsens the average sediment texture at the seafloor in those areas.

Subbottom profiles from Megasite 1 also show interesting aspects of mound morphology. Many mounds appear asymmetric in profile with the steepest slopes on the seaward sides. The data show that this is caused by sediment dammed on the landward sides of the topographic features. Furthermore, on some lines there appears to be a 6 to 8 m depth offset across the mounds, becoming deeper seaward. Across the large flat-top mound where Site 1 is located, for example, the erosional horizon beneath the transparent layer is at about 70 m depth on the north side of the mound and 76 m on the south side. This observation suggests that some of the mounds may sit atop a scarp.

Within Megasite 1 are three small, linear to sub-linear ridges, located in the northern part of the survey area. In the subbottom records, these ridges are asymmetric, with sediment dammed on their north sides and a slight erosional hole on their south sides. Typically the depth offset across these ridges is 1.5 to 2.0 m. The origin of these features is unclear, although previous speculation was that similar ridges are ancient shoreline features (Sager et al. 1992).

Megasite 2

In Megasite 2, the underlying erosional unconformity is not visible in many places. Above this horizon, two more-or-less homogeneous layers are visible, the upper one acoustically transparent and the lower acoustically turbid. This configuration is most obvious to the north of the mounds, and is often not seen to the south. These layers are typically about 1 to 2 m in thickness, occasionally 5 to 10 m. The surficial sediments lie atop mound flanks in most places. In particular, the linear, high-backscatter area in the northeast part of the megasite is a buried ridge with small mounds on the tops of the larger mounds showing through. In many places the upper sediment layers are upturned on the mound flanks and pinch out, leaving the mound top exposed. These sediments typically bury the north sides of low, flat carbonate hard bottoms but leave the south sides exposed.

Megasite 2 profiles show no obvious correlation between high-backscatter areas and erosion, in contrast to Megasite 1. This fits the observation from the mosaic that the high-backscatter areas have no preferred direction. Because these areas fringe the mounds, it is likely that the high backscatter is caused by textural differences owing to material shed from the mounds.

Megasite 3

In Megasite 3, the surficial sediments also appear as a thin transparent layer, typically 1 to 2 m thick. Like those of Megasite 2, the two low, flat carbonate hard bottoms are buried on their north sides and show a 1.5 to 2.0 m scarp on their south sides. The tops appear even with surrounding sediments and there are small, thin, transparent areas that suggest sediment ponds.

The linear mounds in the western part of Megasite 3 show an asymmetric profile with low slopes on their north sides and steep slopes on the south sides. In part this is a result of sediments ponded on the north sides. However, the mounds themselves appear asymmetric and often have a low hump on the north sides and a pinnacle on the south side. Many profiles show a small erosional hole at the base of the south side, with a total height of about 10 m from bottom to pinnacle top.

The profiles show that at least one of the mounds in the eastern part of Megasite 3 has an asymmetric shape, but others have flat tops. In this region the dark high-backscatter areas to the southwest of the larger mounds can be seen as an erosional feature on subbottom profiles, as at Megasite 1.

Megasite 4

Like its sonar image data, the subbottom data from Megasite 4 are unique. In this area, seaward-dipping delta foreset beds are regularly seen beneath a thin transparent layer, 1 to 2 m in thickness. Penetration here is greater than at any other megasite and it is possible to see delta beds 10 to 15 m below the seafloor.

The curvilinear high-backscatter feature in the southern part of the Megasite 4 mosaic corresponds to a zone of steeper slopes in the subbottom profiles. This is consistent with the bathymetry, which shows closer contours at this location. Interestingly, this zone is at different depths on different profiles. It is deepest on the east side of the megasite and shallows approximately 17 m to the west. This is also consistent with the bathymetry data.

In Megasite 4, it was not possible to match high-backscatter areas with mounds or other features of the subbottom profiles, such as erosional areas, because the seafloor in the subbottom profiles usually appears uniform and few mounds are evident. Apparently most of the backscatter features in the side-scan sonar mosaic arise from textural variations at the seafloor.

Megasite 5

As at other sites, the upper transparent layer in Megasite 5 is nearly uniform and 1 to 2 m thick. In some places this layer is seen atop erosionally-truncated delta foreset beds. According to Sydow and Roberts (1994), these beds are part of the Lagniappe Delta. In the subbottom profiler records, this erosional surface is often irregular, a characteristic noted for the Lagniappe Delta top by Sydow and Roberts (1994).

The shelf edge in Megasite 5 has two unusual features. First, the dark band seen in the side-scan sonar mosaic corresponds to a reflection-free zone in the subbottom records. The seaward edge of this zone often appears as dipping reflectors and the landward edge sometimes matches with erosional “notches” in the seafloor. These observations imply this dark band is an exposed delta-front layer. As the dark band widens to the west, the shelf edge develops a large, flat mound of transparent sediments. The origin of this mound is unclear. The other unusual features are asymmetric troughs near the shelf edge with steep landward and shallow seaward walls. Usually just one is seen on a given line, although occasionally two occur. The depth and widths are several meters by 100 to 200 m. The asymmetric shapes suggest this might be a fault caused by an incipient delta-front slump. Sometimes mounds appear associated with the top of the landward wall of this trough.

Like the dark high-backscatter “tails” trending southwest from mounds in other megasites, those in Megasite 5 also appear to be erosional gullies. Similarly, high-backscatter areas are preferentially located to the southwest of many of the larger mounds, and the subbottom profiles often show slight erosion, especially on the southwest side of the curvilinear mound trend.

Grain Size Data

Grain size data show that sediments recovered in grab samples are typically sands with some gravel and clay. The median mean grain size for the 229 samples taken on Cruises 1C and M1-M3 is 2.8ϕ (**Fig. 3.51**), with most samples having mean grain sizes between 1.75ϕ and 4ϕ . Many samples show a bi- or trimodal distribution. Often the size distribution is peaked around 1ϕ to 3ϕ (fine sand) with a significant fraction in the smallest size class, $>10\phi$ (fine clay). Few samples contain a significant silt fraction. Many samples also have a large contribution in the largest size class, $<-1.5\phi$ (gravel). These particles are typically shells, shell fragments, and other biologic detritus.

Ternary plots echo these characteristics (**Fig. 3.52**). On a sand-silt-clay plot, samples show a nearly linear scatter from sand to clay. Only those samples with moderate amounts of clay have significant fractions in the silt size range, and even then the largest contribution is less than 20% (**Fig. 3.52**). The nearly linear trend implies two sediment sources, one sand and the other clay, that are intermixed. On a gravel-sand-mud ternary plot (**Fig. 3.52**), samples still tend to cluster near the sand apex, but considerably more scatter is apparent owing to variable gravel fractions up to about 50%. The variability of

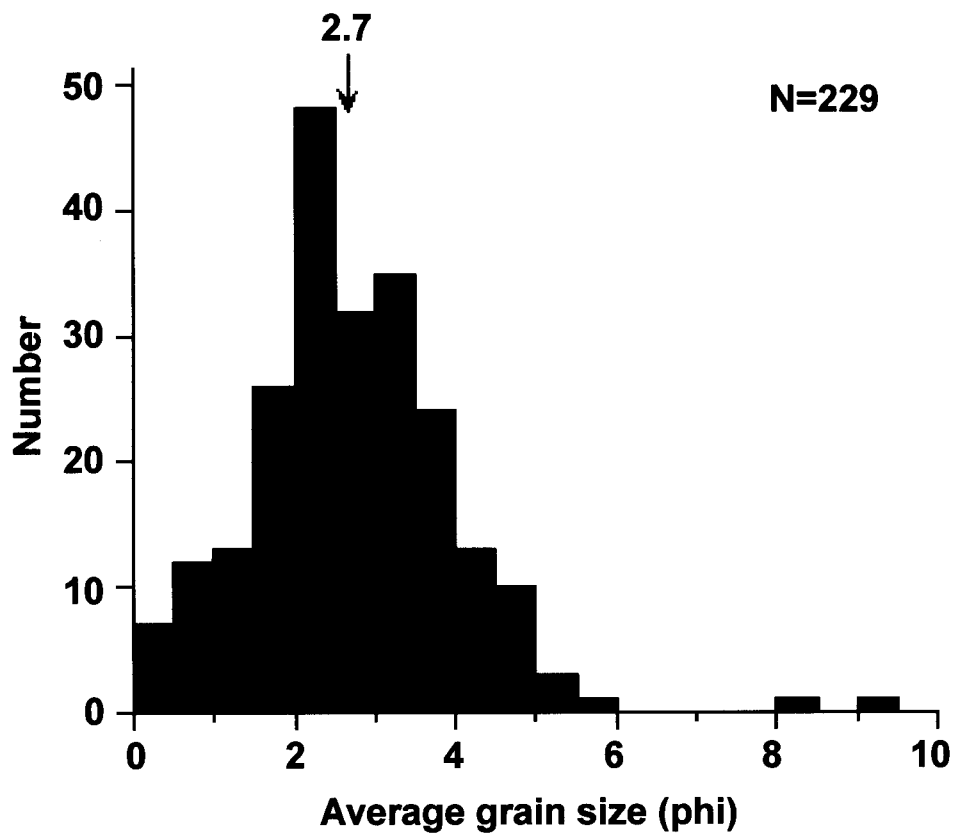


Fig. 3.51. Histogram of mean grain sizes for the 229 grab samples from all cruises. Average grain size for all samples is 2.7ϕ .

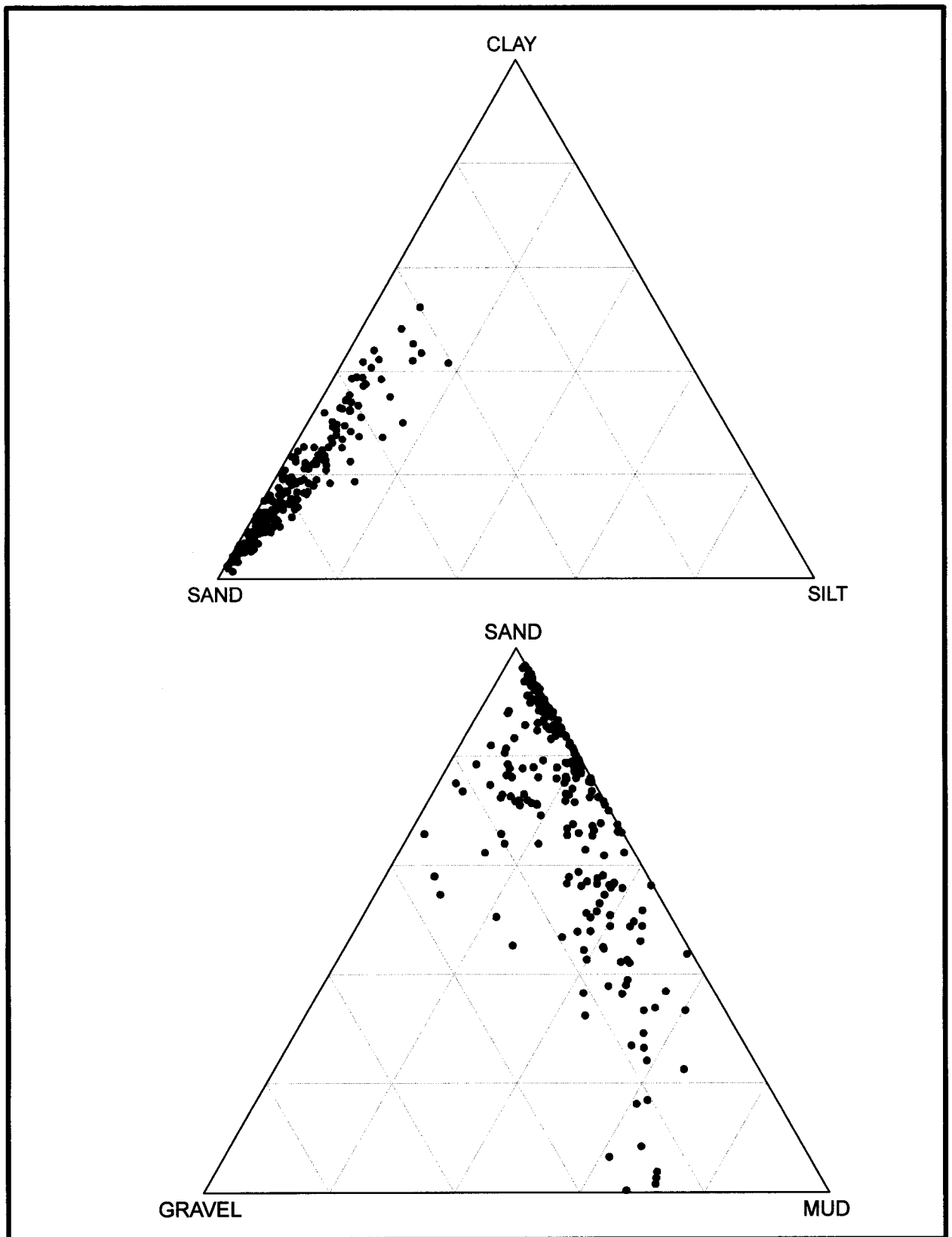


Fig. 3.52. Ternary diagrams showing size classifications of 229 grab samples from all cruises. (Top) Sand-silt-clay ternary diagram. Samples were normalized to 100% after subtracting the gravel fraction. (Bottom) Gravel-mud-sand ternary diagram (Note: mud is combined silt and clay fraction).

the gravel fractions and their biogenic compositions implies they are controlled by local factors.

Owing to high lateral variability in sediment character and uncertainty in the precise location of many grab stations in relation to the side-scan mosaics, it is difficult to tell what type of seafloor backscatter characteristic corresponds to a particular grab. In general, samples from higher-backscatter seafloor tend to be enriched in both gravel and clay. This is seen particularly well comparing grabs from around Site 7 (**Fig. 3.53**). Samples from east of the mound, where the seafloor backscatter is low, are typically 70%-80% sand, with negligible amounts of gravel. In contrast, grabs from west of the mound, where seafloor backscatter is high, contain only 40%-60% sand and the gravel content has increased to 10%-30%. This observation is consistent with the “rule of thumb” that coarser sediments give higher backscatter. Other observations reinforce this connection between backscatter and the presence of debris. ROV observations of the seafloor at Sites 5, 7, and 9 found areas of high backscatter associated with zones of otherwise flat seafloor mantled with carbonate debris (**Figs. 3.31, 3.37, and 3.43**). In some instances, the highest gravel-content samples tend to be located near mound edges, implying the mound as a source. For example, Grab 7 in Site 7 is the sample with the highest gravel content and is located closest to the mound on the western side. At other sites, this connection is not always as clear. Lateral variability among samples at a given site is as high as variability between sites, so the processes that control sediment sorting are probably complex.

Discussion

From prior MMS-funded surveys in the Mississippi-Alabama outer shelf region, we knew that carbonate mounds were often clustered with sizes ranging from several meters on a side to hundreds of meters wide and 10 to 18 m high (Brooks 1991; Continental Shelf Associates, Inc. 1992; Sager et al. 1992). We also knew that areas of high acoustic backscatter were associated with many mounds (Brooks 1991; Laswell et al. 1992) and that in some cases these areas were preferentially located to the southwest of the mounds. This new study has emphasized and broadened these findings. In addition, we are beginning to get a better understanding of the relationship of sonar backscatter to the mounds and the sediment characteristics.

Although we knew previously that many of the carbonate mounds are subcircular in plan view, our new side-scan sonar data show the details of mound flanks and co-occurrences with far greater resolution than previously. In prior studies, we found a difference between mounds at the shelf edge, in water depths of about 105 to 120 m and those shallower. The former seemed to have sharper peaks (they were the original Ludwick and Walton [1957] “pinnacles”) and the latter sometimes had flat tops (Sager et al. 1992). Our new data show that flat or nearly flat tops are not uncommon among large mounds located in the 70 to 90 m depth band. These data also have extended the range westward by mapping several such mounds in Megasite 5 (**Fig. 3.54**). The side-scan sonar data also show that the shelf-edge “pinnacle” mounds are unlike the shallower mounds in that

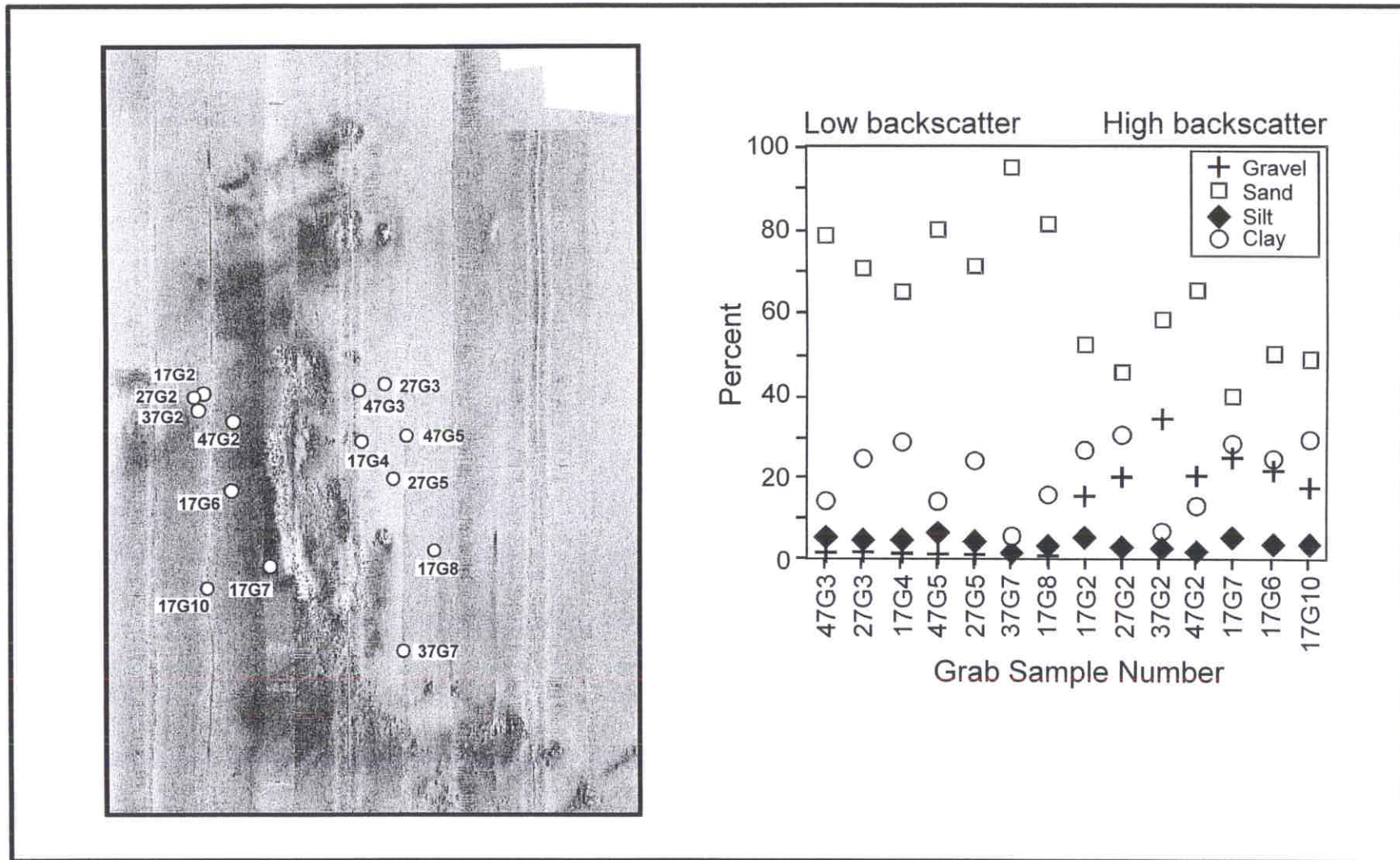


Fig. 3.53. Comparison of grain size data with side-scan sonar backscatter near Site 7. Image at left shows side-scan sonar mosaic around large mound in northwest Megasite 5. Site 7 is located at its north end. Circles show grab sample locations. Plot at right shows grain size distributions (percent gravel, sand, silt and clay) from samples from plot at left. Samples are arranged with those from low-backscatter seafloor at left and those from high-backscatter seafloor at right. The most obvious difference is a greater percentage of gravel at the expense of sand in those samples from high-backscatter seafloor.

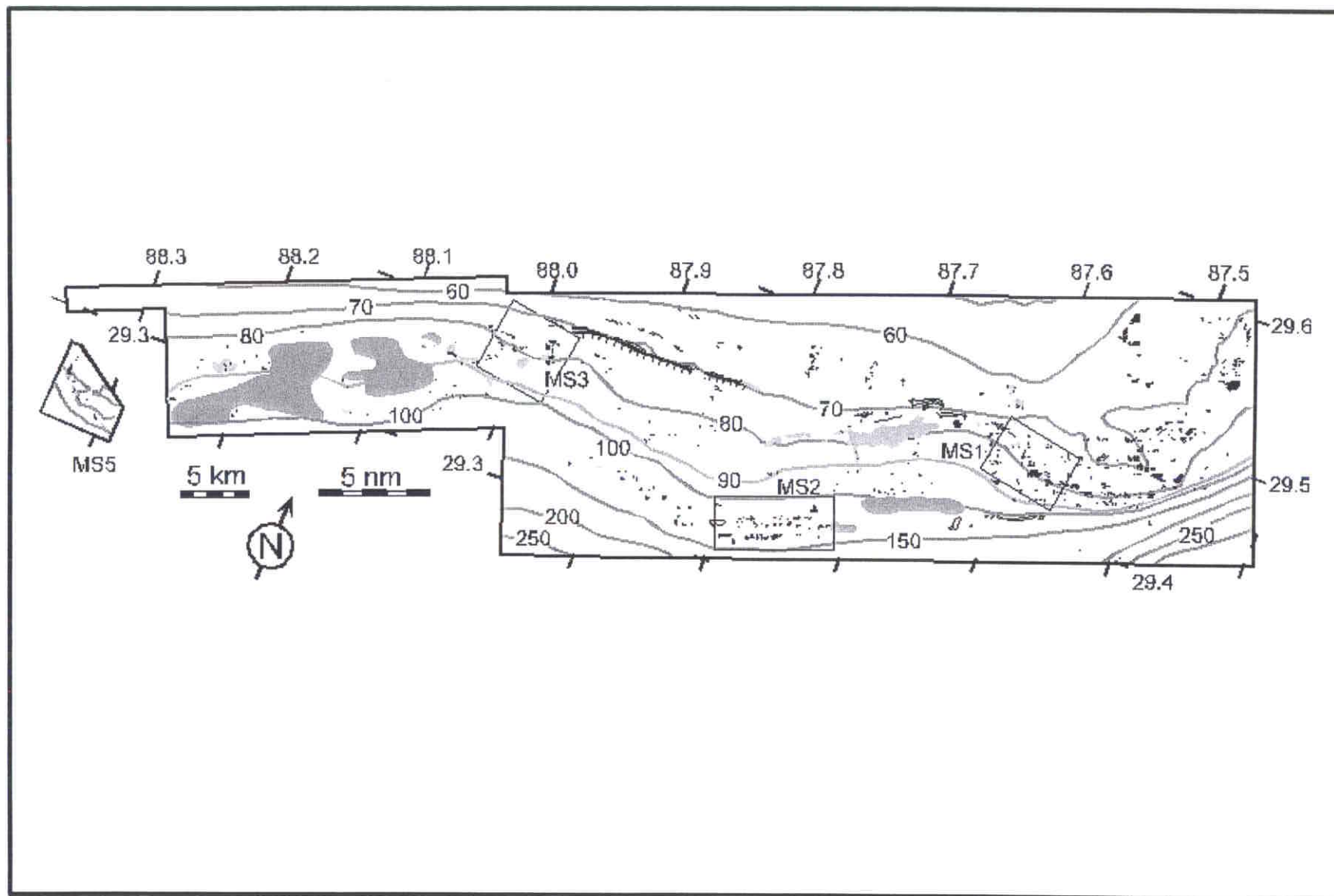


Fig. 3.54. Mound distribution on the Mississippi-Alabama outer continental shelf and megasite locations. Black objects represent mounds. Dark, heavy lines denote submerged ridges. Dark gray areas show regions of seafloor pockmarks. Light gray denotes areas zones with thousands of small mounds. Bathymetric contours shown in gray at 10-m intervals to 100 m depth and at 50-m intervals deeper. Boxes labeled "MS" show megasite boundaries. (Modified from Sager et al., 1992).

the pinnacle mounds are often irregular or linear in plan view, whereas the shallower mounds are usually subcircular in plan view and often made up of clusters of smaller subcircular “unit mounds.” What is more, the new data imply a third class of mounds: low, wide, carbonate hard bottoms hundreds of meters in diameter but only a few meters in height. These features are particularly notable near the shelf edge in Megasite 2, but are also seen in at shallower depths in Megasites 1 and 3. These mounds often have tops with bumps a few meters or less in height that make them appear to be made up of many smaller “mini-mounds” and in this sense they are similar to many of the other, shallower subcircular mounds.

The morphologic differences among mounds suggest differences in development. The low, wide carbonate hard bottoms imply slow upward growth over a large area, perhaps indicating stable sea level or slow sea-level rise. We previously speculated that such mounds grew at the shelf edge during the slow sea level rise after the last ice age (Sager et al. 1992), but now we know them to be even more widespread (**Fig. 3.54**). Perhaps they are indicators of periods of nearly constant sea level, during which the broad carbonate banks can grow and spread. The tall, steep-sided “pinnacle” mounds suggest rapid upward growth during faster sea level rise (Sager et al. 1992). Because many of these mounds apparently sit atop the low, wide hard bottoms, this possibly indicates a switch in mound growth from lateral to vertical aggradation owing to acceleration in sea level rise. The widely-dispersed, shallower mounds, which are highly-variable in size and height, may represent a short period of sea level stabilization in the middle of the deglaciation (Sager et al. 1992).

Our new data also give some insights about the location of carbonate mound formation. Prior data implied the mounds formed atop erosional unconformities on the two deltas in the MAMES survey area (Sager et al. 1992). The new data have strengthened this observation. Although layers cannot be traced beneath the mounds, owing to the scattering of acoustic energy they cause, in many places delta foreset beds beneath appear continuous when traced from one side to the other of a mound or mound cluster. This would probably not occur if the mound had formed prior to the deposition of the delta beds; instead, the beds would be distorted. Our new data also imply that in some places, larger mound groups formed on bathymetric scarps, as shown by depth offsets, or atop carbonate hard bottoms. These observations imply that the mounds formed where suitable substrates were available. This is consistent, for example, with organisms requiring hard substrates for attachment.

Subbottom profiles over the mounds frequently show asymmetric profiles, another clue about mound formation. Often large mounds have a peak at the seaward edge and have sediments dammed up on their landward sides. These characteristics suggest that mound growth was most intense on the side facing the sea, where perhaps nutrients are highest and sediments least. This is similar to the formation of coral reefs in shallow water and lends credence to the hypothesis that the mounds were formed by biologic action in shallow water. The damming of sediments indicates that the mounds existed when the surficial sediment layer was deposited. Since it is generally accepted that this layer was formed from reworked sediments when sea level was much lower, this implies that the

mounds existed when sea level was lower; in other words, they formed nearer to sea level.

Results from our sediment studies give some significant insights about sediment distribution and sedimentary processes. The upper acoustically-transparent layer, which apparently represents relict sands deposited by reworking during lower sea level, is more uniform than expected. At Megasite 2, nearest the shelf edge, this layer sometimes sits atop another layer that displays greater acoustic reverberation and changes in thickness. This layer is often absent, but attains thicknesses of more than 5 m at the edges and in between the large mounds at the shelf edge. These sediments probably formed at an earlier time and their source may be the mounds, as suggested by proximity. These observations imply that the deposition of the more recent layer was not highly variable around the mounds. Because normal bottom currents are relatively slow and the benthic nepheloid layer does not carry a large suspended sediment load (see Chapters 5 and 6), we think that the sediment layers evident on the chirp sonar subbottom profiles were deposited before sea level reached its current height and are presently mostly static.

While normal sedimentation is not very active, several lines of evidence imply there are high-current events that cause significant reworking of the sediments. Sediment grain size data imply the surficial sediments are composed of three end-members. Most sediments are mainly sand, with a smaller variable amount of clay added. The linear nature of the size data on the sand-silt-clay ternary diagram implies two end-members, sand and clay, that are intermixed. Since the sediments currently being deposited in the region are fine clays, this could occur owing to resuspension events that mix the clay with the sand near the surface. The third component consists of gravel-size fragments, usually shells, shell fragments, or other biogenic debris. The gravel content is usually highest near mounds, indicating the mounds as a potential source or suggesting the mound proximity is an important factor for controlling the presence of organisms. Because we find no simple correlation between mound proximity and gravel content (many near-mound stations show no enhancement in gravel-size fragments), the gravel may be shed from the mounds and there are some indications that bottom currents help determine where gravel is deposited.

Scour marks seen in the side-scan sonar mosaics and the chirp sonar profiles imply sediment redeposition during storms. The scour marks are linear troughs, usually pointing southwest and beginning at a small to medium-size mound. They show up as high-backscatter “tails” emanating from the mounds in Megasites 1, 3, and 5 (see **Fig. 3.5**). For many large mounds, the scour is displayed as an asymmetric high-backscatter “halo” on the southwest side of the mound. Frequently, the high-backscatter area corresponds to an erosional swale behind the mound, sometimes cutting completely through the sand layer into the late Pleistocene unconformity. Grab samples and ROV video observations indicate that these areas have a greater concentration of gravel and larger-size debris, which is doubtlessly the cause of the higher than normal backscatter. Clearly these scour marks are caused by currents perturbed by the topography of the mounds.

Although bottom currents in the study areas are not highly directional under normal circumstances, the situation appears to change during large storms (see Chapter 6). Two hurricanes passed through the study area in September 1998 (Earl and Georges) and both created strong currents, with speeds >1 m/sec, that flowed southwest in approximately the same direction as the linear scour marks. What is more, sediment trap data indicate that the storm currents cause resuspension fluxes 10-50 times higher than normal (see Chapter 5). These large storm events created currents in the right direction to cause the scour marks and had the power to move the sediments. When a current impinges upon a submerged obstacle, it causes eddies that can be detached from the obstacle and move downstream if the current velocity is sufficient (e.g., Roden 1991). We believe such eddies are responsible for the current scour. In addition, the strong currents may explain the observation that sediments are piled up against the north sides of many mounds even though there is no obvious movement of large quantities of sediment seaward. Strong southwesterly currents that cause widespread resuspension and sediment movement in the same direction may be the cause of the sediment damming. Such resuspension events may also explain the mixture of sand and clay observed in the grab samples.

In summary, the Mississippi-Alabama OCS mounds present a relatively unchanging environment under most circumstances. The mounds appear to have formed more than 10,000 years ago before sea level rose to its present height. Although there appears to be some ongoing bioerosion on the mounds, it does not seem to be pervasive or rapid. Most sediments around the mounds also were deposited in the geologic past. The surface sediments appear to be a relict sand, reworked during the last rise in sea level, mixed with clay from the present-day nepheloid layer and biogenic debris from benthic organisms and the mounds. On occasion, this environment seems to be perturbed by storms that cause rapid bottom currents and resuspension. At these times there is erosion at the sea bottom and reworking, mixing, and redeposition of the surficial sediments.

Chapter 4: Geochemistry

Mahlon C. Kennicutt II

Introduction

The geochemistry component includes a combination of hydrocarbon, metal, grain size, total organic carbon (TOC), and total inorganic carbon (TIC) measurements in sediments and sediment trap materials. Contaminant measurements are intended to document the current hydrocarbon and metal concentrations within the study sites. Sediment characteristics (grain size, TOC, TIC) aid in determining the origins of sediment and discerning the relationship between sediment texture and biological patterns at the study sites. Metals, TOC, TIC, mass, and grain size are also measured in sediment trap materials to determine the origins of sediments at the sites and to document whether contaminants are accumulating at the sites during the duration of the study (see Chapter 5).

The two most common contaminants derived from platforms are hydrocarbons and metals (Middleditch 1981; Boesch and Rabalais 1987; Boothe and Presley 1987; Continental Shelf Associates, Inc. 1983, 1989). The release of petroleum from a platform to the surrounding environment can occur during drilling and production. Petroleum hydrocarbons are potentially present in a variety of discharges including drilling fluids, cuttings, produced water, spills, deck drainage, and other releases (Kendall 1990). Petroleum hydrocarbons released to the environment can be differentiated from naturally occurring, background biogenic hydrocarbons (Brassell et al. 1978; Philp 1985; Boehm and Requejo 1986; Kennicutt and Comet 1992). Petroleum contains (1) a homologous series of n-alkanes with 1 to more than 30 carbons with odd and even carbon number n-alkanes present in nearly equal amounts; (2) a complex mixture of branched and cycloalkanes; and (3) a suite of polycyclic aromatic hydrocarbons (PAHs). Aliphatic hydrocarbons synthesized by organisms (both planktonic and terrestrial) include a suite of normal alkanes with odd numbers of carbons from 15 to 33. Complex branched and cycloalkanes are rare in organisms. Petroleum PAH mixtures are differentiated from PAHs synthesized by organisms by the structural complexity of the mixture and the presence of substantial amounts of alkyl substituted PAHs. PAHs are the most toxic components of oil and concentrations can indicate potential biological effects. Based on considerations of petroleum chemistry, biological occurrences, and toxicological effects, aliphatic and aromatic hydrocarbons were chosen as tracers of petroleum contamination for this study (Kennicutt 1995).

Metals are also released during offshore drilling and production activities (Lake Buena Vista Symposium 1981; Boesch and Rabalais 1987; Boothe and Presley 1987). Metal contamination can affect both infauna and epifauna in the vicinity of platforms (Southwest Research Institute 1978). Many metals are EPA priority pollutants (antimony [Sb], arsenic [As], cadmium [Cd], chromium [Cr], copper [Cu], lead [Pb], mercury [Hg], nickel [Ni], selenium [Se], silver [Ag], and zinc [Zn]) and are known to be toxic to organisms. These metals are often constituents of drill muds (Houghton et al. 1981; Rubinstein et al. 1981; Tornberg et al. 1981). Tin (Sn) is known to be toxic and is

present in antifouling paints used on platform structures. Barium (Ba) is used as a tracer of the particulate fraction of discharged drilling fluids and cuttings because it occurs in high concentrations in drilling muds and has a low, natural background in ambient sediments (200 to 500 ppm dry weight; Chow and Snyder 1981; Boothe and James 1985; Boothe and Presley 1987). Barium (as barite, barium sulfate) is the dominant component of drill mud (up to 90% on a dry weight basis). Aluminum and iron are major constituents of alumino-silicate minerals and are used to detect changes in sediment type. Vanadium (V) is of interest because it can occur in significant concentrations in some crude oils.

Methods

The geochemistry portion of this study relied on prior study information and a hierarchical approach to select the analysis to be used. For hydrocarbons, a simple measure of the presence or absence of oil was used. Total petroleum hydrocarbons (TPH) determined by gas chromatography/flame ionization detection (GC/FID) and a gravimetric measurement of extractable organic matter (EOM) accurately reflect oil contamination (Kennicutt et al. 1996). The origin of hydrocarbons within a site was determined on a single composite of all samples collected at a site. Fingerprinting using PAH compositions was the method of choice to define the origins of any PAH detected at the study sites. Metals (Ba, Cd, Cr, Pb, Hg, and Zn), most closely related to platform discharges, were measured as well. As an indicator of sediment mineralogy, aluminum (Al) and iron (Fe) were also measured. Crustal elements (Fe, Al) were used to normalize the concentration of metals to detect anthropogenic additions.

Collection

Sediments were collected by grab as described in Chapter 3, Geologic Characterization. The top 5 cm of sediment were sampled. Samples for geochemistry were collected concomitantly with geological samples. The collection of sediment trap materials is described in Chapter 5.

Total Inorganic and Organic Carbon

Sediment carbonate content (0.2 to 0.5 g) was determined by treatment with concentrated HCl. Residual organic carbon was converted to CO₂ and analyzed with a non-dispersive infrared spectrophotometer (Leco WR-12 Total Carbon System). Calcium carbonate was determined as the difference between a treated (acidified) and untreated sample. Acidification was carried out in the crucible used for analysis and the residual acid was evaporated in place to avoid the loss of acid soluble organic matter.

Hydrocarbon Analyses

TPHs were determined by GC/FID analysis of sediment extracts. EOM was determined by weighing the extracts.

PAHs were determined by the National Oceanic and Atmospheric Administration (NOAA) National Status and Trends methods (Wade et al. 1988). Briefly, deuterated PAHs were added before the extraction and were used to calculate analyte concentrations. Sediment samples were mixed with anhydrous sodium sulfate and extracted with methylene chloride/acetone in an Automated Solvent Extractor (ASE). The petroleum hydrocarbons were separated from interfering compounds by silica/alumina columns. The purified extracts were analyzed on an HP 5890/5970 gas chromatograph with a mass selective detector (GC/MS) using a selected ion detection technique. The GC/MS was calibrated with known concentrations of analytes at five different concentration levels and average response factors were used for determination of PAH concentrations. Concentrations of parent and alkylated PAHs were reported as nanogram/gram (ng/g) on a dry weight basis for sediment samples. Each sample batch of 20 samples included a procedural blank, a matrix spike, a matrix spike duplicate, and a standard reference material. Quality assurance samples ensure that the analytical results are valid and of acceptable accuracy and precision.

Trace Metal Analyses

Sediment and sediment trap samples were analyzed for Ba, Cd, Cr, Fe, Hg, Pb, and Zn. Analyses were conducted by National Status and Trends methods. The methods included atomic absorption spectroscopy (AAS), instrumental neutron activation analysis (INAA), and/or inductively coupled plasma spectrometry (ICP), depending on the metal and the concentration (e.g., Taylor and Presley 1998). INAA was used to determine Ba, Cr, and Fe. The precision and accuracy by INAA is excellent regardless of the matrix. A more sensitive method was used when needed for other metals to ensure accurate and precise values.

A freeze-dried representative INAA sediment aliquot was ground to a fine powder. No further treatment was needed. For INAA, 0.5 g aliquots of the powdered samples were weighed directly into plastic vials and heat-sealed. The samples were irradiated for 12 hours in the 1 megawatt TRIGA reactor. After a 10-day cooling period to allow Na, Cl, and other interfering isotopes to decay to low levels, the samples were counted using a hyper-pure germanium detector coupled to a Nuclear Data Corp. model 9900 multichannel analyzer integrated with a Digital VAX II/GPX graphics workstation. Concentrations were obtained by comparing counts for each sample with those for sediment and rock reference materials of accurately known elemental composition. Details of this method are given in Boothe and James (1985), including information on counting geometry, reference materials, spikes, blanks and other aspects of quality assurance.

National Status and Trends Program methods were used in the AAS/ICP analysis (Lauenstein et al. 1993). The method for Hg included a sulfuric acid-permanganate digestion of the dry powdered sample followed by stannous chloride reduction to Hg metal and detection by cold vapor atomic absorption. For other metals, 200 mg aliquots of the powdered sediment samples were weighed into Teflon[®] “bombs” and completely dissolved in a mixture of nitric, hydrofluoric, and boric acids at 130°C. Various dilutions were made of the clear digests to bring them into the working range of the AAS or ICP.

A Perkin-Elmer Corp. model 3300DV (dual view) ICP was used when element concentrations permitted. When concentrations were too low for this instrument, a Perkin-Elmer 3030Z AA equipped with an HGA-600 graphite furnace and an auto sampler were used. Details of furnace programs, matrix modifiers, blanks, spikes, reference materials, and other quality assurance information can be found in the reference given above. The proposed methods ensured that the matrix spike recovery for all elements was greater than 90% and that recoveries of certified values for reference materials from the National Research Council of Canada were 90% or better as well.

Results and Discussion

To survey the monitoring sites for the presence of contaminants, 10 grab samples were collected at each site during the first monitoring cruise (1C). Each grab sample was analyzed for EOM, TOC and TIC content, gas chromatographically resolvable and unresolvable (UCM) hydrocarbons, and metals (Ba, Cd, Cr, Fe, Hg, Pb, and Zn). A composite grab sample at each site was analyzed for total PAHs. The measures of hydrocarbons at the sites were low and relatively uniform. Little or no evidence of petroleum related hydrocarbons was observed at any of the nine study sites (**Table 4.1**). The slight increase in EOM and PAH towards the west most likely represents a general fining of sediments (because silts and clays tend to have higher concentrations of EOM and PAH). Metals indicative of contamination were at or near background levels at all sites as well (**Table 4.1**). Barium, a tracer of drill mud discharges, was at background levels and only a few samples might be interpreted as containing slightly elevated barium levels. A slight increase in a few metals (Ba, Cr, Fe, Zn) towards the west most likely represents a general fining of sediments.

TOC in sediments at the study sites was low and relatively uniform (**Table 4.2**). In most instances, TOC was less than 0.5%, occasionally reaching 1.0% or more. Sedimentary carbon was primarily in the form of carbonate. TIC ranged from ~3.5% to more than 8% (pure calcium carbonate would be 12% carbon). Carbonate content decreased from east to west by nearly a factor of two, reflecting proximity to riverine inputs of particulate matter.

Table 4.1. Summary of average sediment characteristics at the study sites during Cruise 1C.

Site	EOM (ppm)	TPH (ppm)	PAH (ppb)	UCM (ppm)	Total Resolved Hydrocarbons (ppm)
1	43.2	11.2	8.2	7.7	9.5
2	35.7	12.0	8.3	9.7	3.2
3	42.1	10.4	10.8	8.6	1.8
4	74.1	20.1	21.5	12.7	7.5
5	59.2	18.4	15.3	13.7	4.7
6	59.2	16.2	15.5	11.3	4.9
7	73.1	21.2	25.7	16.3	4.9
8	33.6	13.2	12.2	10.2	3.0
9	70.9	20.0	20.4	12.7	7.3

Site	Ba (ppm)	Cd (ppm)	Cr (ppm)	Fe (ppm)	Hg (ppm)	Pb (ppm)	Zn (ppm)
1	123.3	0.10	21.0	8858	0.02	7.8	26.2
2	120.1	0.05	21.0	7616	0.02	7.9	22.8
3	111.2	0.07	26.8	8665	0.02	6.7	24.7
4	357.1	0.12	40.0	18,729	0.03	15.0	60.4
5	499.5	0.08	33.8	17,316	0.03	12.3	50.6
6	471.6	0.08	32.0	17,578	0.03	12.5	60.0
7	497.3	0.07	38.0	18,344	0.03	15.3	58.4
8	240.0	0.05	23.5	10,397	0.02	10.6	30.1
9	465.9	0.07	40.6	19,565	0.03	15.3	60.8

Abbreviations: EOM = extractable organic matter; TPH = total petroleum hydrocarbons; PAH = polycyclic aromatic hydrocarbons; UCM = unresolved complex mixture.

Table 4.2. Summary of the average total organic (TOC) and inorganic (TIC) carbon content (%) of sediments at the study sites during Cruises 1C, M2, M3, and M4.

Cruise	Site	n=	TOC	TIC	Cruise	Site	n=	TOC	TIC	Cruise	Site	n=	TOC	TIC	Cruise	Site	n=	TOC	TIC
1C	1	8	0.1	8.0	M2	1	5	0.2	6.9	M3	1	6	0.2	7.5	M4	1	5	0.2	7.2
	2	10	0.2	5.1		2	5	0.1	5.7		2	5	0.0	5.0		2	5	0.2	4.3
	3	10	0.2	5.0		3	5	0.1	5.9		3	5	0.0	5.9		3	5	0.2	6.6
	4	9	1.1	7.3		4	5	0.4	8.0		4	11	1.3	7.0		4	5	0.3	9.3
	5	10	1.1	6.1		5	5	0.24	6.16		5	5	0.6	5.3		5	5	0.2	5.5
	6	10	0.2	5.7		6	5	0.4	4.6		6	5	1.2	4.7		6	5	0.3	5.8
	7	10	0.3	5.0		7	5	0.	3.9		7	5	0.2	3.1		7	5	0.2	4.7
	8	10	0.2	3.1		8	5	0.2	3.4		8	5	0.4	3.3		8	5	0.2	4.8
	9	10	0.3	6.1		9	5	0.3	5.1		9	5	0.2	3.8		9	5	0.2	4.3

The conclusion of the survey is that contaminants, if detected at all, were present in very low concentrations in sediments from the study area. Therefore, anthropogenic influences at the study sites are negligible and are not likely to influence biological patterns in the study area. PAHs were at or below the method detection limits and appear to be derived from low-level, background contamination from atmospheric deposition that is seen Gulf-wide. The levels detected are several orders of magnitude below concentration levels that are thought to invoke biological responses. PAH concentrations are compared with concentrations from a previous MMS study in the western Gulf of Mexico in similar water depths in **Figure 4.1**. Sediment contaminant concentrations were measured in sediments near and far from three oil and gas producing platforms in similar water depths (30 to 150 m) as part of the Gulf of Mexico Offshore Operations Monitoring Experiment (GOOMEX Phase 1; Kennicutt 1995). In the GOOMEX program, elevated levels of PAHs were only detected in sediments near to platforms, and sediments beyond ~100 m from the platform were considered to be background levels. As can be seen in **Figure 4.1**, the PAH concentrations at the study sites are equal to or lower than concentrations detected at undisturbed sites in the western Gulf of Mexico far from platforms.

In most cases, trace metals were also detected at levels that are commonly detected in unimpacted Gulf of Mexico sediments. In a comparison of the study site results with those from the GOOMEX program (**Figure 4.2**), it is clear that sediment trace metal concentrations are similar to those observed far from platforms in the western Gulf of Mexico in similar water depths. In particular, concentrations of Ba, a sensitive tracer of drilling mud discharges, at the study sites are significantly below levels detected at 3,000 to 5,000 m from platforms. These comparisons suggest that the study sites have been exposed to little or no contamination and that the concentrations observed are well below levels known to induce biological responses.

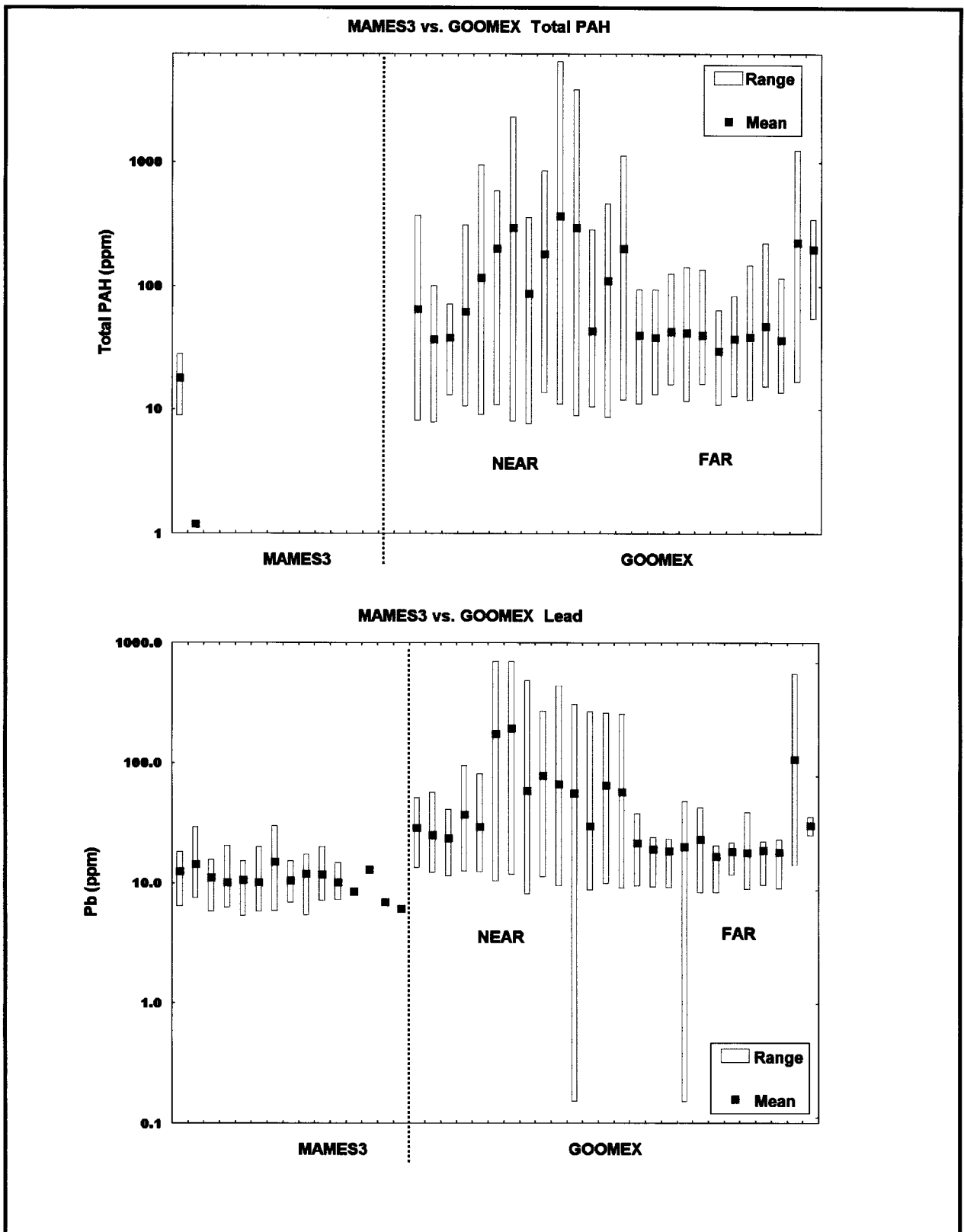


Fig. 4.1. Comparison of total polycyclic aromatic hydrocarbon (PAH) and lead (Pb) concentrations in sediments at sites sampled during this study (labeled MAMES3) and at sites sampled near and far from platforms in the western Gulf of Mexico during GOOMEX Phase 1 (Kennicutt 1995).

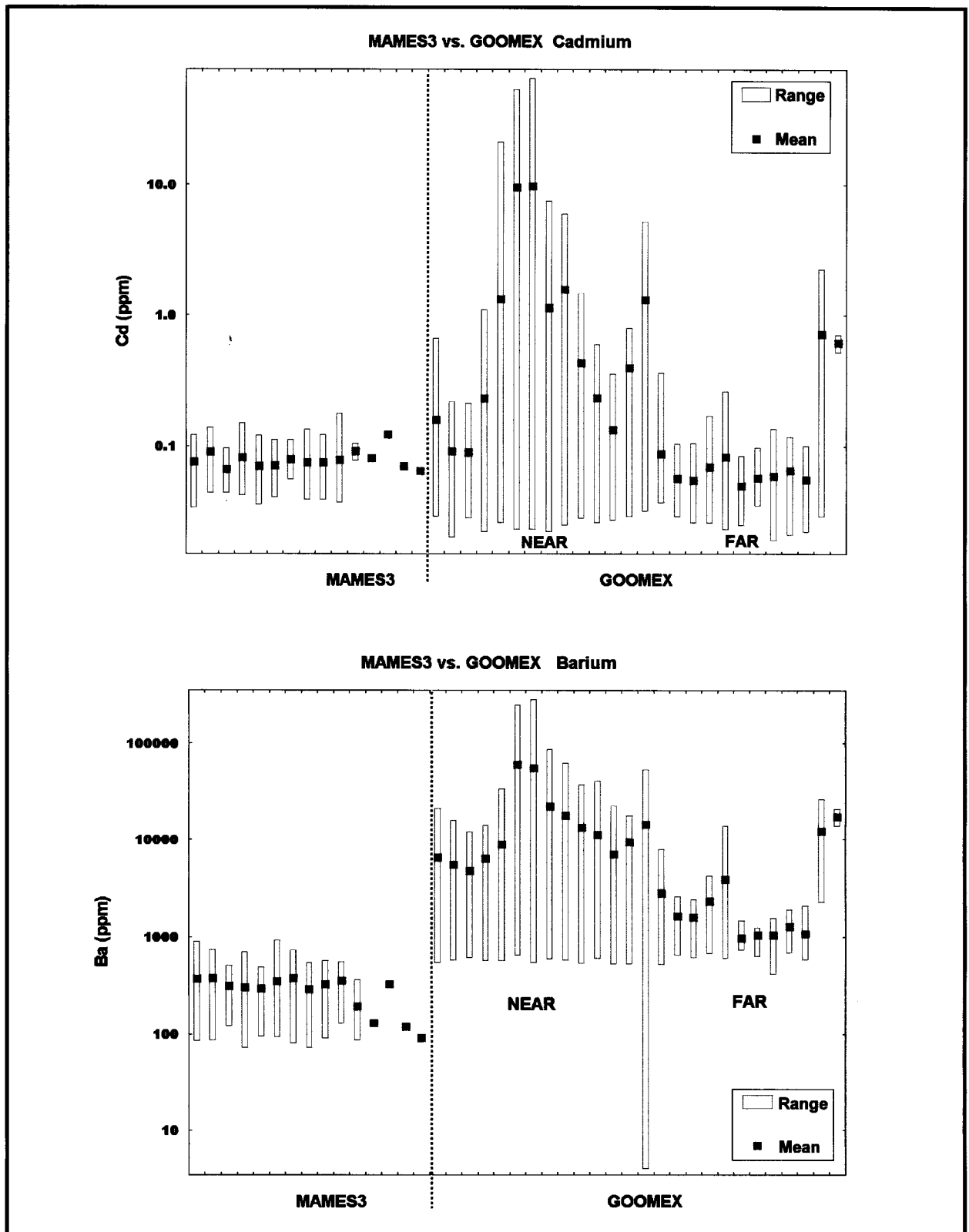


Fig. 4.2. Comparison of cadmium (Cd) and barium (Ba) concentrations in sediments at sites sampled during this study (labeled MAMES3) and at sites sampled near and far from platforms in the western Gulf of Mexico during GOOMEX Phase 1 (Kennicutt 1995).

Chapter 5: Sediment Dynamics

Ian D. Walsh

Introduction

The objectives of the sediment dynamics component in collaboration with the geochemistry and geology components were to (1) provide quantitative and qualitative measurements of the extent and occurrence of the nepheloid layer; (2) determine sedimentation and resuspension rates; (3) determine how topographic highs affect present-day sedimentation; (4) determine temporal variations in sediment texture; and (5) relate short term sediment dynamics to long term sediment accumulation. To address these goals, sediment traps, optical instruments, and conductivity-temperature-depth/dissolved oxygen (CTD/DO) sensors were used to assess and monitor the extent and variability of the nepheloid layer sediment and resuspension.

The goals as outlined above were met by documenting particle distributions and dynamics with several techniques. Data on the spatial and vertical distribution, intensity, and short time-scale variability of the nepheloid layer were acquired with a transmissometer interfaced to the CTD/DO system. Profiles of beam attenuation were recorded during the cruises. Sediment traps were deployed with the physical oceanography moorings to quantify particle flux. Vertically separated sediment traps were used to sample particulates from the nepheloid layer and higher waters to derive short term sedimentation and resuspension rates. Particles from the traps were compared with sediments from the seafloor to characterize the depositional process. The extent and occurrence of the nepheloid layer was determined by CTD/DO/transmissometer/optical backscatter (OBS) casts around the study sites during monitoring cruises along with casts taken at each mooring site during the mooring servicing cruises. Long term variations were to be addressed by OBS instruments deployed on mooring stations, providing comparisons with current meter records.

Most changes in the optical properties of seawater are caused by particles suspended or settling through the water. Light attenuation as measured with a beam transmissometer is one of the easiest to use and most versatile optical instruments now in use to measure inherent optical properties in seawater. A Seatech 25-cm pathlength transmissometer was used to provide measurements of optical attenuation coincident with CTD casts. Gross, large-scale measurements can be made easily with this instrument, but to make precise quantitative measurements considerable care must be exercised in cleaning the optical windows, in correcting for the decay of the LED light source, and in calibration with in-situ particle concentration from filtered samples (Bartz et al. 1978; Gardner et al. 1983). Beam attenuation is an inherent property of seawater and is the sum of light scattering and absorption (Gordon et al. 1984). At the 660 nm wavelength used in the Seatech transmissometer, the scattering function is small. Attenuation is usually considered to be the sum of attenuation of seawater (c_w), yellow matter (c_y), and particles (c_p). In the open ocean, c_y is negligible and c_w is constant, so changes in total attenuation result from changes in particles (Morel 1974; Jerlov 1976; Pak et al. 1988; Gardner et al. 1995; Walsh et al. 1995). The properties of particles that affect attenuation are their

concentration, size distribution, index of refraction, and shape, with concentration and size being most important. If the size distribution, index of refraction, and shape of particles are constant, beam attenuation is linearly related to particle concentration (Spinrad et al. 1983; Baker and Lavelle 1984; Moody et al. 1986). Particle characteristics vary between regions, however, so in order to estimate particle mass concentration from attenuation data it is necessary to calibrate the data by filtering water for total particle concentration.

Transmissometers are also effective in locating areas of resuspension of bottom sediments and production of bottom and intermediate nepheloid layers (Gardner and Walsh 1990; Walsh 1990). Because resuspended sediments form the bulk of nepheloid layer particles (Gardner et al. 1983, 1985), monitoring of the nepheloid layer by use of beam attenuation data can be used to infer spatial and temporal variability of both particle concentrations and resuspension (Gardner and Walsh 1990; Walsh 1990; Walsh et al. 1995).

Field and Laboratory Methods

CTD/DO/Transmissometer/OBS Data Sets

The R/V TOMMY MUNRO was used to collect beam attenuation profiles on eight cruises over the course of the program. Filtration of water samples for calibration of the transmissometer was completed on four of these cruises. Results from the CTD/DO data sets are discussed in Chapter 6.

Using the transmissometer interfaced to the CTD, profiles were made prior to recovery of each mooring and after redeployment on the mooring servicing cruises. Particle concentration profiles for calibration of the transmissometer beam attenuation data were made at each mooring site by filtration from Niskin bottles. One-liter samples were drawn from nine bottles from each filtration cast and vacuum filtered onto pre-weighed 47-mm, 0.4- μm pore size Poretics filters. The filters were rinsed with filtered distilled water to remove salts and dried. On shore, the filters were weighed again, and the difference between the pre- and post-weighing yields the particle mass concentration per liter. Blank filters were used for quality control at all stages of the analysis.

Four calibration data sets were produced from the mooring service cruises in January 1998 (Cruise S2), July 1998 (Cruise S3), October 1998 (Cruise S4), and April 1999 (Cruise M4). Regression analysis of filtered particle concentration on particle beam attenuation from the transmissometer profiles from each cruise separately yielded a range in slopes of less than 20% with significant correlations within each data set and intercepts close to the origin (**Fig. 5.1**). When combining the data sets and treating the four cruises as a single sample, the regression was highly significant with a slope of 1.45 and an r^2 of 0.94 (**Fig. 5.2**). The slope is within the range reported for the Texas-Louisiana Shelf Circulation and Transport Process (LATEX) Program data sets [1.2 to 1.9 (Zhang 1997)]. Beam attenuation values for the entire data set were adjusted to yield a c_p of zero for a concentration of zero.

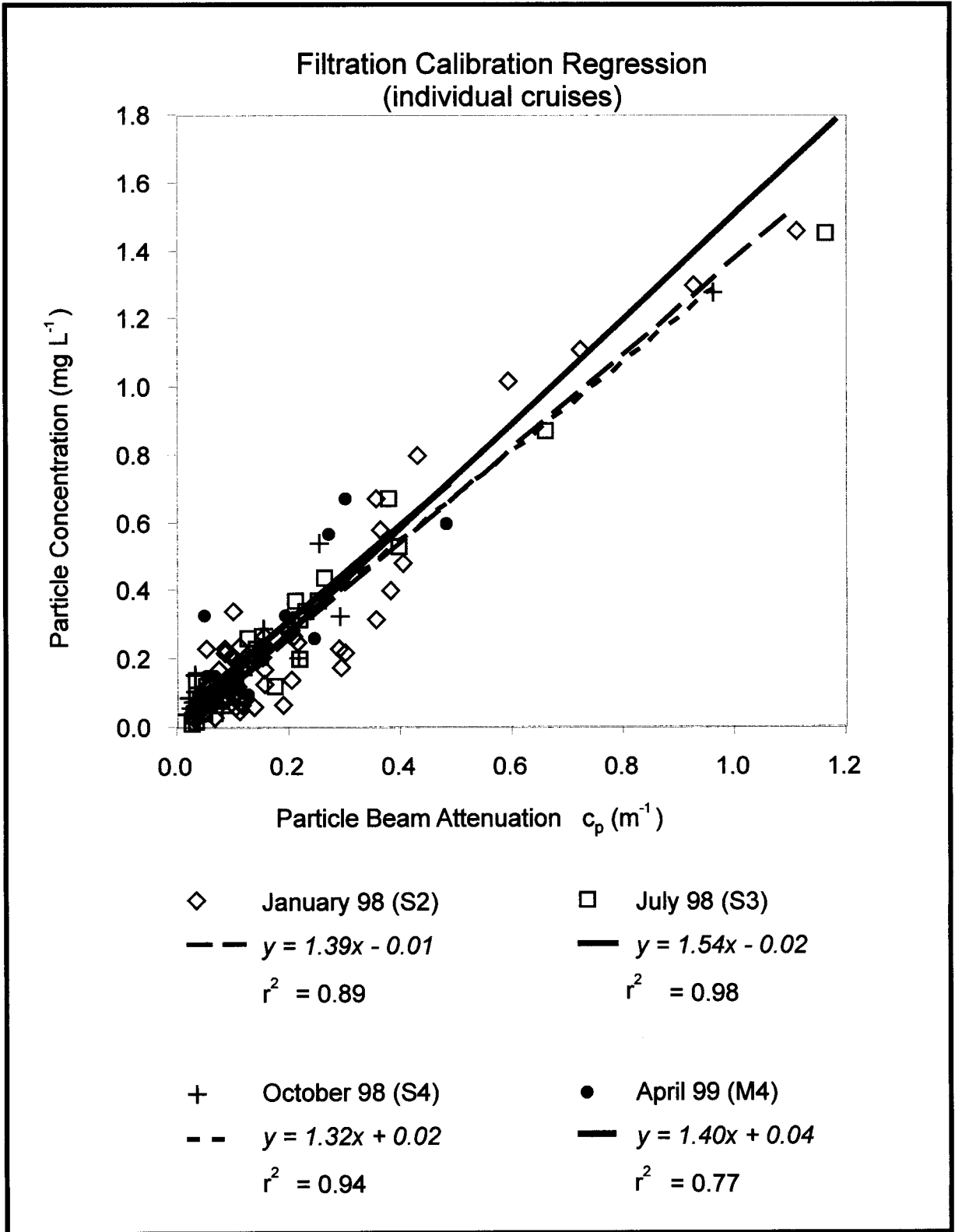


Fig. 5.1. Calibration plot of Niskin bottle particle concentration against the particle beam attenuation data from the transmissometer for the same depths and cast by cruise for four mooring servicing cruises. Least squares regressions and goodness of fit statistics are given for each cruise's data set. Regressions were not forced through the origins.

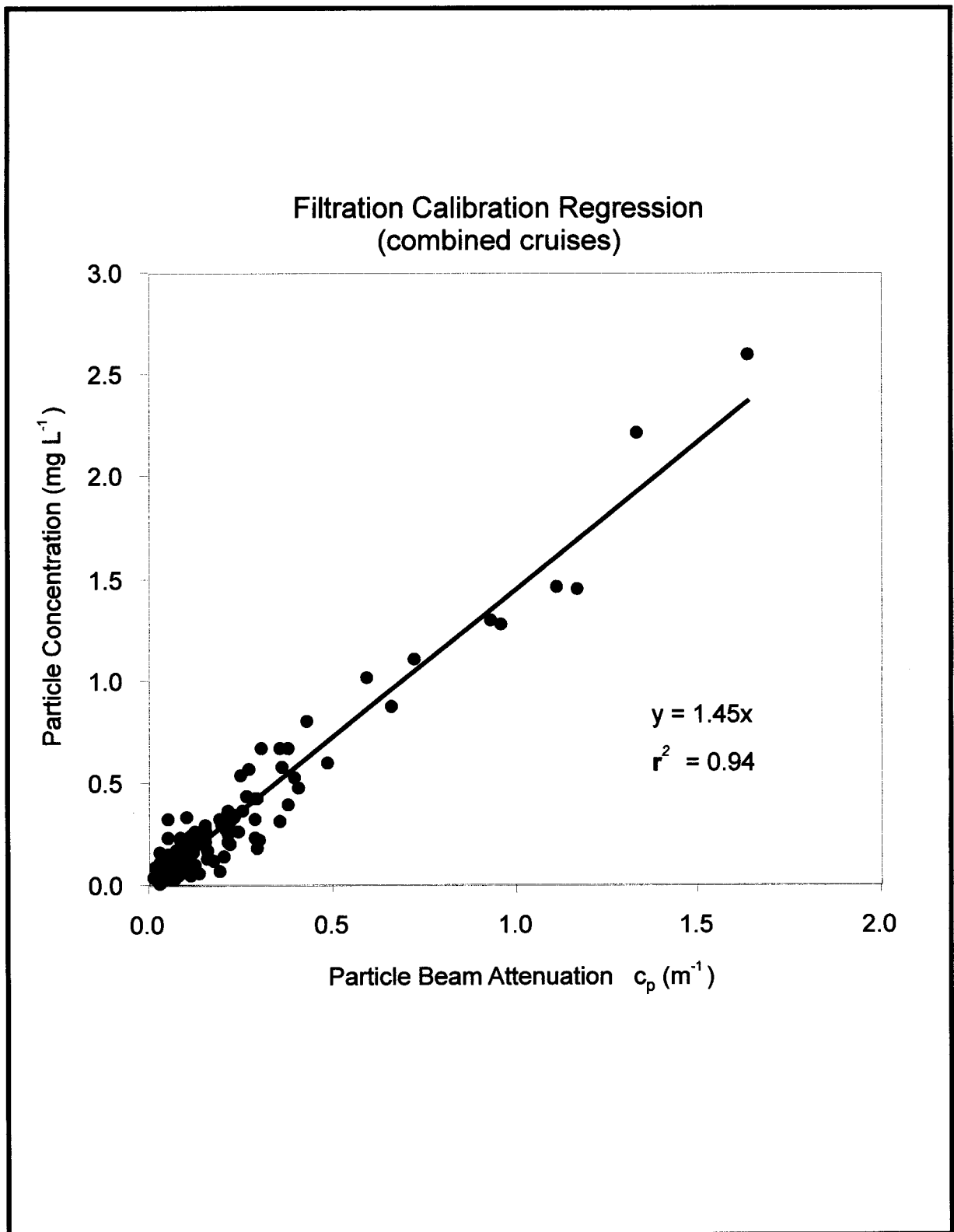


Fig. 5.2. Calibration plot of data from Fig. 5.1 treated as a single set. The regression was forced through the origin.

Correlation of the OBS sensor data (a Seatech light scattering sensor [LSS]) on the CTD package with the transmissometer data was performed by plotting LSS voltage versus the calibrated particle beam attenuation data (c_p) as shown for a representative cast in **Fig. 5.3**. There was good agreement between the two sensors, though the upper and midwater LSS data have considerably more data spiking than the transmissometer data set. Further discussion is based on the transmissometer data set. The OBS data set from the mooring program did not yield a sufficiently robust data set to correlate the particle profiling and moored data sets. The moored instruments did not appear to be sufficiently sensitive to the concentrations of particulates at the sites and the resultant data set was not coherent enough for analysis.

Sediment Traps

The sinking flux of particulate material was collected using sediment traps. Simple core-tube sediment traps were deployed on each of the moorings to monitor particle flux and resuspension during the monitoring period. This type of sediment trap has been proven both effective and cost-effective during the Texas-Louisiana Shelf Circulation and Transport Process (LATEX) Program on the shelf of the western Gulf of Mexico (Zhang 1997). The traps were placed at 2.5 m, 7 m, and 15 m above the bottom (mab).

Sediment traps were deployed from May 1997 through April 1999, supplying almost continuous records of sedimentation over 2 years. Of the 144 total potential samples (3 depths x 6 moorings x 8 cruises = 144 samples), 133 samples were recovered, for a 92% recovery rate (**Table 5.1**). Five samples were lost due to fish bites through the sediment trap end caps, spillage at sea, or the loss of the trap. Two moorings failed to release during the project. Mooring C5C7 was not recovered and those samples were lost from the analysis. However, in the case of the first deployment of the mooring at Site 4 (C4A1), the mooring was recovered on the subsequent cruise and the data are reported for periods 1 and 2 (**Table 5.2**). In that case, while samples were lost, the complete time series was maintained. In terms of the time series, 136 of 144 sample periods were sampled, for a coverage rate of 94%.

Sediment trap samples were decanted and refrigerated at sea, with subsequent processing occurring in the laboratory ashore. In the lab, the supernatant was drawn off and the samples were wet sieved through a 1 mm nylon screen. The >1 mm fraction was visually inspected during processing and archived. In all samples, the >1 mm fraction was a small proportion (<<5%) of the total sample. Two sample splitting procedures were used. For the first four sets of samples, the <1 mm fraction was split into six fractions using a forced air, constant-stirring splitter. For the rest of the samples, a rotating splitter was used to split the sample into 10 fractions. Two splits were combined and archived at this stage (dark refrigeration). Two splits were used for grain size analysis. The remaining splits in pre-weighed centrifuge tubes were centrifuged at 15 krpm for 10 minutes. Supernatant was drawn off and samples were resuspended with distilled water to remove salts and centrifuged again. The supernatant was drawn off and the tubes with sample weighed. The samples are frozen and freeze-dried for 24 to 48 hours depending on the volume of sample. After freeze-drying, the tubes were weighed to measure the water

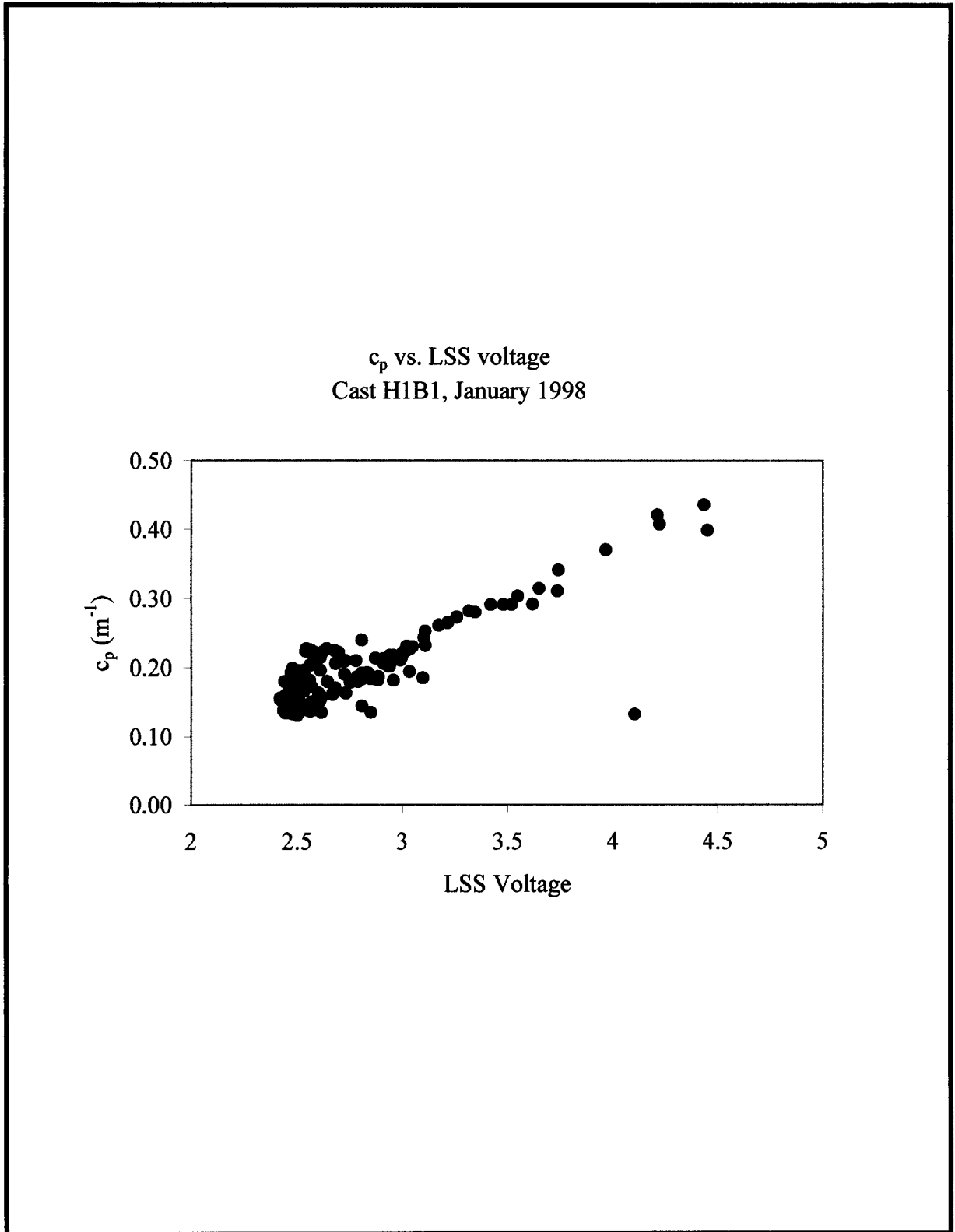


Fig. 5.3. Particle beam attenuation (c_p) plotted against the LSS (Seatech Light Scattering Sensor) data from a representative cast showing the correlation between the two data sets. The high values (i.e., voltage >3) are from the nepheloid layer.

Table 5.1. Matrix of recovered sediment trap samples. Periods are individual deployments. See Table 5.2 for specific deployment and recovery dates. “Lost” indicates that either the trap was not recovered or the sample was lost due to fish bites through the end caps or spillage.

Site	Depth (mab)	Period							
		1	2	3	4	5	6	7	8
1	15	lost	C1A2	C1A3	C1A4	C1A5	C1A6	C1A7	C1A8
	7	C1A1	C1A2	lost	C1A4	C1A5	C1A6	C1A7	C1A8
	2.5	C1A1	C1A2	C1A3	C1A4	C1A5	C1A6	C1A7	C1A8
1	15	C1B1	C1B2	C1B3	lost				
	7	C1B1	C1B2	C1B3	C1B4				
	2.5	C1B1	C1B2	C1B3	C1B4				
1	15	C1C1	C1C2	C1C3	lost				
	7	C1C1	C1C2	C1C3	C1C4				
	2.5	C1C1	C1C2	C1C3	C1C4				
4	15		C4A1 ^a	C4A3	C4A4	C4A5	C4A6	C4A7	C4A8
	7		C4A1 ^a	C4A3	C4A4	C4A5	C4A6	C4A7	C4A8
	2.5		C4A1 ^a	C4A3	C4A4	C4A5	C4A6	C4A7	C4A8
5	15	C5A1	C5A2	C5A3	C5A4	C5A5	C5A6	C5A7	C5A8
	7	C5A1	C5A2	C5A3	C5A4	C5A5	C5A6	C5A7	C5A8
	2.5	C5A1	C5A2	C5A3	C5A4	C5A5	C5A6	C5A7	C5A8
5	15					C5B5	C5B6	C5B7	C5B8
	7					C5B5	C5B6	C5B7	C5B8
	2.5					C5B5	C5B6	C5B7	C5B8
5	15					C5C5	C5C6		lost
	7					C5C5	C5C6		C5C8
	2.5					C5C5	C5C6		C5C8
9	15	C9A1	C9A2	C9A3	C9A4	C9A5	C9A6	C9A7	C9A8
	7	C9A1	C9A2	C9A3	C9A4	C9A5	C9A6	C9A7	C9A8
	2.5	C9A1	C9A2	C9A3	C9A4	C9A5	C9A6	C9A7	C9A8

mab = meters above bottom

^a Mooring C4A1 could not be recovered at the end of period 1 but was recovered at the end of the period 2.

Table 5.2. Matrix of deployment (D) and recovery (R) dates for each sediment trap during the time series. Mooring C4A1 was recovered on a second attempt. Mooring C5C7 was not recovered. Data from C4A1 are reported here over the entire deployment period.

Site	Depth (mab)	Mooring	Period															
			1 D	1 R	2 D	2 R	3 D	3 R	4 D	4 R	5 D	5 R	6 D	6 R	7 D	7 R	8 D	8 R
1	15	C1A	5/15/97	lost	7/26/97	10/2/97	10/2/97	1/29/98	1/29/98	4/24/98	4/24/98	7/20/98	7/21/98	10/13/98	10/13/98	2/9/99	2/9/99	4/13/99
	7	C1A	5/15/97	7/26/97	7/26/97	10/2/97	10/2/97	lost	1/29/98	4/24/98	4/24/98	7/20/98	7/21/98	10/13/98	10/13/98	2/9/99	2/9/99	4/13/99
	2.5	C1A	5/15/97	7/26/97	7/26/97	10/2/97	10/2/97	1/29/98	1/29/98	4/24/98	4/24/98	7/20/98	7/21/98	10/13/98	10/13/98	2/9/99	2/9/99	4/13/99
1	15	C1B	5/15/97	7/26/97	7/26/97	10/2/97	10/2/97	1/29/98	1/29/98	lost								
	7	C1B	5/15/97	7/26/97	7/26/97	10/2/97	10/2/97	1/29/98	1/29/98	4/24/98								
	2.5	C1B	5/15/97	7/26/97	7/26/97	10/2/97	10/2/97	1/29/98	1/29/98	4/24/98								
1	15	C1C	5/15/97	7/26/97	7/26/97	10/2/97	10/2/97	1/29/98	1/30/98	lost								
	7	C1C	5/15/97	7/26/97	7/26/97	10/2/97	10/2/97	1/29/98	1/30/98	4/24/98								
	2.5	C1C	5/15/97	7/26/97	7/26/97	10/2/97	10/2/97	1/29/98	1/30/98	4/24/98								
4	15	C4A	5/15/97			10/29/97	10/30/97	1/30/98	1/30/98	5/1/98	5/1/98	7/21/98	7/22/98	10/13/98	10/13/98	2/9/99	2/9/99	4/13/99
	7	C4A	5/15/97			10/29/97	10/30/97	1/30/98	1/30/98	5/1/98	5/1/98	7/21/98	7/22/98	10/13/98	10/13/98	2/9/99	2/9/99	4/13/99
	2.5	C4A	5/15/97			10/29/97	10/30/97	1/30/98	1/30/98	5/1/98	5/1/98	7/21/98	7/22/98	10/13/98	10/13/98	2/9/99	2/9/99	4/13/99
5	15	C5A	5/15/97	7/26/97	7/26/97	10/5/97	10/6/97	1/30/98	1/30/98	5/1/98	5/1/98	7/21/98	7/22/98	10/13/98	10/13/98	2/9/99	2/9/99	4/13/99
	7	C5A	5/15/97	7/26/97	7/26/97	10/5/97	10/6/97	1/30/98	1/30/98	5/1/98	5/1/98	7/21/98	7/22/98	10/13/98	10/13/98	2/9/99	2/9/99	4/13/99
	2.5	C5A	5/15/97	7/26/97	7/26/97	10/5/97	10/6/97	1/30/98	1/30/98	5/1/98	5/1/98	7/21/98	7/22/98	10/13/98	10/13/98	2/9/99	2/9/99	4/13/99
5	15	C5B								5/1/98	7/21/98	7/22/98	10/13/98	10/13/98	2/9/99	2/9/99	4/13/99	
	7	C5B								5/1/98	7/21/98	7/22/98	10/13/98	10/13/98	2/9/99	2/9/99	4/13/99	
	2.5	C5B								5/1/98	7/21/98	7/22/98	10/13/98	10/13/98	2/9/99	2/9/99	4/13/99	
5	15	C5C								5/1/98	7/21/98	7/22/98	10/13/98	10/13/98		2/10/99	lost	
	7	C5C								5/1/98	7/21/98	7/22/98	10/13/98	10/13/98		2/10/99	4/13/99	
	2.5	C5C								5/1/98	7/21/98	7/22/98	10/13/98	10/13/98		2/10/99	4/13/99	
9	15	C9A	5/15/97	7/26/97	7/26/97	10/31/97	10/31/97	1/30/98	1/30/98	5/1/98	5/1/98	7/21/98	7/21/98	10/14/98	10/14/98	2/10/99	2/10/99	4/14/99
	7	C9A	5/15/97	7/26/97	7/26/97	10/31/97	10/31/97	1/30/98	1/30/98	5/1/98	5/1/98	7/21/98	7/21/98	10/14/98	10/14/98	2/10/99	2/10/99	4/14/99
	2.5	C9A	5/15/97	7/26/97	7/26/97	10/31/97	10/31/97	1/30/98	1/30/98	5/1/98	5/1/98	7/21/98	7/21/98	10/14/98	10/14/98	2/10/99	2/10/99	4/14/99

mab = meters above bottom

loss. The samples were removed from the centrifuge tubes and ground to a powder in a mortar. Ground samples were placed into preweighed petri dishes and weighed. The empty centrifuge tubes also were weighed to estimate the remaining sample on the wall and as a double check on the petri dish weight. Mass flux was calculated using the dry weight divided by the area of the tube and the elapsed time of deployment in days (**Table 5.2**).

Dry splits of the ground samples were made to provide subsamples for chemical analysis. Total inorganic carbon (TIC) and total organic carbon (TOC) analyses were made on all samples for which adequate material was available. Trace metal analysis for barium, chromium, and iron were made on combined samples from periods 1 and 2, 3 and 4, and 7 and 8. Samples were combined based on the time weighted mass fluxes for each period. Because of the large amount of material collected during sampling period 6, subsamples for trace metal analysis were made from both periods 5 and 6.

Results and Discussion

Water Column

The water column particulate data collected indicates that the study area has high spatial and temporal variability as illustrated at Site 1 during the January 1998 mooring servicing cruise (S2) (**Fig. 5.4**). Two casts were made at mooring site B just prior to recovery and immediately after redeployment of the mooring. The two casts, though only a few hours apart, demonstrate that advective processes are important at this site. Below the surface layer the particle concentration reached a minimum in both casts near 40 m. However, a warm saline layer between 20 m and 60 m appears in the H1B2 cast but not the H1B1 cast. An intermediate nepheloid layer is associated with the base of this layer and is separated from the benthic nepheloid layer by a thin layer of lower salinity water. The warm saline layer and its associated intermediate nepheloid layer were found in both of the profiles made at mooring C to the southwest of B, while the profiles at mooring site A to the south of B were similar to H1B1.

While variability was high, a benthic nepheloid layer (defined as an increase in particle beam attenuation above a midwater column minimum) was present at all sites during all casts, though with a wide range in concentrations. The benthic nepheloid layer was found to be associated with lower bottom water temperatures (**Fig. 5.5**), indicating that intrusions of slope water were commonly accompanied by bed shear stresses exceeding the sediment resuspension threshold.

The spatial and temporal variability in the beam attenuation/particle concentration profiles was analyzed from the available transmissometer profile data. All the available profiles from the eight cruises during which casts were made ($n = 20$ to 34 per site) were averaged on half-meter intervals to derive a mean profile for each site with standard deviations (**Fig. 5.6**). There was little difference in the mean particle concentration in the mid-water column (i.e., 40 m) among the sites, though Site 4 had the lowest mid-water average particle concentration, a function of its relatively offshore location. Absolute

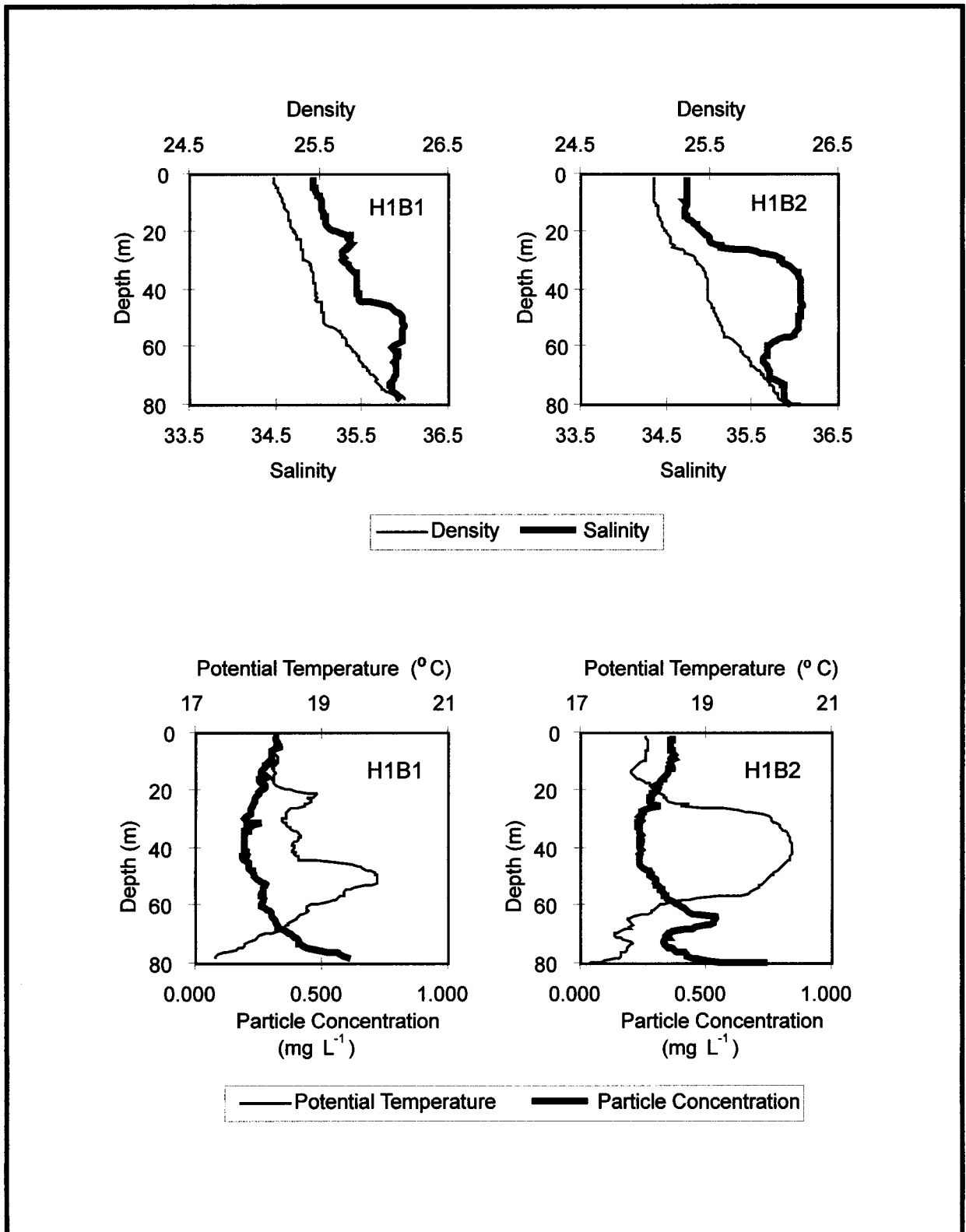


Fig. 5.4. Profiles of density, salinity, potential temperature, and particle concentration from the calibrated beam attenuation data from two casts at the Site 1 mooring taken during the January 1998 mooring service cruise (S2). Note the presence of the warm saline intermediate layer in H1B2 and the associated intermediate nepheloid layer.

T vs C_p profiles - January 1998 (Cruise S2)

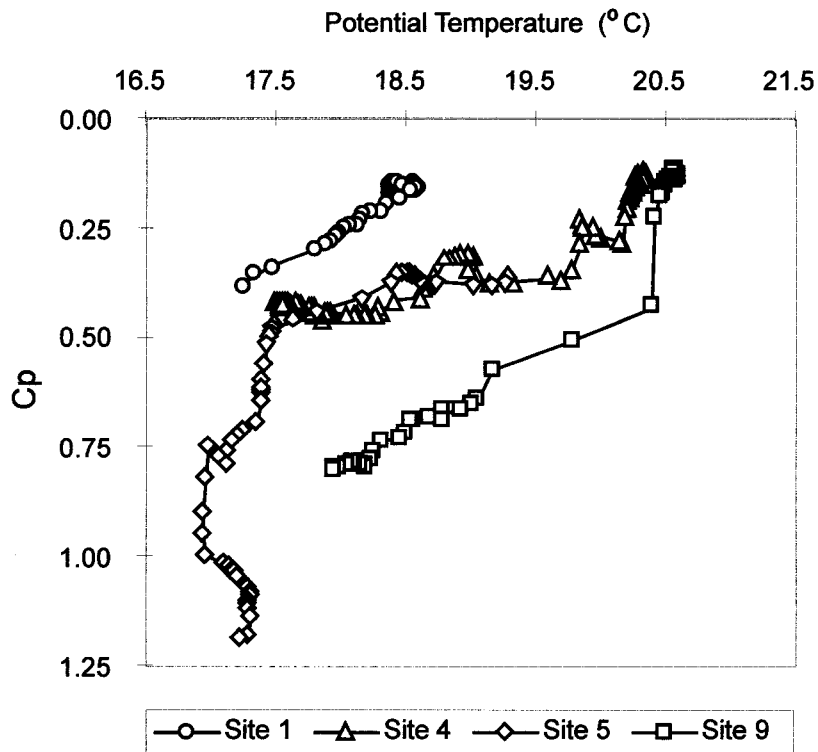


Fig. 5.5. Plot of particle beam attenuation (c_p) versus potential temperature for selected casts taken during the January 1998 mooring servicing cruise (S2). Note the increase in beam attenuation with decreasing temperature. [Note: Potential temperature is the temperature that a parcel of water would have if it were moved adiabatically (i.e., with no heat added or removed) to the surface where pressure is assumed to be 1 atmosphere.]

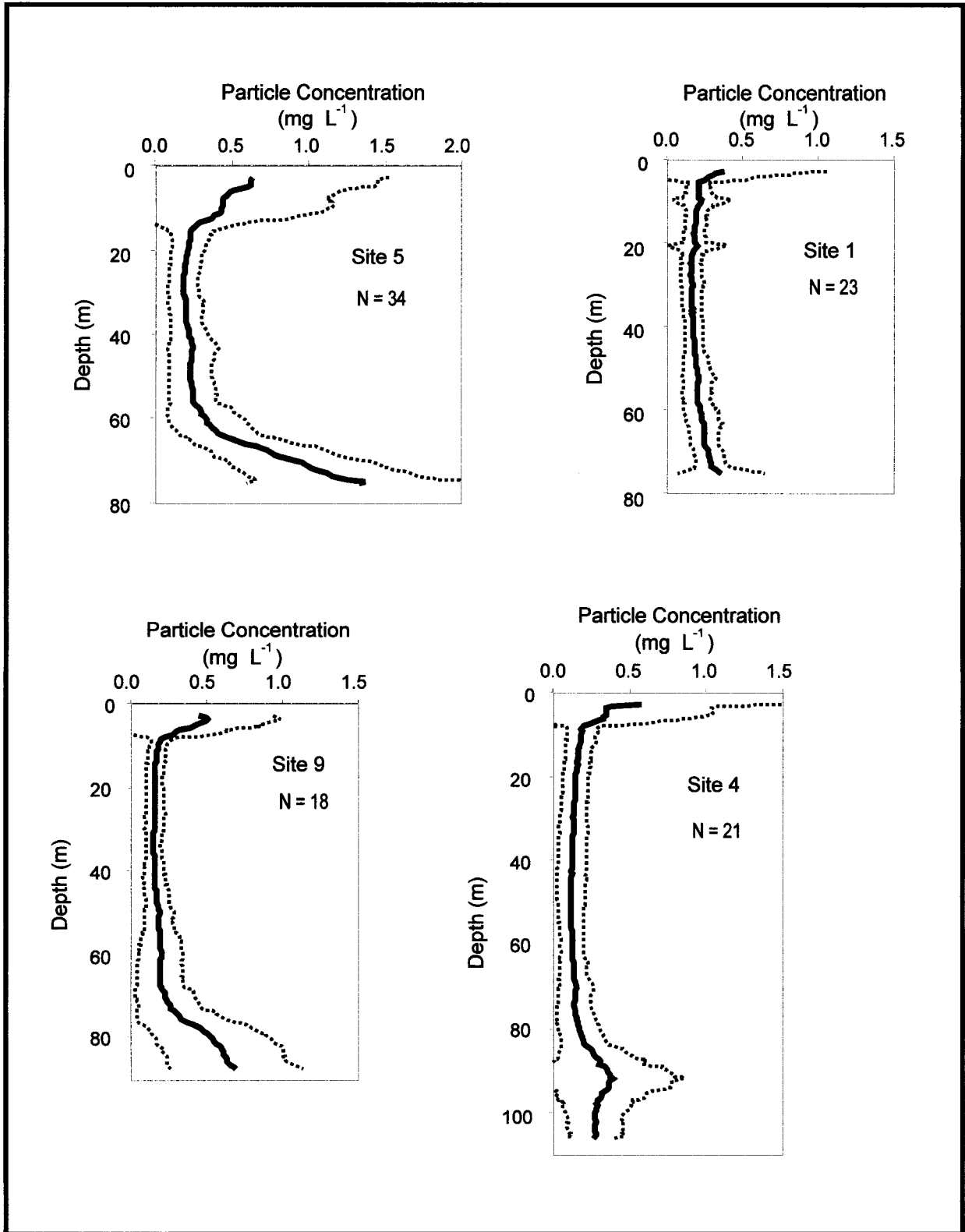


Fig. 5.6. Mean particle profiles compiled from all available transmissometer casts at each site. Beam attenuation was converted to particle mass concentration using the calibration from Fig. 5.2.

standard deviations were highest in the surface layer, reflecting variability in production and the presence of low salinity layers that were commonly found to have very high particle loads. Comparing the nepheloid layers between the sites (**Fig. 5.7**), Site 5 was the location of the most persistently intense (higher concentration) nepheloid layer, while Sites 1 and 4 had weak mean but occasionally robust nepheloid layers. The westernmost site (9) fell in between. The absolute standard deviations increased towards the bottom from the minima in the midwater column, but when normalized to the mean were found to decrease towards the bottom at all sites, reflecting the fact that a nepheloid layer was present in all profiles (**Fig. 5.7b**).

Normalized variance was greatest at Site 4. Site 4 was the most unique in that an intermediate nepheloid layer centered approximately 15 mab is reflected in the mean profile. This intermediate nepheloid layer is most likely produced on the shallower shelf just to the north and advected over the site. The higher particle concentration in the intermediate nepheloid layer reflects the higher energy on the shallower shelf, which leads to development of higher concentration nepheloid layers (e.g., Site 5).

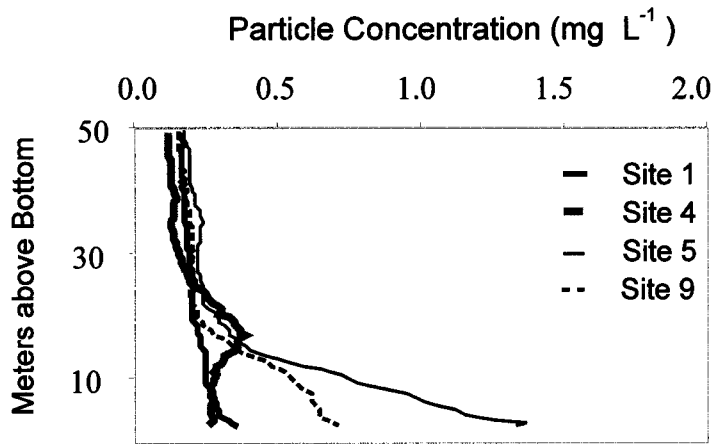
The stability of the particle concentration/beam attenuation correlation among the four sampling cruises indicates that the particles in the nepheloid layer had similar size distributions and adsorption properties throughout the study period. This argues strongly for a local origin for the nepheloid layer particles, and against significant wide-scale advection of sediments through these sites. Rather, the local surface sediments probably have a rapid cycling between the water column following resuspension events and the surface sediments following deposition.

Sediment Traps

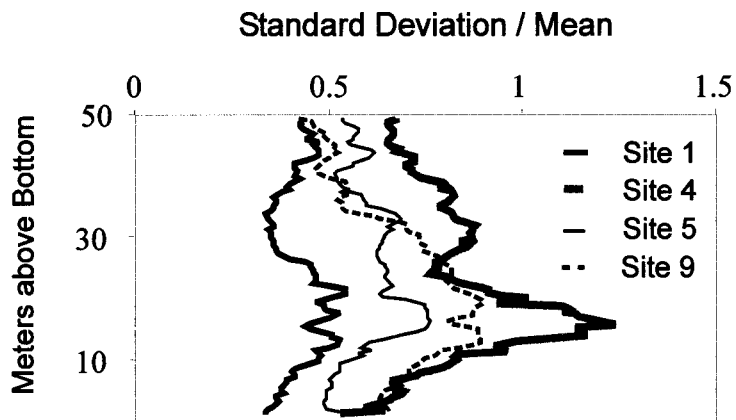
The sediment trap results during the study period reflect the influence of resuspension input at the study sites. As with the persistent nepheloid layer found in the transmissometer data set, bulk fluxes increased to the bottom for all moorings and time periods (**Fig. 5.8**). The dominant temporal signal in the entire data set is the extremely high fluxes recorded during period 6 (7/21-10/13/98) (**Fig. 5.8**). During this period, Hurricane Georges passed near the mooring sites and energetic southwestward currents were recorded (Chapter 6). Fluxes during this period were the highest recorded for each site and depth during the study, and ranged from 4 to 70 times the average fluxes recorded, excluding period 6.

Study-long average fluxes excluding period 6 ranged from 1.5 to 6 g m⁻² d⁻¹ in the traps 15 mab to 6.7 to 29.3 g m⁻² d⁻¹ in the 2.5 mab traps. Comparing between the sites, the study average fluxes increased from Site 1 to Site 4 to Site 5, with Site 9 essentially the same as Site 5 at 15 and 7 mab but with a lower average flux at 2.5 mab. This trend of increasing fluxes towards the west reflects the trend in the water column particle load discussed above. No seasonal trends are apparent at all the sites over the study period, which may reflect the dominance of storm- and event-driven resuspension.

Total organic carbon concentrations consistently decreased with depth at each of the sites for all time periods with the exception of period 6. Considering that little degradation of



(a)



(b)

Fig. 5.7. Mean particle profiles from Fig. 5.6 presented on a common height above bottom scale (a) and the variance for that data presented as the standard deviation divided by the mean (b).

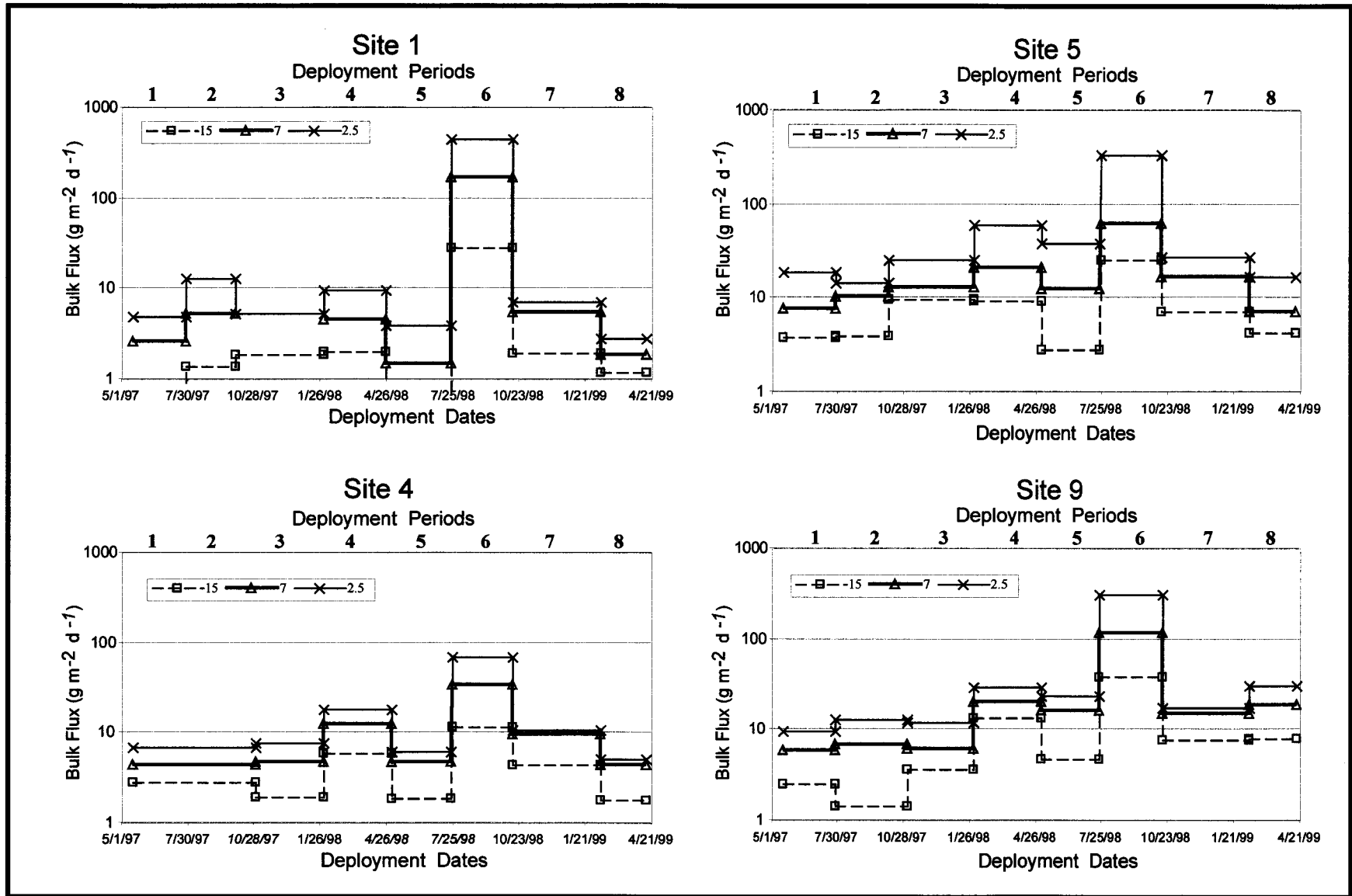


Fig. 5.8. Bulk fluxes recorded during the study at Sites 1, 4, 5, and 9.

organic carbon would be expected during a transit time through 15 m of water column (Walsh et al. 1988), the decrease in concentration is a function of the dilution of the water column flux by the lower TOC concentration sediment resuspension flux. Comparing the 15 mab data set, which is the least influenced by local resuspension, the highest TOC concentrations and widest range of values was found at Site 1, with the lowest concentration and range at Site 5, in keeping with the relative degree of resuspension seen in the water column data set above. Since the local resuspension at Site 4 is similar to that at Site 1, it would be expected that Site 4 would have a similar range of TOC concentrations as Site 1. However, at Site 4 only the period 2 TOC concentration is greater than the range recorded at Site 5, and the total range is essentially the same as Site 9, suggesting that the intermediate nepheloid layer seen in the water column data set (Figs. 5.6 and 5.7) is a significant contributor to the sediment trap flux at this site.

As discussed above, period 6 fluxes were the highest recorded during the study. The lowest sediment trap TOC concentrations, similar to sediment values (see Chapter 4), were measured during period 6 with little vertical gradient in concentration at any of the sites (Fig. 5.9). The implication is that the storm events during this period resulted in massive resuspension such that the water-column-derived particle flux was minimal compared to the resuspension (sediment-derived) flux.

Within-site variability in sediment fluxes was studied by deploying three sets of sediment traps on the three moorings (A, B, C) at Site 1 during the first year (periods 1-4), and Site 5 during the second year (periods 5-8). Bulk fluxes from Site 1 are plotted in Fig. 5.10. While variability between samples increased with depth, there was no consistent pattern between periods. This suggests that while the regional dynamics control the sedimentation dynamics 15 mab (i.e., the top of the benthic nepheloid layer) highly local roughness elements and flow dynamics (on the order of tens of meters) modulate the nepheloid layer and sedimentation dynamics very close to the bottom. This is hardly surprising, as any detailed analysis of sedimentation on such a close scale would be expected to reflect the highly local dynamics, but it does suggest that the topographic highs of the features within the study area will modulate local sedimentation on similar time and length scales (i.e., meters and months). The lack of a persistent pattern between periods probably reflects that variability of the mesoscale physical oceanographic events (i.e., intrusions, filaments, and storms) has a controlling influence on the resultant sedimentation.

The TOC concentrations and fluxes from Site 5 for periods 5-8 are plotted in Fig. 5.11. There is little variability among any set of samples for a given time period and depth of the TOC concentration data set. The persistent decrease in TOC concentration with depth reflects the dilution of the water-column-derived flux of organic carbon with the resuspended sediments that is seen at all sites (Fig. 5.9). The TOC concentrations are at a minimum (< 2%) for period 6 and there is little vertical gradient. This pattern persists across all sites (Fig. 5.9) and reflects the intense resuspension events associated with the tropical storms and hurricane that transited across the study area during this time period (see Chapter 6). There is more variability between moorings with respect to the TOC flux at Site 5 in any given period than was observed at Site 1. However, in contrast to

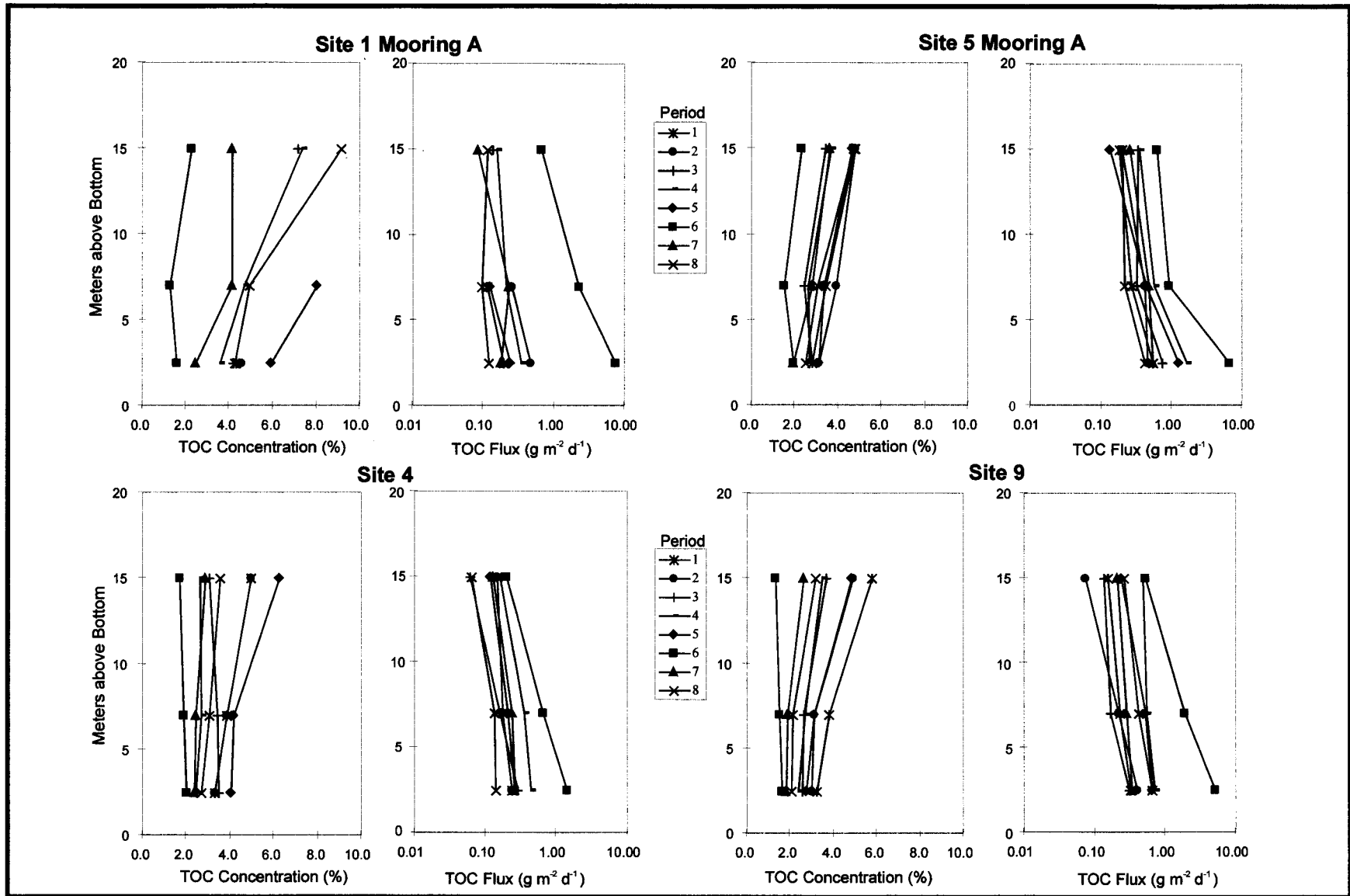


Fig. 5.9. Total organic carbon (TOC) concentrations and TOC fluxes presented for each sample period at each site.

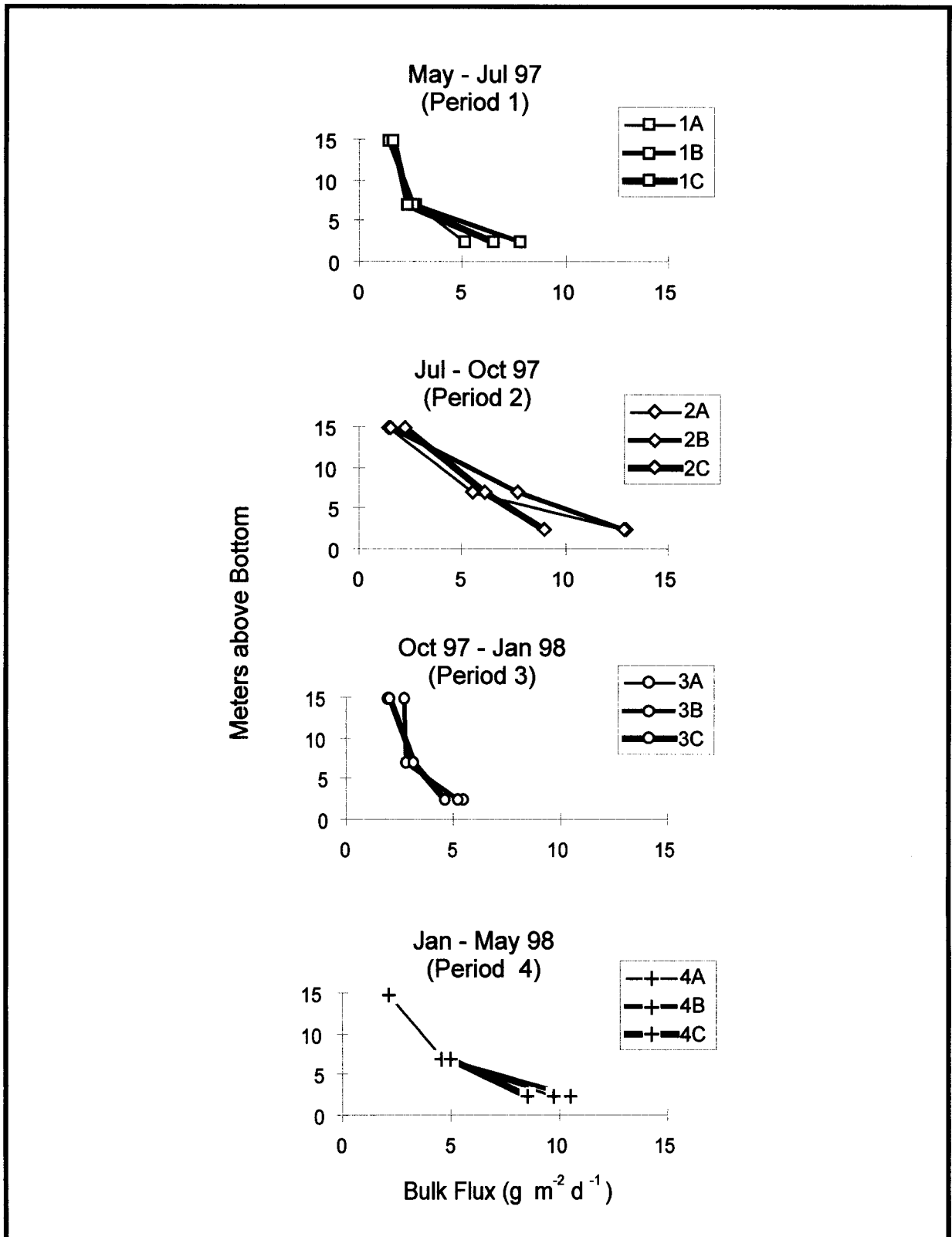


Fig. 5.10. Comparison of bulk fluxes measured during the first year of the program at three moorings at Site 1.

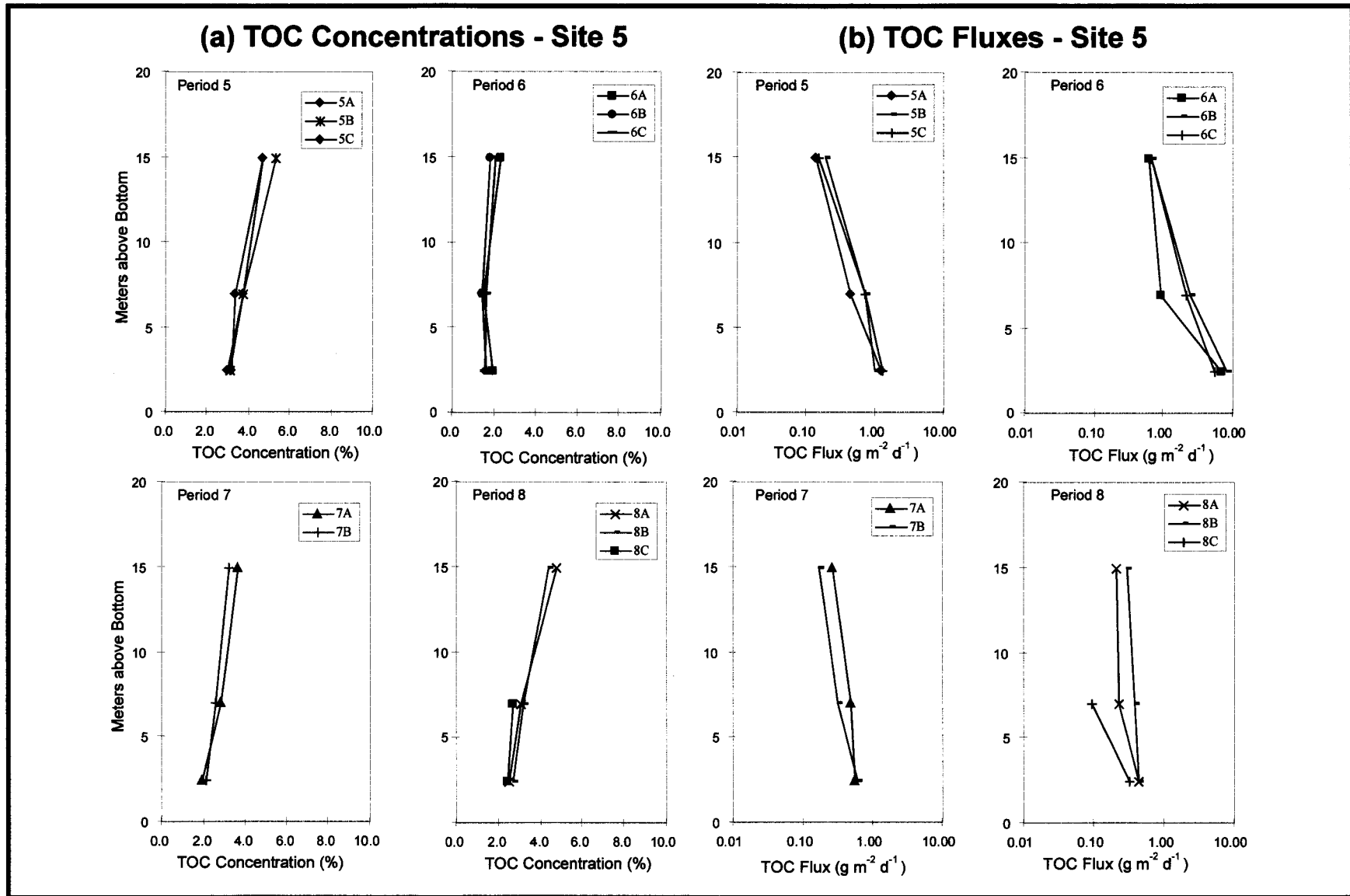


Fig. 5.11. Comparison of (a) total organic carbon (TOC) concentrations and (b) TOC fluxes measured during the second year of the program at Site 5.

Site 1, the TOC fluxes among the 2.5 mab samples were more similar in any given period than the 15 and 7 mab samples. As with Site 1, there was no consistent pattern between moorings, e.g., during period 7 mooring A recorded higher TOC fluxes than mooring B at 15 and 7 mab, but the opposite relationship was found during period 8. As at Site 1, mesoscale variability probably results in within-site variability in the sedimentation and nepheloid layer dynamics. The lack of variability in the near bottom sediment traps at Site 5 may reflect a saturation effect in either an upper limit of particle concentration in the water column or the ability of the sediment trap design to adequately sample such high concentrations. It is unlikely that the 2.5 mab sediment traps significantly undertrapped relative to the 7 and 15 mab traps, however, as the gradient in sediment flux at Site 5 is matched by the gradient in the nepheloid layer at Site 5 (**Fig. 5.7**). Furthermore, the relationship between the sediment trap fluxes and average nepheloid layer concentrations between sites is consistent among all four sites (**Fig. 5.7**). It is more likely that advection and site-wide resuspension at Site 5 is more important than resuspension dynamics and roughness elements on the scale of tens of meters.

Barium sources are both natural and anthropogenic (drilling muds). Barium concentrations (along with chromium and iron) were measured in the pooled sediment trap samples to yield a time series of data at each site (**Fig. 5.12**). Site 1 had consistently lower barium concentrations, while the western and shallower sites (9 and 5) were consistently higher. Resuspended sediment had a lower barium concentration than the water column material, as reflected in the minimum barium concentration recorded at all sites for period 6 and the general decrease in concentration with depth for any given period and site.

Conclusions

Both the water column particulate measurements and the sediment trap data set reflect the variation in resuspension and nepheloid layer dynamics between the sites. Within the sites there was no consistent trend in the sediment trap data set at any given depth level, suggesting that mesoscale variability was more important than local effects averaged over a mesoscale time period (i.e., the trapping period).

A persistent and energetic nepheloid layer at Site 5 resulted in the highest average bulk fluxes and lowest TOC concentrations in the settling material. Sites 1 and 4 had the lowest rates of resuspension and the lowest fluxes, though Site 1 had the highest sediment trap TOC concentrations. Site 9 had a robust and persistent nepheloid layer, with a peak mean concentration twice that found at Site 1 and 4, though half of the peak mean was found at Site 5. Similarly, Site 9 fluxes fell between the low fluxes measured at Sites 1 and 4 and the high fluxes measured at Site 5.

Storm events of hurricane scale cause extreme responses in the sedimentation rates at all of the sites. During period 6, the highest fluxes were recorded at Site 1, while for all other periods it was either the lowest or was similar to Site 4. This probably reflects the southwestward flow of the currents during this time period, which put Site 1 closest to the sediment source.

Chapter 6: Physical Oceanography/Hydrography

F. J. Kelly, Norman L. Guinasso, Jr., and Les C. Bender

Introduction

This component of the program monitored oceanographic conditions (i.e., currents, temperature, salinity, turbidity, dissolved oxygen, etc.) at four sites along the Mississippi-Alabama OCS. Specific objectives were to characterize the regional and local currents in the study area; to determine the dynamics of important oceanographic parameters; and, in concert with the other project components, to define the relationship of currents and oceanographic conditions to the geological and biological processes.

To address the objectives, the oceanographic processes effort consisted of three elements: instrument moorings, hydrographic stations, and collateral data. Six 18-m high, bottom-mounted, instrument moorings were deployed at selected hard bottom sites to continuously measure current velocity, temperature, conductivity/salinity, dissolved oxygen, and turbidity. The moorings also had sediment traps to collect samples of settling suspended particulate matter (see Chapter 5 for results). Discrete vertical profiles of conductivity-temperature-depth (CTD), dissolved oxygen, transmissivity, and optical backscatter were collected by the same instrument package used during the Texas-Louisiana Shelf Circulation and Transport Process Program (LATEX; Nowlin et al. 1998). Collateral data, such as satellite advanced very high resolution radiometer (AVHRR) images, satellite altimetry, river discharge, coastal wind and sea level data, and buoy observations of wind, waves, barometric pressure, air and sea temperature, were gathered to summarize the primary physical forcing mechanisms.

Moored instruments provide information about the temporal scales of physical processes that affect biota associated with benthic habitats in the study area. The variables of greatest interest are current speed and direction, suspended sediments, water temperature, dissolved oxygen, and salinity. The semi-annual monitoring cruises recorded the cumulative results of interactions on various time scales among the physical and chemical variables and the biological communities. The continuous *in situ* data provided additional information about variability and capture the details of events such as the passage of a hurricane or the intrusion of a Loop Current-associated water mass.

Vertical profiles of the above-mentioned time-series variables were taken during the monitoring and servicing cruises to provide details about vertical structure. Previous studies (Kelly 1991) indicated that water masses in the study area undergo changes both in the near-surface and at depth. The CTD profiles indicated the presence of near-bottom nepheloid layers that vary quite markedly over the area in both space and time. Vertical variations are induced by Loop Current intrusions, seasonal heating and cooling, wind forcing, fresh water input from the local rivers, and the passage of storms. To assess the magnitude of these variations, multiple vertical profiles of conductivity, temperature, photosynthetically active radiation (PAR), transmissivity, backscattered light, and oxygen concentrations were collected at each study site. Vertical profiles were made at three locations around each site to determine short scale variability in space and time scale that

may be related to flow past the topographic features. Water samples were collected for determination of total suspended matter (see Chapter 5). From these measurements, the depth of the nepheloid layer was inferred and the water masses enveloping the features were characterized. These data were also used to provide quality control for time-series measurements made at the moorings.

This report covers data collected by moored instruments during all deployment periods and vertical profiles collected on all cruises. Selected results and analyses are used to summarize and synthesize the suite of observations. The complete set of data collected by the instruments used during this project and the standard graphs and tables that display the observations are available on the project's CD-ROM.

Methods

Overview

From a physical point of view, the hard bottom features of interest in the study area are flow obstacles that extend up to about 20 m above the surrounding seafloor. Water depth in the region ranges from 70 to 120 m. Six moorings measured currents, conductivity/salinity, temperature, dissolved oxygen, turbidity, and sediment flux. The mooring design is illustrated in **Fig. 6.1**. Current, temperature, and conductivity/salinity, dissolved oxygen, and turbidity were recorded by a suite of sensors at 2.5–3.5 meters above bottom (mab); at 16 mab, only current, temperature, and conductivity/salinity were recorded. Sediment traps were attached at three heights above the bottom (see Chapter 5).

One mooring was placed at each of four of the nine study sites (**Figs. 6.2–6.5**). Moorings at Sites 1 and 5 were located near large, flat-top mounds in water depths of about 80 m. Site 4 was located near medium-relief “pinnacle” mounds along the shelf edge; this was the deepest site, with the mooring at about 112 m. At Site 9, the mooring was located near low-relief hard bottom at about 92 m depth. (See Chapter 3 for bathymetric maps.) These four mooring locations were permanent and maintained throughout the two-year field program to provide long-term time-series data. The fifth and sixth moorings were re-locatable. During the first year, they were placed at Site 1 to form, in conjunction with the permanent mooring, a triangular pattern. They were moved to Site 5 in May 1998 (Cruise M3).

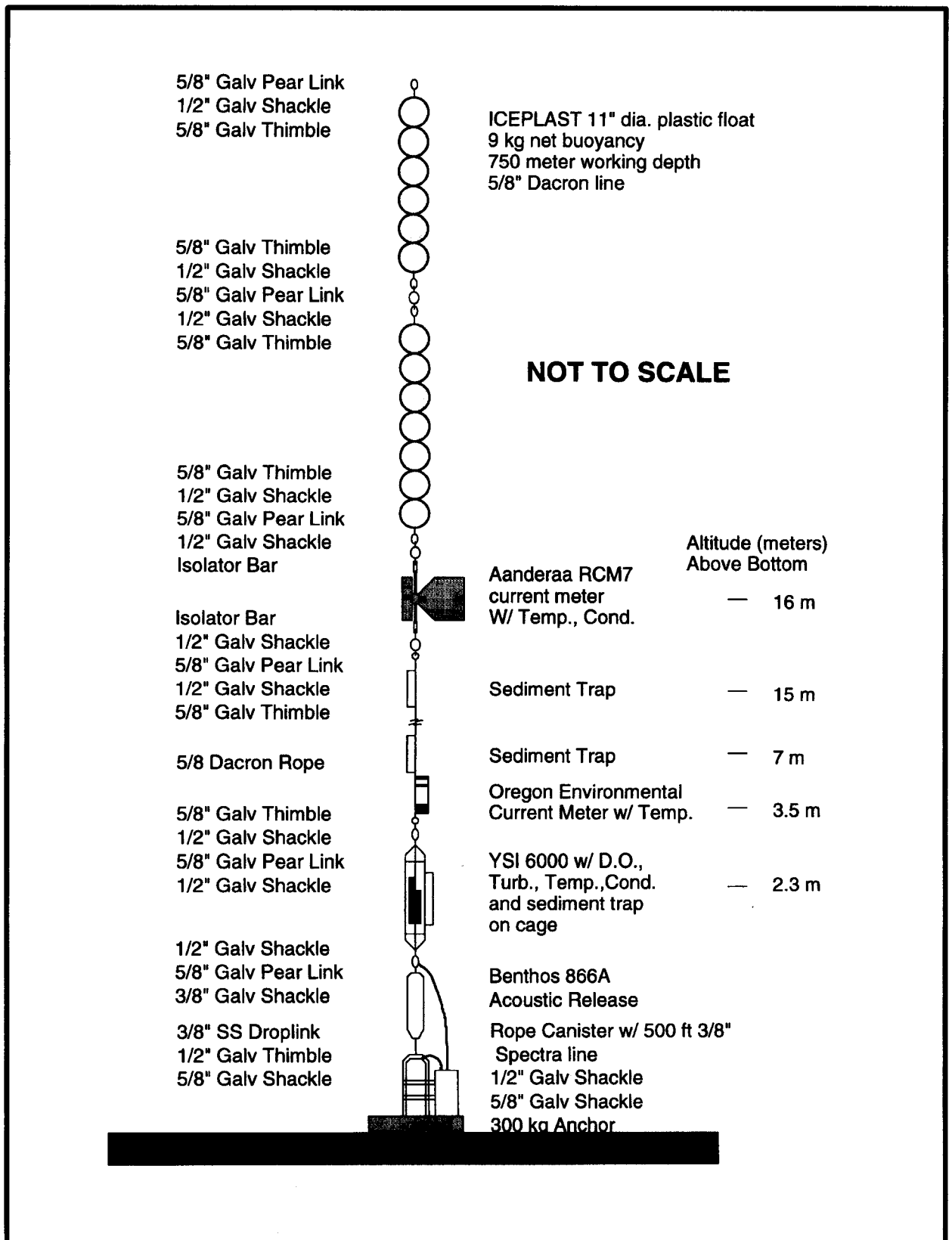


Fig. 6.1. Schematic drawing of the instrument mooring.

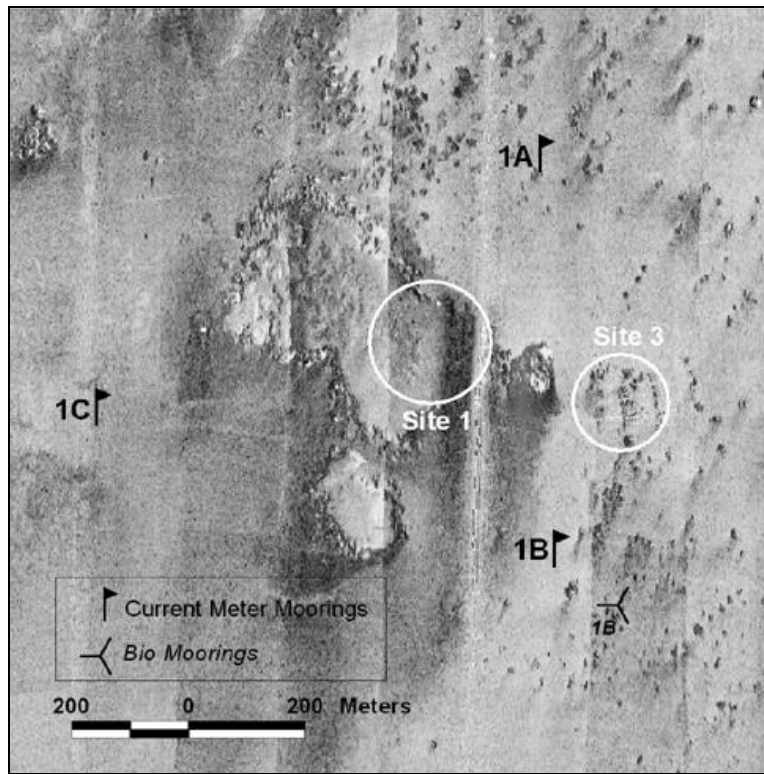


Fig. 6.2. Current meter mooring locations at Site 1 (indicated by flags). Mooring 1A was in place throughout the program (periods 1–8), whereas 1B and 1C were present only for periods 1–4. Triad indicates biomooing (see Chapter 10).

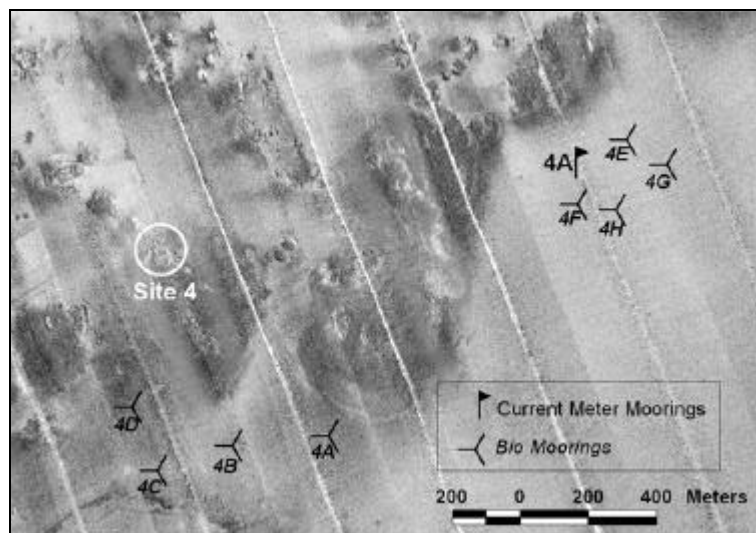


Fig. 6.3. Current meter mooring location at Site 4 (indicated by flag). Mooring 4A was in place throughout the program (periods 1–8). Triads indicate biomoorings (see Chapter 10).

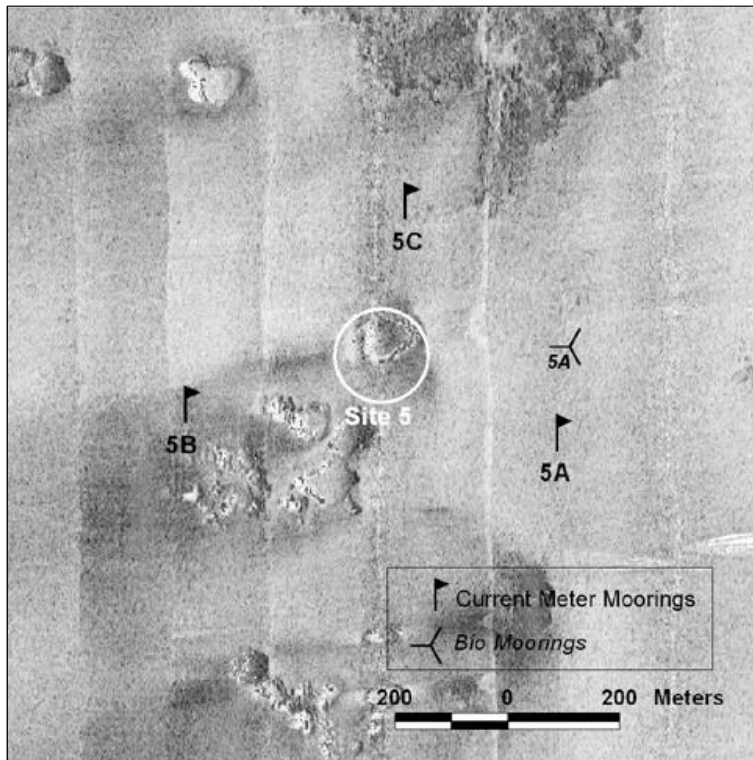


Fig. 6.4. Current meter mooring locations at Site 5 (indicated by flags). Mooring 5A was in place throughout the program (periods 1–8), whereas moorings 5B and 5C were present only for periods 4–8. Triad indicates biomoooring (see Chapter 10).

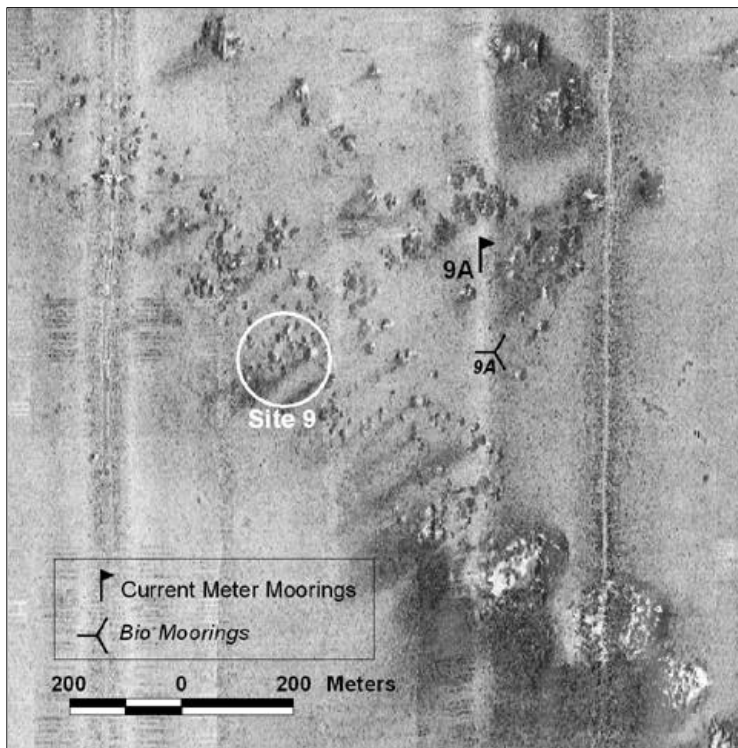


Fig. 6.5. Current meter mooring location at Site 9 (indicated by flag). Mooring 9A was in place throughout the program (periods 1–8). Triad indicates biomoooring (see Chapter 10).

Nine cruises were conducted to collect CTD profiles and to deploy and service the moorings over eight deployment periods. Cruise dates, type of CTD and number of casts by cruise are summarized in **Table 6.1**. (The table lists 10 entries because sampling was conducted on both legs of Cruise M4.) CTD casts were made at all nine sites during the monitoring cruises (1C, M2, M3, and M4), but only at four sites during mooring servicing cruises. The details of the operations and logistics for each cruise are presented in Chapter 2. The locations, dates, and times of deployment of the instrument moorings are summarized in **Table 6.2**.

Table 6.1. Cruise dates, designations, and CTD cast information.

Cruise	Seq.	Start	End	CTD Casts	Instrument type
1C	c1	5/21/97	5/24/97	29	SBE-911
S1	c2	7/28/97	7/29/97	11	SBE 19 SEACAT
M2	c3	9/30/97	10/31/97	25	SBE-911
S2	c4	1/29/98	1/30/98	12	SBE-911
M3	c5	4/24/98	5/3/98	31	SBE-911
S3	c6	7/20/98	7/22/98	11	SBE-911
S4	c7	10/13/98	10/14/98	12	SBE-911
S5	c8	2/9/99	2/10/99	12	SBE-911
M4 Leg 1	c9	4/14/99	4/15/99	6	SBE-911
M4 Leg 2	c10	7/29/99	8/6/99	30	SBE 19 SEACAT

During monitoring cruises, three CTD casts were conducted around each site, weather and time permitting, and additional casts were made to support the mooring operations, yielding 25–31 casts. On mooring service cruises, only the six mooring sites were visited, yielding 11–12 casts. (The April 1999 cruise [M4 Leg 1] was a recovery-only cruise.) At sites with moorings, CTD locations were chosen to be close to the moorings. Usually, a cast was made before a mooring was released, and a cast was made after a new mooring was deployed. The CTD was always lowered as close to the bottom as the sea state would permit, so that the CTD data could be used as a quality control check on the data recorded at the beginning and end of the moored records.

During the February 1999 cruise (S5), mooring 5C would not surface. A fishing boat off Destin, Florida found the mooring's flotation and top (RCM7) current meter in May 1999. The data are good through about the beginning of February 1999. The bottom instruments and acoustic release were lost. A spare mooring with an upper and lower RCM7 current meter (but no YSI oxygen/turbidity meter) was deployed at Site 5C during the February 1999 cruise.

Equipment

Moorings

Six multi-parameter physical oceanography moorings were deployed. Their principal components are shown in **Fig. 6.1**.

Table 6.2. Locations, dates, and times of deployment of the instrument moorings.

ID	Depth	Date In	Time (UTC)	Date Out	Time (UTC)	Easting	Northing	Lat Degree	Lat Min	Lat Sec	Lon Degree	Lon Min	Lon Sec
C1A1	78	05/23/97	0339	07/28/97	1231	444520.7	3256839.9	29	26	28.75	87	34	19.32
C1A2	78	07/28/97	1433	10/03/97	0230	444555.0	3256881.2	29	26	30.09	87	34	18.05
C1A3	80	10/04/97	0826	01/29/98	1656	444532.0	3256877.9	29	26	29.98	87	34	18.91
C1A4		01/29/98	1912	04/04/98	1521	444587.9	3256837.3	29	26	28.67	87	34	16.82
C1A5	77	04/24/98	1925	07/20/98	2332	444704.4	3256821.1	29	26	28.16	87	34	12.50
C1A6	77	07/21/98	0203	10/13/98	1548	444721.0	3256824.0	29	26	28.26	87	34	11.89
C1A7	78	10/13/98	1809	02/09/99	1233	444703.5	3256832.3	29	26	28.53	87	34	12.53
C1A8	75	02/09/99	1454	04/14/99	0348	444700.0	3256831.0	29	26	28.50	87	34	12.65
C1B1	81	05/23/97	0457	07/28/97	1509	444544.5	3256163.9	29	26	6.79	87	34	18.31
C1B2	79	07/28/97	1637	10/03/97	0140	444608.6	3256226.7	29	26	8.84	87	34	15.95
C1B3	83	10/04/97	0717	01/29/98	2104	444581.1	3256249.9	29	26	9.59	87	34	16.97
C1B4		01/29/98	2252	04/24/98	2034	444523.3	3256180.3	29	26	7.31	87	34	19.10
C1C1	82	05/23/97	0109	07/28/97	1739	443761.2	3256406.8	29	26	14.56	87	34	47.43
C1C2	82	07/28/97	1913	10/03/97	0333	443793.8	3256445.8	29	26	15.83	87	34	46.23
C1C3	83	10/03/97	1206	01/30/98	0027	443792.9	3256456.9	29	26	16.18	87	34	46.26
C1C4	81	01/30/98	0205	04/25/98	0035	443879.4	3256453.1	29	26	16.07	87	34	43.06
C4A1	115	05/21/97	2121	10/29/97	1730	426583.3	3244597.2	29	19	47.66	87	45	22.15
C4A2	na	na	na	na	na								
C4A3	112	10/30/97	0643	01/30/98	0540	426551.2	3244767.9	29	19	53.20	87	45	23.38
C4A4		01/30/98	0906	05/01/98	1800	426721.2	3244688.8	29	19	50.66	87	45	17.06
C4A5	113	05/01/98	1957	07/21/98	0512	426675.8	3244722.9	29	19	51.76	87	45	18.75
C4A6	113	07/21/98	2157	10/13/98	2032	426681.0	3244824.0	29	19	55.05	87	45	18.58
C4A7	111	10/13/98	2229	02/09/99	1649	426657.8	3244812.6	29	19	54.67	87	45	19.44
C4A8	112	02/09/99	1927	04/14/99	0709	426651.0	3244816.0	29	19	55.09	87	45	19.69

Table 6.2. (continued).

ID	Depth	Date In	Time (UTC)	Date Out	Time (UTC)	Easting	Northing	Lat Degree	Lat Min	Lat Sec	Lon Degree	Lon Min	Lon Sec
C5A1	81	05/23/97	1303	07/29/87	0206	405132.8	3251628.7	29	23	30.94	87	58	39.59
C5A2	82	07/29/97	0340	10/06/97	0426	405132.8	3251592.8	29	23	29.77	87	58	39.58
C5A3	82	10/06/97	0717	01/30/98	1221	405119.8	3251578.2	29	23	29.29	87	58	40.06
C5A4		01/30/98	1403	05/01/98	1348	405088.9	3251517.0	29	23	27.29	87	58	41.18
C5A5	79	05/01/98	1618	07/21/98	1724	405074.4	3251623.1	29	23	30.74	87	58	41.75
C5A6	79	07/22/98	0659	10/14/98	0315	405129.3	3251625.0	29	23	30.82	87	58	39.71
C5A7	78	10/14/98	0515	02/10/99	0037	405134.1	3251632.0	29	23	34.28	87	58	39.54
C5A8	78	02/10/99	0322	04/14/99	1220	405134.0	3251637.0	29	23	31.20	87	58	39.50
C5B5	82	05/01/98	1137	07/21/98	1551	404551.0	3251700.6	29	23	33.11	87	59	1.19
C5B6	78	07/22/98	0737	10/14/98	0235	404473.1	3251710.2	29	23	33.40	87	59	4.09
C5B7	78	10/14/98	0558	02/09/99	2358	404451.3	3251715.9	29	23	33.58	87	59	4.90
C5B8	78	02/10/99	0454	04/14/99	1142	404462.0	3251703.0	29	23	33.18	87	59	4.50
C5C5	79	05/01/98	1250	07/21/98	1456	404864.7	3252078.8	29	23	43.33	87	58	49.67
C5C6	78	07/22/98	0823	10/14/98	0205	404862.0	3252075.7	29	23	45.38	87	58	49.78
C5C7	79	10/14/98	0650	na	na	404878.5	3252069.8	29	23	45.20	87	58	49.16
C5C8	78	02/10/99	1405	04/14/99	1115	405010.0	3252201.0	29	23	49.50	87	58	44.33
C9A1	91	05/23/97	2030	07/29/97	0718	371417.2	3235151.9	29	14	24.89	88	19	23.29
C9A2	93	07/29/97	0900	10/31/97	0600	371400.2	3235151.4	29	14	24.78	88	18	23.92
C9A3	94	10/31/98	0858	01/30/98	1818	371134.1	3235538.5	29	14	37.35	88	19	33.94
C9A4	93	01/30/98	1957	05/02/98	0000	371053.6	3235704.3	29	14	42.70	88	19	36.98
C9A5	92	05/02/98	0158	07/22/98	0224	371252.9	3235236.2	29	14	27.57	88	19	29.41
C9A6	88	07/22/98	0339	10/14/98	1144	371226.2	3235241.2	29	14	27.73	88	19	30.40
C9A7	91	10/14/98	1254	02/10/99	0824	371197.2	3235253.4	29	14	28.11	88	19	31.48
C9A8	90	02/10/99	1033	04/14/99	1530	371190.0	3235250.0	29	14	28.00	88	19	31.73

Abbreviations: UTC = Coordinated Universal Time.

A mooring was constructed using 5/8-inch Dacron rope. The linkage between the acoustic release and the anchor was also rope, rather than chain, so that it could be cut by an ROV should the release fail. The rope canister contained 152 m of 3/8-inch Spectra line, a length that permitted the mooring to rise to the surface and be recovered before pulling up the anchor. Strings of ICEPLAST Model 1102 plastic floats (9 kg of net buoyancy each) provided flotation. Static mooring analysis was computed for the mooring using the program BUOY2.41 developed by Specialty Devices Inc. The amount of flotation was selected to assure that mooring “blow-over” was less than 1.0 m for current profiles up to 40 cm/s. (However, peak current speed at the upper current meter exceeded this value at times and was more than double it during Hurricane Georges.) A Benthos Model 866A Continental Shelf Release was used on each current mooring.

Current Meters

The bottom current meter on each mooring was an Oregon Environmental, Inc. (OEI) Model 9407 with temperature sensor. The top current meter on each mooring was an Aanderaa Model RCM7 with conductivity and temperature sensors. On occasion, a spare RCM7 replaced the OEI current meter. Both types vector-averaged currents, recorded into battery-backed solid-state memory, and downloaded directly to PC-type computers. Each instrument was serviced according to the manufacturers’ instructions before and after deployment.

The OEI current meter suffered from firmware bugs and a fragile compass. The former caused no data to be recorded sometimes. The latter has resulted in uncertainty in the quality of the direction values in many of the OEI meters during the second field year. Unfortunately, OEI went out of business in February 1999. We conducted a calibration of the OEI meters and a review of all the data collected by these instruments. Unfortunately, much of the direction data must be rejected, as indicated in **Table 6.3**.

Dissolved Oxygen and Turbidity Recorders

A YSI Model 6000 recording system with oxygen, turbidity, temperature, and conductivity sensors was immediately below the OEI current meter. The YSI 6000 also recorded internally. An external battery pack extended the instrument’s total battery life to at least four months.

To reduce biofouling, the standard sensor-guard of the YSI 6000 (conceptually, a cup with holes in it) was replaced with an “anti-fouling sensor-guard” custom manufactured by Oceanographic Industries of Miami Beach, FL. The inside of the guard was covered with an antifouling gel. Freshly coated guards were installed during each servicing cruise. Used guards were returned to the manufacturer for re-coating.

The dissolved oxygen sensor was calibrated to 100% saturation, following the manufacturer’s instructions, just prior to deployment. The turbidity sensor was calibrated using distilled water and a solution of standard turbidity provided by the manufacturer. The standard was a 100 nephelometric turbidity unit (NTU) \pm 2% solution made with Styreen/DVB Copolymer. The turbidity sensor was quite linear between 0 and 100 NTU, but the turbidity in the study region was low, usually less than 10 NTU. Therefore, a 10 NTU substandard was created by precision dilution.

Table 6.3. Summary of the time-series data return, sorted by deployment period and instrument locations.

ID	Start	UTC	Stop	UTC	Sensors	Comments
Mooring 1A						
C1A1 16 mab	05/23/97	4:30	07/28/97	12:00	V,T,C	--
C1A2 16 mab	07/28/97	16:00	10/03/97	1:30	V,T,C	Data gap 8/4 - 9/3
C1A3 16 mab	10/04/97	9:00	01/29/98	16:30	V,T,C	--
C1A4 16 mab	1/29/98	19:30	4/24/98	15:00	V,T,C	--
C1A5 16 mab	4/24/98	20:00	7/20/98	23:00	V,T,C	--
C1A6 16 mab	7/21/98	2:30	10/13/98	15:30	V,T,C	--
C1A7 16 mab	10/13/98	18:30	2/9/99	12:00	V,T,C	--
C1A8 16 mab	2/9/99	15:30	4/14/99	3:30	V,T,C	--
C1A1 4 mab	05/23/97	4:00	07/28/97	12:00	V,T	--
C1A2 4 mab	07/28/97	15:00	10/03/97	2:00	V,T	--
C1A3 4 mab	10/04/97	9:00	01/29/98	15:30	V,T	--
C1A4 4 mab	na	na	na	na	na	No data
C1A5 4 mab	4/24/98	20:00	7/20/98	12:00	V,T	--
C1A6 4 mab	7/21/98	2:30	10/13/98	15:30	V,T	Direction questionable, speed ok
C1A7 4 mab	na	na	na	na	na	No data
C1A8 4 mab	2/9/99	15:30	4/14/99	3:30	V,T	Direction bad; speed ok
O1A1	05/23/97	4:00	07/28/97	12:00	DO,Turb,T,C	--
O1A2	7/28/97	16:00	10/3/97	1:30	DO,Turb,T,C	Oxygen bad; turbidity ends 9/13/97
O1A3	na	na	na	na	na	Connector leaked - no data
O1A4	1/29/98	19:30	4/24/98	15:00	DO,Turb,T,C	--
O1A5	4/24/98	19:30	7/20/98	23:30	DO,Turb,T,C	Oxygen bad
O1A6	7/21/98	2:52	10/13/98	15:22	DO,Turb,T,C	--
O1A7	na	na	na	na	na	Connector leaked - no data
O1A8	2/9/99	15:30	4/14/99	3:30	DO,Turb,T,C	--

Table 6.3. (Continued).

ID	Start	UTC	Stop	UTC	Sensors	Comments
Mooring 1B						
C1B1 16 mab	05/23/97	4:00	07/28/97	13:00	V,T,C	--
C1B2 16 mab	07/28/97	17:30	10/03/97	0:30	V,T,C	No cond. data
C1B3 16 mab	10/04/97	8:00	01/29/98	20:30	V,T,C	--
C1B4 16 mab	1/29/98	23:00	4/24/98	21:00	V,T,C	--
C1B1 4 mab	05/23/97	5:30	07/28/97	15:00	V,T	--
C1B2 4 mab	07/28/97	17:00	10/03/97	0:00	V,T	Velocity ends 9/18/97 due to fouling
C1B3 4 mab	10/04/97	8:00	01/29/98	20:00	V,T	Velocity ends 1/17/98 due to fouling
C1B4 4 mab	na	na	na	na	na	No data
O1B1	05/23/97	5:30	07/28/97	15:00	DO,Turb,T,C	Turbidity data bad after 7/16/97
O1B2	7/28/97	17:30	10/3/97	0:30	DO,Turb,T,C	Turbidity bad
O1B3	10/04/97	8:00	01/29/98	20:30	DO,Turb,T,C	Turbidity bad
O1B4	1/29/98	23:00	4/24/98	20:00	DO,Turb,T,C	--
Mooring 1C						
C1C1 16 mab	05/23/97	7:00	07/28/97	17:30	V,T,C	--
C1C2 16 mab	07/28/97	19:30	10/03/97	3:00	V,T,C	--
C1C3 16 mab	10/03/97	12:30	01/30/98	0:00	V,T,C	--
C1C4 16 mab	01/30/98	2:30	04/25/98	0:00	V,T,C	--
C1C1 4 mab	na	na	na	na	na	No data recorded by OEI 9407
C1C2 4 mab	na	na	na	na	na	No data recorded by OEI 9407
C1C3 4 mab	10/03/97	12:30	01/30/98	0:00	V,T,C	RCM7 instead of 9407; velocity ends 10/29/97 -- fouling
C1C4 4 mab	1/30/98	2:30	4/25/98	0:30	V,T,C	RCM7 instead of 9407
O1C1	05/23/97	7:00	07/28/97	17:00	DO,Turb,T,C	--
O1C2	07/28/97	17:00	10/03/97	3:00	DO,Turb,T,C	--
O1C3	10/03/97	12:00	01/30/98	0:00	DO,Turb,T,C	Oxygen questionable
O1C4	1/29/98	23:00	4/24/98	20:00	DO,Turb,T,C	--

Table 6.3. (Continued).

ID	Start	UTC	Stop	UTC	Sensors	Comments
Mooring 4A						
C4A1 16 mab	05/22/97	3:00	08/04/97	12:30	V,T,C	Recording stopped by low battery; cond. sensor failed
C4A2 16 mab	na	na	na	na	na	Mooring not rotated during July 97 cruise
C4A3 16 mab	10/30/97	7:00	01/30/98	5:00	V,T,C	--
C4A4 16 mab	na	na	na	na	na	Bad Data Storage Unit
C4A5 16 mab	05/01/98	19:59	05/03/98	6:34	V,T,C	1-minute sample interval
C4A6 16 mab	7/21/98	22:30	10/13/98	19:30	V,T,C	--
C4A7 16 mab	10/13/98	23:00	2/9/99	16:30	V,T,C	--
C4A8 16 mab	2/9/99	20:00	4/14/99	6:30	V,T,C	--
C4A1 4 mab	na	na	na	na	na	No data recorded by OEI 9407
C4A2 4 mab	na	na	na	na	na	Mooring not rotated during July 97 cruise
C4A3 4 mab	10/30/97	7:00	01/30/98	5:00	V,T	--
C4A4 4 mab	1/30/98	9:30	5/1/98	18:00	V,T	--
C4A5 4 mab	na	na	na	na	na	No data
C4A6 4 mab	7/21/98	22:30	10/13/98	22:00	V,T	Direction bad; speed ok
C4A7 4 mab	10/13/98	23:00	2/9/99	11:30	V,T	Fouled after 12/1/98
C4A8 4 mab	2/9/99	20:00	4/14/99	6:30	V,T	--
O4A1	05/22/97	3:00	09/19/97	12:00	DO,Turb,T,C	Turbidity bad beginning 8/1/97
O4A2	na	na	na	na	na	Mooring not rotated during July 97 cruise
O4A3	na	na	na	na	na	Connector leaked - no data
O4A4	1/29/98	23:00	4/24/98	20:00	DO,Turb,T,C	Turbidity bad; oxygen bad after 2/15/98
O4A5	na	na	na	na	na	No data
O4A6	7/21/98	22:30	10/13/98	19:30	DO,Turb,T,C	--
O4A7	10/13/98	23:00	2/9/99	16:30	DO,Turb,T,C	--
O4A8	2/9/99	20:00	4/14/99	6:30	DO,Turb,T,C	--

Table 6.3. (Continued).

ID	Start	UTC	Stop	UTC	Sensors	Comments
Mooring 5A						
C5A1 16 mab	05/23/97	18:30	07/29/97	2:00	V,T,C	--
C5A2 16 mab	07/29/97	4:30	10/06/97	4:00	V,T,C	--
C5A3 16 mab	10/06/97	7:00	01/30/98	11:00	V,T,C	--
C5A4 16 mab	na	na	na	na	na	No data
C5A5 16 mab	05/01/98	16:19	05/03/98	6:35	V,T,C	1-minute sample interval
C5A6 16 mab	7/22/98	7:30	10/14/98	2:30	V,T,C	--
C5A7 16 mab	10/14/98	6:00	2/10/99	0:00	V,T,C	--
C5A8 16 mab	2/10/99	4:00	4/14/99	12:00	V,T,C	--
C5A1 4 mab	05/23/97	18:00	07/29/97	1:30	V,T	--
C5A2 4 mab	07/29/97	4:00	10/06/97	4:00	V,T	--
C5A3 4 mab	10/06/97	7:30	01/30/98	11:00	V,T	Velocity ends 12/1/97 due to fouling
C5A4 4 mab	1/30/98	15:00	5/1/98	13:30	V,T,C	RCM7
C5A5 4 mab	05/01/98	16:19	05/03/98	6:35	V,T,C	RCM7; 1-minute sample interval
C5A6 4 mab	7/22/98	7:30	10/14/98	3:00	V,T	Fouling problems
C5A7 4 mab	10/14/98	6:00	2/10/99	0:00	V,T	Fouling problems
C5A8 4 mab	2/10/99	4:00	4/13/99	12:00	V,T	--
O5A1	05/23/97	18:00	07/29/97	1:30	DO,Turb,T,C	--
O5A2	07/29/97	4:00	10/06/97	4:00	DO,Turb,T,C	Turbidity bad
O5A3	10/06/97	7:30	01/30/98	11:00	DO,Turb,T,C	--
O5A4	na	na	na	na	na	Not deployed
O5A5	5/1/98	13:00	7/21/98	14:30	DO,Turb,T,C	T, C, Oxygen end 6/11/98
O5A6	7/22/98	8:00	10/14/98	2:30	DO,Turb,T,C	--
O5A7	na	na	na	na	na	No data
O5A8	2/10/99	4:00	4/14/99	12:00	DO,Turb,T,C	Oxygen bad

Table 6.3. (Continued).

ID	Start	UTC	Stop	UTC	Sensors	Comments
Mooring 5B						
C5B5 16 mab	05/01/98	11:39	05/03/98	6:35	V,T,C	1-minute sample interval
C5B6 16 mab	7/22/98	8:00	10/14/98	2:00	V,T,C	--
C5B7 16 mab	10/14/98	6:30	2/9/99	23:30	V,T,C	--
C5B8 16 mab	2/10/99	5:30	4/14/99	11:00	V,T,C	--
C5B5 4 mab	5/1/98	12:00	7/21/98	15:30	V,T	--
C5B6 4 mab	7/22/98	8:00	10/14/98	2:00	V,T	Direction questionable
C5B7 4 mab	10/14/98	6:30	2/10/99	0:00	V,T	Direction, temperature bad; speed ok
C5B8 4 mab	2/10/99	5:30	4/14/99	11:00	V,T	Direction questionable; speed ok
O5B5	5/1/98	12:30	6/28/98	8:00	DO,Turb,T,C	--
O5B6	7/22/98	8:00	9/5/98	5:30	DO,Turb,T,C	--
O5B7	na	na	na	na	na	--
O5B8	na	na	na	na	na	--
Mooring 5C						
C5C5 16 mab	5/1/98	13:30	7/21/98	14:30	V,T,C	--
C5C6 16 mab	7/22/98	9:00	10/14/98	1:30	V,T,C	--
C5C7 16 mab	10/14/98	7:30	2/10/99	0:00	V,T,C	--
C5C8 16 mab	2/10/99	14:30	4/14/99	10:30	V,T,C	--
C5C5 4 mab	na	na	na	na	na	No data
C5C6 4 mab	7/22/98	8:30	10/14/98	2:00	V,T	Direction questionable; speed ok
C5C7 4 mab	na	na	na	na	na	Instrument lost
C5C8 4 mab	2/10/99	14:30	4/14/99	10:30	V,T,C	RCM7
O5C5	5/1/98	16:55	7/21/98	16:55	DO,Turb,T,C	--
O5C6	7/22/98	9:00	8/10/98	15:30	DO,Turb,T,C	--
O5C7	na	na	na	na	na	Instrument lost
O5C8	na	na	na	na	na	Instrument not deployed

Table 6.3. (Continued).

ID	Start	UTC	Stop	UTC	Sensors	Comments
Mooring 9A						
C9A1 16 mab	05/24/97	2:00	07/29/97	7:00	V,T,C	--
C9A2 16 mab	07/28/97	10:00	10/02/97	2:30	V,T,C	--
C9A3 16 mab	10/31/97	9:30	01/30/98	18:00	V,T,C	--
C9A4 16 mab	1/30/98	20:30	5/2/98	14:30	V,T,C	--
C9A5 16 mab	5/2/98	2:30	5/24/98	21:00	V,T,C	--
C9A6 16 mab	7/22/98	4:00	10/14/98	11:00	V,T,C	--
C9A7 16 mab	10/14/98	13:30	2/10/99	8:00	V,T,C	--
C9A8 16 mab	2/10/99	11:00	4/14/99	15:00	V,T,C	--
C9A1 4 mab	05/24/97	2:00	07/29/97	7:00	V,T	--
C9A2 4 mab	na	na	na	na	na	No data recorded by OEI 9407
C9A3 4 mab	10/31/97	9:30	01/30/98	18:00	V,T	--
C9A4 4 mab	1/30/98	20:30	3/11/98	4:00	V,T	--
C9A5 4 mab	5/2/98	2:30	7/22/98	2:00	V,T	--
C9A6 4 mab	7/22/98	4:00	10/14/98	11:30	V,T	Direction questionable; speed ok
C9A7 4 mab	na	na	na	na	na	No data
C9A8 4 mab	2/10/99	11:00	4/14/99	15:00	V,T,C	RCM7
O9A1	05/24/97	2:00	07/29/97	7:00	DO,Turb,T,C	Turbidity questionable
O9A2	07/28/97	10:00	10/02/97	2:30	DO,Turb,T,C	--
O9A3	10/31/97	9:30	01/30/98	18:00	DO,Turb,T,C	--
O9A4	1/30/98	21:00	5/1/98	23:30	DO,Turb,T,C	--
O9A5	5/2/98	2:30	7/22/98	2:00	DO,Turb,T,C	Turbidity bad
O9A6	na	na	na	na	na	No data
O9A7	10/14/98	14:00	11/29/98	13:30	DO,Turb,T,C	--
O9A8	2/10/99	11:00	4/14/99	15:00	DO,Turb,T,C	Oxygen bad

Abbreviations: mab = meters above bottom; na = not applicable; C = conductivity; DO = dissolved oxygen; T = temperature; V = velocity; UTC = Coordinated Universal Time.

Profiling Instruments

The primary system for continuous measurements was a Sea-Bird Electronics, Inc. SBE-911 CTD system with a SBE-11 deck unit. The Sea-Bird SBE-911 CTD is a research grade system that profiles temperature, salinity, and density at all ocean depths. The SBE-911 uses stable time-response matched sensors and fast, high-resolution parallel sampling for data acquisition. A SBE-19 SEACAT CTD was used on the July 1997 and July–August 1999 cruises.

In addition to providing precise measurements of temperature and salinity with depth, the TAMU/GERG Sea-Bird CTD system had other sensors integrated into its data acquisition unit. Continuous profiles of dissolved oxygen were measured with a Beckman polarographic type *in situ* dissolved oxygen sensor, manufactured by Sensor Medics, Inc. Mounted in the Sea-Bird SBE-911 Plus CTD, the oxygen sensor was attached to a manifold that permitted active pumping of water past the membrane. Great care was taken between each cast and between each cruise to assure that oil or grease did not foul the membrane. After each cruise, the standard Sea-Bird software was used to convert the oxygen sensor voltages into dissolved oxygen concentrations from which vertical profiles could be plotted. A sensor time delay of 3 seconds was used. These data are available for eight of the cruises.

Downwelling irradiance was measured with a Biospherical Instruments, Inc. Model QSP-200L irradiance profiling sensor. Particle scattering was measured with a Sea Tech light scattering sensor. In addition to the light scattering sensor, the CTD was equipped with a SeaTech, Inc. 25-cm transmissometer. Samples for discrete measurements of suspended particulate concentration (Chapter 5) were drawn from the 10-liter PVC Niskin bottles mounted on the General Oceanics rosette sampler, which was part of the CTD profiling system.

Collateral Data

Altimetry

Sea surface altimetry and computed geostrophic flows for the Gulf of Mexico were obtained from the University of Colorado's Colorado Center for Astrodynamic Research. The Center provides near real-time and archived maps of the sea surface height or height anomaly with superimposed velocity vectors at <http://www-ccar.colorado.edu/~realtime/gom-real-time vel/>. An analysis product is produced every weekday, based on the latest 10 days of TOPEX and 17 days of ERS-2 sampling.

Meteorological Buoy

The National Data Buoy Center (NDBC) buoy 42040 is a 3-m discus buoy that is located approximately 7 km from Site 9. The buoy supplies wind direction, wind speed, air temperature, water temperature, wave height, and wave period. We obtained the

hourly-averaged data for 1 January 1997 through 31 December 1999 from the NDBC Website at <http://www.ndbc.noaa.gov/>. The buoy's data are representative of the surface conditions at Megasite 5. They are the best available estimate of conditions at the other sites, with the possible exception of water temperature, because the distance to Megasite 1 (75 km) is less than the spatial scale of synoptic weather patterns that force the winds and waves, except for short time scales of a few hours.

Sea Surface Temperature (SST)

Sea surface temperatures for the Gulf of Mexico are made available by the Ocean Remote Sensing Group of the Johns Hopkins University Applied Physics Laboratory for research purposes. The Ocean Remote Sensing Group records and processes imagery from the AVHRR on the National Oceanic and Atmospheric Administration (NOAA) polar-orbiting satellites. Multi-day composite images for specific periods of interest were obtained from their website at <http://fermi.jhuapl.edu/avhrr/gm/index.html> and were used to help in the analysis of conditions occurring during cruises.

NEGOM Cruises

During the period of this study, five of the nine Northeast Gulf of Mexico (NEGOM) Chemical Oceanography and Hydrography cruises were also conducted (Jochens and Nowlin 2000) (**Table 6.4**). Figures (not shown) of dynamic height, gridded winds, sea surface salinity and sea surface temperature were obtained for use in this synthesis.

Table 6.4. Dates of NEGOM cruises relevant to this study.

Cruise	Date
N1	11/16/97 – 11/26/97
N2	5/4/98 – 5/15/98
N3	7/25/98 – 8/9/98
N4	11/12/98 – 11/25/98
N5	5/15/98 – 5/28/98

River Discharge

River discharge data were obtained for all the major rivers that empty into the Gulf between the Mississippi Delta and Cape San Blas: the Mississippi, the Pearl, the Pascagoula, the Tombigbee, the Alabama, the Escambia, and the Choctawatchee. These rivers contribute about 95% of the long-term freshwater flow onto the Mississippi-Alabama shelf. The daily-averaged discharge data for these rivers for 1 January 1997 to 30 September 1999 were obtained from the following seven sources. All except sources 4 and 5 are the last gauging stations prior to their respective rivers entering the Gulf.

1. The United State Army Corps of Engineers (USA COE) gauge 01100 on the Mississippi River at Tarbert Landing, near River Mile 306.3.
2. The United States Geological Service (USGS) station 02488500 on the Pearl River near Monticello, MS.
3. The USGS station 02479310 on the Pascagoula River at Graham Ferry, MS.
4. The USGS station 02467000 on the Tombigbee River at the Demoplois Lock and Dam.
5. The USGS station 02428400 on the Alabama River near Clairborne, AL.
6. The USGS station 02376033 on the Escambia River near Molino FL.
7. The USGS station 02366500 on the Choctawatchee River near Bruce, FL.

A time-series of combined freshwater flow onto the Mississippi-Alabama shelf was created (**Fig. 6.6**) from the above river discharge data. In keeping with convention used in the LATEX study (M. Howard, personal communication), we made the assumption that 50% of the Mississippi discharge measured at Tarbert Landing goes east when it reaches the Gulf. The Tombigbee and Alabama River discharges were combined into a proxy flow out of Mobile Bay using the same formula that was utilized for the LATEX program: $(1.07*(1.03*Alabama_Discharge+1.284*Tombigbee_Discharge))$.

Results

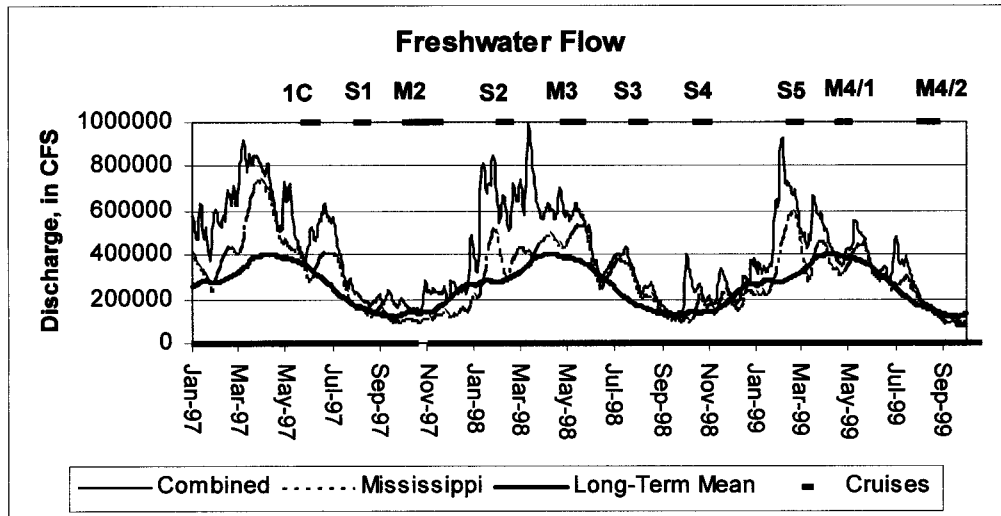
Time-Series Data

Each mooring nominally had three different instruments recording time series data. The upper one, at 16 mab, was always an Aanderaa RCM7 current meter with temperature and conductivity sensors (one vector and two scalar series). The current meter at 4 mab was usually an OEI 9407 current meter with a temperature sensor (one vector and one scalar series). On occasion, it was replaced with a RCM7. Just below it was a YSI 6000 Monitor with temperature, conductivity, dissolved oxygen, and turbidity sensors (four scalar series). For record keeping and graphical display purposes, a file naming convention identifies instrument type, site, position at site, deployment period, and for current meters, the height above bottom, e.g., C1B2 16 mab. The coding is as follows:

Instrument type: C = current meter, O = oxygen/turbidity system
 Site: 1, 4, 5, or 9
 Position at site: A, B, or C; generally, A is NNE of mound, B is SSE, C is W
 Deployment: 1, 2, 3, ...
 Height: 16 mab, or 4 mab (for instrument type C)

For basic data reporting, each instrument's time series data are plotted and reported as a group by deployment. A summary page (e.g., **Fig. 6.7**) for a current velocity record displays basic statistics, a scatter plot, and a table of joint frequency for speed and direction, which is the tabular version of a current rose. The start and stop times at the top of the summary page include all times for which the instrument's sensors produced good records. The number of points refers specifically to the velocity record, which may be shorter than the instrument's deployment period. Current velocity data are then

(a)



(b)

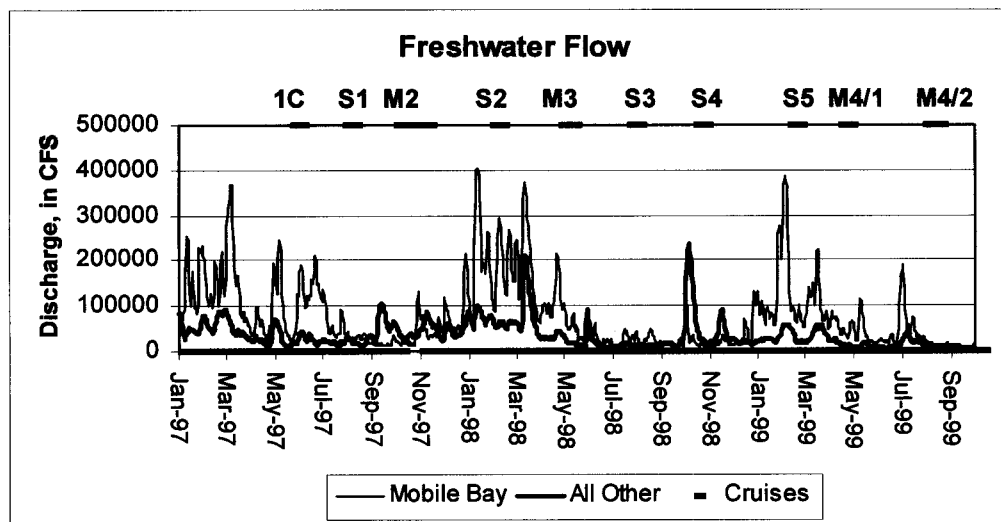
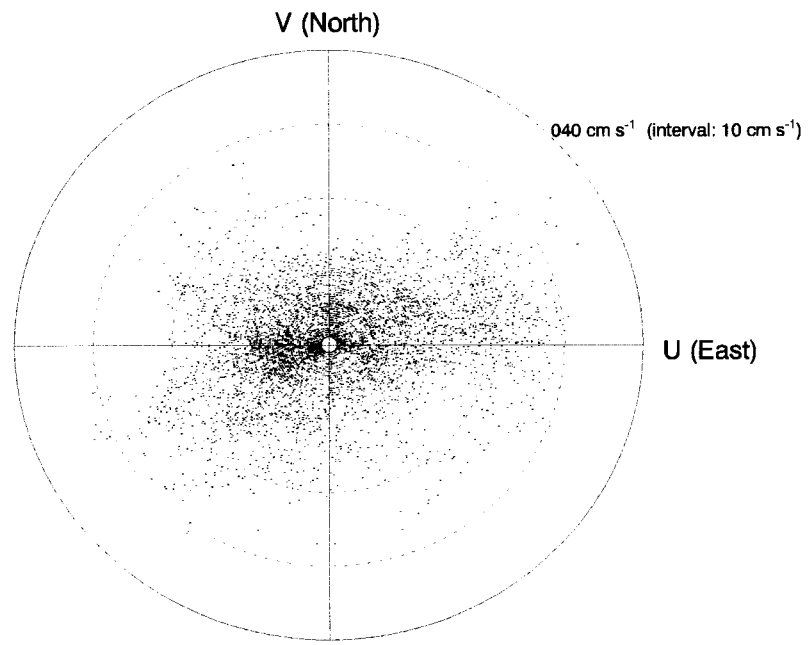


Fig. 6.6. Freshwater flow onto the Mississippi-Alabama shelf. (a) Combined flow for all seven major rivers, the 50% contribution from the Mississippi River, and the daily long-term mean flow contribution (50% of the total) of the Mississippi from 1961 - 1998. (b) Freshwater flow from Mobile Bay, which is calculated from the Tombigbee and Alabama Rivers, and the other four rivers, Pearl, Pascagoula, Escambia, and Choctawatchee Rivers.

C1A7 - 16 mab					
START TIME: 10/13/1998 18:30			STOP TIME: 02/09/1999 12:00 GMT		
	Num pts.	Mean	Std Dev	Minimum	Maximum
SPEED:	5700	9.80	6.56	1.10	34.50
U COMP:	5700	0.41	9.96	-29.99	31.65
V COMP:	5700	0.23	6.30	-26.99	24.73
MEAN CURRENT VECTOR:			0.47 cm s ⁻¹ @ 60.7° True		



	N	NE	E	SE	S	SW	W	NW	TOTAL
< 5	3.58	2.51	3.05	1.60	2.93	4.47	4.98	2.37	25.48
5 - 10	3.91	4.61	4.31	2.68	1.72	4.77	7.73	3.58	33.32
10 - 15	1.68	3.44	3.89	1.05	1.49	3.14	4.16	2.63	21.48
15 - 20	0.16	1.17	3.00	0.40	0.77	1.95	1.75	1.02	10.22
20 - 25	0.02	1.30	2.98	0.42	0.07	1.10	0.53	0.37	6.79
25 - 30	0.00	0.23	1.37	0.11	0.07	0.40	0.09	0.11	2.37
30 - 35	0.00	0.09	0.05	0.02	0.02	0.09	0.07	0.02	0.35
> 35	0.00	0.00	0.00	0.00	0.00	0.00	0.00	0.00	0.00
TOTAL	9.35	13.34	18.66	6.28	7.07	15.92	19.31	10.08	

Fig. 6.7. Example of a Summary Page (C1A7) for a current velocity time series.

plotted in time series format, together with scalar data collected at the same time by the current meter (e.g., **Fig. 6.8**). The scale is one month per page to visually resolve the tidal and inertial fluctuations in speed and direction. The four parameters measured by the YSI 6000 are also plotted as a time series group, but at a scale of one deployment period per page. With this latter format, the variability in dissolved oxygen and turbidity during the deployment can be seen (e.g., **Fig. 6.9**).

Only selected examples of the graphical records are used in this report to illustrate the principal features of the time-series records. A complete set of the data is published on a CD-ROM containing all project data.

The time-series data returned by the instruments are summarized in **Table 6.3**, sorted by deployment period and instrument location. Note that the period of a time-series record is usually shorter than the total period of deployment (**Table 6.2**) because of instrument equilibration at the beginning or other editing. The time between recovery and redeployment of instruments was usually a few hours. It was up to several days in duration during multidisciplinary monitoring cruises because of the logistical demands. Fouling, individual sensor failure, or total instrument failure also caused data gaps in the records. Fouling can bias the speed and/or direction sensors by causing drag or complete lock-up of the rotors and/or vanes. Fouling can bias the inductive-type conductivity sensors on the RCM7 by changing the effective cell constant. Each instrument was inspected upon recovery, and observations about the degree and effects of fouling were noted on the mooring log sheet. Several velocity records have been manually truncated after initial processing, based on these recovery notes and a subjective inspection of the time series plot. Most of the RCM7 current meters for the April–October 1999 deployment period were set incorrectly to a one-minute sample interval, which filled up memory in a few days.

Some of the OEI 9407 and YSI 6000 meters suffered total instrument failure. In the case of the OEI 9407, firmware bugs caused no data to be recorded at times. The YSI 6000 had some problems with waterproof connectors and fittings. Saltwater leakage caused some individual sensors to fail or the main logger to lose all data.

Tables of the joint frequency distribution (JFD) of speed and direction (tabular version of the current rose) and basic statistics provide a compact method of summarizing the large volume of observations of current velocity and other parameters collected at each location. For example, **Table 6.5a** gives the JFD for mooring 1A at 16 mab for all good current velocity data. Gaps and bad points are excluded in the analysis. The JFD gives the percentage of good observations that fell in each bin defined by the given speed range and direction octant. Rows and columns are summed to give the total percentage of observations that occurred in a given speed range or direction octant, respectively. The mean scalar speed for each direction octant is also listed. **Table 6.5b** lists the basic statistics for scalar variables and the mean velocity vector, based on the mean east and north components. Comparing the scalar mean speed and the vector mean velocity gives an idea of directional variability. The data are half-hourly, so the maximum number of points in a time series if all data were good is about 34,650. The same analyses for mooring 1A at 4 mab is given in **Table 6.6**. Because the upper and lower locations on the mooring have different lengths of reliable data, the analyses are also performed for

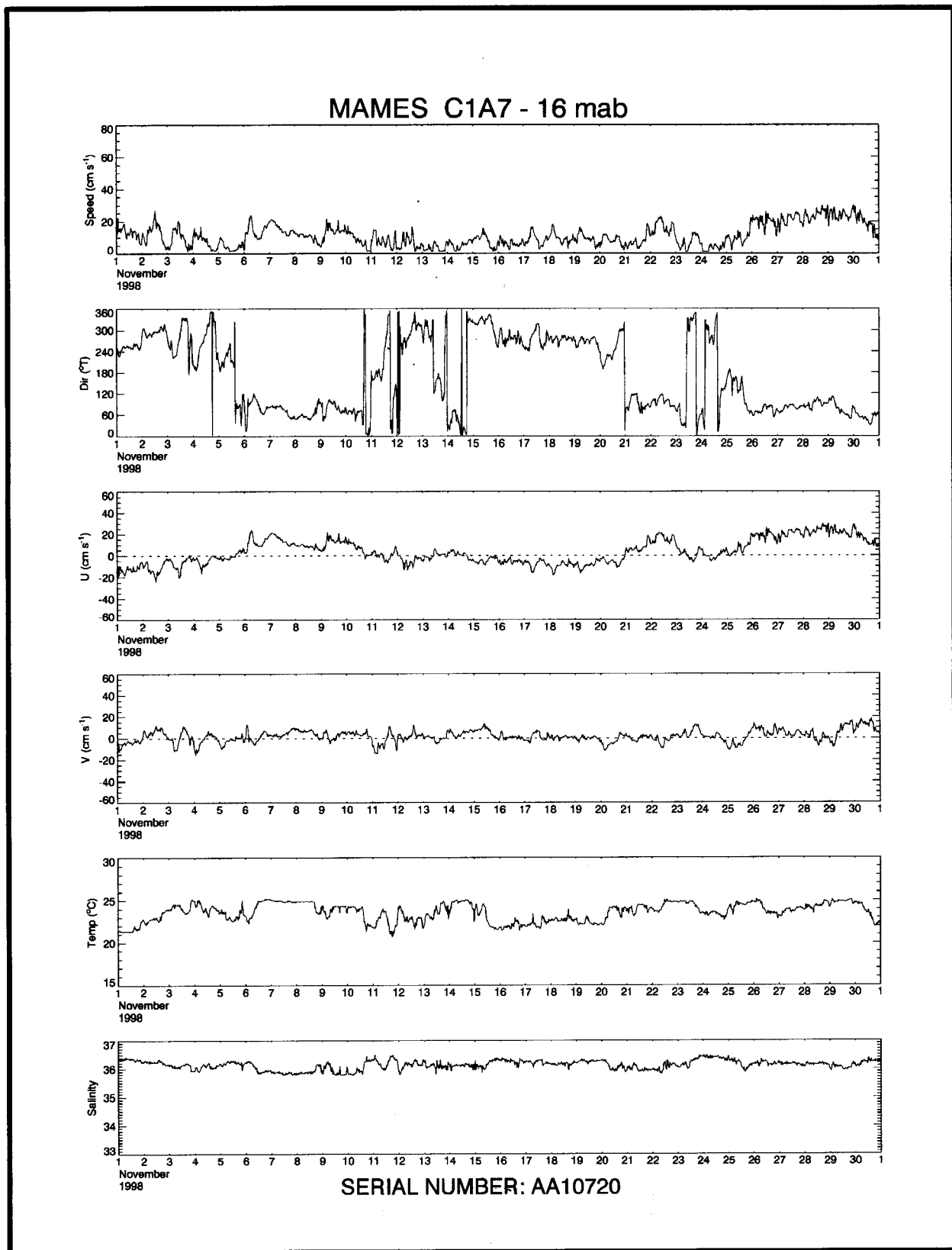


Fig. 6.8. Example of a monthly time-series plot (C1A7) for data recorded by a current meter.

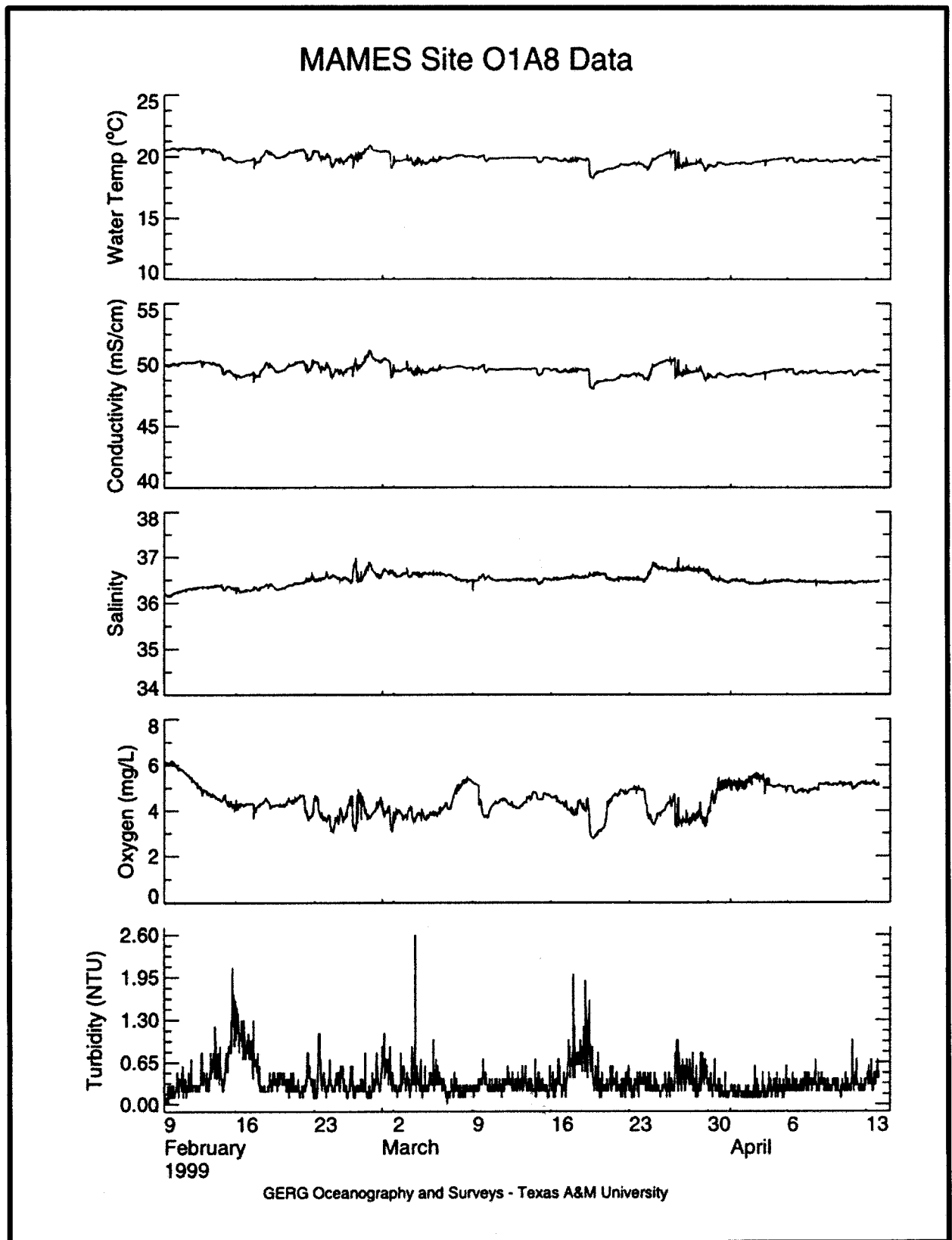


Fig. 6.9. Example of a plot of data (O1A8) collected by the YSI 6000 monitor.

Table 6.5. Data summary for mooring C1A, 16 mab, all good periods: C1A1, C1A3, C1A4, C1A5, C1A6, C1A7, and C1A8. (a) Joint Frequency Distribution (JFD) of speed and direction; (b) Basic statistics of scalar variables, mean current vector, principal axis orientation (deg. T), and magnitudes of major and minor axes (cm/s).

a)

Percent Occurrence in Each Speed-Direction Cell (No. Obs = 29351)

RANGE (CM/S)	N	NE	E	SE	S	SW	W	NW	ROW TOT
<=5	2.56	3.38	3.42	2.12	2.11	3.18	4.46	3.09	24.32
>5 <=10	3.14	4.96	5.12	2.69	3.14	4.57	5.52	3.74	32.87
>10 <=15	1.51	2.81	3.69	1.40	1.85	2.29	2.59	1.96	18.10
>15 <=20	0.52	2.31	3.48	0.70	0.80	1.80	1.34	0.66	11.59
>20 <=25	0.20	1.81	3.07	0.36	0.15	1.86	0.88	0.22	8.55
>25 <=30	0.04	0.48	0.98	0.04	0.04	0.93	0.39	0.09	3.01
>30 <=35	0.00	0.16	0.35	0.00	0.01	0.34	0.11	0.01	0.99
>35 <=40	0.00	0.03	0.05	0.00	0.01	0.14	0.01	0.00	0.25
>40	0.00	0.00	0.01	0.00	0.00	0.31	0.01	0.00	0.33
COL TOTALS	7.97	15.95	20.17	7.32	8.11	15.41	15.30	9.77	100.00
AVG. SPEED	7.9	11.3	13.0	8.7	8.7	13.2	9.2	8.1	

b)

Basic Stats

	Min.	Max.	Mean	Std.	Nobs.
SPEED:	1.1	96.7	10.6	7.8	29351
U (East):	-69.1	40.0	0.9	10.8	29351
V (North):	-73.5	29.9	-0.0	7.5	29351
T (Deg.C):	15.4	27.4	20.6	1.6	29351
Salinity:	35.0	37.0	36.2	0.3	29351

Mean Current Vector: 0.9 cm/s at 91.8 deg. True
Princax= 66.2 major= 11.5 minor= 6.5

Table 6.6. Data summary for mooring C1A, 4 mab, all good periods: C1A1, C1A2, C1A3, C1A5, and C1A8. (a) Joint Frequency Distribution (JFD) of speed and direction; (b) Basic statistics of scalar variables, mean current vector, principal axis orientation (deg. T), and magnitudes of major and minor axes (cm/s).

a)

Percent Occurrence in Each Speed-Direction Cell (No. Obs = 17881)

RANGE (CM/S)	N	NE	E	SE	S	SW	W	NW	ROW TOT
<=5	8.51	3.55	5.83	6.23	8.25	5.06	3.64	3.19	44.25
>5 <=10	4.38	3.13	4.26	7.35	8.15	4.32	1.76	2.37	35.71
>10 <=15	1.57	1.47	2.66	2.77	4.46	2.07	0.46	0.31	15.78
>15 <=20	0.31	0.43	0.79	0.16	1.12	0.39	0.05	0.01	3.25
>20 <=25	0.05	0.25	0.36	0.00	0.11	0.07	0.02	0.01	0.87
>25 <=30	0.03	0.02	0.08	0.00	0.00	0.00	0.00	0.01	0.13
>30 <=35	0.00	0.00	0.01	0.00	0.00	0.00	0.00	0.00	0.01
>35 <=40	0.00	0.00	0.00	0.00	0.00	0.00	0.00	0.00	0.00
>40	0.00	0.00	0.00	0.00	0.00	0.00	0.00	0.00	0.00
COL TOTALS	14.85	8.83	13.99	16.51	22.10	11.90	5.93	5.91	100.00
AVG. SPEED	4.7	7.2	7.2	6.5	7.1	6.5	4.6	5.0	

b)

Basic Stats

	Min.	Max.	Mean	Std.	Nobs.
SPEED:	0.0	30.8	6.3	4.5	17881
U (East):	-23.0	29.4	1.2	4.9	17881
V (North):	-22.9	26.6	-1.6	5.7	17881
T (Deg.C):	12.5	24.1	20.0	1.5	17881

Mean Current Vector: 2.0 cm/s at 142.7 deg. True
Princax= 20.3 major= 5.8 minor= 4.7

just the common periods (**Tables 6.7–6.8**), which allow an examination of vertical differences. In addition, the JFD from the common period can be compared with that from its longer “parent” data set to examine the temporal stability of the results. **Tables 6.9–6.20** give the JFDs and basic statistics in the same manner for moorings 4A, 5A, and 9A.

Principal axis analysis was performed for each vector time series to find the main orientation of fluid flow at the current meter location (**Table 6.21**). In this method, the orientations of the orthogonal axes are found that maximize and minimize the variances in the observed velocity fluctuations. The relative size of the magnitude of the major and minor axes indicates the ellipticity in a scatter plot of the data. Over the continental shelf, the mean and low frequency currents are generally “steered” parallel to the local bottom contours, and, as a result, the major axis is usually larger than the minor axis.

Vertical Profiles

CTD casts were taken during each of the monitoring and servicing cruises to assess the vertical profiles of salinity, temperature, PAR, transmissivity, backscattered light, and oxygen concentrations. During the monitoring cruises, three profiles were generally taken around each site to assess variability at each site. A total of 179 CTD stations were completed during the various cruises (**Table 6.1**). The data have been processed using the Seabird standard software. Plots of temperature, salinity, and sigma-theta have been prepared for all casts and are available, along with the data on the project’s CD-ROM. Temperature-salinity plots for each cruise are presented later in the Discussion section. Optical properties measured by the CTD are discussed in Chapter 5.

Unique Weather Events

The episodic spikes seen in the freshwater flow onto the Mississippi-Alabama shelf (**Fig. 6.6**) are indicative of weather events that had the potential to influence the study area, through either freshwater runoff or high winds. The following weather events had the potential to affect the physical oceanographic conditions in and around the study area.

July 1997

Hurricane Danny passed over the study area on 18 July. This was 10 days before the commencement of Cruise S1. A slow-moving hurricane, Danny stalled for 18 hours over southern Alabama and resulted in extremely high rainfall totals. A 24-hour rainfall total of 32.51 inches was officially recorded at Dauphin Island Sea Lab’s observing site. Dauphin Island is approximately 64 nmi to the north of Site 9. This is the fifth largest rainfall recorded in United States history and the largest in Alabama’s. Doppler radar estimates confirm maximum storm total precipitation amounts were around 43 inches near Dauphin Island. The Tropical Prediction Center of the National Weather Service estimated that most of the extreme precipitation occurred over ungauged regions near the coast or over water near southwestern Mobile Bay. This is evident in the relatively small amount of gauged river runoff associated with this storm.

Table 6.7. Data summary for mooring C1A, 16 mab, for periods in common with 4 mab: C1A1, C1A3, C1A5, and C1A8. (a) Joint Frequency Distribution (JFD) of speed and direction; (b) Basic statistics of scalar variables, mean current vector, principal axis orientation (deg. T), and magnitudes of major and minor axes (cm/s).

a)										
Percent Occurrence in Each Speed-Direction Cell (No. Obs. = 16048)										
RANGE (CM/S)	N	NE	E	SE	S	SW	W	NW	ROW TOT	
<=5	2.47	4.49	4.22	2.43	1.94	2.68	3.74	3.46	25.43	
>5 <=10	3.05	6.03	5.90	2.85	3.43	4.28	4.49	3.71	33.75	
>10 <=15	1.63	3.30	4.02	1.61	1.76	1.74	1.63	1.61	17.30	
>15 <=20	0.45	3.26	4.27	0.56	0.69	1.28	0.68	0.45	11.66	
>20 <=25	0.24	2.35	3.88	0.22	0.15	0.99	0.40	0.09	8.33	
>25 <=30	0.00	0.69	1.15	0.02	0.02	0.32	0.11	0.06	2.37	
>30 <=35	0.00	0.24	0.63	0.00	0.02	0.04	0.02	0.02	0.98	
>35 <=40	0.00	0.06	0.09	0.00	0.02	0.00	0.00	0.00	0.17	
>40	0.00	0.00	0.01	0.00	0.00	0.00	0.00	0.00	0.01	
COL TOTALS	7.85	20.43	24.17	7.70	8.03	11.35	11.07	9.42	100.00	
AVG. SPEED	7.9	11.6	13.3	8.0	8.6	10.1	7.8	7.3		

b)					
Basic Stats	Min.	Max.	Mean	Std.	Nobs.
SPEED:	1.1	40.6	10.2	7.2	16048
U (East):	-31.7	40.0	3.2	9.9	16048
V (North):	-36.4	23.8	1.0	6.8	16048
T (Deg.C):	15.6	23.4	20.5	1.1	16048
Salinity:	35.0	37.0	36.3	0.3	16048
Mean Current Vector:	3.4 cm/s at 73.1 deg. True				
Princax=	69.1 major= 10.4 minor= 6.1				

Table 6.8. Data summary for mooring C1A, 4 mab, for periods in common with 16 mab: C1A1, C1A3, C1A5, and C1A8. (a) Joint Frequency Distribution (JFD) of speed and direction; (b) Basic statistics of scalar variables, mean current vector, principal axis orientation (deg. T), and magnitudes of major and minor axes (cm/s).

a)										
Percent Occurrence in Each Speed-Direction Cell (No. Obs. = 15064)										
RANGE (CM/S)	N	NE	E	SE	S	SW	W	NW	ROW TOT	
<=5	9.38	3.80	5.48	5.51	7.59	4.65	3.34	3.08	42.82	
>5 <=10	4.75	3.60	4.45	6.49	7.35	4.31	1.85	2.30	35.10	
>10 <=15	1.65	1.73	3.09	2.64	4.69	2.46	0.55	0.34	17.15	
>15 <=20	0.31	0.50	0.93	0.15	1.32	0.46	0.06	0.01	3.74	
>20 <=25	0.06	0.29	0.43	0.00	0.13	0.08	0.02	0.01	1.03	
>25 <=30	0.03	0.02	0.10	0.00	0.00	0.00	0.00	0.01	0.16	
>30 <=35	0.00	0.00	0.01	0.00	0.00	0.00	0.00	0.00	0.01	
>35 <=40	0.00	0.00	0.00	0.00	0.00	0.00	0.00	0.00	0.00	
>40	0.00	0.00	0.00	0.00	0.00	0.00	0.00	0.00	0.00	
COL TOTALS	16.18	9.94	14.48	14.79	21.08	11.95	5.82	5.76	100.00	
AVG. SPEED	4.6	7.4	7.7	6.5	7.4	7.0	4.9	5.0		

b)					
Basic Stats	Min.	Max.	Mean	Std.	Nobs.
SPEED:	0.0	30.8	6.5	4.7	15064
U (East):	-23.0	29.4	1.3	5.1	15064
V (North):	-22.9	26.6	-1.4	5.9	15064
T (Deg.C):	12.5	24.1	20.0	1.6	15064
Mean Current Vector:	1.9 cm/s at 137.7 deg. True				
Princax=	25.8 major= 6.1 minor= 4.9				

Table 6.9. Data summary for mooring 4A, 16 mab, all good periods: C4A1, C4A3, C4A6, C4A7, and C4A8. (a) Joint Frequency Distribution (JFD) of speed and direction; (b) Basic statistics of scalar variables, mean current vector, principal axis orientation (deg. T), and magnitudes of major and minor axes (cm/s).

a)										
Percent Occurrence in Each Speed-Direction Cell (No. Obs = 20758).										
RANGE (CM/S)	N	NE	E	SE	S	SW	W	NW	ROW TOT	
<=5	1.61	2.58	3.08	2.60	1.94	3.09	3.47	2.46	20.84	
>5 <=10	1.89	4.76	7.25	2.61	2.14	7.14	5.97	1.58	33.34	
>10 <=15	0.39	2.64	6.30	0.87	0.50	5.60	3.37	0.28	19.94	
>15 <=20	0.09	1.36	5.03	0.53	0.08	5.25	2.41	0.03	14.77	
>20 <=25	0.02	0.84	2.12	0.17	0.03	3.69	1.64	0.00	8.51	
>25 <=30	0.00	0.12	0.33	0.05	0.01	1.13	0.20	0.00	1.85	
>30 <=35	0.00	0.00	0.10	0.00	0.00	0.30	0.04	0.00	0.44	
>35 <=40	0.00	0.00	0.03	0.01	0.00	0.06	0.02	0.00	0.12	
>40	0.00	0.00	0.01	0.00	0.00	0.09	0.09	0.00	0.18	
COL TOTALS	4.01	12.30	24.24	6.84	4.71	26.35	17.20	4.36	100.00	
AVG. SPEED	6.2	9.9	12.0	7.5	6.2	13.4	10.8	4.9		

b)						
Basic Stats	Min.	Max.	Mean	Std.	Nobs.	
SPEED:	1.0	65.9	10.8	6.9	20758	
U (East):	-60.1	41.4	-0.6	11.3	20758	
V (North):	-33.8	22.6	-1.7	5.8	20758	
T (Deg.C):	10.9	22.6	19.0	1.3	20758	
Salinity:	35.4	36.8	36.4	0.2	17186	
Mean Current Vector:	1.8 cm/s at 199.6 deg. True					
Princax=	70.4 major= 11.8 minor= 4.5					

Table 6.10. Data summary for mooring 4A, 4 mab, all good periods: C4A3, C4A4, C4A7, and C4A8. (a) Joint Frequency Distribution (JFD) of speed and direction; (b) Basic statistics of scalar variables, mean current vector, principal axis orientation (deg. T), and magnitudes of major and minor axes (cm/s).

a)										
Percent Occurrence in Each Speed-Direction Cell (No. Obs = 12074)										
RANGE (CM/S)	N	NE	E	SE	S	SW	W	NW	ROW TOT	
<=5	3.29	2.58	2.75	1.97	4.17	4.71	3.78	1.94	25.19	
>5 <=10	1.97	3.41	2.49	2.18	3.88	7.77	3.96	1.14	26.80	
>10 <=15	1.18	1.54	1.75	1.08	3.95	10.40	4.27	0.65	24.81	
>15 <=20	0.27	0.41	0.84	0.27	1.83	6.99	2.48	0.12	13.21	
>20 <=25	0.14	0.12	0.29	0.02	0.92	3.43	0.61	0.02	5.57	
>25 <=30	0.08	0.04	0.11	0.06	0.27	1.53	0.35	0.01	2.44	
>30 <=35	0.00	0.02	0.03	0.02	0.12	0.75	0.06	0.00	0.99	
>35 <=40	0.00	0.00	0.02	0.03	0.03	0.38	0.11	0.00	0.57	
>40	0.00	0.00	0.02	0.00	0.03	0.30	0.07	0.00	0.42	
COL TOTALS	6.92	8.13	8.30	5.63	15.19	36.26	15.69	3.88	100.00	
AVG. SPEED	6.4	7.7	8.8	7.5	10.1	13.6	10.6	6.0		

b)						
Basic Stats	Min.	Max.	Mean	Std.	Nobs.	
SPEED:	0.0	52.7	10.6	7.4	12074	
U (East):	-50.6	40.9	-3.9	8.5	12074	
V (North):	-46.5	28.3	-4.4	7.8	12074	
T (Deg.C):	10.8	21.1	17.7	2.1	12074	
Mean Current Vector:	5.9 cm/s at 221.6 deg. True					
Princax=	50.6 major= 9.9 minor= 5.9					

Table 6.11. Data summary for mooring 4A, 16 mab, for periods in common with 4 mab: C4A3, C4A7 (through 11-30-98), and C4A8. (a) Joint Frequency Distribution (JFD) of speed and direction; (b) Basic statistics of scalar variables, mean current vector, principal axis orientation (deg. T), and magnitudes of major and minor axes (cm/s).

a)									
Percent Occurrence in Each Speed-Direction Cell (No. Obs. = 9765)									
RANGE (CM/S)	N	NE	E	SE	S	SW	W	NW	ROW TOT
<=5	1.38	1.88	2.09	2.88	1.83	3.68	3.68	2.46	19.88
>5 <=10	1.98	4.26	7.37	2.73	1.83	8.80	7.05	1.75	35.77
>10 <=15	0.36	2.08	5.05	0.95	0.44	6.35	3.90	0.38	19.51
>15 <=20	0.09	1.02	3.57	0.54	0.08	5.84	2.44	0.06	13.65
>20 <=25	0.05	0.73	1.77	0.20	0.03	3.86	2.46	0.00	9.10
>25 <=30	0.00	0.15	0.38	0.05	0.02	0.80	0.31	0.00	1.71
>30 <=35	0.00	0.00	0.11	0.01	0.00	0.11	0.03	0.00	0.27
>35 <=40	0.00	0.00	0.06	0.00	0.00	0.02	0.01	0.00	0.09
>40	0.00	0.00	0.02	0.00	0.00	0.00	0.00	0.00	0.02
COL TOTALS	3.86	10.13	20.43	7.37	4.24	29.45	19.87	4.65	100.00
AVG. SPEED	6.5	10.0	11.9	7.5	6.2	12.5	10.9	5.2	

b)					
Basic Stats	Min.	Max.	Mean	Std.	Nobs.
SPEED:	1.0	41.7	10.6	6.6	9765
U (East):	-34.0	41.4	-1.6	10.9	9765
V (North):	-27.4	22.6	-2.0	5.5	9765
T (Deg.C):	10.9	21.4	18.8	1.6	9765
Salinity:	35.5	36.8	36.4	0.2	9765
Mean Current Vector: 2.6 cm/s at 219.5 deg. True					
Princax= 71.8 major= 11.3 minor= 4.5					

Table 6.12. Data summary for mooring 4A, 4 mab, for periods in common with 16 mab: C4A3, C4A7 (through 11-30-98), and C4A8. (a) Joint Frequency Distribution (JFD) of speed and direction; (b) Basic statistics of scalar variables, mean current vector, principal axis orientation (deg. T), and magnitudes of major and minor axes (cm/s).

a)									
Percent Occurrence in Each Speed-Direction Cell (No. Obs. = 9235)									
RANGE (CM/S)	N	NE	E	SE	S	SW	W	NW	ROW TOT
<=5	4.03	3.15	3.39	2.41	4.32	4.41	3.83	2.17	27.71
>5 <=10	2.14	4.18	3.10	2.56	4.02	6.62	3.91	1.02	27.54
>10 <=15	1.32	1.80	2.22	1.17	3.64	10.29	4.80	0.58	25.81
>15 <=20	0.25	0.47	1.03	0.27	1.40	6.48	2.96	0.12	12.96
>20 <=25	0.13	0.11	0.35	0.02	0.58	2.46	0.61	0.03	4.29
>25 <=30	0.04	0.01	0.12	0.08	0.10	0.64	0.39	0.01	1.39
>30 <=35	0.00	0.00	0.04	0.02	0.03	0.08	0.03	0.00	0.21
>35 <=40	0.00	0.00	0.02	0.04	0.00	0.01	0.00	0.00	0.08
>40	0.00	0.00	0.02	0.00	0.00	0.00	0.00	0.00	0.02
COL TOTALS	7.92	9.71	10.29	6.57	14.09	30.97	16.52	3.93	100.00
AVG. SPEED	5.9	7.4	8.8	7.4	9.0	12.2	10.5	5.6	

b)					
Basic Stats	Min.	Max.	Mean	Std.	Nobs.
SPEED:	0.0	41.8	9.6	6.3	9235
U (East):	-31.4	40.9	-2.8	8.1	9235
V (North):	-30.9	26.3	-3.3	6.8	9235
T (Deg.C):	10.8	21.1	18.3	2.0	9235
Mean Current Vector: 4.3 cm/s at 220.7 deg. True					
Princax= 56.4 major= 9.0 minor= 5.7					

Table 6.13. Data summary for mooring 5A, 16 mab, all good periods: C5A1, C5A2, C5A3, C5A6, C5A7, and C5A8. (a) Joint Frequency Distribution (JFD) of speed and direction; (b) Basic statistics of scalar variables, mean current vector, principal axis orientation (deg. T), and magnitudes of major and minor axes (cm/s).

a)										
Percent Occurrence in Each Speed-Direction Cell (No. Obs. = 24838)										
RANGE (CM/S)	N	NE	E	SE	S	SW	W	NW	ROW TOT	
<=5	2.74	3.89	4.44	2.88	2.04	3.16	4.33	3.08	26.57	
>5 <=10	2.45	6.03	6.28	2.88	2.25	4.65	5.70	3.18	33.42	
>10 <=15	1.09	3.70	4.89	1.29	1.22	2.67	3.58	1.06	19.50	
>15 <=20	0.26	2.60	4.28	0.50	0.33	1.51	2.03	0.37	11.88	
>20 <=25	0.09	1.28	2.80	0.22	0.06	0.60	0.81	0.17	6.02	
>25 <=30	0.02	0.40	0.88	0.06	0.02	0.15	0.32	0.03	1.88	
>30 <=35	0.00	0.06	0.16	0.01	0.00	0.06	0.10	0.04	0.42	
>35 <=40	0.00	0.01	0.00	0.00	0.00	0.06	0.05	0.02	0.14	
>40	0.00	0.00	0.00	0.00	0.00	0.06	0.10	0.00	0.17	
COL TOTALS	6.66	17.97	23.72	7.85	5.91	12.93	17.02	7.94	100.00	
AVG. SPEED	6.8	10.4	12.0	7.7	7.5	9.9	10.0	7.1		

b)					
Basic Stats	Min.	Max.	Mean	Std.	Nobs.
SPEED:	1.1	95.3	9.8	6.9	24838
U (East):	-92.6	33.1	1.6	10.2	24838
V (North):	-33.2	35.0	0.5	5.9	24838
T (Deg.C):	13.8	27.2	20.8	1.4	24838
Salinity:	34.9	37.3	36.3	0.4	24838
Mean Current Vector:	1.7 cm/s at 72.4 deg. True				
Princax=	74.4 major= 10.5 minor= 5.4				

Table 6.14. Data summary for mooring 5A, 4 mab, all good periods: C5A1, C5A2, C5A3, C5A4, C5A6, C5A7, and C5A8. (a) Joint Frequency Distribution (JFD) of speed and direction; (b) Basic statistics of scalar variables, mean current vector, principal axis orientation (deg. T), and magnitudes of major and minor axes (cm/s).

a)										
Percent Occurrence in Each Speed-Direction Cell (No. Obs. = 17692)										
RANGE (CM/S)	N	NE	E	SE	S	SW	W	NW	ROW TOT	
<=5	3.91	4.71	3.59	2.20	2.83	4.47	4.00	2.53	28.22	
>5 <=10	3.95	5.51	3.82	2.51	3.65	9.02	5.69	2.72	36.85	
>10 <=15	1.36	3.27	2.99	0.86	1.88	7.12	2.55	0.64	20.68	
>15 <=20	0.42	2.00	1.68	0.37	1.01	3.48	1.32	0.11	10.39	
>20 <=25	0.05	0.71	0.70	0.12	0.38	0.73	0.19	0.02	2.91	
>25 <=30	0.00	0.10	0.17	0.02	0.00	0.11	0.05	0.00	0.45	
>30 <=35	0.00	0.01	0.04	0.01	0.00	0.12	0.02	0.02	0.22	
>35 <=40	0.00	0.00	0.04	0.00	0.00	0.05	0.06	0.01	0.15	
>40	0.00	0.00	0.02	0.10	0.00	0.01	0.01	0.00	0.13	
COL TOTALS	9.70	16.30	13.06	6.19	9.74	25.10	13.88	6.04	100.00	
AVG. SPEED	6.5	8.9	9.8	7.9	8.5	10.2	8.2	6.0		

b)					
Basic Stats	Min.	Max.	Mean	Std.	Nobs.
SPEED:	0.0	60.0	8.7	5.9	17692
U (East):	-38.5	52.5	-0.6	8.0	17692
V (North):	-31.0	23.9	-1.0	6.7	17692
T (Deg.C):	14.7	27.4	19.3	1.3	17692
Mean Current Vector:	1.1 cm/s at 209.8 deg. True				
Princax=	55.8 major= 9.0 minor= 5.4				

Table 6.15. Data summary for mooring 5A, 16 mab, for periods in common with 4 mab: C5A1, C5A2, and C5A3 (to 11/30/99). (a) Joint Frequency Distribution (JFD) of speed and direction; (b) Basic statistics of scalar variables, mean current vector, principal axis orientation (deg. T), and magnitudes of major and minor axes (cm/s).

a)										
Percent Occurrence in Each Speed-Direction Cell (No. Obs. = 9165)										
RANGE (CM/S)	N	NE	E	SE	S	SW	W	NW	ROW TOT	
<=5	2.61	3.36	4.40	2.97	2.01	2.42	3.42	3.31	24.48	
>5 <=10	2.64	8.52	7.70	2.89	2.11	3.27	6.11	3.83	37.08	
>10 <=15	1.19	5.31	5.53	0.95	0.82	1.89	3.04	0.83	19.56	
>15 <=20	0.27	3.45	5.66	0.52	0.23	0.68	0.94	0.34	12.09	
>20 <=25	0.09	1.21	3.09	0.05	0.04	0.36	0.60	0.16	5.61	
>25 <=30	0.03	0.23	0.48	0.00	0.00	0.08	0.21	0.02	1.05	
>30 <=35	0.00	0.07	0.03	0.00	0.00	0.00	0.01	0.02	0.13	
>35 <=40	0.00	0.00	0.00	0.00	0.00	0.00	0.00	0.00	0.00	
>40	0.00	0.00	0.00	0.00	0.00	0.00	0.00	0.00	0.00	
COL TOTALS	6.83	22.15	26.90	7.39	5.20	8.70	14.33	8.51	100.00	
AVG. SPEED	7.1	10.6	11.9	6.8	6.7	8.8	9.0	6.8		

b)					
Basic Stats	Min.	Max.	Mean	Std.	Nobs.
SPEED:	1.1	34.5	9.5	6.1	9165
U (East):	-28.7	30.6	3.0	9.3	9165
V (North):	-21.1	25.8	1.5	5.4	9165
T (Deg.C):	18.4	22.8	20.8	0.7	9165
Salinity:	36.0	36.8	36.4	0.1	9165
Mean Current Vector: 3.4 cm/s at 64.2 deg. True					
Princax= 74.5 major= 9.5 minor= 5.0					

Table 6.16. Data summary for mooring 5A, 4 mab, for periods in common with 16 mab: C5A1, C5A2, and C5A3 (to 11/30/99). (a) Joint Frequency Distribution (JFD) of speed and direction; (b) Basic statistics of scalar variables, mean current vector, principal axis orientation (deg. T), and magnitudes of major and minor axes (cm/s).

a)										
Percent Occurrence in Each Speed-Direction Cell (No. Obs = 8494)										
RANGE (CM/S)	N	NE	E	SE	S	SW	W	NW	ROW TOT	
<=5	3.77	3.47	2.79	2.39	2.63	3.56	3.32	1.87	23.79	
>5 <=10	3.61	4.74	3.25	2.80	3.97	7.88	5.84	3.26	35.35	
>10 <=15	1.62	3.32	2.31	1.13	2.33	7.85	2.84	0.69	22.10	
>15 <=20	0.69	2.60	1.74	0.64	1.70	5.06	1.58	0.11	14.12	
>20 <=25	0.08	1.22	0.87	0.16	0.69	0.98	0.16	0.00	4.18	
>25 <=30	0.00	0.13	0.27	0.00	0.00	0.05	0.00	0.00	0.45	
>30 <=35	0.00	0.00	0.01	0.00	0.00	0.00	0.00	0.00	0.01	
>35 <=40	0.00	0.00	0.00	0.00	0.00	0.00	0.00	0.00	0.00	
>40	0.00	0.00	0.00	0.00	0.00	0.00	0.00	0.00	0.00	
COL TOTALS	9.78	15.49	11.24	7.12	11.31	25.37	13.74	5.93	100.00	
AVG. SPEED	7.1	10.4	10.4	7.8	9.7	10.9	8.6	6.6		

b)					
Basic Stats	Min.	Max.	Mean	Std.	Nobs.
SPEED:	0.0	30.6	9.5	5.6	8494
U (East):	-22.9	29.9	-0.7	8.0	8494
V (North):	-23.3	23.0	-1.3	7.4	8494
T (Deg.C):	16.8	21.7	19.5	1.0	8494
Mean Current Vector: 1.5 cm/s at 209.5 deg. True					
Princax= 49.4 major= 9.4 minor= 5.6					

Table 6.17. Data summary for mooring 9A, 16 mab, all good periods: C9A1, C9A2 (to 10/3/97), C9A3, C9A4 (to 4/24/98), C9A5 (to 5/24/98), C9A6, C9A7, and C9A8. (a) Joint Frequency Distribution (JFD) of speed and direction; (b) Basic statistics of scalar variables, mean current vector, principal axis orientation (deg. T), and magnitudes of major and minor axes (cm/s).

a)										
Percent Occurrence in Each Speed-Direction Cell (No. Obs. = 28634)										
RANGE (CM/S)	N	NE	E	SE	S	SW	W	NW	ROW TOT	
<=5	2.54	3.05	3.62	2.88	2.71	2.99	3.22	2.35	23.37	
>5 <=10	2.62	4.52	4.54	3.43	2.98	3.54	4.05	2.27	27.94	
>10 <=15	0.88	2.82	3.71	1.60	1.37	2.46	2.91	0.94	16.69	
>15 <=20	0.36	2.25	4.50	1.02	0.54	1.78	1.93	0.36	12.74	
>20 <=25	0.16	1.69	4.25	0.46	0.27	1.55	2.36	0.18	10.92	
>25 <=30	0.04	0.66	2.64	0.13	0.02	0.93	1.43	0.05	5.89	
>30 <=35	0.00	0.26	1.05	0.02	0.01	0.18	0.26	0.01	1.79	
>35 <=40	0.00	0.07	0.17	0.00	0.00	0.04	0.06	0.00	0.34	
>40	0.00	0.00	0.03	0.00	0.00	0.15	0.12	0.01	0.32	
COL TOTALS	6.60	15.31	24.51	9.55	7.89	13.62	16.34	6.17	100.00	
AVG. SPEED	7.2	12.0	15.4	8.9	7.8	12.7	13.3	7.6		

b)					
Basic Stats	Min.	Max.	Mean	Std.	Nobs.
SPEED:	1.0	91.7	11.9	8.6	28634
U (East):	-79.8	43.4	2.0	12.8	28634
V (North):	-54.9	48.3	-0.3	6.9	28634
T (Deg.C):	14.7	26.9	20.0	1.4	28634
Salinity:	34.8	36.9	36.2	0.3	27540
Mean Current Vector: 2.0 cm/s at 97.5 deg. True					
Princax= 75.5 major= 13.2 minor= 6.3					

Table 6.18. Data summary for mooring 9A, 4 mab, all good periods: C9A1, C9A3, C9A4 (to 3/11/98), C9A5 (to 5/29/98), C9A6, C9A7 (to 12/21/98), and C9A8. (a) Joint Frequency Distribution (JFD) of speed and direction; (b) Basic statistics of scalar variables, mean current vector, principal axis orientation (deg. T), and magnitudes of major and minor axes (cm/s).

a)										
Percent Occurrence in Each Speed-Direction Cell (No. Obs. = 20333)										
RANGE (CM/S)	N	NE	E	SE	S	SW	W	NW	ROW TOT	
<=5	4.69	2.62	2.91	2.33	3.08	3.83	3.38	1.59	24.41	
>5 <=10	2.11	4.86	4.07	2.31	2.92	5.06	3.86	1.23	26.43	
>10 <=15	1.34	5.19	4.50	3.24	3.79	4.96	2.86	0.57	26.45	
>15 <=20	0.32	2.57	2.19	3.20	2.08	3.26	1.13	0.06	14.80	
>20 <=25	0.04	1.14	0.52	1.53	0.61	1.48	0.20	0.00	5.51	
>25 <=30	0.01	0.21	0.13	0.57	0.10	0.38	0.04	0.00	1.44	
>30 <=35	0.00	0.07	0.01	0.21	0.04	0.17	0.00	0.00	0.52	
>35 <=40	0.00	0.07	0.01	0.05	0.01	0.05	0.01	0.00	0.21	
>40	0.00	0.01	0.00	0.01	0.03	0.04	0.10	0.02	0.22	
COL TOTALS	8.50	16.75	14.36	13.45	12.66	19.23	11.57	3.48	100.00	
AVG. SPEED	5.2	11.3	10.3	13.2	10.4	11.3	8.8	6.2		

b)					
Basic Stats	Min.	Max.	Mean	Std.	Nobs.
SPEED:	0.0	60.0	10.3	6.8	20333
U (East):	-56.1	40.4	1.4	9.2	20333
V (North):	-49.8	36.2	-2.2	7.9	20333
T (Deg.C):	13.1	26.0	19.1	1.3	20333
Mean Current Vector: 2.6 cm/s at 146.5 deg. True					
Princax= 60.7 major= 9.7 minor= 7.2					

Table 6.19. Data summary for mooring 9A, 16 mab, for periods in common with 4 mab: C9A1, C9A3, C9A4 (to 3/11/98), C9A5 (to 5/24/98), C9A6, C9A7 (to 12/21/98), and C9A8. (a) Joint Frequency Distribution (JFD) of speed and dir.; (b) Basic statistics of scalar variables, mean current vector, principal axis orientation (deg. T), and magnitudes of major and minor axes (cm/s).

a)									
Percent Occurrence in Each Speed-Direction Cell (No. Obs. = 20909)									
RANGE (CM/S)	N	NE	E	SE	S	SW	W	NW	ROW TOT
<=5	2.38	2.20	2.99	2.24	2.16	1.91	2.11	1.97	17.95
>5 <=10	2.41	4.41	5.05	3.71	2.94	3.16	3.86	2.16	27.68
>10 <=15	0.99	3.08	4.27	1.81	1.27	2.27	2.81	1.00	17.50
>15 <=20	0.48	2.75	5.57	1.23	0.60	1.65	1.91	0.42	14.62
>20 <=25	0.22	2.25	5.26	0.55	0.33	1.32	2.21	0.19	12.33
>25 <=30	0.05	0.90	3.42	0.17	0.02	0.78	1.32	0.07	6.74
>30 <=35	0.00	0.35	1.42	0.03	0.01	0.20	0.24	0.02	2.28
>35 <=40	0.00	0.09	0.23	0.00	0.00	0.05	0.08	0.00	0.46
>40	0.00	0.00	0.05	0.00	0.00	0.21	0.16	0.02	0.44
COL TOTALS	6.53	16.04	28.25	9.74	7.34	11.55	14.70	5.84	100.00
AVG. SPEED	7.8	13.5	16.5	9.8	8.5	13.8	14.1	8.3	

b)					
Basic Stats	Min.	Max.	Mean	Std.	Nobs.
SPEED:	1.0	91.7	13.1	8.8	20909
U (East):	-79.8	43.4	3.4	13.5	20909
V (North):	-54.9	48.3	0.1	7.3	20909
T (Deg.C):	14.7	26.9	20.1	1.5	20909
Salinity:	35.4	36.9	36.3	0.2	19815
Mean Current Vector:	3.4 cm/s at 88.8 deg. True				
Princax=	75.8 major= 13.9 minor= 6.7				

Table 6.20. Data summary for mooring 9A, 4 mab, for periods in common with 16 mab: C9A1, C9A3, C9A4 (to 3/11/98), C9A5 (to 5/24/98), C9A6, C9A7 (to 12/21/98), and C9A8. (a) Joint Frequency Distribution (JFD) of speed and dir.; (b) Basic statistics of scalar variables, mean current vector, principal axis orientation (deg. T), and magnitudes of major and minor axes (cm/s).

a)									
Percent Occurrence in Each Speed-Direction Cell (No. Obs. = 20117)									
RANGE (CM/S)	N	NE	E	SE	S	SW	W	NW	ROW TOT
<=5	4.13	2.64	2.94	2.35	3.11	3.82	3.11	1.60	23.70
>5 <=10	2.13	4.92	4.12	2.34	2.95	5.11	3.81	1.25	26.61
>10 <=15	1.35	5.25	4.55	3.27	3.83	5.02	2.89	0.58	26.74
>15 <=20	0.32	2.60	2.22	3.23	2.10	3.29	1.14	0.06	14.96
>20 <=25	0.04	1.15	0.52	1.55	0.62	1.49	0.20	0.00	5.57
>25 <=30	0.01	0.21	0.13	0.58	0.10	0.39	0.04	0.00	1.46
>30 <=35	0.00	0.07	0.01	0.21	0.04	0.17	0.00	0.00	0.52
>35 <=40	0.00	0.07	0.01	0.05	0.01	0.05	0.01	0.00	0.21
>40	0.00	0.01	0.00	0.01	0.03	0.04	0.10	0.02	0.22
COL TOTALS	7.99	16.92	14.51	13.60	12.80	19.38	11.30	3.50	100.00
AVG. SPEED	5.6	11.3	10.3	13.2	10.4	11.4	9.0	6.3	

b)					
Basic Stats	Min.	Max.	Mean	Std.	Nobs.
SPEED:	0.0	60.0	10.4	6.8	20117
U (East):	-56.1	40.4	1.5	9.2	20117
V (North):	-49.8	36.2	-2.2	7.9	20117
T (Deg.C):	13.1	26.0	19.0	1.3	20117
Mean Current Vector:	2.7 cm/s at 146.3 deg. True				
Princax=	60.6 major= 9.8 minor= 7.2				

Table 6.21. Summary of principal axes analysis. Angle of the major axis relative to north, amplitudes of the major and minor axes, number of observations in each analysis, and the magnitude and sense of rotation of the 4 mab axis relative to the 16 mab axis, looking down. (Note: the angle of the major axis is only defined for 0-180°; it is not a vector quantity. Thus, predominantly SW flow would have a NE angle.)

	Major Axis Angle (°CW from N) and dir. octant	Major Axis Amplitude (cm/s)	Minor Axis Amplitude (cm/s)	No. Observ.	Rotation (°) 4 mab relative to 16 mab	Sense of rotation
All Good						
16 mab						
C1A	66.2 (NE)	11.5	6.5	29,351	--	--
C4A	70.4 (E)	11.8	4.5	20,758	--	--
C5A	74.4 (E)	10.5	5.4	24,838	--	--
C9A	75.5 (E)	13.2	6.3	28,634	--	--
All Good						
4 mab						
C1A	20.3 (N)	5.8	4.7	17,881	45.9	CCW
C4A	50.6 (NE)	9.9	5.9	12,074	19.8	CCW
C5A	55.8 (NE)	9.0	5.4	17,692	18.6	CCW
C9A	60.7 (NE)	9.7	7.2	20,333	14.8	CCW
Common						
16 mab						
C1A	69.1 (E)	10.4	6.1	16,048	--	--
C1B	64.3 (NE)	9.4	4.9	10,626	--	--
C1C	66.6 (NE)	9.9	5.5	4076	--	--
C4A	71.8 (E)	11.3	4.5	9765	--	--
C5A	74.5 (E)	9.5	5.0	9165	--	--
C5C	73.7 (E)	8.8	3.9	3017	--	--
C9A	75.8 (E)	13.9	6.7	20,909	--	--
Common						
4 mab						
C1A	25.8 (NE)	6.1	4.9	15,064	43.3	CCW
C1B	34.6 (NE)	11.0	5.0	9424	29.7	CCW
C1C	19.1 (NE)	8.4	3.8	4076	47.5	CCW
C4A	56.4 (NE)	9.0	5.7	9235	15.4	CCW
C5A	49.4 (NE)	9.4	5.6	8494	25.1	CCW
C5C	54.7 (NE)	6.8	3.4	3017	19.0	CCW
C9A	60.6 (NE)	9.8	7.2	20,117	15.2	CCW

Abbreviations: CW = clockwise; CCW = counterclockwise.

January 1998

During the week of 5–9 January 1998, the eastern U.S. and eastern Canada were severely affected by a storm system with a southerly flow and abundant moisture. This resulted in flooding rains from the lower Mississippi valley through the southeast and into the northeast. Because of this storm, a local peak in the Mississippi River flow is seen in the freshwater flow (**Fig. 6.6**). The maximum freshwater flow from Mobile Bay occurred on 10 January. Cruise S2 commenced on 29 January.

March 1998

A late-winter snowstorm passed through the Midwest and Plains states between 6 March 1998 and 9 March 1998. The maximum combined freshwater flow onto the Mississippi-Alabama shelf and the individual maximums for the Escambia and Choctawhatchee Rivers are associated with this weather event.

June/July 1998

During June and July 1988, numerous instances of unusually cool bottom waters were reported along the Florida coast west of Cape San Blas. In some cases, low oxygenated water bottom waters were reported. Prior to that period, NEGOM cruise N2 was conducted from 5 to 15 May. The cruise recorded the presence of an anomalous cold-water event. Our Cruise M3, conducted from 24 April to 3 May, recorded bottom temperatures of 17 to 18.5°C at the study sites and dissolved oxygen levels from 3.0 to 4.0 mL/L. None of these values was particularly unusual for spring conditions.

September 1998

Meteorologically speaking, September of 1998 was an unusual month. Hurricane Earl, a Category 2 storm on the Saffir/Simpson Hurricane Scale, crossed the eastern side of the study area on 3 September. Maximum one-minute surface winds of 85–87 knots were recorded for the day. Rainfall totals of three to six inches were common near the path of the storm, although much higher amounts were recorded in a few areas. For example, Panama City, Florida recorded 16.38 inches.

Tropical Storm Hermine passed to the west of the study area on 20 September. Hermine produced rains of about 0.5–1.0 inches. The 42040 NDBC buoy recorded a maximum significant wave height of 1.74 m on 20 September at 1600 UTC and a maximum hourly-averaged wind speed of 10.4 m/s in the same hour.

The eye of Hurricane Georges passed directly over Site 5 on 29 September. Georges was the second strongest hurricane within the Atlantic basin during the 1998 season. The hurricane was a substantial rain producer along the central and eastern Gulf of Mexico. Rainfall totals generally ranged from to 20 inches over most of southern Mississippi and Alabama and the Florida Panhandle. In response to the heavy rains, widespread flooding occurred in Southern Mississippi from 30 September through 2 October. There is a

distinctive spike seen in the combined freshwater flow record because of this storm (**Fig. 6.6**). Cruise S4 commenced on 13 October.

January 1999

On 17 January, a severe weather outbreak began over north-central Arkansas. The fast-moving storm system swept through the northeast sections of Arkansas and then across western and central Tennessee with high winds, hail and heavy rain. The upper watershed for the Tombigbee River drained much of the resulting precipitation and a significant increase in flow is seen in the downstream gauges beginning on 23 January and peaking on 3 February. This storm consequently resulted in the second largest freshwater flow from Mobile Bay.

Discussion

Flow at 16 mab

The current meters at 16 mab measure the mesoscale flow just above the mounds. Across the entire study region there is substantial similarity in the percentages and statistics of observed flow. For example, **Tables 6.5** and **6.17** show the JFDs and basic statistics for Sites 1 and 9, which are 72 km apart and span the east-west extent of the study. Both sites have a good data return (>83%) at 16 mab for the two-year period. At both sites, the most frequent direction octant is E (20% at Site 1 and 25 % at Site 9), as is the direction of the mean current vector. The NE, SW, and W sectors are the next most frequent at about 15% each. This reflects the generally NE/SW nature of the flow at the 16 mab level, which is above the bottom Ekman layer. The most frequent speed range is 5–10 cm/s, (33% at Site 1 and 28% at Site 9), and the overall mean speeds are similar at 11–12 cm/s. However, the magnitudes of the mean current vectors are small, i.e., 0.9 cm/s at Site 1, and 2.0 cm/s at Site 9. Strong currents, i.e., greater than 40 cm/s, are most frequently directed SW or W, particularly during Hurricane Georges (97 cm/s at Site 1 and 92 cm/s at Site 9). The results at Site 5 (**Table 6.13**), located about midway across the study region, are very similar to those at the each end. The depths at all three sites are similar (78–92 m).

At Site 4, located farther out on the shelf in deeper water (112 m), the speed distribution and statistics at 16 mab (**Table 6.9**) are similar to the other three sites, with 5–10 cm/s being most frequent (33%). Because of the greater depth at this site, the maximum speed, recorded during Hurricane Georges, is only 66 cm/s. The distribution of direction has a slight southwesterly bias compared to the other three sites, as the most frequent direction octant is SW (26%). It is followed closely by E (24%), which is the most frequent octant at the other sites. The mean current vector flow is S, i.e., toward 200° at 1.8 cm/s. The SW bias is a result of speeds greater than 20 cm/s, which are most frequently in the SW octant.

Principal axis analysis (**Table 6.21**) shows a slight east-west trend in the orientation of the major axes, i.e., 66.2° at Site 1 to 75.5° at Site 9, which probably is related to the

large-scale trend of the bathymetry, rather than the mesoscale-scale topography near each site. The angles of the major axes are consistent with the most frequent directions in the JFDs (E plus W). (When comparing the principal axis angle with the JFD one combines an octant and its reciprocal because the angle of the principal axis is only determined between 0° and 180°.) The similarity in orientation of the major axes across the study region reinforces the conclusion that at 16 mab the sites experience similar flow regimes (but not the same flow at any given instant). The ratios of major-to-minor axis amplitudes are 1.7, 2.6, 1.9, and 2.1 at Sites 1, 4, 5, and 9, respectively. The larger ratio for Site 4 indicates greater directionality in the flow, which could be a result of either steeper bottom slope or the ridgeline that lies just north of the site.

Flow at 4 mab

Compared with the flow at 16 mab, the near-bottom flow is more site-specific. Bottom friction and the local topography influence the flow, particularly at Site 1. A comparison is again made between Sites 1 and 9 (**Tables 6.6** and **6.18**), the high-relief eastern site and the low-relief western site. The most frequent speed range at Site 9 is a virtual tie between the 5–10 cm/s range and the 10–15 cm/s range, at 26% each. At Site 1, on the other hand, the most frequent range is 0–5 cm/s (44%). The overall mean speed is also lower at Site 1, i.e., 6.3 cm/s compared to 10.3 cm/s. Observations of direction also differ significantly between the two sites. The most frequent direction octants are S at Site 1 and SW at Site 9, and the angles of the principal axes are 20.3° (N/S) and 60.7° (NE/SW), respectively. However, the mean current vectors at both sites are oriented SE and virtually identical in magnitude and direction (2.0 cm/s at 143° and 2.6 cm/s at 147°, respectively).

At Site 4 and 5 (**Tables 6.10** and **6.14**), the flow statistics at 4 mab are similar to those at Site 9 (**Table 6.18**). The dominant speed ranges are 5–10 cm/s, the most frequent directions sectors are SW, the angles of the principal axes are NE/SW (50.6° and 55.8°, respectively), and the directions of the mean current vectors are SW (222° and 210°, respectively). However, the vector mean speed at Site 5 is only 1.1 cm/s, while at Site 4 it is 5.9 cm/s, a value that also exceeds the overlying flow at 16 mab.

Vertical and Horizontal Flow Comparisons

To provide a more precise comparison between the flow at 16 mab and 4 mab, the JFDs, basic statistics, and principal axis analyses are also presented by site for just the contemporaneous periods of reliable data at the two current meter levels, which substantially reduces the number of observations used in the computations. A comparison of the results for the reduced data set for each meter location with those of its larger “parent” data set shows similar results as long as several deployment periods are still involved. This is not the case when the statistics for an individual deployment period of about three months are compared with those for longer combined periods, as discussed below. The results suggest that the statistics of the time series are relatively stationary over longer periods but not necessarily over single deployment periods. The most interesting result between the two levels lies in the difference between the angles of the principal axes (**Table 6.21**). At Sites 4, 5, and 9 the axis at 4 mab is rotated 15–20°

counterclockwise (CCW) from that at 16 mab, i.e., to the left, looking down. This is what one would expect because of friction in the bottom Ekman layer. At Site 1, however, the vertical difference in angles is 45.9° , considerably larger than at the other three sites.

Mooring 1A is located about one “mound” diameter northeast of Site 1 (**Fig. 6.2**). The topographic surveys found a steep slope on the east and northeast sides of the mound. As discussed above, several factors differentiate the near-bottom flow observed at mooring 1A from the near-bottom flow at other sites; we conclude that the extent of the flow disturbance created by the topography of Site 1 extends at least the distance to the mooring. Moorings were deployed at similar distances at two other locations around Site 1 during the first field year, designated moorings 1B and 1C (**Fig. 6.2**). Principal axis (**Table 6.21**) and JFD (**Tables 6.22–6.25**) analyses were calculated for the times for which reliable data exist simultaneously at both meter depths for moorings 1B and 1C. (Fouling and instrument malfunction limit the extent of the common records.)

At mooring 1B, located southeast of the site, the distributions and statistics for 16 mab (**Table 6.22**) are similar to those at mooring 1A and at the other sites discussed above—eastward flows (30%) at speeds in the 5–10 cm/s range (33%) dominate, and the angle of the major axis is 64.3° . Near the bottom (**Table 6.23**), the most frequent speed range is also 5–10 cm/s, but the principal direction octants are S and NE at 25% each, and the angle of the principal axis is 34.6° . Thus, there is a significant CCW rotation in direction between 16 and 4 mab, but not as much as at mooring 1A (43° vs. 30°). The large percentage of near-bottom observations in the 0–5 cm/s range observed at 1A is not seen at 1B (44% vs. 21%).

At mooring 1C, located west of the site, only the fourth deployment period has useful data at both levels (C1C4, February–April 1998). For this particular deployment, both current meters were RCM7 instruments. The flow statistics at 16 mab for this short period (**Table 6.24**) are significantly different from those for the longer data sets for 1A and 1B. The differences are largely related to the differences in record length, because observations for just the fourth deployment period for mooring 1A (deployment C1A4, **Table 6.26**) yield results for direction that are similar to those for deployment C1C4. At mooring 1C, the most frequent octant is W (29%), and the second most frequent is SW (19%). The W and SW octants also contain most of the speed observations greater than 20 cm/s. The angle of the principal axis is 66.6° (246.6° reciprocal). Significant differences between the two sides of the site are found in some of the speed statistics. The most frequent speed range is 0–5 cm/s (44%) at mooring 1C on the west side of the mound (**Table 6.24**), but 5–10 cm/s (26%) at mooring 1A on the northeast side (**Table 6.26**). The mean speeds are 8.5 cm/s and 12.5 cm/s, respectively. However, the mean current vectors are almost identical (~ 3 cm/s at 250 – 258°). Thus, at 16 mab, the flow for the isolated period February–April 1998 is dominantly west-southwest, and on the downstream or lee side of the mound, there is a significant increase in very low or stagnant flow compared to the upstream side.

Table 6.22. Data summary for mooring 1B, 16 mab, for periods in common with 4 mab: C1B1, C1B2, and C1B3 (to 12/31/97). (a) Joint Frequency Distribution (JFD) of speed and direction; (b) Basic statistics of scalar variables, mean current vector, principal axis orientation (deg. T), and magnitudes of major and minor axes (cm/s).

a)										
Percent Occurrence in Each Speed-Direction Cell (No. Obs = 10626)										
RANGE (CM/S)	N	NE	E	SE	S	SW	W	NW	ROW TOT	
<=5	2.80	3.98	5.01	4.71	3.36	4.23	3.49	1.76	29.32	
>5 <=10	2.06	6.16	7.58	2.80	3.33	6.61	3.16	1.43	33.13	
>10 <=15	0.42	3.76	5.27	0.63	1.28	1.21	0.75	0.30	13.64	
>15 <=20	0.14	5.09	7.35	0.26	0.39	0.32	0.36	0.27	14.18	
>20 <=25	0.04	2.04	3.13	0.02	0.24	0.44	0.16	0.10	6.17	
>25 <=30	0.02	0.80	1.26	0.00	0.03	0.08	0.07	0.04	2.29	
>30 <=35	0.00	0.40	0.52	0.00	0.00	0.00	0.07	0.02	1.01	
>35 <=40	0.00	0.15	0.10	0.00	0.00	0.00	0.00	0.00	0.25	
>40	0.00	0.01	0.00	0.00	0.00	0.00	0.00	0.00	0.01	
COL TOTALS	5.48	22.41	30.22	8.41	8.62	12.88	8.06	3.92	100.00	
AVG. SPEED	5.6	12.5	12.9	5.3	7.1	7.0	6.8	6.8		

b)						
Basic Stats	Min.	Max.	Mean	Std.	Nobs.	
SPEED:	1.0	41.1	9.8	7.2	10626	
U (East):	-10.0	38.0	5.8	8.7	10626	
V (North):	-25.3	30.4	1.1	6.0	10626	
T (Deg.C):	18.0	23.2	20.9	0.7	10626	
Salinity:	34.8	36.6	36.2	0.5	7443	
Mean Current Vector:	5.9 cm/s at 79.3 deg. True					
Princax=	64.3 major= 9.4 minor= 4.9					

Table 6.23. Data summary for mooring 1B, 4 mab, for periods in common with 16 mab: C1B1, C1B2, and C1B3 (to 12/31/97). (a) Joint Frequency Distribution (JFD) of speed and direction; (b) Basic statistics of scalar variables, mean current vector, principal axis orientation (deg. T), and magnitudes of major and minor axes (cm/s).

a)										
Percent Occurrence in Each Speed-Direction Cell (No. Obs. = 9424)										
RANGE (CM/S)	N	NE	E	SE	S	SW	W	NW	ROW TOT	
<=5	2.56	2.40	2.15	1.74	3.60	3.85	2.21	2.11	20.62	
>5 <=10	3.23	4.26	2.15	1.58	5.74	6.65	1.76	2.03	27.40	
>10 <=15	1.57	6.12	2.88	0.51	7.17	5.45	0.66	0.57	24.94	
>15 <=20	0.53	9.18	1.75	0.07	6.95	2.35	0.06	0.04	20.94	
>20 <=25	0.01	2.71	0.41	0.00	1.68	0.23	0.00	0.00	5.04	
>25 <=30	0.00	0.49	0.08	0.00	0.30	0.15	0.00	0.00	1.02	
>30 <=35	0.00	0.00	0.00	0.00	0.05	0.00	0.00	0.00	0.05	
>35 <=40	0.00	0.00	0.00	0.00	0.00	0.00	0.00	0.00	0.00	
>40	0.00	0.00	0.00	0.00	0.00	0.00	0.00	0.00	0.00	
COL TOTALS	7.89	25.15	9.43	3.90	25.49	18.69	4.69	4.75	100.00	
AVG. SPEED	7.5	13.9	10.5	6.0	12.2	9.5	5.9	5.8		

b)						
Basic Stats	Min.	Max.	Mean	Std.	Nobs.	
SPEED:	0.1	34.1	10.8	6.0	9424	
U (East):	-17.2	27.1	1.9	7.5	9424	
V (North):	-34.1	23.3	-1.4	9.5	9424	
T (Deg.C):	13.1	21.8	19.9	1.1	9424	
Mean Current Vector:	2.4 cm/s at 126.9 deg. True					
Princax=	34.6 major= 11.0 minor= 5.0					

Table 6.24. Data summary for mooring 1C, 16 mab, for the period in common with 4 mab, which is just deployment C1C4. (a) Joint Frequency Distribution (JFD) of speed and direction; (b) Basic statistics of scalar variables, mean current vector, principal axis orientation (deg. T), and magnitudes of major and minor axes (cm/s).

a)										
Percent Occurrence in Each Speed-Direction Cell (No. Obs. = 4076)										
RANGE (CM/S)	N	NE	E	SE	S	SW	W	NW	ROW TOT	
<=5	3.83	4.96	6.99	2.92	4.15	7.14	10.23	3.66	43.87	
>5 <=10	1.86	2.43	1.94	0.71	1.86	3.26	7.63	1.99	21.69	
>10 <=15	0.64	1.89	1.25	0.81	1.42	3.43	5.52	0.81	15.78	
>15 <=20	0.44	0.81	1.15	0.47	0.56	2.21	2.53	0.52	8.68	
>20 <=25	0.37	0.88	0.47	0.22	0.22	1.23	1.42	0.32	5.13	
>25 <=30	0.12	0.42	0.27	0.00	0.00	0.69	1.20	0.00	2.70	
>30 <=35	0.00	0.15	0.07	0.00	0.02	0.54	0.64	0.00	1.42	
>35 <=40	0.00	0.00	0.00	0.00	0.00	0.27	0.15	0.00	0.42	
>40	0.00	0.00	0.00	0.00	0.00	0.25	0.07	0.00	0.32	
COL TOTALS	7.26	11.53	12.14	5.13	8.24	19.01	29.39	7.29	100.00	
AVG. SPEED	6.6	8.5	6.5	6.4	6.6	10.7	9.6	6.5		

b)						
Basic Stats	Min.	Max.	Mean	Std.	Nobs.	
SPEED:	1.1	47.6	8.5	8.1	4076	
U (East):	-43.4	29.7	-2.9	9.3	4076	
V (North):	-29.0	26.6	-0.6	6.4	4076	
T (Deg.C):	15.0	20.2	18.5	0.8	4076	
Salinity:	34.5	36.5	36.0	0.2	4076	
Mean Current Vector: 3.0 cm/s at 257.7 deg. True						
Princax= 66.6 major= 9.9 minor= 5.5						

Table 6.25. Data summary for mooring 1C, 4 mab, for the period in common with 16 mab, which is just deployment C1C4. (a) Joint Frequency Distribution (JFD) of speed and direction; (b) Basic statistics of scalar variables, mean current vector, principal axis orientation (deg. T), and magnitudes of major and minor axes (cm/s).

a)										
Percent Occurrence in Each Speed-Direction Cell (No. Obs. = 4076)										
RANGE (CM/S)	N	NE	E	SE	S	SW	W	NW	ROW TOT	
<=5	6.21	3.39	2.89	3.93	10.13	9.84	12.93	9.79	59.10	
>5 <=10	1.74	0.17	0.10	0.47	7.14	4.12	1.67	1.08	16.49	
>10 <=15	0.25	0.00	0.02	0.00	6.75	2.92	0.34	0.17	10.45	
>15 <=20	0.12	0.00	0.10	0.00	3.88	1.99	0.29	0.10	6.48	
>20 <=25	0.10	0.00	0.00	0.00	2.31	0.71	0.20	0.02	3.34	
>25 <=30	0.00	0.00	0.00	0.00	1.42	0.96	0.05	0.00	2.43	
>30 <=35	0.00	0.00	0.00	0.00	0.22	0.54	0.00	0.00	0.76	
>35 <=40	0.00	0.00	0.00	0.00	0.00	0.22	0.02	0.00	0.25	
>40	0.00	0.00	0.00	0.00	0.12	0.59	0.00	0.00	0.71	
COL TOTALS	8.42	3.56	3.12	4.39	31.97	21.88	15.51	11.16	100.00	
AVG. SPEED	3.9	2.2	2.4	2.6	10.4	9.9	3.1	2.9		

b)						
Basic Stats	Min.	Max.	Mean	Std.	Nobs.	
SPEED:	1.1	51.4	6.9	7.9	4076	
U (East):	-38.4	17.7	-2.3	4.6	4076	
V (North):	-44.8	22.4	-4.4	8.0	4076	
T (Deg.C):	14.3	19.7	18.0	1.1	4076	
Salinity:	33.8	36.3	35.8	0.2	4076	
Mean Current Vector: 5.0 cm/s at 207.8 deg. True						
Princax= 19.1 major= 8.4 minor= 3.8						

Table 6.26. Data summary for mooring 1A, 16 mab, for just deployment C1A4 (for comparison with Tables 6.24 and 6.25). (a) Joint Frequency Distribution (JFD) of speed and direction; (b) Basic statistics of scalar variables, mean current vector, principal axis orientation (deg. T), and magnitudes of major and minor axes (cm/s).

a)

Percent Occurrence in Each Speed-Direction Cell (No. Obs. = 3544)

RANGE (CM/S)	N	NE	E	SE	S	SW	W	NW	ROW TOT
<=5	1.81	1.61	1.52	1.58	1.61	3.39	7.20	2.40	21.11
>5 <=10	1.98	3.33	4.01	2.17	2.57	3.41	6.09	2.34	25.90
>10 <=15	1.13	1.41	3.19	0.90	1.86	2.43	4.51	1.95	17.38
>15 <=20	1.04	1.98	2.12	0.99	0.96	3.19	3.72	0.99	14.98
>20 <=25	0.51	2.17	1.86	1.04	0.25	2.31	3.10	0.59	11.85
>25 <=30	0.37	0.51	0.56	0.11	0.08	2.17	1.64	0.31	5.76
>30 <=35	0.00	0.08	0.00	0.00	0.00	1.24	0.51	0.00	1.83
>35 <=40	0.00	0.00	0.00	0.00	0.00	0.40	0.11	0.00	0.51
>40	0.00	0.00	0.00	0.00	0.00	0.62	0.06	0.00	0.68
COL TOTALS	6.83	11.09	13.26	6.80	7.34	19.16	26.95	8.58	100.00
AVG. SPEED	10.7	13.1	12.7	10.8	9.6	16.4	11.8	10.0	

b)

Basic Stats	Min.	Max.	Mean	Std.	Nobs.
SPEED:	1.1	49.6	12.5	8.6	3544
U (East):	-45.1	27.8	-2.9	12.3	3544
V (North):	-31.0	29.9	-1.0	8.4	3544
T (Deg.C):	15.4	20.4	18.5	0.7	3544
Salinity:	35.5	36.4	36.0	0.1	3544

Mean Current Vector: 3.1 cm/s at 250.0 deg. True
 Princax= 67.6 major= 12.9 minor= 7.3

At 4 mab on the west side of Site 1 (**Table 6.25**), the lee effect seems to be even greater. The frequency of occurrence of low speed (0–5 cm/s) increases to 59%, and the scalar mean speed drops to 6.9 cm/s. Direction rotates 47.5° CCW compared to the 16 mab level. The most frequent octant is S (32%); the angle of the principal axis is 19.1° (199.1° reciprocal); and the mean current vector is 5 cm/s at 208°. Note that the magnitude of the mean vector is larger than that at 16 mab, but the scalar mean speed is lower. The increase in the vector mean speed near the bottom is a result of greater directionality for the flow.

At Site 5 on the southeast side (mooring 5A), there is no indication of flow disruption in either the total data sets or those for the upper/lower common period because the statistics are similar to the other sites. However, on the north side, mooring 5C has one deployment period (C5C8) with simultaneous common data at 16 and 4 mab. This happens to be approximately the same period but different year (February–April 1999) as that for mooring 1C discussed above. Again, both current meters were RCM7 instruments. The observations yield an inconclusive interpretation for possible flow effects. The results at the upper level (**Table 6.27**) show that while the most frequent speed range is 5–10 cm/s (36%), the 0–5 cm/s range is a close second (33%). The frequency of low flow increases to 40% at the near-bottom level (**Table 6.28**). These high percentages of low flow would suggest a lee effect. However, the direction data show that W and SW flows dominate at the upper meter (27% and 17%) and SW and W flows dominate at the lower meter (26% and 17%). Mean current vectors and principal axes are consistent with these JFD results. The direction data thus suggest that the mooring 5C is upstream of Site 5 much of the time during this period.

The observations from the deployed current meters provide a good, quantitative description of the mesoscale flow conditions between the bottom and 16 m above the bottom in the study region. The results also indicate some possible flow perturbation at a distance of one “mound” diameter from Sites 1 and 5. A detailed observational study of the flow on the sides and tops of the sites was beyond the scope of the study. However, a qualitative picture of what such flow might look like can be inferred from other work. A general discussion of the possible effects of the study features on the near-bottom flow follows.

Flow Structure over Generalized Mounds

The general character of flow past small three-dimensional obstacles is quite complex and depends on the geometry of the obstacle, the flow speed, and the stratification of the fluid. The features of interest in this study have small vertical and horizontal extent. Their horizontal characteristic length scale (width), L , is about 200 m. A characteristic horizontal current velocity, U , at 16 mab is about 0.1 m/s. Using a mean latitude of 29.3°, the Coriolis parameter, f , is 7.1×10^{-5} . Thus, the Rossby number, U/fL , is 7.0. A characteristic time scale, L/U , is less than one hour. Such a large Rossby number and a short time scale in relation to a pendulum day mean that the effect of the earth’s rotation, i.e., the Coriolis acceleration on the flow, can be ignored. In this case, the studies and models of flow around larger scale obstacles such as seamounts (e.g., Hogg 1973; Ou 1991) are not applicable. The Flower Garden Banks, for example, are large enough

Table 6.27. Data summary for mooring 5C, 16 mab, for the period in common with 4 mab, which is just deployment C5C8. (a) Joint Frequency Distribution (JFD) of speed and direction; (b) Basic statistics of scalar variables, mean current vector, principal axis orientation (deg. T), and magnitudes of major and minor axes (cm/s).

a)										
Percent Occurrence in Each Speed-Direction Cell (No. Obs. = 3017)										
RANGE (CM/S)	N	NE	E	SE	S	SW	W	NW	ROW TOT	
<=5	3.41	2.68	2.29	2.19	3.28	6.07	8.85	4.24	33.01	
>5 <=10	1.66	6.36	6.46	1.99	3.02	6.70	6.46	3.22	35.86	
>10 <=15	0.30	3.22	4.21	1.09	0.70	2.55	5.80	0.43	18.30	
>15 <=20	0.00	2.09	1.36	0.07	0.10	1.43	4.97	0.30	10.31	
>20 <=25	0.00	0.60	0.40	0.00	0.00	0.33	1.06	0.00	2.39	
>25 <=30	0.00	0.00	0.00	0.00	0.00	0.00	0.13	0.00	0.13	
>30 <=35	0.00	0.00	0.00	0.00	0.00	0.00	0.00	0.00	0.00	
>35 <=40	0.00	0.00	0.00	0.00	0.00	0.00	0.00	0.00	0.00	
>40	0.00	0.00	0.00	0.00	0.00	0.00	0.00	0.00	0.00	
COL TOTALS	5.37	14.95	14.72	5.34	7.09	17.07	27.28	8.19	100.00	
AVG. SPEED	4.1	9.6	9.6	6.4	5.3	7.4	9.4	5.3		

b)						
Basic Stats	Min.	Max.	Mean	Std.	Nobs.	
SPEED:	1.1	26.1	8.0	5.5	3017	
U (East):	-25.7	22.9	-1.1	8.5	3017	
V (North):	-17.5	14.9	-0.1	4.5	3017	
T (Deg.C):	18.7	20.7	19.8	0.3	3017	
Salinity:	35.7	36.8	36.2	0.2	3017	
Mean Current Vector:	1.1 cm/s at 264.4 deg. True					
Princax=	73.7 major= 8.8 minor= 3.9					

Table 6.28. Data summary for mooring 5C, 4 mab, for the period in common with 16 mab, which is just deployment C5C8. (a) Joint Frequency Distribution of speed and direction; (b) Basic statistics of scalar variables, mean current vector, principal axis orientation (deg. T), and magnitudes of major and minor axes (cm/s).

a)										
Table of Percent Occurrence in Each Speed-Direction Cell (No. Obs. = 3017)										
RANGE (CM/S)	N	NE	E	SE	S	SW	W	NW	ROW TOT	
<=5	3.35	6.40	6.03	2.85	4.61	6.86	5.54	4.77	40.40	
>5 <=10	1.39	7.72	4.44	1.13	4.44	10.37	7.19	2.39	39.08	
>10 <=15	0.17	4.08	0.43	0.00	0.99	7.46	4.14	0.56	17.83	
>15 <=20	0.03	0.36	0.00	0.00	0.00	1.52	0.36	0.00	2.29	
>20 <=25	0.00	0.00	0.00	0.00	0.00	0.27	0.13	0.00	0.40	
>25 <=30	0.00	0.00	0.00	0.00	0.00	0.00	0.00	0.00	0.00	
>30 <=35	0.00	0.00	0.00	0.00	0.00	0.00	0.00	0.00	0.00	
>35 <=40	0.00	0.00	0.00	0.00	0.00	0.00	0.00	0.00	0.00	
>40	0.00	0.00	0.00	0.00	0.00	0.00	0.00	0.00	0.00	
COL TOTALS	4.94	18.56	10.90	3.98	10.04	26.48	17.37	7.72	100.00	
AVG. SPEED	4.3	7.3	4.9	3.8	5.7	8.4	7.5	4.6		

b)						
Basic Stats	Min.	Max.	Mean	Std.	Nobs.	
SPEED:	1.1	21.7	6.7	4.0	3017	
U (East):	-21.2	13.8	-1.5	5.9	3017	
V (North):	-16.9	16.5	-1.0	4.8	3017	
T (Deg.C):	18.5	20.1	19.5	0.3	3017	
Salinity:	35.4	36.7	36.2	0.2	3017	
Mean Current Vector:	1.8 cm/s at 237.6 deg. True					
Princax=	54.7 major= 6.8 minor= 3.4					

($L \sim 4$ km) for rotational effects to be important, and Rezak et al. (1985) investigated the possible formation of Taylor columns over the banks.

Here, the results of laboratory studies of three-dimensional, stratified, non-rotating flow over a small obstacles provide the best conceptual pictures of flow details one might expect over the topographic features of this study. Baines (1995) reviews the current state of the theoretical and laboratory models of stratified flow over small obstacles. Much of Baines' discussion of three-dimensional flow is based on the experiments of Hunt and Snyder (1980), hereafter referred to as HS. The most important non-dimensional parameter in this field of study is the internal Froude number, $F = U/Nh$, where h is the height above bottom of the obstacle, U is a characteristic upstream speed at the level of h , and

$$N = \sqrt{-\frac{g}{\rho_o} \frac{d\rho}{dz}}$$

is the buoyancy frequency (also called the Brunt-Väisälä frequency) in radians per second. It is the frequency of unforced gravity waves on the stratification and is, thus, a measure of stratification. It is computed from the vertical density gradient at the level of the obstacle, gravitational acceleration, g , density, ρ , and mean water column density ρ_o . (Note: HS use the Froude number, U/Nh , while Baines uses the inverse of the Froude number, Nh/U . We use the HS convention.) The value of F indicates, based on experiments and models, whether streamlines from upstream impinge on the hill, go around it, or go over the top. It also indicates, as a function of stratification, where to expect the locations of internal hydraulic jumps and their size, and the region of separated or recirculating flow in the lee of the hill.

HS conducted a set of laboratory experiments to observe the flow structure over a bell-shaped hill at values of F from 0.1 to 1.7 and at $F = \infty$. The hill's shape was defined by the inverse of a fourth-order polynomial. Topographic slope of this hill is not small: the ratio of hill's height to half-width scale is 0.5. **Figs. 6.10–6.14**, taken from HS, present their collation of the results of various visualization techniques. The figures represent HS's somewhat subjective summary of mean flow over the hill. They note that instantaneous flow may differ substantially from the mean picture. The following is a condensation of the results of HS.

- a) **Fig. 6.10.** At $F = 0.2$ (low speed/strong stratification), the fluid flows horizontally around the hill, except in a narrow region near the top. In this region, fluid parcels have enough kinetic energy to overcome the stability and rise up and over the top. A slight hydraulic jump occurs just downstream of the top of the hill. Downstream, there is a symmetric pair of more or less vertically oriented vortices causing upstream flow on the centerline. On the downstream face of the hill, the flow is primarily perpendicular to the free-stream flow direction and oscillates from one side to the other. There is a very weak upslope component to the flow on the lower part of the leeward slope. The flow around the sides of the hill separates from the hill at about 110° from the upstream stagnation line.

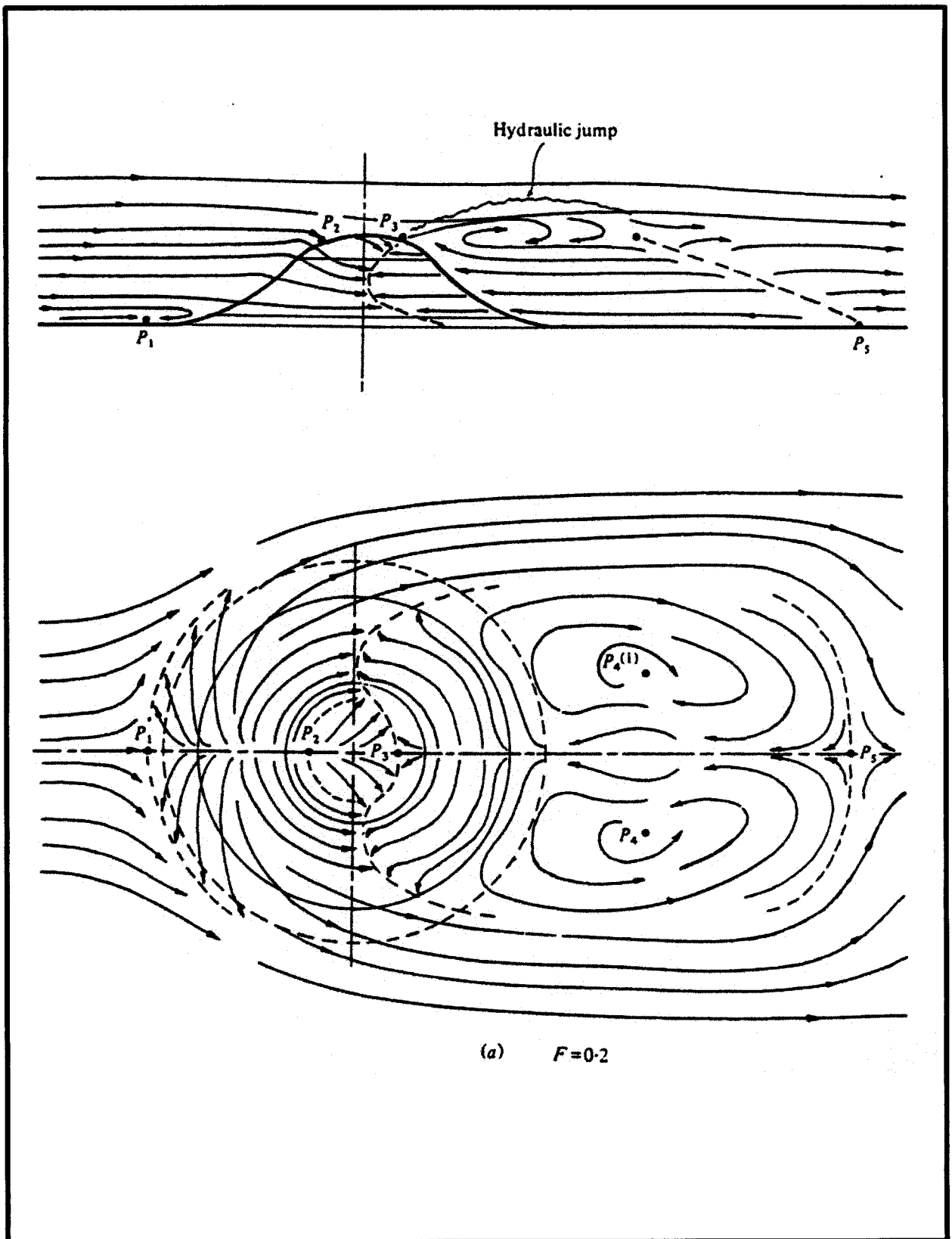


Fig. 6.10. Derived center-plane streamline (top) and surface shear-stress patterns (bottom) for a Froude number (U/Nh) $F=0.2$ (From: Hunt and Snyder 1980; reprinted with the permission of Cambridge University Press).

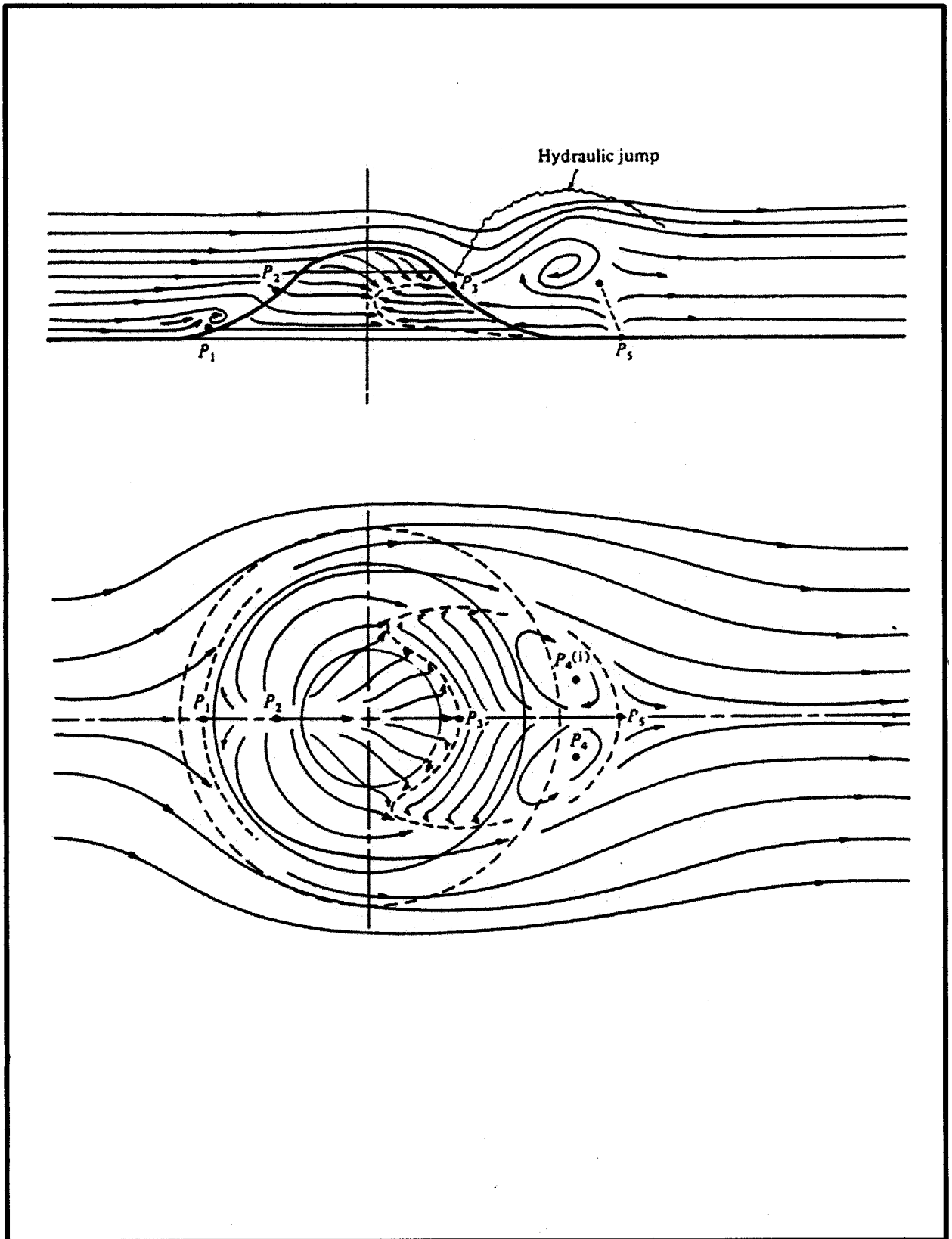


Fig. 6.11. Derived center-plane streamline (top) and surface shear-stress patterns (bottom) for a Froude number (U/Nh) $F=0.4$ (From: Hunt and Snyder 1980; reprinted with the permission of Cambridge University Press).

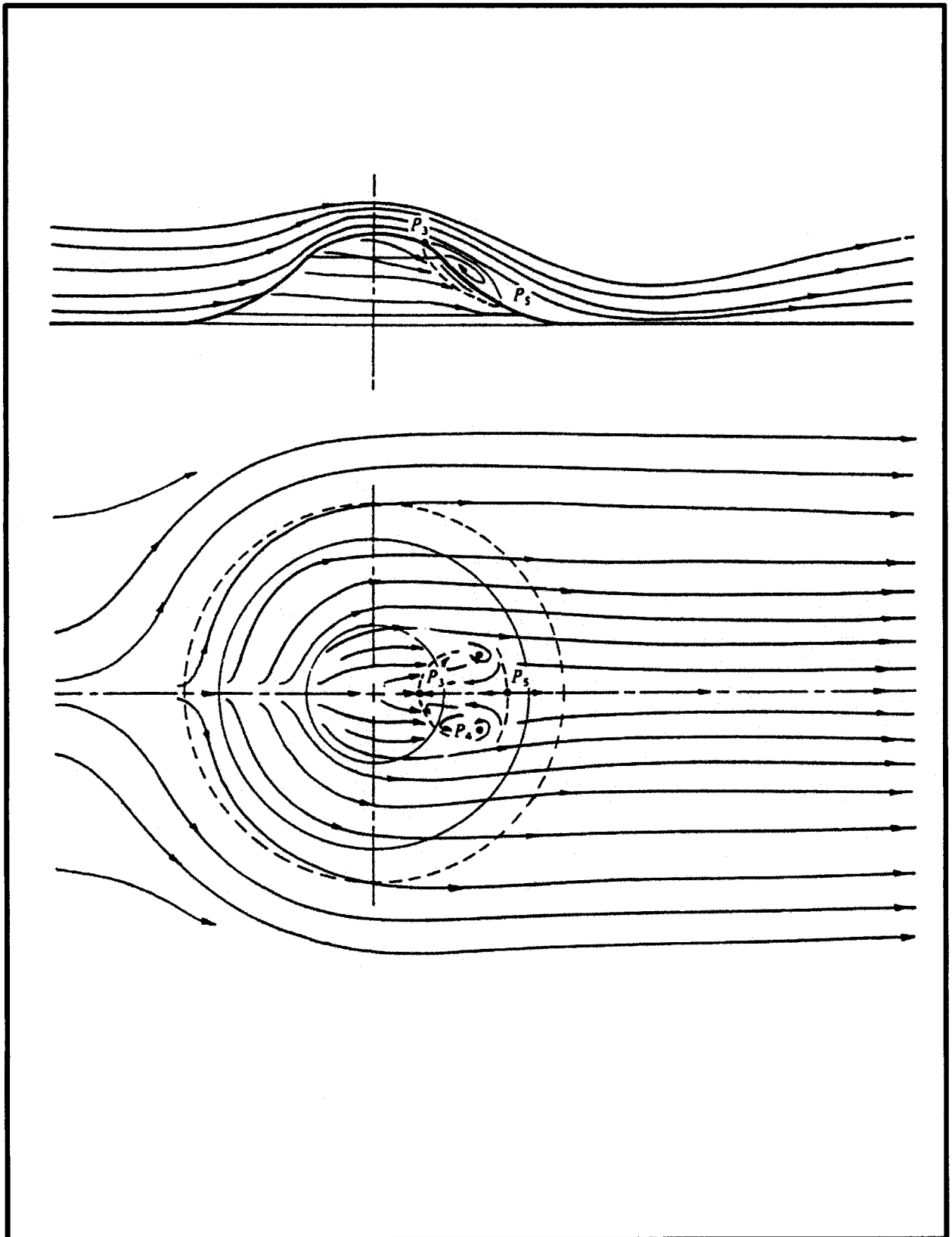


Fig. 6.12. Derived center-plane streamline (top) and surface shear-stress patterns (bottom) for a Froude number (U/Nh) $F=1.0$ (From: Hunt and Snyder 1980; reprinted with the permission of Cambridge University Press).

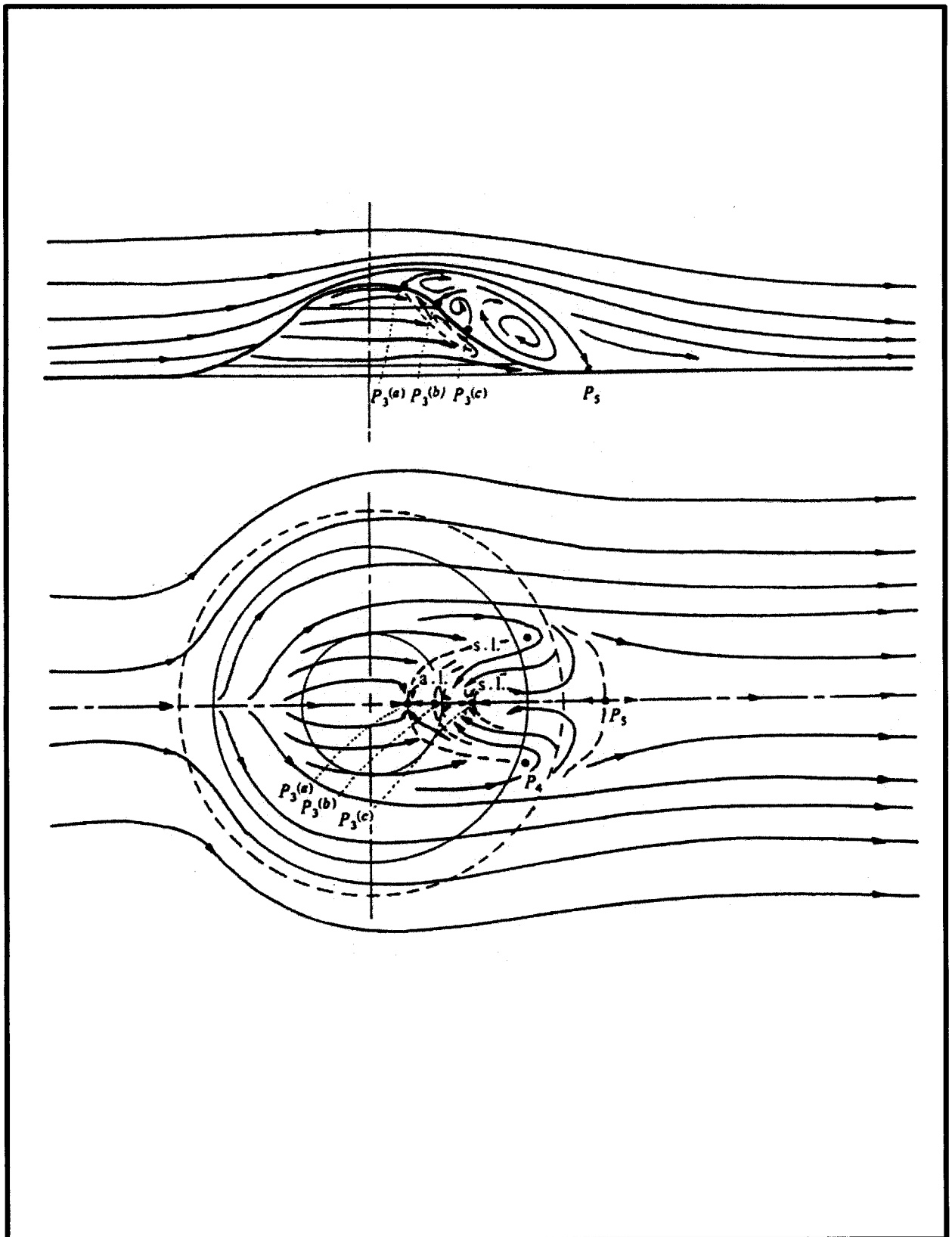


Fig. 6.13. Derived center-plane streamline (top) and surface shear-stress patterns (bottom) for a Froude number (U/Nh) $F=1.7$ (From: Hunt and Snyder 1980; reprinted with the permission of Cambridge University Press).

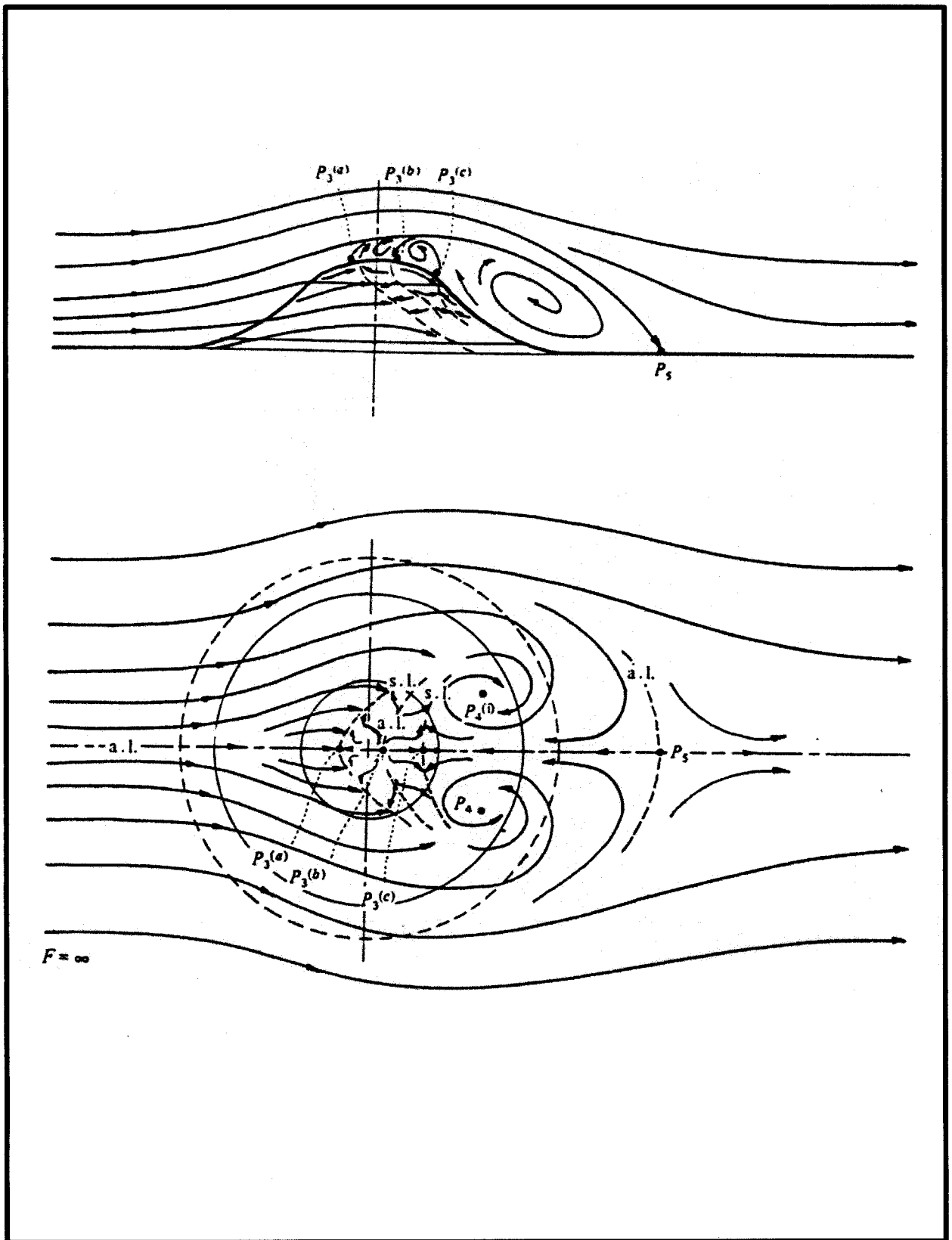


Fig. 6.14. Derived center-plane streamline (top) and surface shear-stress patterns (bottom) for a Froude number (U/Nh) $F = \infty$ (infinity) (From: Hunt and Snyder 1980; reprinted with the permission of Cambridge University Press).

- b) **Fig. 6.11.** At $F = 0.4$ (increasing speed/decreasing stratification), the flow has more energy to move in the vertical direction. The region where the flow goes over the top of the hill is now broader, and a plume (dye) emanating from an upstream point at a height of $0.6h$ (where “ h ” is the height of the hill) would spread thinly to cover the entire upper half of the hill. In going over the top, however, the flow does not separate until it is roughly halfway down the lee slope. There is a strong hydraulic jump just downstream of this separation point. Downstream, the symmetric pair of vertically oriented vortices still causes an upstream flow on the centerline. However, they are smaller and closer to the base of the hill. Flow around the sides still separates at about 110° .
- c) $F = 0.6$ to 0.9 . (No Figures). As F moves from 0.6 toward 0.9 , the separation point associated with the hydraulic jump begins near the downstream base of the hill and moves even farther downstream with increasing F . The hydraulic jump peaks two to three hill heights downstream. At $F = 0.9$ all the flow in the center plane goes over the top of the hill. A plume (dye) emitted upstream at ground level on the centerline would spread out and cover nearly the entire hill surface. The flow goes down the lee side without separating (no hydraulic jump), and a lee wave forms.
- d) **Fig. 6.12.** At $F = 1.0$ the flow begins separating from the top of the lee side of the hill. The critical value of F at which this separation begins depends on a number of factors. As F is increased further, the size of the recirculating region on the lee side grows, and the wake dimensions grow laterally and vertically. The pair of vortices disappears and a horseshoe pattern begins to develop. A large-scale lee wave develops downstream (not seen in figure) with wavelength $\sim 6L$.
- e) **Fig. 6.13.** At $F = 1.7$ (high speed/weak stratification) the flow separates just past the top of the hill, resulting in a large recirculating region on the leeward slope. A plume (dye) emitted at ground level on the upstream centerline would spread thinly over the entire hill surface. The horseshoe pattern on the lee side continues to expand. The wavelength of the lee wave is $\sim 10L$.
- f) **Fig. 6.14.** At $F = \infty$ (the homogeneous case, i.e., no stratification or $N = 0$) flow is broadly similar to the case when $F = 1.7$. Separation first occurs on the centerline before the summit of the hill is reached. The streamlines rise farther above the top compared to the case of $F = 1.7$.

In addition to the qualitative observations, HS report some quantitative results. The criterion for determining whether the plume will impact the hill surface and go around the sides or over the top is, roughly, $H_s = h(1-F)$, where H_s is the dividing streamline height. If the upstream plume height is lower than H_s , it will impact on the hill surface; otherwise, it will go over the top. The speedup over the top, which can be seen in the patterns for $F = 1.0$ and greater, is roughly 1.3 for the specific case of neutral flow ($F = \infty$). HS also note in **Figs. 6.11–6.14** some of the features of the topology of the flow, i.e., nodes and saddles of attachment and separation. Baines (1995) discusses in detail the topology of flow on the surface of a three-dimensional obstacle. Both HS and Baines

(1995) discuss experiments and theory for other obstacle shapes. A key parameter is the slope. Steep sides and sharp corners induce substantial additional complexity in the flow upstream of the obstacle, over the top and in the lee, but the most general characteristics still obtain for other shapes at similar Froude numbers.

Assuming the topographic obstacles of this study are grossly similar to the hill used by HS, one can use the above results to compute typical ranges for the Froude number. “Hill” heights in the study region are typically 1 to 15 m; we use 5 and 15 m as two examples. The frequency of various observed speed ranges at 16 mab are discussed above. The maximum observed speed is 96.7 cm/s (at Site 1 during Hurricane Georges). The third Froude parameter is the buoyancy frequency, N . Selected examples of the vertical profile of N , computed from CTD cast data, are shown in **Fig. 6.15**. Typically, the profile of N computed from raw CTD data is very noisy and must be smoothed. Therefore, N was computed from the 0.5-m, bin-averaged values of pressure, temperature and salinity, and then the profile was further smoothed with a running 10-point mean. The CTD casts were typically made to within 2 m of the bottom, so after all the smoothing, the deepest value for N in **Fig. 6.15** is about 8 mab. For all CTD casts, values of N (smoothed) near 16 mab are ~ 0.001 – 0.025 rad/s. Typical values are 0.01–0.02 rad/s. Even though salinity may be almost uniform near the bottom, there is usually a temperature gradient to provide vertical stability. The accuracies of the temperature and salinity sensors from the moored instruments are too coarse (compared to the CTD) to use in a detailed computation of N , but note that mean values, for example, from the first deployment period at Site 1A yield a mean N of 0.01 rad/s. To relate the observed laboratory flow patterns reported by HS to specific sites of this study, one must make assumptions about the frequency of occurrence of various ranges of the value of N . A reasonable assumption would seem to be that $N \geq 0.01$ much of the time. Lower values obtain when a very homogeneous bottom water mass advects through a site or when very strong turbulent vertical mixing occurs, such as during a hurricane.

Because of the ranges of the parameters used to compute the buoyancy frequency, the near-bottom values of the Froude number cover at least two orders of magnitude. In **Fig. 6.16(a)** and **(b)**, the Froude number is plotted as a function of N and U for hill heights of 5 m and 15 m, respectively. The values of F near 1.0 are of particular interest because near this critical value the flow changes from a hill-hugging lee flow to a separated lee flow. For a 15-m hill and $N = 0.025$ rad/s (strong stratification), the Froude number is subcritical (less than 1.0) for speeds up to 37.5 cm/s. At $N = 0.001$ rad/s (very weak stratification), the flow is subcritical only for the weakest currents, i.e., for speeds less than 1.5 cm/s.

At Site 1, assuming $N \geq 0.01$ rad/s most of the time and $h = 13$ m, the frequency occurrence of values of F can be estimated from that of speed (**Table 6.29**). The flow will be subcritical ($F < 1.0$) for speeds up to 13 cm/s, which occurs almost 75% of the time. In this case the flow pattern over the site probably looks something like **Figs. 6.10–6.11**. Near 13 cm/s ($F \sim 1.0$), the flow might resemble that in **Fig. 6.12**. Between 13 cm/s and 30 cm/s ($1.0 < F < 2.0$), the flow depicted in **Fig. 6.13** might occur, and at the maximum observed speed of 96.7 cm/s ($F = 7.4$), the flow in **Fig. 6.14** is probably a

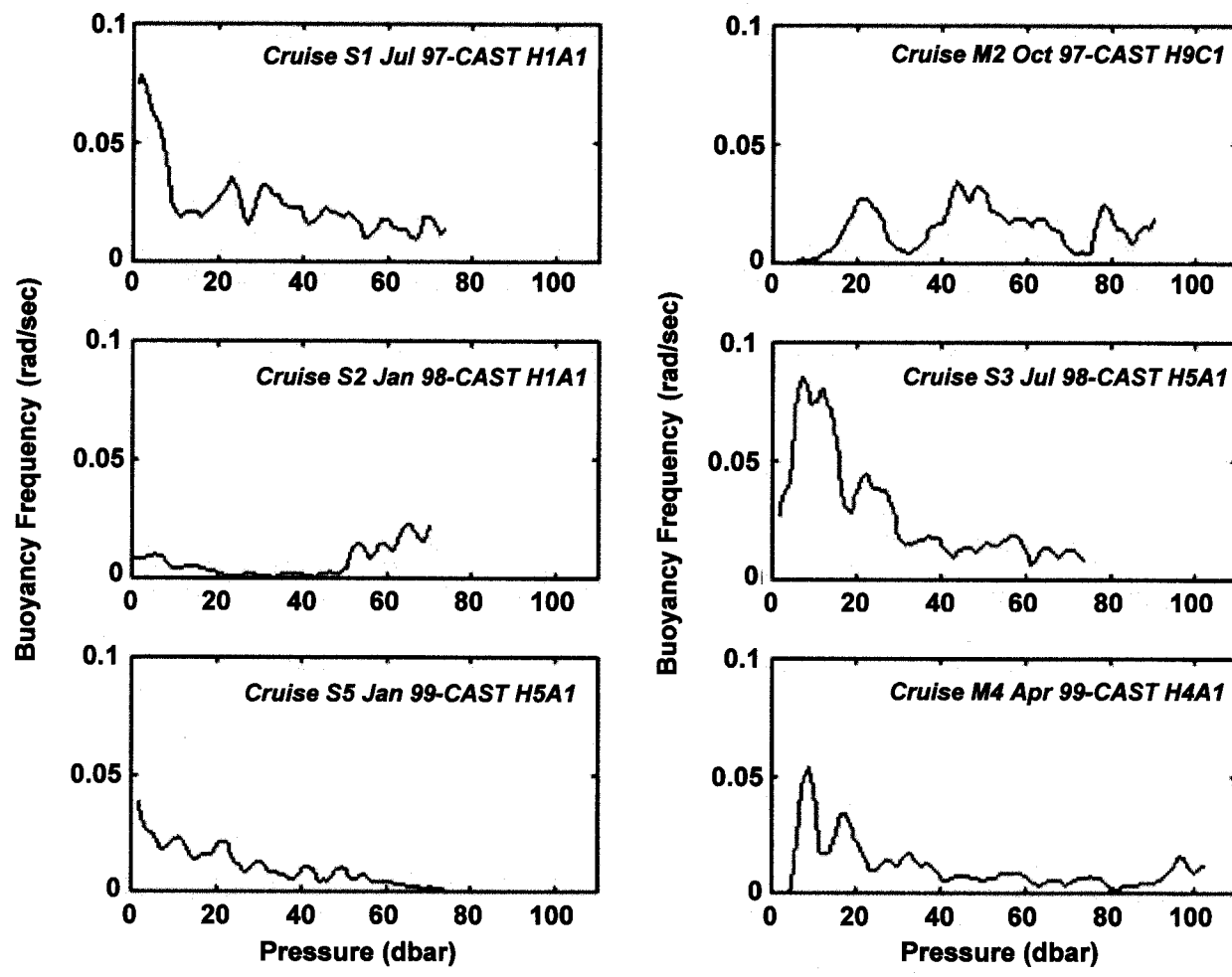


Fig. 6.15. Selected examples of smoothed vertical profiles of buoyancy frequency.

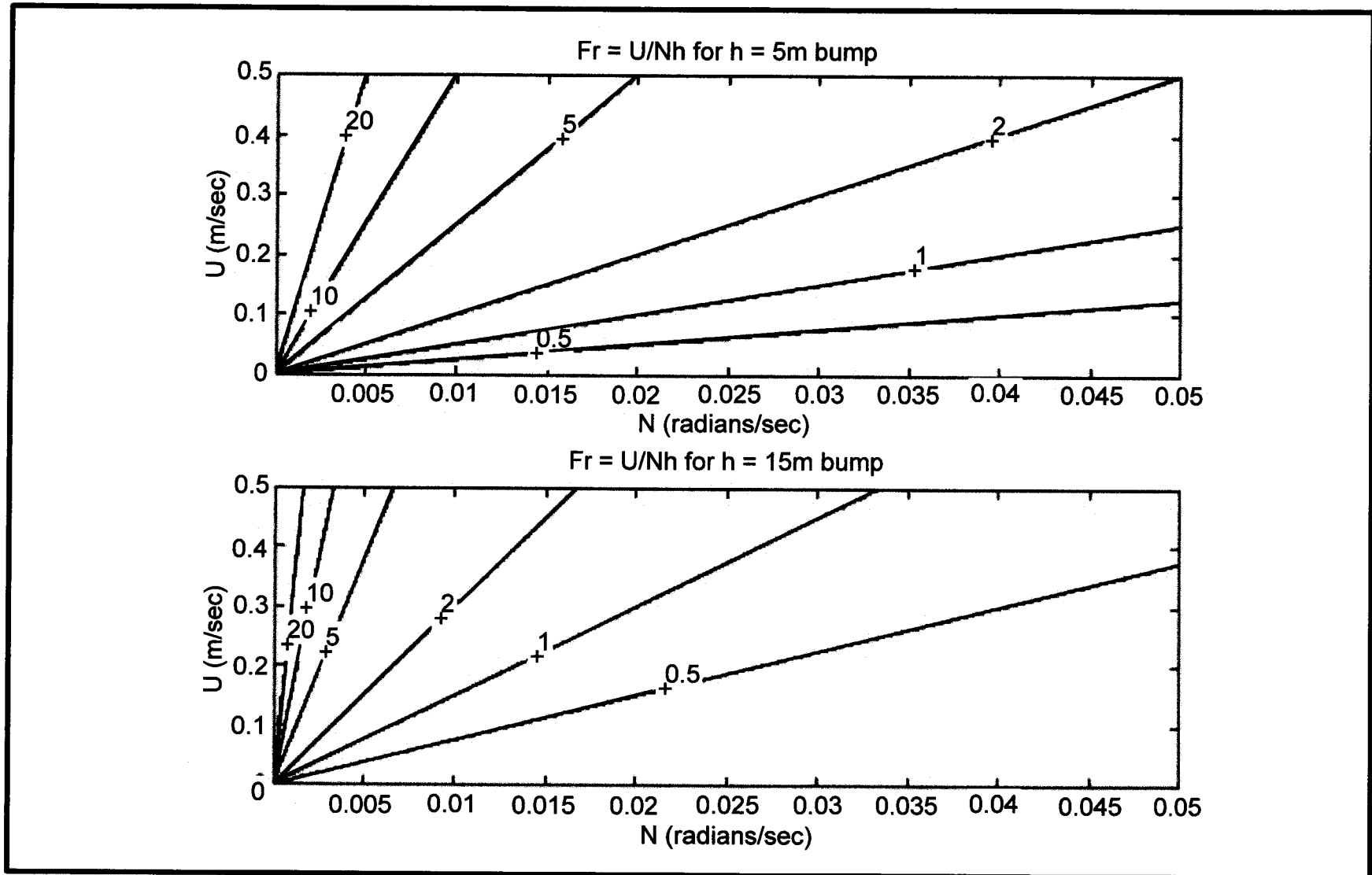


Fig. 6.16. Froude number (U) plotted as a function of buoyancy frequency (N) and current speed; (a) for a hill height of 15 m; (b) for a hill height of 5 m.

reasonable depiction, especially because turbulent mixing would decrease the value of N below the assumed value of 0.01, making F even larger.

Over the much lower relief feature at Site 9, where the height is only a few meters, the Froude number is higher to begin with. Assuming $N \geq 0.01$ rad/s and $h = 3$ m, the flow will be subcritical only at speeds less than 3 cm/s. More than about 80% of the time (Table 6.17), the flow will be supercritical, and Figs. 6.13–6.14 would be appropriate flow models. The maximum observed speed of 91.7 cm/s yields a Froude number of 30.6, but the turbulent mixing would probably create near neutral ($F = \infty$) flow.

Table 6.29. Froude number for Sites 1, 4, 5, and 9 computed from mound height (13 m, 10 m, 10 m, and 3 m, respectively), an assumed N of 0.01 rad/s, and the upper limit of each speed range in the joint frequency distribution (JFD) tables of speed vs. direction. Also shown is the figure number of the flow pattern that corresponds to the value of F and the percentage of observations at that F , based on the speed percentages in the JFD tables. Note: values in this table are intended to provide only a gross picture of possible flow patterns at various speeds and should not be used in a quantitative way.

	Speed Upper Limit (cm/s)							
	5.0	10.0	15.0	20.0	25.0	30.0	35.0	40.0
Site 1								
Froude number (F)	0.4	0.8	1.2	1.5	1.9	2.3	2.7	3.1
Flow Pattern Fig.	6.11	6.11	6.13	6.13	6.13	6.13	6.14	6.14
% Occurrence	24.3	32.9	18.1	11.6	8.6	3.0	1.0	0.3
Site 4								
Froude number (F)	0.5	1.0	1.5	2.0	2.5	3.0	3.5	4.0
Flow Pattern Fig.	6.11	6.12	6.13	6.13	6.13	6.14	6.14	6.14
% Occurrence	19.9	35.8	19.5	13.7	9.1	1.7	0.3	0.1
Site 5								
Froude number (F)	0.5	1.0	1.5	2.0	2.5	3.0	3.5	4.0
Flow Pattern Fig.	6.11	6.12	6.13	6.13	6.13	6.14	6.14	6.14
% Occurrence	26.6	33.4	19.5	11.9	6.0	1.9	0.4	0.1
Site 9								
Froude number (F)	1.7	3.3	5.0	6.7	8.3	10.0	11.7	13.3
Flow Pattern Fig.	6.13	6.14	6.14	6.14	6.14	6.14	6.14	6.14
% Occurrence	23.4	27.9	16.7	12.7	10.9	5.9	1.8	0.3

Waves

Surface gravity waves can affect water properties, particularly in the bottom boundary layer, if the maximum orbital wave velocity is high enough to cause sediment resuspension. Accepted convention states that a deep-water wave ‘feels’ the bottom when the water depth is less than half the wavelength. For each of the study sites, the following table (Table 6.30) shows the minimum wave period for a wave to influence the ocean bottom and the top of a feature.

Table 6.30. Minimum wave period for a wave to influence the bottom and top of each site.

Site	Minimum Wave Period (s)	
	Seafloor	Top of Mound
1	9.9	9.0
2	10.2	9.4
3	10.1	9.9
4	11.7	11.0
5	10.0	8.9
6	10.0	9.8
7	10.6	9.4
8	11.1	10.6
9	11.1	10.7

The dominant wave period (recorded by the NDBC 42040 buoy) during the duration of each of the cruises was between 4.19 and 6.22 seconds. These waves would not influence the bottom. The distribution of the hourly-averaged dominant wave period between 1 January 1997 and 31 December 1999 (**Table 6.31**) shows that the median wave period is between 5 and 6 seconds.

Table 6.31. Distribution of wave period observed at NDBC Buoy 42040 during 1 January 1997 through 31 December 1999.

Wave Period (s)	Individual %	Cumulative %
3 - 4	10.81	100.00
4 - 5	19.29	89.19
5 - 6	31.30	69.90
6 - 7	17.80	38.60
7 - 8	13.18	20.80
8 - 9	4.34	7.62
9 - 10	2.26	3.28
10 - 11	0.61	1.02
11 - 12	0.17	0.41
12 - 13	0.13	0.24
13 - 14	0.00	0.11
14 - 15	0.10	0.11
15 - 20	0.00	0.00

Waves with periods greater than 9 seconds, which could influence the bottom at the shallower sites, occurred only 3.28% of the time. Waves with periods greater than 10 seconds only occurred 1.0% of the time and waves with periods greater than 11 seconds only occurred 0.4% of the time. Such longer-period waves occur during the passage of hurricanes, which are infrequent. If the wave height is also large, the orbital wave velocity at the bottom is sufficient to cause vertical mixing in the wave bottom boundary layer. Three such hurricanes occurred during the study period. One was

Hurricane Danny in July 1998. Hurricanes Earl and Georges are discussed in the next section.

During Hurricane Danny in July 1997, the NDBC 42040 buoy began recording the arrival of swell (9-second period waves with a significant wave height of 0.3 m) generated by the hurricane approximately four days before passage of the storm. These swell waves would only be capable of producing orbital wave velocities of 0.6 cm/s at the top of the shallowest mound (Site 5) and velocities less than 0.15 cm/s at the deepest mound (Site 4). The velocities at the bottom would be less. At hurricane passage on 0000 UTC 19 July, the hourly winds peaked at 16.32 m/s. The dominant period wave had a period of 7.7 seconds and a maximum significant wave height was 3.34 m. This would only be capable of producing orbital wave velocities of 2.25 cm/s at the shallowest site (Site 5) and velocities less than 0.25 cm/s at the Site 4, the deepest site.

September 1998 Events

September 1998 was the most unusual month of the study because of several events. Hurricane Earl's path (**Fig. 6.17**) crossed the eastern side of the study area on 3 September and the eye of Hurricane Georges (**Fig. 6.18**) passed directly over Site 5 on 29 September. The resulting currents at 16 mab are shown in stick vector form in **Fig. 6.19**. The speeds recorded at 4 mab during September 1998 are shown in **Fig. 6.20**. (Speeds are shown for 4 mab rather than stick vectors because of a problem with the compasses in the OEI current meters. The instruments' rotors are believed to have functioned properly.) The effect of the strong bottom currents on sediment during the hurricanes at Site 5 is shown in **Fig. 6.21**. Only during these events did turbidity values exceed normal background ranges.

Hurricane Georges

The 42040 NDBC buoy recorded a maximum significant wave height of 10.88 m on 27 September at 1900 UTC and a maximum hourly-averaged wind speed of 27.9 m/s in the same hour. The dominant wave period was 12.5 seconds. This would be capable of producing orbital wave velocities on the order of 80 cm/s at the shallowest mound (Site 5) and 36 cm/s velocities at the deepest site (Site 4). Over the period of the storm, the orbital wave velocity at the site (Site 5) continuously exceeded 25 cm/s for 32 hours. The orbital wave velocity at the deepest site (Site 4) exceeded 25 cm/s for 27 hours. Without a doubt, these orbital velocities are high enough to cause sediment resuspension. In addition, this storm was capable of uniformly mixing the entire water column.

Currents were strongest during Hurricane Georges. At Site 1, speed reached 96.7 cm/s at the 16-mab level. The direction of the hurricane driven currents was mainly southwest at Sites 1 and 4, and shifted between southwest and northwest at Sites 5 and 9. At 4 mab the response was strongest at Site 4, reaching 60 cm/s. Since the eye of Georges passed directly over Site 5, a barotropic response to sea level fluctuations is exhibited by the near-bottom current.

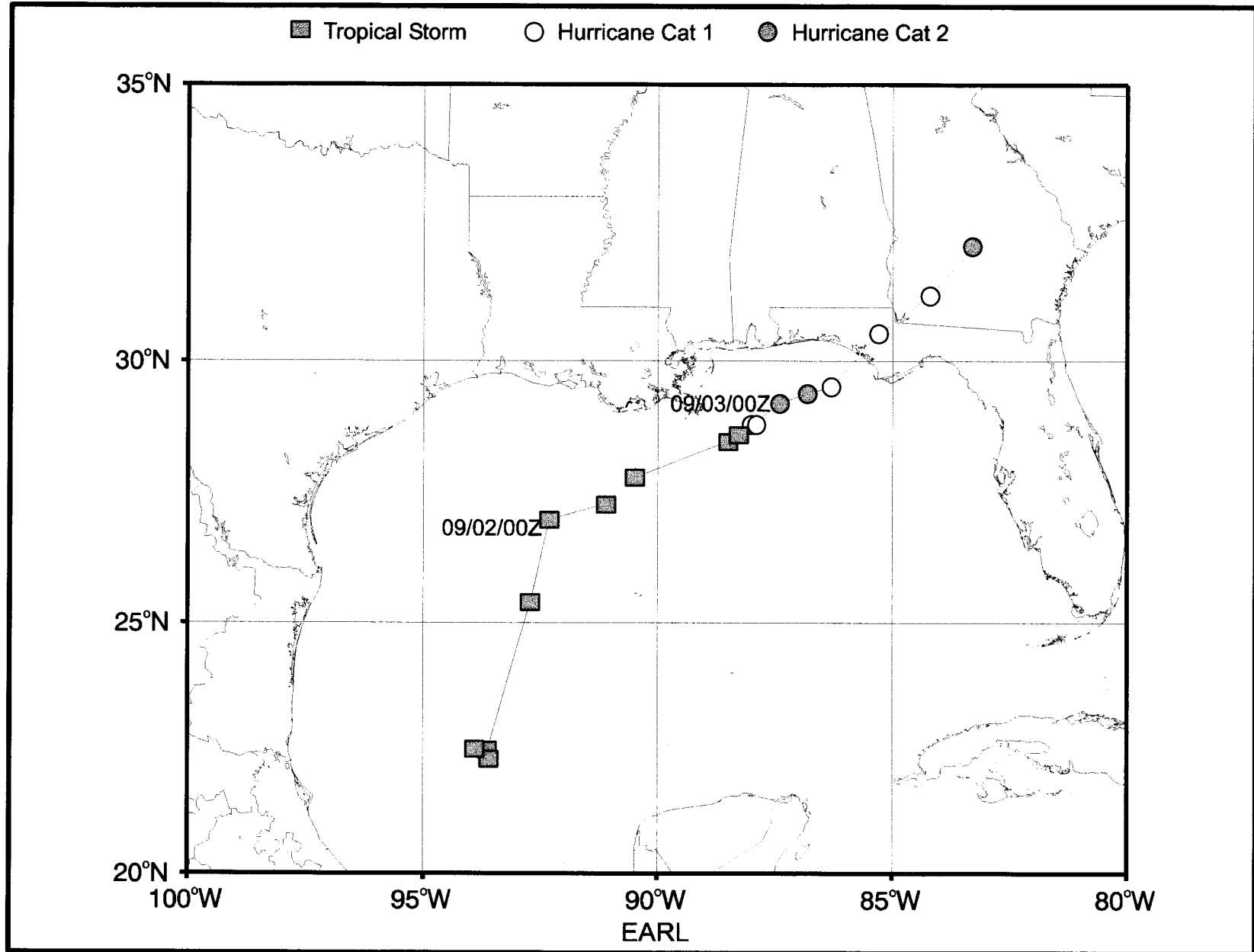


Fig. 6.17. Map showing the path of Hurricane Earl.

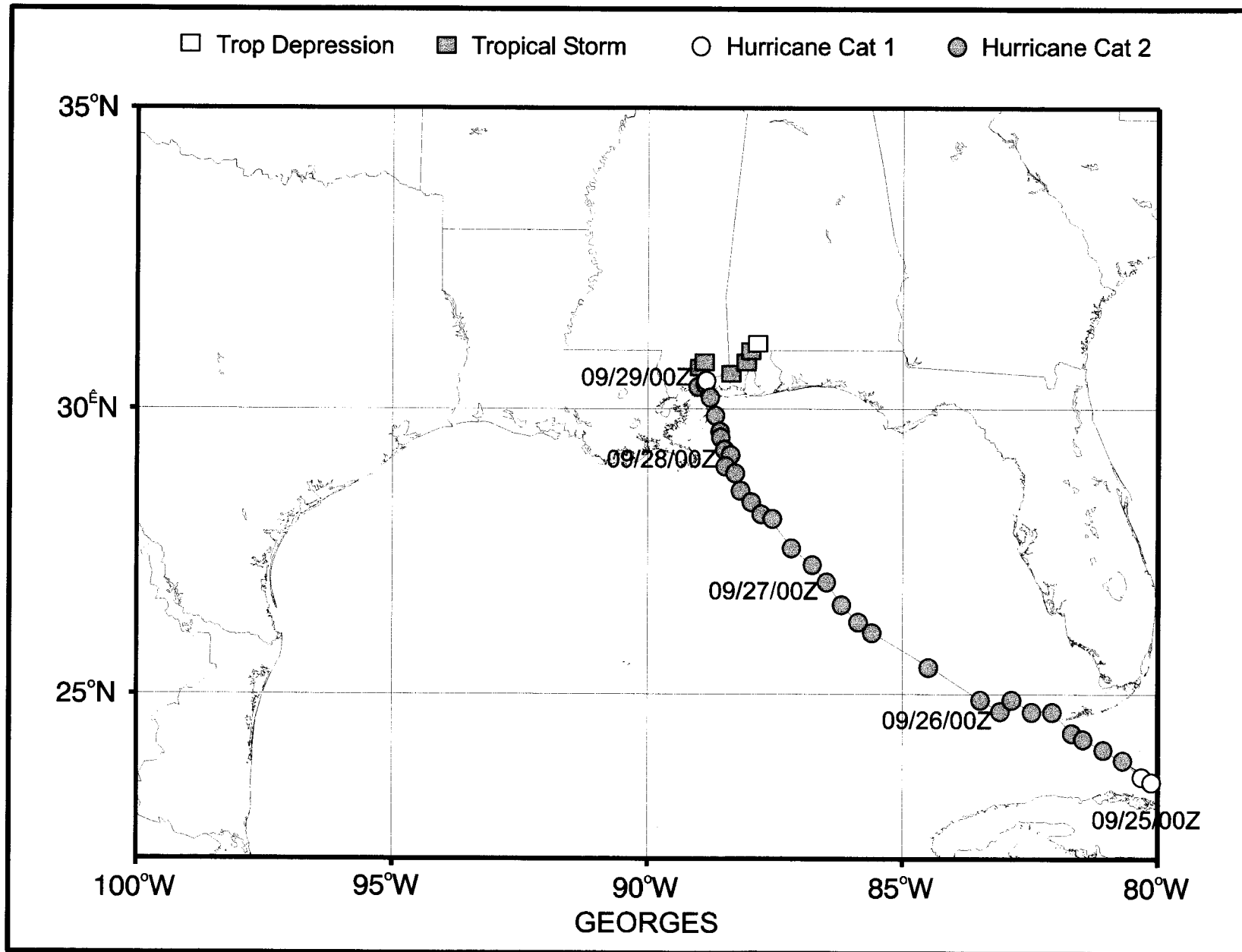


Fig. 6.18. Map showing the path of Hurricane Georges.

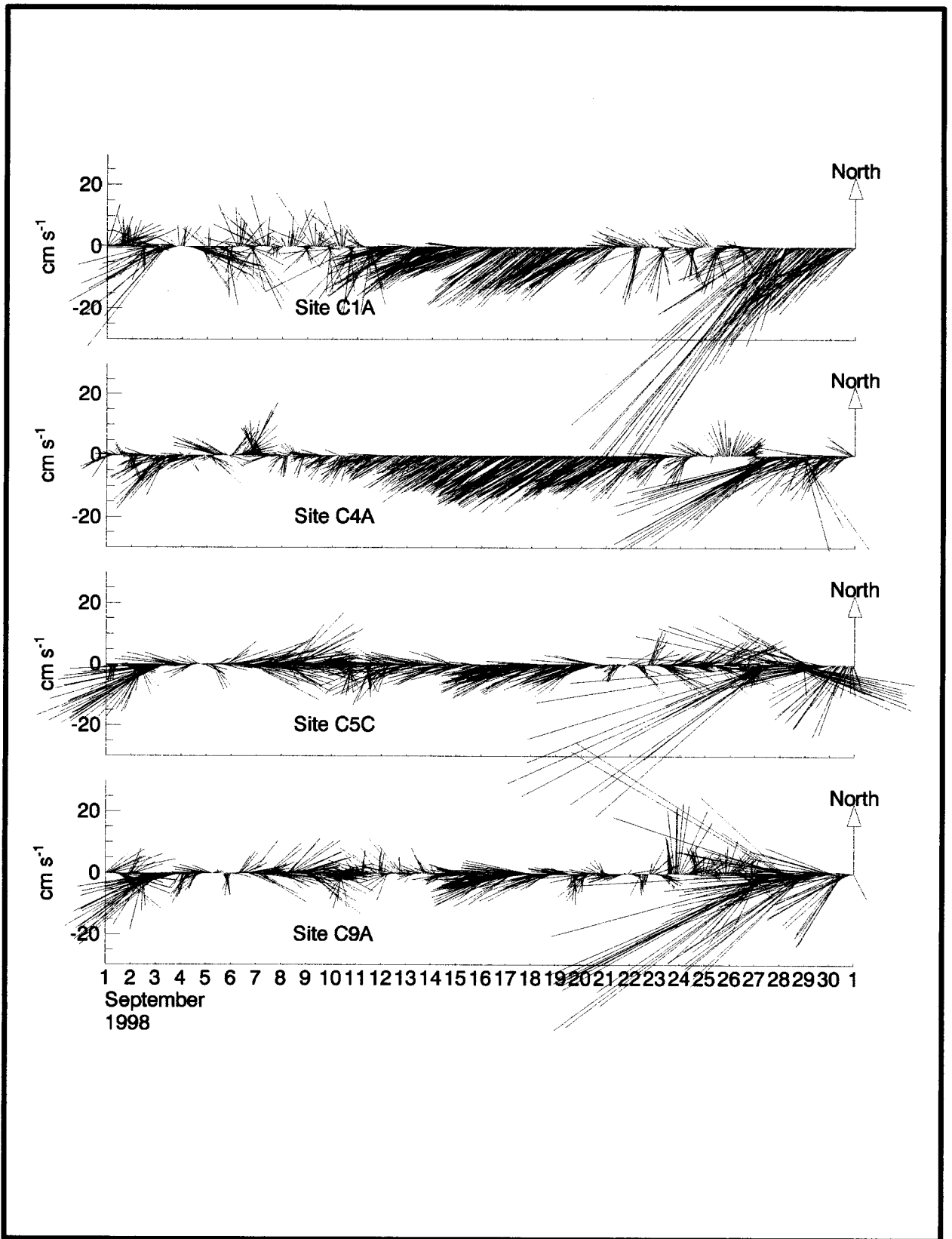


Fig. 6.19. September 1998 stick vector plot of currents recorded at 16 meters above the bottom (mab) at Sites 1, 4, 5, and 9. North is vertically upward, and a scale for the magnitude is in the left side of each panel.

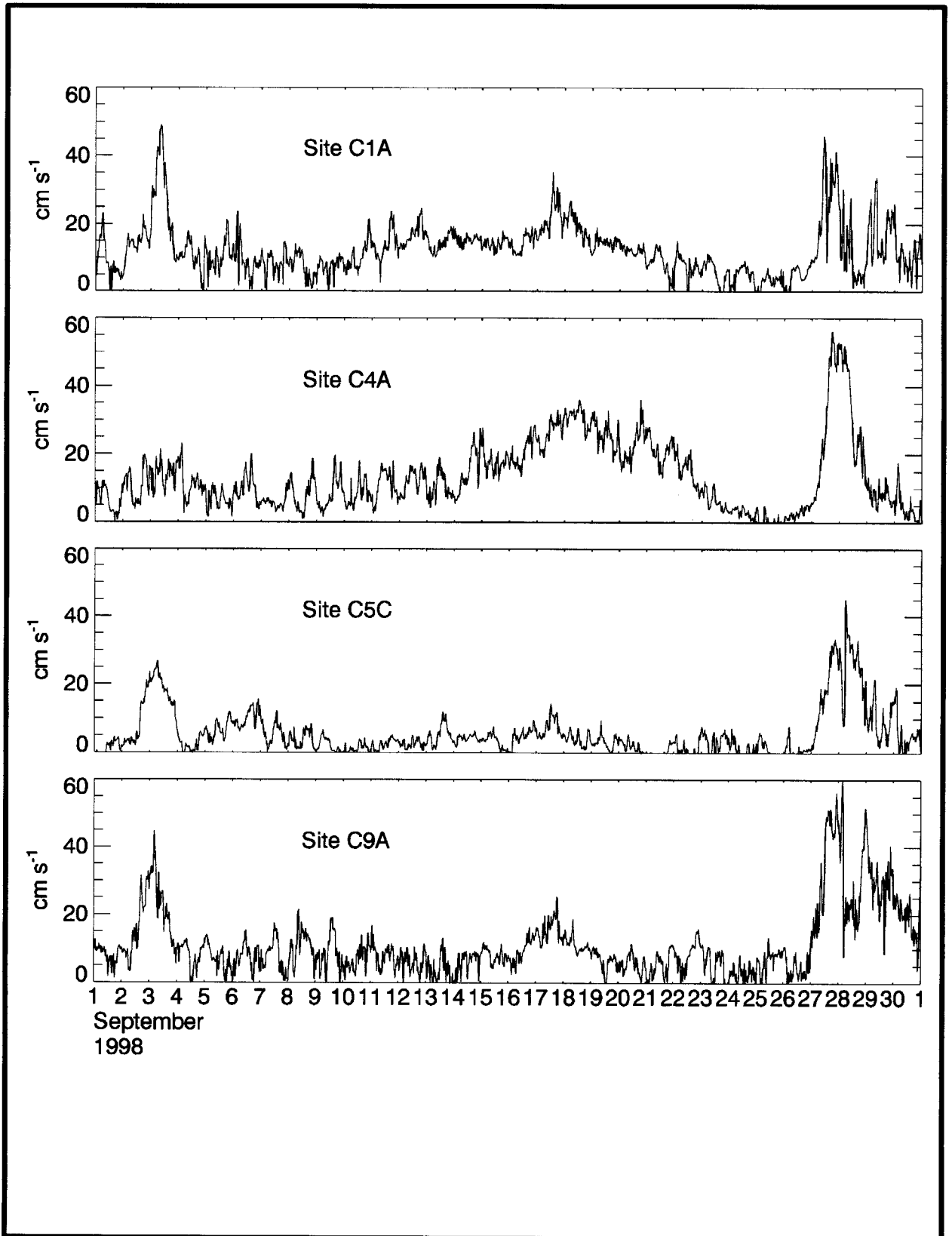


Fig. 6.20. September 1998 current speeds recorded at 4 meters above the bottom (mab) at Sites 1, 4, 5, and 9.

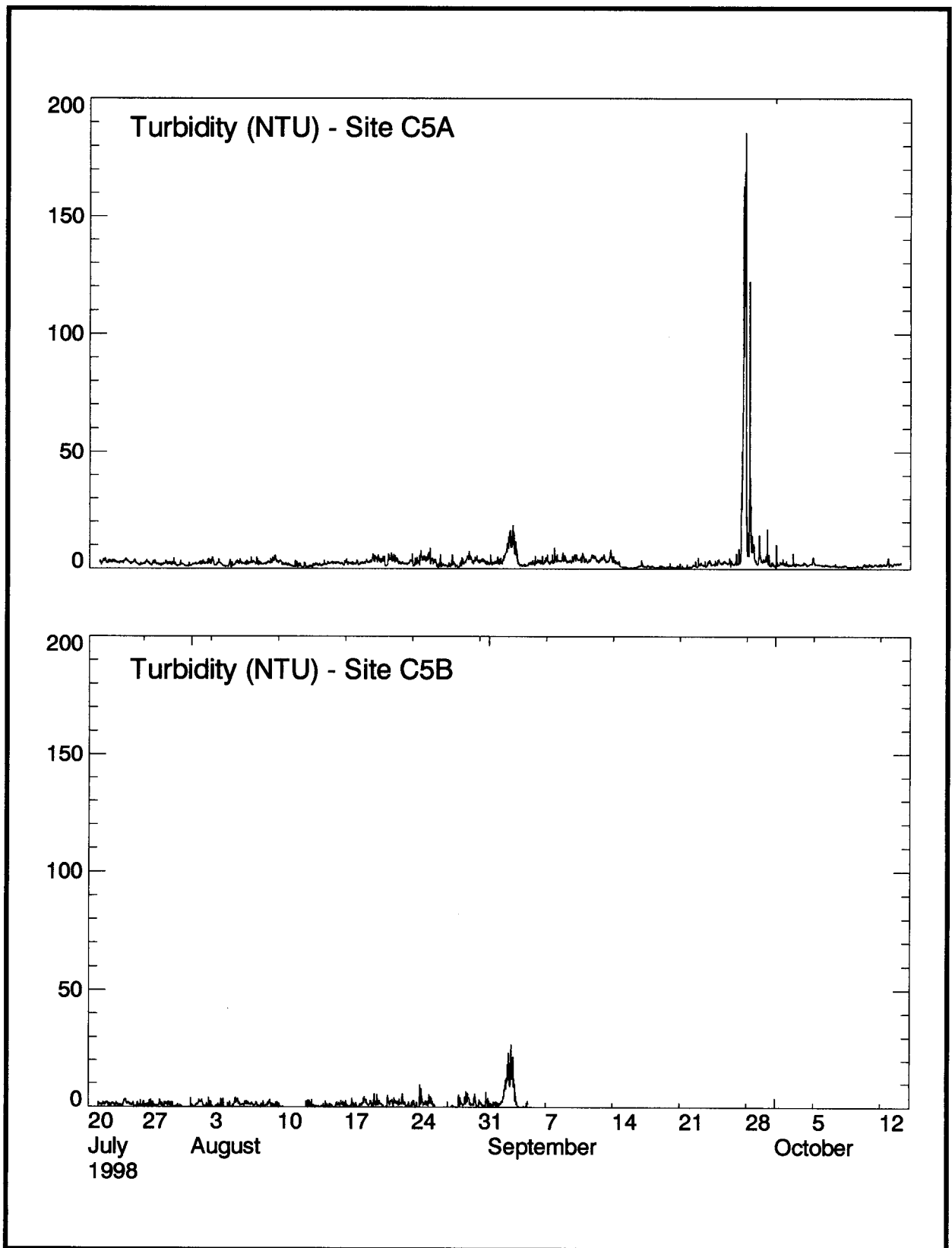


Fig. 6.21. Turbidity (NTU) recorded at Sites 5A and 5B at 2.3 meters above the bottom during 20 July through 14 October 1998.

Hurricane Earl

Hurricane Earl, which moved more quickly across the shelf, forced a response of about half the intensity forced by Hurricane Georges. The response to Hurricane Earl at 4 mab was strongest at Site 1, reaching about 50 cm/s, and almost nonexistent at Site 4. The NDBC 42040 buoy began recording the arrival of swell (6.25-second period waves with a significant wave height of 0.6 m) generated by the hurricane approximately three days before passage of the storm. These swell waves were incapable of influencing the bottom. At ~ 1500 UTC on 2 September, the hourly winds peaked at 21.1 m/s. At that time, the dominant period wave had a period of 10.0 seconds and a maximum significant wave height was 5.96 m. These swell waves would be capable of producing orbital wave velocities no greater than 20 cm/s at the shallowest site (Site 5) and velocities of 6 cm/s at the deepest site (Site 4). Depending on the local value of the Shields parameter, these velocities may be capable of causing sediment resuspension.

Possible Loop Current-Related Intrusion

Between September's two hurricane events, an oceanic circulation feature may have intruded onto the shelf. Currents were persistently southwestward during 11-21 September at Sites 1 and 4, with speeds of 15-20 cm/s. This signature was also observed at Sites 5 and Site 9 for briefer periods. The intrusion event between the hurricanes is most evident at Site 4, where current speed exceeded 20 cm/s for eight days.

Freshwater Input

The presence of river runoff in the surface layer can affect water properties. The total freshwater flow onto the Mississippi-Alabama shelf is shown in **Fig. 6.6**. The figure also shows the daily long-term mean Mississippi River contribution from 1961 to 1998. The long-term flow reaches a maximum in the middle of April and a minimum in late September. Probably as a result of frequent winter storms in the lower Mississippi basin, the long-term record shows a secondary maximum in early January. Compared to the long-term daily mean contribution (50% of the total) of 253,000 cubic feet per second (cfs), the actual Mississippi discharge in 1997, 1998, and 1999 contributed 20% more than typical. However, there appears to be a linear trend that shows the discharge contribution increasing from 200,000 cfs in 1961 to 300,000 cfs in 1998.

The total freshwater flow onto the Mississippi-Alabama shelf, averaged over the period 1 January 1997 to 30 September 1999, was 413,164 cfs. Of this total, the Mississippi contributed 73%, Mobile Bay 18.9%, and all other rivers 8.4%. Of that 8.4%, the Pearl River contributed 1.8%, the Pascagoula 2.6%, the Escambia 2.1%, and the Choctawatchee 2.0%. As expected, the Mississippi River is the largest contributor of freshwater to the Mississippi-Alabama Shelf. Mobile Bay is the second largest.

The Mississippi River contribution had a maximum of 740,000 cfs that occurred on 26 March 1997. It is conceivable that this peak was the result of a 1 March 1997 storm that brought record rainfalls in excess of 10 inches and severe flooding to the Ohio Valley. The maximum combined freshwater flow onto the Mississippi-Alabama Shelf

occurred on 12 March 1998. The peak flow of 988,700 cfs was the result of a late winter storm that caused the highest flows seen for the Escambia and the Choctawhatchee Rivers. The Escambia River maximum flow of 100,000 cfs occurred on 11 March 1998 and the Choctawhatchee River maximum flow of 93,900 cfs occurred on 13 March 1998. The Mobile Bay flow had a coincident peak of 373,000 cfs. The storm that generated these large runoffs was not particularly severe, but it did have a large geographical coverage. The Pearl River maximum flow of 47,300 cfs occurred on 29 April 1997, coincident with a local peak in the Mobile Bay flow. There are no readily available records of a spring storm that may have caused this event. The Pascagoula River maximum flow of 102,000 cfs occurred on 13 January 1998 and the Mobile Bay maximum flow of 404,385 cfs occurred on 10 January 1998. Both of these events are associated with a severe winter storm. A local peak in the Mobile Bay flow occurred on 3 February 1999 and is associated with storms that produced severe tornadoes in Arkansas and Tennessee. A local peak in the Escambia and the Choctawhatchee Rivers in early October 1998 was the result of flooding due to the passage of Hurricane Georges. A minor peak in the Mobile Bay flow that occurred on 23 July 1997 is due to the passage of Hurricane Danny.

As an estimate of the amount of freshwater deposited onto the shelf prior to a cruise, the combined freshwater flow data were averaged over the 30 days preceding the start of a cruise (**Table 6.32**). The average refers to the average flow for the period from 1 January 1997 to 31 September 1999.

Table 6.32. Combined freshwater flow data averaged over the 30 days preceding the start of each cruise.

Cruise	Discharge (cfs)	Difference from Average (%)
1C	573788	+39%
S1	373974	-9%
M2	195602	-53%
S2	656664	+59%
M3	608669	+47%
S3	390617	-5%
S4	220956	-47%
S5	575514	+39%
M4-Leg 1	517267	+25%
M4-Leg 2	345826	-16%

In Situ Measurements of Water Properties

Temperature and Salinity

The moored instruments collected time series temperature and conductivity, which together yield a time series of calculated salinity. Temperature at the depth of the

instrument moorings followed a small seasonal cycle with superposed variability caused by short-term vertical motion under stratified conditions, and by advective changes from tidal and inertial currents and possible intrusions by mesoscale water mass motion (cf. **Figs. 6.8–6.9**). At Site 1 at 16 mab, the monthly mean low occurred in February 1998 at 18.1°C, and the monthly mean high occurred in November 1998 at 23.6°C (**Fig. 6.8**). The lowest recorded temperature was 15.4°C in February 1998 and the highest was 27.5°C in September 1998.

At Site 1 at 16 mab, the mean temperature is 20.6°C, and the standard deviation is 1.6°C (**Table 6.5**). To the west at Site 9, the values are 20.0°C and 1.4°C, for a similar size data set (**Table 6.17**). The 0.6°C difference in mean values at 16 mab is mostly a result of the ~ 13 m greater depth at Site 9. The 16 mab current meter at Site 9 and the 4 mab one at Site 1 are at about the same depth and have identical means of 20.0°C (**Table 6.6** and **Table 6.17**).

Salinity ranged from about 34.9 to 36.8 but generally was in the 36.2 to 36.4 range. Values above 36.5 suggest possible intrusion of Loop Current related water. (Note: Salinity as currently defined by the Practical Salinity Scale, has no units. Values are given simply as a number.)

Dissolved Oxygen and Turbidity

Time series of dissolved oxygen and turbidity were collected at a height of ~ 2.3 mab at each mooring. Data return is good for dissolved oxygen, but not for turbidity. Sensor or instrument malfunction rather than fouling are responsible for data loss. Dissolved oxygen values were generally near or above 4 mg/L (e.g. **Fig. 6.9**), except at Site 5 during the second deployment period. In this record, values were below 3.0 mg/L much of the time and fell below 2.0 mg/L during 18–28 August and 5–13 September 1997. Turbidity values were generally quite low, i.e., 0–2 NTU, with brief periods during which turbidity rose to the 2–10 NTU range. Values exceeding 10 NTU occurred during Hurricane Georges (**Fig. 6.21**). Turbidity is discussed further in Chapter 5.

Vertical Profiles

Fig. 6.22 summarizes the temperature-salinity relationships for the nine cruises. A composite T-S plot is given for each cruise (**Fig. 6.22a-i**), and for all casts of all cruises (**Fig. 6.22j**). A synopsis of each cruise that includes both the contemporaneous collateral data from other sources (meteorology, river discharge, waves, etc.) and the vertical profile results is presented in **Appendix D**. These synopses are summarized in **Table 6.33**.

Oxygen

Unlike LATEX, where bottle titrations were performed at approximately half the hydrographic stations, no titrations were performed to determine discrete dissolved oxygen values. LATEX found substantial problems existed with the application of the standard calibration method to the LATEX data set. They surmised that the major

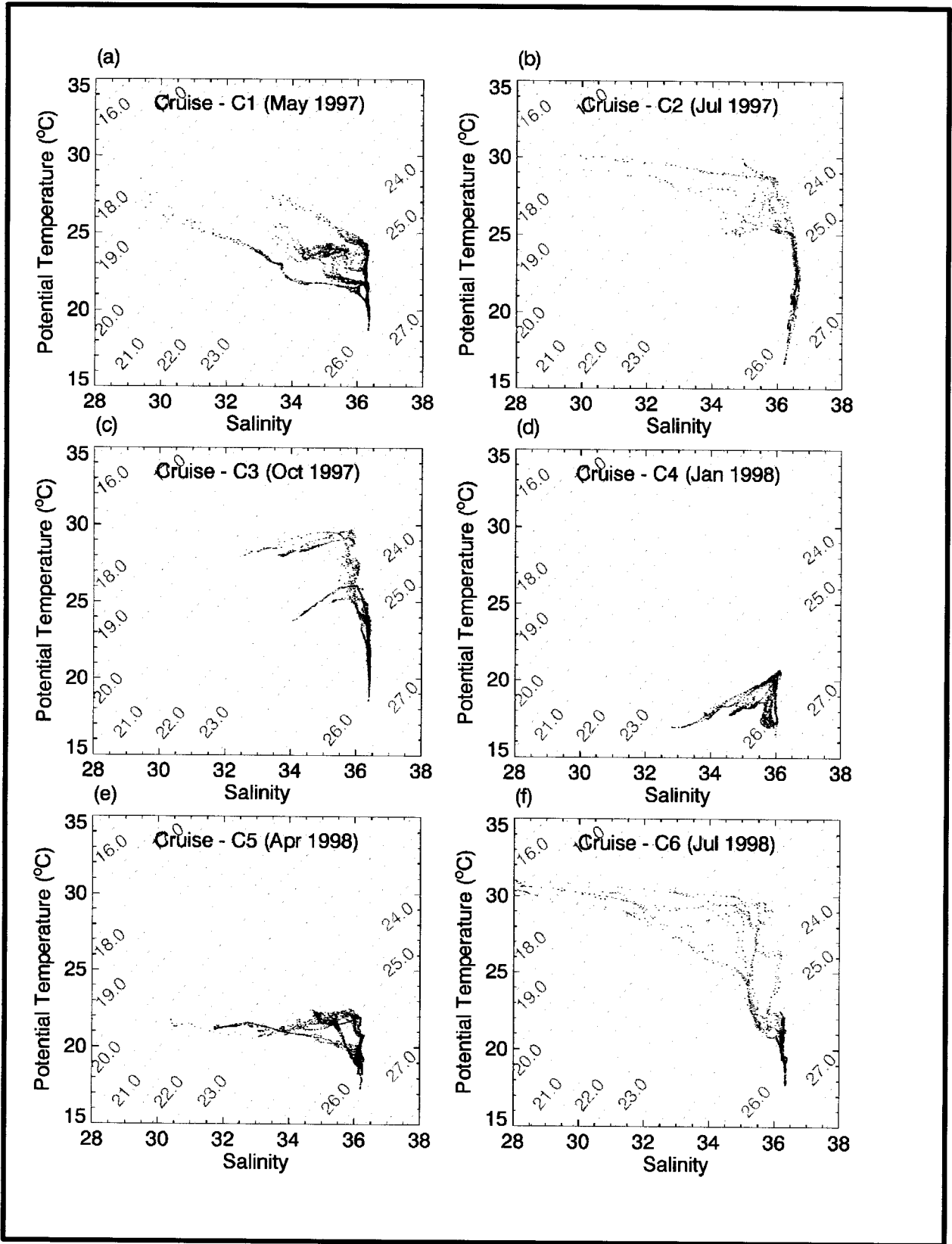


Fig. 6.22. Temperature-salinity (T-S) relationships for the nine cruises thus far in the program. A composite T-S plot is given for each cruise (a-i), and for all casts of all cruises (j).

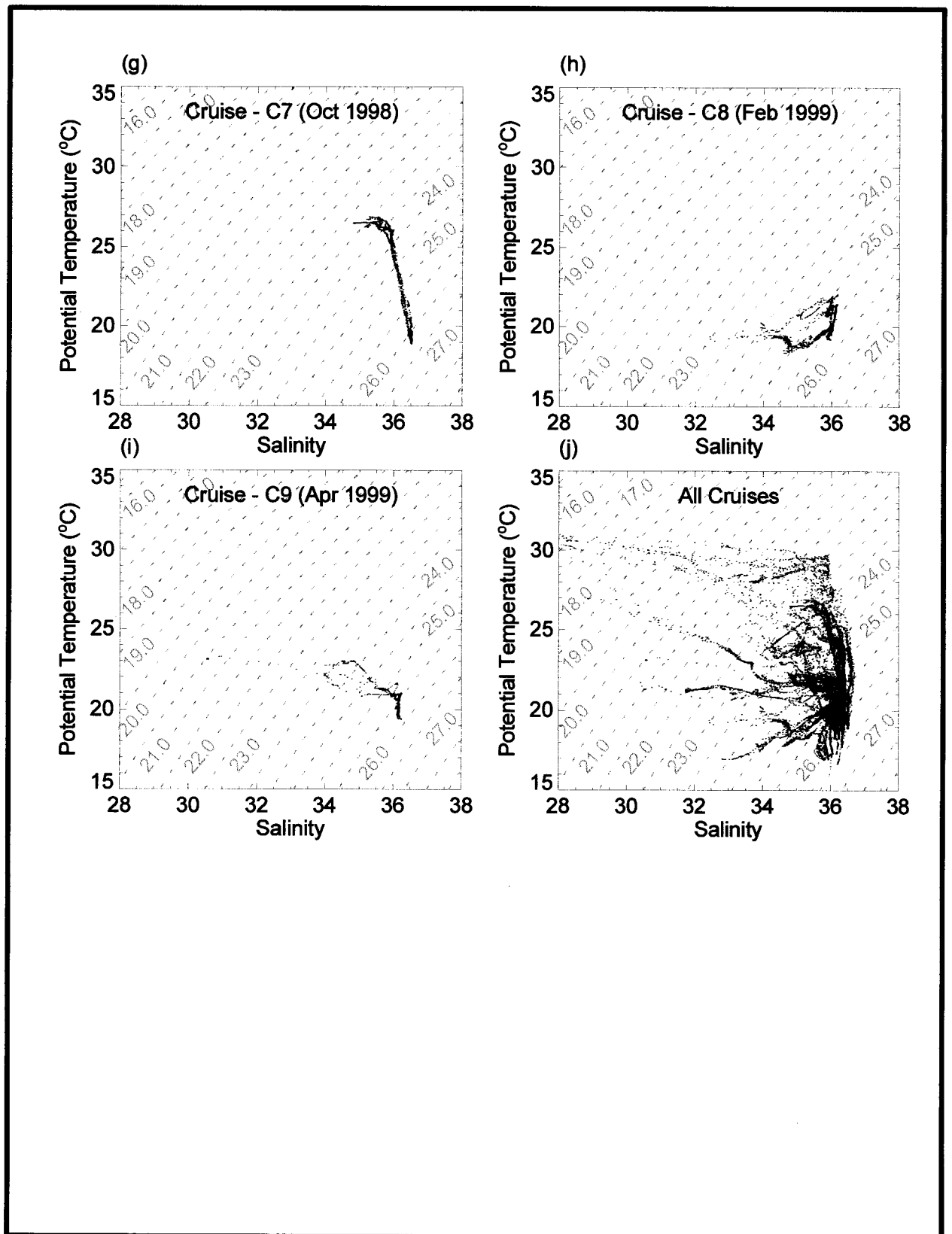


Fig. 6.22. (Continued).

Table 6.33. Summary of oceanographic results and observations from each cruise together with contemporaneous collateral data from other sources.

Cruise: Date:	Winter		Spring			Summer			Autumn	
	S2 Jan-98	S5 Feb-99	IC May-97	M3 Apr-98	M4 – Leg 1 Apr-99	S1 Jul-97	S3 Jul-98	M4 – Leg 2 Aug-99	M2 Oct-97	S4 Oct-98
Weather	Winter storm	Winter storm	--	Late-winter storm	--	Hurricane Danny	Cool bottom waters	--	--	Hurricanes Earl & Georges
Freshwater Discharge	+ 59 %	+ 39 %	+ 39 %	+ 47 %	+ 25%	- 9 %	- 5 %	- 16%	- 53 %	- 47 %
Wind Direction (°) (from)	315	225	167	310	0	210	210	225	285	40
Wind Speed (m/s)	3.36	4.46	2.76	4.82	7.85	2.74	3.85	4.20	4.11	5.67
Wave Height (m)	0.27	0.55	0.28	0.69	1.29	0.3	0.52	0.71	0.62	0.84
Dominant Wave Period (s)	5.16	4.19	4.67	4.78	5.71	6.22	4.40	4.31	4.52	5.31
Average Wave Period (s)	4.15	3.74	3.97	4.01	4.65	4.34	3.77	3.90	3.65	4.21
Geostrophic Flow (cm/s)	Upshef: weak	Easterly: weak	Upshef: 10-15	Onshelf: 25	Easterly: weak	Downshef: weak	Upshef: 50	Upshef: 25	Onshelf: 20	Upshef: weak
River Runoff Signature?	N	N	Y Sites 5,6,7,8,9	N	Y Site 9	Y All sites	Y All sites	Y All sites	N	N
Loop Current Intrusion?	N	N	N	N	N	Y All sites	N	N	N	N
AVHRR Surface T (°C)	18 – 21	24	26 – 28	22	26	Clouds	32	32	29	26
NDBC Surface T (°C)	17.2	19.7–25.6	26	21.1	23.3	29.7	30.6	30.6	27.8	26.1
CTD Surface T (°C)	17.5 – 18.5	19.2 – 21.1	23 – 27	20.5 – 22.0	22.1 – 23.1	30	30.5 – 30.9	30 – 31	24.5 – 28.5	25.5 – 27.0
CTD Bottom T (°C)	17.0 – 18.0	19.0 – 20.5	19 – 20.5	17.0 – 18.5	19.5 – 20.0	16.5 – 20	17.5 – 19.0	19.0 – 22.0	18.5 – 20.0	19.0 – 20.5
CTD Surface Salinity	33.0 – 35.5	33.4 – 35.7	30.0 – 34.0	32.0 – 35.0	30.6 – 34.6	< 30.0	~28	26.2 – 33.0	32.5 – 35.5	35.0 – 36.0
CTD Bottom Salinity	~36.0	~36.0	36.4 – 36.5	36.1 – 36.2	36.1	36.0 – 36.5	36.0 – 36.3	36.2 – 36.4	~36.4	~36.5

Table 6.33. (continued).

Cruise: Date:	Winter			Spring			Summer			Autumn	
	S2 Jan-98	S5 Feb-99	1C May-97	M3 Apr-98	M4 – Leg 1 Apr-99	S1 Jul-97	S3 Jul-98	M4 – Leg 2 Aug-99	M2 Oct-97	S4 Oct-98	
CTD Surface DO	3.7 – 5.5	4.5 – 6.5	3.5 – 5.25	4.0 – 5.5	5.7 – 6.6	No Data	4.75 – 5.75	1.6 – 4.1	3.75 – 4.5	4.5 – 5.0	
CTD Bottom DO	3.0 – 3.25	5.0 – 5.75	3.5 – 4.0	3.5 – 4.5	6.6 – 7.1	No Data	3.5 – 4.0	2.75 – 4.5	3.0	3.5 – 4.0	
Density Structure, Surface											
Site 1	Stratified	Stratified	5 m – well mixed	10 m – well mixed	10 m – well mixed	5 m – well mixed	10 m – well mixed	5 m – well mixed	30 m – well mixed	40 m – well mixed	
Site 4	20 m – well mixed	5 m – well mixed	5 m – well mixed	10 m – well mixed	10 m – well mixed	5 m – well mixed	10 m – well mixed	10 m – well mixed	40 m – well mixed	30 m – well mixed	
Site 5	10 m – well mixed	5 m – well mixed	5 m – well mixed	10 m – well mixed	10 m – well mixed	5 m – well mixed	10 m – well mixed	5 m – well mixed	20 m – well mixed	15 m – well mixed	
Site 9	Stratified	5 m – well mixed	5 m – well mixed	10 m – well mixed	10 m – well mixed	5 m – well mixed	10 m – well mixed	10 m – well mixed	20 m – well mixed	40 m – well mixed	
Density Structure, Middle											
Site 1	1 water mass	Stratified	1 water mass	1 water mass	Stratified	Stratified	Stratified	Stratified	Stratified	1 water mass	
Site 4	1 water mass	1 water mass	1 water mass	1 water mass	1 water mass	Stratified	Stratified	Stratified	Stratified	1 water mass	
Site 5	Stratified	Stratified	2 water masses	Stratified	Stratified	Stratified	Stratified	Stratified	2 water masses	Stratified	
Site 9	1 water mass	1 water mass	Stratified	2 water masses	Stratified	Stratified	Stratified	Stratified	2 water masses	Stratified	
Density Structure, Bottom											
Site 1	Stratified	1 water mass	Stratified	Stratified	1 water mass	Stratified	1 water mass	Stratified	Stratified	1 water mass	
Site 4	1 water mass	1 water mass	Stratified	Stratified	1 water mass	Stratified	1 water mass	Stratified	Stratified	1 water mass	
Site 5	Stratified	1 water mass	Stratified	Stratified	1 water mass	1 water mass	1 water mass	Stratified	1 water mass	Stratified	
Site 9	1 water mass	1 water mass	1 water mass	1 water mass	1 water mass	1 water mass	1 water mass	Stratified	1 water mass	No Data	
Variability, Bottom Density											
Site 1	Extreme	Small	Average	Very Large	--	Large	Small	Average	Very Large	Small	
Site 4	Average	Small	Large	Large	--	Small	Average	Large	Large	Small	
Site 5	Small	Small	Average	Average	--	Average	Average	Average	Average	Average	
Site 9	Small	Small	Large	Small	--	Small	Average	Small	Small	Small	

Abbreviations: AVHRR = advanced very high resolution radiometer; CTD = conductivity-temperature-depth; DO = dissolved oxygen; NDBC = National Data Buoy Center.

problem was the combination of substantial vertical gradients coupled with sensor time delays and decided that the computation of oxygen concentration from the raw oxygen sensor data should be left to potential users.

We corrected the oxygen sensor against the Levitus 94 climatology for the one-degree square that encompasses the study region. This approach assumes that (a) the Levitus data are the combination of reliable and accurate measurements, including bottle titrations, and (b) the climatology experienced during our cruises is statistically similar to the Levitus climatology. Yearly-averaged, dissolved oxygen concentrations are provided in the Levitus 94 database for the surface, 10 m, 20 m, 30 m, 50 m, and 75 m depths. A climatology for the same depths was constructed by averaging the CTD data from the eight cruises that used the same oxygen sensor. The results are plotted in **Fig. 6.23** for each depth. It clearly shows that this study's climatology is biased low by a nearly constant offset of ~ 0.468 mL/L from the surface to 30-m depth. The 50- and 75-m depths for this study's climatology are likely influenced by the bottom to a greater degree than the Levitus 94 climatology, since the Levitus 94 one-degree square encompassed water deeper than 100 m. In order to correct the oxygen sensor, each oxygen profile was increased by 0.4679 mL/L. This matched our climatology to the Levitus 94 climatology. The values in Table 6.33 reflect the corrected oxygen concentrations.

A review of the corrected seasonal climatology (**Fig. 6.24**) shows that, in general, the dissolved oxygen level for the winter and spring cruises is slightly higher than the Levitus climatology, and the summer and autumn cruises are noticeably lower. This trend held for all depths. During the summer and winter cruises, the dissolved oxygen concentration at the surface was significantly lower than the Levitus climatology.

Salinity

Yearly and monthly-averaged salinity data are also available in the Levitus 94 climatology for the same depths as above. A climatology for this study for the same depths was constructed by averaging the CTD data from all cruises. Unlike the dissolved oxygen data, there is no need to correct the salinity data. The results (**Fig. 6.25**) show that during this study the water column was noticeably fresher than Levitus, particularly at the surface. This is probably due to the 20% higher than average river runoff recorded for each of the three years. A review of the seasonal climatology (**Fig. 6.26**) shows a strong summertime halocline down to the 20 m depth. This layer will significantly inhibit vertical mixing of momentum, salt, and heat. The highest salinity occurs during wintertime, while autumn salinities are nearly as high as the winter. Regardless of season or cruise, the salinity near the bottom at 75 m was relatively constant. Only during the winter did it fall slightly below 36.0. Evidence of Loop Current intrusions is seen in the summer data for the 20 and 30 m depths. The salinity is slightly higher than climatology would indicate.

Temperature

Similarly for temperature, a climatology for this study for the same depths was constructed by averaging the CTD data from all cruises. The results (**Fig. 6.27**) show that

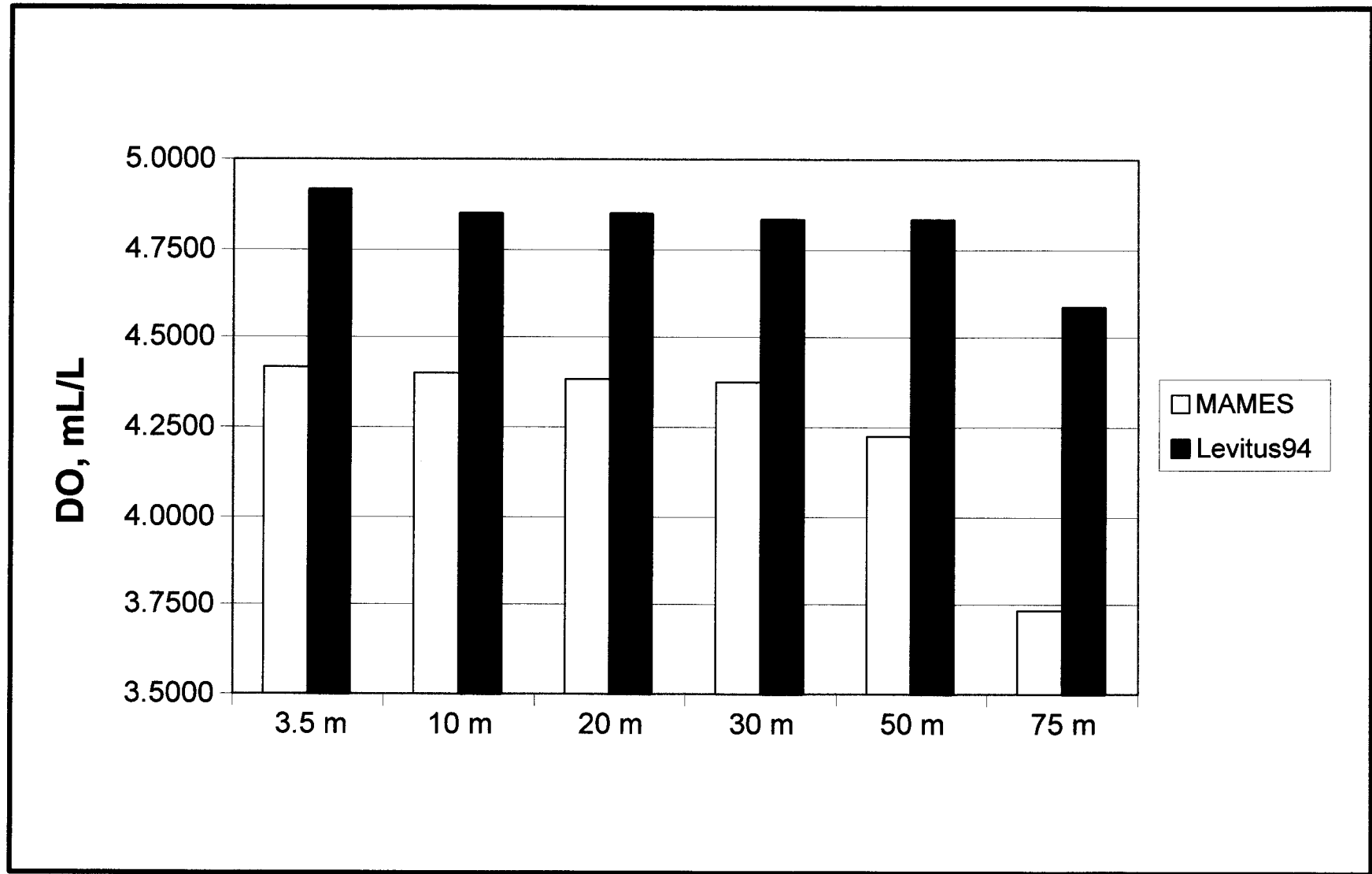


Fig. 6.23. Comparison of dissolved oxygen concentrations for the combined cruises during this study versus the Levitus 94 climatology for the one-degree square encompassing the study region. A constant offset of 0.47 mL/L is evident in the 3.5 m, 10 m, 20 m, and 30 m depths.

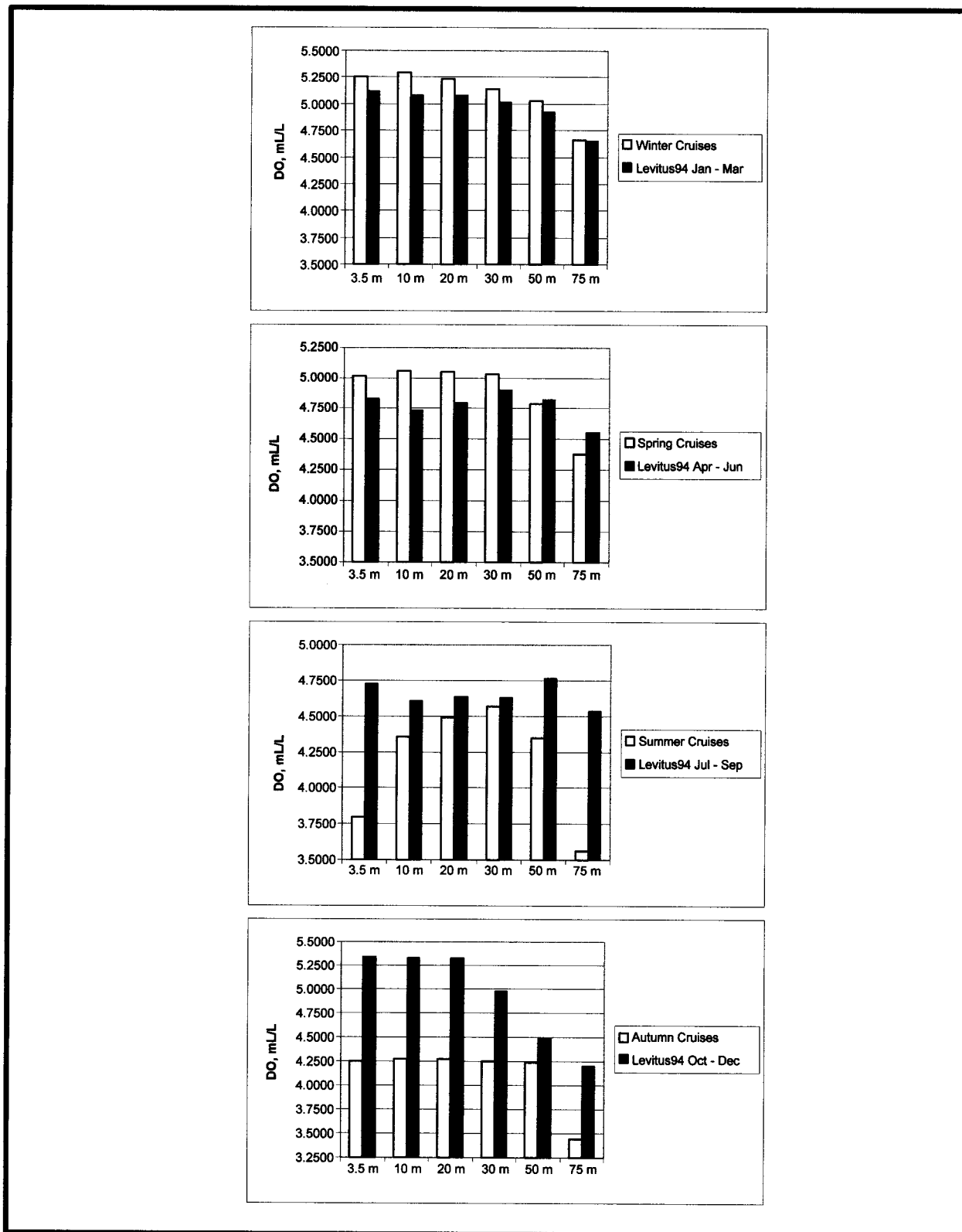


Fig. 6.24. Comparison of corrected dissolved oxygen concentration for the cruises during this study versus the Levitus climatology by season. The Levitus climatology encompasses the one-degree square encompassing the study region.

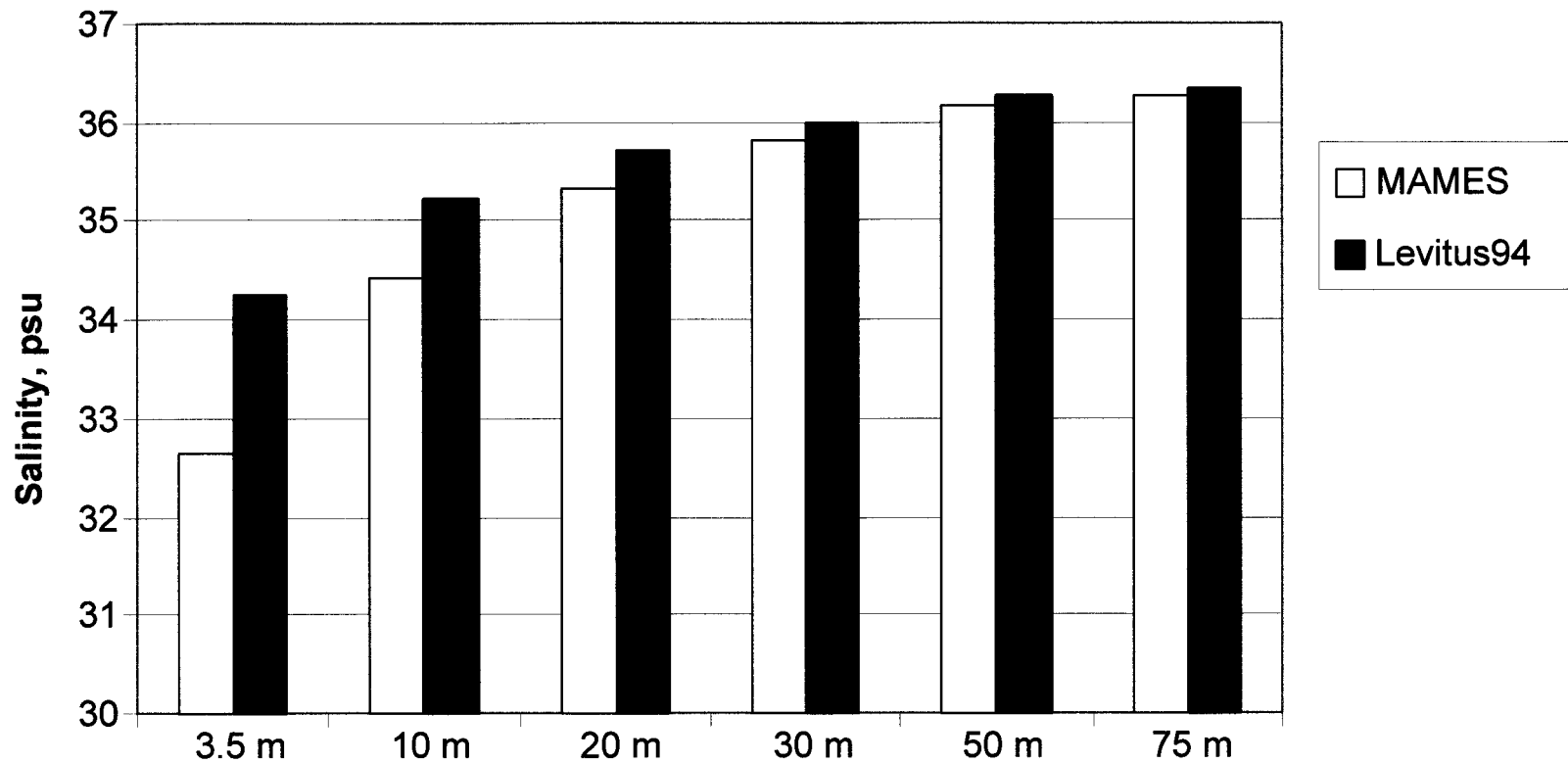


Fig. 6.25. Comparison of salinity for the combined cruises during this study versus the Levitus 94 climatology for the one-degree square encompassing the study region. The surface is noticeably fresher than climatology.

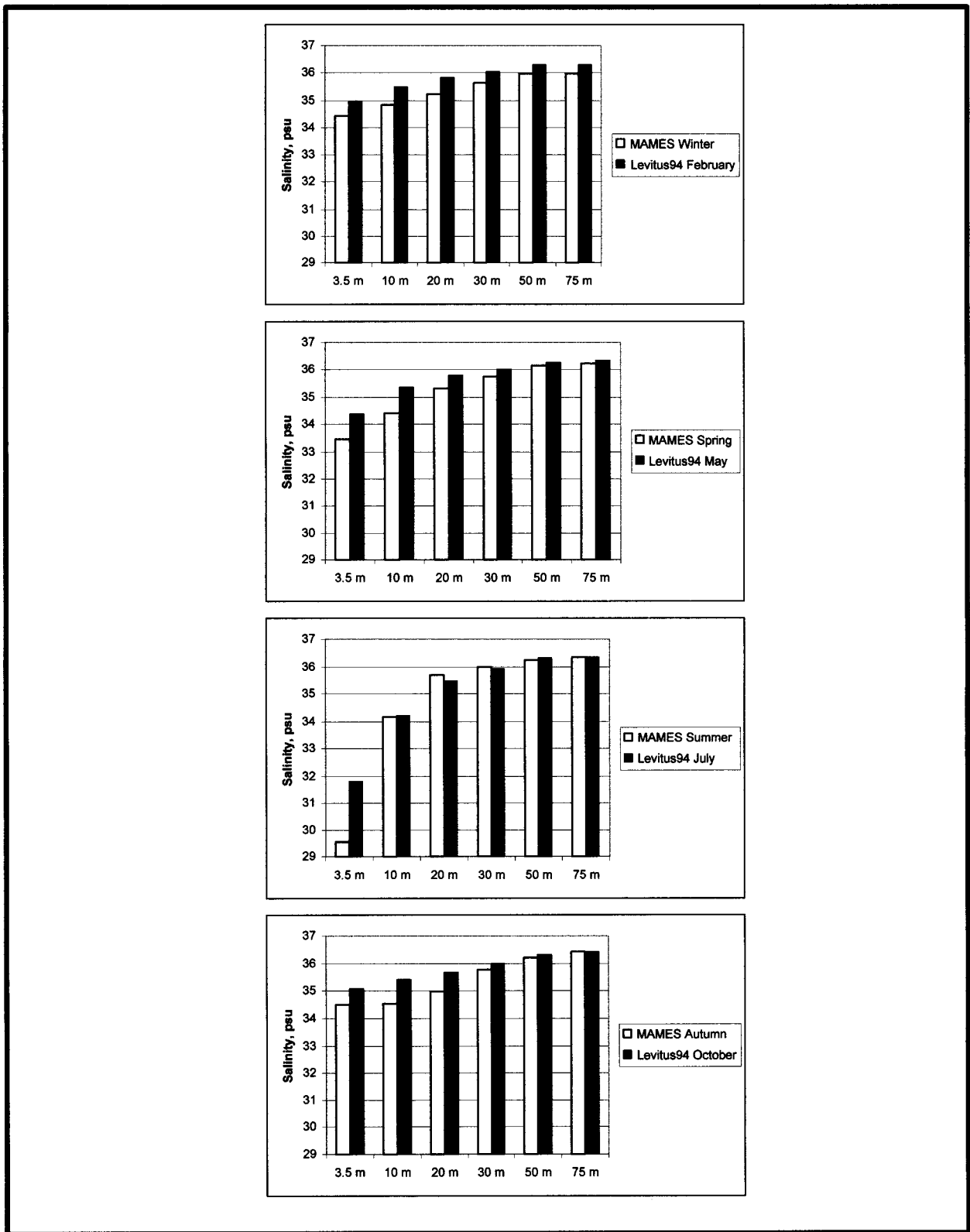


Fig. 6.26. Comparison of salinity for the cruises during this study versus the Levitus climatology by season. The Levitus climatology encompasses the one-degree square encompassing the study region.

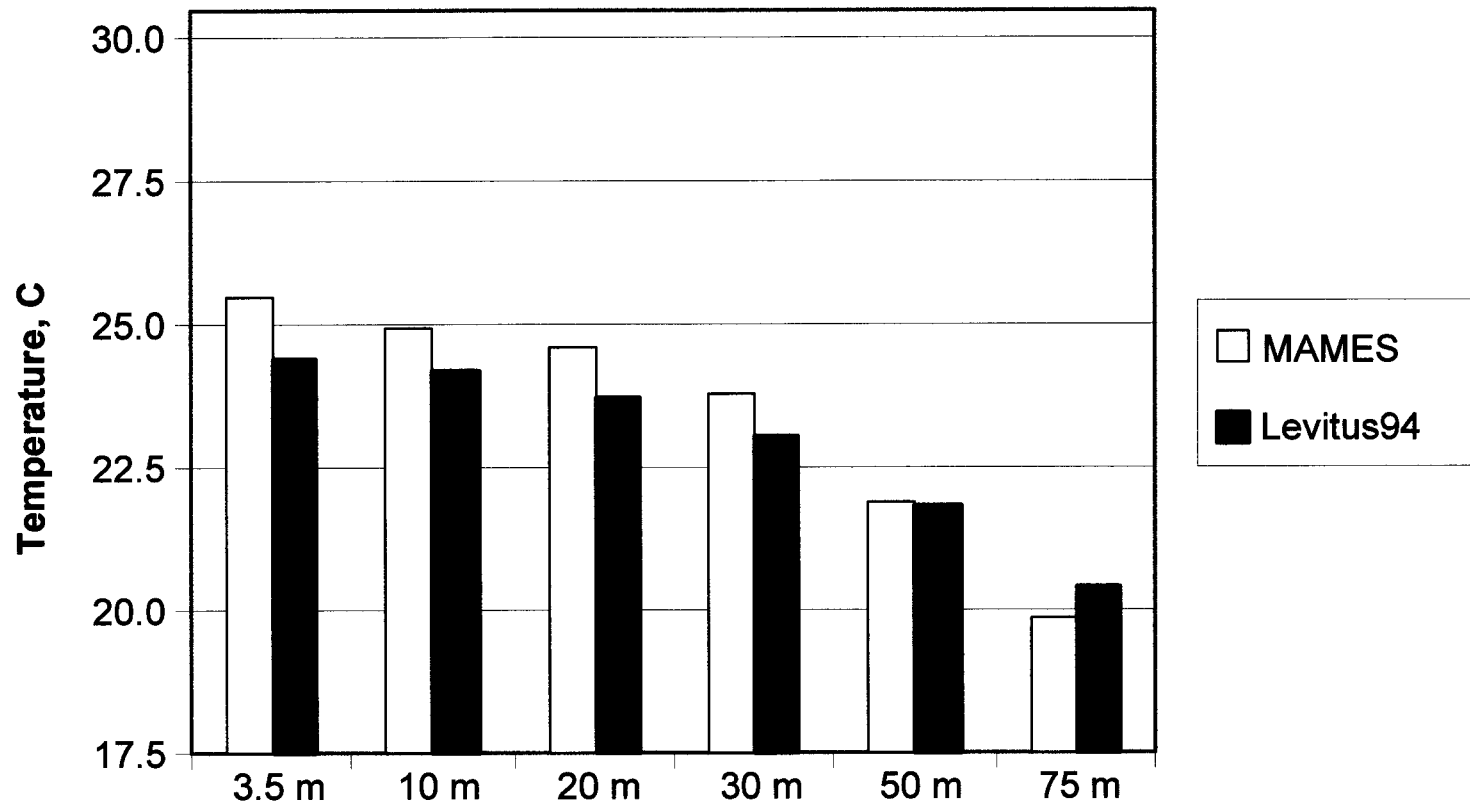


Fig. 6.27. Comparison of temperature for the combined cruises during this study versus the Levitus 94 climatology for the one-degree square encompassing the study region. The water column is noticeably warmer than climatology.

the water column is noticeably warmer than Levitus 94 climatology, particularly at the surface. A review of the seasonal climatology (**Fig. 6.28**) shows the water column is vertically uniform and coldest during winter. In spring, the water column begins to heat up and a thermocline starts to develop. The water column is at its warmest during summer and the thermocline is well established. There is approximately a 10°C vertical gradient from top to bottom. Then in autumn the thermocline begins to break down, but the heat content in the water column remains nearly the same as in the summer. The high heat trapped in the surface levels is mixed down as the strong summertime halocline breaks down. However, through each season and each year the temperature near the bottom (75 m) remains within a fairly tight band of 18.11°C to 20.79°C. On the other hand, the surface temperature ranges from a low of 17.86°C to a high of 30.62°C. Both winter cruises show a mid-depth temperature higher than the surface or the bottom, yet the surface is slightly colder than the bottom.

Discussion

From a review of the temperature, salinity, and density profiles for each of the cruises, it is apparent that the density of the water in the upper part of the water column is mainly controlled by the salinity. This suggests water properties determined by coastal processes. In the lower half of the water column, the density is mainly controlled by the temperature, which suggests water properties determined by the presence of Gulf waters. The bottom salinity always ranged from 36.0 to 36.5 regardless of site depth, site location, season, or year. Water with this salinity is indicative of common Gulf water. Furthermore the salinity was generally uniform in the bottom half of the water column. Any temporal variations in the density, which are frequently seen, are the result of temperature variations.

The intrusion of Loop Current water, with its signature salinity greater than 36.5, occurs only for one cruise, during the summer (July 1997) Cruise S1. That intrusion was seen across the study region (**Fig. 6.29**). The presence of Mississippi River plume water in the surface layer is seen in every summer cruise at every site. It is probably transported from the delta by favorable winds and currents. During the spring cruises, plume water is seen sporadically at the western sites. Plume water is not seen during the autumn and winter cruises.

The upper half of the water column is warmer and less saline than the Levitus 94 climatology indicates. This is a clear indication of the effect of the increased amount of river runoff experienced during the study period. The period of greatest river runoff (Winter and Spring) is not associated with the minimum surface salinity (Summer).

Both winter cruises occurred at a time when cold shelf water was being pulled off the shelf, to the east of the study area. Both winter cruises show the presence of a warm subsurface layer associated with a homogeneous water mass.

It is apparent from a review of the temperature, salinity, and density profiles that temporal variations in water properties can be quite significant, even at the bottom. An example of the range of temporal variations that can occur in salinity for example, at a

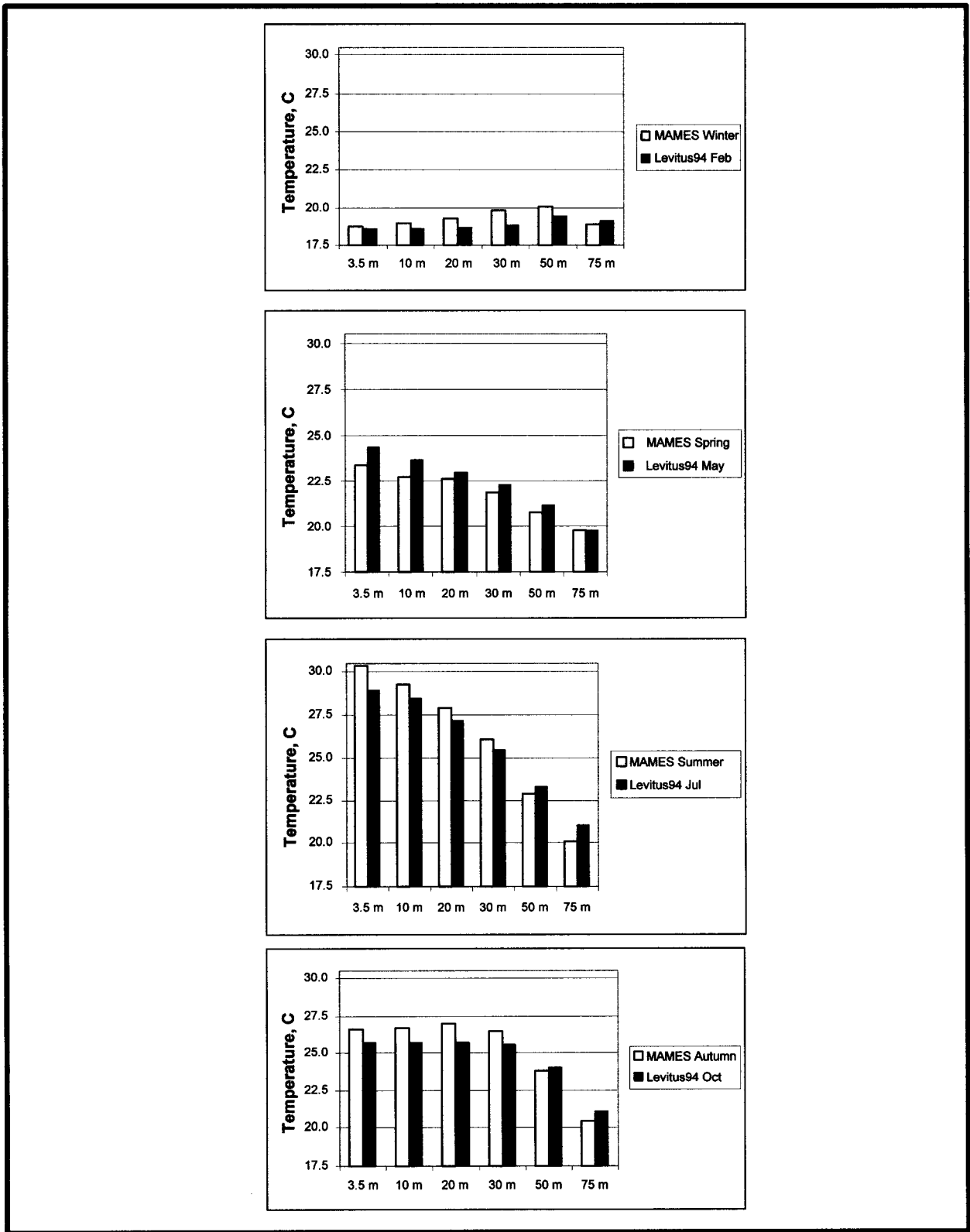
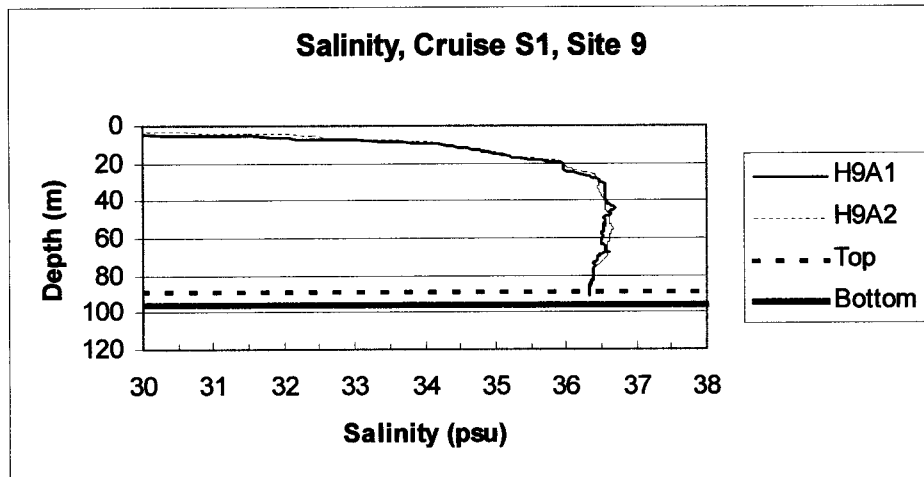


Fig. 6.28. Comparison of temperature for the cruises during this study versus the Levitus climatology by season. The Levitus climatology encompasses the one-degree square encompassing the study region.

(a)



(b)

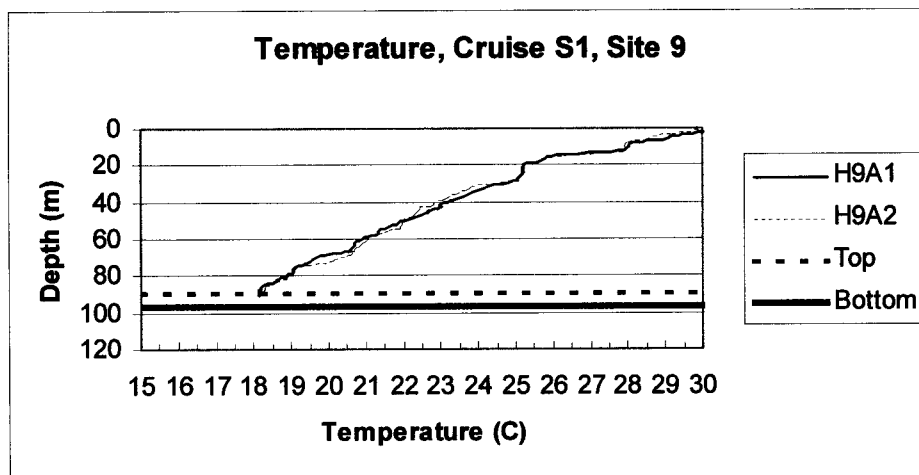


Fig. 6.29. Vertical profiles at Site 9 during Cruise S1 that shows the intrusion of the Loop Current with its signature of salinity greater than 36.5. The legend 'Top' indicates the top of the pinnacle and 'Bottom' the sea floor. Panel (a) shows salinity and (b) shows temperature.

single site is shown in **Fig. 6.30**. Yet even at the same site, in the same season, but different years, the variability over several hours can be quite small or it can be quite large. The greatest temporal variability in the bottom density over a four to six hour time frame consistently occurred at Site 1, where the bottom density structure was usually stratified. The least amount of temporal variability in bottom density over a four to six hour time frame consistently occurred at Site 9, where the bottom density structure was vertically uniform due to the presence of a uniform water mass.

The CTD profiles suggest that spatial variations in the vicinity of a site are small. **Fig. 6.31** shows the small spatial variation that occurred at the three CTD locations around Site 5 during Cruise S4. The three locations, A, B, and C, were rapidly sampled prior to servicing the mooring, and again afterwards. There is little variation from location to location over the short period of approximately 45 minutes. Other examples of limited spatial variation when a site is rapidly sampled are seen at Site 1 (Cruise M3), Site 9 (Cruise M3), and Site 4 (Cruise M2). Furthermore, spatial variations from Site to Site within a megasite are also small. The extent of spatial variations among megasites is difficult to judge because of the non-synoptic nature of the sampling. During the summer, the data suggest that the profiles of temperature, salinity, and density are similar across the study area. The shapes of the summer density profiles are quite uniform from site-to-site and year-to-year. The surface mixed layer is consistently 5–10 m thick and contains river runoff. Below the surface, the water column is continuously stratified to near the bottom, where the water becomes relatively homogeneous (**Fig. 6.32**). The short-term temporal variability near the bottom at a site is related to the degree of vertical stratification, i.e., the slope of the density profile. The greater the slope the greater the temporal variability induced by small vertical motions, which are related to a variety of processes, including possibly the flow over the mounds.

Conclusions

The results from the analyses of the full data set are quite similar to those reported in the Second Annual Report and the Third Annual Report (Continental Shelf Associates, Inc. and Texas A&M University, Geochemical and Environmental Research Group 1998b, 1999). The principal new result comes from a detailed examination of the near-bottom currents (4 mab) from the perspective of results from laboratory studies of three-dimensional, stratified, non-rotating flow over small obstacles. The laboratory studies provide the best conceptual pictures of flow details one might expect over the topographic features of this study. The most important non-dimensional parameter for stratified non-rotating flow is the internal Froude number, $F = U/Nh$, where h is the height above bottom of the obstacle, U is a characteristic upstream speed at the level of h , and N is the buoyancy frequency (also called the Brunt-Väisälä frequency) in radians per second. The value of F indicates, based on experiments and models, whether streamlines from upstream impinge on the hill, go around it, or go over the top. It also indicates, as a function of stratification, where to expect the locations of internal hydraulic jumps and their size, and the region of separated or re-circulating flow in the lee of the hill.

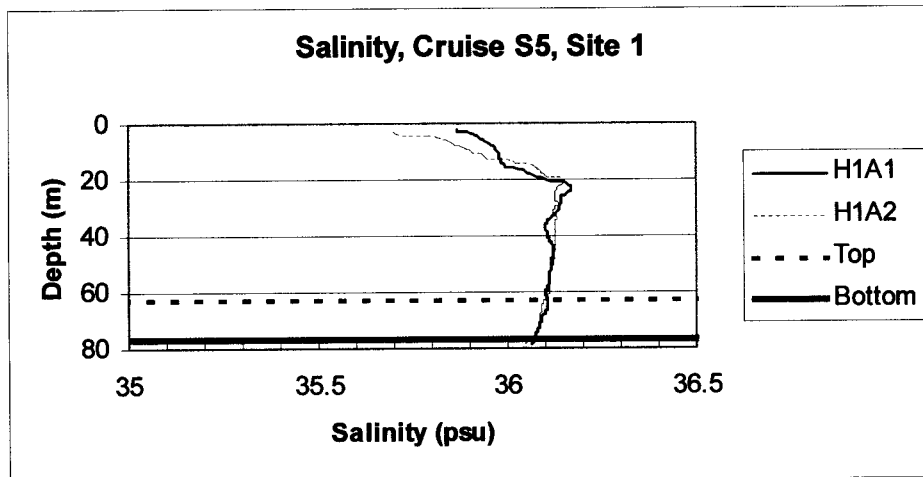
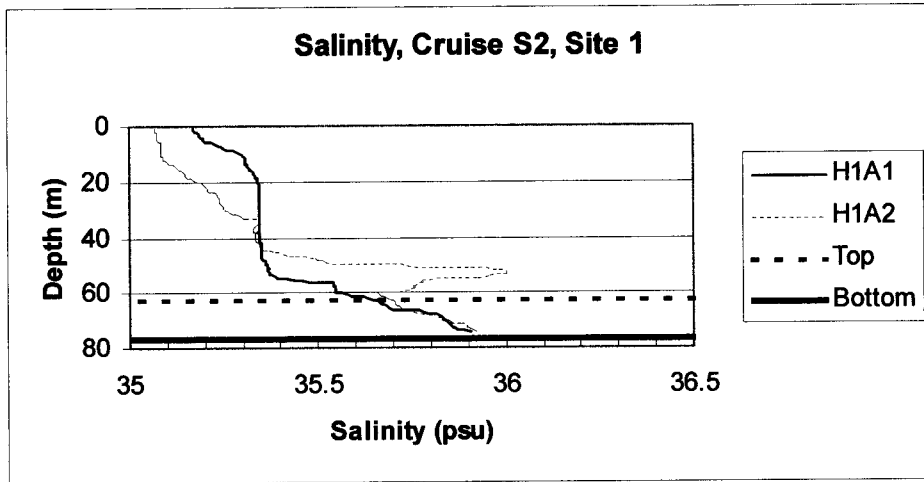
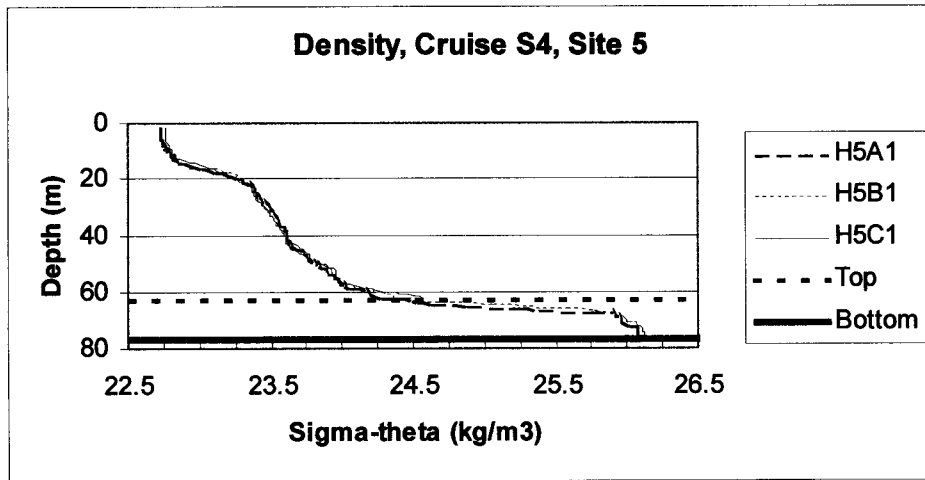


Fig. 6.30. Salinity profile at Site 1 showing the range of temporal variations that can occur. Both cruises were conducted in winter. The time difference between the two casts in Cruise S2 was three hours, eight minutes. The time difference between the two casts in Cruise S5 was exactly five hours. The legend 'Top' indicates the top of the pinnacle and 'Bottom' the sea floor.

(a)



(b)

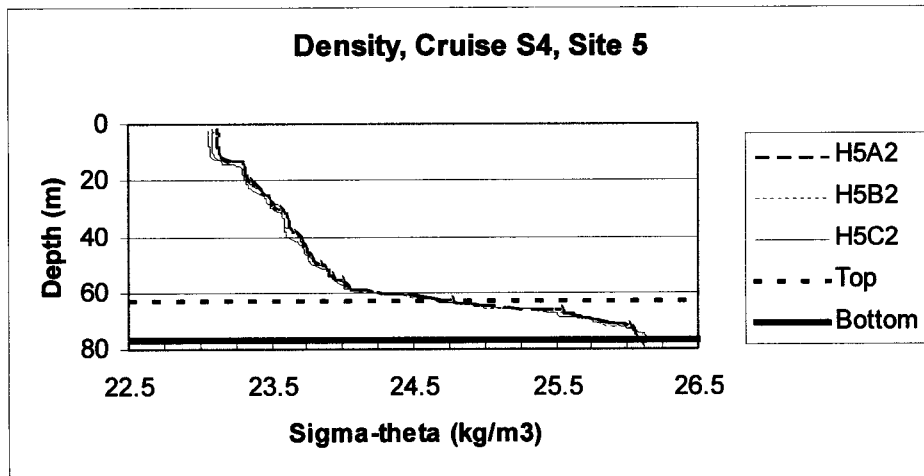


Fig. 6.31. Density profiles at Site 5 showing small spatial variations. All six casts were made during Cruise S4 on 14 October 1998. Cast H5A1 was started at 0058 UTC, cast H5B1 sixteen minutes later at 0114 UTC, and cast H5C1 twenty minutes later at 0134 UTC. Cast H5C2 commenced at 0725 UTC, cast H5B2 seventeen minutes later at 0742 UTC, and cast H5A2 nineteen minutes later at 0801 UTC. A comparison of both panels shows that some temporal changes occurred in the upper half of the water column. The legend 'Top' indicates the top of the pinnacle and 'Bottom' the sea floor.

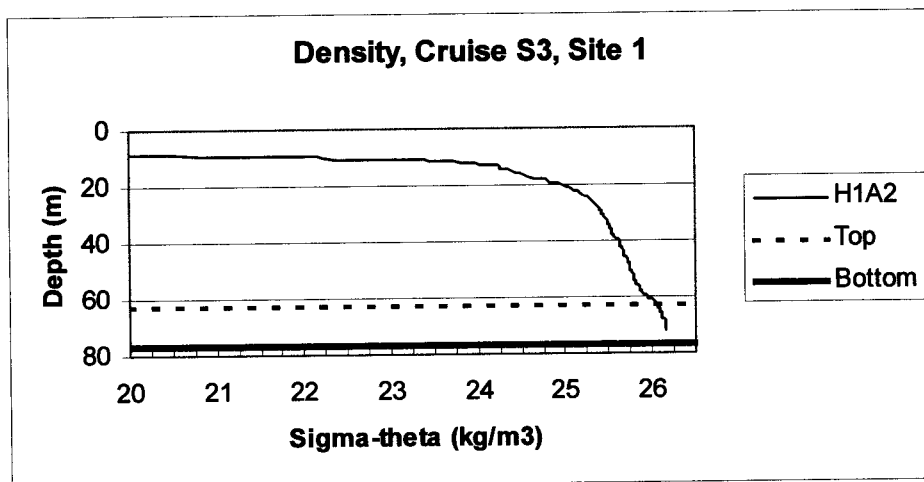
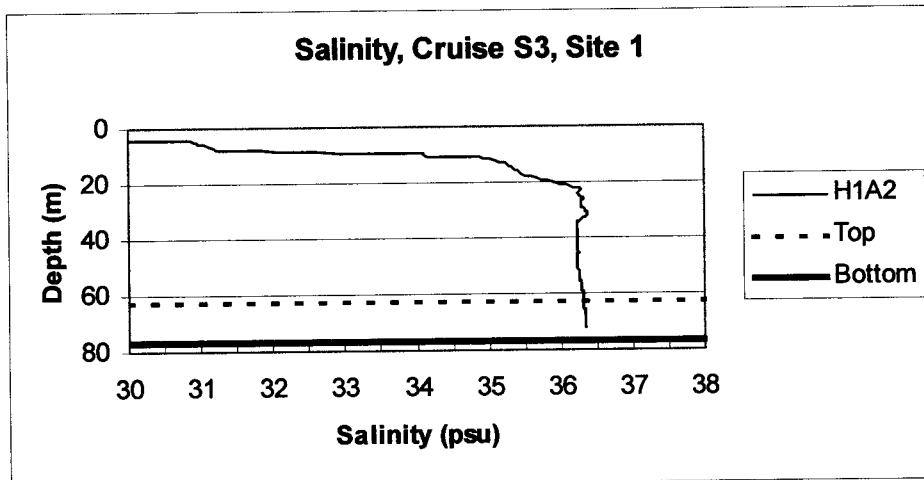
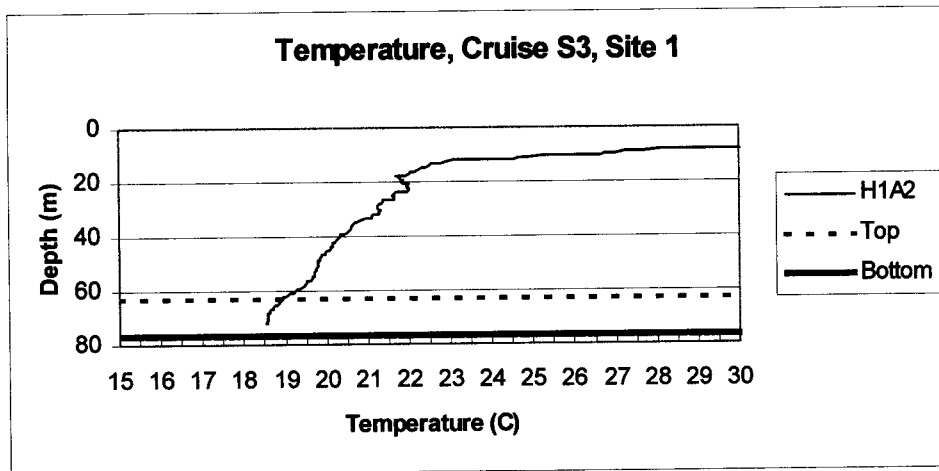


Fig. 6.32. A typical summer profile of temperature, salinity, and density collected at Site 1 during Cruise S3. The legend 'Top' indicates the top of the pinnacle and 'Bottom' the seafloor.

There is measurable flow disturbance at 4 mab at Site 1, which is a high-relief site ($h = 13$ mab). Compared to the other three sites, the 4 mab currents at mooring Site 1A (located about one “mound diameter” northeast of Site 1) have (a) a lower mean speed, (b) a greater percentage of near stagnant conditions, and (c) a much larger counter-clockwise rotation of the principal axis.

These observed characteristics are consistent with the downstream flow disruption observed in laboratory experiments of stratified non-rotating flow over small hills. Furthermore, the measurements of temperature and salinity from CTD casts and *in situ* sensors indicate that typically, $N \geq 0.01$ rad/s much of the time. Based on mound height, an assumed value for N of 0.01 rad/s and the observed currents at 4 mab, one can compute the percentage of time that various ranges of Froude values obtain.

If the laboratory results apply to the “hills” in this study, the following might describe the general characteristics of the flow on and around Site 1. At Site 1, the flow is probably subcritical ($F < 1.0$) up to 13 cm/s, which occurs $\sim 75\%$ of the time. At very low speed, the fluid flows horizontally around the hill, except in a narrow region near the top. In this region, fluid parcels have enough kinetic energy to overcome the stability and rise up and over the top. A slight hydraulic jump occurs just downstream of the top of the hill. Downstream, there is a symmetric pair of more or less vertically oriented vortices causing upstream flow on the centerline. On the downstream face of the hill, the flow is primarily perpendicular to the free-stream flow direction and oscillates from one side to the other. There is a very weak upslope component to the flow on the lower part of the leeward slope. As speed increases, the flow has more energy to move in the vertical direction. The region where the flow goes over the top of the hill broadens. A plume (dye) emanating from an upstream point near the base would spread thinly to cover a greater portion of the hill. A strong hydraulic jump develops downstream of the lee separation point. Downstream, a symmetric pair of vertically oriented vortices causes an upstream flow on the centerline. However, they become smaller and move closer to the base of the hill as speed increases. Near 13 cm/s ($F = 1$, i.e., critical), the flow begins separating from the top of the lee side of the hill. At higher speeds (super critical), the flow separates on or before the top of the hill, and a large re-circulating region develops on the leeward slope. The pair of vortices disappears and a horseshoe pattern develops. Over the much lower relief feature at Site 9, where the height is only a few meters, the Froude number is higher to begin with. The flow will be subcritical only at speeds less than 3 cm/s. More than about 80% of the time, the flow will be supercritical.

Chapter 7: Hard Bottom Communities

*Dane D. Hardin, Keith D. Spring, Stephen T. Viada,
Alan D. Hart, Bruce D. Graham, and Michael B. Peccini*

Introduction

Hard bottom communities at greater than 50 m water depth include organisms that are slow growing (Carricart-Ganivet et al. 1994; Parker et al. 1997; Mortensen and Rapp 1998), long lived (Gili et al. 1989; Parker et al. 1997), and sensitive to physical disturbance (Hardin et al. 1993). Studies near several offshore petroleum platforms off Point Conception in California (Hyland et al. 1994) measured decreased abundances of some epifaunal species associated with fluxes of drilling muds near the seabed. In the same area, Hardin et al. (1994) reported variation in the distribution and abundance of hard bottom epibiota related to depth, vertical relief of hard bottom features, position on hard bottom features, and flux of suspended sediments. The slow growth and possible sensitivity of hard bottom epibiota to drilling muds and/or suspended sediments suggest the importance of investigating the factors that may control these communities in areas affected by petroleum development, such as the Gulf of Mexico.

A number of studies have focused on hard bottom epibiota in the northern Gulf of Mexico. In the northwestern Gulf of Mexico, Rezak et al. (1990) studied hard bottom communities from 15 m to over 200 m deep. They reported that these communities were depth-stratified, probably in response to temperature, light penetration, and the thickness of the nepheloid layer. Minnery (1990) studied crustose coralline algae in the same area, at the Flower Garden Banks, and described depth zones related to grazing pressure by fishes, current speed, and the nepheloid layer. Gittings et al. (1984) examined hard bottom assemblages associated with a brine seep at the East Flower Garden Bank and postulated that assemblages not affected by the seep may be food limited. Observations made by Gittings et al. (1992) of hard bottom communities within the current study area indicated variation in epibiota related to habitat relief, substrate complexity, and distance from the Mississippi River. They concluded that this variation was due to differences in sedimentation.

The current study is designed to expand on the observations made by Gittings et al. (1992). In addition to the overall program objectives (see Chapter 1), this chapter addresses the following specific objectives:

- Describe hard bottom community structure and temporal dynamics at each site;
- Describe and interpret zonation patterns and differences in hard bottom community structure among sites differing in relief (high/medium/low), longitude (east/central/west), depth, etc.;

- Describe and interpret relationships between community structure and environmental parameters such as small-scale habitat variability, sediment cover, sediment flux, and other geologic and oceanographic variables;
- Describe and interpret ecological interrelationships and processes within hard bottom communities, including evidence of predation, competition, disease, recent settlement and growth, etc.;
- Make a general assessment of health and condition of hard bottom communities; and
- Compare results with other pinnacle studies, Northwestern Gulf bank studies, Southwest Florida Shelf Ecosystems Study, Eastern Gulf live bottom surveys, California OCS Monitoring Program (CAMP) reports, and other studies as appropriate.

Field Methods

Hard bottom communities were sampled at nine sites by a remotely operated vehicle (ROV). Sampling sites were chosen to fall within three categories of relief (i.e., low, medium, and high; see Chapter 2) in three regions from east to west. Site selection was based on data from geophysical surveys and ROV reconnaissance surveys.

Four cruises for sampling hard bottom communities were conducted during the study, according to the schedule presented in **Table 7.1**. Several types of samples were collected at each site, as indicated in **Table 7.2**.

Table 7.1. Schedule of cruises for sampling hard bottom communities.

Cruise	Date
1C	May 1997
M2	October 1997
M3	August 1998
M4	July-August 1999

Table 7.2. Types and purposes of samples collected.

Sample Type	Purpose
Random 35-mm photographs	Estimates of percent cover and abundances (densities) of epibiota at each site
Fixed 35-mm photographs	Descriptions of temporal changes in epibiota related to growth, recruitment, intra- and interspecific competition, disease, and mortality
Video transects and ancillary observations	Descriptions of motile and more widely dispersed macrofauna, such as fishes (see Chapter 8), and to assist in broad characterizations of substrates and corresponding epibenthic species composition
Biological voucher specimens	Assistance in the identification of organisms appearing in video and photographs and to assist in identifying and characterizing substrates

Equipment

A Benthos open frame SeaROVER ROV was used to collect random and fixed quadrats and biological voucher specimens and photographs. The ROV was equipped with a color-imaging scanning sonar for long range (100 m) detection of seafloor features with topographic relief, and object detection and avoidance in conditions of low ambient light and water clarity. The ROV was outfitted with two manipulators: a single-function unit (jaw open/close) and a three-function unit (jaw open/close; raise/lower arm, rotate arm; and extend/retract arm). These manipulators were used to collect biological voucher specimens and to deploy site markers.

For visual navigation and photography, the ROV also was outfitted with two video cameras and a 35-mm still camera. A high-resolution standard VHS camera with pan-and-tilt was used for ROV piloting and recording general and qualitative observations. Lighting for this video camera was provided by two fixed 250-watt quartz halogen underwater lamps mounted on the front of the ROV frame. The second video camera was mounted with the still camera on a pan-and-tilt unit on the lower front of the ROV frame. Lighting for the still camera was provided by a 150-watt-second electronic flash and lighting for the video camera was provided by a 200-watt quartz halogen underwater lamp, also mounted on the pan-and-tilt unit. The still camera and strobe were triggered manually from the shipboard controller.

Various data were recorded on still and video images. Overlaid on the video imagery were station/site number, transect number, ROV heading, and ROV depth. The still camera was equipped with an LED data chamber that placed the date, time (in seconds), and run number on each frame.

The video and 35-mm still cameras were adjusted to the same field of view so the image on the shipboard video monitor indicated the image captured by the still camera. The still camera was adjusted to minimum focus, a distance of 60 cm. This distance provided the highest resolution possible for the identification and quantification of biota of small size, especially in conditions of limited visibility. Each photograph station covered an area of approximately 0.3 m².

A low-power laser system, consisting of four laser projectors, was employed to provide distance and scale information in the video and still images. The four projectors were mounted on the pan-and-tilt unit. Three of the projectors were aimed in parallel to form an inverted equilateral triangle of known and consistent dimensions. The fourth projector was mounted on the bottom of the pan-and-tilt unit and its beam adjusted to converge with the lower parallel beam of the laser triangle at the 35-mm still camera's focal distance of 60 cm. The converging laser beams allowed the ROV pilot to adjust the distance of the ROV and camera from the substrate, ensuring sharp focus and constant sampler size in still images. The distance of separation between the three, parallel laser beams, visible as red dots on the substrate in video and still images, provided a precise indicator of scale.

Quality Assurance

Several measures were taken to ensure the quality of video and still records. Multiple video recorders were used to record the imagery from each of the two video cameras as well as the scanning sonar. The signal from the primary data-recording video camera was split to allow simultaneous recording of multiple original-quality sets of video data. Exposed lengths of still film from each completed roll were developed onboard the vessel to ensure proper exposure and focus.

Navigation

Navigation of the survey vessel was accomplished using a Differential Global Positioning System (DGPS) receiver coupled with a beacon receiver to obtain differential corrections broadcast by the U.S. Coast Guard. The three-dimensional distance and direction of the ROV and the voucher specimen basket from the ship were determined with an acoustic underwater tracking system using acoustic transponders on the ROV and specimen basket. This system was interfaced with a shipboard system of computer software and hardware that integrated various data collection sensors, still and video records with the DGPS.

Site Definitions

Each site was defined as a circular area of a certain diameter. Site diameters were based on an analysis of the digital elevation data collected during Cruise 1A. In this analysis, the standard deviation of the slope magnitude, slope direction, and depth were iteratively calculated for progressively larger areas of each feature, starting at the center of the study site. Plots of these calculated standard deviations versus area were examined to ascertain the areas around the center points of each study site over which the standard deviations stabilized. This examination ensured that the variability in elevation that the feature added to the surrounding background elevation was appropriately considered in the determining the site boundary. Resulting site diameters ranged from 100 to 200 m (see Results, General Observations).

Random Quadrats

Locations for photographing random quadrats were determined prior to each monitoring cruise. One hundred random locations were selected at each site using the digital elevation models for each of the sites. Each of the nine monitoring sites was defined as a circular area with a site-specific diameter. Each circular site was divided into eight sectors (Fig. 7.1), with 16 points randomly positioned in each sector. Stratifying by sector was done to help distribute points throughout each site and did not reflect an *a priori* hypothesis about differences among sectors. When on site, the ROV was maneuvered between each of the random locations in a sector. At each pre-selected random location, the ROV operator used the converging laser images to ensure the video and 35-mm still cameras were the proper distance and perpendicular to the substrate. Data for each photograph and the corresponding ROV position were recorded both manually and automatically. If the random point did not fall on hard substrate, additional random points were sampled until approximately 100 were obtained. Upon the completion of a sector, the ROV was maneuvered to an adjacent sector and the sampling process was repeated until all of the eight sectors were completed. Additional photographs were taken of specific features or biota along video transects to aid in bottom characterization or individual species identifications.

Fixed Quadrats

The locations of the fixed quadrats were randomly selected during Cruise 1C and permanently marked at each monitoring site. Fixed quadrat markers consisted of low-profile lead weights that were molded into the shape of numerals corresponding to the quadrat numbers. The size of the fixed quadrat markers was consistent among sites and thus served as a reference scale. The five fixed quadrats at each site were generally positioned near a marker buoy, which consisted of a plastic float anchored approximately five feet off the seafloor. The positions of these marker buoys were randomly selected. After deployment of fixed quadrat markers by the ROV, the position of each fixed quadrat was recorded with the navigation system to facilitate resampling during subsequent surveys. Detailed maps also were drawn of each fixed quadrat

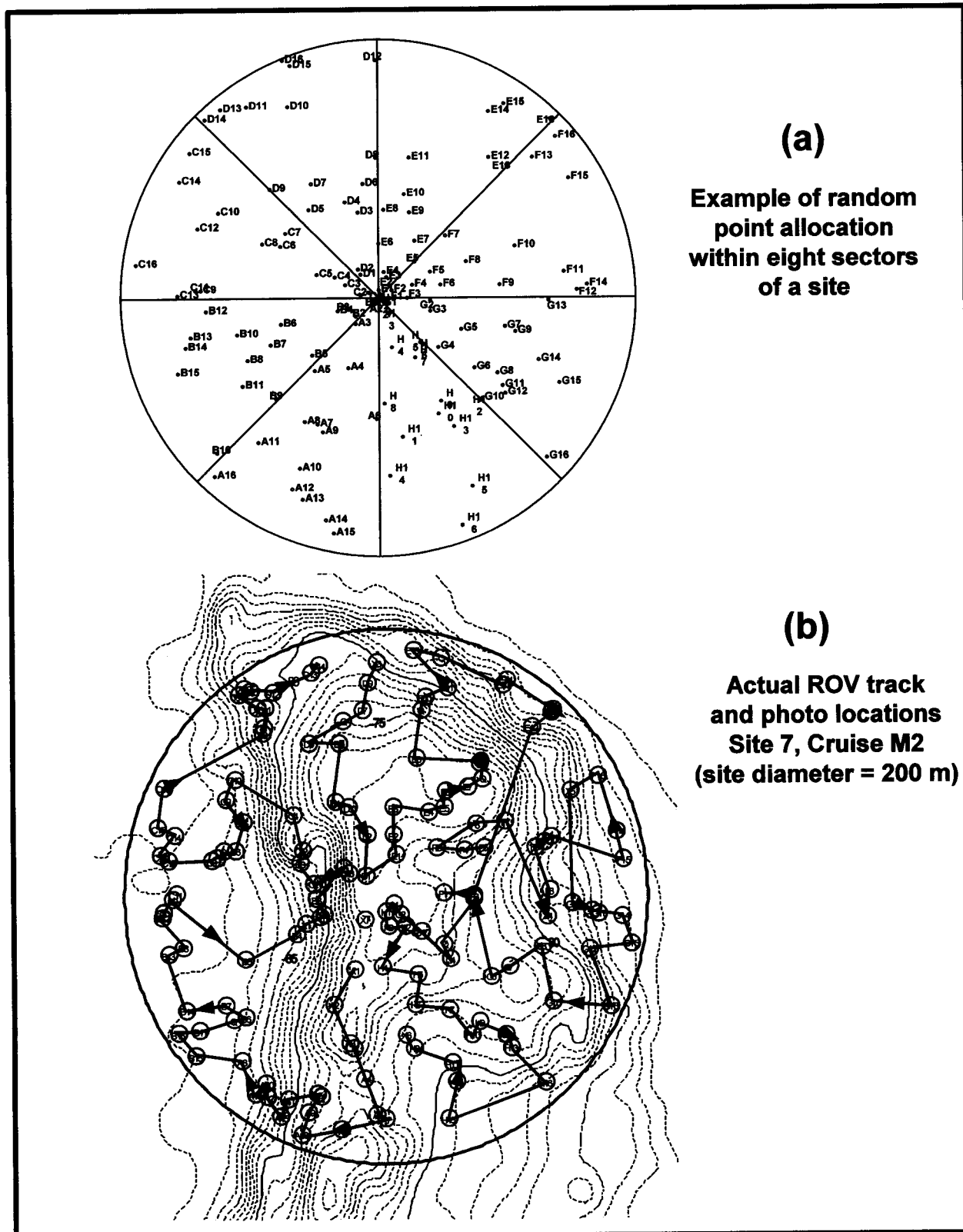


Fig. 7.1. (a) Example of random point allocation within eight sectors of a site. A quantitative photograph was to be taken at each random point. (b) Actual ROV track and photograph locations at Site 7 on Cruise M2. Qualitative and quantitative video and additional photographs were collected along transects between random points.

location, showing the marker buoy and other identifiable natural features and clusters of characteristic epibiota. These maps assisted the ROV pilot in relocating the fixed quadrats and facilitated consistent ROV orientation for subsequent photo and video images.

As with the random quadrats, each fixed quadrat covered an area of approximately 0.3 m², and the laser system was used to ensure the proper distance between the camera and the substrate. At each fixed quadrat site, a series of still photographs and corresponding segments of video images were collected in various positions around the quadrat marker to maximize the probability that images from subsequent cruises would overlap.

Video Records

The ROV was also used to collect video records. Video records were collected along the transects between each of the random still photo locations. One video camera was aimed ahead for navigating the ROV, and the second video camera was oriented perpendicular to the substrate. Each random location served as the endpoint of the preceding video transect and the starting point of the next transect.

Voucher Specimens

Voucher specimens were usually collected using the ROV's manipulators, but some specimens were also collected using a rock dredge, sediment grabs, and opportunistically from oceanographic and biological moorings. Specimens collected by ROV were placed in an aluminum basket that was equipped with an acoustic transponder to facilitate its relocation and spring-loaded doors to prevent the specimens from washing out of the basket during recovery. The basket was usually carried to the seabed and recovered by the ROV. Notes were taken regarding *in situ* color(s), site, depth, and specific habitat of all collected specimens in an effort to correlate these voucher identifications with similar organisms seen in photographs. After recovery, voucher specimens were assigned a unique identification number and were photographed and preserved in labeled sealed containers. Other specimens were labeled and preserved.

Laboratory Methods

Random Quadrats

Following each survey, the exposed 35-mm bulk film rolls were developed and the images digitized and stored on photographic CDs. Additional CDs were made to provide backup and extra working copies of all random photographs.

One hundred random photographs were selected for analysis from each sampling site. All random quadrats photographed within each sector were assigned a random number and then organized in numerical order. The analysis of the random photographs followed this numerical ordering. Extra photographs beyond the requisite 100 per site were used as backups when any of the images in the selected group were rejected due to poor image quality.

Coverage of biota and substrate within random quadrats was estimated using the random point-contact method developed by Bohnsack (1976, 1979). Randomly spaced points are superimposed over a photograph, and the number of points contacting each taxon or substrate type is recorded. The percent cover of each taxon and substrate type within an image is estimated as the percentage of the total points that contact the taxon or substrate type. Some of the random points may fall on deep shadows or areas that are out of focus and are therefore unreadable. In these cases, the denominator in the percent cover calculations is reduced by the number of points overlaying the shadowed or blurred areas. Some emergent or erect branching colonial organisms, such as certain sponges, hydroids, octocorals, and antipatharians, which commonly attach to the substrate at a single point, can produce a canopy covering the turf of epibiota when viewed from above. Although the percent cover estimates for these organisms include more area than that by which they are attached to the substrate, such estimates are commonly used as measures of importance in multi-layered assemblages (Foster et al. 1991). In addition to estimates of percent cover, numbers of individuals of solitary organisms were also counted and all species that were present in the image were recorded. Species that were present but not contacted by a random point were assigned a default percent cover of 0.5.

The analysis of random quadrats was performed using desktop publishing software. The images were displayed on a large, high-resolution color monitor, and the brightness and contrast were enhanced to most effectively reveal details of the seafloor, without overexposing bright or light-colored biota. Photographic images of poor quality, typically resulting from high turbidity, were rejected and alternate images were selected. Two series (one purple and one green) of nine random patterns of 25 points (dots) were designed and saved as separate electronic files prior to the analysis of the photographic images. A different set was used for each site. The selection of color series depended upon the predominant background of each enhanced photograph, with purple dots appearing more vividly in bright areas and green dots appearing more vividly in dark or high-contrast areas. Selections of the nine random dot patterns were made using a

random number table. Two of the selected patterns of 25 dots were electronically superimposed as separate, sequentially analyzed layers over each photograph.

Fixed Quadrats

The analysis of fixed quadrats required several steps. First, a set of comparable, sequential images was assembled for each of the five fixed quadrats from each cruise at each study site. Individual, digitized images were electronically captured from video footage. Digitized images from Cruise 1C (or Cruise M2 in some cases) were displayed on a computer monitor as baseline images for the capture of images that were as close as possible in distance and orientation from subsequent surveys. Identifiable prominent organisms were selected from the baseline image of each quadrat to facilitate selection of images that were as similar as possible in orientation and to provide a basis for analysis. Selected biota included solitary and colonial scleractinian corals (especially *R. manuelensis*), octocorals, sponges, and coralline algae. Taxonomic identifications of the selected prominent biota were facilitated by examining corresponding 35-mm still photographs of the fixed quadrats that were collected along with video data. Comparisons of sequential fixed quadrat images were made using two computers with separate monitors. The sequential images were displayed together and were individually enhanced, as for the random quadrats. The images were examined for evidence of settlement or recruitment of biota, growth, recession, death, or disease, and changes in the quantity or depth of loose sediment cover from survey to survey.

Taxonomy

Many of the relatively deepwater organisms observed within random quadrats, especially the sessile epibenthic organisms, are poorly known. Many of these organisms exhibit significant morphological variability or comprise sets of very similar congeners or conspecifics that require microscopic examination to identify. Consequently, the identifications assigned to unidentified epibiota within random quadrats were based on the use of the lowest accurate taxonomic categories, and the level of category assigned depended on the familiarity of the analysts with the organisms in question. Further separation of identifiable varieties within taxonomic categories, above genus necessitated the use of supplemental descriptive terms, usually based on color and morphology. Monochromatic organisms were labeled with basic color names. Polychromatic organisms exhibiting separate, distinct colors were labeled by the use of a forward slash (/) between the two colors (e.g., red/white indicating distinct red and white components). If the organism exhibited an obvious blend of colors, it was noted with the use of a dash (-) between the colors (e.g., yellow-brown). Descriptive terms for morphologies were derived from the taxonomic literature specific for each group. Nomenclature of organisms identified to genus or species followed standard taxonomic protocol. Organisms of a probable yet unverified genus were marked with a question mark preceding the genus name (e.g., *?Astrocyclus caecilia*). The nomenclature of an organism of a known genus and indeterminate species included the following three choices, based on available information:

- Known genus with indeterminate species (e.g., *Antipathes* spp.);
- Known genus with probable yet not verified species identification (e.g., *Antipathes ?furcata*); and
- Known genus containing two closely resembled (and difficult to differentiate) species, both of which may occur within the project area (e.g., *Antipathes atlantica/gracilis*).

All collected specimens were identified to the lowest taxonomic category. Specimens that could not be identified were sent to taxonomic specialists. Specimens of particular interest (i.e., rare or potentially new species, and species exhibiting range extensions) were retained and archived by the taxonomic specialists. All other specimens have been retained and archived by Continental Shelf Associates, Inc.

Statistical Analyses

Sources and Uses of Physical Data

Several physical variables were developed for use in analyzing linear models to determine the relationships between organisms and their environment. Much of the data that was the basis for these variables was provided by other components of this program.

Effects of vertical sediment flux (see Chapter 5) were evaluated in two ways. First, because of the assumed longevity of most of the organisms, the mean “normal” vertical sediment flux was examined. For this evaluation, mean data from all deployments not influenced by Hurricanes Earl and Georges were used to approximate normal, long-term conditions that might affect organism distributions. Second, vertical sediment flux during Hurricanes Earl and Georges was examined to determine whether organism distributions were affected by more extreme events. In both cases, the relationship between sediments collected in sediment traps and other variables, such as height above the bottom, proximity to the Mississippi River, and depth were determined using stepwise multiple regressions. Significant regressions were used to estimate normal and hurricane sediment fluxes for each random quadrat. The regressions used were as follows:

Non-hurricane periods (periods 1-5, 7, and 8 using Chapter 5 terminology):

$$\log_{10} \text{ vertical flux (g m}^{-2} \text{ d}^{-1}) = 1.8930 - 0.0453 \text{ (meters above bottom) - } \\ 0.00626 \text{ (kilometers from Mississippi River mouth)} \\ (r^2 = 0.872, p < 0.0001)$$

Hurricane periods (period 6 using Chapter 5 terminology):

$$\log_{10} \text{ vertical flux (g m}^{-2} \text{ d}^{-1}) = 3.58557 - 0.0752 \text{ (meters above bottom) - } \\ 0.0179 \text{ (water depth in meters) - 0.00544 (kilometers from Mississippi River} \\ \text{mouth)} (r^2 = 0.949, p < 0.0001)$$

Current speed and direction data (Chapter 6) were used to evaluate causes of variation in organism distribution on medium and high relief features. Because the mean depths of sites within these relief categories fell between 66 and 92 m (Table 7.3), current data from Sites 1, 5, and 9 were used to represent the range of depths and longitudes for these sites within the study area.

Effects of currents also were evaluated in three ways using an average joint frequency distribution (JFD) of current speed and direction based on JFDs for Sites 1, 5, and 9 (see Chapter 6). First, the percentages of all current records falling within each of eight direction bins were compared to the percent cover of organisms found within eight corresponding bins of bearing from the center of the feature (i.e., a rough approximation of the side of the feature on which the organisms were found). Second, because currents can also affect sessile organisms by controlling the flux of food particles, a derived variable called "food flux" was generated to estimate this effect. For this variable, it was assumed that currents from all directions had equal concentrations of food and that food flux varied according to current speed (i.e., currents of 20 cm/sec provide twice the food of currents of 10 cm/sec, etc.). The percentage of food flux accounted for by currents from each direction was compared to organism distributions. This comparison did not consider possible species-specific variation in feeding efficiencies at different current speeds. Third, because the kinetic energy in currents may prevent suspended sediments from settling onto epibiota, the percentage of kinetic energy accounted for by currents from each direction was also compared to organisms distributions. For this comparison, it was assumed that the kinetic energy in currents is proportional to the square of the current speed.

Several other physical variables were determined for each random quadrat through examination of both video and still images, many of which were developed by M. Peccini as part of the microhabitat study (Chapter 9), as follows:

- Location on feature – At medium and high relief sites, the location on the feature of each random quadrat was determined according to the following five categories: 1) surrounding seafloor, 2) base, 3) side, 4) top edge, or 5) top interior.
- Bearing – Also at medium and high relief sites, the bearing of each random quadrat from the center of the feature was determined to approximate the side of the feature on which the sample was taken. The coordinates recorded for each photograph were overlaid on the depth elevation model of the site (Chapter 9) and the quadrat was placed into one of eight bins or categories (S, SW, W, NW, N, NE, E, or SE).
- Slope – Also at medium and high relief sites, the overall substrate slope of each random quadrat was estimated according to the following three categories and their respective numerical values: 1) horizontal (0°), 2) moderate (45°), or 3) vertical (90°).

Table 7.3. Physical characteristics for each hard bottom site. Means were calculated from observed or estimated values for each photo.

Characteristic	Site 1	Site 2	Site 3	Site 4	Site 5	Site 6	Site 7	Site 8	Site 9
Region	East	East	East	Central	Central	Central	West	West	West
Relief Category	High	Medium	Low	Medium	High	Low	High	Medium	Low
Percentage Rock Outcrop ^a	91.5	42.6	18.9	48.8	50.6	41.9	68.0	46.9	29.9
Distance of Site Center from Mississippi River, Main Pass (km)	146.6	143.8	146.8	124.8	108.0	108.4	70.0	70.7	70.3
Mean Height Above Bottom (i.e., vertical relief) (m) ^b	12	5	3	7	10	3	10	6	3
Mean Depth (m) ^c	66	78	80	102	68	73	78	92	92
Mean Sediment Veneer Category ^d	1.08	1.93	1.93	1.93	1.80	2.00	1.78	1.96	1.96
Mean Slope Category ^e	4.31	19.11	18.45	5.69	23.97	1.83	31.02	21.13	12.69
Mean Medium-scale Substrate Roughness Category ^f	1.12	1.57	1.50	1.49	1.36	1.22	1.58	1.68	1.56
Mean Small-scale Substrate Roughness Category ^g	1.84	1.54	1.46	1.39	1.77	1.21	1.63	1.67	1.49
Mean Normal Flux of Suspended Sediment (g/m ² /day) ^h	2.98	6.22	7.03	6.81	6.27	12.45	11.31	17.94	20.69
Mean Hurricane Flux of Suspended Sediment (g/m ² /day) ⁱ	7.90	19.81	23.17	6.15	16.58	53.11	20.20	26.83	34.95

^a Estimated percentage of rock outcrop for each site based upon microhabitat measurements (see Chapter 9).

^b Height above bottom for each photo was calculated by subtracting the depth of the photo from the maximum depth of any photo from a given site in a given cruise.

^c Depth recorded for each photo from the depth sensor on the ROV.

^d Numerical values were given to two categories of sediment veneer: light = 1, heavy = 2.

^e Numerical values were given to three categories of slope: horizontal = 0, moderate = 45, vertical = 90.

^f Numerical values were given to three categories of medium-scale roughness: low = 1, medium = 2, high = 3.

^g Numerical values were given to three categories of small-scale roughness: low = 1, medium = 2, high = 3.

^h The normal (non-hurricane) flux of suspended sediments was estimated for each photo using sediment trap data from Chapter 5 (for all periods except period 6 during which Hurricanes Earl and Georges passed over the study area), the height above bottom of the photo and the distance from the site to the Mississippi River ($\log_{10} \text{flux} = 1.8930 - 0.0453 \text{ height above bottom} - 0.00626 \text{ distance from Mississippi}$; $r^2 = 0.872$, $p < 0.0001$).

ⁱ The sediment flux during hurricanes was estimated for each photo using sediment trap data from Chapter 5 for deployment period 6 (when Hurricanes Earl and Georges passed over the study area), the height above bottom of the photo, the depth of the photo and the distance from the site to the Mississippi River ($\log_{10} \text{flux} = 3.58557 - 0.0752 \text{ height above bottom} - 0.0179 \text{ depth} - 0.00544 \text{ distance from Mississippi}$; $r^2 = 0.949$, $p < 0.0001$).

- Sediment veneer – The thickness of sediment veneer overlaying the substrate within each random quadrat was initially estimated according to the following four categories: 1) none, 2) light, 3) moderate, or 4) heavy. These four categories were subsequently collapsed into two categories of light and heavy that were assigned numerical values of 1 and 2, respectively.
- Depth – The depth of each random quadrat was determined from the ROV’s depth sensor.
- Height above bottom – This was calculated for each random quadrat by subtracting the depth of the quadrat from the maximum depth of any photograph at that site during that cruise. Use of cruise-specific maxima corrected for slight cruise-to-cruise variation in the ROV depth sensor, as indicated by repeated measurements made at fixed locations.
- Small-scale roughness – This variable describes the surface texture of the substrate visible in the photographs at a centimeter scale. Random quadrats were assigned one of the following three categories, with corresponding numerical values: 1) low, 2) medium, or 3) high. These categories approximated a continuum from smooth substratum to substratum characterized by narrow irregular pits or tunnels deep enough for small fish to use as shelter.
- Medium-scale roughness – This variable describes substrate texture at a scale of a meter or more. Random quadrats were placed into one of the following three categories, with corresponding numerical values: 1) low, 2) medium, or 3) high. These categories also approximated a continuum from smooth substrate to substrate characterized by dramatic indentations and tunnels which gave it a very irregular “Swiss cheese” appearance when viewed from a wider-angle perspective than that of the random photographs.

Linear Models

Statistical analyses used percent cover (rather than density) estimates because percent cover incorporates variation in organism size. The cover data for the 40 taxa with the overall highest mean percent cover and major taxonomic groups were analyzed with linear models. In addition, total biotic cover was also analyzed. For one set of analyses, analysis of variance was used to examine differences with respect to cruise, region (eastern, central and western), and relief (high, medium and low). All two-way interactions and the three-way interaction were included in the model. Cover data were transformed with the arcsine transformation to normalize the data.

A second set of linear model analyses was performed to examine the relationships between biological and physical/environmental variables. Biological variables were abundances (percent cover) of the 40 dominant taxa, abundances of major taxonomic groups, and total cover. These analyses were conducted for three sets of sites:

- all sites;
- Sites 1, 2, 5, 7, and 8 (sites with higher relief); and
- Sites 3, 4, 6, and 9 (sites with lower relief).

Cover data were transformed with the arcsine transformation to normalize the data. The environmental variables included in all of the analysis were cruise, depth, sediment veneer, small-scale roughness, medium-scale roughness, distance from the Mississippi River, sediment flux, and sediment flux during periods when hurricanes passed in the vicinity of the study area. Location on the feature, substrate slope at the location of the random quadrat, and bearing of the random quadrat from the center of the feature were included in the analyses of the higher relief sites (Sites 1, 2, 5, 7, and 8).

Canonical Correspondence Analysis

Canonical correspondence analysis (CCA) was used to analyze patterns of species abundance and species composition among “samples” as well as relationships between species data and environmental variables. Individual photographs were not used as samples because the large number of observations would make plotting and interpretation infeasible. Instead, composite samples were created by pooling the cover estimates for a site, cruise, and depth interval. Depth intervals were defined in 5-m increments beginning at 60 m. CCA is a direct ordination method in which the environmental variables define the axes in the ordination analysis. It is a combination of regression and ordination where the species scores are constrained as linear combinations of the environmental variables (Ter Braak 1986; Palmer 1993). A taxon/samples matrix and an environmental/samples matrix are combined in the ordination to convey the influence of environmental variables on the taxa and samples data. The 40 dominant taxa were included in the analysis. Environmental variables were cruise, silt veneer, slope, medium-scale roughness, small-scale roughness, distance from the Mississippi River, depth, height above bottom, normal sediment flux, and sediment flux for periods when hurricanes passed. Categorical variables were converted to numerical values for inclusion in the analysis.

Chi-Square Tests

Chi-square tests were used to compare the observed and expected frequencies of the following types of observations in the fixed quadrats:

- organism growth or recruitment versus damage or mortality; and
- decrease in sediment veneer (erosion) versus increase in sediment veneer (deposition).

The tests were performed using only the observations that indicated either growth/recruitment or damage/mortality and either erosion or deposition. The tests used expected frequencies based upon a hypothesis extrinsic to the sampled data (Sokal and Rohlf, 1998). This hypothesis stated that the conditions of prominent organisms and sedimentation in the fixed quadrats were stable over the study period, leading to equal frequencies of observations in each class for these two types of observations. (i.e., the frequencies of observations of growth/recruitment and damage/mortality should be equal and the frequencies of observations of erosion and deposition should be equal).

Results

General Observations

A thorough review of video records provided qualitative descriptions of the rock features and biological communities at each site. This review suggested a large amount of biological variation that is not always associated with obvious physical differences. The results of this review follow.

Site 1

Site 1 is a large flat-top mound (see Chapter 3 for geological terminology) located at the eastern end of the study area at 29°26'19.131"N and 87°34'27.273"W. Water depth ranges from approximately 60 m on top of the feature down to 78 m at the base along the east and northeast. This is one of the largest features of the nine monitoring sites, extending for more than 400 m in a northwest-southeast direction. The 200-m diameter monitoring site extends across the top of this feature and down the nearly vertical northeastern and eastern flanks to the flat seafloor (see Chapter 3, Figure 3.17). The northeastern and eastern faces of the feature drop off nearly 10 m in some locations, while in other areas the slopes consist of what appears to be large rock outcrops that may have broken loose from the main structure. The flat top of the feature is covered with low relief rock outcrops and patches of coarse-grained sediments up to several meters in diameter filling the low-lying areas. Bioturbation is evident within these sandy areas.

The epibiota associated with the top of the feature appears very diverse and with greater percent cover than at any other site. The community is visibly dominated by small octocorals, sponges, ectoprocts, coralline and other red algae, and crinoids. The most common taxa observed included the octocorals *Bebryce cinerea/grandis*, *Nicella* spp., members of the genus *Thesea*, unidentified tan/orange fans (Stenogorgiinae), and the octocoral whip *Ctenocella (Ellisella)* spp. Also observed were the sponges *Ulosa* sp., *Dysidea* sp., and *Ircinia campana*; crinoids; the ectoprocts ?*Cellaria* sp. and ?*Idmidronea* sp.; and the antipatharian spiral whip *Stichopathes ?lutkeni*. Most of the octocorals on the top interior of the feature appear to be less than approximately 15 cm in height, although near the northeastern and eastern top edges of the feature there appear to be higher densities of larger colonies.

The vertical faces of the feature have a substantially lower density of epibiota. The ahermatypic coral *Rhizopsammia manuelensis* was the only organism visible in most of these locations. It was more common on the tops of rock outcrops and boulders at the base of the vertical faces, along with small octocoral fans, the coral *Madracis/Oculina* sp., and *Ctenocella (Ellisella)* spp. More gradually sloping areas along the edge of the feature were colonized by taxa common to the top interior including small and large octocoral fans, *Ctenocella (Ellisella)* spp., the antipatharian spiral whip *Stichopathes ?lutkeni*. Coralline algae were also found on the gradual slopes down to at least 75 m. A distinct characteristic of the vertical eastern face of this feature was its recently eroded appearance, with an almost regular pattern of concave, scalloped depressions. If these concave depressions were due to recent exfoliation, it would explain the depauperate epibiota on these surfaces.

Site 2

Site 2 is approximately 3.3 km west-northwest of Site 1 at 29°26'41.053"N and 87°36'26.512"W. The monitoring site is 120 m in diameter and ranges in depth from approximately 70 m at the top to 78 to 82 m at the base. The feature is somewhat arc-shaped and falls into the composite mound category (Chapter 3). It appears to consist of tens of unit mounds clustered together that range in size from 1 m to greater than 5 m in height and up to 5 to 10 m in diameter. Distances between the bases of unit mounds range from much less than a meter up to 1 to 2 m, with the tops being separated by up to 5 to 10 m. Some of the unit mounds are larger in diameter and may be connected. The individual unit mounds are tallest at the western edge of the feature and decrease to 1 to 2 m in height in the east. There is a general rounded appearance to the individual unit mounds and their tops are somewhat irregular in many cases. Nevertheless, overall there are relatively few jagged edges, protrusions, or overhangs. The bases of the mounds are generally silt-covered with much lower densities of epibiota than was observed on the sides and tops of the mounds.

The dominant species observed at this site was the ahermatypic coral *R. manuelensis*. It occurs on all surfaces of the mounds but has lower densities near the bases and on the lower-relief features. Other common species include various other solitary ahermatypic corals such as the unidentified solitary scleractinian and *Madrepora carolina*, Stenogorgiinae, the ectoproct *Stylopoma spongites*, the octocoral fan *Nicella* spp., antipatharians, such as *Stichopathes ?lutkeni* and the genus *Antipathes* spp.; unidentified sponges, *Ctenocella (Ellisella)* spp., and the coral *Madracis/Oculina* sp. The lower-relief mounds on the eastern side of the site are also colonized by *R. manuelensis*, although at lower densities. Other fauna common on the lower relief mounds include *Stichopathes ?lutkeni* and members of the genus *Antipathes* spp., and several small octocoral species.

Site 3

Site 3 is an area of low relief rock features immediately to the east of Site 1 at 29°26'15.901"N and 87°34'15.266"W. The monitoring site is 150 m in diameter and ranges in depth from approximately 74 to 83 m. This site consists of patchy low relief rock outcrops with diameters ranging from <1 m to approximately 10 m, with heights from <1 m up to nearly 5 m. The majority of the features at the site are 1 to 2 m high. The smallest outcrops were usually observed in shallow depressions and did not extend much above the surrounding seafloor. The largest, up to 5 m high, occur in the southeast section of the site and have almost vertical sides with rounded tops and rugged or rough surfaces with overhangs and holes (i.e., high medium-scale roughness). All rock features have various amounts of silt cover with the lowest-relief structures having the thickest veneer. Horizontal surfaces on all the structures have visibly thicker layers of silt than vertical surfaces.

Epibiota varied according to the height of the outcrops. The lowest relief features were inhabited by *Stichopathes ?lutkeni*, various small octocorals, crinoids, and ectoprocts. The medium-sized features had a more diverse assemblage including *Stichopathes ?lutkeni*, *Madrepora carolina*; *Stylopoma spongites*, *Bebryce cinerea/grandis*, *Ctenocella (Ellisella) spp.*, *Nicella spp.*, the genus *Thesea*, Stenogorgiinae, members of the genus *Antipathes*, crinoids, and the ophiuroid basket star *?Astrocyclus caecilia*. The highest features were characterized by high abundances of *R. manuelensis*, which was observed at much lower densities on features less than 2 m high. On the taller features *R. manuelensis* was observed on the sides, from just above the bases up to the top edge. *Madracis/Oculina sp.* was also present along the top edges of the larger features, particularly on and under overhangs. Other biota observed on the larger features included *Stichopathes ?lutkeni*, the genus *Antipathes*, *Bebryce cinerea/grandis*, *Ctenocella (Ellisella) spp.*, *Nicella spp.*, crinoids; the long-spined echinoid *Diadema antillarum*, and *?Astrocyclus caecilia*.

There was substantial variation in the biological communities on individual features, despite their relative physical similarity. For example, one feature approximately 2 m high and 4 to 5 m in diameter had over 100 colonies of *Madrepora carolina*, while no other feature observed within this site had more than approximately 10 colonies. Another example of this variation involved *R. manuelensis*. There were relatively high numbers of this organism on the sides of the taller features in the southeastern part of the site but much lower abundances throughout the remainder of the site.

Site 4

Site 4 is located on a large diameter, medium height mound at 29°19'39.041"N and 87°46'07.849"W. The sampling site has a diameter of 140 m and is the deepest site, ranging in depth from approximately 96 to 109 m. The sampling site encompasses the top of a broad mound, with the surface gradually sloping down from the center of the site to the west-southwest and to the north. The majority of the site is low relief hard substrate with a sediment veneer ranging from fine sand to shell hash. Scattered across the site are individual features extending from <1 m to almost 3 m above the surrounding platform. The individual features range from elongate ridges 1 to 2 m high with either rounded or rough tops to patchy, very rough irregular structures with overhangs, ledges, and jagged protrusions.

The most abundant taxa on the elevated features at this site were *R. manuelensis*, *Madracis/Oculina* sp., *Madrepora carolina*, *Ctenocella (Ellisella)* spp., *Nicella* spp., crinoids, basket stars, and the unidentified solitary scleractinian. The surrounding low relief hard bottom was characterized by the antipatharians *Antipathes ?furcata* and *Antipathes* spp., *Ctenocella (Ellisella)* spp., *Nicella* spp., and crinoids. The highest faunal abundances occurred on the edges of the rock overhangs and protrusions.

Site 5

Site 5 is located at 29°23'35.930"N and 87°58'51.055"W. The feature is a flat-topped mound ranging in depth from approximately 62 m at the top up to 78 m at the base. The mound has a diameter of about 60 to 75 m and the monitoring site diameter is 160 m. The top of the mound is relatively flat, with less than approximately 0.2 m vertical relief at any single location. A fine sediment veneer occurred on all horizontal rock surfaces and was particularly evident on the top of the mound, filling all depressions. The sides of the mound are nearly vertical walls up to 10 m in height, and slightly rounded off near the top edge. Unit mounds, ranging in size from 1 m to 7 m in height and 2 m to 5 m in diameter, flank almost the entire periphery of the larger mound and are separated from it by less than 1 m to approximately 15 m. Because of the sizes, shapes, and proximity of these smaller features, it appears some of them may have broken off from the main structure. Many of the unit mounds are very rugose, with jagged protrusions and holes, especially near the seafloor.

As observed at Site 1, there are distinct assemblages in different locations on the features. Conspicuous taxa on the top interior of the large feature were Stenogorgiinae, *Swiftia exserta*, *Stichopathes ?lutkeni*, the genus *Antipathes*, *Bebryce cinerea/grandis*, *Ctenocella (Ellisella)* spp. and *Hypnogorgia pendula*, and other unidentified gorgonian corals. There were very few hermatypic or ahermatypic corals on the top interior, perhaps due to the heavy accumulations of fine sediments, which could cover any organisms not able to project above them. *R. manuelensis* was very abundant on the vertical sides from near the base up to the top edge. Coincident with increased cover of sediment veneer on the

top interior of the feature, it was observed at very low abundances, and only on the upper edges of more exposed outcrops.

Rhizopsammia manuelensis was the dominant taxon on virtually all surfaces of the smaller mounds. Other conspicuous taxa on the vertical face of the main feature and adjacent mounds included *Madracis/Oculina* sp., *Madrepora carolina*, members of the genus *Antipathes* and *Stichopathes ?lutkeni*. Other taxa included the sea urchins *Stylocidaris affinis* and *Diadema antillarum*, a few unidentified sponge species, and small colonies of bryozoans.

Site 6

Site 6 is located at 29°23'52.887"N and 87°58'42.610"W, approximately 525 m to the north-northwest of Site 5. The monitoring site diameter is 150 m and water depths within the site range from approximately 68 m to 76 m. The features within this site consist of low relief rock outcrops ranging from barely exposed to approximately 1.5 m high. The exposed outcrops are widely scattered across the site and appear to project from a continuous carbonate bottom, most of which is covered by a sediment veneer. The features' surface morphologies range from relatively smooth, low mounds to very irregular surfaces with overhangs, protrusions, and cavities. A fine layer of silt covered all horizontal surfaces and the surficial sediments range from fine up to coarse with shell fragments.

The biological community on these low relief features was not very diverse. The most conspicuous taxa include the *Bebryce cinerea/grandis*, members of the genus *Thesea*, *Ctenocella (Ellisella)* spp., members of the genus *Antipathes* and *Stichopathes ?lutkeni*. *Madracis/Oculina* sp. and *Madrepora carolina* were also occasionally observed, while *R. manuelensis* was relatively common on the few features with more than 1 m of relief.

Site 7

Site 7 is located at the northern end of an elongate north-south feature known as "36 Fathom Ridge" at 29°15'24.844"N and 88°20'21.455"W. With a diameter of 200 m, the monitoring site ranged in depth from 69 m at the top to 88 m along the western side. The top interior of the feature is relatively flat, although not as distinctly flat as at Sites 1 and 5. Unlike Sites 1 and 5, there is localized relief of up to approximately 0.5 m scattered across the top. Pockets of sediments ranging from silt to sand-sized fractions also are scattered across the top. At the edges of the flat-topped area, the relief becomes more irregular with surface features exhibiting 1 to 2 m of relief, and this relief increases with distance from the top of the feature. The sides of the feature range from nearly vertical walls stepping down to the seafloor to large attached monolithic structures that decrease in height further from the site center. Along the western side of the site, there are numerous large rock overhangs and ledges several meters wide and deep, with some

tilted at acute angles. Large, distinct sediment-filled depressions and channels were observed along the southern edge of the monitoring site.

As at Sites 1 and 5, there is a distinct difference between the community on the flat top of the structure and that associated with the sloping sides and flanks. Biota observed on the top of the feature include *Bebryce cinerea/grandis*, *Ctenocella (Ellisella) spp.*, *Nicella spp.*, crinoids, the genus *Antipathes*, *Stichopathes ?lutkeni*, coralline algae, several species of sponges; *?Astrocyclus caecilia*, and *R. manuelensis*. The occurrence of *R. manuelensis* on the top of this feature and not in similar habitat at Sites 1 and 5 may be due to the less uniform topography at this site, where this taxon occurred on elevations above the surrounding surface. The species does not appear in the areas of lowest relief atop the feature. On the edges, sides, and adjacent rock structures, *R. manuelensis* is the dominant epibiota, with crinoids, the genus *Antipathes*, *Stichopathes ?lutkeni*, coralline algae (down to approximately 76 m), *Madracis/Oculina sp.*, the unidentified solitary scleractinian, and several sponge species also observed. Along the exposed edges of the large rock overhangs, *Madracis/Oculina sp.* and the unidentified solitary scleractinian were abundant. In the areas of scattered shell and rubble surrounding the feature, crinoids, with small colonies of *Antipathes*, also were conspicuous.

Site 8

Site 8 is located at 29°13'53.857"N and 88°19'01.565"W, approximately 3,700 m to the southeast of Site 7. The monitoring site is 100 m in diameter, encompassing a primary feature that is approximately 40 to 45 m across and 87 to 97 m deep. A group of lower relief mounds occurs along the northwest edge of the monitoring site, approximately 40 m from the primary feature. These mounds range in height from 0.5 to 2.5 m and fauna similar to the primary site. The primary feature has a roughly oval outline and appears to be a composite mound comprised of tightly clustered unit mounds. The unit mounds are approximately 1 m high at the periphery, increasing in 1 to 2 m increments to an irregular summit with several 1 m to 3 m deep crevices crossing the feature. The unit mounds have overhangs near the base of the feature, and there are numerous cavities and deep holes throughout the main feature. The entire feature is covered by silt with areas of thicker deposits on horizontal surfaces and in depressions and crevices.

Rhizopsammia manuelensis was conspicuous on the entire structure from just above the base to the top, with lower densities observed on horizontal surfaces with a heavier silt accumulation. Other observed epibiota included the *Ctenocella (Ellisella) spp.*, *Hypnogorgia pendula*, *Nicella spp.*, the genus *Thesea*, the genus *Antipathes*, *Stichopathes ?lutkeni*, and *Madrepora carolina*. There is no obvious zonation of any of these taxa except for higher abundances of *Hypnogorgia pendula* occurring near the top of the feature. The arrow crab, *Stenorhynchus seticornis*, *?Astrocyclus caecilia*, crinoids and the sea urchins *Diadema antillarum* and *Stylocidaris affinis* were also observed on the mounds. The species colonizing the lower relief mounds appear similar in composition to those on the primary feature.

Site 9

Site 9 is an area of low relief rock features located at 29°14'19.499"N and 88°19'36.859"W, approximately 1,250 m to the northwest of Site 8. The diameter of the monitoring site is 150 m and water depths range from 87 to 96 m. The rock features within the monitoring site are widely scattered and are generally 0.5 to 1.5 m high and up to 10 m in diameter. A few outcrops are much larger with heights up to 5 m and diameters greater than 10 m. Many of the medium to large structures are flattened and greatly undercut with wide overhangs and vertical holes down through the mounds. The bases of the features are covered with silt up to a height of about 0.5 m. Some areas of low rock are completely covered, and the buried hard substrate is only apparent from the gorgonian fans and whips protruding through the silt.

Biota on the lower relief structures includes *Bebryce cinerea/grandis*, *Hypnogorgia pendula*, *Nicella* spp., *Swiftia exserta*, the genus *Thesea*, *Ctenocella (Ellisella)* spp., the genus *Antipathes*, *Madrepora carolina*, and occasional crinoids. *Ctenocella (Ellisella)* spp. had visibly higher abundances at this site than at the other eight sites, especially on the low relief rock outcrops. While smaller mounds up to 1 m in height had few colonies of *R. manuelensis*, the larger mounds had very high numbers of *R. manuelensis* on the upper 2 to 3 m of the structure, along with larger octocoral fans.

Random Quadrats

A total of 2,997 random photos were analyzed from four cruises. At least 85 random photos were analyzed from each site on each cruise, except for Site 9 on Cruise 1C, where only nine samples were analyzed; and Site 5 on Cruise M3 and Site 6 on Cruises M3 and M4, where no samples were obtained. High turbidity caused these reductions in samples.

Variation among sites in physical characteristics substantiated the initial categorization of sites by region and relief (**Table 7.3**). The eastern, central, and western sites ranged from 143.8–146.8 km, 108.0–124.8 km, and 70.0–70.7 km from the Mississippi River, respectively. Mean height above bottom (of random quadrats) for high, medium, and low relief sites were 10–12 m, 5–7 m, and 3 m, respectively. Microhabitat analysis of substrate types also indicated descending percentages of rock outcrop within the circular site boundaries from high relief sites down to low relief sites within each region. High-relief sites also had the lowest sediment veneer and normal and hurricane fluxes of suspended sediments within regions. Within relief categories, normal fluxes of suspended sediments increased from east to west. Such a trend among regions did not exist for hurricane fluxes of suspended sediments, because of the effects of depth on this parameter.

Some physical parameters, such as depth, slope, and substrate roughness, varied inconsistently among relief categories and regions. These inconsistent differences suggest a number of factors may confound interpretations of differences among sites that rely exclusively on relief, region, and cruise as main effects. While application of multiple statistical approaches (e.g., ANOVA, linear models, and cononical correspondence analysis) in subsequent analyses was designed to account for the other sources of variation, relief and region remained as convenient descriptors for categorizing the habitat preferences of numerically dominant taxa.

Taxonomic Composition

The 40 taxa with the highest overall mean percent cover values were selected for statistical analysis (Table 7.4). Twenty-seven of the 40 dominant taxa were found at all nine sites. All but 4 of the remaining 13 taxa were found at seven or eight sites. The 4 taxa that were found at two, three, or four sites (i.e., *Peysonnelia* spp., unidentified rhodophyta, *Ulosa* sp., and *Pseudoceratina crassa*) were included in subsequent analyses because of their relatively high overall mean percent cover and because they appeared to reflect the effects of either region or relief. An additional indication that these 40 dominant taxa are representative of the hard bottom communities in the study area is provided by Fig. 7.2, which shows they contributed nearly 90% of the mean total biological cover.

These 40 dominant taxa comprised 14 taxon groups. Although octocorals were the most diverse taxon group, ahermatypic corals were the most abundant group, due to the overall dominance of *R. manuelensis*. Numbers of taxa and overall mean percent cover for each group were as follows:

	<u>Number of Taxa</u>	<u>Percent Cover</u>
Octocorallia	10	3.819
Porifera	6	1.115
Ahermatypic corals	4	6.756
Antipatharia	4	3.194
Ectoprocta	4	1.129
Algae	3	0.921
Echinoidea	2	0.280
Hermatypic corals	1	0.182
Ascidiacea	1	0.094
Crinoidea	1	1.080
Hydroida	1	0.470
Natantia	1	0.049
Ophiuroidea	1	0.174
Reptantia	1	0.169

Table 7.4. Mean percent areal cover of the 40 most abundant hard bottom taxa, as indicated by mean percent cover at nine sites in the northeastern Gulf of Mexico.

Taxon	Taxon Group ^a	Site 1	Site 2	Site 3	Site 4	Site 5	Site 6	Site 7	Site 8	Site 9	Overall Mean	Number of sites
<i>Rhizopsammia manuelensis</i>	Aherm	0.096	4.579	0.728	4.230	12.028	1.248	13.178	10.104	8.038	6.025	9
<i>Antipathes ?furcata</i>	Anti	0.071	0.428	0.412	15.949	0.176	0.030	0.542	0.541	3.057	2.356	9
<i>Nicella</i> spp.	Octo	2.636	0.558	0.603	1.386	0.014	0.000	0.483	2.296	1.824	1.089	8
Crinoidea	Crin	1.044	0.446	0.929	3.908	0.061	0.000	3.056	0.178	0.101	1.080	8
Stenogorgiinae	Octo	1.477	0.698	1.431	0.519	1.040	0.756	0.301	1.795	0.746	0.974	9
Porifera, yellow encrusting	Por	0.563	0.546	0.741	0.285	0.590	0.320	0.850	0.408	0.653	0.551	9
<i>Ctenocella (Ellisella)</i> spp.	Octo	0.809	0.320	0.532	0.577	0.023	0.179	0.093	1.006	1.209	0.528	9
Corallinaceae	Alg	1.868	1.125	0.201	0.026	0.547	0.000	0.799	0.137	0.028	0.526	8
Scleractinia (solitary)	Aherm	0.034	0.481	0.253	0.296	1.322	0.656	0.430	0.718	0.454	0.516	9
<i>Antipathes ?atlantica/gracilis</i>	Anti	0.000	1.189	0.223	0.047	1.262	0.183	1.373	0.193	0.047	0.502	8
Bryozoa, unidentified	Ecto	0.754	0.343	0.379	0.246	0.446	1.515	0.421	0.056	0.086	0.472	9
Hydroida, unidentified	Hydr	0.491	0.078	0.220	0.128	0.644	1.510	0.483	0.408	0.272	0.470	9
<i>Bebryce cinerea/grandis</i>	Octo	0.472	0.154	0.539	0.207	0.004	1.441	0.444	0.182	0.301	0.416	9
<i>?Idmidronea</i> sp.	Ecto	0.050	0.084	0.186	0.005	0.088	3.000	0.000	0.005	0.000	0.380	7
Porifera, orange encrusting	Por	0.464	0.407	0.341	0.111	0.447	0.171	0.559	0.167	0.188	0.317	9
<i>Antipathes</i> spp.	Anti	0.023	0.364	0.233	0.271	0.443	0.199	0.082	0.135	0.409	0.240	9
<i>Swiftia exserta</i>	Octo	0.294	0.029	0.218	0.108	0.787	0.000	0.122	0.037	0.317	0.213	8
<i>Peyssonnelia</i> spp.	Alg	1.431	0.041	0.000	0.009	0.000	0.000	0.379	0.000	0.000	0.207	4
<i>Stylocidaris affinis</i>	Ech	0.019	0.042	0.064	0.063	0.507	0.008	0.293	0.433	0.294	0.191	9
Rhodophyta, unidentified	Alg	1.294	0.037	0.173	0.000	0.000	0.000	0.000	0.000	0.000	0.188	3
<i>Madracis/Oculina</i> sp.	Herm	0.029	0.248	0.203	0.167	0.474	0.005	0.226	0.162	0.121	0.182	9
<i>?Astrocyclus caecilia</i>	Oph	0.005	0.072	0.305	0.260	0.022	0.000	0.060	0.394	0.452	0.174	8
Galatheidae	Rep	0.003	0.327	0.163	0.059	0.061	0.278	0.156	0.116	0.364	0.169	9
<i>Madrepora carolina</i>	Aherm	0.001	0.094	0.457	0.210	0.209	0.035	0.000	0.162	0.181	0.169	8

Table 7.4. (Continued).

Taxon	Taxon Group ^a	Site 1	Site 2	Site 3	Site 4	Site 5	Site 6	Site 7	Site 8	Site 9	Overall Mean	Number of sites
<i>Stylopoma spongites</i>	Ecto	0.066	0.299	0.422	0.024	0.078	0.307	0.197	0.064	0.062	0.169	9
<i>Thesea</i> spp.	Octo	0.036	0.065	0.343	0.071	0.083	0.280	0.014	0.174	0.277	0.149	9
<i>Thesea/Scleracis</i> spp.	Octo	0.584	0.094	0.202	0.140	0.002	0.003	0.006	0.039	0.271	0.149	9
<i>Thesea</i> sp. (red)	Octo	0.001	0.062	0.207	0.032	0.029	0.048	0.085	0.280	0.444	0.132	9
<i>Homotrema rubrum</i>	Ecto	0.041	0.242	0.267	0.005	0.094	0.264	0.005	0.048	0.002	0.108	9
<i>Stichopathes ?lutkeni</i>	Anti	0.008	0.285	0.270	0.004	0.072	0.036	0.146	0.031	0.018	0.096	9
?Didemnidae	Asci	0.015	0.046	0.190	0.137	0.065	0.114	0.150	0.073	0.053	0.094	9
<i>Diadema antillarum</i>	Ech	0.004	0.126	0.282	0.056	0.010	0.005	0.227	0.014	0.078	0.089	9
<i>Thesea</i> sp. (white)	Octo	0.241	0.004	0.023	0.031	0.016	0.327	0.009	0.087	0.063	0.089	9
Porifera, amorphous indistinct	Por	0.541	0.075	0.051	0.001	0.010	0.035	0.003	0.028	0.003	0.083	9
<i>Hypnogorgia pendula</i>	Octo	0.032	0.017	0.039	0.006	0.018	0.008	0.003	0.182	0.419	0.080	9
Porifera, orange amorphous	Por	0.312	0.075	0.107	0.009	0.029	0.035	0.014	0.005	0.003	0.065	9
<i>Ulosa</i> sp.	Por	0.539	0.001	0.002	0.000	0.000	0.000	0.000	0.000	0.000	0.060	3
<i>Stenorhynchus seticornis</i>	Nat	0.012	0.039	0.097	0.003	0.079	0.020	0.062	0.052	0.081	0.049	9
? <i>Javania cailleti</i>	Aherm	0.000	0.018	0.005	0.159	0.027	0.000	0.018	0.088	0.101	0.046	7
<i>Pseudoceratina crassa</i>	Por	0.205	0.000	0.000	0.000	0.000	0.000	0.150	0.000	0.000	0.039	2
All Taxa		21.987	15.567	13.454	30.628	23.038	13.681	26.892	22.219	22.232		

^a = Taxon group abbreviations: Aherm = ahermatypic corals; Alg = alga; Anti = antipatharia; Asci = ascidiacea; Crin = crinoidea; Ech = echinoidea; Ecto = ectoprocta; Herm = hermatypic corals; Hydr = hydroida; Nat = natantia; Octo = octocoralia; Oph = ophiuroidea; Por = porifera; Rep = reptantia.

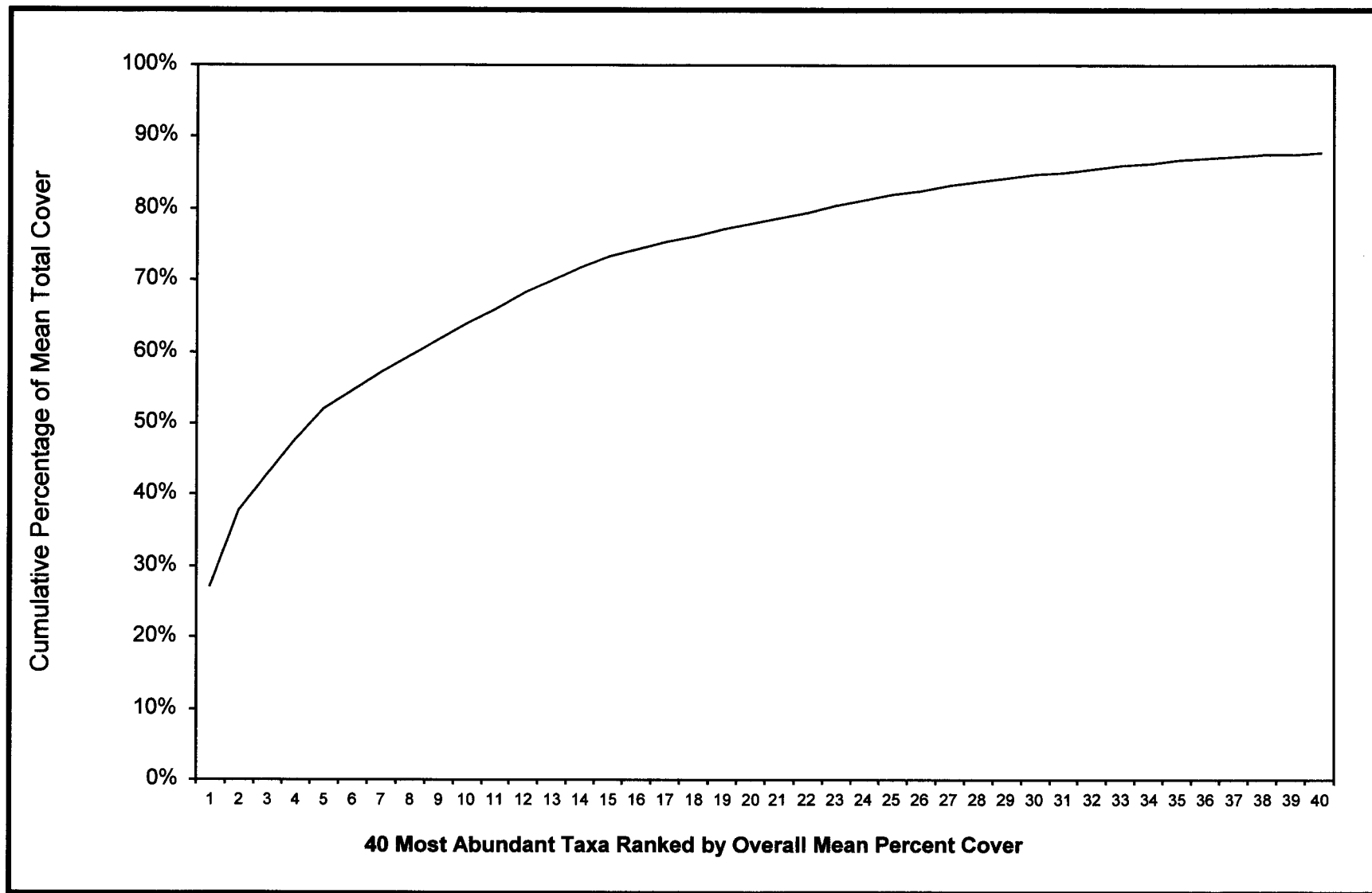


Fig. 7.2. Cumulative percentage of mean total cover contributed by the 40 most abundant hard bottom taxa.

Linear Model Analyses

Three-way ANOVAs indicated numerous significant differences in the 40 dominant hard bottom taxa according to categories of relief, region, and cruise and numerous significant interactions (**Table 7.5**). This high number of significant differences and interactions is not surprising given the large number of random quadrats analyzed. Based on the number of significant results, relief had the greatest effect, followed by region and cruise. Thirty-five taxa varied significantly among relief categories, 32 varied significantly among region categories, and 28 varied significantly among cruises. Nevertheless, this model accounted for generally small percentages of variation, with the highest r^2 value being 0.500 for *?Idmidronea*. Interpretation of these results is complicated by the high number of significant interactions. Every taxon had at least one significant two-way interaction, and most taxa had three significant two-way interactions and a significant three-way interaction. It also must be remembered that because a large number of taxa and taxon groups were tested, a small number of the significant results could be due to chance.

Very few of the significant differences among cruises shown in **Table 7.5** indicated systematic abundance changes through time. Corallinaceae, *Madrepora carolina*, both the yellow and orange encrusting poriferans, the red *Thesea* sp., the unidentified *Thesea* spp., and total poriferans increased through time. Conversely, *?Idmidronea* and Stenogorgiinae were the only taxa to exhibit consistent declines. Temporal changes due to seasonal effects probably would be indicated by Cruises 1C and M2 being on opposite ends of the cruise rankings, because they represent the earliest and latest sampling seasons, spring and fall, respectively (see **Table 7.1**). Only *Ctenocella (Ellisella)* spp., the orange amorphous poriferan, unidentified rhodophyta, and the unidentified solitary scleractinian suggested seasonal differences, with the last three having highest abundances in spring and lowest abundances in fall.

Twelve taxa and two taxon groups varied systematically from east to west, suggesting strong effects of region (**Table 7.5**). Unidentified bryozoa, *Homotrema rubrum*, *Madrepora carolina*, the amorphous indistinct and orange amorphous porifera, unidentified rhodophyta, *Ulosa* sp., and total ectoprocts had highest percent cover in the east and lowest in the west. Conversely, *?Didemnidae*, *?Javania cailleti*, *R. manuelensis*, the unidentified solitary scleractinian, *Stylocidaris affinis*, and total ahermatypic corals had highest percent cover in the west and lowest in the east.

Sixteen taxa, three taxon groups, and total cover varied systematically from high to medium to low relief, suggesting a strong effect of relief (**Table 7.5**). *Antipathes ?atlantica/gracilis*, Corallinaceae, Crinoidea, *Madracis/Oculina* sp., *Peysonnelia* spp., the amorphous indistinct porifera, *Rhizopsammia manuelensis*, *Stylocidaris affinis*, total algae, total hermatypic corals, and total cover were greatest in high relief and lowest in low relief. Conversely, *?Astrocyclus caecilia*, *Ctenocella (Ellisella)* spp., galatheidae, *Homotrema rubrum*, *Madrepora carolina*, *Stylopoma spongites*, the red *Thesea* sp., the

Table 7.5. ANOVA results for differences among categories of habitat relief, region and cruise for the percent cover of 40 hard bottom taxa, the aggregate cover for five taxon groups, and the total aggregate cover for all hard bottom taxa.

Taxa	r^2	Relief		Region		Cruise		Significant Interactions ^a
		p	rank ^b	p	rank ^b	p	rank ^b	
<i>Antipathes ?atlantica/gracilis</i>	0.105	<0.0001	H M L	0.5279	W E C	0.7027	4 3 2 1	C*RI, C*Rg, RI*Rg, C*RI*Rg
<i>Antipathes ?furcata</i>	0.486	<0.0001	M L H	<0.0001	C W E	0.1369	4 3 2 1	RI*Rg
<i>Antipathes</i> spp.	0.085	0.0149	M L H	0.5517	C E W	<0.0001	1 3 2 4	C*Rg, RI*Rg, C*RI*Rg
<i>?Astrocyclus caecilia</i>	0.060	<0.0001	L M H	0.0078	W E C	0.0199	4 2 3 1	RI*Rg
<i>Bebryce cinerea/grandis</i>	0.086	<0.0001	L H M	0.2111	E C W	0.1378	1 3 2 4	C*RI, C*Rg, RI*Rg
Bryozoa, unidentified	0.247	<0.0001	H L M	<0.0001	E C W	<0.0001	1 3 4 2	C*RI, C*Rg, RI*Rg, C*RI*Rg
Corallinaceae	0.339	<0.0001	H M L	<0.0001	E W C	<0.0001	4 3 2 1	C*RI, C*Rg, RI*Rg, C*RI*Rg
Crinoidea	0.214	<0.0001	H M L	0.1354	C W E	0.2432	1 3 2 4	C*Rg, RI*Rg, C*RI*Rg
<i>Ctenocella (Ellisella)</i> spp.	0.139	<0.0001	L M H	<0.0001	W E C	0.0305	2 3 4 1	C*RI, C*Rg, RI*Rg, C*RI*Rg
<i>Diadema antillarum</i>	0.032	0.6608	L H M	0.0175	W E C	0.4301	3 2 4 1	C*RI, RI*Rg
?Didemnidae	0.124	0.0046	L H M	<0.0001	W C E	<0.0001	2 3 1 4	C*RI, C*Rg, RI*Rg, C*RI*Rg
Galatheidae	0.316	<0.0001	L M H	0.0001	W E C	<0.0001	3 4 1 2	C*RI, C*Rg, RI*Rg, C*RI*Rg
<i>Homotrema rubrum</i>	0.461	<0.0001	L M H	<0.0001	E C W	<0.0001	1 3 2 4	C*RI, C*Rg, RI*Rg, C*RI*Rg
Hydroida	0.157	<0.0001	H L M	<0.0001	C W E	<0.0001	2 1 3 4	C*RI, C*Rg, RI*Rg, C*RI*Rg
<i>Hypnogorgia pendula</i>	0.025	0.0693	L M H	0.0213	W E C	0.5665	3 2 4 1	RI*Rg
<i>?Idmidronea</i>	0.500	<0.0001	L H M	<0.0001	C E W	<0.0001	1 2 3 4	C*RI, C*Rg, RI*Rg, C*RI*Rg
<i>?Javania cailleti</i>	0.178	<0.0001	M L H	<0.0001	W C E	<0.0001	3 4 1 2	C*RI, C*Rg, RI*Rg, C*RI*Rg
<i>Madrepora carolina</i>	0.081	<0.0001	L M H	0.0372	E C W	0.0017	4 3 2 1	C*RI, C*Rg, RI*Rg, C*RI*Rg
<i>Madracis/Oculina</i> sp.	0.044	0.0001	H M L	0.1788	C W E	0.0914	1 3 2 4	C*RI, C*Rg, RI*Rg
<i>Nicella</i> spp.	0.176	<0.0001	M H L	<0.0001	W E C	0.0738	3 4 2 1	RI*Rg
<i>Peysonnelia</i> spp.	0.349	<0.0001	H M L	<0.0001	E W C	0.0010	1 2 4 3	C*RI, C*Rg, RI*Rg, C*RI*Rg
Porifera, amorphous indistinct	0.233	<0.0001	H M L	<0.0001	E C W	<0.0001	3 1 4 2	C*RI, C*Rg, RI*Rg, C*RI*Rg
Porifera, orange amorphous	0.223	<0.0001	H L M	<0.0001	E C W	<0.0001	1 3 4 2	C*RI, C*Rg, RI*Rg, C*RI*Rg
Porifera, orange encrusting	0.223	<0.0001	H L M	<0.0001	E W C	<0.0001	4 3 2 1	C*RI, C*Rg, RI*Rg, C*RI*Rg
Porifera, yellow encrusting	0.125	<0.0001	H L M	<0.0001	W E C	<0.0001	4 3 2 1	C*RI, C*Rg, RI*Rg
<i>Pseudoceratina crassa</i>	0.028	0.0002	H L M	0.0084	E W C	0.9382	2 1 3 4	RI*Rg
<i>Rhizopsammia manuelensis</i>	0.323	<0.0001	H M L	<0.0001	W C E	<0.0001	4 3 1 2	C*RI, C*Rg, RI*Rg, C*RI*Rg

Table 7.5. (Continued).

Taxa	r^2	Relief		Region		Cruise		Significant Interactions ^a
		p	rank ^b	p	rank ^b	p	rank ^b	
Rhodophyta, unidentified	0.395	<0.0001	H L M	<0.0001	E C W	<0.0001	1 4 3 2	C*RI, C*Rg, RI*Rg, C*RI*Rg
Scleractinia, solitary	0.318	0.0014	M L H	<0.0001	W C E	<0.0001	1 4 3 2	C*RI, C*Rg, RI*Rg, C*RI*Rg
Stenogorgiinae	0.115	0.0525	L M H	<0.0001	E W C	<0.0001	1 2 3 4	C*RI, C*Rg, RI*Rg, C*RI*Rg
<i>Stenorhynchus seticornis</i>	0.034	0.4201	L H M	0.1098	W E C	0.1330	3 1 4 2	RI*Rg, C*RI*Rg
<i>Stichopathes ?lutkeni</i>	0.066	0.1368	L M H	<0.0001	E W C	0.0271	3 1 4 2	C*Rg, RI*Rg, C*RI*Rg
<i>Stylocidaris affinis</i>	0.128	0.0008	H M L	<0.0001	W C E	0.0002	4 3 1 2	C*Rg, RI*Rg
<i>Stylopoma spongites</i>	0.141	0.0040	L M H	<0.0001	E W C	0.0668	2 1 3 4	C*RI, C*Rg, RI*Rg, C*RI*Rg
<i>Swiftia exserta</i>	0.044	<0.0001	H L M	0.9007	C W E	<0.0001	2 1 4 3	C*RI, RI*Rg, C*RI*Rg
<i>Thesea</i> sp. (red)	0.125	<0.0001	L M H	<0.0001	W E C	<0.0001	4 3 2 1	C*Rg, RI*Rg, C*RI*Rg
<i>Thesea</i> sp. (white)	0.218	<0.0001	L H M	<0.0001	C E W	<0.0001	1 3 2 4	C*RI, C*Rg, RI*Rg, C*RI*Rg
<i>Thesea</i> spp.	0.070	<0.0001	L M H	0.5387	W E C	0.0031	4 3 2 1	C*Rg, RI*Rg, C*RI*Rg
<i>Thesea/Scleracis</i> spp.	0.211	<0.0001	H L M	<0.0001	E W C	<0.0001	3 4 2 1	C*RI, C*Rg, RI*Rg, C*RI*Rg
<i>Ulosa</i> sp.	0.259	<0.0001	H L M	<0.0001	E C W	0.1593	1 3 2 4	C*RI, C*Rg, RI*Rg, C*RI*Rg
Total Ahermatypic Corals	0.331	<0.0001	M H L	<0.0001	W C E	<0.0001	4 1 3 2	C*Rg, RI*Rg, C*RI*Rg
Total Algae	0.446	<0.0001	H M L	<0.0001	E W C	<0.0001	4 3 1 2	C*RI, C*Rg, RI*Rg, C*RI*Rg
Total Antipatharians	0.375	<0.0001	M L H	<0.0001	C W E	0.8155	3 4 2 1	C*Rg, RI*Rg
Total Ectoprocts	0.434	<0.0001	L H M	<0.0001	E C W	<0.0001	1 3 2 4	C*RI, C*Rg, RI*Rg, C*RI*Rg
Total Hermatypic Corals	0.043	0.0001	H M L	0.1841	C W E	0.0893	1 3 2 4	C*RI, C*Rg, RI*Rg
Total Octocorals	0.202	<0.0001	L M H	<0.0001	W E C	0.2429	3 2 1 4	C*Rg, RI*Rg, C*RI*Rg
Total Poriferans	0.328	<0.0001	H L M	<0.0001	E W C	0.0235	4 3 2 1	C*RI, C*Rg, RI*Rg, C*RI*Rg
Total Cover	0.197	<0.0001	H M L	<0.0001	C W E	<0.0001	1 3 4 2	C*RI, C*Rg, RI*Rg, C*RI*Rg
Total Number of Taxa	0.327	<0.0001	M L H	<0.0001	W E C	<0.0001	4 3 2 1	C*RI, C*Rg, RI*Rg, C*RI*Rg

^a = Interactions are listed for which probabilities were <0.0500. Abbreviations: C = cruise; RI = relief; Rg = region.

^b = Relief categories (H = high, M = medium, L = low), regions (E = east, C = central, W = west) and cruises (1 = 1C, 2 = M2, 3 = M3, 4 = M4) are arranged with the highest means on the left and the lowest means on the right.

unidentified *Thesea* spp., and total octocorals were greatest in low relief and lowest in high relief.

The ANOVA results for relief and region (**Table 7.5**) provided the basis for categorizing taxa according to habitat preferences (**Table 7.6**). Although fewer than 50% of the significant effects for relief indicated consistent trends, previous studies (Hardin et al. 1994) and our video observations have shown that biological differences associated with habitat relief may occur over differences of less than 2 m. Consequently, a conservative approach to assigning habitat preferences was applied, and those taxa with highest abundances at either medium or high relief sites were combined into a single category. All taxa that had highest mean percent cover at low relief sites were placed in the low relief category. Taxa that varied significantly according to region and had highest mean percent cover in the west or east were placed into west and east categories, respectively, regardless of whether an east-to-west gradient was evident.

A majority of the 40 dominant taxa preferred medium-high relief habitat (**Table 7.6**). Ten taxa and two taxon groups preferred eastern medium-high relief; 7 taxa, two taxon groups and total cover were highest at either the central region or no region; and 6 taxa and two taxon groups preferred western medium-high relief. Of the 12 taxa and two taxon groups that preferred low relief, 4 taxa preferred the central or no region, 3 taxa and total ectoprocts preferred the east, and 5 taxa and total octocorals preferred the west.

These groupings were subjected to linear model tests to determine the effects of physical variables other than categories of region and relief. Some of the physical variables (i.e., location on feature, bearing from center of feature and slope) were expected to have small effects in low relief habitat, so separate tests were run for all taxa at all sites, medium-high relief taxa at medium-high relief sites, and low relief taxa at low relief sites. Because initial observations at Site 4 indicated it was a low mound with gradually sloping sides, this site was placed in the low relief category for these linear model tests.

Although the linear model test for effects of eight variables on all taxa at all sites explained generally low amounts of variation, all tests were highly significant, probably due to the large numbers of replicates (i.e., 2,653) (**Table 7.7**). The taxa that preferred medium-high relief tended to have higher amounts of explained variation (mean $r^2 = 0.208$) than did taxa that preferred low relief (mean $r^2 = 0.163$). Those taxa with no relief preference had consistently low amounts of variation explained by this linear model (mean $r^2 = 0.051$). There were also generally more significant variables for medium-high relief taxa than for low relief taxa. Taxa with no relief preference had no more than four significant variables.

Table 7.6. Habitat and region preferences of taxa based upon ANOVA results for the effects of relief and region (see Table 7.5). Individual taxa are ranked in each category of habitat preference according to their overall mean percent cover (see Table 7.4).

Habitat	Region	Taxa	Taxon Number ^a	
Medium-High Relief	Central or None	<i>Antipathes ?furcata</i>	6	
		Crinoidea	11	
		<i>Antipathes ?atlantica/gracilis</i>	5	
		<i>Antipathes</i> spp.	7	
		Hydroida, unidentified	16	
		<i>Swiftia exserta</i>	35	
		<i>Madracis/Oculina</i> sp.	18	
		Total Antipatharians	--	
		Total Hermatypic Corals	--	
		Total Cover	--	
	East	Corallinaceae	10	
		Bryozoa, unidentified	9	
		Porifera, orange encrusting	24	
		<i>Peysonnella</i> spp.	21	
		Rhodophyta, unidentified	28	
		<i>Thesea/Scleracis</i> spp.;	39	
		Porifera, amorphous indistinct	22	
		Porifera, orange amorphous	23	
		<i>Ulosa</i> sp.	40	
		<i>Pseudoceratina crassa</i>	26	
		Total Algae	--	
		Total Poriferans	--	
		West	<i>Rhizopsammia manuelensis</i>	27
	<i>Nicella</i> spp.		20	
	Porifera, yellow encrusting		25	
	Scleractinia, solitary		29	
	<i>Stylocidaris affinis</i>		33	
? <i>Javania caillieti</i>	4			
Total Ahermatypic Corals	--			
Total Number of Taxa	--			
Low Relief	Central or None		<i>Bebryce cinerea/grandis</i>	8
			? <i>Idmidronea</i>	3
		<i>Thesea</i> spp.	38	
		<i>Thesea</i> sp. (white)	37	
	East	<i>Madrepora carolina</i>	19	
		<i>Stylopoma spongites</i>	34	
		<i>Homotrema rubrum</i>	15	
		Total Ectoprocts	--	
	West	<i>Ctenocella (Ellisella)</i> spp.	12	
		? <i>Astrocyclus caecilia</i>	1	
		Galatheidae	14	
		<i>Thesea</i> sp. (red)	36	
		? <i>Didemnidae</i>	2	
		Total Octocorals	--	
	None	None	<i>Stenorhynchus seticornis</i>	31
		East	Stenogorgiinae	30
			<i>Stichopathes?lutkeni</i>	32
West		<i>Diadema antillarum</i>	13	
		<i>Hypnogorgia pendula</i>	17	

^a = Taxon numbers refer to Figs. 7.12 and 7.13.

Table 7.7. General linear models results for the effects of eight variables on the percent cover of 40 hard bottom taxa, the aggregate cover for five groups, and the total aggregate cover for all hard bottom taxa at all sites listed according to taxa preferences for habitat relief and region. Individual taxa are ranked according to their overall mean percent areal cover (see Table 7.4). Variables are shown from left to right in order of the number of significant correlations.

Relief	Region	Taxa	r ²	p	Significant Variables ^a							
					Dist	Cruise	Ruffs	Depth	Flux	Ven	Hflux	Ruffm
Medium-High	Central or None	<i>Antipathes ?furcata</i>	0.443	<0.0001	X	--	X	X	--	--	X	X
		Crinoidea	0.240	<0.0001	X	X	X	X	X	--	X	--
		<i>Antipathes ?atlantica/gracilis</i>	0.123	<0.0001	X	X	--	X	--	--	--	--
		<i>Antipathes</i> spp.	0.064	<0.0001	X	X	--	--	X	--	X	--
		Hydroida, unidentified	0.101	<0.0001	X	X	--	X	X	--	X	--
		<i>Swiftia exserta</i>	0.039	<0.0001	X	X	--	X	--	--	--	X
		<i>Madracis/Oculina</i> sp	0.128	<0.0001	X	X	X	X	X	X	--	X
		Total Antipatharians	0.332	<0.0001	X	--	--	--	--	--	X	X
		Total Hermatypic Corals	0.129	<0.0001	X	X	X	X	X	X	--	X
	Total Cover	0.252	<0.0001	X	X	X	--	--	X	--	X	
	East	Corallinaceae	0.348	<0.0001	X	X	X	X	X	X	X	--
		Bryozoa, unidentified	0.210	<0.0001	X	X	X	X	X	--	X	X
		Porifera, orange encrusting	0.255	<0.0001	X	X	X	--	--	X	--	--
		<i>Peysommelia</i> spp.	0.362	<0.0001	X	X	--	X	X	X	--	X
		Rhodophyta, unidentified	0.332	<0.0001	X	X	X	--	X	X	X	--
		<i>Thesea/Scleracis</i> spp.	0.109	<0.0001	X	X	--	X	X	--	--	--
		Porifera, amorphous indistinct	0.182	<0.0001	X	X	X	--	--	X	--	--
		Porifera, orange amorphous	0.210	<0.0001	X	X	X	X	--	--	--	--
		<i>Ulosa</i> sp.	0.242	<0.0001	X	X	X	X	X	--	--	--
<i>Pseudoceratina crassa</i>		0.023	<0.0001	X	--	--	X	--	--	--	--	
Total Algae	0.500	<0.0001	X	X	X	X	X	--	X	--		
Total Poriferans	0.382	<0.0001	X	X	X	X	X	X	--	--		
West	<i>Rhizopsammia manuelensis</i>	0.474	<0.0001	X	X	X	X	X	X	X	X	
	<i>Nicella</i> spp	0.187	<0.0001	X	--	--	--	--	X	X	--	
	Porifera, yellow encrusting	0.170	<0.0001	X	X	X	X	--	X	--	X	
	Scleractinia, solitary	0.270	<0.0001	X	X	X	--	--	--	X	X	
	<i>Stylocidaris affinis</i>	0.141	<0.0001	X	X	X	X	X	X	X	X	
	<i>?Javania cailleti</i>	0.136	<0.0001	X	X	--	--	--	--	--	--	
	Total Ahermatypic Corals	0.479	<0.0001	X	X	X	X	X	X	--	X	
	Total Number of Taxa	0.321	<0.0001	X	X	X	X	X	--	X	X	

Table 7.7. (Continued).

Relief	Region	Taxa	r ²	p	Significant Variables ^a							
					Dist	Cruise	Ruffs	Depth	Flux	Ven	Hflux	Ruffm
Low	Central or None	<i>Bebryce cinerea/grandis</i>	0.071	<0.0001	X	--	--	X	--	--	--	X
		? <i>Idmidronea</i>	0.399	<0.0001	X	X	--	X	X	--	X	X
		<i>Thesea</i> spp.	0.050	<0.0001	X	X	--	--	--	X	--	--
		<i>Thesea</i> sp. (white)	0.167	<0.0001	X	X	--	--	X	--	X	--
	East	<i>Madrepora carolina</i>	0.084	<0.0001	X	--	--	X	X	--	--	X
		<i>Stylopoma spongites</i>	0.122	<0.0001	X	--	--	--	X	X	X	X
		<i>Homotrema rubrum</i>	0.305	<0.0001	X	X	X	--	X	X	X	--
		Total Ectoprocts	0.339	<0.0001	X	X	X	--	X	--	X	--
	West	<i>Ctenocella (Ellisella)</i> spp.	0.137	<0.0001	X	X	X	X	X	X	X	X
		? <i>Astrocyclus caecilia</i>	0.053	<0.0001	X	X	--	--	--	--	--	--
		Galatheidae	0.219	<0.0001	X	X	X	--	X	--	X	--
		<i>Thesea</i> sp. (red)	0.126	<0.0001	X	X	--	X	X	--	--	--
		?Didemnidae	0.057	<0.0001	X	X	X	--	--	X	X	--
		Total Octocorals	0.216	<0.0001	X	--	X	X	X	X	--	--
None	None	<i>Stenorhynchus seticornis</i>	0.039	<0.0001	X	--	X	--	--	X	--	X
	East	Stenogorgiinae	0.092	<0.0001	X	X	X	--	--	X	--	--
		<i>Stichopathes ?lutkeni</i>	0.054	<0.0001	X	--	--	--	--	--	--	--
	West	<i>Diadema antillarum</i>	0.045	<0.0001	X	--	--	--	--	X	--	X
		<i>Hypnogorgia pendula</i>	0.024	<0.0001	--	--	--	--	--	--	--	--

^a Variables marked (X) are those for which probabilities were <0.0500. Variable abbreviations: Dist = distance from the Mississippi River; Cruise = cruise; Ruffs = small-scale substratum roughness; Depth = depth; Flux = normal (non-hurricane) flux of suspended sediments; Ven = sediment veneer; Hflux = flux of suspended sediments during hurricanes; and Ruffm = medium-scale substratum roughness.

Results of the linear model test for the effects of 11 variables on medium-high relief taxa and taxon groups at medium and high relief sites indicated 21 taxa or taxon groups for which location on feature, bearing from center of feature and slope were significant variables (**Table 7.8**). Nevertheless, the variation explained per taxon (mean $r^2 = 0.207$) was similar to that for these taxa at all sites without including these variables.

A comparison of the percentage of medium-high relief taxa for which each variable was significant shows that the effects of some variables were more widespread among these taxa at all sites than at medium-high relief sites (**Table 7.9**). Sediment veneer, depth, normal flux, and medium-scale roughness decreased substantially in the percentage of taxa for which they were significant at medium-high relief sites, compared to all sites. This suggests that these variables may be strong determinants in the preference of some medium-high relief taxa for medium-high relief habitat. The decline in the percentage of taxa for which sediment veneer and depth was significant was especially marked in those taxa preferring eastern or western regions. The decline in importance of medium-scale roughness was similar among all region preferences.

There were substantial differences in the percentages of medium-high relief taxa affected by different variables. Cruise and distance from the Mississippi River were consistently significant for medium-high relief taxa at all sites and at medium-high relief sites. Because distance from the Mississippi did not vary among random quadrats within sites, this variable is synonymous with site and may simply reflect consistent differences among sites. Small-scale substrate roughness was also significant for a majority of medium-high relief taxa at all sites and at medium-high relief sites. At just medium-high relief sites, location on feature and hurricane flux of suspended sediments were next most important, followed by normal flux of suspended sediments, substrate slope, depth, sediment veneer, and medium-scale substrate roughness.

Restriction of the linear model test for low relief taxa to low relief sites (**Table 7.10**) slightly increased the amount of variation explained (mean $r^2 = 0.190$) over the amount explained when all sites were included. Nevertheless, there were small differences in the percentages of taxa for which each variable was significant between the analysis with all sites and the analysis with only low relief sites (**Table 7.11**). This suggests that there are not substantial differences in the importance of these variables for low relief taxa among sites with different vertical relief.

Distribution Patterns

There were several, distinct distribution patterns for those medium-high relief taxa and taxon groups that varied significantly according to location on feature. The unidentified solitary scleractinian and *R. manuelensis* both were most abundant on the sides of medium-high relief features (**Fig. 7.3**). The abundances of *Ulosa* sp., unidentified rhodophyta, the orange amorphous and amorphous indistinct porifera, crinoidea, corallinaceae, and unidentified bryozoa were all highest on the top interiors of

Table 7.8. Results of general linear models for effects of 11 variables on the percent cover of hard bottom taxa and taxon groups that have highest abundances at medium and high relief sites listed according to region preference. Test was performed on data from five medium and high relief sites (1, 2, 5, 7 and 8). Individual taxa are ranked according to their overall mean percent cover (see Table 7.4). Variables are shown from left to right in order of the number of significant correlations.

Region Preference	Taxa	r^2	p	Significant Variables ^a											
				Dist	Cruise	Ruffs	Loc	Flux	Hflux	Slope	Depth	Bear	Ruffm	Ven	
Central or None	<i>Antipathes ?furcata</i>	0.030	0.0080	X	X	--	--	--	--	--	--	--	--	--	--
	Crinoidea	0.252	<0.0001	X	--	X	X	X	X	--	X	X	--	--	--
	<i>Antipathes ?atlantica/gracilis</i>	0.137	<0.0001	X	X	--	--	--	--	--	--	X	--	--	--
	Hydroida, unidentified	0.062	<0.0001	X	--	--	--	--	--	--	X	X	--	--	--
	<i>Antipathes</i> spp.	0.089	<0.0001	X	X	--	--	--	X	--	--	--	--	--	--
	<i>Swiftia exserta</i>	0.053	<0.0001	X	--	X	--	--	--	--	--	--	--	--	--
	<i>Madracis/Oculina</i> sp	0.153	<0.0001	X	X	X	--	X	X	X	--	X	X	--	--
	Total Antipatharians	0.158	<0.0001	X	X	--	--	--	--	--	--	X	--	--	--
	Total Hermatypic Corals	0.152	<0.0001	X	X	X	--	X	--	X	--	X	X	--	--
Total Cover	0.231	<0.0001	X	X	X	X	--	--	X	X	X	--	X	--	
East	Corallinaceae	0.338	<0.0001	X	X	X	X	X	X	X	X	X	X	--	--
	Bryozoa, unidentified	0.180	<0.0001	X	X	X	X	X	X	X	X	X	--	--	--
	Porifera, orange encrusting	0.271	<0.0001	X	X	X	X	--	--	--	--	--	--	--	X
	<i>Peysonnelia</i> spp.	0.348	<0.0001	X	X	X	--	X	X	X	X	--	--	--	X
	Rhodophyta, unidentified	0.362	<0.0001	X	X	X	X	X	X	--	--	--	--	--	--
	<i>Thesea/Scleracis</i> spp.	0.165	<0.0001	X	X	--	--	X	X	--	--	--	--	--	--
	Porifera, amorphous indistinct	0.191	<0.0001	X	X	X	X	--	--	--	--	--	--	--	--
	Porifera, orange amorphous	0.253	<0.0001	X	X	X	X	--	--	--	--	--	--	--	--
	<i>Ulosa</i> sp.	0.243	<0.0001	X	X	X	X	X	X	--	--	--	--	--	--
	<i>Pseudoceratina crassa</i>	0.028	0.0130	X	--	--	--	--	--	--	--	--	--	--	--
	Total Algae	0.484	<0.0001	X	X	X	--	X	X	X	X	X	--	--	--
Total Poriferans	0.387	<0.0001	X	X	X	X	X	X	--	X	--	--	X	X	
West	<i>Rhizopsammia manuelensis</i>	0.540	<0.0001	X	X	X	X	--	--	X	--	X	X	--	--
	<i>Nicella</i> spp.	0.232	<0.0001	X	--	X	--	--	--	--	--	--	--	--	--
	Porifera, yellow encrusting	0.202	<0.0001	X	X	X	--	--	--	X	--	--	--	--	X
	Scleractinia, solitary	0.375	<0.0001	X	X	X	X	X	X	--	--	X	--	--	--
	<i>Stylocidaris affinis</i>	0.148	<0.0001	X	X	X	--	--	--	--	--	--	X	--	--
	<i>?Javania cailleti</i>	0.105	<0.0001	X	X	--	--	--	--	X	--	--	--	--	--
	Total Ahermatypic Corals	0.573	<0.0001	X	X	X	X	--	--	X	X	X	X	X	--
	Total Number of Taxa	0.373	<0.0001	X	X	X	--	--	--	--	--	X	--	X	X

^a Variables marked (X) are those for which probabilities were <0.0500. Variable abbreviations: Dist = distance from the Mississippi River; Cruise = cruise; Ruffs = small-scale substratum roughness; Loc = location on rock feature; Flux = normal (non-hurricane) flux of suspended sediments; Hflux = flux of suspended sediments during hurricanes; Slope = substratum slope; Depth = depth; Bear = bearing from site center; Ruffm = medium-scale substratum roughness; and Ven = sediment veneer.

Table 7.9. Number and percentage of the medium-high relief hard bottom taxa for which 11 environmental variables were significant in two models (see Tables 7.7 and 7.8) tested for effects of the variables on taxa abundances.

Variable	Region	Med-High Relief Taxa at All Sites		Med-High Relief Taxa at Med-High Relief Sites	
		Number Significant	Percentage Significant	Number Significant	Percentage Significant
Cruise	Central or None	6	85.7	4	57.1
	East	9	90.0	9	90.0
	West	5	83.3	5	83.3
	Overall	20	87.0	18	78.3
Location on Feature	Central or None	NA ^a	--	1	14.3
	East	NA ^a	--	7	70.0
	West	NA ^a	--	2	33.3
	Overall	NA ^a	--	10	43.5
Sediment Veneer	Central or None	1	14.3	0	0
	East	5	50.0	2	20.0
	West	4	66.7	1	16.7
	Overall	10	43.5	3	13.0
Bearing	Central or None	NA ^a	--	4	57.1
	East	NA ^a	--	1	10.0
	West	NA ^a	--	2	33.3
	Overall	NA ^a	--	7	30.4
Depth	Central or None	6	71.4	2	28.6
	East	7	70.0	3	30.0
	West	3	50.0	0	0
	Overall	16	69.6	5	21.7
Normal Flux	Central or None	4	57.1	2	28.6
	East	6	60.0	6	60.0
	West	2	33.3	1	16.7
	Overall	12	52.2	9	39.1
Hurricane Flux	Central or None	4	57.1	3	42.9
	East	3	30.0	6	60.0
	West	4	66.7	1	16.7
	Overall	11	47.8	10	43.5
Small-scale Substrate Roughness	Central or None	3	42.9	2	28.6
	East	7	70.0	8	80.0
	West	4	66.7	5	83.3
	Overall	14	60.9	15	65.2
Medium-scale Substrate Roughness	Central or None	3	42.9	1	14.3
	East	2	20.0	0	0
	West	4	66.7	2	33.3
	Overall	9	39.1	3	13.0
Distance from Mississippi	Central or None	7	100.0	7	100.0
	East	10	100.0	10	100.0
	West	6	100.0	6	100.0
	Overall	23	100.0	23	100.0
Substrate Slope	Central or None	NA ^a	--	1	14.3
	East	NA ^a	--	3	30.0
	West	NA ^a	--	3	50.0
	Overall	NA ^a	--	7	30.4

^a = Not analyzed.

Table 7.10. Results of general linear models for the effects of eight variables on the percent cover of hard bottom taxa and taxon groups that have highest abundances at low relief sites listed according to region preference. Tests were performed on data from four medium and low relief sites (3, 4, 6 and 9). Individual taxa are ranked according to their overall mean percent cover (see Table 7.4). Variables are shown from left to right in order of the number of significant correlations.

Region Preference	Taxa	r^2	p	Significant Variables ^a							
				Cruise	Dist	Flux	Hflux	Depth	Ruffm	Ven	Ruffs
Central or None	<i>Bebryce cinerea/grandis</i>	0.107	<0.0001	X	X	--	--	--	--	--	X
	? <i>Idmidronea</i>	0.471	<0.0001	X	X	X	X	X	X	--	--
	<i>Thesea</i> spp.	0.059	<0.0001	X	--	X	--	--	--	X	--
	<i>Thesea</i> sp. (white)	0.333	<0.0001	X	X	--	X	--	--	--	--
East	<i>Madrepora carolina</i>	0.099	<0.0001	X	X	X	--	X	X	X	--
	<i>Stylopoma spongites</i>	0.165	<0.0001	X	X	X	X	X	X	--	--
	<i>Homotrema rubrum</i>	0.482	<0.0001	X	X	X	X	X	--	X	--
	Total Ectoprocts	0.526	<0.0001	X	X	X	X	X	X	--	--
West	<i>Ctenocella (Ellisella)</i> spp.	0.095	<0.0001	X	X	--	--	--	--	X	X
	? <i>Astrocyclus caecilia</i>	0.046	<0.0001	X	--	--	--	--	--	--	--
	Galatheidae	0.302	<0.0001	X	X	--	X	--	X	--	X
	<i>Thesea</i> sp. (red)	0.118	<0.0001	--	X	X	--	X	X	X	--
	? <i>Didemnidae</i>	0.055	<0.0001	X	X	X	X	X	--	--	--
	Total Octocorals	0.105	<0.0001	--	X	X	X	--	X	X	--

^a Variables marked (X) are those for which probabilities were <0.0500. Variable abbreviations: Cruise = cruise; Dist = distance from the Mississippi River; Flux = normal (non-hurricane) flux of suspended sediments; Hflux = flux of suspended sediments during hurricanes; Depth = depth; Ruffm = medium-scale substratum roughness; Ven = sediment veneer; and Ruffs = small-scale substratum roughness.

Table 7.11. Number and percentage of low relief hard bottom taxa for which eight environmental variables were significant in two models (see Tables 7.7 and Table 7.10) tested for effects of the variables on taxa abundances.

Variable	Region	Low-Relief Taxa at All Sites		Low-Relief Taxa at Low-Relief Sites	
		Number Significant	Percentage Significant	Number Significant	Percentage Significant
Cruise	Central or None	3	75.0	4	100.0
	East	1	33.3	3	100.0
	West	5	100.0	4	80.0
	Overall	9	75.0	11	91.7
Sediment Veneer	Central or None	1	25.0	1	25.0
	East	1	33.3	2	66.7
	West	2	40.0	2	40.0
	Overall	4	33.3	5	41.7
Depth	Central or None	2	50.0	1	25.0
	East	1	33.3	3	100.0
	West	2	40.0	2	40.0
	Overall	5	41.7	6	50.0
Normal Flux	Central or None	2	50.0	2	50.0
	East	3	100.0	3	100.0
	West	3	60.0	2	40.0
	Overall	8	66.7	7	58.3
Hurricane Flux	Central or None	2	50.0	2	50.0
	East	2	66.7	2	66.7
	West	3	60.0	2	40.0
	Overall	7	58.3	6	50.0
Small-scale Substratum Roughness	Central or None	0	0	1	25.0
	East	1	33.3	0	0
	West	3	60.0	2	40.0
	Overall	4	33.3	3	25.0
Medium-scale Substratum Roughness	Central or None	2	50.0	1	25.0
	East	2	66.7	2	66.7
	West	1	20.0	2	40.0
	Overall	5	41.7	5	41.7
Distance from Mississippi	Central or None	4	100.0	3	75.0
	East	3	100.0	3	100.0
	West	5	100.0	4	80.0
	Overall	12	100.0	10	83.3

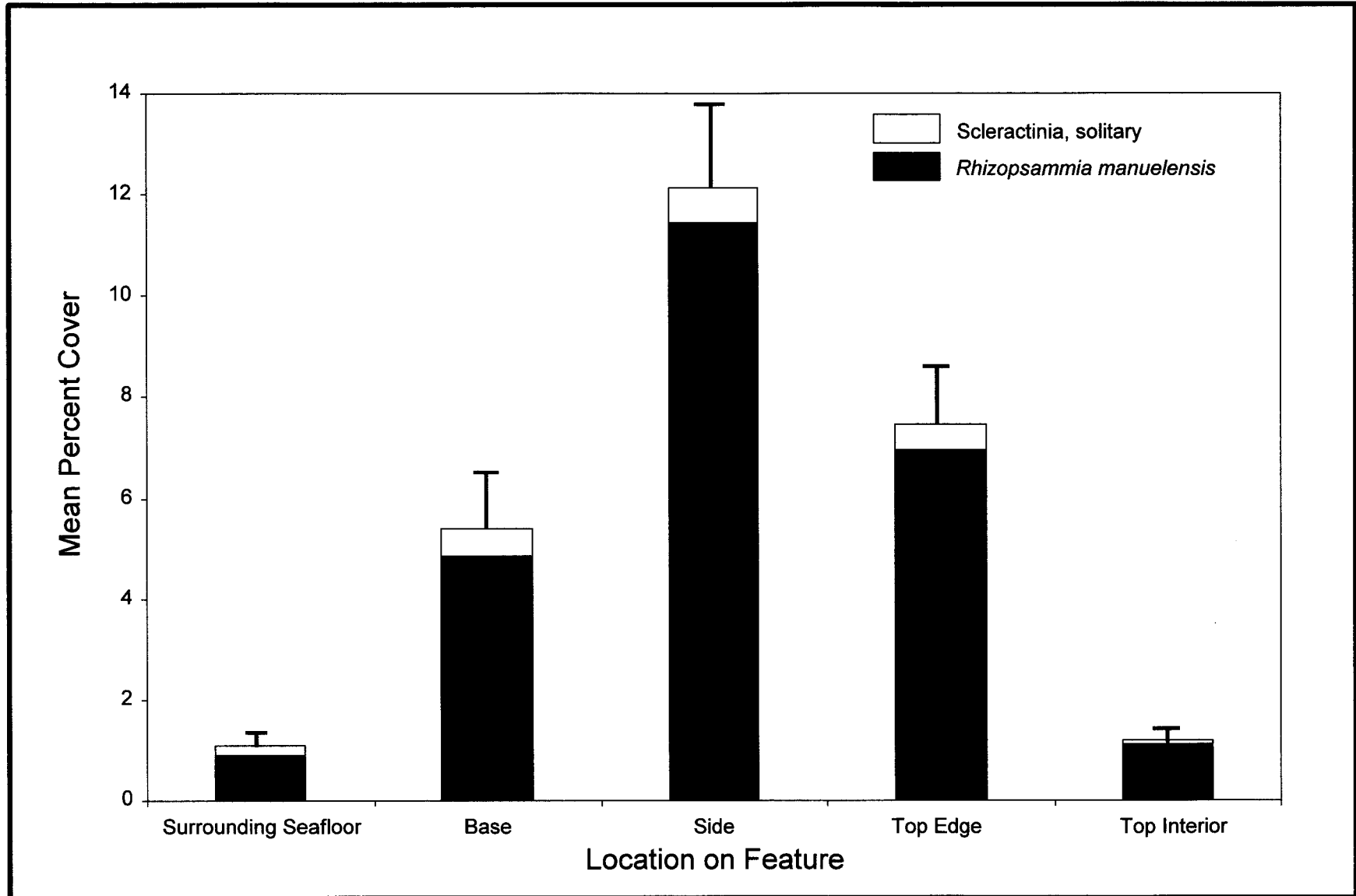


Fig. 7.3. Distribution of solitary Scleractinia and *Rhizopsammia manuelensis* according to location on hard bottom features. Bars indicate one standard error for the two groups combined, using data combined from all sites with surveys as replicates.

medium-high relief features (**Fig. 7.4**). Total cover suggested the combination of these two patterns, increasing from the surrounding seafloor, through the base and up the sides to the top interiors of medium-high relief features (**Fig. 7.5**).

There also were several distribution patterns for those medium-high relief taxa that varied according to bearing from the center of medium-high relief features. Corallinaceae had highest percent cover south of feature centers, with other minor modes to the west and southeast (**Fig. 7.6**). Hydroida were most abundant to the northwest of feature centers, with minor modes to the southwest and northeast-east (**Fig. 7.7**). The unidentified solitary scleractinian and *R. manuelensis* had higher abundances from the south clockwise through the northeast and lower abundances to the east and southeast (**Fig. 7.8**). *Madracis/Oculina* sp., crinoidea, and total antipatharians had highest percent covers to the west, northwest, or north of feature centers (**Fig. 7.9**).

Some of these distribution patterns that varied according to bearing from the feature center may be related to currents. Two potentially important effects of currents on epibiota involve the kinetic energy and flux of food provided by the currents. Kinetic energy, which suspends sediments and may bend or break tall, upright organisms, is proportional to the square of the current speed. The flux of food particles available to suspension feeding organisms is proportional to the current speed. These two indicators of current effects have slightly different percent distributions among different headings (i.e., the directions toward which the currents flow), and each is slightly different from the percent distribution of currents (**Fig. 7.10**). Mean percent cover data from each cruise were regressed as replicate independent variables against overall mean values for currents, kinetic energy, and food flux. These analyses indicated that the combined abundances of *Madracis/Oculina* sp., crinoidea, and total antipatharians were significantly related to both kinetic energy and food flux (**Table 7.12**), although the amount of variation explained was low. None of the other organism distribution patterns were related to current parameters.

Canonical Correspondence Analysis

CCA was performed to help examine the complex patterns of variation revealed by the linear model. Composite samples were created by pooling the cover estimates for a site, cruise, and depth interval. Depth intervals were defined in 5-m increments according to **Table 7.13**.

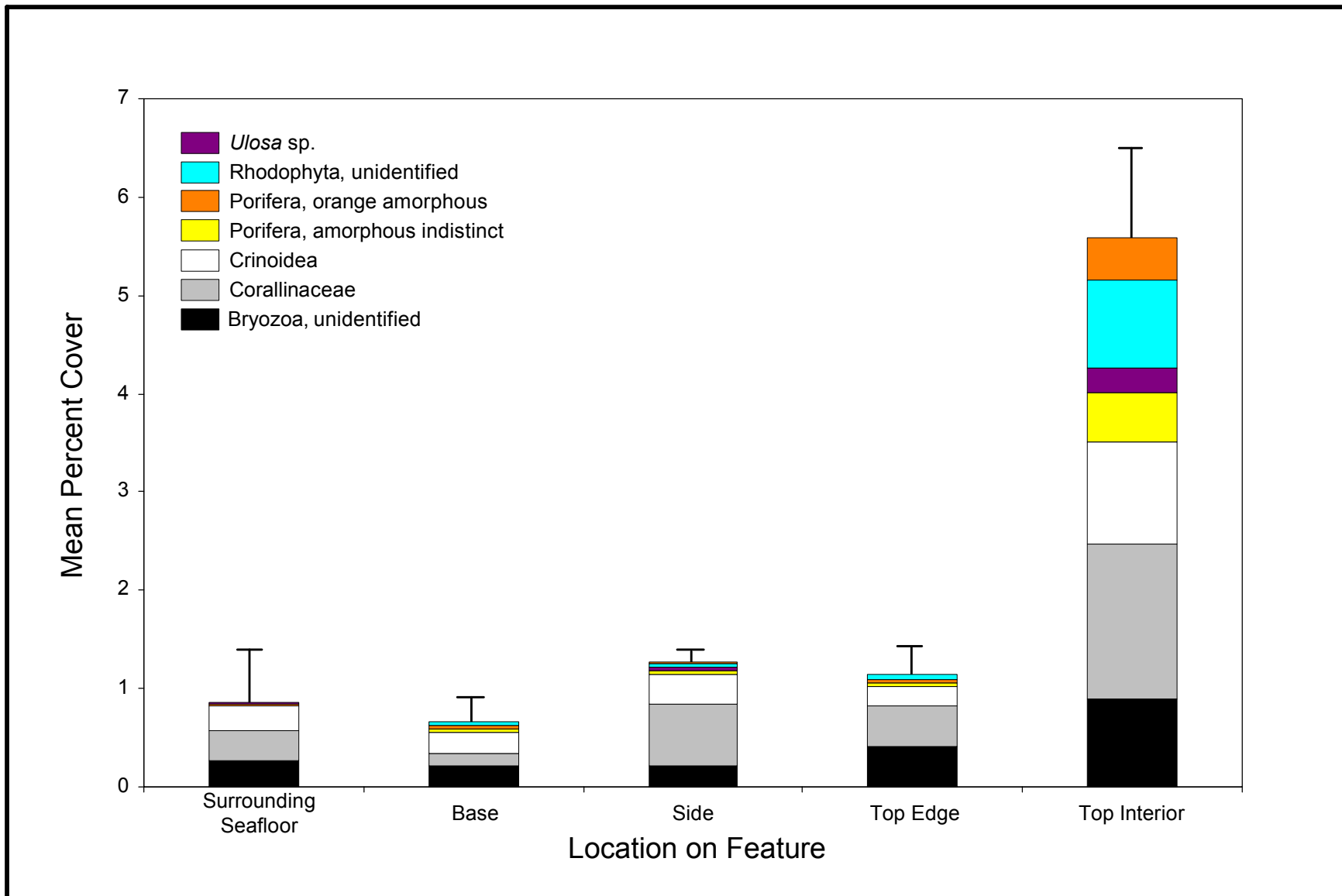


Fig. 7.4. Distribution of *Ulosa* sp., unidentified Rhodophyta, orange amorphous Porifera, amorphous indistinct Porifera, Crinoidea, Corallinaceae, and unidentified Bryozoa according to location on hard bottom features. Bars indicate one standard error for all groups combined, using data combined from all sites with surveys as replicates.

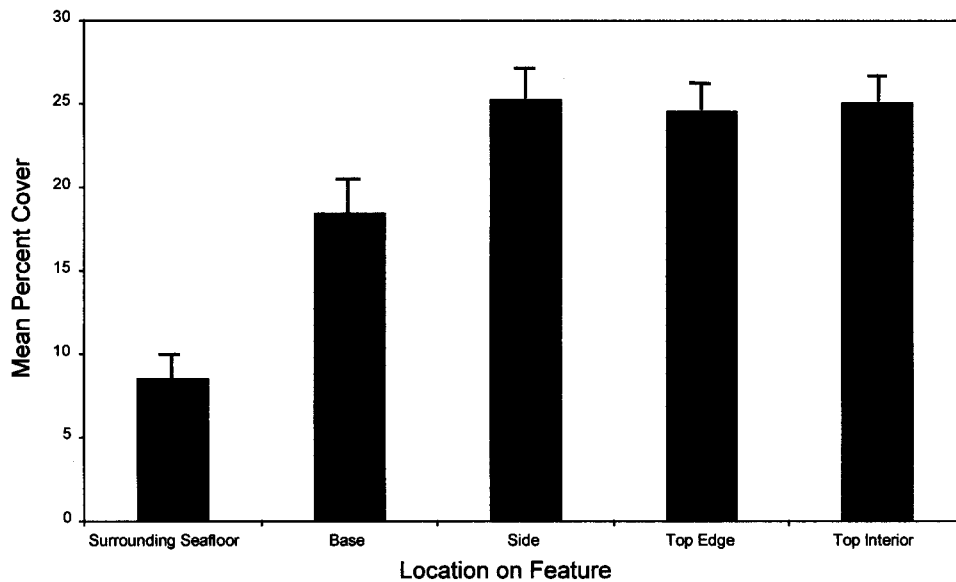


Fig. 7.5. Distribution of total cover according to location on hard bottom features. Bars indicate one standard error, using data combined from all sites with surveys as replicates.

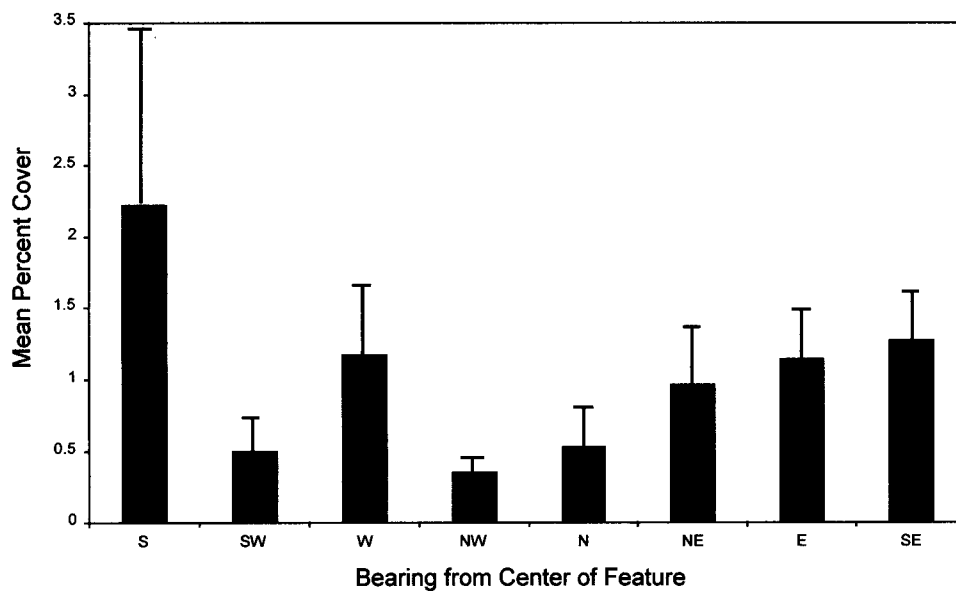


Fig. 7.6. Distribution of coralline algae (*Corallinaceae*) according to bearing from the center of hard bottom features. Bars indicate one standard error, using data combined from all sites with surveys as replicates.

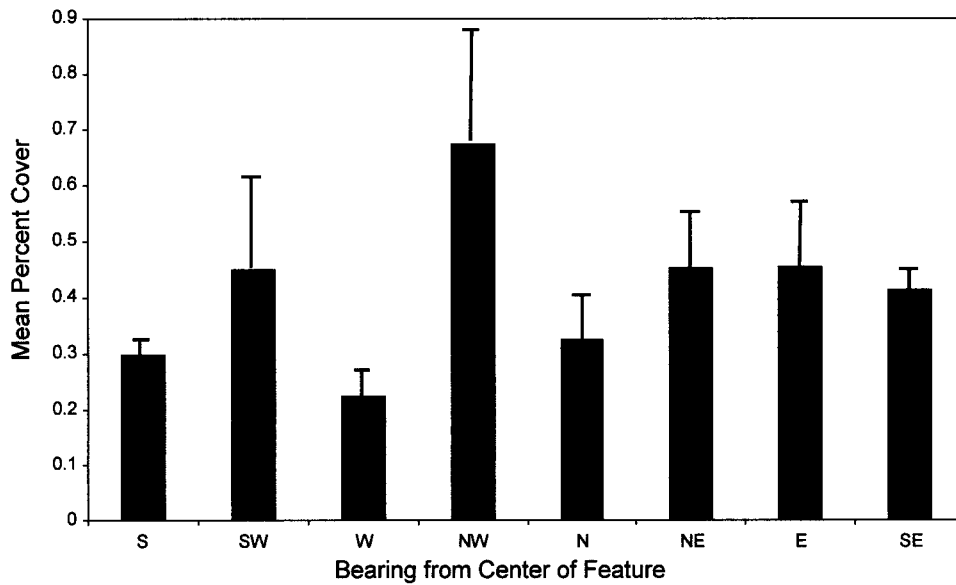


Fig. 7.7. Distribution of Hydroida according to bearing from the center of hard bottom features. Bars indicate one standard error for both groups combined, using data combined from all sites with surveys as replicates.

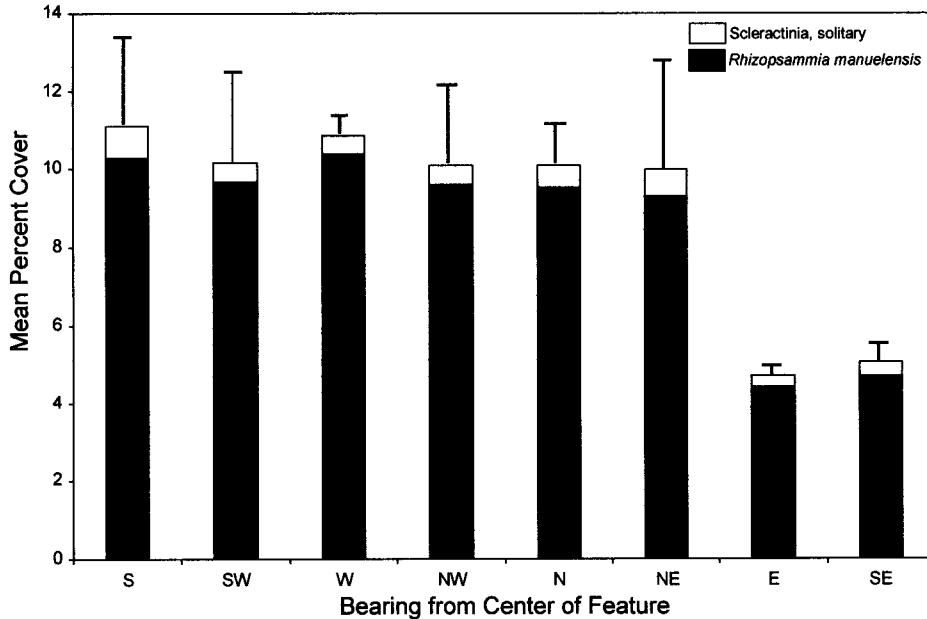


Fig. 7.8. Distribution of solitary Scleractinia and *Rhizopsammia manuelensis* according to bearing from the center of hard bottom features. Bars indicate one standard error for both groups combined, using data combined from all sites with surveys as replicates

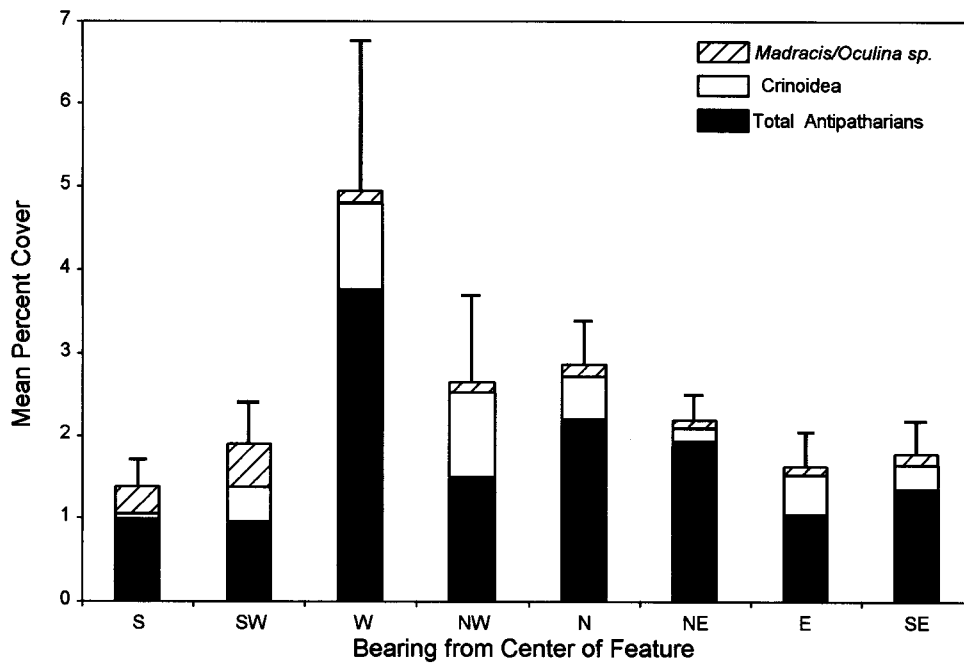


Fig. 7.9. Distribution of *Madracis/Oculina* sp., Crinoidea, and total antipatharians according to bearing from the center of hard bottom features. Bars indicate one standard error for the three groups combined, using data combined from all sites with surveys as replicates.

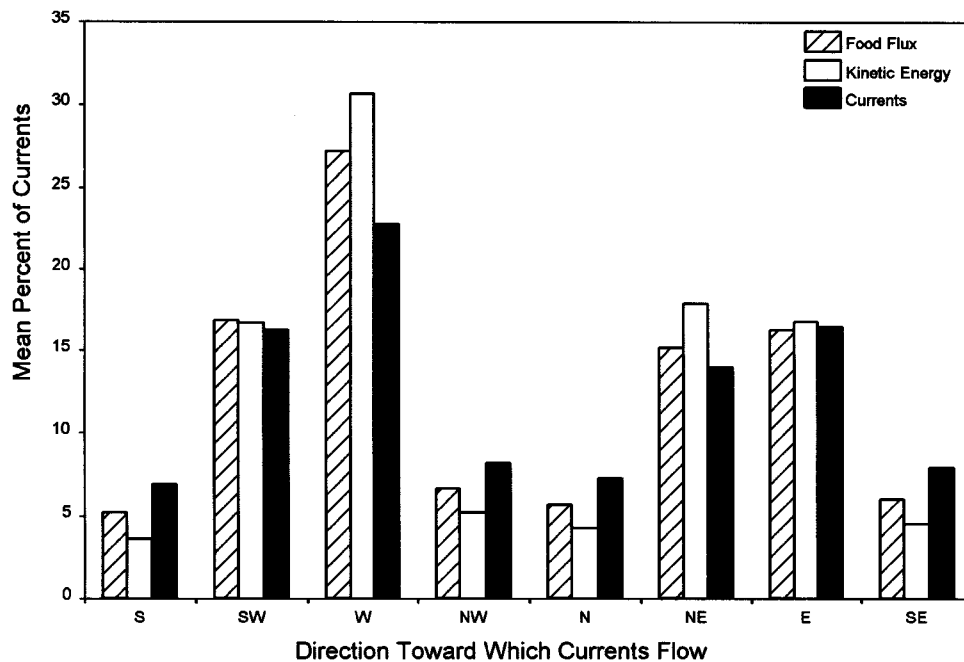


Fig. 7.10. Comparison of the percentages of currents, kinetic energy in currents, and food flux provided by currents that flow toward different directions. Values were calculated using an average joint frequency distribution of current speed and direction from the current meters located at 16 meters above bottom (mab) at Sites 1, 5, and 9 over all deployments.

Table 7.12. Results of linear regressions to determine the relationships between taxa abundances on each side of features (i.e., at different bearings from the center, the dependent variable) and the currents, current kinetic energy, and food flux flowing toward those sides of the features (independent variables).

Taxa	Currents		Kinetic Energy		Food Flux	
	r^2	p	r^2	p	r^2	p
Corallinaceae	0.003	0.7820	0.001	0.8401	0.002	0.8049
Hydroida	0.026	0.3807	0.034	0.3157	0.033	0.3196
Solitary Scleractinian + <i>Rhizopsammia manuelensis</i>	0.001	0.8940	0.006	0.6767	0.004	0.7153
Crinoidea + <i>Macracis/Oculina</i> sp. + Total Antipatharians	0.112	0.0610	0.139	0.0354	0.138	0.0363

Table 7.13. Depth intervals used for pooling data to define samples in canonical correspondence analysis.

Depth Interval (meters)	Site-Depth Category
60–65	01
65–70	02
70–75	03
75–80	04
80–85	05
85–90	06
90–95	07
95–100	08
100–105	09
105–110	10

Correlations between environmental variables and the ordination axes suggested that depth (axis 1), sediment veneer (axis 2), hurricane flux of suspended sediments (axis 3), and height above bottom and normal flux of suspended sediments (axis 4) were the most important variables (**Table 7.14**). Nevertheless, coefficients for axes 3 and 4 were low. The four axes accounted for 34.6% of the variation in the taxa, with over 70% of that due to axes 1 and 2 (**Table 7.15**).

Table 7.14. Correlation coefficients between environmental variables and canonical correspondence analysis ordination axes. Variables are presented in order of the strength of the correlation coefficient with axis 1. The strongest correlation coefficient (absolute magnitude) for each axis is indicated in bold.

Variable	Axis Number			
	1	2	3	4
Depth	0.7134	-0.4556	-0.0250	0.2157
Slope	-0.5081	-0.3500	-0.2379	-0.0483
Small-scale substrate roughness	-0.3701	-0.0235	-0.3672	0.1818
Distance from the Mississippi River	0.2785	0.5506	0.0444	-0.0955
Hurricane flux of suspended sediments	-0.2596	-0.1728	0.4333	0.4290
Height above bottom	-0.1672	0.2485	-0.2905	-0.5487
Medium-scale substrate roughness	-0.1441	-0.4529	-0.2647	0.1793
Sediment veneer	0.1385	-0.6897	0.2792	-0.0168
Normal flux of suspended sediments	-0.0803	-0.4191	0.1304	0.5079

Table 7.15. Results of the canonical correspondence analysis using nine environmental variables.

	Axes				Total Inertia
	1	2	3	4	
Eigenvalues	0.408	0.312	0.203	0.092	2.934
Taxa-environment correlations	0.910	0.884	0.790	0.722	
Cumulative Percentage Variance					
of Taxa data	13.9	24.5	31.5	34.6	
of Taxa-environment relation	35.9	63.4	81.3	89.4	
Sum of all unconstrained eigenvalues					2.934
Sum of all canonical eigenvalues					1.136

Samples from Cruise M2, the only cruise in which all sites were sampled, suggest that Site 4 is most strongly affected by depth, and Site 1, especially the shallower parts, tends to have low thickness of sediment veneer (**Fig. 7.11a**). The deeper parts of Site 6 experience higher fluxes of suspended sediments from hurricanes, and random quadrats from deeper parts of Sites 1 and 8 are very close to the seafloor and probably also experience higher normal flux of suspended sediments (**Fig. 7.11b**). Conversely, samples from the shallower parts of Sites 1 and 5 were farther off the seafloor and experienced lower normal flux of suspended sediments (**Fig. 7.11b**).

The distribution of taxa along the ordination axes also suggest the effects of depth, sediment veneer, hurricane flux of suspended sediments, height above the bottom, and normal flux of suspended sediments (**Fig. 7.12** and **Fig. 7.13**). Superimposition onto these figures of vectors, depicting the direction of effects for each environmental variable, helps determine which taxa are most affected by which variables (**Fig. 7.14**). In these analyses, the head of a vector is indicated by the vector label, and the length of a vector generally indicates its importance in explaining variation in the taxa. The strength of the influence of a variable on a taxon can be estimated by drawing a perpendicular line from the taxon to the vector. The distance from the origin where the perpendicular line intersects the vector indicates the strength of the variable's influence on the taxon. Negative effects of a variable are inferred by extending its vector in a reciprocal direction through the origin. *Antipathes ?furcata*, *?Javania cailleti* and *Antipathes* spp. appear to increase in response to depth, whereas *?Idmidronea* appears to decrease in response to depth. *Hypnogorgia pendula*, and to a lesser extent, *?Astrocyclus caecilia* increase in response to increasing sediment veneer (**Fig. 7.14a**). Conversely, *Ulosa* sp., unidentified rhodophyta, the amorphous indistinct and orange amorphous poriferans, *Peysonnelia* spp., *Pseudoceratina crassa*, *Thesea/Scleracis* spp., the white *Thesea* sp., corallinaceae, and unidentified bryozoa decrease in response to sediment veneer. Although axis 3 did not have strong variable correlations (**Table 7.14**), vectors for normal flux and hurricane flux point in the same general direction, and unidentified *Thesea* spp. and the red *Thesea* sp. both appeared tolerant of high fluxes of suspended sediments (**Fig. 7.14b**). *Pseudoceratina crassa*, crinoidea, unidentified *Antipathes* spp., *Antipathes ?atlantica/gracilis*, and *Swiftia exserta* increased in abundance with increasing height above the bottom and decreasing flux of suspended sediments.

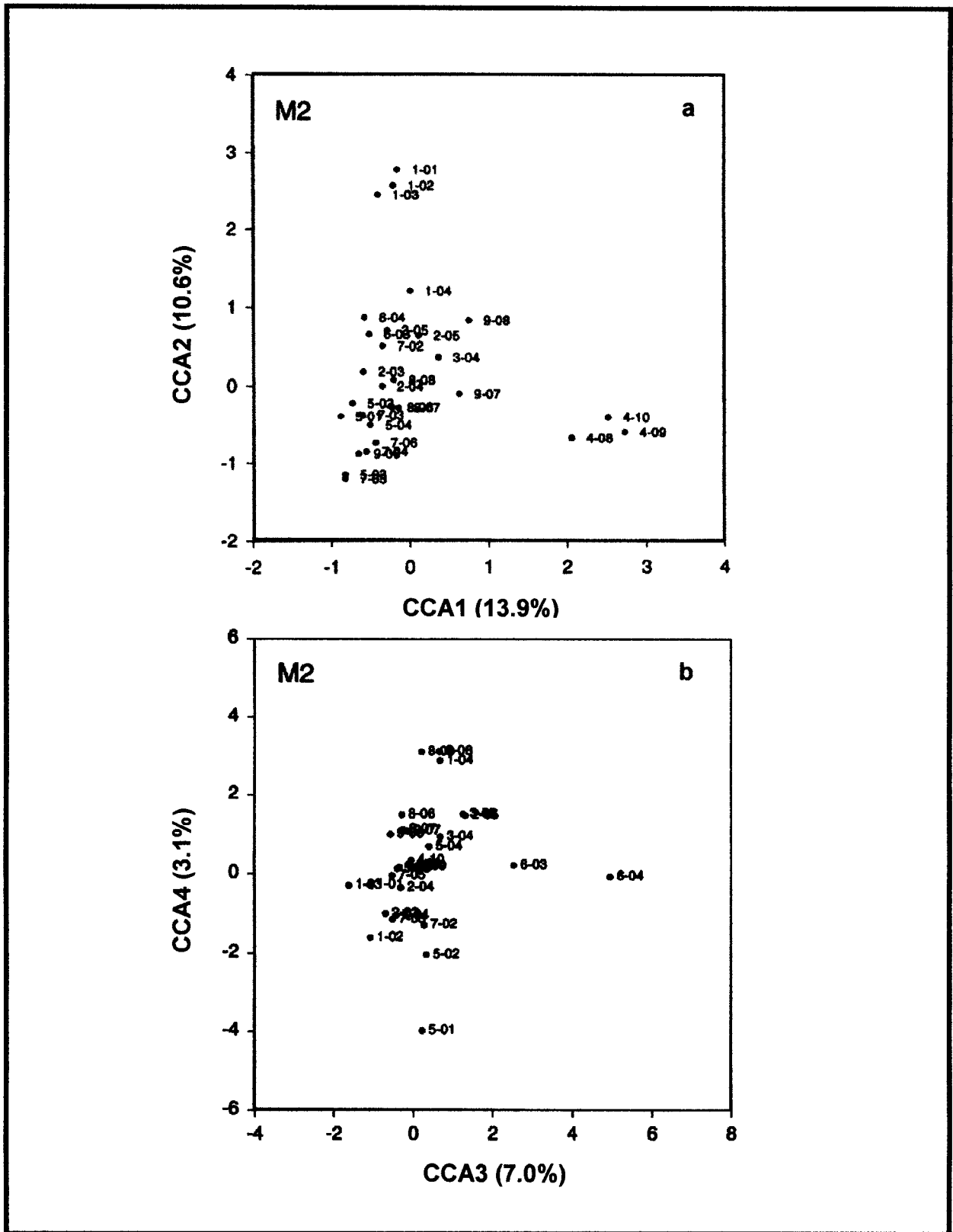


Fig. 7.11. Distribution of sites along canonical correspondence axes on Cruise M2. First number indicates site number, and numbers after the dash indicate depth interval (see Table 7.13).

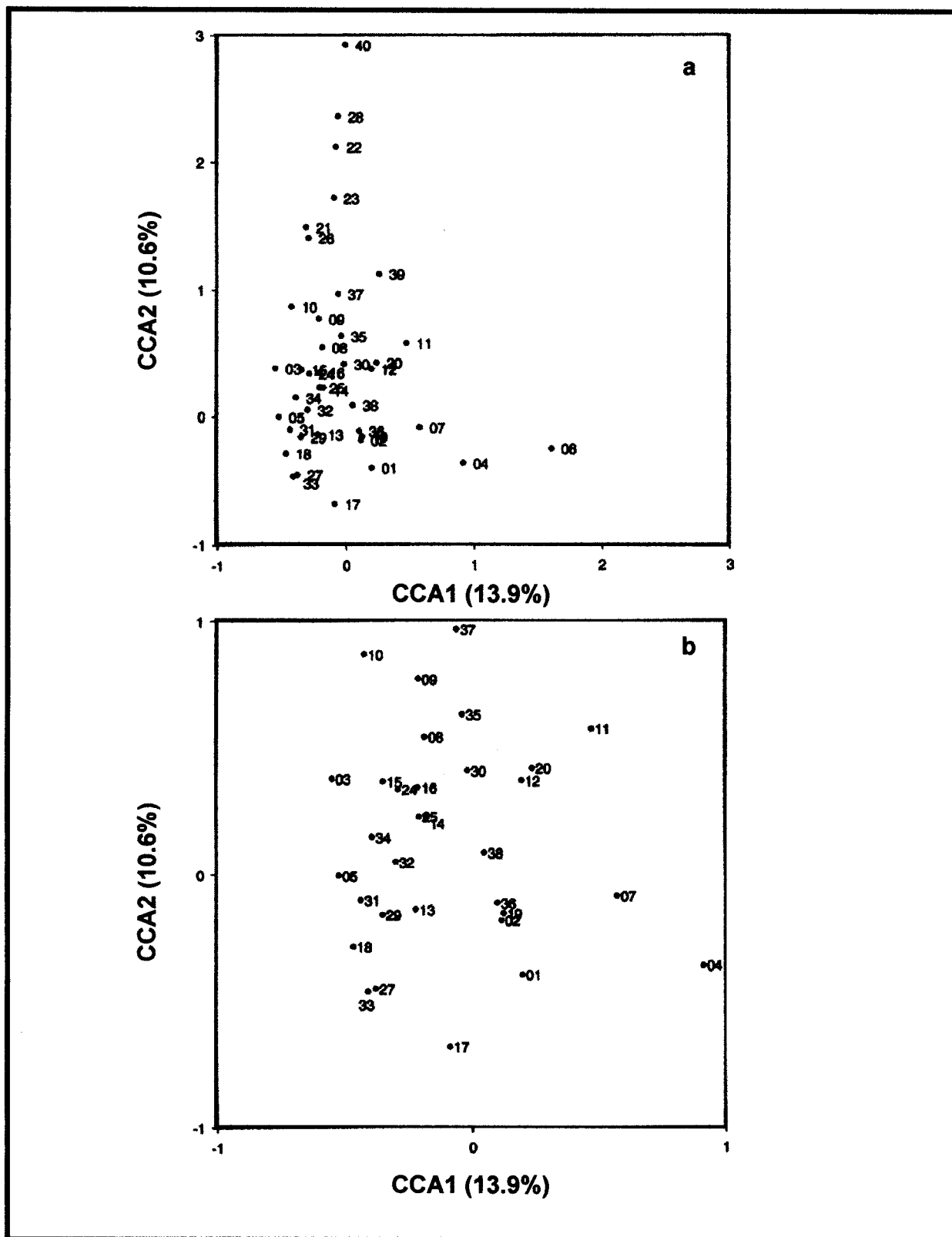


Fig. 7.12. (a) Distribution of 40 dominant hard bottom taxa along canonical correspondence axes 1 and 2 and (b) magnification of the region near the origin. Taxa numbers are as shown in Table 7.7.

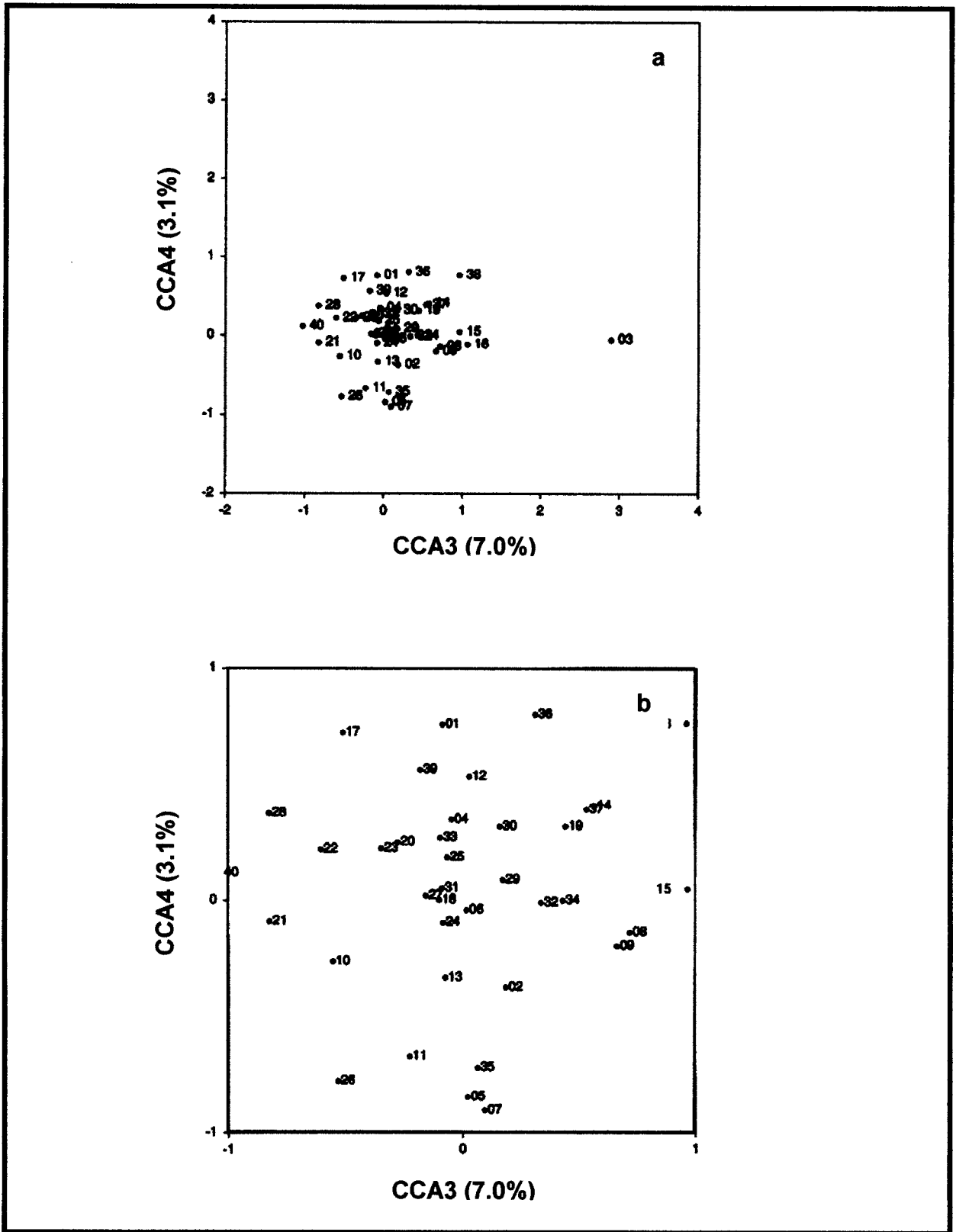


Fig. 7.13. (a) Distribution of 40 dominant hard bottom taxa along canonical correspondence axes 3 and 4 and (b) magnification of the region near the origin. Taxa numbers are as shown in Table 7.7.

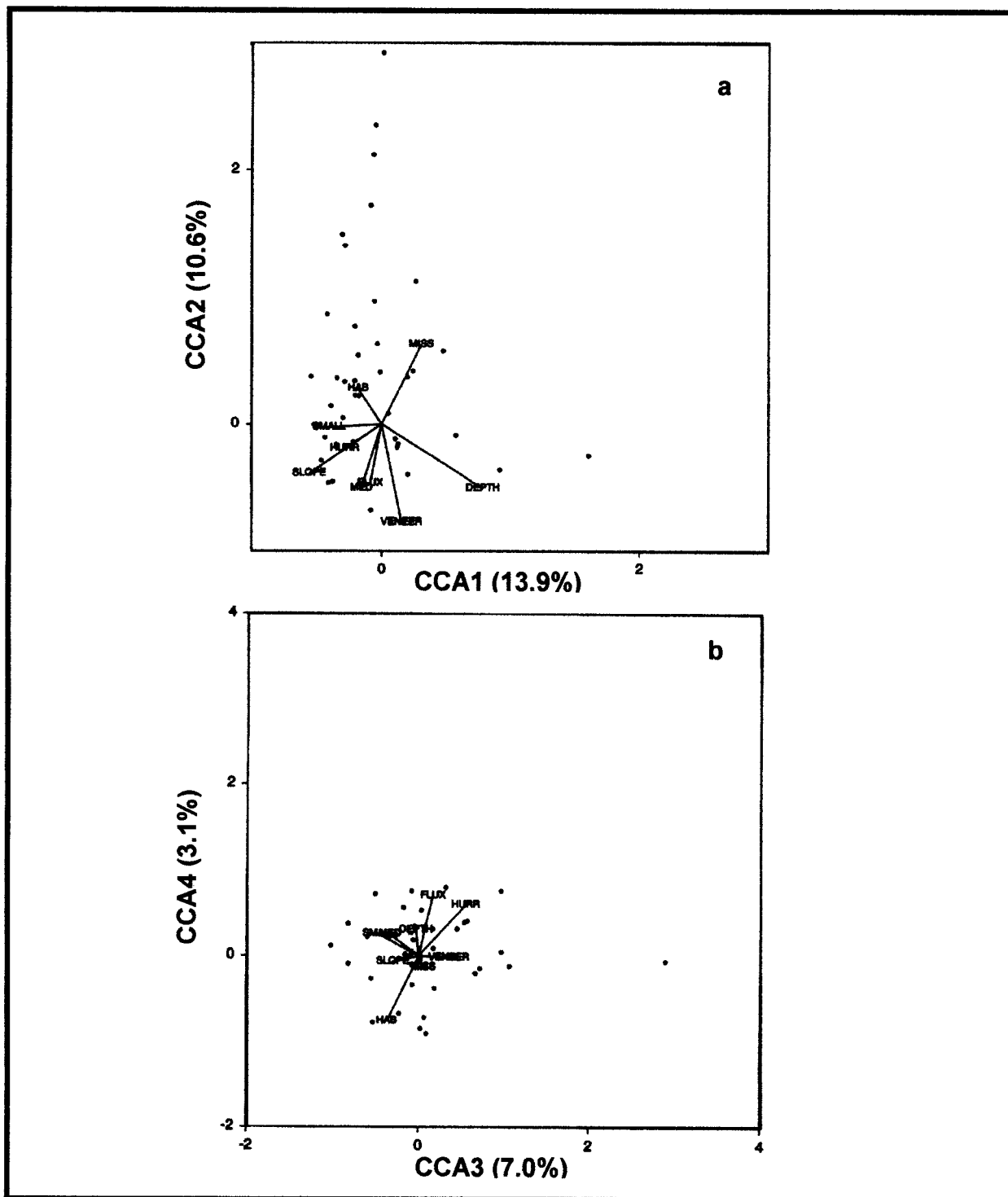


Fig. 7.14. Relationship between 40 dominant hard bottom taxa and environmental variables along four canonical correspondence analysis axes. Abbreviations: DEPTH = water depth; FLUX = normal (non-hurricane) flux of suspended sediments; HAB = height above bottom; HURR = hurricane flux of suspended sediments; MED = medium-scale substrate roughness; MISS = distance from the Mississippi River; SLOPE = substrate slope; SMALL = small-scale substrate roughness; and VENEER = sediment veneer on substrate.

Fixed Quadrats

Repetitive sampling of fixed quadrats was challenging. Variable currents and underwater visibility complicated efforts to obtain photographic and video records of fixed quadrats that could be matched well across surveys. Nevertheless, of a total possible 130 samples, a 66.7% completion rate was achieved (**Table 7.16**). One hundred percent of the samples from Sites 2, 4, and 8 were obtained.

Table 7.16. Number of observations of fixed quadrats that were repeatable from the previous cruise. The maximum number for each site on each cruise is five.

Site	Cruise			Total
	M2	M3	M4	
1	0	3	4	7
2	5	5	5	15
3	3	5	0	8
4	5	5	5	15
5	5	0	0	5
6	5	0	0	5
7	0	5	5	10
8	5	5	5	15
9	0	5	5	10
Total	28	33	29	90

Observations from the fixed quadrats reveal a very dynamic near-bottom environment. Using the complete records for Sites 2, 4, and 8 as an example, numerous instances of sediment deposition, occasional instances of erosion, organism growth, and damage or mortality were noted (**Table 7.17**). Moreover, these observations suggest that many sessile organisms become buried and may remain that way for extended periods, while other taxa thrived in an environment characterized by frequent sediment movement. While low-growing *R. manuelensis* were being buried in a fixed quadrat, taller antipatharians were growing. None of the prominent colonies of the ahermatypic coral *R. manuelensis* showed evidence of tissue loss or disease during the project period, despite their apparently chronic inundation with fine sediments. We also observed that massive spherical or amorphous sponges seemed to be capable of removing loose sediment from their surfaces.

Table 7.17. Representative observations from fixed quadrats at three sites.

Site	Quadrat	Cruise Interval		
		1C – M2	M2 – M3	M3 – M4
2	1	One antipatharian colony grew.	Large increase in fine sediment. New colony of <i>Antipathes ?atlantica/gracilis</i> observed. Encrusting sponges and coralline algae covered with sediment.	Further increase in fine sediment. Antipatharian colonies all grew substantially. <i>R. manuelensis</i> colonies and all other encrusting epibiota were covered.
	2	Increase in fine sediments. Many <i>R. manuelensis</i> colonies and most coralline algae partially or completely buried	No change in sediment cover. One antipatharian colony increased in size approximately 60%.	Further increase in fine sediment. Coralline algae totally covered. Additional growth of the antipatharian noted, but at slower rate than previous.
	3	Slight increase in fine sediment.	No changes observed.	Large increase in fine sediment. <i>R. manuelensis</i> colonies and coralline algae partially or completely buried.
	4	Slight increase in fine sediment.	No changes observed.	Large increase in fine sediment. Both antipatharians grew.
	5	Slight increase in fine sediment.	Slight decrease in fine sediment.	Large increase in fine sediment.
4	1	Increase in fine sediment.	No changes observed.	Further increase in fine sediment.
	2	No changes observed.	Increase in fine sediment.	No changes observed.
	3	No changes observed.	No changes observed.	Decrease in fine sediment.
	4	No changes observed.	No changes observed.	Decrease in fine sediment.
	5	No changes observed.	Large increase in fine sediment.	Further increase in fine sediment. Many <i>R. manuelensis</i> colonies completely buried.
8	1	Increase in fine sediment.	No changes observed.	No changes observed.
	2	Increase in fine sediment. Stenogorgiinae disappeared.	Further increase in fine sediment.	No changes observed.
	3	Increase in fine sediment.	Further increase in fine sediment.	Large decrease in fine sediment. <i>B. cinerea/grandis</i> colony found broken at basal stem.
	4	Increase in fine sediment. Stenogorgiinae disappeared.	Further increase in fine sediment.	No changes observed.
	5	Increase in fine sediment.	Further increase in fine sediment.	No changes observed.

Over all sites and all fixed quadrat observations, the observed frequency of sediment deposition exceeded that of sediment erosion (**Table 7.18**). Chi-square tests determined that observed frequencies of sediment deposition and erosion were different from expected frequencies (**Table 7.19**). Deposition exceeded erosion overall and during the period before Hurricanes Earl and Georges passed over the study area. Observations made in Cruise M4, after the hurricanes passed over the area, indicated no overall difference in the frequencies of deposition and erosion, although erosion during this period was only observed in the central and west regions (**Fig. 7.15**). While we do not know how long observed deposition remains or its cumulative effects, these results suggest that extreme events, such as hurricanes, may limit sediment deposition in these hard bottom habitats.

While frequencies of deposition and erosion differed, frequencies of damage or mortality and growth or recruitment were not very different (**Table 7.18**). Chi-square tests determined that observed frequencies of damage/mortality and growth/recruitment were similar overall, before the hurricanes and after the hurricanes (**Table 7.20**). No examples of direct competition were observed and only three observations of tissue regression were made suggesting predation. Two of these were in Cruise M4, after the hurricanes, and one was in Cruise M2. Although the two observations in Cruise M4 were made at high relief Sites 1 and 7 where higher abundances of epibenthic feeding fishes occur (Chapter 8), we cannot be sure that predation was the cause of the tissue regression.

Discussion

Analysis of a complete data set, with attendant higher statistical power, has revealed more patterns than we previously reported (Continental Shelf Associates and Texas A&M University, Geochemical and Environmental Research Group 1999). Although we previously reported very few effects of habitat relief, these earlier results were based upon ANOVAs that used site means from each cruise as replicates. The current analytical effort, employing a number of different statistical approaches and high numbers of replicates, has substantially expanded the investigation of effects of environmental variables on hard bottom communities. This effort has shown that most of the 40 most abundant hard bottom taxa varied with respect to both relief category and region and that environmental variables related to relief and region are also important.

The results from linear model tests and CCA to determine the effects of environmental variables on hard bottom communities differed slightly, although this is not surprising. For example, of the three taxa that increased in response to depth along ordination axis 1 (**Fig. 7.12a**), only *Antipathes ?furcata*, which appeared to be most strongly affected, had a significant effect of depth in the linear model (**Table 7.7**). Moreover, many more taxa had significant depth effects in the models than were suggested by CCA. The methodological differences for these two types of analyses explain the differences in results. The linear models used biological and environmental data for each random

Table 7.18. Number of observations of sediment deposition, sediment erosion, organism growth or recruitment, and organism damage or mortality in fixed quadrats.

Site	Cruise Interval															
	1C to M2				M2 to M3				M3 to M4				Total			
	Depo	Eros	Growth/ Rec	Dmg/ Mort	Depo	Eros	Growth/ Rec	Dmg/ Mort	Depo	Eros	Growth/ Rec	Dmg/ Mort	Depo	Eros	Growth/ Rec	Dmg/ Mort
1	0	0	0	0	3	0	0	0	4	0	0	0	7	0	0	0
2	4	0	1	0	1	1	2	0	5	0	3	0	10	1	6	0
3	1	0	0	1	3	0	0	2	--	--	--	--	4	0	0	3
4	1	0	0	0	2	0	0	0	2	2	0	0	5	2	0	0
5	1	0	0	0	--	--	--	--	--	--	--	--	1	0	0	0
6	1	0	0	0	--	--	--	--	--	--	--	--	1	0	0	0
7	--	--	--	--	5	0	0	1	0	1	0	1	5	1	0	2
8	5	0	0	2	4	0	0	0	0	1	0	1	9	1	0	3
9	--	--	--	--	5	0	0	1	0	3	0	1	5	3	0	2
TOTAL	13	0	1	3	23	1	2	4	11	7	3	3	47	8	6	10

Abbreviations: Dep = sediment deposition; Eros = sediment erosion; Growth/Rec = organism growth or recruitment; and Dmg/Mort = organism damage or mortality. -- indicates no data.

Table 7.19. Results of chi-square tests for differences between observed and expected frequencies of sediment deposition and sediment erosion in fixed quadrats over all times and from before and after Hurricanes Earl and Georges.

Classes	Observed	Expected	χ^2	<i>p</i>
Overall				
Deposition	47	27.5	27.6545	<0.001
Erosion	8	27.5		
Pre-hurricanes				
Deposition	36	18.5	33.1081	<0.001
Erosion	1	18.5		
Post-hurricanes				
Deposition	11	9	0.8889	>0.05
Erosion	7	9		

Table 7.20. Results of chi-square tests for differences between observed and expected frequencies of epifaunal growth or recruitment and damage or mortality in fixed quadrats over all times and from before and after Hurricanes Earl and Georges.

Classes	Observed	Expected	χ^2	<i>p</i>
Overall				
Growth/Recruitment	6	8	1.0000	>0.05
Damage/Mortality	10	8		
Pre-hurricanes				
Growth/Recruitment	3	5	1.6000	>0.05
Damage/Mortality	7	5		
Post-hurricanes				
Growth/Recruitment	3	3	0.0000	>0.05
Damage/Mortality	3	3		

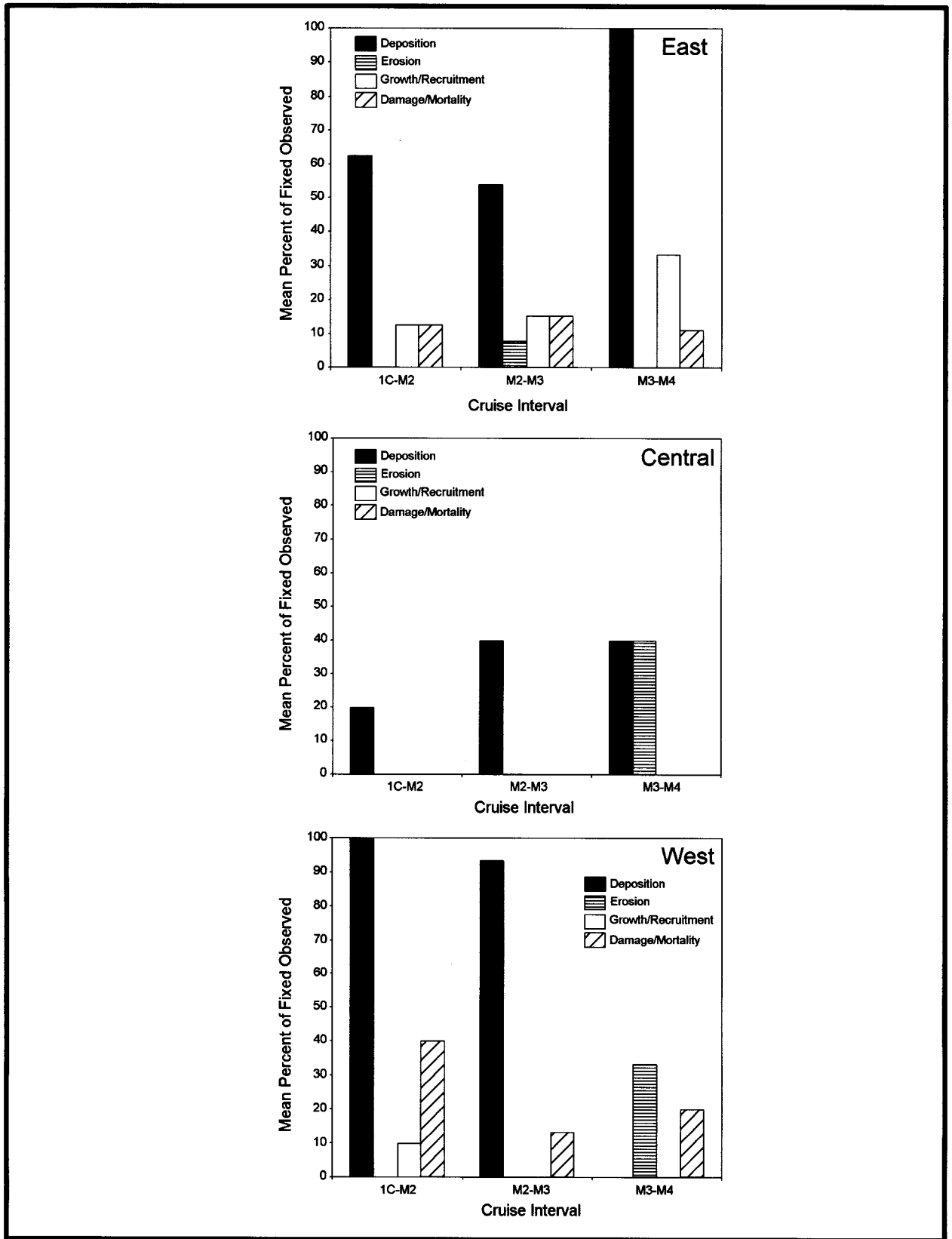


Figure 7.15. Percent of fixed quadrats observed that included sediment deposition, sediment erosion, organism growth or recruitment, and organism damage or mortality.

quadrat, achieving high statistical power through analysis of nearly 3,000 replicates. The CCA analysis compared biological and environmental data among samples comprised of means from within depth-site-cruise combinations and, thus, were based on a much smaller number of replicates. It is possible that this definition of samples with the CCA analyses will mean that some taxon-variable relationships might appear less strong than they actually are. For example, if a taxon is restricted to a very narrow range for a variable (e.g., no sediment veneer) but most site-depth-cruise samples have overall means for that variable that are substantially different from this narrow requirement, then the taxon will not appear to be strongly affected by the variable. Including every random quadrat in the CCA analyses would have solved this problem, but the resulting plots would have been impossible to read. Ordination methods that accommodate every random quadrat are not as robust as CCA in reducing the effects on results of colinearity among variables.

The generally low amount of variation accounted for by the linear models suggest that stochastic or unexamined processes contribute substantially to distribution patterns of hard bottom communities. Our observations of very patchy occurrences of dominant taxa, such as *Madrepora carolina* and *Rhizopsammia manuelensis* at Site 3, also support this suggestion. Recent exfoliation of rock features, as suggested by video observations, is one possible source of unexplained variation.

Despite slight differences in results, both the linear models and CCA analyses indicated an important effect of sediment veneer, especially for medium-high relief taxa. Others have also proposed sediment veneer as a strong controlling factor in the region (Phillips et al. 1990; Gittings et al. 1992). The effect of sediment veneer, as indicated by the number of taxa for which it was a significant linear model variable (**Table 7.9**), declined when the model test was restricted to medium-high relief sites. Similar declines also occurred in the importance of depth and medium-scale substrate roughness. We suggest the importance of depth for medium-high relief taxa across all sites results from their occurrence higher above the surrounding seafloor and its associated sediments at low relief sites. Although height above bottom was not used in the linear models because of colinearity with estimates of vertical sediment flux, all five taxa that appeared to increase with height above the bottom in the CCA (**Fig. 7.14b**) were medium-high relief taxa. Moreover, depth was a significant variable in the linear model at all sites for four of these five taxa, but only two were affected by depth in medium-high relief sites. A greater preference by medium-high relief taxa for substrate with greater medium-scale roughness at low relief sites also is consistent with avoidance of thick sediment veneer. Greater medium-scale substrate roughness likely provides microhabitats that would be relatively free of accumulated sediments, even where overall accumulations of sediment veneer are high.

CCA results indicated that 25% of the 40 dominant taxa were negatively related to the vector for sediment veneer (**Fig. 7.14a**). All but one of these taxa (i.e., the unidentified white *Thesea* sp.) preferred eastern medium-high relief habitat (**Table 7.6**) and six of the ten preferred the top interiors of medium-high relief features (**Fig. 7.4**). Site 1, the eastern high relief site, had a substantially lower mean sediment veneer than did any other site (**Table 7.3**).

Many taxa were found in higher abundances farther from the Mississippi River (**Table 7.5** and **Table 7.6**). These findings are consistent with the observations of Gittings et al. (1992), who attributed these trends to higher concentrations of suspended sediments and probability of sedimentation near the river. In the current study, higher abundances of many medium-high relief taxa in the eastern region are consistent with sensitivity to suspended sediments. Many of these taxa were located along the same general axis as the CCA vector for distance from the Mississippi River and along the reciprocal of the CCA vector for normal flux of suspended sediments (**Fig. 7.14a**). Moreover, we have documented a strong combined influence of proximity to the Mississippi River and height above the bottom on normal fluxes of suspended sediments ($r^2 = 0.872$, $p < 0.0001$).

Converse to the pattern of increasing abundances with distances from the Mississippi River, some taxa increased with proximity to the Mississippi River. Three of four ahermatypic coral taxa and total numbers of taxa were highest in the west region, although our study area did not extend into the area where Gittings et al. (1992) observed an effect (i.e., less than 70 km). Higher abundances near the river may be due to higher primary productivity associated with discharged nutrients. High chlorophyll concentrations have been documented in the Mississippi River plume (Hitchcock et al. 1997) and discharges from the river have been related to historic increases in primary production on the northern Gulf of Mexico shelf (Rabalais et al. 1996; Lohrenz et al. 1997). The area influenced by the river plume, while highly variable, can be more than 2,200 km² (Walker and Rouse 1993).

We observed highest overall abundance at high relief sites (**Table 7.5**), which was distributed primarily on the sides and tops of features (**Fig. 7.5**). These observations substantiate previous findings of high organism abundances on features elevated above the surrounding seafloor (Pequegnat 1964; Mullineaux 1989; Messing et al. 1990; Gittings et al. 1992; Hardin et al. 1994; Genin et al. 1986) (see also Chapter 9 of this report). This pattern primarily has been attributed to increased food flux associated with current acceleration (Genin et al. 1986; Hardin et al. 1994) and reduced sedimentation and flux of suspended sediments (Gittings et al. 1992; Hardin et al. 1994). Our results suggest that both are important. The orientation of sea fans perpendicular to current direction (Chapter 9) and the relationship of some taxa with predicted food fluxes associated with currents (**Fig. 7.9**, **Fig. 7.10**, **Table 7.12**) support the importance of current acceleration and food fluxes. The significant relationship of the same taxa with kinetic energy in currents and the dominant effect of sediment veneer on these hard

bottom communities support the importance of sedimentation processes. The reciprocal vectors for sediment veneer and height above the bottom (**Fig. 7.14a**) and both normal and hurricane flux of suspended sediments and height above the bottom (**Fig. 7.14b**) also support the importance of sedimentation and sediment flux. Actual measurements of food fluxes should be made to partition the variation in hard bottom communities due to these two processes.

The detrimental effects of sediment deposition and high fluxes of suspended sediments on hard bottom communities, especially corals, have been widely documented (Babcock and Davies 1991; Rice and Hunter 1992; Van Katwijk et al. 1993; Carney et al. 1999; Wesseling et al. 1999; Cox et al. 2000). The high frequency of deposition observed in fixed quadrats suggests that the normal condition of many hard bottom habitats in the current study area may be slightly depositional. Some dominant taxa appear adapted to this condition, even surviving periods of burial and there is some evidence that corals can utilize the organic carbon in sediment as a food source (Rosenfeld et al. 1999). Nevertheless, the biological stability suggested by similar frequencies of growth or recruitment and damage or mortality (see **Table 7.19**) is based on measurements made over less than two and a half years. Our results also suggest that extreme events, such as hurricanes, may reduce or reverse the depositional trends (**Table 7.18**), presumably by resuspending and advecting sediments away from hard bottom. An accurate assessment of the long-term trends in these communities and the role of sedimentation require studies over a longer period than was encompassed by this program. In particular, long-term observations of fixed quadrats would be especially enlightening.

Chapter 8: Fish Communities

David B. Snyder

Introduction

Because the biological program focused primarily on epibiota, no “dedicated” fish censusing or sampling was conducted. Nevertheless, the photographs and video collected provided images suitable to qualitatively analyze fish assemblages associated with the study sites. The use of archived videotapes to characterize deep dwelling biota has been used successfully in other situations (e.g., Felley et al. 1989; Felley and Vecchione 1995). Given the considerable cost of exploration in deep waters and given that so little is known about the fishes associated with deep reef habitats such as the study area, any contribution is valuable to our understanding of the composition and organization of these assemblages.

The use of photographic data to characterize fish assemblages is subject to the same limitations that affect visual censuses by divers in shallower waters (Kingsford and Battershill 1998). These limitations include attraction/avoidance by certain species, varying visibility of fishes in some habitats, variation in water visibility, and undersampling of cryptic species such as blennies, gobies, and eels. For community-level analyses the biggest drawback is that cryptic species are underrepresented and diversity may be greatly underestimated. Accordingly, the assemblage described here from video and still photographic images is the visually conspicuous assemblage. With these caveats in mind, the objectives of this program component were to

- describe richness and composition of the fish assemblages at each site;
- identify differences in fish species richness and assemblage composition among sites differing in relief, location, and other environmental variables;
- identify habitat association by fishes at three spatial scales; and
- identify trophic relationships among fishes, as well as between fishes and the epibenthic biota (through literature review only).

Methods

Field Methods

Because qualitative data were extracted opportunistically from video transects not specifically made for fishes, the field methods were identical to those described for hard bottom community assessment in Chapter 7. Only the aspects of these methods most important to fish assessment need to be restated. Two videocameras simultaneously recorded the path taken by the remotely operated vehicle (ROV) during its operations; one was forward-viewing for piloting the ROV, while the other was downward-viewing perpendicular to the substrate for recording quantitative benthic data. A 35-mm Benthos camera equipped with a Nikkor 28-mm lens and a 200-watt-second electronic strobe was

used to collect still photographs. The camera was aligned perpendicular to the substrate for all quantitative photographs, and aligned parallel with the downward-viewing video camera. A coordinate laser system mounted on the ROV estimated proper distance for still photographs and provided a scale for the images. Random photographs were collected within eight sectors of a single circular plot that defined each study site. The paths recorded on video by the ROV as it moved from photograph to photograph provided the best data available for characterizing the fish taxa present at each site. These paths represented random, non-overlapping transects through each of eight sectors at all sites.

Laboratory Analysis

Video and still photographic data collected during ROV operations were reviewed to generate a master fish species list. The photographs (35-mm transparencies) were viewed on a large-screen film viewer. All fishes in the quantitative photographs were identified to the lowest practical taxon and added to the species list for a particular site or sector from which the photograph was taken. Identifications were confirmed for some species by hook-and-line sampling for specimens. Each taxon in the master table was assigned a trophic category based upon Bohnsack et al. (1987).

Video data collected during the random photographic sampling were used to assess assemblage composition and richness. Videos from both videocameras were examined simultaneously for the presence of fishes. Videotapes from both of these cameras were useful because they produced complementary observations. The forward-viewing camera often recorded larger fishes such as amberjacks, snappers, groupers, or sharks that were not seen by the downward camera. On the other hand, the downward-viewing camera recorded small reef-associated species (streamer basses, damselfishes, squirrelfishes) not discernable by the forward-viewing camera. Fish species occurrences were recorded for each random path taken within a sector of a site (these paths are hereafter referred to as transects). The final data included fish frequency of occurrence (transects) by site and cruise.

Habitat use by 17 common fishes was evaluated using a procedure modified from Syms (1995). The species included were

- *Centropristis ocyurus* (bank sea bass)
- *Chaetodon aya* (bank butterflyfish)
- *C. sedentarius* (reef butterflyfish)
- *Chromis enchrysurus* (yellowtail reeffish)
- *Corniger spinosa* (spinycheek soldierfish)
- *Decodon puellaris* (red hogfish)
- *Gonioplectrus hispanus* (Spanish flag)
- *Holacanthus bermudensis* (blue angelfish)
- *Liopropoma eukrines* (wrasse bass)
- *Mycteroperca phenax* (scamp)
- *Paraques iwamotoi* (black-bar drum)
- *P. umbrosus* (cubbyu)
- *Priacanthus arenatus* (bigeye)
- *Pristigenys alta* (short bigeye)
- *Pronotogrammus martinicensis* (rougtongue bass)
- *Scorpaena* sp. A (scorpionfish)
- *Serranus phoebe* (tattler)

Habitat use by these fishes was assessed at three spatial scales: **large scale** (tens of kilometers to hundreds of meters), **meso-scale** (tens of meters to 1 m), and **small scale** (1 m to centimeters). Video transects were reviewed for the occurrence of fishes from a list of 17 common species. Once an individual was encountered on the videotape, its position in the environment was recorded at each of these three scales.

The large scale was represented by the nine study sites that were selected *a priori* to represent three relief categories (high, medium, and low) and three geographic locations (designated as eastern, central, and western).

The meso-scale was represented by habitats within sites, including entire hard bottom features as well as hard bottom/sand. Terminology similar to that used in the microhabitat study (Chapter 9) was adopted. Small mounds 1 m or less in diameter interspersed over a level sand bottom were termed sand/small mound bottom. Hard bottom features included medium size outcrops called mounds (1 to 10 m diameter) and larger features termed monoliths (tens of meters in diameter). Categories used described fish position relative to a particular feature (i.e., top, side, or base). Continuous hard bottom described the upper surface of large flat-topped monoliths such as Site 1. Continuous hard bottom consisted of low relief hard bottom with a sand veneer. The meso-scale habitat categories used in the analysis of videotapes were as follows:

- Continuous hard bottom
- Mound (top)
- Mound (side)
- Mound (base)
- Monolith (top)
- Monolith (side)
- Monolith (base)
- Sand/small mounds

Small scale habitat categories included holes of three different size classes (estimated using the paired lasers on the ROV), ledges, crevices, sediment types, and biota (soft corals, sponges, crinoids). These categories were as follows:

- Small hole (<5 cm)
- Medium hole (6 -10 cm)
- Large hole (>10 cm)
- Under ledge
- Crevice
- Bare rock
- Burrow in sediment
- Shell hash
- Medium sediment
- Fine sediment
- Massive sponge
- Finger sponge
- Crinoid
- Soft coral

For each occurrence of a target fish species in the video transects, the habitat was noted at each of the three scales. Large scale habitats were known *a priori* from the categorization of each site by relief and location. For the meso-scale and small scale habitats, videotapes collected during Cruise M2 were analyzed because the most consistent water clarity was observed across all sites during this cruise and all sites were sampled. Viewing time for the sector transects was standardized to 25 min of continuous viewing by the ROV. Segments of tape where the ROV did not move or hovered in place

for 2 min or more were not used. Only videotapes recorded during daylight hours (0800 to 1600) were reviewed. For this reason, some video segments from Cruises M3 and M4 were used for Sites 5 and 6. The sampling universe consists only of the habitats occupied by the 17 fishes included in the analysis—not all habitats present at a site (Syms 1995). Syms (1995) pointed out that for the all-occurrence sampling scheme to work, the sampling had to be unbiased with respect to the target fishes. Here, bias was minimized because sampling was randomized and the program was designed to characterize epibiota rather than fishes (i.e., the ROV pilots and on-board scientist had no bias relative to fish distribution).

Data Analysis

All fish data analyzed for this report, with the exception of the overall species list that included taxa observed in still photographs, were from videotape analyses. These data consist of presence-absence and frequency of occurrence of fish taxa by transect within the nine study sites.

Environmental variables available for each site included location category (east, west, or central); relief category (high, medium, or low); distance from Mississippi River mouth; maximum water depth (based on depth recorded at photograph locations); and vertical relief (based on standard deviation of depths recorded at photograph locations). In addition, several variables measured in other program components were brought into the analysis. These were substrate classifications, including percentages of continuous hard bottom, monolith, and mound at each site (from Chapter 9); total biotic cover (mean over all cruises, from Chapter 7); and sediment flux (mean over all deployment periods, from Chapter 5). Values of environmental variables used in the data analysis are listed in **Table 8.1**.

In addition to these variables that apply to each site as a whole, each fish occurrence has a corresponding habitat category at the large, meso-, and small scales as defined previously. These data were used for the analysis of fish-habitat associations.

Analysis of Variance

The total number of taxa recorded for each site within each cruise was used as an estimate of taxonomic richness. The hypothesis of no difference in richness among sites classified as high, medium, or low relief was tested using one-way analysis of variance (ANOVA). The hypothesis of no relationship between categorical location (east, central, and west) also was examined by one-way ANOVA. Relationships between richness and several environmental variables (water depth, distance from the Mississippi River, and relief) were estimated for each site with Pearson's product-moment correlation coefficient.

Detrended Correspondence Analysis

Patterns of co-occurrence among species and similarity of species composition among samples as well as relationships between species data and environmental variables were

Table 8.1. Environmental variables used in analyses of fish communities.

Variable	Source	Site								
		1	2	3	4	5	6	7	8	9
Location category (east, central, or west)	<i>A priori</i> category (experimental design)	East	East	East	Central	Central	Central	West	West	West
Relief category (high, medium, or low)	<i>A priori</i> category (experimental design)	High	Med	Low	Med	High	Low	High	Med	Low
Distance from Mississippi River mouth (km)	Measured map distance	146.6	143.8	146.8	124.8	107.9	108.4	70	70.9	70.3
Maximum water depth (m)	Depths recorded at photo locations (see Chapter 8)	78.2	82.3	83.2	108.7	78.1	75.7	88	97	95.5
Relief (standard deviation of photo depths)	Depths recorded at photo locations (see Chapter 8)	3.7	3	1.15	2.56	4.62	1.54	4.68	2.25	1.49
Substrate classification (% of site area)										
Continuous hard bottom	Habitat analysis of all nine sites done by M. Peccini (see Chapter 9)	72.9	0	0	0	26.7	0	18.4	0	0
Monolith	(same)	14.7	32.6	9.4	18.4	21.1	3.1	43.2	33.2	22.9
Mound	(same)	3.9	10.1	9.4	30.4	2.8	38.8	6.4	13.7	6.9
Sediment flats	(same)	8.5	57.4	81.1	51.2	49.4	58.1	32.8	53.1	70.1
Biotic cover (%)	Quantitative photographs (see Chapter 7). Mean over all cruises.	25.6	17.2	14.6	31.0	24.1	15.0	27.0	22.4	21.5
Mean sediment flux (g/m ² /day)	Sediment trap data (see Chapter 5). Mean over all periods.	3.0	6.2	7.0	6.8	6.3	12.4	11.3	17.9	21.4

analyzed by several ordination methods based upon correspondence analysis (CA). The first method applied to the data was Detrended Correspondence Analysis (DCA). DCA summarizes a species-by-samples data matrix using a weighted averaging procedure (Hill and Gauch 1980). Sample scores from DCA are reported in standard deviation (sd) units that can be used to estimate faunal turnover or beta diversity among samples (e.g., Gauch 1982; Ibarra and Stewart 1989). DCA provides an estimate of gradient length in sd units (Gauch 1982; ter Braak and Smilauer 1998). Gauch (1982) suggested that the sd units represent half changes in species composition and that a gradient length of 4 sd indicated a complete (100%) turnover in species composition. Also, axes with high sd values (≥ 4.0) indicate that species distributions along the sampled gradient tend to be unimodal rather than linear. The site scores of DCA axis 1 were used as variables in one-way ANOVAs to test the hypothesis of no difference between relief (high, medium, and low) or location (east, central, and west) categories with respect to assemblage composition.

Canonical Correspondence Analysis

While DCA is considered an indirect ordination method because the environmental significance of the resulting axes must be inferred correlatively, canonical correspondence analysis (CCA) is a direct ordination method whereby supplied environmental variables define the resulting axes in the ordination analysis. CCA is a combination of regression and ordination where the species scores are constrained as linear combinations of the environmental variables (Palmer 1993). The analysis combines a species-by-samples matrix and an environmental-by-samples matrix to produce ordinations that convey the influence of environmental variables on the species and samples data. Environmental variables used in the analysis included percentage morphology (continuous hard bottom, monolith, mound, sediment flats), percent biotic cover (estimated from quantitative photographs), sediment flux (estimated from sediment trap data), distance from the Mississippi River, relief (standard deviation of photograph depths), and water depth. In CCA, relief and location were input as continuous rather than categorical variables; relief was estimated using the standard deviation of individual quantitative photograph depths at each site and location was input as distance in kilometers from the Mississippi River mouth. These variables were subjected to a forward selection process that chose variables that contributed most to the variance explained by the analysis. Each variable was evaluated statistically by Monte Carlo permutation tests following a stepwise selection process. All Monte Carlo tests used 1,000 random permutations of the environmental data. Once a subset of meaningful environmental variables was selected, the CCA was re-run to produce ordinations of species scores and sample scores with environmental variables superimposed as arrows indicating the strength and direction of correlation with the ordination axes. DCA and CCA were performed on a taxa-by-samples data matrix consisting of species frequencies (summed across the eight transects for each site) by station-time (= site-cruise). Pelagic species such as amberjacks, sharks, and mackerels and taxa not identified below the family level were not included in the matrix. This produced a matrix of 33 samples by 48 taxa. The number of station-times was 33 (instead of 36) because Sites 5 and 6 were not sampled during Cruise M3 and Site 6 was not sampled during Cruise M4. DCA and CCA were performed with the program CANOCO 4.0 (ter Braak and Smilauer 1998).

Fish-Habitat Associations

CA was used to analyze the results of the multi-scale fish habitat utilization. Three separate data sets (contingency tables) were generated during the fish habitat analysis. Separate CAs were run for large scale, meso-scale, and small scale untransformed data sets. The scores of the first two CA axes, when plotted, depicted the relationship of habitat categories based upon the species composition and simultaneously the similarity among species based upon their patterns of habitat use.

Results

Analysis of still photographs and video transects from four cruises yielded 76 fish taxa in 33 families (**Table 8.2**). The most speciose families observed were sea basses (Serranidae), squirrelfishes (Holocentridae), morays (Muraenidae), lizardfishes (Synodontidae), jacks (Carangidae), wrasses (Labridae), and butterflyfishes (Chaetodontidae). The most frequently occurring taxa in the videotapes were *Pronotogrammus martinicensis*, *Pristigenys alta*, *Chaetodon aya*, *Hemanthias vivanus* (red barbier), *Scorpaena* sp. and *Serranus phoebe* (**Table 8.3**). Rank order of the most frequently occurring taxa at each site is shown in **Table 8.4**. Two-letter species abbreviations used in ordination diagrams are listed in **Table 8.5**.

Descriptive Statistics and ANOVAs

Taxonomic richness for each cruise and site is shown in **Fig. 8.1**. Numbers of fish taxa per cruise varied as follows:

Cruise	Minimum	Maximum	Mean
• 1C	5 (Site 9)	22 (Site 7)	15.3
• M2	13 (Site 6)	30 (Site 1)	20.7
• M3	19 (Site 8)	37 (Site 1)	28.1
• M4	9 (Site 3)	23 (Site 1)	15.2

One-way ANOVAs were conducted to evaluate whether mean numbers of fish taxa varied among sites, cruises, relief categories (high, medium, or low), or location categories (east, central, or west). There were no significant differences among cruises ($F = 0.65$, $p = 0.589$, $df = 3$) or sites ($F = 1.02$, $p = 0.4477$, $df = 8$). There also were no significant differences among relief categories ($F = 0.49$, $p = 0.6198$) or location categories ($F = 0.76$, $p = 0.4743$). The number of taxa observed during each cruise and at each site was weakly correlated with relief ($r = 0.185$), distance from the Mississippi ($r = 0.029$), water depth ($r = -0.100$), percent biotic cover ($r = -0.149$), and sediment flux ($r = -0.144$).

Table 8.2. Fish taxa observed (●) in still photographs and videotapes from each site during Cruises 1C, M2, M3, and M4. Trophic categories are from Bohnsack et al. (1987), as follows: Herbivores (H), Planktivores (P), Carnivorous Browsers (B), Microinvertivore (Mi), Macroinvertivores (Ma), and Piscivores (F).

Scientific Name	Common Name	Trophic Category	Occurrence at Sites									
			1	2	3	4	5	6	7	8	9	
SYLIORHINIDAE	CAT SHARKS											
<i>Syliorhinus retifer</i>	chain dogfish	Ma, F	--	--	--	--	--	--	--	--	--	●
CARCHARHINIDAE	REQUIEM SHARKS											
<i>Mustelus</i> sp.	dogfish	Ma, F	--	--	--	●	●	--	●	--	--	--
<i>Rhizoprionodon terraenovae</i>	Atlantic sharpnose shark	Ma, F	--	--	--	--	--	--	●	--	--	--
RAJIIDAE	SKATES											
<i>Raja</i> sp.	skate	Ma	--	--	--	--	--	--	--	--	--	●
MURAENIDAE	MORAYS											
<i>Gymnothorax kolpos</i>	blacktail moray	F	--	--	--	●	--	--	--	--	--	--
<i>Gymnothorax nigromarginatus</i>	blackedge moray	F	--	--	--	●	--	--	●	--	--	--
<i>Muraena retifera</i>	reticulate moray	F	--	●	●	--	--	--	--	--	--	--
Muraenid sp.	moray	F	--	●	--	--	--	--	--	--	--	--
SYNODONTIDAE	LIZARDFISHES											
<i>Saurida</i> sp.	lizardfish	Ma	--	●	●	--	●	--	--	--	--	●
<i>Synodus intermedius</i>	sand diver	Ma, F	--	●	●	--	--	--	--	--	--	--
<i>Synodus</i> sp.	lizardfish	Ma, F	--	--	●	--	--	●	--	--	--	--
BATRACHOIDIDAE	TOADFISHES											
<i>Opsanus pardus</i>	leopard toadfish	Ma, F	●	--	●	--	--	--	--	--	●	--
ANTENNARIIDAE	FROGFISHES											
<i>Antennarius ocellatus</i>	ocellated frogfish	F	--	--	--	--	--	--	●	--	--	--
OGCOCEPHALIDAE	BATFISHES											
<i>Ogcocephalus corniger</i>	longnose batfish	Mi	●	●	●	--	--	--	●	●	●	●
<i>Ogcocephalus</i> sp.	batfish	Mi	●	●	--	●	--	--	●	●	●	●
GADIDAE	CODS											
<i>Urophycis</i> sp.	hake	Ma	●	--	--	●	--	--	--	●	--	--

Table 8.2. (Continued).

Scientific Name	Common Name	Trophic Category	Occurrence at Sites								
			1	2	3	4	5	6	7	8	9
OPHIDIIDAE	CUSK-EELS										
<i>Brotula barbata</i>	bearded brotula	Ma, F	--	--	--	●	--	--	--	●	●
HOLOCENTRIDAE	SQUIRRELFISHES										
<i>Corniger spinosus</i>	spinycheek soldierfish	Ma, Mi	●	●	--	●	--	--	●	--	●
<i>Neoniphon marianus</i>	longjaw squirrelfish	Ma, Mi	●	--	--	--	--	--	--	--	--
<i>Holocentrus adscensionis</i>	squirrelfish	Ma, Mi	●	--	--	--	--	--	--	--	--
<i>Sargocentron bullisi</i>	deepwater squirrelfish	Ma, Mi	●	--	--	--	--	--	--	--	--
<i>Holocentrus rufus</i>	longspine squirrelfish	Ma, Mi	●	--	--	●	--	--	--	--	--
FISTULARIIDAE	CORONETFISHES										
<i>Fistularia petimba</i>	red coronetfish	F	●	--	●	--	--	--	●	--	--
SCORPAENIDAE	SCORPIONFISHES										
<i>Scorpaena</i> sp. A	scorpionfish	F	●	●	●	●	●	●	●	●	●
<i>Scorpaena</i> sp. B	scorpionfish	F	--	●	--	●	--	--	●	--	--
SERRANIDAE	SEA BASSES										
<i>Centropristis ocyurus</i>	bank sea bass	Ma, F	--	--	●	--	●	●	--	--	--
<i>Centropristis striata</i>	black sea bass	Ma, F	--	--	--	--	●	--	--	--	--
<i>Epinephelus niveatus</i>	snowy grouper	Ma, F	--	--	●	●	--	●	--	●	●
<i>Epinephelus adscensionis</i>	rock hind	Ma, F	--	--	--	--	●	--	--	--	--
<i>Gonioplectrus hispanus</i>	Spanish flag	Ma	--	●	●	●	--	--	●	●	●
<i>Hemanthias vivanus</i>	red barbier	P	●	●	●	●	●	●	●	●	●
<i>Promotogrammus martinicensis</i>	rougtongue bass	P	●	●	●	●	●	●	●	●	●
<i>Liopropoma eukrines</i>	wrasse bass	Ma, Mi	●	●	--	●	●	●	●	●	●
<i>Mycteroperca phenax</i>	scamp	F	●	●	●	●	--	●	●	●	●
<i>Mycteroperca microlepis</i>	gag	F	--	●	--	--	--	--	--	--	--
<i>Paranthias furcifer</i>	creole-fish	P	●	--	--	--	--	--	●	--	--
<i>Rypticus saponaceous</i>	greater soapfish	Ma, F	--	--	--	--	--	●	--	--	--
<i>Rypticus</i> sp.	soapfish	Ma, F	--	--	--	--	--	●	--	--	--
<i>Serranus atrobrancus</i>	blackear bass	Mi	●	●	●	●	●	--	●	●	●
<i>Serranus phoebe</i>	tattler	Ma, Mi	●	●	●	●	●	●	●	--	--

Table 8.2. (Continued).

Scientific Name	Common Name	Trophic Category	Occurrence at Sites									
			1	2	3	4	5	6	7	8	9	
PRIACANTHIDAE	BIGEYES											
<i>Priacanthus arenatus</i>	bigeye	MA, P	●	--	--	●	●	●	●	--	--	
<i>Pristigenys alta</i>	short bigeye	P	●	●	●	●	●	●	●	●	●	
APOGONIDAE	CARDINALFISHES											
<i>Apogon pseudomaculatus</i>	twospot cardinalfish	P	●	●	●	●	--	●	--	--	--	
MALACANTHIDAE	TILEFISHES											
<i>Caulolatilus</i> sp.	tilefish	Ma	--	--	--	●	--	--	--	--	--	
<i>Malacanthus plumieri</i>	sand tilefish	Ma	●	--	--	--	--	--	--	--	--	
CARANGIDAE	JACKS											
<i>Seriola dumerili</i>	greater amberjack	F	●	●	●	●	●	●	●	●	●	--
<i>Seriola rivoliana</i>	almaco jack	F	●	●	--	--	●	--	●	--	--	
<i>Trachurus lathami</i>	rough scad	P	●	--	●	●	--	--	--	--	--	
LUTJANIDAE	SNAPPERS											
<i>Lutjanus campechanus</i>	red snapper	Ma, F	--	●	●	●	●	●	●	●	●	●
<i>Rhomboplites aurorubens</i>	vermilion snapper	Ma, P	●	●	--	●	●	●	●	●	●	●
SPARIDAE	PORGIES											
<i>Calamus</i> sp.	porgy	Ma	--	●	--	--	●	--	●	--	--	
SCIAENIDAE	DRUMS											
<i>Paraques iwamotoi</i>	black-bar drum	Ma	●	●	●	●	●	●	--	●	●	
<i>Paraques umbrosus</i>	cubbyu	Ma	●	--	--	●	--	●	●	●	●	
CHAETODONTIDAE	BUTTERFLYFISHES											
<i>Chaetodon aya</i>	bank butterflyfish	B	●	●	●	●	●	●	●	●	●	●
<i>Chaetodon ocellatus</i>	spotfin butterflyfish	B	--	●	--	--	--	--	--	--	--	--
<i>Chaetodon sedentarius</i>	reef butterflyfish	B	●	●	●	--	●	--	●	--	--	
POMACANTHIDAE	ANGELFISHES											
<i>Holacanthus bermudensis</i>	blue angelfish	B	●	●	--	●	●	●	●	●	●	--
<i>Holacanthus tricolor</i>	rock beauty	B	●	--	--	--	--	--	--	--	--	--
POMACENTRIDAE	DAMSELFISHES											
<i>Chromis enchrysurus</i>	yellowtail reeffish	P	●	--	●	--	●	●	●	●	●	--

Table 8.2. (Continued).

Scientific Name	Common Name	Trophic Category	Occurrence at Sites									
			1	2	3	4	5	6	7	8	9	
LABRIDAE	WRASSES											
<i>Bodianus pulchellus</i>	spotfin hogfish	Mi	●	●	--	--	--	--	--	●	--	--
<i>Decodon puellaris</i>	red hogfish	Mi	●	--	●	●	--	--	--	●	--	●
<i>Halichoeres</i> sp.	wrasse	Mi	●	--	●	--	--	--	--	--	--	--
GOBIIDAE	GOBIES											
Gobiids	gobies	Mi	●	--	--	--	--	--	--	●	--	--
GEMPYLIDAE	SNAKE MACKERELS											
<i>Trichiurus lepturus</i>	Atlantic cutlassfish	F	●	--	●	--	--	--	--	--	--	--
SCOMBRIDAE	MACKERELS											
<i>Scomberomorus cavalla</i>	king mackerel	F	--	--	--	--	--	--	--	●	--	--
BOTHIDAE	LEFTEYE FLOUNDERS											
<i>Bothid</i> sp.	lefteye flounder	Mi, Ma	--	--	●	●	--	--	--	--	--	--
<i>Cyclopsetta</i> sp.	lefteye flounder	Mi, Ma	--	●	--	--	--	--	--	--	--	--
<i>Syacium</i> sp.	lefteye flounder	Mi, Ma	--	--	--	--	--	--	--	●	--	--
BALISTIDAE	LEATHERJACKETS											
<i>Balistes capriscus</i>	gray triggerfish	Ma	--	--	●	--	--	--	--	--	--	--
<i>Monacanthus</i> sp.	filefish	Mi	●	--	--	--	--	--	--	--	--	--
OSTRACIIDAE	TRUNKFISHES											
<i>Lactophrys polygonia</i>	honeycomb cowfish	B	●	--	--	--	--	--	--	--	--	--
<i>Lactophrys quadricornis</i>	scrawled cowfish	B	--	--	--	●	--	--	--	--	--	--
TETRAODONTIDAE	SMOOTH PUFFERS											
<i>Canthigaster rostrata</i>	sharpnose puffer	B	●	--	--	--	--	--	--	●	--	--
<i>Sphoeroides spengleri</i>	bandtail puffer	Mi, B	●	--	--	--	--	--	--	--	--	--
DIODONTIDAE	SPINY PUFFERS											
<i>Chilomycterus</i> sp.	burrfish	B	--	--	--	●	--	--	--	--	--	--
<i>Diodon holocanthus</i>	balloonfish	B	--	--	--	●	--	--	--	●	●	●
TOTAL TAXA			42	31	30	35	23	22	37	23	23	

Table 8.3. Top 20 fish taxa observed in video transects at all nine sites combined during Cruises 1C, M2, M3, and M4 ranked by frequency of occurrence.

Taxa	Cruise 1C		Cruise M2		Cruise M3		Cruise M4		Total	
	No. of Transects	% of Transects								
Total Transects Available	72	100	72	100	56	100	64	100	264	100
<i>Pronotogrammus martinicensis</i>	39	54.17	56	77.78	49	87.50	54	84.38	198	75.00
<i>Pristigenys alta</i>	36	50.00	44	61.11	52	92.86	48	75.00	180	68.18
<i>Chaetodon aya</i>	23	31.94	35	48.61	40	71.43	29	45.31	127	48.11
<i>Hemanthias vivanus</i>	17	23.61	29	40.28	39	69.64	22	34.38	107	40.53
<i>Scorpaena</i> sp.	5	6.94	34	47.22	12	21.43	17	26.56	68	25.76
<i>Serranus phoebe</i>	16	22.22	17	23.61	15	26.79	16	25.00	64	24.24
<i>Mycteroperca phenax</i>	9	12.50	16	22.22	29	51.79	8	12.50	62	23.48
<i>Holacanthus bermudensis</i>	19	26.39	10	13.89	10	17.86	9	14.06	48	18.18
<i>Liopropoma eukrines</i>	12	16.67	14	19.44	11	19.64	10	15.63	47	17.80
<i>Seriola dumerili</i>	15	20.83	8	11.11	13	23.21	8	12.50	44	16.67
<i>Chaetodon sedentarius</i>	8	11.11	10	13.89	16	28.57	10	15.63	44	16.67
<i>Chromis enchrysurus</i>	13	18.06	11	15.28	10	17.86	9	14.06	43	16.29
<i>Paraques iwamotoi</i>	12	16.67	12	16.67	10	17.86	3	4.69	37	14.02
<i>Corniger spinosus</i>	3	4.17	14	19.44	10	17.86	9	14.06	36	13.64
<i>Paraques umbrosus</i>	3	4.17	16	22.22	5	8.93	8	12.50	32	12.12
<i>Ogcocephalus corniger</i>		0.00	9	12.50	10	17.86	9	14.06	28	10.61
<i>Lutjanus campechanus</i>	17	23.61	1	1.39	9	16.07		0.00	27	10.23
<i>Rhomboplites aurorubens</i>	6	8.33	3	4.17	8	14.29	8	12.50	25	9.47
<i>Serranus atrobranchus</i>	3	4.17	7	9.72	12	21.43		0.00	22	8.33
<i>Priacanthus arenatus</i>	5	6.94	9	12.50	5	8.93	3	4.69	22	8.33

Table 8.4. Top 20 fish taxa observed in video transects during Cruises 1C, M2, M3, and M4 combined at Sites 1 through 9, ranked by frequency of occurrence.

Species	Site 1		Site 2		Site 3		Site 4		Site 5		Site 6		Site 7		Site 8		Site 9		Total	
	No. Transects	%	No. Transects	%	No. Transects	%	No. Transects	%												
Total Transects Available	32	100	32	100	32	100	32	100	24	100	16	100	32	100	32	100	32	100	264	100
<i>Pronotogrammus martinicensis</i>	26	81.25	30	93.75	21	65.62	25	78.12	18	75.00	8	33.33	32	100.00	17	53.13	21	65.63	198	75.00
<i>Pristigenys alta</i>	26	81.25	15	46.88	26	81.25	24	75.00	15	62.50	2	8.33	31	96.88	20	62.50	21	65.63	180	68.18
<i>Chaetodon aya</i>	20	62.50	13	40.63	20	62.50	9	28.12	11	45.83	5	20.83	30	93.75	10	31.25	9	28.13	127	48.11
<i>Hemanthias vivanus</i>	21	65.62	11	34.38	8	25.00	11	34.38	8	33.33	5	20.83	15	46.88	17	53.13	11	34.38	107	40.53
<i>Scorpaena sp.</i>	12	37.50	8	25.00	8	25.00	15	46.88	5	20.83	5	20.83	9	28.13	5	15.63	1	3.13	68	25.76
<i>Serranus phoebe</i>	11	34.38	12	37.50	5	15.62	5	15.62	15	62.50	4	16.67	12	37.50		0.00		0.00	64	24.24
<i>Mycteroperca phenax</i>	4	12.50	9	28.13	3	9.38	15	46.88	3	12.50	2	8.33	9	28.13	10	31.25	7	21.88	62	23.48
<i>Holacanthus bermudensis</i>	12	37.50	3	9.38		0	3	9.38	8	33.33	2	8.33	17	53.13	3	9.38		0.00	48	18.18
<i>Liopropoma eukrines</i>	4	12.50	8	25.00	2	6.25	2	6.25	5	20.83	2	8.33	12	37.50	7	21.88	5	15.63	47	17.80
<i>Seriola dumerili</i>	3	9.38	5	15.63	4	12.50	3	9.38	6	25.00	1	4.17	20	62.50	2	6.25		0.00	44	16.67
<i>Chaetodon sedentarius</i>	19	59.38	5	15.63	1	3.12		0	1	4.17		0.00	16	50.00	1	3.13	1	3.13	44	16.67
<i>Chromis enchrysurus</i>	21	65.62	1	3.13	3	9.38		0	11	45.83	2	8.33	4	12.50	1	3.13		0.00	43	16.29
<i>Paraques iwamotoi</i>	1	3.12	5	15.63	5	15.62	8	25.00	6	25.00	5	20.83	1	3.13	1	3.13	5	15.63	37	14.02
<i>Corniger spinosus</i>	7	21.88	7	21.88		0	4	12.50	1	4.17		0.00	11	34.38	3	9.38	3	9.38	36	13.64
<i>Paraques umbrosus</i>	5	15.62		0.00		0	4	12.50		0.00	7	29.17	5	15.63	8	25.00	3	9.38	32	12.12
<i>Ogcocephalus corniger</i>	7	21.88	1	3.13	2	6.25	1	3.12		0.00		0.00	3	9.38	7	21.88	7	21.88	28	10.61
<i>Lutjanus campechanus</i>		0	2	6.25	3	9.38		0	4	16.67	8	33.33	2	6.25	4	12.50	4	12.50	27	10.23
<i>Rhomboplites aurorubens</i>		0	4	12.50		0	3	9.38	6	25.00	3	12.50	5	15.63	3	9.38	1	3.13	25	9.47
<i>Serranus atrobranchus</i>	2	6.25	6	18.75	9	28.12	2	6.25	1	4.17		0.00	1	3.13		0.00	1	3.13	22	8.33
<i>Priacanthus arenatus</i>	2	6.25		0.00		0	1	3.12	6	25.00	2	8.33	11	34.38		0.00		0.00	22	8.33

Table 8.5. Species and species codes used in ordination plots.

Code	Species Name	Code	Species Name
AP	<i>Apogon pseudomaculatus</i>	LC	<i>Lutjanus campechanus</i>
BB	<i>Brotula barbata</i>	LE	<i>Liopropoma eukrines</i>
BP	<i>Bodianus pulchellus</i>	LP	<i>Lactophrys polygonia</i>
CA	<i>Chaetodon aya</i>	LQ	<i>Lactophrys quadricornis</i>
CD	<i>Chaetodon sedentarius</i>	MM	<i>Mycteroperca microlepis</i>
CE	<i>Chromis enchrysurus</i>	MP	<i>Mycteroperca phenax</i>
CO	<i>Centropristis ocyurus</i>	MR	<i>Muraena retifera</i>
CP	<i>Calamus</i> sp.	MU	<i>Malacanthus plumieri</i>
CR	<i>Canthigaster rostrata</i>	OC	<i>Ogcocephalus corniger</i>
CS	<i>Corniger spinosus</i>	OP	<i>Opsanus pardus</i>
CU	<i>Caulolatilus</i> sp.	OS	<i>Ogcocephalus</i> sp.
DH	<i>Diodon holocanthus</i>	PA	<i>Pristigenys alta</i>
DP	<i>Decodon puellaris</i>	PF	<i>Paranthias furcifer</i>
EN	<i>Epinephelus niveatus</i>	PI	<i>Paraques iwamotoi</i>
FM	<i>Flammeo marinus</i>	PM	<i>Pronotogrammus martinicensis</i>
FP	<i>Fistularia petimba</i>	PR	<i>Priacanthus arenatus</i>
GH	<i>Gonioplectrus hispanus</i>	PU	<i>Paraques umbrosus</i>
GN	<i>Gymnothorax nigromarginatus</i>	RA	<i>Rhomboplites aurorubens</i>
HA	<i>Holocentrus adscensionis</i>	SA	<i>Serranus atrobranchus</i>
HB	<i>Holacanthus bermudensis</i>	SB	<i>Sargocentron bullisi</i>
HR	<i>Holocentrus rufus</i>	SD	<i>Scorpaena dispar?</i>
HS	<i>Halichoeres</i> sp.	SP	<i>Serranus phoebe</i>
HT	<i>Holacanthus tricolor</i>	SS	<i>Scorpaena</i> sp.
HV	<i>Hemanthias vivanus</i>	US	<i>Urophycis</i> sp.

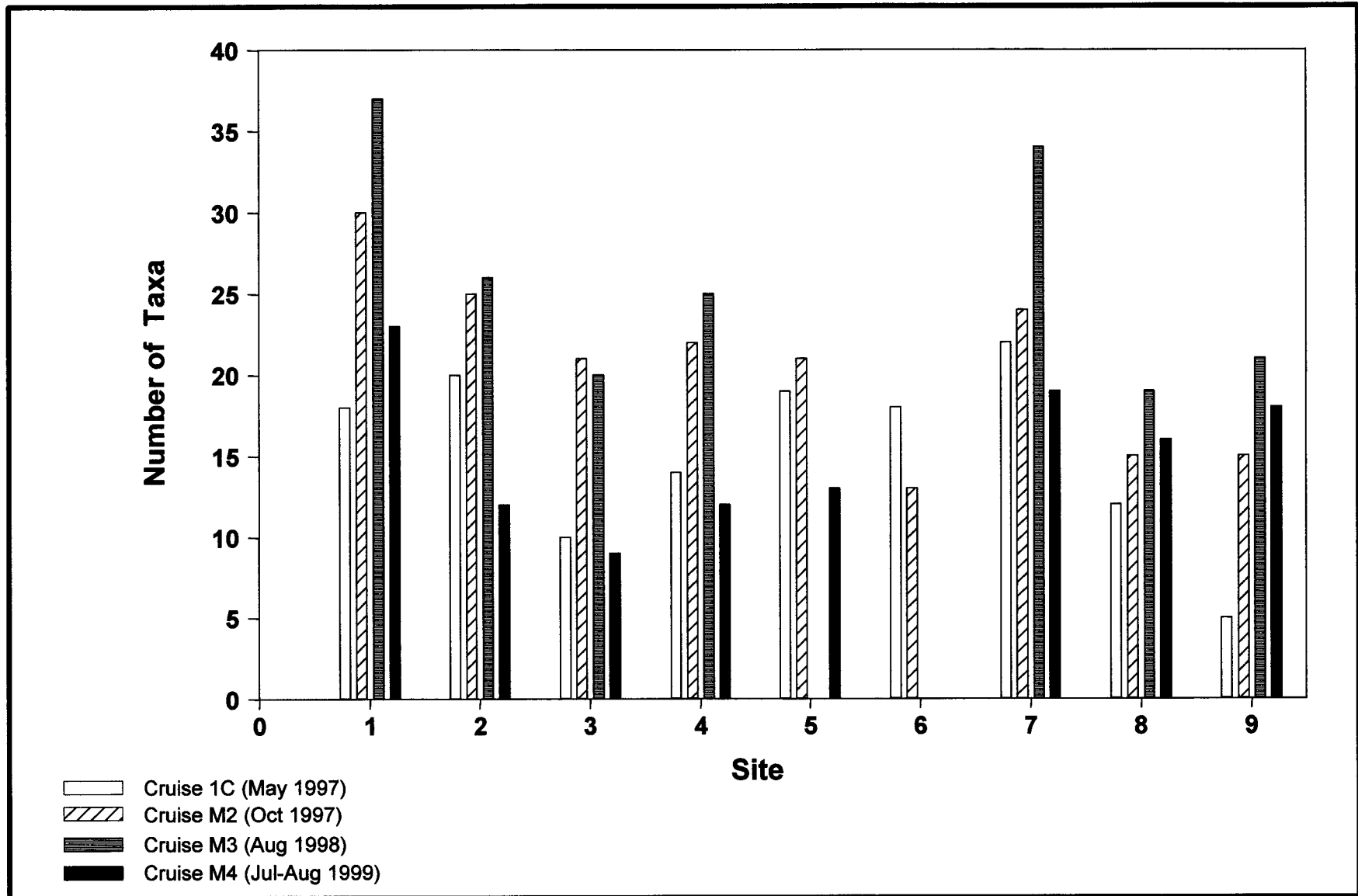


Fig. 8.1. Total fish taxa observed on video transects at Sites 1 through 9 for four monitoring cruises. Analysis of variance indicates there were no significant differences among cruises ($F = 0.65, p = 0.589, df = 3$) or sites ($F = 1.02, p = 0.4477, df = 8$).

Detrended Correspondence Analysis

The first two DCA ordination axes explained 22.1% of the variance in the sample and species data (**Fig. 8.2a** and **b**). Site 1 separated from most of the other samples along axis 1 (**Fig. 8.2a**). The length of gradient determined by DCA was 1.91 sd, indicating less than 50% turnover in species between the most dissimilar samples. The average DCA score (sd) for Site 1 was lower than all other sites and the greatest change in beta diversity was observed between Site 1 and the other eight sites. The ANOVA of axis 1 sample scores was significant for both relief ($F = 18.90, p = 0.000$) and location ($F = 4.23, p = 0.024$).

Taxa responsible for patterns observed in the site scores are shown in the ordination of taxon scores for DCA axes 1 and 2 (**Fig. 8.2b**). Taxa with low scores on DCA axis 1 were *Malacanthus plumieri* (sand tilefish), *Sargocentron bullisi* (deepwater squirrelfish), *Lactophrys polygonia* (honeycomb cowfish), *Holacanthus tricolor* (rock beauty), *Holocentrus adscensionis* (squirrelfish), and *Canthigaster rostrata* (sharpnose puffer). Those exhibiting high DCA axis 1 scores included *Epinephelus niveatus* (snowy grouper), *Brotula barbata* (bearded brotula), *Lutjanus campechanus* (red snapper), *Chilomycterus* sp. (burrfish), *Caulolatilus* sp. (tilefish), *Gonioplectrus hispanus*, and *Paraques iwamotoi*. On DCA axis 2, taxa with the highest scores were *Gymnothorax nigromarginatus* (blackedge moray), *Caulolatilus* sp., and *Scorpaena* sp. A. Taxa with low DCA axis 2 scores were *Paranthias furcifer* (creole-fish), *Fistularia petimba* (red coronetfish), *Scorpaena* sp. B, and *Mycteroperca microlepis* (gag).

Canonical Correspondence Analysis

The influence of environmental variables on fish assemblage composition in videotapes was examined by CCA. The forward selection process selected five of nine variables: percent continuous hard bottom, relief, distance, water depth, and percent monolith as contributing significantly to the variance explained by the analysis. The first four CCA axes accounted for a cumulative 34% of the variance in the species data and 94% of the variance in the species-environment relation. The first two CCA axes accounted for roughly two-thirds (20%) of the species data and 48% of the species environmental relation, respectively. Thus, from here on, the focus will be on the first two axes.

The CCA ordination plots are shown in **Fig. 8.3a** and **b** and canonical coefficients for the environmental variables and the first four CCA axes are given in **Table 8.6**. The biplot arrows in **Fig. 8.3a** depict the strength and direction of the correlation of the variables with the ordination axes. CCA axes 1 and 2 accounted for 14.6% and 8.1% of the variation in the data. The separation of samples along CCA axis 1 reflected a combination of percent continuous hard bottom, relief, and distance from the Mississippi River. Four samples from high-relief eastern Site 1 had the highest scores on CCA axis 1. A less distinctive separation of samples from Sites 4, 8, and 9 occurred along the lower portion of CCA axis 1. Water depth and percent monolith were correlated with these samples. Based upon 1,000 random permutations of the environmental data set, the eigenvalues of CCA axis 1 ($F = 4.088, p = 0.001$) and all CCA axes ($F = 2.567, p = 0.001$) combined were significantly different than expected by chance. Samples

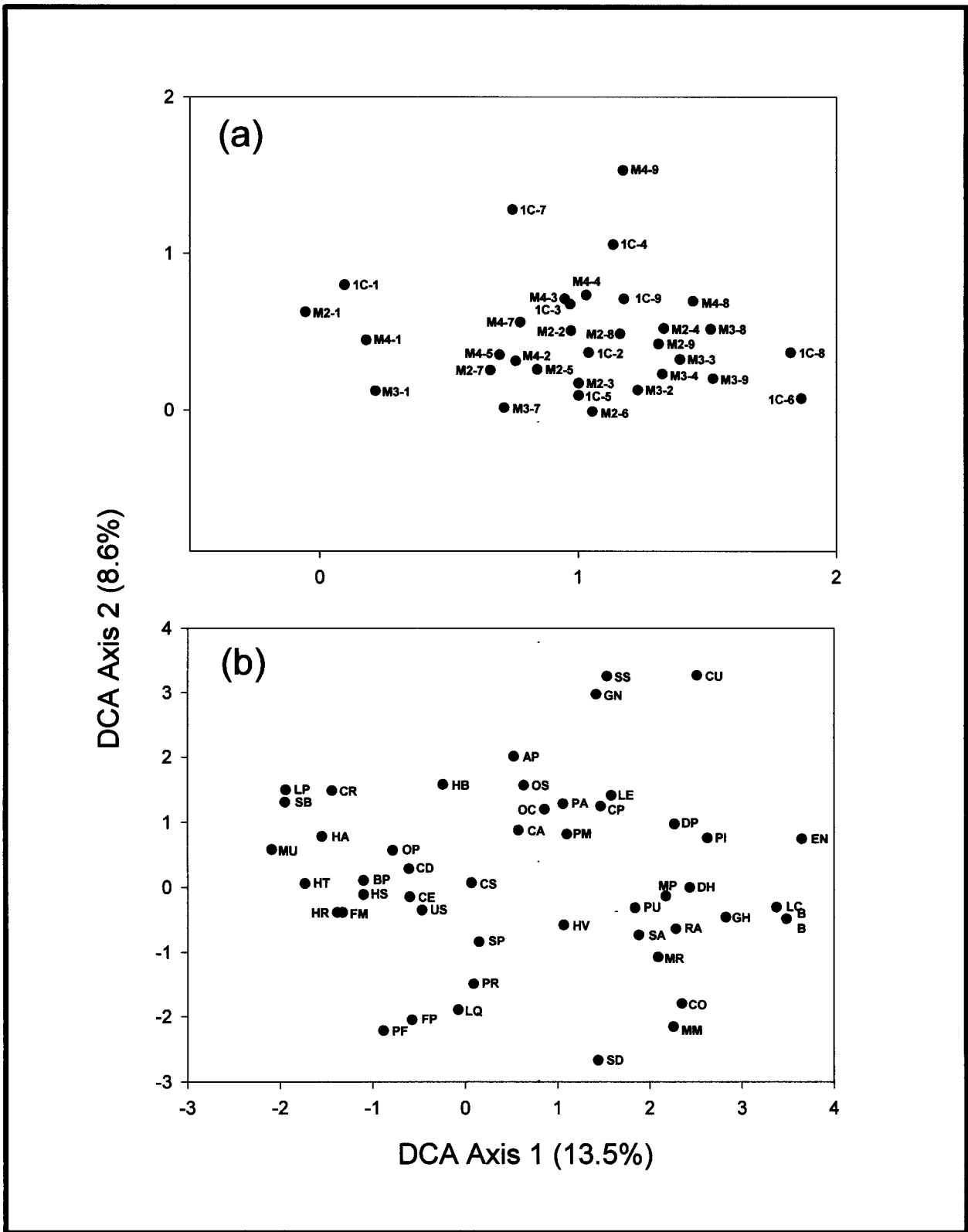


Fig. 8.2. (a) Sample scores from detrended correspondence analysis of taxa-by-samples matrix based on video transects plotted on Axes 1 and 2. Points are labeled by cruise (1C, M2, M3, M4) and site (1-9). (b) Species scores from the same analysis. Labels for species points are given in Table 8.5.

Table 8.6. Canonical coefficients and inter-set correlations for the first four axes of canonical correspondence analysis of fish assemblages and five environmental variables.

Variable	Axis 1	Axis 2	Axis 3	Axis 4
Canonical Coefficients				
Distance from Mississippi River	0.2337	-0.3172	1.2787	-0.0897
Water depth	-0.0275	-0.8024	-0.2263	-0.3281
% Continuous hard bottom	1.0245	-0.8845	-0.4821	-0.217
% Monolith	0.316	-0.9183	0.8419	0.7596
Relief (sd of photo depth)	-0.1482	0.8759	-0.2165	0.3481
Inter-set Correlations				
Distance from Mississippi River	0.4312	0.2086	0.5706	-0.4487
Water depth	-0.5592	-0.6131	-0.1955	-0.0703
% Continuous hard bottom	0.9585	0.0884	-0.1534	-0.06
% Monolith	-0.1328	-0.3513	-0.0017	0.757
Relief (sd of photo depth)	0.4795	0.3054	-0.1293	0.5131

sd = standard deviation.

representing most of the other location and relief categories clustered together near the origin of the ordination, indicating their similarity in species composition. These patterns were very similar to those resolved by DCA, except that the first axes of the two analyses were essentially reversed or “mirrored” (rank correlation between the CCA axis 1 and DCA axis 1 scores was -0.837). The reversal of the scores along the first axis is a common phenomenon with DCA but the interpretation of the axis remains the same (ter Braak and Smilauer 1998).

Fish-Habitat Associations

The total frequencies of occurrence of 17 species by large, meso-scale, and small scale habitat categories are given in **Table 8.7**. The following sections describe the CA results by scale category.

Large Scale

CA plots showed no evidence of a gradient and revealed most of the 17 species were distributed similarly at this scale. Site 5 (central, high relief) and Site 1 (eastern, high relief) separated from the other seven sites along CA axis 1 (**Fig. 8.4a**). The species ordination (**Fig. 8.4b**) showed that the primary species driving the separation of the two sites was *Chromis enchrysurus*. On CA axis 2, Site 3 (eastern, low relief) and Site 6 (central, low relief) had higher scores than the other seven sites. Species responsible for the isolation of these two sites in ordination space were *Centropristis ocyurus* and *Decodon puellaris*. The general pattern that emerges in the plot is that on CA axis 1, Site 1 (eastern) and Site 5 (central) (both high relief) and on CA axis 2, Site 3 (eastern) and 6 (central) (both low relief) separated from the remaining sites. The cluster of sites represented by east, central, and western sites as well as high, medium, and low relief sites supported most species.

Meso-Scale

Correspondence analysis of the data table formed at least three groups of meso-scale habitat categories (**Fig. 8.5a**). The tops and sides of monoliths, mounds, and continuous hard bottom (which is the top of a large monolith) clustered together with negative scores on CA axis 1. The bases of mounds or monoliths clustered together with high scores on CA axis 2. Bottom areas characterized by level sediment or sediment interspersed with small mounds exhibited very high scores on CA axis 1. Thus CA axis 1 contrasted relief: lowest (negative) scores were high relief categories, low positive scores represented lower relief portions of features (bases), and very high scores were for level bottom categories.

The tops and sides of monoliths and mounds provided habitat for *Pronotogrammus martinicensis*, *Holacanthus bermudensis*, *Liopropoma eukrines*, *Mycteroperca phenax*, and *Corniger spinosa*. *Pristigenys alta*, *Chromis enchrysurus*, and *Serranus phoebe* were most common on continuous hard bottom and tops of monoliths (which were essentially the same thing) (**Fig. 8.5b**). *Paraques iwamotoi*, *P. umbrosus*, and *Gonioplectrus*

Table 8.7. Frequency of fishes observed by habitat category for large, meso-, and small scale analyses. A large, meso-, and small scale habitat classification was assigned to each fish occurrence on a videotape transect. Large scale habitat was assigned based on the *a priori* classification of a site according to location (east, central, or west) and relief (high, medium, or low). The meso- and small scale classifications were assigned based on analysis of videotape associated with each fish occurrence.

Large Scale		Meso-Scale		Small Scale	
Category	Frequency	Category	Frequency	Category	Frequency
East (Site 1)	135	Continuous hard bottom	301	Large hole (>15 cm)	24
East (Site 2)	343	Mound top	221	Medium hole (10-15 cm)	155
East (Site 3)	65	Mound side	443	Small hole (<10 cm)	214
Central (Site 4)	416	Mound base	125	Bare rock	1,186
Central (Site 5)	184	Monolith top	153	Crevice	45
Central (Site 6)	176	Monolith side	611	Under ledge	275
West (Site 7)	282	Monolith base	79	Massive sponge	8
West (Site 8)	223	Sand/small mounds	92	Finger sponge	4
West (Site 9)	201			Soft coral	30
				Crinoid	2
				Fine sand	9
				Medium sand	20
				Shell hash	7

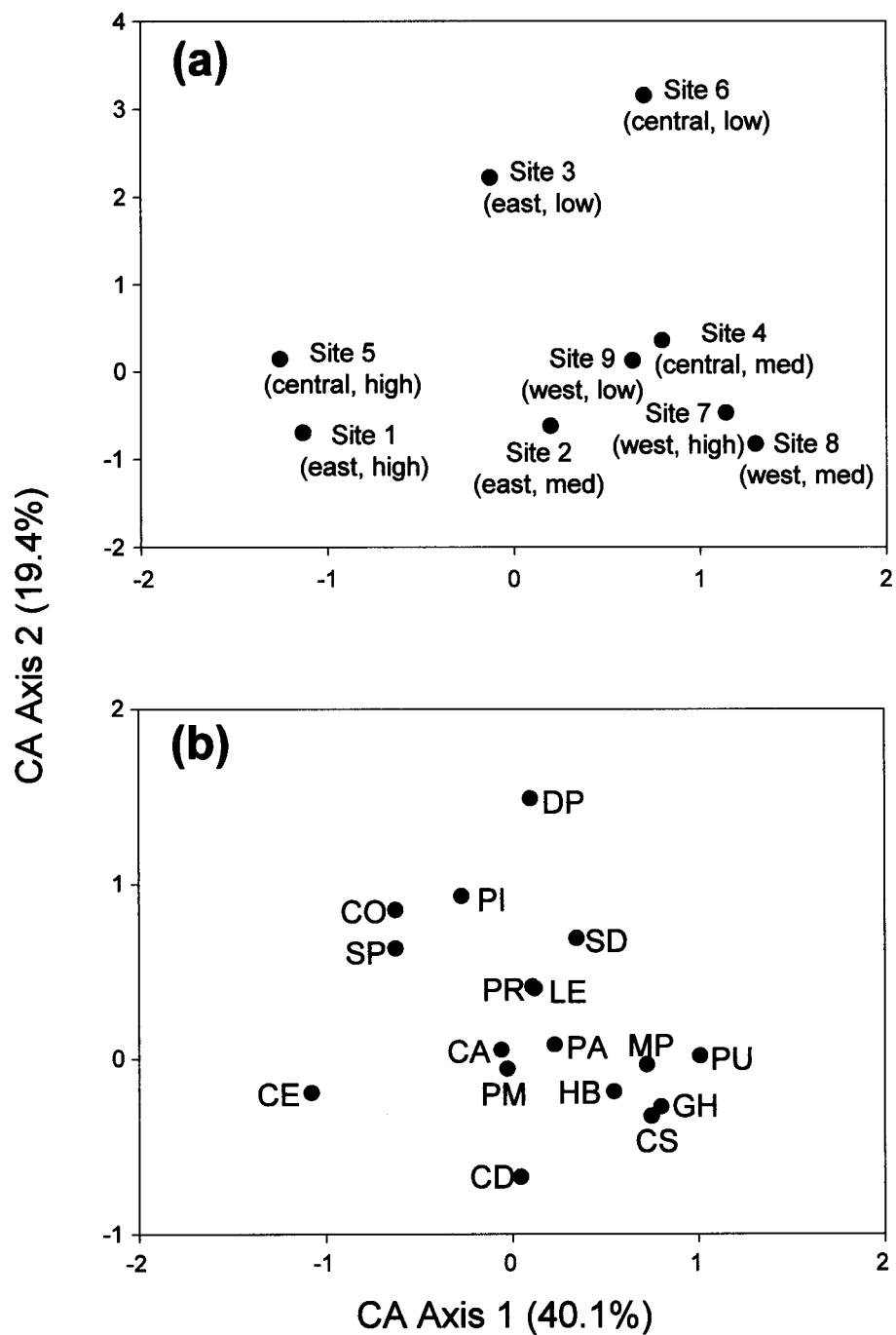


Fig. 8.4. Ordination of (a) large scale habitat classes (sites) and (b) species in large scale habitat classes by correspondence analysis. Sites are designated by location (east, central, west) and relief (high, med, low). Species codes are given in Table 8.5.

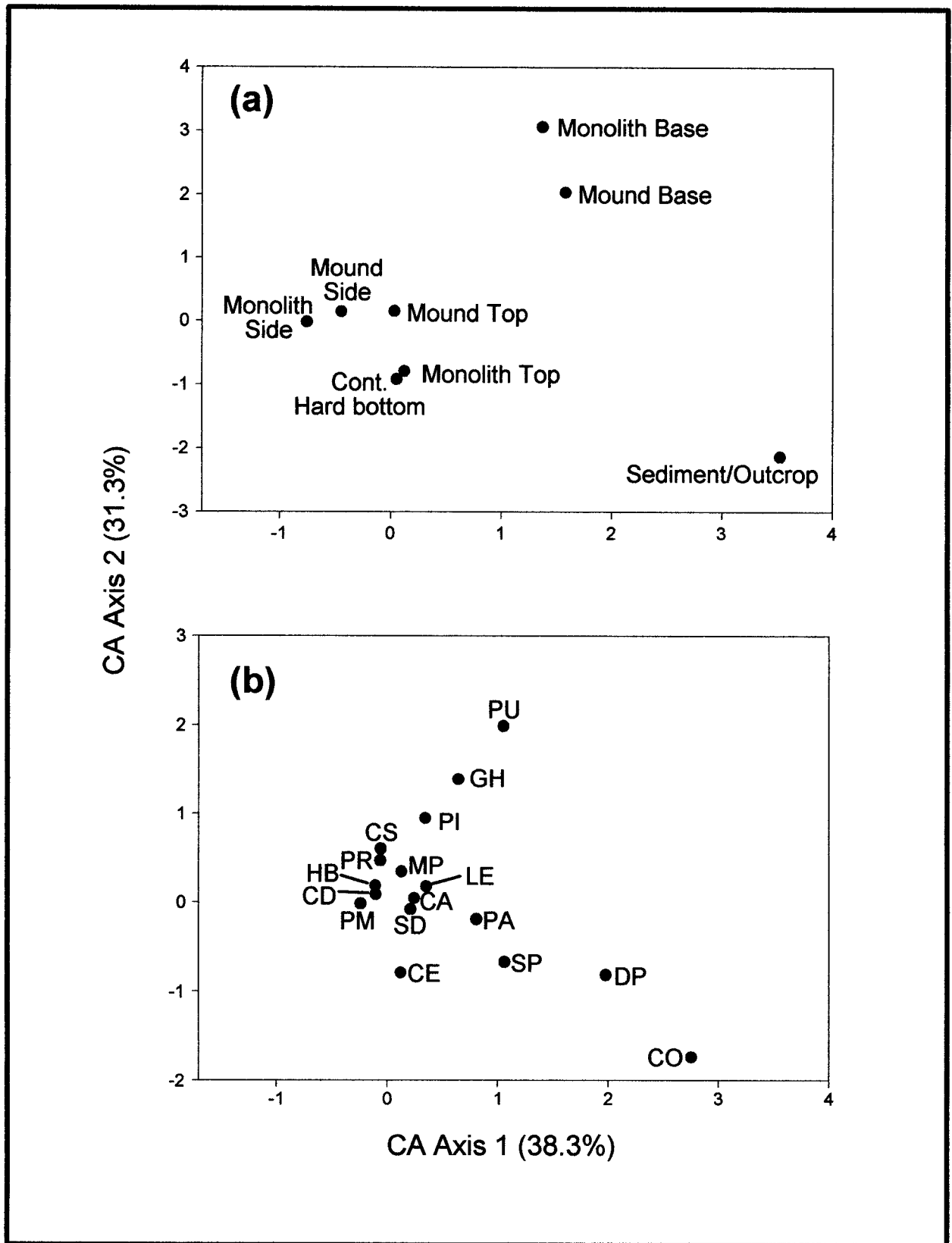


Fig. 8.5. Ordination of (a) meso-scale habitat classes and (b) species in meso-scale habitat classes by correspondence analysis. Species codes are given in Table 8.5.

hispanus used the bases of mounds and monoliths. In the low relief sedimentary habitats, *Centropristis ocyurus*, *Serranus phoebe*, and *Decodon puellaris* were most common.

Small Scale

The most obvious small scale pattern was the separation along CA axis 1 of hard bottom habitat categories from sediment texture categories (**Fig. 8.6a**). This was similar to the pattern observed at the meso-scale. Small scale categories that characterized hard bottom had low scores on CA axis 1, whereas sedimentary habitats exhibited very high scores on CA axis 1. Again, *Centropristis ocyurus* was most common over the sedimentary habitats. The hard bottom habitats were clustered along the negative portion of CA axis 1. These categories were as important as the position around the side or base. Species using the small scale hard bottom categories overlapped considerably (**Fig. 8.6b**). The most conspicuous outliers along CA axis 2 were *Pristigenys alta* and *Corniger spinosa* which exclusively used medium and large holes. Crevices, ledges, and holes were more important as habitat to this suite of fishes than were individual organisms such as corals, sponges, and crinoids.

Trophic Composition

The trophic categories assigned to taxa in **Table 8.2** are subjective and in most cases inferred from food habit studies performed in other areas (i.e., Randall 1967). Despite these limitations, a general picture of trophic composition of the fish assemblage at the study sites can be drawn. A summary of these categories shows that the fish assemblage was primarily composed of carnivores and to a lesser extent planktivores—no herbivores were observed. Although planktivores represented only about 9% of the taxa, the planktivorous taxa, including *Pronotoqrammus martinicensis*, *Hemanthias vivanus*, *Pristigenys alta*, and *Chromis enchrysurus* were among the most frequently occurring. The remaining 91% were carnivores spanning a variety of feeding types. Taxa that feed on exclusively on either macroinvertebrates or microinvertebrates or on combinations of those two categories comprised 36% of all taxa. Microinvertebrate feeders included wrasses and sea basses, whereas lizardfishes (synodontids), serranids, tilefishes (malacanthids), and drums (sciaenids) represented macroinvertebrate feeders. Those taxa categorized as feeding on combinations of micro- and macroinvertebrates include squirrelfishes and left-eye flounders (bothids). Taxa that fed on a combination of macroinvertebrates and fishes contributed 17% of all taxa. These included several serranids, requiem (carcharhinid) and cat (scyliorhinid) sharks, and the cusk-eel (ophidiid) *Brotula barbata*. Another 17% of the taxa were composed of piscivores such as moray eels (muraenids), *Fisturalia petimba*, scorpaenids, carangids, and scombrids. The benthic browser category contributed 13% of the taxa and was represented by butterflyfishes and angelfishes (pomacanthids). These phylogenetically related taxa browse on hydrozoans, sponges, and corals attached to hard surfaces.

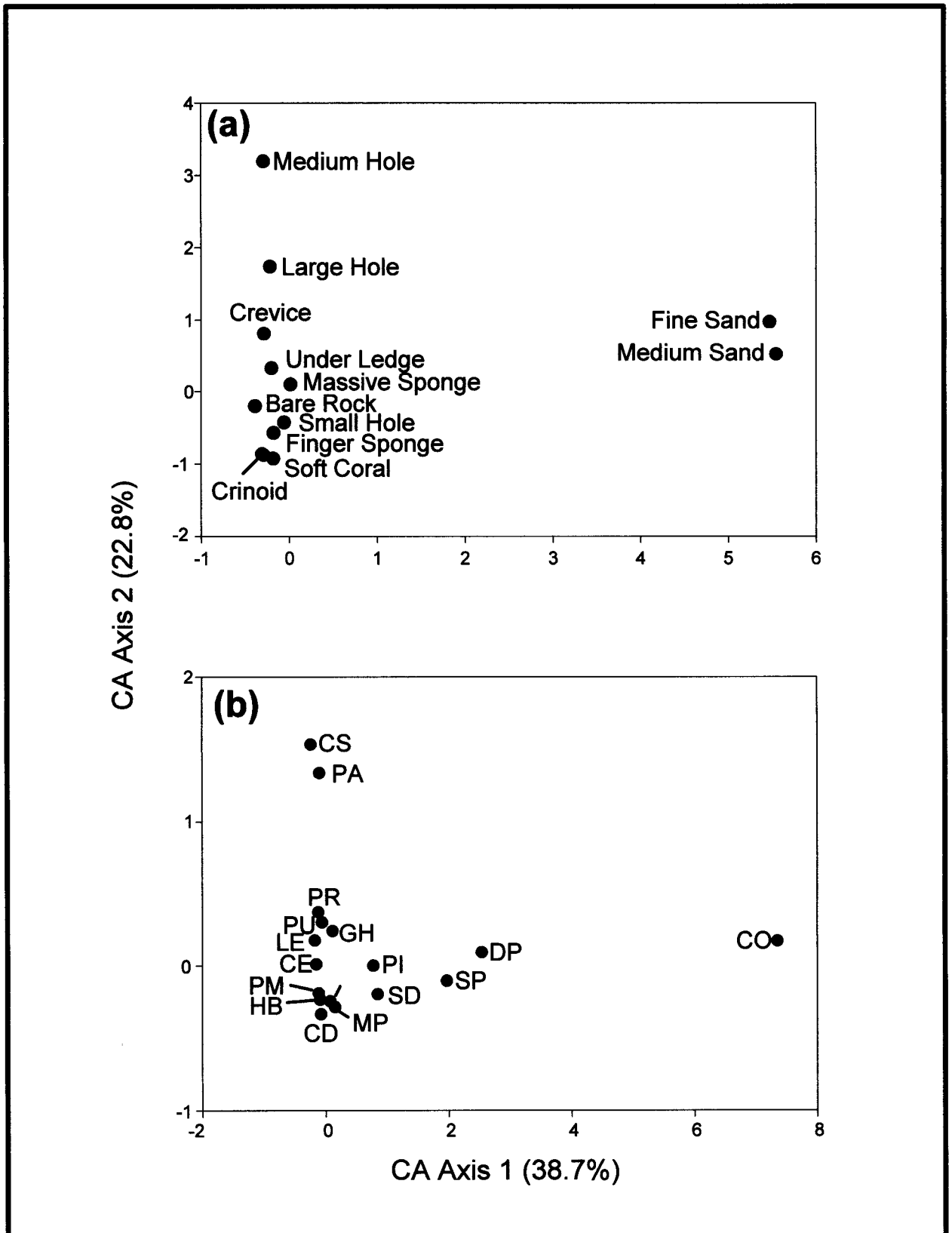


Fig. 8.6. Ordination of (a) small scale habitat classes and (b) species in small scale habitat classes by correspondence analysis. Species codes are given in Table 8.5.

Discussion

Qualitative video data collected during the four monitoring cruises showed that the ichthyofauna inhabiting the carbonate mounds consists primarily of reef fishes. Pelagic (e.g., sharks, jacks, bluefish, and king mackerel) and demersal (flounders) fishes also were observed, but infrequently when compared with reef species. The most commonly occurring reef fish species observed in video and photographs were members of the deep reef fish assemblage reported for water depths of 50 m to over 200 m in the western Atlantic (e.g., Colin 1974, 1976; Parker and Mays 1998). This assemblage is much less diverse than the reef fish assemblages reported for water depths less than 50 m, but is distinctive in its species composition and characterized by the presence of a core group of deep reef forms including *Pronotogrammus martinicensis*, *Liopropoma eukrines*, *Serranus phoebe*, *Pristigenys alta*, *Chromis enchrysurus*, *Chaetodon aya*, *Hemanthias vivanus*, and *Scorpaena* spp. Similar species were reported by previous investigations of the mounds (e.g., Continental Shelf Associates, Inc. 1985; Darnell 1991). Comparable deep reef fish assemblages have been documented off the southeastern U.S. (Miller and Richards 1980; Parker and Ross 1986; Gilmore et al. 1987), on the outer shelf banks in the northwestern Gulf of Mexico (Bright and Pequegnat 1974; Boland et al. 1983; Dennis and Bright 1988a), and near the head of De Soto Canyon (Shipp and Hopkins 1978; Continental Shelf Associates, Inc. 1987b). The total of 76 taxa represents about half of the fish fauna known from the hard banks and reefs of the northern Gulf of Mexico (Cashman 1973; Bright and Pequegnat 1974; Smith et al. 1975; Smith 1976; Sonnier et al. 1976; Boland et al. 1983; Dennis and Bright 1988a,b). The core group of deep reef species, with the possible exception of *Pronotogrammus martinicensis*, generally exhibits a continental distribution pattern *sensu* Robins (1971). The shelf edge banks of the northwestern Gulf, on the other hand, support species from both continental and insular origins (Dennis and Bright 1988a). From this perspective the Mississippi-Alabama trend assemblage may actually be more similar in species composition to the deep reef assemblage found off the southeastern U.S. than with the assemblage occurring in the northwestern Gulf of Mexico.

The fishes assembled on the nine study sites responded to some, but not all, of the environmental variables measured during this study. Two variables of primary importance to the project were distance from the Mississippi River discharge and relief. The interest in these variables was driven by the fact that a persistent nepheloid layer characterizes the outer shelf environment in the central and western Gulf and that this nepheloid layer negatively influences the distribution and abundance of fishes and attached invertebrates associated with hard banks of the same region (Dennis and Bright 1988a; Gittings et al. 1991, 1992). Hard bottom features with high relief would project above the nepheloid layer, and those that were farther from the Mississippi River (a source of fine sediments contributing to the nepheloid layer in the Eastern Gulf) should support the most diverse faunal assemblages.

Relief and distance from the Mississippi River along with several other variables were analyzed using univariate and multivariate techniques. Correlations of both distance and relief with total number of taxa (richness) were weak. However both of these variables

contributed to the explanation of overall assemblage composition in CCA. The most obvious spatial pattern observed with respect to the entire assemblage was that all four samples from Site 1 separated from all other samples in both direct and indirect ordinations. CCA indicated that relief (standard deviation of individual photograph depth), distance from the Mississippi River, and percent continuous hard bottom co-varied to explain the separation of Site 1 samples. Despite these correlations in CCA, in this case relief and distance are not likely related to the presence of a nepheloid layer; in fact, suspended sediment flux, a more direct measure of a nepheloid layer, was not even selected as an important variable by CCA. It appears that the nepheloid layer is not as persistent in this portion of the northern Gulf. Thus, the different species composition observed at Site 1 may be simply due to other factors such as water depth (Site 1 was the shallowest study site) or other unmeasured correlates of shallow water depth rather than distance from the Mississippi River mouth or relief *per se*. The area surveyed by the ROV at Site 1 was the top of a large flat-topped monolith; this area was called continuous hard bottom in the analyses. It consisted of low relief outcrops with sponges, soft corals, and coralline algae and contained large patches of medium and coarse grained sediment. This habitat was reminiscent of a hard bottom area on the shelf in water depths of 40 to 60 m, not the top of a large monolith emanating from the seafloor 20 m below. Characteristics of this habitat may be attractive to settling larvae of both shallow and deepwater fishes and may contribute to the unusual assemblage found at this site.

Ordination results also suggest that the fish assemblage of the nine study sites does not exist as an east-west gradient, but as a relatively homogenous portion of a much larger continuum. Possibly Site 1 represents an area (an ecotone) of faunal change along a larger gradient that extends from the Mississippi River to the southwest Florida shelf. To accurately elucidate the true patterns of along-shelf distribution, a much broader sampling scheme would be needed. Certainly more western sites would be required to resolve the influence of the nepheloid layer on the existing fish assemblages. The other variable of interest, relief (categorical or quantitative), was very simplistic and did not accurately capture the structural complexity of the carbonate features within the study areas. Surface topography and complexity varied on several spatial scales and undoubtedly influenced the adult and juvenile habitat use patterns in ways that were not evident in the analyses.

To some extent, the multi-scale analysis of habitat use by common species provided some insight into this problem of habitat complexity. As with the whole assemblage analyses, large scale habitat use data did not reveal a gradient across sites. Separated by tens of kilometers, the nine study sites were considered the largest spatial scale. This is the scale where one would expect distinct patterns to emerge (e.g., Syms 1995; Menge and Olson 1991). However, patterns of habitat use for most sites clustered together in the ordination diagram showing minimal separation along the first axis. Meso-scale observations showed that species regularly used various sub-divisions (tops, sides, bases) of larger features. These patterns generally reflected the feeding behavior of these species. For example, the planktivore *Pronotogrammus martinicensis* schools near the sides or tops of large- and medium-sized features, presumably to maximize encounters with zooplankton being transported by local currents over and around the features. Other species, including

the benthic invertebrate feeders *Paraques umbrosus* and *P. iwamotoi*, regularly occurred near the bases of mounds and monoliths. Most smaller species examined remained near features of all sizes for shelter from larger groupers (*Epinephelus* spp. and *Mycteroperca* spp.), amberjacks (*Seriola* spp.), and sharks that patrol the structures. A fundamental pattern observed in meso- and small scale analyses was the separation of sedimentary and hard bottom habitats. The considerable overlap in use of the small scale hard bottom habitats also was expected. Small scale habitat use by mobile and schooling species such as *Pronotogrammus martinicensis*, *Mycteroperca phenax*, and *Holacanthus bermudensis* was not as meaningful and usually scored as bare rock. More site-attached species, including *Pristigenys alta*, *Serranus phoebe*, *Liopropoma eukrines*, and *Corniger spinosa*, were accurately categorized.

Food webs in deep reef habitats such as those in the study area share fundamental similarities and differences with food webs functioning on shallower reefs. The most obvious difference between deep reefs and shallow reefs is the absence of herbivores on deep reefs. This is reflected in the absence of surgeonfishes, chubs, and parrotfishes. Currently, Doug Weaver of the U.S. Geological Survey is studying the food web architecture of the Mississippi Alabama pinnacle trend in detail (Weaver and Sulak 2000). His preliminary findings show that several feeding guilds exist on hard bottom features and the adjacent soft bottoms. The numerically dominant species such as *Pronotogrammus martinicensis*, *Pristigenys alta*, and *Chromis enchrysurus* are planktivorous, and therefore much of the fish biomass supported by hard bottom features depends upon water column production. These planktivores feed on eggs and larvae of soft bottom fishes and invertebrates thereby establishing a link with the adjacent soft bottom system. Members of the plankton feeding guild provide an important prey base for larger predators such as amberjacks (*Seriola* spp.), groupers (*Epinephelus* spp., *Mycteroperca* spp.), red snapper (*Lutjanus campechanus*), and sharks (Carcharhinidae).

Large groupers were rarely seen in the video transects of the study sites. *Epinephelus niveatus* was usually observed as sub-adults or juveniles. *Epinephelus nigritus* (Warsaw grouper), largest of the deepwater groupers, was never observed. *Mycteroperca microlepis*, a species that prefers shallower water depths, was only occasionally observed. Scamp and amberjacks (*Seriola* spp.) were the only large predators regularly observed as adults. Certainly larger individuals could have actively avoided the ROV and escaped detection. However, it is also likely that populations of groupers have suffered heavy fishing pressure from commercial and recreational fishers operating in the region. Circumstantial evidence supporting this claim comes from annual commercial landings records for National Marine Fisheries Service statistical grid number 10 (which encompasses the overall study area). Annual landings show that since the early 1970's snowy grouper, Warsaw grouper, red snapper, and amberjack catches have all declined. In addition, fishing gear, anchors, and other debris commonly observed in the video footage of the study sites indicate regular use of the area by fishers. Another trend in landings data that points to overfishing was that catches of the smaller vermilion snapper (*Rhomboplites aurorubens*) have increased during the latter part of the same time period in which catches of other species declined. Collectively these trends resemble a situation called "fishing down the food web" (Pauly et al. 1998). This phenomenon occurs in

areas where overfishing depletes more desirable species (usually top predators), forcing the fishery to target smaller, lower trophic level species in order to meet demands and generate revenue. A much more detailed analysis would be required to support this assertion for the Mississippi-Alabama region.

The data collected here provide only a snapshot of the composition and richness of the fish assemblages. So little is known about deep reef systems that even snapshots are important. It does not provide data with the sensitivity needed to predict effects of oil and gas operations on fishes. Nor does it provide the foundation needed to develop a conceptual model of the organization and structure of the fish assemblages in the study area. Such a model (which would also assist in predicting and assessing anthropogenic effects) requires accurate estimates of numbers of individuals and species replicated over space and time. In the absence of such information, a basic framework of how the deep reef fish assemblages are organized may be adopted from research conducted on shallow water patch reefs (Sale and Douglas 1984; Sale 1991; Sale et al. 1994). There are thousands of carbonate mounds dotting the outer continental shelf offshore of Mississippi-Alabama, and these features share some basic characteristics with isolated patch reefs found in shallow tropical areas. The mounds are discrete, vary in size and structural complexity, and are surrounded by level sand bottoms. On shallow patch reefs with similar attributes, the numbers of species, individuals, and species composition vary considerably over time and space. This pattern has been explained by variability in larval recruitment to the patch reefs within a region (Sale 1991). In essence, species available from the regional species pool recruit independently of each other and at varying rates. Individuals are lost from sites through death or emigration also in a way unstructured with respect to the species composition of the sites (Sale and Douglas 1984; Sale 1991). At small scales, the patterns of abundance and distribution of species would vary greatly, whereas at larger scales the assemblage composition would appear persistent. Other factors such as disturbance, predation, or competition acting at various scales could also produce similar patterns. Ultimately the structure of patch reef assemblages is determined by species-specific characteristics in life history and microhabitat preference of the colonizing species and how these attributes vary in time and across space (Sale et al. 1994).

Chapter 9: GIS and Microhabitat Studies

Ian R. MacDonald and Michael B. Peccini

Introduction

The GIS (geographic information system) and microhabitats study examined relationships between the physical environment and the composition, abundance, and health of a marine, hard bottom ecosystem. The study had two goals. The general goal was to provide uniform mapping products and geographic tools in support of the overall program. Application of ArcView GIS software made it possible flexibly to combine geographic data layers in a single map. Random photo locations and bathymetry, for example, could be overlain upon a side-scan sonar image. Maps have been produced for reporting and to assist individual project investigators with their respective investigations. The maps have included georectified mosaics and bathymetry from the side-scan sonar imagery. Mooring locations and grab samples were also plotted. The specific goal of this study is to perform a detailed analysis of physical and geological attributes at representative sites and to evaluate the influence of these attributes on abundance and distribution of selected groups of species.

GIS techniques have been used to integrate available data into consistent map formats and standardized displays. Essentially, GIS allows the construction of maps with multiple overlays, e.g., depth contours with random photo stations displayed as symbols that indicate the local geology. GIS provides one means by which further integration among the various program elements can be achieved. For this report, GIS was used to evaluate the orientation of gorgonian and antipatharian sea fans in relation to currents at five sites (1, 3, 5, 7, and 9). In addition, the GIS was used to evaluate sea fan distribution in relation to microhabitat (substrate classifications) at four sites (1, 3, 5, and 7).

The direct influence of current direction upon benthic fauna has been documented in several previous studies. Rowe and Menzies (1968) predicted the seafloor extent of the Gulf Stream on the continental slope off North Carolina based on photographs of two decapod species that tended to face into the current. Heezen and Hollister (1971) published numerous photographs in which fishes, sponges, or other deep-sea animals act as current vanes. Time-averaged effects become evident when sessile animals have a fixed and axially asymmetric growth form that enhances survival if turned into prevailing currents. Such effects have been noted in scleractinian corals such as *Agaricia agaricites*, which can display bifacial growth forms (Helmuth and Sebens 1993). Orientation is particularly distinctive among the fan-shaped gorgonians in which the colony of polyps occupies ramie arrayed from a central holdfast along a predominant vertical axis or blade (Barham and Davies 1968). Early investigators proposed that turning the plane of the fan normal to a current would minimize torsional stress to the holdfast (Wainwright and Dillon 1969; Grigg 1972). Subsequent work showed that it also maximized feeding efficiency by the colony of polyps (Leversee 1976; Velimirov 1983; Dai and Lin 1993). MacDonald et al. (in review) have recently measured precisely the distribution and orientation of almost 1,000 gorgonians in an area of approximately one square kilometer and therefore compiled a more comprehensive data set than had

been previously available. They also obtained a diverse set of physical measurements to validate and complement the biological observations. Together, these results demonstrated the influence of circulation patterns at a community level and considered the role of fine-scale topographic features in determining this effect.

Gorgonian and antipatharian sea fans were chosen as representatives of the larger community of sessile, filter-feeding organisms because their size, morphology, and species-specific coloration make them easy to identify in photographic samples. They also serve as good long term indicators of habitat suitability because they are both immobile and long-lived.

The majority of the sea fan taxa found at the study sites belong to the Subclass Octocorallia (Alcyonaria), which are distinguished from other anthozoans by the eight, characteristically pinnate, tentacles of their polyps (Barnes 1980). Within this subclass, the Order Gorgonacea, known as the horny or gorgonian corals, contains the plexaurid and ellisellid families that are common to the study area. Gorgonians are generally found in erect branching colonies with a flexible skeleton that permits bending in currents (Barnes 1980). Colonial branching often occurs within a single flat plane that tends to be orientated at right angles to the current (Wainwright and Dillon 1969; Velimirov 1983; Leversee 1976; Barnes 1980).

Because of functional and morphological similarities, several species from the Subclass Zoantharia also were included in this study. Zoanthids also grow with branching fan-like morphology, but their polyps have more than eight tentacles, which tend not to be pinnate (Barnes 1980). The two species of zoanthid fans (*Antipathes atlantica* and *A. furcata*) included in the study both belong to the Order Antipatharia, Family Antipathidae.

The importance of current flow on the zonation of sea fans has been documented in previous studies. By recording locations of gorgonian and antipatharian colonies found on an extinct deep-sea volcano, Genin et al. (1986) found that the organisms were more abundant on the peaks and exhibited increased densities at the edges of wide peaks where physical theory would predict topographically accelerated flow. In another study of the zonation of deepwater carbonate mounds, Messing et al. (1990) determined that the abundance of zoanthids was greatest along the upcurrent crests of the features, and concluded that zonation was primarily a function of the current flow regime.

The availability of hard substrate also has been shown to have a significant influence on zonation patterns of gorgonians (Gotelli 1988; Dahlgren 1989). Beyond simple availability, the effects of sediment associated with the hard bottom play an important role. In an experiment performed by Gotelli (1988), the placement of exposed and buried stones in the field revealed that sand scour reduced recruitment by 50%. Observations on the southwest Florida shelf (Phillips et al. 1990) found the thickness of the sand veneer likely played a significant role in determining where sessile epifaunal colonies could become established.

The microhabitat study incorporates classification of the relevant physical environment with biological observations. These results combine the descriptive statistics from the hard bottom community structure and dynamics effort with the microhabitat categorizations in a cross-cutting design. The microhabitat study provides a control on the within-site variability of the sessile community that can be used to determine the influence of abiotic factors.

Methods

Geographic Information System

The ArcView GIS analysis incorporated data from various cruises. **Table 9.1** summarizes the GIS data set.

The side-scan sonar mosaics included large images of the entire megasite areas as well as smaller detailed mosaics that were collected in areas of special interest, some of which were later selected as monitoring sites. All bathymetric grids were derived from the smaller mosaics and these grids were crucial for site selection. A minor problem was encountered due to slight but noticeable navigation offsets between the large and small mosaics. The cause was most likely the fact that the track-lines for the large mosaics were north-south while track-lines in the small mosaic ran east-west. This produced slight differences in the correction used for the lay-back of the side-scan sonar tow vehicle. The result was that sampling locations plotted on the uncorrected large mosaics were 20 to 35 m away from the hard bottom feature in some cases. This was corrected, where necessary, by re-registering the large mosaics to the positions of identical features present in the small mosaics.

Table 9.1. Layers of the geographic information system (GIS) database.

Available for All Sites	Available for Sites 1, 3, 5, and 7
<ul style="list-style-type: none"> ▪ Detailed side-scan imagery ▪ Megasite side-scan overview ▪ Bathymetric contours (1 m) ▪ Two-dimensional shaded bathymetric surface ▪ Three-dimensional bathymetric surface ▪ Random photo locations for first 3 monitoring cruises with hotlinks to photo CDs ▪ Approximate ROV paths between random photo points for Cruises 1C and M3 (categorized by videotape) ▪ Bottom classifications based on Cruise M2 photos and video records ▪ Layout maps of all detail and megasite side-scan views with graticule, scale bars, site boundaries, grab and mooring locations ▪ Grab and mooring locations ▪ 300 m square site boundaries ▪ Overview map with GOM coastline, megasite locations and all side-scan imagery 	<ul style="list-style-type: none"> ▪ Random photo geological characterizations for first three monitoring cruises ▪ Boundaries of morphological regions defined from videotape analysis ▪ Locations of distinctive geological features identified in video analysis ▪ Sea fan locations categorized by species and colony numbers per photograph

Measurement of Gorgonian Orientation

Colony orientations were measured opportunistically using video records of random photo dives. Adequate numbers of measured colonies were compiled at five of the nine sampling sites: Site 1 (high relief), Site 3 (low relief), Site 5 (high relief), Site 7 (high relief), and Site 9 (low relief). Whenever a colony was visible with sufficient resolution from a direct overhead perspective, the orientation of the colony's major axis was measured as it appeared on the video monitor (angles were measured between 0° and 180°). The orientation of the ROV at the time of each measurement was also determined using the on-screen compass overlay. The measured colony angle was then corrected to give an actual orientation. The angle perpendicular to the major axis of the fans was used for the analysis.

The colony numbers were summed in 10° bins and plotted as a circular histograms. Because of the symmetry in fan morphology, the distribution was taken to be diametrically bimodal and each bin from 0° to 180° was plotted with its mirror image from 180° to 360°.

Table 9.2 lists the gorgonian and antipatharian species that were examined to test for the influence of microhabitat and the consistency of orientation. All species of planar gorgonian and antipatharian colonies were included in the measurements.

Statistical Methods

Methods of circular statistics were used to compile unbiased averages for current direction and gorgonian orientation (see Batschelet 1981; Zar 1999). Tests of significance were developed from chi-square comparisons under the assumption of a bimodal distribution of current direction and colony orientation. Logistic regression was used to examine the effect of microhabitat factors upon gorgonian or antipatharian abundance at the selected sites. Tests of significance were developed from chi-square comparisons under the assumption that colony abundance followed a Poisson distribution. Tests and plots were developed with use of routines in the S-Plus software package (Mathsoft 1999).

Table 9.2. Taxonomic designations for gorgonians and antipatharians used in microhabitat investigations. Groups in bold face have planar growth forms. Orientation of these colonies was measured where practical.

<i>Bebryce cinera/grandis</i>	<i>Thesea</i> spp.
<i>Antipathes ?atlantica/gracilis</i>	<i>?Hypnogorgia pendula</i>
<i>Nicella</i> spp.	<i>Stichopathes ?lutkeni</i>
Subfamily Stenogorgiinae	<i>Ctenocella (Ellisella) spp.</i>
<i>Antipathes ?furcata</i>	<i>Swiftia exserta</i>

Current Meter Analysis

Suspect data from the Oregon Environmental, Inc. (OEI) current meters (see Chapter 6) were discarded. All other available data were used. It is important to note that data from different current meters were not necessarily taken during the same deployment periods or for the same lengths of time. Data were sorted by angle and partitioned among 36 10° bins. Individual current speed records (s_i), in units of centimeters per second, were summed within each of the 36 bins. Mean flow was calculated by dividing current speed records by the total number of current measurements taken during the deployment period (1), where s_i is the individual measurement of current speed and n is the total number of measurements. These units are used mainly to correct summed velocities for the varying deployment times between current meters. Flow values were plotted in polar coordinates.

$$\text{Mean flow} = \sum_{i=1}^n s_i / n \quad (1)$$

To calculate mean angles and angular dispersion (r), current meter data were folded (by summing fluxes of opposite angles) into a 180° distribution; the data were then treated like the fan data as a diametrically bimodal distribution. Mean angles were calculated using methods from Zar (1999). Folding and unfolding makes directional data symmetrical and permits calculation of bimodal circular statistics.

Normalized frequency distributions for the flux data were used to arrive at an “expected” frequency distribution for the fan data, testing the hypothesis that the fans and the current flux should have similar distributions.

Selection of Microhabitat and Classification of Substrata

The microhabitat study focused on four of the nine monitoring sites: Site 1 (high relief), Site 3 (low relief), Site 5 (high relief) and Site 7 (high relief). These sites were principally selected to allow comparison of the effects of relief. Additionally, the side-scan and bathymetric data available for these sites were largely free of artifacts.

For the microhabitat characterization, the Gittings et al. (1991) classifications were adapted and simplified for the specific conditions at Site 7 and used to classify each random photo. Classification of substratum was carried out by first determining the major category, i.e., whether the station contained an **outcrop** (i.e., evident rocky substratum), or was a **flat** region (generally the areas away from the base of the mounds). Subsequent classification of subcategories used a controlled vocabulary to describe specific attributes of outcrops or flats. A detailed description of the classifications and terms is given below. Examples of classified random photos are shown in **Figs. 9.1, 9.2, and 9.3** following the classification descriptions.

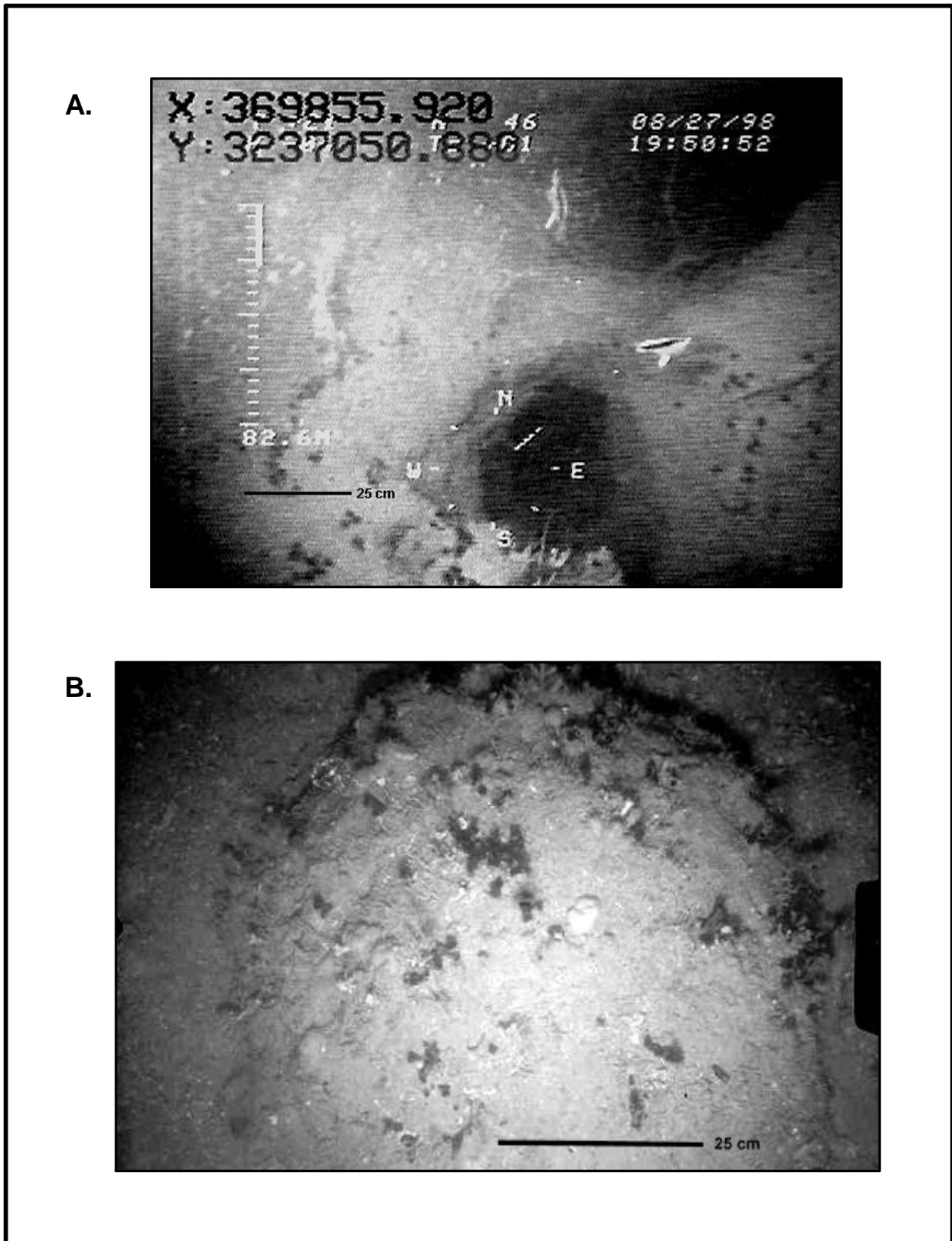
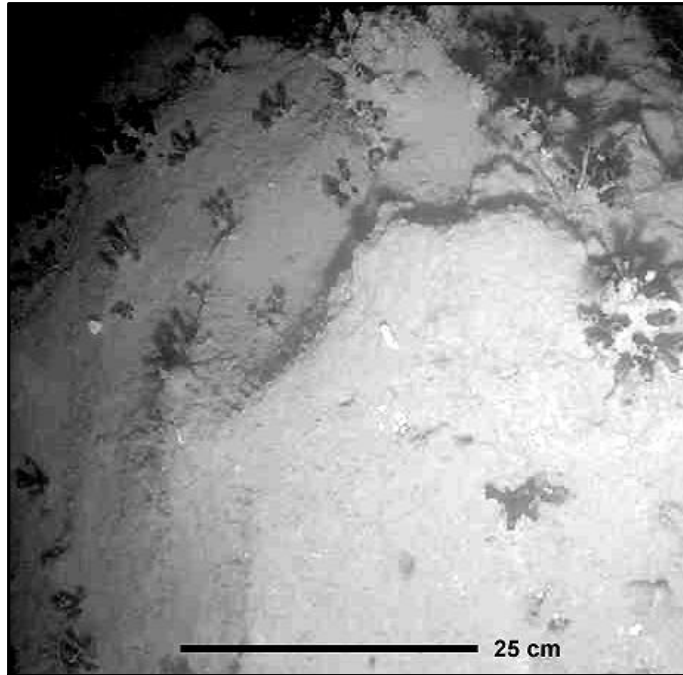


Fig. 9.1. Substrate classifications. A. Vertical outcrop, thick, silty veneer and large-scale perforation with medium surface roughness. B. Mounded outcrop, moderate silty veneer and no sand-fill.

A.



B.

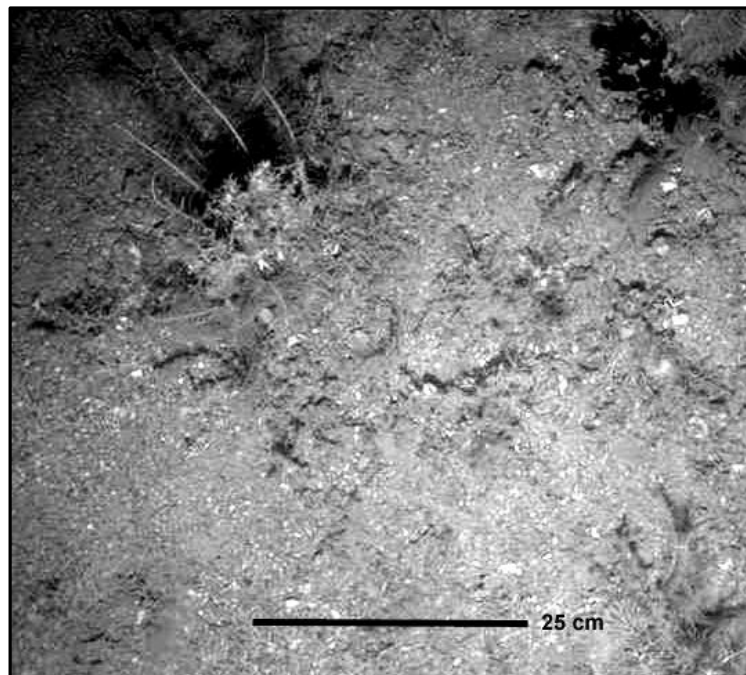
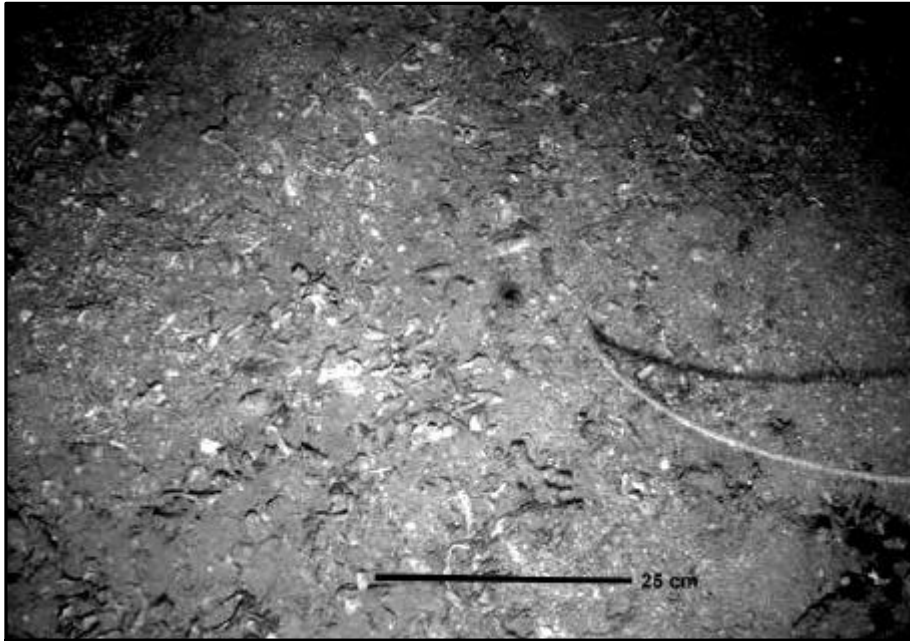


Fig. 9.2. Substrate classifications. A. Fine sediment as thick, silty veneer on outcropped surface. B. Coarse sediment as sandy fill with near-complete burial of outcropped surface.

A.



B.

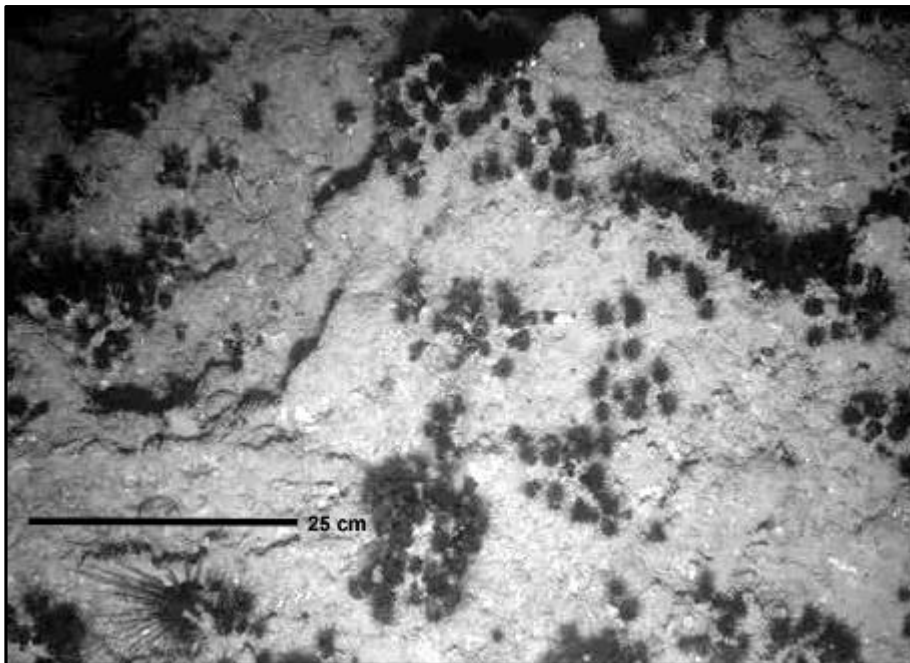


Fig. 9.3. Substrate classifications. A. Combination of fine, coarse, and rubble sediment on area of no outcropping. B. Outcropping with high surface roughness and moderate silty veneer.

Major Category: Flat

Subcategory criterion: Location on feature - Standard terms were as follows:

- Top Interior: on the upper portion of the mound, away from any edge effects
- Top Edge: on the upper portion of the mound, at the crest of a drop-off
- Side: on the slope of the mound
- Base: at the base of the mound

Subcategory criterion: Sediment Components - Standard terms were as follows:

- Fine means silty sediments
- Coarse means sand and shell-hash
- Rubble indicates small rocks and debris

Major Category: Outcrop

Subcategory criterion: Morphology - Three common morphological features are defined as follows:

- Mound - Sediment flats feature sediment accumulation in cracks, channels, or flat terraces that has completely buried any underlying structure. Within these flats are often found small “tip-of-the-iceberg” outcroppings less than a meter in extent and relief. Mounds occur frequently in the photographic sampling and are likely over-represented because of the inclination of ROV pilots to avoid areas of sediment devoid of structure or biology.
- Monolith - A monolith is a large (several meters in relief and extent) isolated feature. Monoliths often have very high relief and even sheer faces. They are distinguished as “isolated” because of their separation from other features by deep channels or wide cracks. The size of these features often makes it difficult to determine their overall extent so it is possible that they may occur as part of an elongated ridge, however in at least one direction their peaks become valleys within a distance of several meters.
- Continuous hard bottom - The central area of Sites 1 and 7 consists of a large expanse (tens of meters) of relatively consolidated, flat or consistently sloping outcrop. When the ROV is on a feature where no dramatic changes in relief or depth occur within a large area, the feature is defined as an area of continuous hard bottom. Cracks or narrow channels are frequently visible, however they lack the width and depth that distinguishes monoliths as separate features. The size of the feature (i.e., continuous hard bottom vs. monolith) is often not immediately evident so definitions are sometimes applied only after the ROV has continued some distance beyond the site.

Subcategory criterion: Height Above Bottom - Where a site was on a feature that rose out of an area of unconsolidated sediment, the height above this sediment surface was estimated whenever possible.

Subcategory criterion: Sediment Cover - Silt veneer conformed with uniform thickness to the surface morphology of the outcrop.

Subcategory criterion: Roughness small-scale. This describes the surface texture of the outcrop features visible in the photographs at a centimeter scale. It is classified as low, medium, or high, where the latter indicates narrow irregular pits and tunnels deep enough for small fishes to use as shelter.

Subcategory criterion: Roughness medium-scale. This was characterized by dramatic indentations and tunnels that gave structures a very irregular “swiss cheese” appearance on a scale visible from a wider angle perspective than that of the random photographs. Also subjectively classified as small, medium, or large.

Results and Discussion

Orientation of Gorgonian Colonies and Predominant Water Transport

Orientations of gorgonian colonies were measured opportunistically at five of the nine study sites, i.e., Sites 1, 3, 5, 7, and 9 (Table 9.3). These sites were chosen for detailed study because of the quality of available data and because they represented the nominal and actual range of site morphology from “high relief” (Sites 1, 5, and 7) to “low relief” (Sites 3 and 9). Fig. 9.4 recapitulates the regional morphology of the sites and shows the relative locations of current meter moorings. Factors that limited the measurements were water clarity, altitude and attitude of the ROV as it transited over colonies sites, and availability of usable heading data in the video records. Despite these limitations, graphic depictions of the location and orientation data (Figs. 9.5 to 9.9) show that the exercise achieved a fairly uniform distribution of measurements across the circular site boundaries.

Table 9.3. Circular statistics for gorgonian orientations at selected study sites. Results from individual sites are shown in Figs. 9.5 to 9.9. N indicates the number of gorgonian colonies for which orientation was measured. Mean vector is given in folded compass degrees in the range 0° to 180°, where, for example, the clockwise range 0° to 90° folded degrees is the equivalent of 0° to 90° T and 180° to 270° T. Vector length can range from 0 to 1 and is a measure of the spread of the data where zero would indicate that each value was different and one would indicate that all values were the same. The p-values for the Rayleigh test indicate the probability that a given distribution could arise by chance. Confidence interval gives the range about the means for two standard intervals and extends over the full range of 0° to 359° T.

Site	N	Mean Vector (μ)	Vector Length (r)	SE of Mean (deg.)	Rayleigh Test (p)	Confidence interval			
						95%		99%	
						Min	Max	Min	Max
1	120	41°	0.54	6.3°	<0.01	28.5°	53.3°	24.6°	57.2°
3	66	179°	0.63	6.9°	<0.01	165.6°	192.6°	161.4°	196.8°
5	60	83°	0.50	9.7°	<0.01	63.6°	101.6°	57.7°	107.5°
7	57	88°	0.39	13.1°	<0.01	62.7°	114.1°	54.6°	122.2°
9	65	42°	0.53	8.8°	<0.01	24.7°	59.3°	19.2°	64.8°

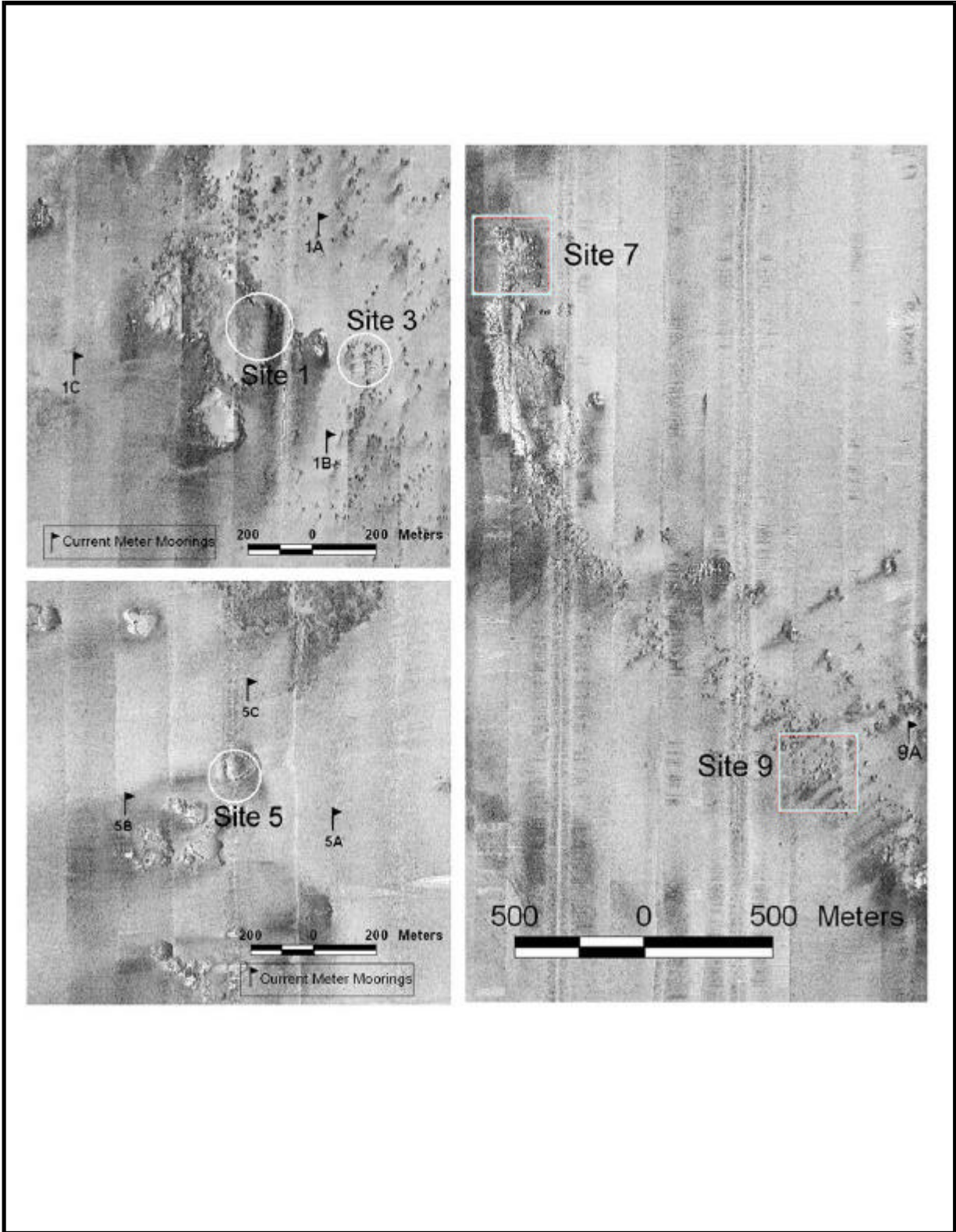


Fig. 9.4. Overview of study sites discussed in this chapter.

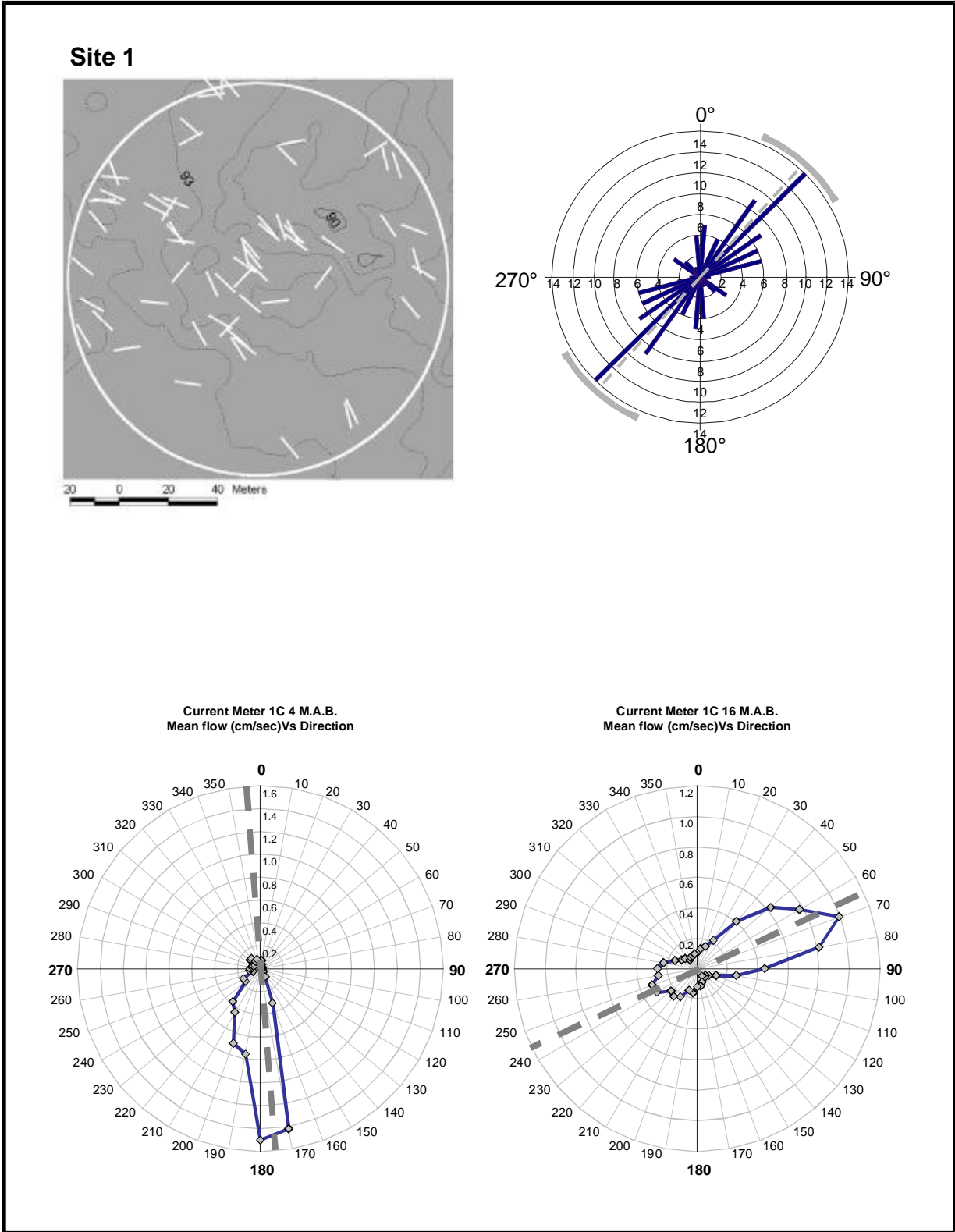
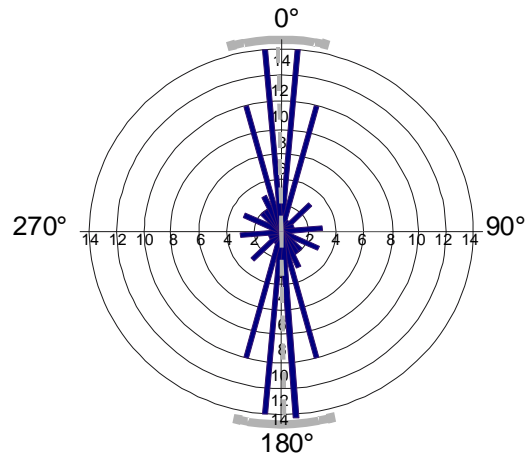
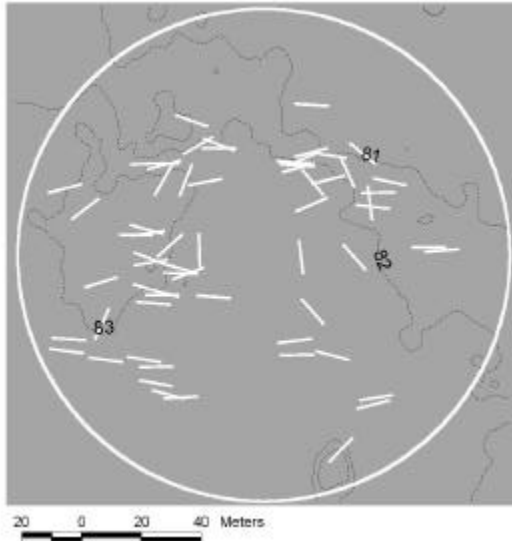
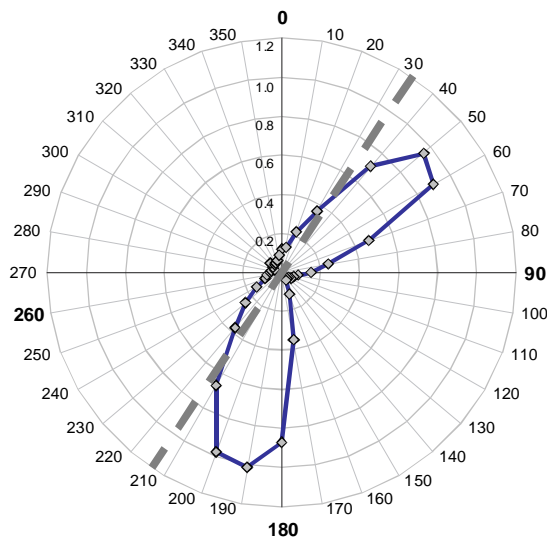


Fig. 9.5. Gorgonian orientations and mean directional water flow at Site 1. Clockwise from upper left, the panels show the locations and orientations of sea fan colonies and site bathymetry (contours in meters), a circular histogram of orientation frequencies, and mean flow recorded at Mooring 1C 4 m above bottom and 16 m above bottom.

Site 3



Current Meter 1B 4 M.A.B.
Mean flow (cm/sec) Vs Direction



Current Meter 1B 16 M.A.B.
Mean flow (cm/sec) Vs Direction

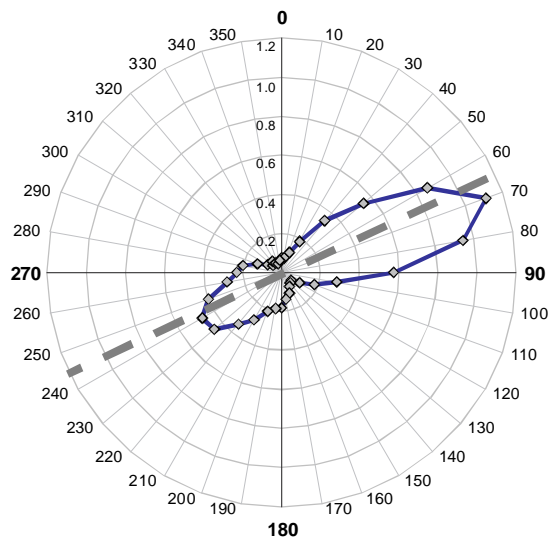
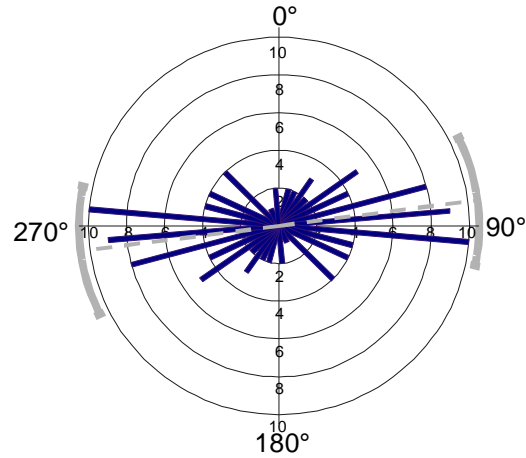
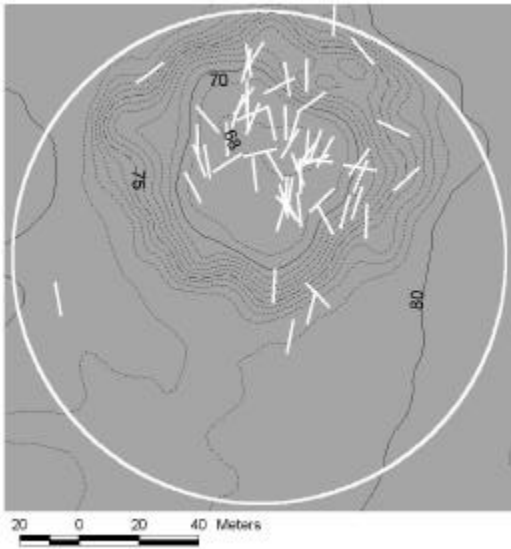
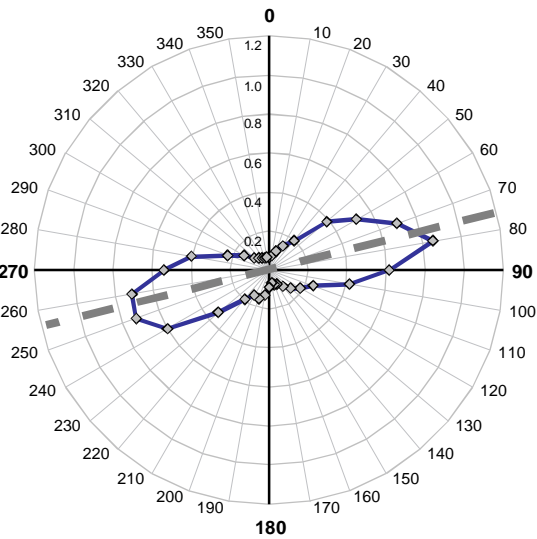


Fig. 9.6. Gorgonian orientations and mean directional water flow at Site 3. Clockwise from upper left, the panels show the locations and orientations of sea fan colonies and site bathymetry (contours in meters), a circular histogram of orientation frequencies, and mean flow recorded at Mooring 1B 4 m above bottom and 16 m above bottom.

Site 5



Current Meter 5C 16 M.A.B.
Mean flow (cm/sec)Vs Direction



Current Meter 5B 16 M.A.B.
Mean flow (cm/sec)Vs Direction

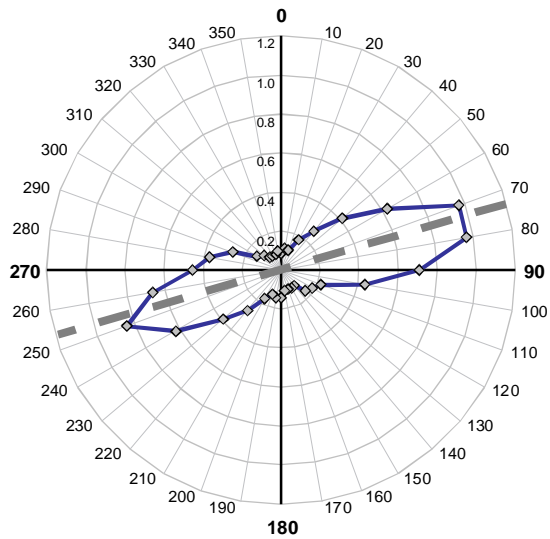


Fig. 9.7. Gorgonian orientations and mean directional water flow at Site 5. Clockwise from upper left, the panels show the locations and orientations of sea fan colonies and site bathymetry (contours in meters), a circular histogram of orientation frequencies, and mean flow recorded at Mooring 5C 16 m above bottom and Mooring 5B 16 m above bottom.

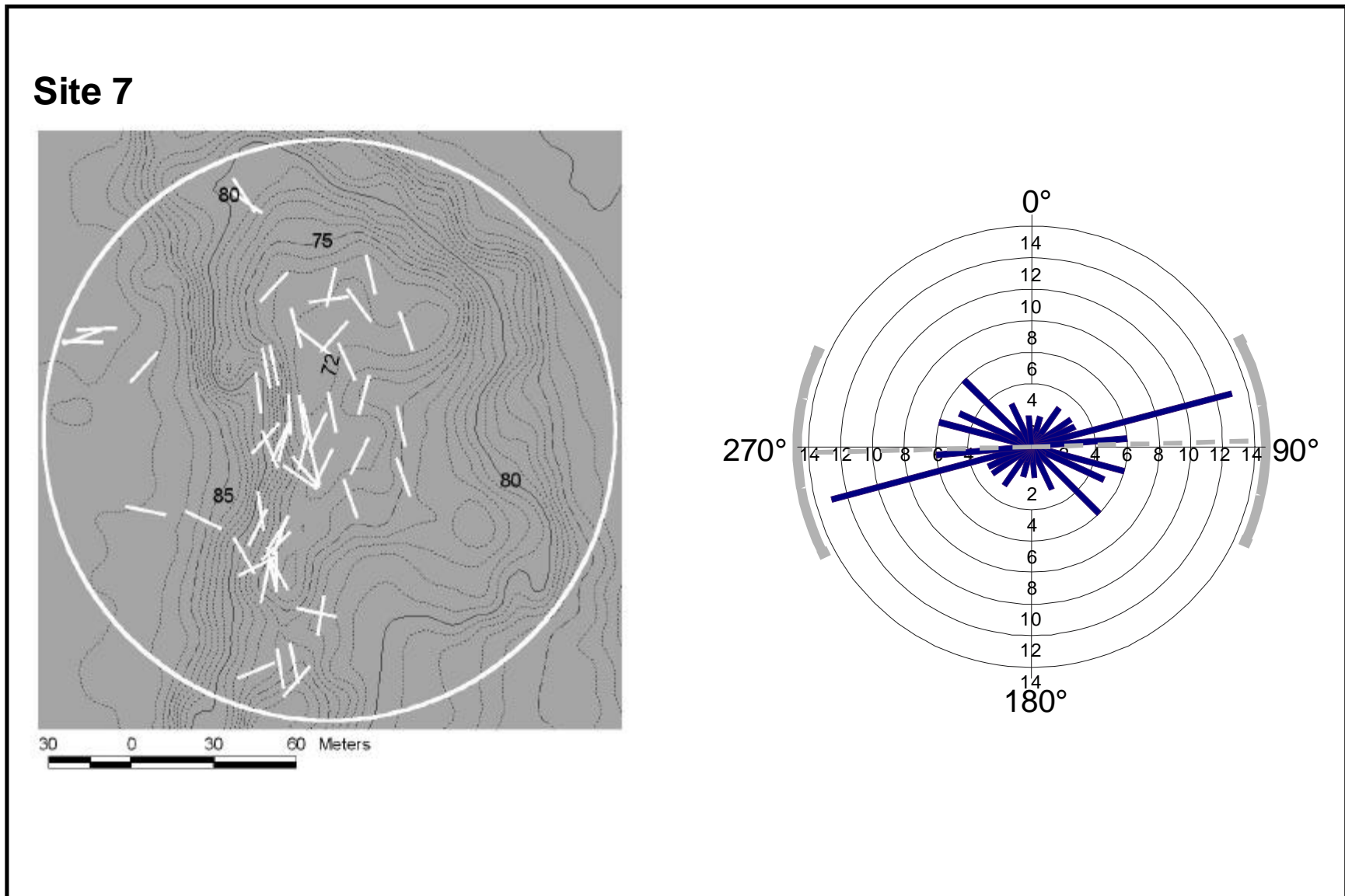


Fig. 9.8. Gorgonian orientations and mean directional water flow at Site 7. Left panel shows the locations and orientations of sea fan colonies and site bathymetry (contours in meters). Right panel shows a circular histogram of orientation frequencies. Mean flow is shown in Fig. 9.9.

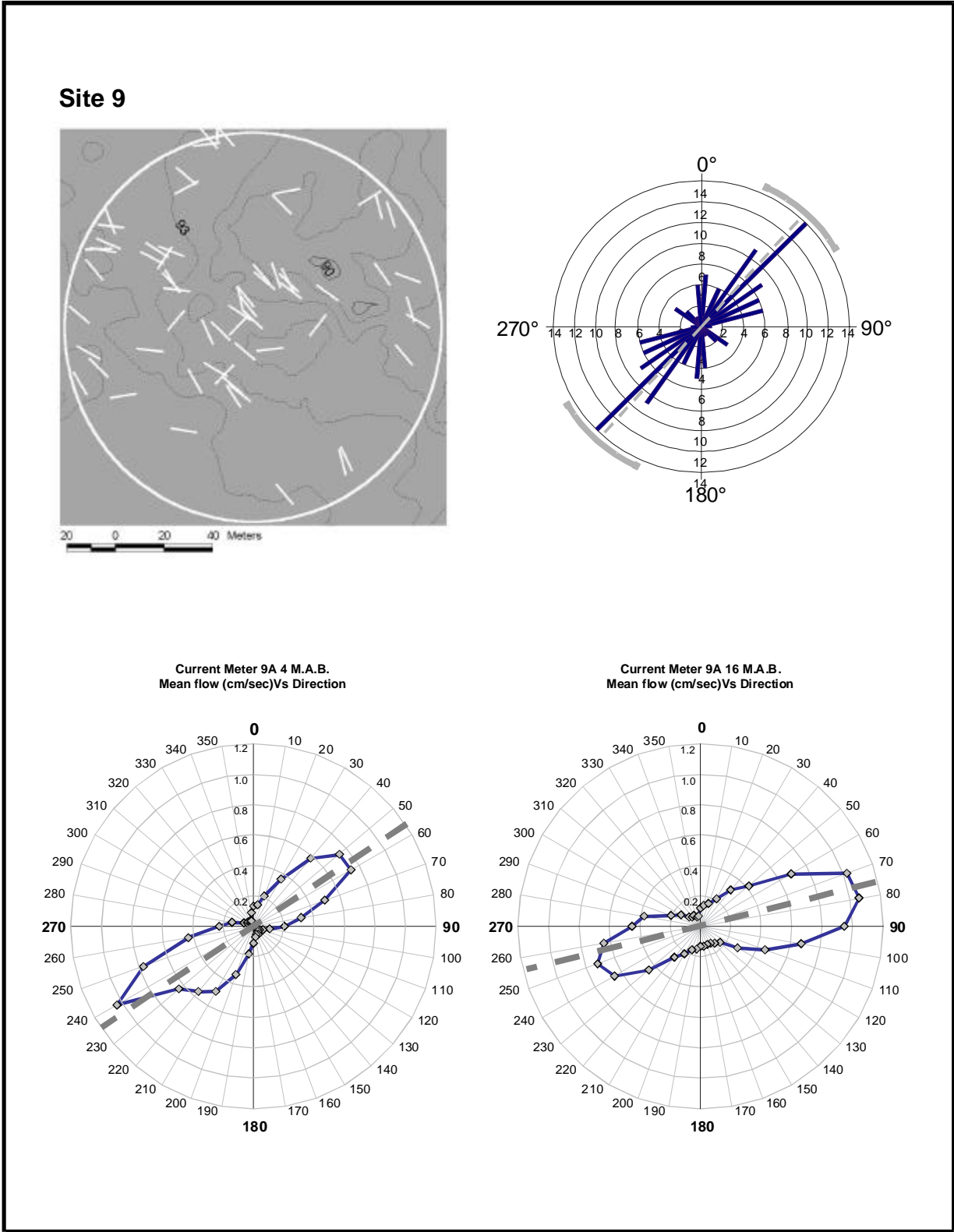


Fig. 9.9. Gorgonian orientations and mean directional water flow at Site 9. Clockwise from upper left, the panels show the locations and orientations of sea fan colonies and site bathymetry (contours in meters), a circular histogram of orientation frequencies, and mean flow recorded at Mooring 9A 4 m above bottom and 16 m above bottom.

The general result for these measurements is that, in every site, a large sample of gorgonian orientations exhibited non-random distributions with a distinct and unimodal central tendency (**Table 9.3**). A Rayleigh test of the distributions (Zar 1999) showed that in every case the probability of the distributions arising by random chance was less than 0.01. A reasonable conclusion is that the population of gorgonians is responding similarly to an environmental constant acting on the site as a whole. Evidence from the separate site and from available current records indicates that the predominant direction of water movement at the site is a strong determinant of colony orientation, as discussed below. Individually, there are distinct differences among the sampled populations that may arise due to the interaction of water flow and site topography. The circular statistic r , the length of the mean vector, is a measure of the spread of the distribution. Higher values indicate a narrower distribution. The sites with the higher values for vector length (Sites 1, 3, and 9) are characterized by large expanses of relatively flat topography.

To examine the possibility that water movement was influencing gorgonian orientations, the current meter data were processed to quantify the direction of the water transport. The assumption was that for filter-feeding animals dependent upon suspended particles, an optimal strategy would be to orient the filtering apparatus perpendicular to the direction of flow. To calculate the current flux, the water speed and direction data were binned into 10° sectors. Within each sector, the current speed, recorded in centimeter per second at 30 minute intervals, was summed over the available data set. The result quantifies the biologically available flow in a given direction whereas a simple scatter-plot of the current data tends to emphasize the most energetic events. For statistical comparison to colony orientation results, the water flow data were folded into the range 0° to 180° to calculate the mean vectors (**Table 9.4**). In plotting the data (**Figs. 9.5 to 9.9**), the full range of compass degrees was employed to illustrate non-uniform distributions in the bimodal data (e.g., **Fig. 9.6**).

Table 9.4. Circular statistics for current flux measured at current meter moorings. Asterisk indicates data not shown; all other data are shown graphically (**Figs. 9.5 to 9.9**). (See **Fig. 9.4** for mooring locations.) The number of days (N) of data is shown for each mooring. Mean vector is given in folded compass degrees in the range 0° to 180°, where the clockwise range 0° to 90° folded degrees is the equivalent of 0° to 90° T and 180° to 270° T. Vector length can range from zero to one and is a measure of the spread of the data where zero would indicate that each value was different and one would indicate that all values were the same.

Mooring	Height above Bottom (m)	Associated Site	N (days)	Mean Vector (μ)	Vector Length (r)
1A *	16	1	629.7	69°	0.40
1B	16	1	335.2	65°	0.52
1C	16	1	336.2	65°	0.47
1A*	4	3	250.2	171°	0.31
1B	4	3	222.0	32°	0.54
1C	4	3	110.4	176°	0.62
5A *	16	5	517.5	74°	0.49
5B	16	5	265.8	74°	0.52
5C	16	5	343.4	76°	0.54
9A	16	7	589.4	76°	0.50
9A	4	9	275.5	54°	0.61

As with the colony orientation data, the general conclusion from this presentation of current flow is that there is a distinctly non-random distribution to the movement of water across the study sites. Because the current directions could be measured over the full range of the compass—unlike gorgonian orientations—it is possible to see that the water movements were strongly bimodal in most cases and that the modes were often distinct. Discussion of the regional and seasonal factors that influence water flow is beyond the scope of this discussion. However, an examination of the agreement or lack of agreement between the mean vector of colony orientation and the mean vector of water flow illustrates instances where local topography may be acting to steer water flow over the mounds in ways that are not captured by the mooring data.

At Site 1 (**Fig. 9.5**), the study area is situated on the top of a mound that extends well beyond the study site boundaries (**Fig. 9.4**). Consequently, except for a sharp drop-off in the northeast portion of the site, most of the study area is at a uniform elevation with respect to the surrounding seafloor. Water flow measured by the 16 m above bottom instrument is distinctly bimodal, with the dominant mode oriented to the northeast (65°). Note that the results from the 16 m above bottom instrument at Mooring 1A were in close agreement with results from 1B and 1C and are not plotted. In effect, Site 1 is downstream from relatively unobstructed flows arriving from the west-southwest. The gorgonian orientations at the site, which were significantly non-random, were rotated by about 15° counterclockwise from the mean vector of the water flow. This rotation is beyond the range of the 95% or 99% confidence intervals. While the bottom Eckman effect can be expected to produce counterclockwise rotation approaching the bottom, it is not clear from the present data whether all of observed rotation is due to this. Flows recorded by the instrument at 4 m above bottom at Mooring 1C are almost perpendicular to the upper current meter (**Fig. 9.5**).

Site 3 is a low-relief site characterized by numerous boulders or outcrops that rise 1 to 2 m above the surrounding seafloor. The gorgonian orientations at the site have a mean vector of 179° and agree quite well with the mean vectors of water flow recorded by the bottom instruments at moorings 1A and 1C (**Tables 9.3 and 9.4**). Here, however, the rotation in the orientations is clockwise with respect to currents. Moreover, the orientation data have a different mean vector from that of the flow recorded by the bottom instrument at Mooring 1B (**Fig. 9.6**). The bottom current meter at 1B apparently recorded a persistent jet to the northeast. Possibly, this flow is an artifact of the adjacent topography. There is no evidence that the northeasterly jet affected the gorgonian colonies at Site 3.

Site 9 is a “low-relief” feature similar to Site 3. Colony orientations at the site had a mean vector of 42° and a vector length of 0.53 (**Table 9.3**). Colony orientations (**Fig. 9.9**) were rotated counterclockwise from the mean flow (54°) (**Table 9.4**), which is consistent with Eckman effect upon the near-bottom flow.

Boundaries for Sites 5 and 7 both fully encompass “high-relief” features. Consequently, localized deflections of water flow across the features undoubtedly occur as the angle and

direction of the bottom slope changes. The vector lengths for the orientation data reflect this greater variability in deflection (**Table 9.3**). Orientations agree with the mean vector of the water flow data. The mooring closest to Site 7 (Mooring 9A upper—see **Fig. 9.9**) was located nearly 4 km from the site; the gorgonian orientations (**Fig. 9.8**) agree well with the mean flow despite this offset.

In conclusion, filter feeding sea fans display characteristic orientations, which can be readily determined from video imaging. A very modest field effort dedicated to measuring gorgonian orientations could probably collect a sample adequate for determining the mean orientation of a specific feature within 5° to 10°. These mean orientations appear to be strongly influenced by mean directional water flow. Deviation from the current meter readings probably indicates local topographic steering. These subtleties in the flow field around a feature will always be present, but will be difficult or impossible to determine without extensive measurement and modeling. If management needs determine the localized flow around a mound to manage discharge impacts, for example, a robust estimate of flow could be obtained from the gorgonian population. Under many circumstances, such an approach might be time- and cost-effective relative to a full-blown program of physical oceanography.

Gorgonian Distribution and Microhabitat Factors

After review of the complete photographic series, it was determined that six habitat categories were evaluated with sufficient consistency and frequency to be used for further analysis. These were *morphology*, *location on feature*, *silt veneer*, *roughness small-scale*, *roughness medium-scale*, and *slope*. Other categories, e.g., *rubble*, occurred infrequently or proved difficult to evaluate in available imagery. Colony abundance observed in random photographs from the selected sites (1, 3, 5, and 7) were then compared against habitat factors following a set of standardized routines. Partial ANOVA tests of a simple effects model were completed for the pooled abundance of all taxonomic groups (total colonies) and for the most abundant groups at each site. The results of these tests are presented in **Tables 9.5** through **9.8**. The numbers of colonies per photograph were plotted to confirm the occurrence of a long-tailed distribution that could be modeled with a Poisson distribution (**Figs. 9.10** through **9.13**). The chi-square probability that a given result could occur by random chance under a Poisson distribution was used to screen for significant habitat factors. Box and whisker diagrams (Cleveland 1985) were plotted for the total colonies and for the three most abundant groups. In these plots, the horizontal bar in the box shows the 50th percentile of the data, the lower and upper ends of the box indicate the respective quartiles, and the whiskers show the 10th and 90th percentiles. Outliers are plotted as individual values.

In all cases, designated characteristics of the habitat were significant factors in determining the abundance of gorgonian or antipatharian colonies. Morphology, which distinguished among types of attachment substrata, was nearly always a significant factor in determining colony abundance. Although colonies—particularly the antipatharians—did occur at photo-stations where there was no visible hard substratum, the overwhelming majority of colonies were associated with a hard structure on the seafloor. Comparison

Table 9.5. Partial analysis of variance for influence of microhabitat factors upon abundance of gorgonian and antipatharian colonies at Site 1. Setting $\alpha = 0.05$, chi-square values can be used to evaluate significance of selected factors in a simple effects model for all colonies and for the three most abundant groups.

Microhabitat Factor	df	Deviance	Residual df	Residual Deviance	Pr (Chi)
Terms added sequentially (first to last)					
Response: Total colonies (N=1308)					
NULL			480	1276.737	
morphology	3	268.2118	477	1008.525	0.0000000
location on feature	3	44.0329	474	964.492	0.0000000
silt veneer	3	5.1624	471	959.330	0.1602847
roughness-small scale	2	3.1604	469	956.170	0.2059306
roughness-medium scale	2	7.5278	467	948.642	0.0231932
slope	2	18.1387	465	930.503	0.0001151
Response: <i>Nicella</i> spp. (N=510)					
NULL			480	910.8282	
morphology	3	122.0078	477	788.8204	0.0000000
location on feature	3	7.0142	474	781.8062	0.0714467
silt veneer	3	5.2673	471	776.5389	0.1532396
roughness-small scale	2	14.3117	469	762.2273	0.0007803
roughness-medium scale	2	3.0846	467	759.1427	0.2138881
slope	2	8.3773	465	750.7653	0.0151666
Response: <i>Ctenocella</i> (<i>Ellisella</i>) other (N=224)					
NULL			480	437.5762	
morphology	3	42.72188	477	394.8543	0.0000000
location on feature	3	12.75216	474	382.1022	0.0052044
silt veneer	3	5.46752	471	376.6347	0.1405941
roughness-small scale	2	0.25692	469	376.3777	0.8794481
roughness-medium scale	2	1.31296	467	375.0648	0.5186731
slope	2	1.09155	465	373.9732	0.5793920
Response: White Stenogorgiinae (N=112)					
NULL			480	418.3128	
morphology	3	25.97583	477	392.3370	0.0000096
location on feature	3	3.73560	474	388.6014	0.2914668
silt veneer	3	1.48455	471	387.1169	0.6858397
roughness-small scale	2	4.72297	469	382.3939	0.0942801
roughness-medium scale	2	0.68539	467	381.7085	0.7098538
slope	2	16.10415	465	365.6044	0.0003184

Table 9.6. Partial analysis of variance for influence of microhabitat factors upon abundance of gorgonian and antipatharian colonies at Site 3. Setting $\alpha = 0.05$, Chi-square values can be used to evaluate significance of selected factors in a simple effects model for all colonies and for the three most abundant groups.

Microhabitat Factor	df	Deviance	Residual df	Residual Deviance	Pr (Chi)
Terms added sequentially (first to last)					
Response: Total colonies (N=737)					
NULL			491	1415.669	
morphology	2	532.3508	489	883.318	0.0000000
location on feature	2	10.7776	487	872.540	0.0045674
silt veneer	2	17.6161	485	854.924	0.0001495
roughness small	2	5.8335	483	849.091	0.0541106
roughness medium	2	11.2598	481	837.831	0.0035889
slope	2	6.9108	479	830.920	0.0315749
Response: <i>Nicella</i> spp. (N=150)					
NULL			491	706.2993	
morphology	2	193.2250	489	513.0743	0.0000000
location on feature	2	32.3288	487	480.7455	0.0000001
silt veneer	2	8.9046	485	471.8409	0.0116517
roughness small	2	2.7097	483	469.1312	0.2579852
roughness medium	2	7.6933	481	461.4379	0.0213509
slope	2	17.2754	479	444.1625	0.0001773
Response: <i>Bebryce</i> spp. (N=114)					
NULL			491	462.9459	
morphology	2	134.8138	489	328.1321	0.0000000
location on feature	2	7.5749	487	320.5572	0.0226533
silt veneer	2	11.4479	485	309.1093	0.0032668
roughness small	2	2.3124	483	306.7969	0.3146803
roughness medium	2	0.1858	481	306.6110	0.9112669
slope	2	2.0695	479	304.5415	0.3553067
Response: <i>Thesea</i> spp. (N=113)					
NULL			491	405.4872	
morphology	2	90.5848	489	314.9024	0.0000000
location on feature	2	2.2033	487	312.6991	0.3323273
silt veneer	2	15.8747	485	296.8244	0.0003572
roughness small	2	0.7549	483	296.0695	0.6856081
roughness medium	2	9.3902	481	286.6793	0.0091399
slope		0.7391	479	285.9402	0.6910372

Table 9.7. Partial analysis of variance for influence of microhabitat factors upon abundance of gorgonian and antipatharian colonies at Site 5. Setting $\alpha = 0.05$, chi-square values can be used to evaluate significance of selected factors in a simple effects model for all colonies and for the three most abundant groups.

Microhabitat Factor	df	Deviance	Residual df	Residual Deviance	Pr (Chi)
Terms added sequentially (first to last)					
Response: Total colonies (N=140)					
NULL			422	668.5906	
morphology	3	207.3797	419	461.2110	0.0000000
location on feature	3	22.0455	416	439.1654	0.0000638
silt veneer	3	4.5425	413	434.6229	0.2085301
roughness-small scale	2	8.9382	411	425.6847	0.0114574
roughness-medium scale	2	2.2943	409	423.3904	0.3175480
slope	2	2.5353	407	420.8551	0.2814940
Response: <i>Antipathes ?atlantica</i> (N=66)					
NULL			422	270.1720	
morphology	3	39.9148	419	230.2573	0.0000000
location on feature	3	0.4815	416	229.7758	0.9229428
silt veneer	3	1.4147	413	228.3611	0.7020884
roughness-small scale	2	0.3993	411	227.9618	0.8190302
roughness-medium scale	2	0.2911	409	227.6707	0.8645426
slope	2	6.6322	407	221.0385	0.0362940

Table 9.8. Partial analysis of variance for influence of microhabitat factors upon abundance of gorgonian and antipatharian colonies at Site 7. Setting $\alpha = 0.05$, chi-square values can be used to evaluate significance of selected factors in a simple effects model for all colonies and for the three most abundant groups.

Microhabitat Factor	df	Deviance	Residual df	Residual Deviance	Pr (Chi)
Terms added sequentially (first to last)					
Response: Total colonies (N=661)					
NULL			514	1717.560	
morphology	3	410.6978	511	1306.862	0.0000000
location on feature	3	21.1592	508	1285.703	0.0000976
silt veneer	3	26.8597	505	1258.843	0.0000063
roughness-small scale	2	71.2694	503	1187.574	0.0000000
roughness-medium scale	2	51.5587	501	1136.015	0.0000000
slope	2	33.7812	499	1102.234	0.0000000
Response: <i>Bebryce</i> spp. (N=221)					
NULL			514	1089.636	
morphology	3	265.7020	511	823.934	0.0000000
location on feature	3	44.2762	508	779.658	0.0000000
silt veneer	3	35.2173	505	744.441	0.0000001
roughness-small scale	2	40.1389	503	704.302	0.0000000
roughness-medium scale	2	30.0885	501	674.213	0.0000003
slope	2	10.5732	499	663.640	0.0050589
Response: <i>Nicella</i> spp. (N=216)					
NULL			514	1036.006	
morphology	3	124.7051	511	911.301	0.0000000
location on feature	3	11.0744	508	900.227	0.0113304
silt veneer	3	23.3672	505	876.859	0.0000339
roughness-small scale	2	83.2179	503	793.641	0.0000000
roughness-medium scale	2	34.8880	501	758.753	0.0000000
slope	2	57.4114	499	701.342	0.0000000
Response: <i>Antipathes ?atlantica</i> : (N=132)					
NULL			514	476.7785	
morphology	3	77.24959	511	399.5289	0.0000000
location on feature	3	12.35202	508	387.1769	0.0062696
silt veneer	3	0.28436	505	386.8925	0.9629425
roughness-small scale	2	0.28860	503	386.6039	0.8656261
roughness-medium scale	2	4.61253	501	381.9914	0.0996327
slope	2	3.49265	499	378.4987	0.1744139

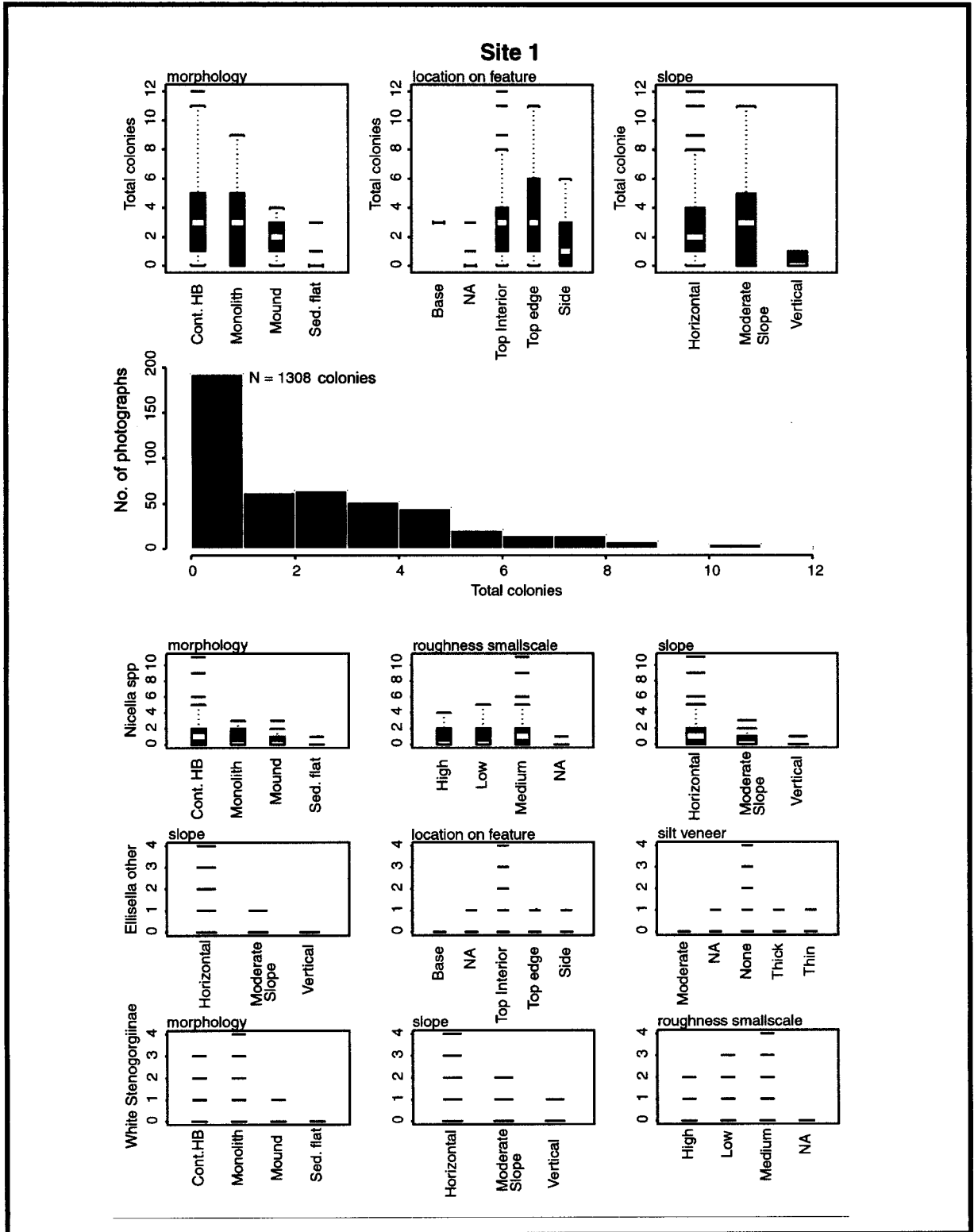


Fig. 9.10. Microhabitat utilization by gorgonians and antipatharians at Site 1. Upper panel shows numbers of colonies associated with microhabitat factors in individual random photographs. See text for descriptions of factors. Histogram shows frequencies of colonies in photographs. Lower three panels show colony numbers and habitat features for the most abundant groups. In box-and-whisker diagrams (Cleveland 1985), the horizontal bar in the box shows the 50th percentile of the data, the lower and upper ends of the box indicate the respective quartiles, and the whiskers show the 10th and 90th percentiles. Outliers are plotted as individual values.

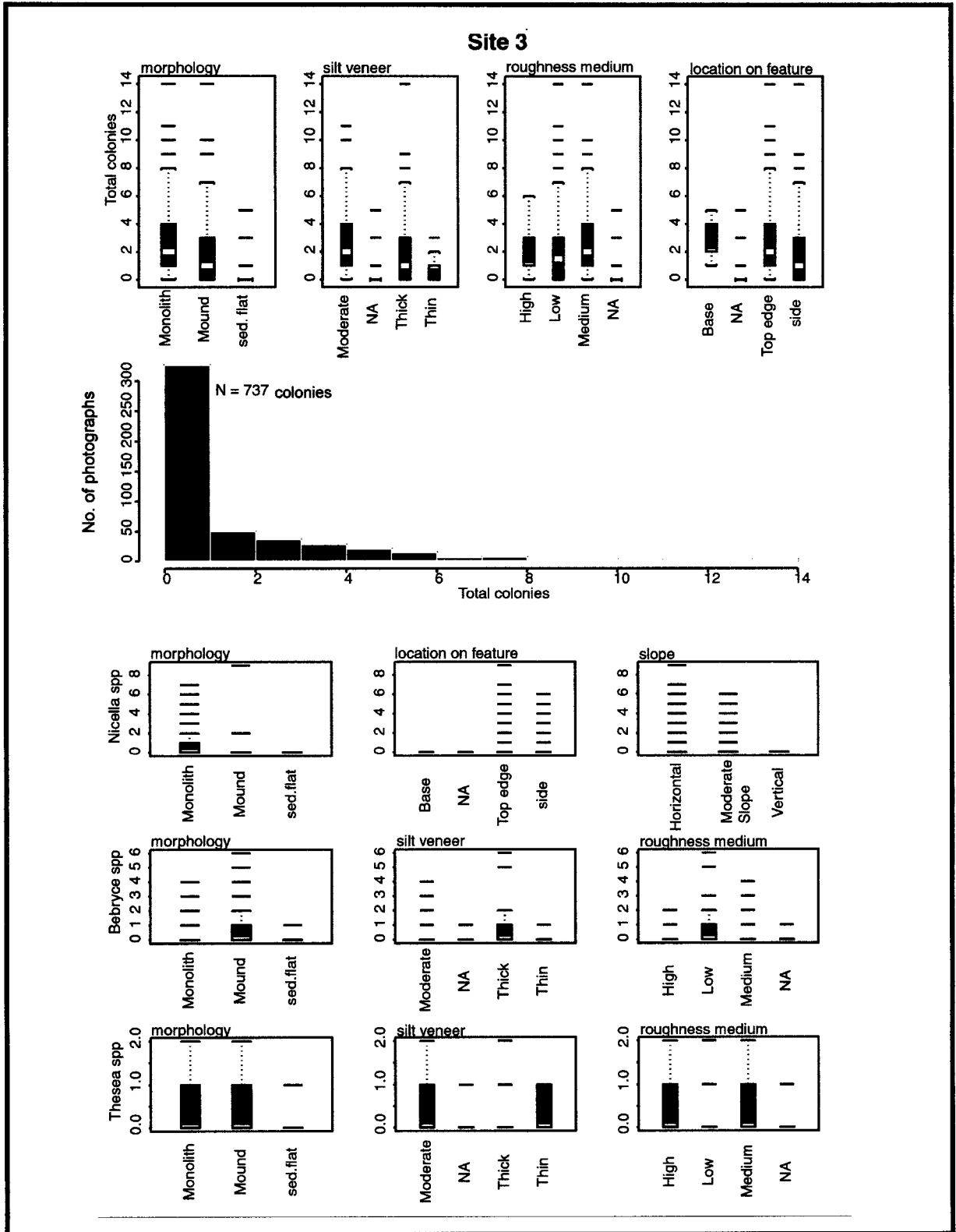


Fig. 9.11. Microhabitat utilization by gorgonians and antipatharians at Site 3. Upper panel shows numbers of colonies associated with microhabitat factors in individual random photographs. See text for descriptions of factors. Histogram shows frequencies of colonies in photographs. Lower three panels show colony numbers and habitat features for the most abundant groups. See Fig. 9.10 for explanation of box-and-whisker diagrams.

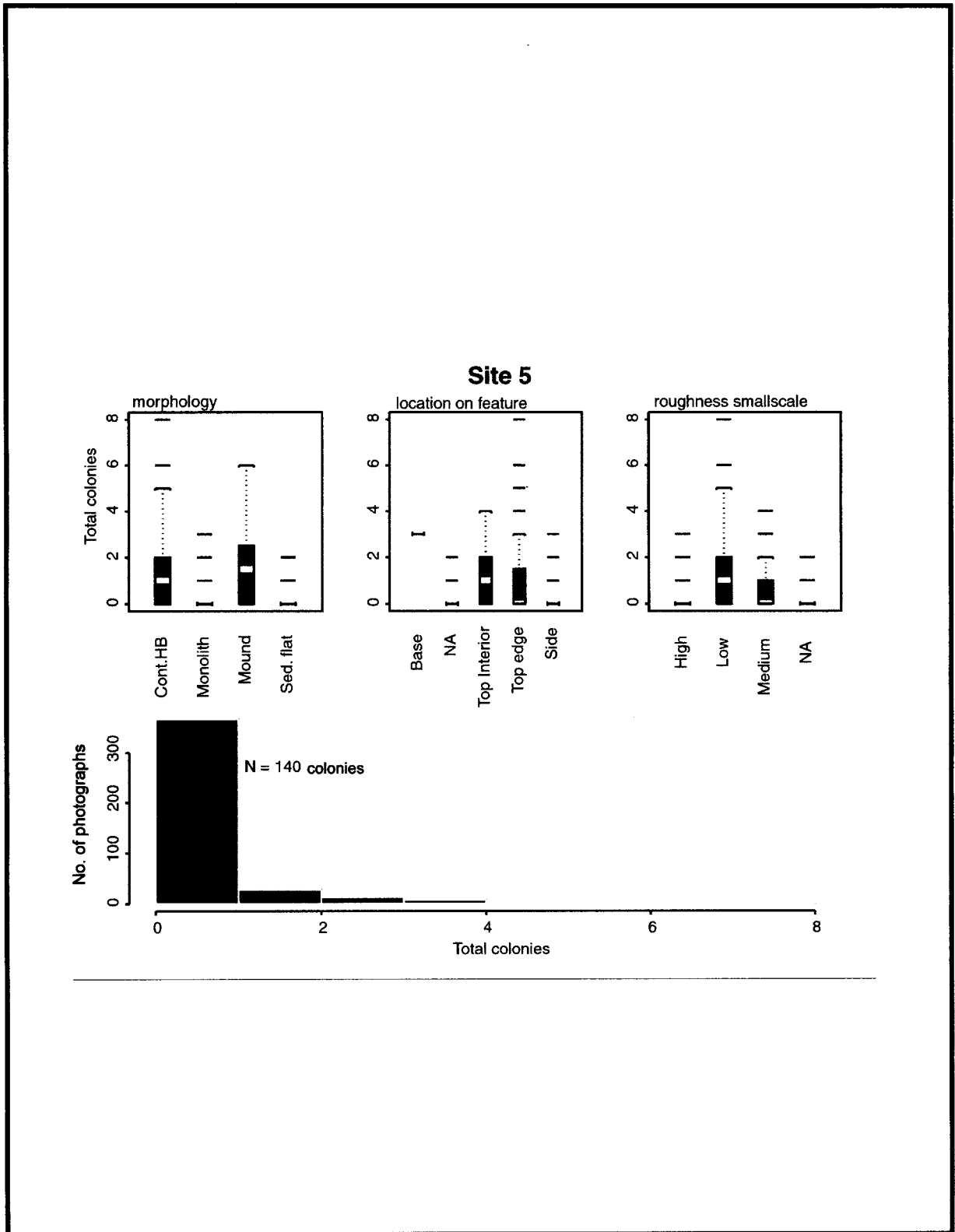


Fig. 9.12. Microhabitat utilization by gorgonians and antipatharians at Site 5. Upper panel shows numbers of colonies associated with microhabitat factors in individual random photographs. See text for descriptions of factors. See Fig. 9.10 for explanation of box-and-whisker diagrams. Histogram shows frequencies of colonies in photographs.

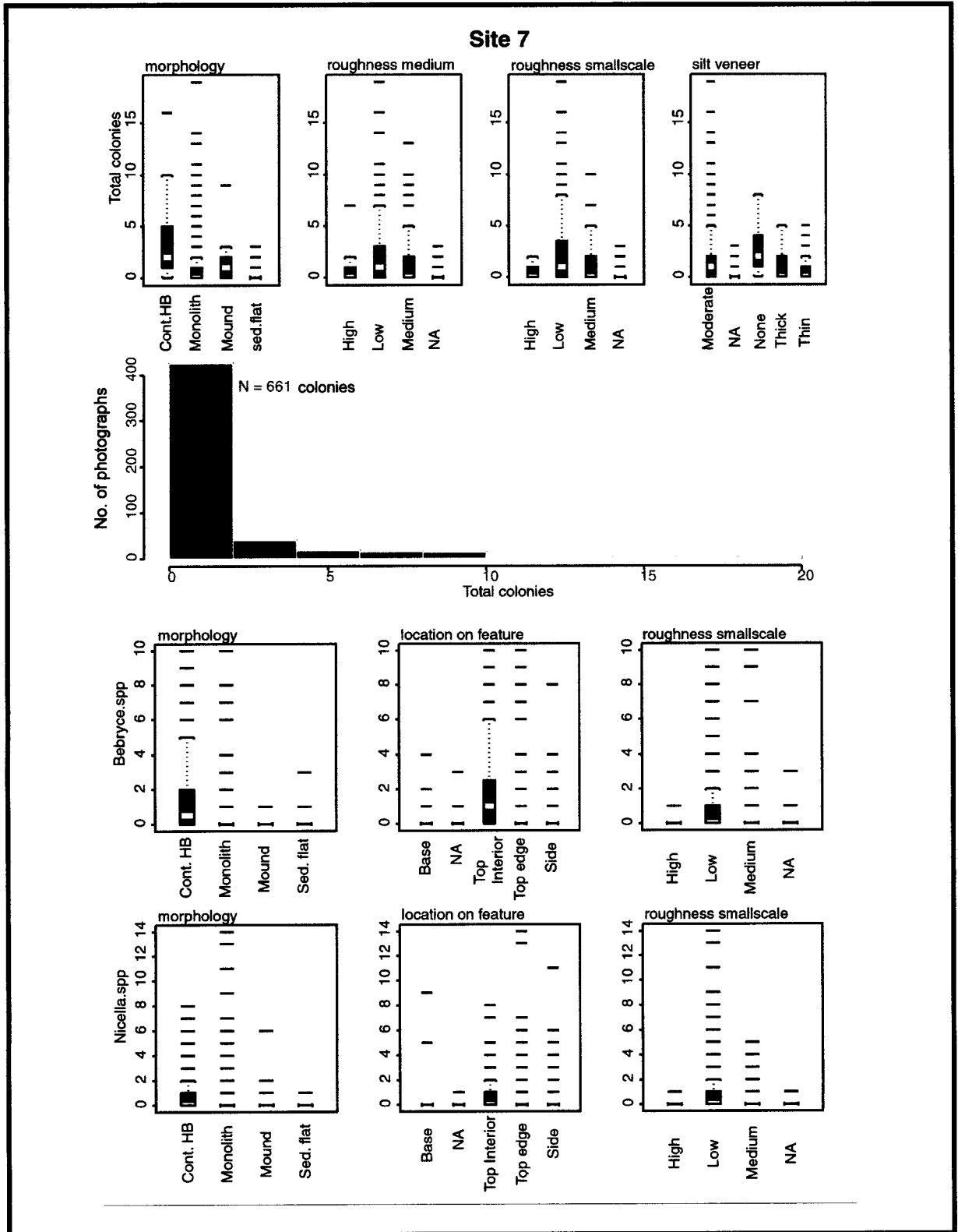


Fig. 9.13. Microhabitat utilization by gorgonians and antipatharians at Site 7. Upper panel shows numbers of colonies associated with microhabitat factors in individual random photographs. See text for descriptions of factors. Histogram shows frequencies of colonies in photographs. Lower three panels show colony numbers and habitat features for the most abundant groups. See Fig. 9.10 for explanation of box-and-whisker diagrams.

of the types of structures utilized at different sites and by different taxonomic groups provides an indication of habitat preferences.

Overall, location on the feature was also a significant factor for the total abundance of all groups. Consistent with previous findings (Messing et al. 1990), the top edges and sides of features were preferred locations. Individual groups occupied a wider range of locations. The *Bebryce* and *Ctenocella* (*Ellisella*) groups, for example, were frequently found on the interior of the hard bottom features.

Other significant factors differed among the sites. Some of these differences clearly resulted from the relief-type of the respective feature. Silt veneer was a significant factor primarily at Site 3, the low-relief feature. This is consistent with a regime in which partial burial of hard bottom was common. Silt veneer was also significant at Site 7 where the sediment flats beyond the edges of the mound occupied a substantial portion of the study area.

Small- and medium-scale roughness also emerged as significant factors in the microhabitats associated with gorgonian colonies. As with all the habitat characteristics, it cannot be determined from the present data whether colony abundance on a particular roughness group resulted from settlement choice and preferential survival or simply adaptation to the prevailing characteristics of a given site. These results confirm the preliminary finding of Gittings et al. (1991) that subsets of the mound environment can be reliably classified from video and photographic images and that components of the hard-bottom community tend to occur on predictable habitat subregions. Work by Messing et al. (1990) indicated that gorgonians occur at the edges of mounds. Present results confirm this, but also show that individual groups are also prevalent on the interior tops of the mounds, thereby expanding the range of microhabitats for filter feeding soft corals in the hard bottom community.

Chapter 10: Epibiont Recruitment

Tara J. Holmberg and Paul A. Montagna

Introduction

The goal of this study was to support the descriptive and monitoring portions of the program with experiments (based upon testable hypotheses) that define ecological mechanisms causing spatial and temporal changes in hard bottom epifaunal communities. Most hard bottom experimental studies have been conducted in rocky intertidal or on shallow coral reefs less than 30 m in depth, because of the accessibility to control and manipulate these communities. However, the few deepwater projects conducted on hard bottom substrates have demonstrated that many of the same abiotic and biotic ecological processes affecting spatial and temporal patterns of well-studied intertidal epifaunal communities also affect deep-sea organisms (Mullineaux 1989; Genin et al. 1992; Rogers 1994). Spatial and temporal variation of hard bottom communities are functional responses to biotic and abiotic processes. These processes are often called a "disturbance."

The extent, magnitude, and effect of biotic or abiotic disturbance varies, often depending on which species are being investigated (Sousa 1985). A vast array of ecological processes, both biotic and abiotic, can affect a given hard bottom community at the same time. Temperature, salinity, and nutrients are all relatively stable in deeper water. Desiccation is not an applicable process because organisms are continuously submerged. Turbidity, turbulence, abrasion (e.g., sand scour, whiplashing), and stochastic physical disturbance events (e.g., hurricanes, internal waves, eddies), however, may all play an important role in changes of coverage, abundance, biomass, and diversity of hard bottom communities in deep water.

As with some abiotic processes, biological disturbances vary temporally and spatially and affect hard bottom communities within the deep sea (Underwood and Denley 1984; Connell and Keough 1985). There are primarily four biological processes that have been described and measured in the rocky intertidal: recruitment, competition (inter- or intraspecific), predation, and indirect interference (e.g., whiplashing, bulldozing, or shading).

Development of an epibiont community is the net result of interactions between biotic and abiotic processes through time. Open space in hard bottom habitats is often the primary limiting factor. The greatest role of disturbance is in forcing predictable patterns of community development to deviate (Pickett and White 1985). Succession is the directional process of initial colonization of bare substrate and subsequent community changes over time.

Open space in a hard bottom community is referred to as a patch. Two types of patches have been identified and described in the ecological literature. Type I patches are bordered by surrounding stands of organisms (Sousa 1985). A predator moving through a community clearing only those organisms in its path creates a Type I patch. These patches are typically recolonized quickly by neighboring colonial organisms (Connell and Keough 1985). Resulting communities are characteristic of early successional stages. If the patch is created

in a stand of solitary, immobile organisms, however, settlement of the patch can only come about via propagules or survivable fragments of individuals (e.g., sponges, algae).

Type II patches are isolated from other areas of colonized substrate (Sousa 1985). This is the most common type of patch created in the subtidal marine environment (Connell and Keough 1985). A diapir pushing through the sediment at the ocean floor creates a Type II patch. These patches are outside the reach of colonial animals and are typically recolonized only by larvae of dispersing organisms (Sousa 1985). They also may be resettled by fragments of adults that move through the patch.

Methods

Experimental Design

For the current study, null hypotheses were formed to develop the experimental design. These hypotheses were based on factors discussed above that govern communities in rocky intertidal zones, which would be applicable to the deep sea. The null hypotheses were

- H₀₁: Epibiont coverage, abundance, and diversity do not change over time.
- H₀₂: Epibiont coverage, abundance, and diversity are not different between study sites.
- H₀₃: Epibiont coverage, abundance, and diversity do not change with increasing height above bottom.
- H₀₄: Epibiont coverage, abundance, and diversity are not affected by disturbance.
- H₀₅: Epibiont coverage, abundance, and diversity are not affected by differences in small-scale turbulence.
- H₀₆: Epibiont coverage, abundance, and diversity are not affected by orientation of settling surface.

The hypotheses were tested with settling plate experiments. Settlement, exclusion, and control treatments were used to study the biotic and abiotic interactions that regulate ecological processes. The settling plates were attached to a mooring and the entire device is called a "biomooring." There were two major deployments: one for a spatial study and one for a temporal study. The original major elements of the settling plate experiment studies were as follows:

1. Spatial study at four stations (Sites 1, 4, 5, and 9) to last for 1 year;
2. Replication of the spatial study during the second year;
3. Three settling plate treatments: uncaged, caged, partially-caged;
4. Two heights, or distances, from the bottom (3 m and 13 m), and;
5. Time series study at one station (Site 4), retrieval every 3 months for 2 years.

Although details of the project were modified because of equipment failure and bad weather, the original hypotheses were still tested. Only elements 4 and 5 were changed:

4. Three heights, or distances, from the bottom (0, 3, and 13 m), and;
5. Time series study at one station (Site 4), cruise every year for retrieval.

Study sites (**Fig. 10.1**) were chosen to correspond with the physical oceanography experiments (see Chapter 6) in order to gather as much information about the ambient environment as possible. The specific study location within the study site was randomly chosen near a carbonate mound. All targeted sites had been previously surveyed by ROV to ensure that hard bottom communities were present on the corresponding mounds. Four sites were chosen to represent a range of vertical relief, water depth, and distance from the Mississippi River Delta. Sites 1 and 5 were characterized by flat-topped mounds of high relief; Site 4 represented steep-sided pinnacles of medium relief; and Site 9 represented low relief hard bottom. Site 9 was located in the western part of the study area, Sites 4 and 5 were in the central part of the area, and Site 1 was in the eastern part of the study area farthest from the Mississippi River.

The spatial experiment was designed to test for differences among habitats. One biomoooring was deployed at Sites 1, 4, 5, and 9 at approximately the same water depth (**Table 10.1**). This experiment was completed as originally planned.

The temporal experiment was designed to test for differences in recruitment and growth over time, with quarterly retrievals over a 2-year period. Eight biomoorings were deployed at Site 4 during Cruise 1C and one biomoooring was to be retrieved on each of the subsequent cruises (**Table 10.2**). Due to shackle failure, the first set of biomoorings deployed was resting on the bottom substrate (0 m height), while the second set of biomoorings deployed was suspended at the originally planned heights of 3 and 13 m from the bottom. This change enhanced the project because sampling was done at three heights from the bottom (0, 3, and 13 m). Because of sampling difficulties and logistical problems, one cruise per year was allotted for retrieval of the temporal samples (**Tables 10.1** and **10.2**). Replicate biomoorings were retrieved during each cruise, which increased the power to determine change over time and space. The slow recruitment rates observed from the first set also indicate annual sampling was better than quarterly sampling. Sampling more frequently would not have detected significant differences among treatments because of slow growth rates.

Settlement Plates and Mooring Design

Designs commonly employed in the intertidal zone were adapted for use in the study area to evaluate effects of time, space, height of substrate above bottom, orientation of substrate, and other ecological controls on succession and community development. Artificial hard bottom settlement plates, representing Type 2 patches, were deployed. Cage and control experiments were used to manipulate the ecological processes affecting settlement plates, and to identify what processes control the community of the hard bottom features in the study area.

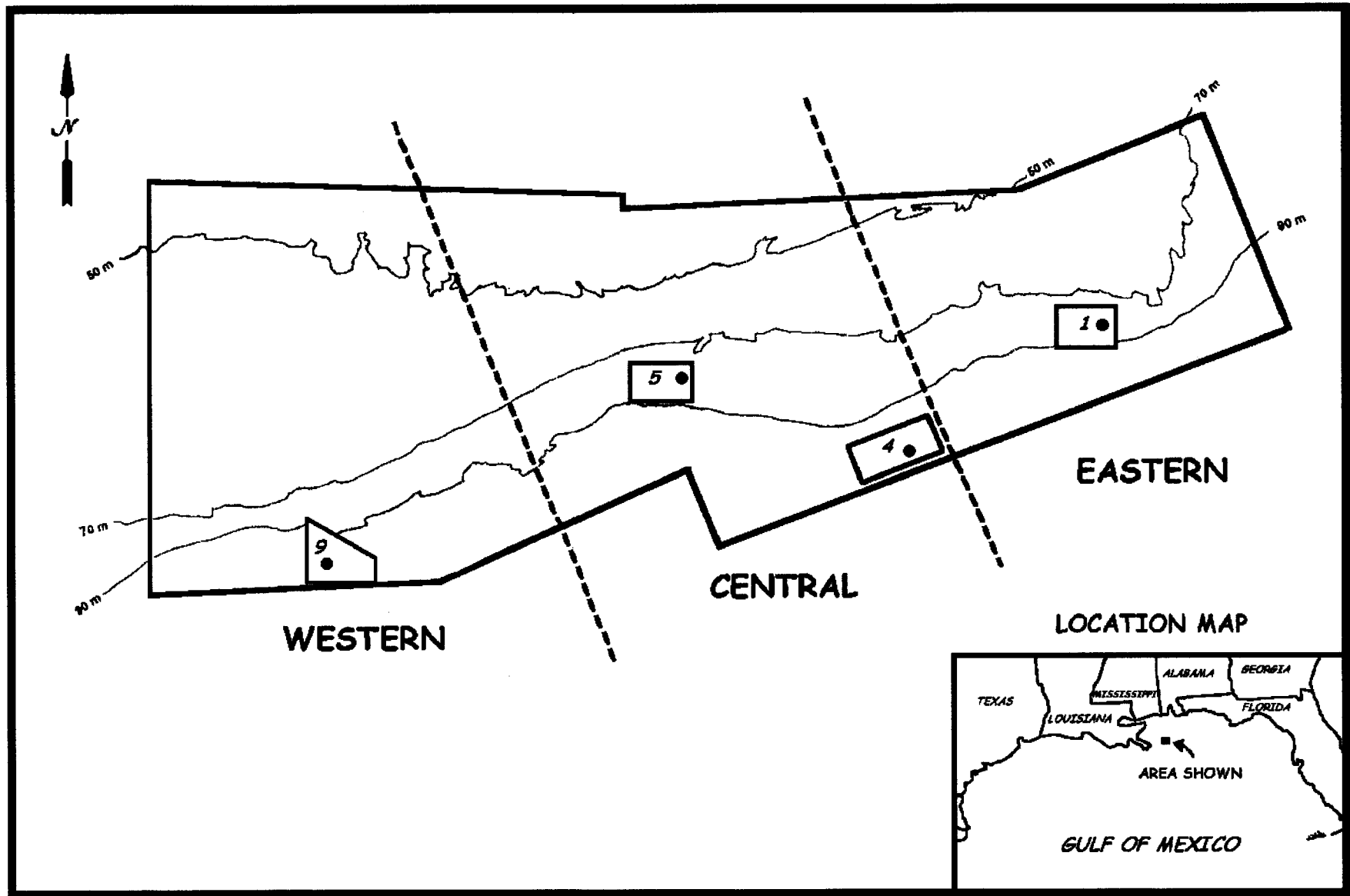


Fig. 10.1. Location of study sites.

Table 10.1. Temporal study time line and sampling schedule for biomonitoring deployments and retrievals at Site 4. Table indicates date of deployments, duration of deployment, and retrievals where D = deployed, --- = submerged, and R = retrieved. Total exposure of biomonitorings, in months (mo.), is indicated in parenthesis. All samples are from 0 meters above bottom.

Sampling Schedule: Date (Months Exposed)			
May 97	Oct 97	Aug 98	Aug 99
D	R (5 mo.)		
D	-----	R (15 mo.)	
D	-----	R (15 mo.)	
D	-----	R (15 mo.)	
D	-----	-----	R (27 mo.)
D	-----	-----	R (27 mo.)

Table 10.2. Spatial study time line and sampling schedule for biomonitoring deployments and retrievals. Table indicates dates of deployment, duration of deployment, and retrieval where D = deployed, --- = submerged, and R = retrieved. Total exposure, in months (mo.), and depth of biomonitorings, in meters above bottom (mab), are indicated in parentheses.

Site	Sampling Schedule: Date (Months Exposed and Depth)			
	May 97	Jan 98	Aug 98	Aug 99
1		D	-----	R (19 mo.) (3, 13 mab)
4	D	-----	R (15 mo.) (0 mab)	
		D	-----	R (19 mo.) (3, 13 mab)
	D	-----	-----	R (27 mo.) (0 mab)
5		D	-----	R (19 mo.) (3, 13 mab)
	D	-----	-----	R (27 mo.) (0 mab)
9	D	-----	R (15 mo.) (0 mab)	
		D	-----	R (19 mo.) (3, 13 mab)

Settlement plates were deployed at different length exposure periods to examine successional changes. Plates also were deployed at several locations within the study area to determine spatial effects of the Mississippi River Delta on community structure. Plates were suspended at different heights above bottom to examine effects of nepheloid layers on community structure. Orientation was examined by incorporating vertical and horizontal settlement surfaces into the experimental design. Additionally, the specific ecological processes of general disturbance and small-scale water flow disruption were investigated.

Unglazed ceramic tiles measuring 116.64 cm² were used as settling surfaces. The use of ceramic tile has been debated in the past, but recent field and laboratory studies have shown that unglazed ceramic tiles had the highest settlement, metamorphosis (90%-100% of settled larvae), and recruitment rates, along with concrete, among 12 settling surfaces studied (Petrie and Keith 2000). These rates were similar to the rates of settlement, metamorphosis, and recruitment in coral reef habitats. Tiles also provide a uniform, replicable surface desirable for experimentation.

Settling plate experiments with exclusion, settlement, and control manipulations were used to study the biotic and abiotic interactions that regulate ecological processes. Settling plates were grouped in three experimental manipulations: an uncaged manipulation (U), a caged manipulation (C), and a partially-caged control manipulation (P). These three manipulations were arranged in a “Y”-shaped triad (**Fig. 10.2**). The acronyms U, C, and P refer to the experimental manipulations, which were used to measure effects of ecological processes.

Each manipulation consisted of three replicated settling plates attached to the triad in “top,” “bottom,” and “side” orientations with the unglazed side of the tile facing outward. Because plates in this study were exposed for periods of 5, 15 or 27 months, it was impossible to determine the effects of each individual ecological process on the epifaunal community studied. As a result, all processes except for small-scale water disruption were combined as general disturbance (D). This does not mean that theories cannot be hypothesized from the data. A basic understanding of the susceptibility of the community to any disturbance event can be determined as described below.

Disturbance (D) is generally defined as any process that opens a space for colonization or recruitment (Sousa 1985). Any or all ecological processes, abiotic or biotic, can cause or contribute to disturbance of a community. Understanding the regulation of a community’s structure requires knowledge of the role of each ecological process in that community’s development. Most inferences of competition effects in the intertidal zone are made by observing individuals or individual colonies competing day after day or week after week. Observations shortly before and after a storm event help observers deduce storm effects on a community.

The uncaged manipulation (U) measured net recruitment (S) with biotic and abiotic disturbances (D). Net recruitment (S) included gross larval settlement, growth, competition, mortality from all sources, and community development. The disturbances experienced by the uncaged manipulation included predation, scour due to turbidity and currents, and indirect-interference (e.g., bulldozing by non-predators). Therefore, the effect of an uncaged manipulation can be determined by the sum of disturbance (D) effects and net recruitment (S):

$$U = S + D$$

The caged manipulation (C) was enclosed on all six sides with 388 mm² plastic mesh. Enclosures occasionally had encrusting bivalves and basket stars living on them, but the area covered by these organisms was never more than a small portion (~5%) of the total surface area of any enclosure. The caging manipulations (C) were used to exclude larger predators (e.g., crabs, fishes, starfishes, urchins, etc.). A common problem with enclosures is that water (W) flow rates and circulation patterns at the settling plate surface are changed. This may either enhance or inhibit settlement, recruitment, and growth of organisms depending on taxa (Menge 1976). Unlike many other disturbances encountered by epibionts, the specific effects of small-scale water flow disruption can be detected via manipulations. The caged manipulation can be represented by the sum of net recruitment (S) and water flow disruption (W):

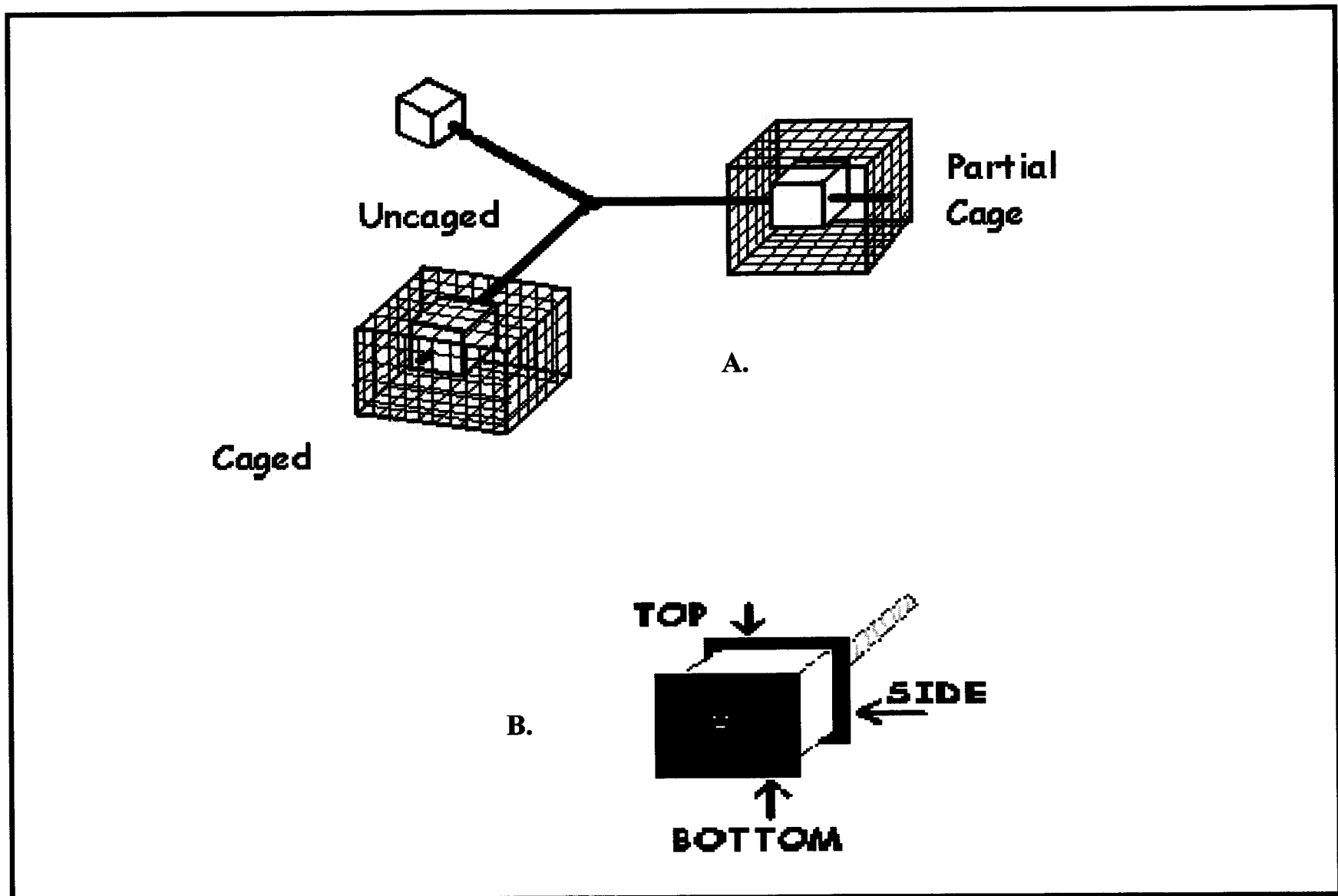


Fig. 10.2. Experimental settling plate manipulations. A. Triad with each of the three manipulations. B. Detail of the uncaged (U) manipulation showing four orientations.

$$C = S + W$$

A partially-caged control manipulation (P) was added to subtract any effects due to the enclosure. This control had the same effects on water flow, but allowed all predators access to the experimental manipulation. Thus, the control manipulation included net recruitment (S + D) in addition to small-scale water flow disruption (W):

$$P = S + D + W$$

Determination of Process Effects

Mathematical combinations of the experimental manipulations described above were used to calculate the effects of ecological process on rates of recruitment. The effects of small-scale water flow disruption (W) can be determined by subtracting the results of the uncaged manipulation (U) from the partially-caged control manipulation (P):

$$W = P - U$$

Both the uncaged and control manipulations are subjected to disturbance (D) and net recruitment (S), while only the control manipulation (C) experiences water flow disruption (W). Therefore, water flow disruption effects are calculated by the difference between the two manipulations.

Similarly, the affects of disturbance (D) can be determined by subtracting those manipulations experiencing both water flow disruption (W) and recruitment (S) from each other. The partially-caged control (P) also experiences general disturbance, while the caged manipulation (C) does not, so the difference between the two manipulations retains the general disturbance effects (D):

$$D = P - C$$

Net recruitment (S) is obtained by calculating the additive effects of the uncaged (U) and caged (C) manipulations while subtracting those effects of the partially-caged control manipulation (P):

$$S = U + C - P$$

Experimental moorings were designed to resemble, and were placed closely to, a corresponding current meter mooring within each site (Figs. 10.3, 10.4, 10.5, and 10.6). This ensured that physical oceanography data could be used to interpret biological data. Thus, the experimental moorings of this study were called “biomoorings.”

A common problem in these types of experiments is pseudoreplication, where the manipulation levels (a triad of U, C, and P manipulations) are not replicated. To avoid pseudoreplication, three replicate triads were used for each treatment cell. Triplicate triads were deployed at two different heights: 3 and 13 m above bottom (“mab”) (Fig. 10.7). Different triad heights were incorporated into the biomoring designs to examine the effects

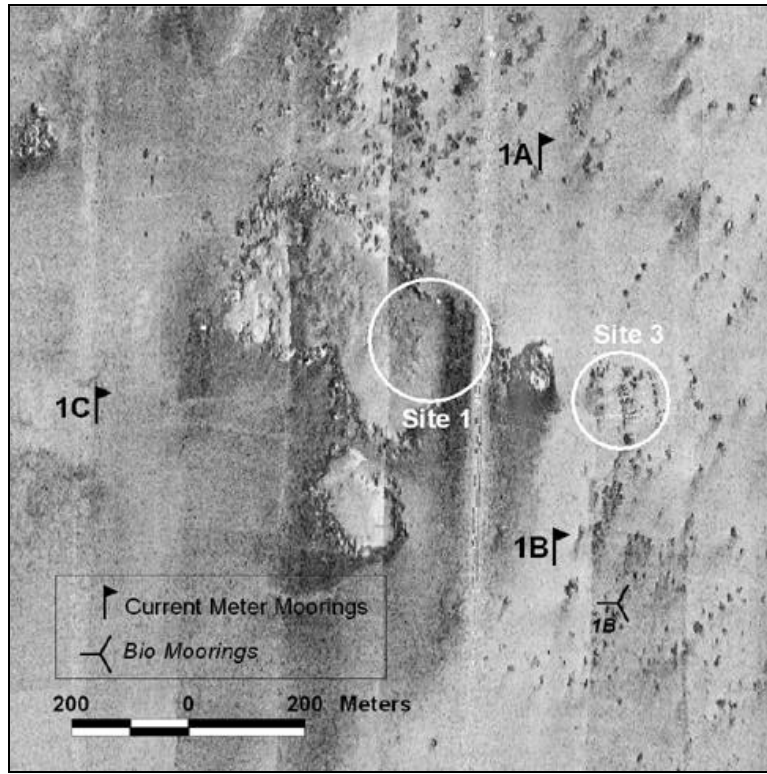


Fig. 10.3. TAMU² side-scan sonar mosaic of Site 1. Current meter mooring locations are indicated by flags. Biomoring location is indicated by triad.

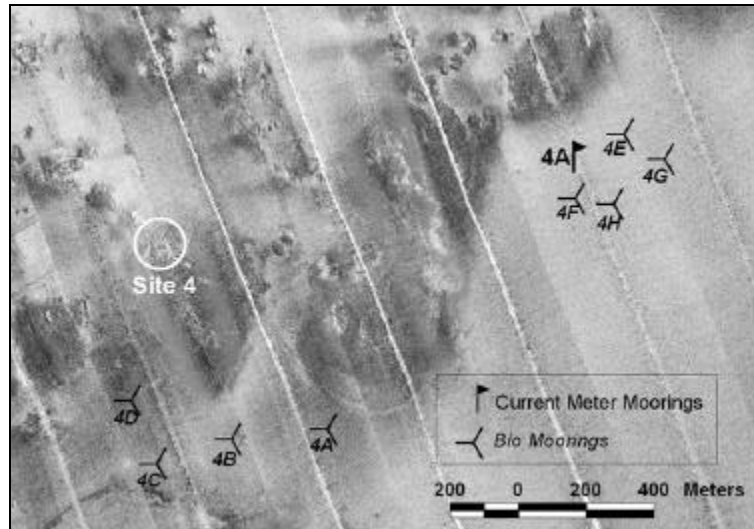


Fig. 10.4. TAMU² side-scan sonar mosaic of Site 4. Current meter mooring location is indicated by flag. Biomoring locations are indicated by triads.

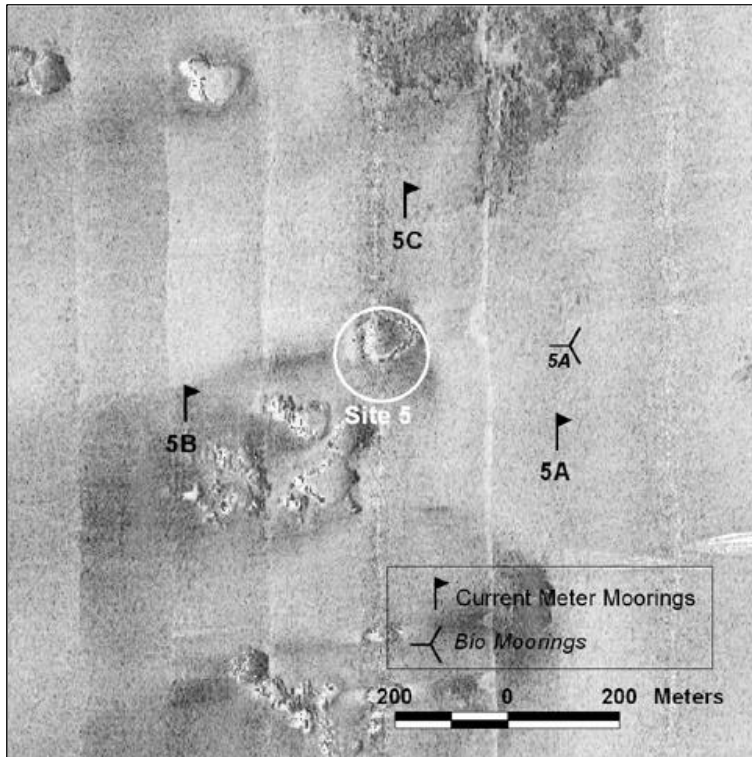


Fig. 10.5. TAMU² side-scan sonar mosaic of Site 5. Current meter mooring locations are indicated by flags. Biomoorings location is indicated by triad.

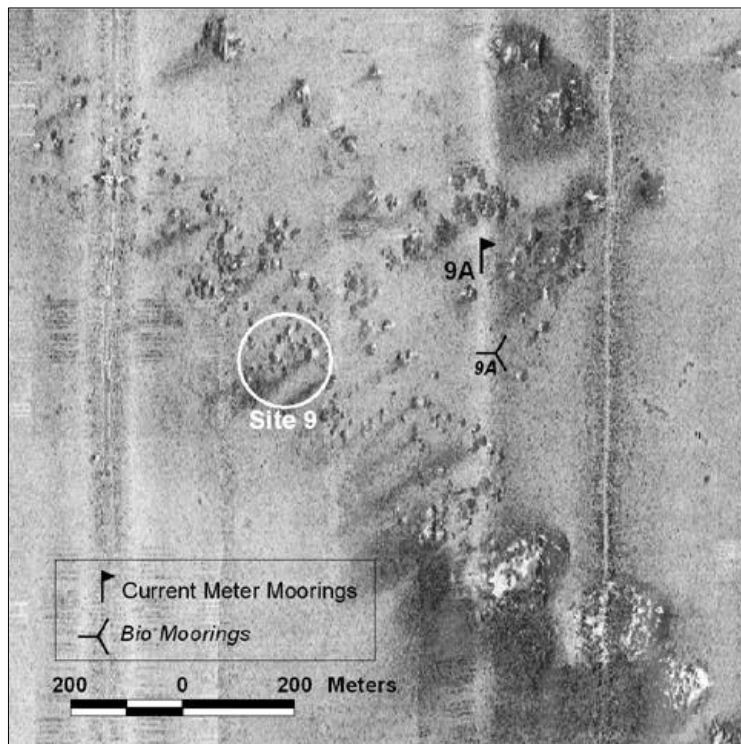


Fig. 10.6. TAMU² side-scan sonar mosaic of Site 9. Current meter mooring location is indicated by flag. Biomoorings location is indicated by triad.

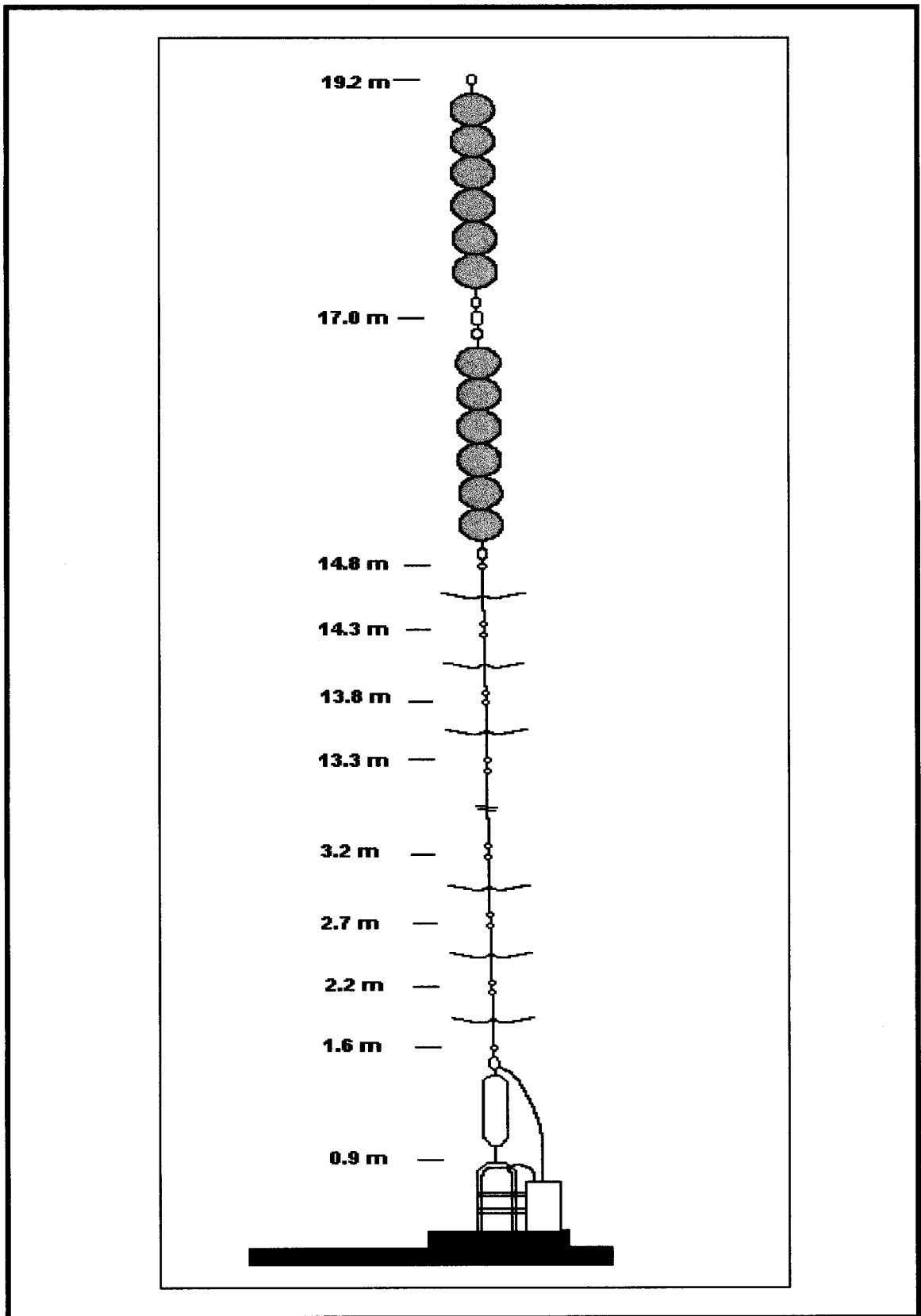


Fig. 10.7. Biomoooring with three replicate triads at two heights above bottom.

of nepheloid layers sometimes present in the region. Therefore, the biomoooring design contains three replicated triads in the nepheloid layer and three above.

Replicate triads were connected to one another with shackles. The triads at 3 mab were connected to an acoustic release and anchor at one end and a rope to separate them from the 13 mab replicates at the other (**Fig. 10.7**). The 13 mab replicate triads were attached to the other end of the separation rope and to floats at the other end. The floats were designed to ensure that the biomoorings would remain suspended throughout exposure periods.

Each triad contained 12 settling plate samples (3 experimental manipulation replicates \times 4 plate orientations). At each height there were 36 samples (3 manipulations \times 4 orientations within each manipulation \times 3 replicate manipulations). Therefore, each orientation for each manipulation was replicated 3 times at a given height. In total, biomoorings consisted of 72 samples (2 heights \times 36 samples).

Biomoooring deployment and retrieval cruises were scheduled to coincide with ROV surveys to efficiently utilize ship time and labor. Weather and equipment failure often led to rescheduling of deployments and retrievals. Therefore, actual deployment and retrievals were not conducted on the designed schedule (every 3 months) and biomoooring exposure periods ended up spanning many months and seasons.

During the first retrieval cruise, the acoustic soundings failed to release the biomoorings. Upon ROV inspection, it was discovered that shackles had failed and the floats of the biomoorings were lost. Shackle failure caused all biomoorings deployed before January 1998 to fall to the bottom. There were between one and four triads remaining at each location from which to collect samples. The orientation information from these biomoorings was unretrievable but an additional height, 0 mab, was gained. The entire temporal study was represented by the 0 mab height, as are some site replicates of the spatial study.

Biomoorings deployed later in the project were constructed with shackles from a different source and reinforced with nylon line strung through the anchor, shackles, triads, and floats to prevent further loss of data. These biomoorings were deployed following the original design of two heights at 3 and 13 mab. These deployments allow comparisons of three different heights (0, 3, and 13 mab) instead of the original plan for two heights.

A temporal study was conducted at Site 4 with retrievals at 5, 15, and 27 months (**Table 10.1**). All biomoorings from the temporal study are from 0 mab. The spatial study incorporated biomoorings from all sites (**Table 10.2**). All upright biomoorings (3 mab and 13 mab) were exposed for 19 months at all sites, and this is referred to the “elevated spatial study.” These biomoorings can be analyzed for differences between sites, water column depths, height above bottom, manipulations, and orientations.

Additional biomoorings from Sites 1, 4, and 9 (0 mab) were exposed for 15 months and for 27 months at Sites 4 and 5 (0 mab). These biomoorings represent two bottom spatial studies. While they cannot be statistically compared, the bottom spatial study with 15 month

exposure can be qualitatively compared to the elevated spatial study of 19 month exposure at the same sites.

Upon retrieval, the location of each biomoooring was recorded with GPS and settling plates removed from the triads. Each settling plate was assigned a unique sample number and a code tag labeling the exact site, height, manipulation, and orientation of each sample. To avoid processing bias, sample numbers were the only identification used for each settling plate during analysis. While in the field, sample numbers and code tags were entered into a deck log. Each sample was then placed in an individually labeled storage container matching both its sample number and identification tag. Before statistical analysis, the sample numbers were paired back with their identification tag with the log book to ensure proper analysis of data.

Laboratory Analysis

The first biomoooring retrieved was placed directly into 2% formalin for preservation. All later samples were placed in standing seawater on the deck to reduce shock and to free motile organisms. After the tiles were removed from the triads, they were placed in a 7% MgCl₂ solution for approximately 2 hours to relax tentacles, valves, and polyps. Next, a buffered formalin solution was added to the sample containers to achieve a final dilution of 2% formalin. The samples then were transported to the laboratory for analysis. Representatives of all motile organisms found in or around the triads, and all organisms attached to the current moorings, were collected and preserved for identification.

In the laboratory, formalin was removed with a 63- μ m sieve and retained mud, shell fragments, etc., were placed into small, individually labeled vials. Sieved samples were used as a reference to help identify unknown organisms. Motile organisms retained from these same samples were stored in vials labeled with the sample number to identify potential predators at each height and site. The tiles then were transferred to a 50% ethanol solution for long-term storage.

Settling plates were scored for abundance as percent cover using quadrat analysis. Quadrat analysis can yield precision error estimates of less than 10% (Menge 1976). Plates were scored by taxa and category (e.g., sediment, uncolonized) to the lowest taxonomic level possible. Areal coverage was measured for colonial and clonal organisms, and individual abundance was measured for solitary organisms.

Samples were stained with rose bengal for ease of identification and a 14.7 mm²-mesh grid with 625 cells was placed over the entire settlement plate. Grid size was chosen by comparing several mesh sizes early in the study. The mesh size chosen optimized precision and analysis time by ensuring coverage of a majority of organisms would not be overestimated, while reducing the difficulty in analyzing an exorbitant number of grid cells. Samples were analyzed with a dissecting scope at 16X magnification.

Total coverage of samples may exceed 100% due to overgrowth and competitive interactions. It is possible that several categories of organisms (stolons, hydroids, and foraminiferans) were overestimated by the grid size. However, most of these organisms have

defense strategies that make settlement near them difficult and, therefore, most may take up more space in colonization than their anatomy indicates.

Edges (outer 8 mm) of samples were not analyzed because slight shifting of the plate while in the triad could have possibly altered exposure period along the edges of the sample. Presence of a colonial organism in any part of a cell counted for the entire cell. Coverage of non-colonial organisms was measured similarly. Abundances were collected for all non-colonial organisms. The non-colonial organisms include solitary scleractinian corals, solitary sea anemones, bivalves, polychaetes, and barnacles.

Statistical Analysis

The design of this study was complex, with five major sources of variation (i.e., main effects): orientation, experimental manipulations, heights above bottom, time, and site. This was not a complete block design, however, so data were analyzed separately for spatial and temporal effects. This reduces the design to a 2- or 4-way analysis of variance (ANOVA), which is still too complex. Complex designs often have many significant interactions, which make interpretation of main effects difficult, if not impossible. An additional complexity in analysis existed in the two distinct kinds of metrics: percent cover of colonial forms, and abundance of individual forms. These were analyzed separately and individual abundances (n) were log transformed ($\ln n + 1$). All analyses were performed using SAS software (SAS Institute, Inc. 1989).

For the temporal study, a 2-way ANOVA was used to distinguish among manipulation and exposure period effects. In addition, variance component analysis was utilized to determine the percent of the variance contributed by each source of variation. The sample plates were retrieved 5, 15, and 27 months after deployment (**Table 10.1**). All samples came from Site 4 at 0 mab, so site and height above bottom are not included in the model. There were 114 samples included in the temporal study.

In the spatial study, samples that were on the bottom due to shackle failure (0 mab) and at two heights (3 and 13 mab) were treated in separate analyses due to different exposure periods. For samples from the bottom spatial study (0 mab), orientation was not recoverable, so 2-way ANOVAs of site and experimental manipulation and variance component analysis were performed on these data. There were 62 samples in the bottom spatial study.

Differences due to height above bottom (3 and 13 mab), site (1, 4, 5, and 9), manipulation (C, P, and U), and orientation (top, bottom, and side) effects were successfully tested in the second biomoorings deployment (**Table 10.2**). This deployment was retrieved after 19 months for all samples, so time was not included in the model. Coverage and abundances were analyzed with a 4-way ANOVA (site, height above bottom, experimental manipulation, and orientation). Variance component analysis was also used in examining the data. There were 216 samples from the elevated spatial study.

Tukey tests, a post-hoc multiple comparison test, were performed to determine significant differences between levels of exposure periods, sites, heights, treatments or orientations. Tukey tests were performed with all ANOVA tests.

Principal components analysis (PCA) was performed on the spatial study data to determine if community differences existed between sites, heights, experimental manipulations, and orientation. The PCA was performed on the covariance matrix of the data to account for covarying non-occurrence of taxa, which is common in ecological data. For percent cover, PCA analysis was run on the 15 major taxa and categories found in the spatial study. For abundances, the analysis was run on the six major taxa composed of solitary organisms.

Results

Taxa and Categories

A total of nine phyla were found in the temporal and elevated spatial studies (**Table 10.3**). All phyla except Porifera were present at every study site. Sponges were found on only a handful of samples from 3 and 13 mab at Sites 1 and 4. Sponges were not found on any samples from 0 mab.

The taxonomic level used for analysis was determined by the lowest level that could consistently be accurately identified. In addition, morphologies and life histories were used to distinguish differences between related, but ecologically different, taxa. For example, zoanthids, anemones, and scleractinian corals are all closely related (Class Anthozoa) and share some behavioral, morphological, and life history traits, but were analyzed separately. Anemones are solitary and may be able to move location if resources are inadequate or if threatened by a predator. In contrast, zoanthid colonies and scleractinian corals are fixed to the substrate and must adapt to the surrounding habitat if changes occur. Scleractinian corals (solitary disk corals in the study area) can withdraw into a calcium carbonate skeleton for protection, an adaptation that zoanthids and anemones do not possess. These morphologies and behaviors are different enough to indicate possible differences in presence and success of taxa.

Bivalves were separated into the orders Pterioidea (winged oysters) and Ostreoida (scallops and oysters) for analysis (**Table 10.3**). Winged oysters are attached by byssal threads, which allow them to move freely from the substrate and suspend above many of the other epibenthic organisms. By feeding well above the substrate, winged oysters are able to access resources not available to other competing organisms. In contrast, scallops (Family Pectinidae) and other oyster-like bivalves (Family Dimyidae) present in the study area are permanently attached to the substrate by one valve and feed very near the substrate surface. Dimyidae are able to feed slightly above the substrate surface somewhat as they grow larger, due to valves which grow in an upward curve. However, they never achieve the vertical relief of winged oysters and as young, small bivalves, they feed much the same way that scallops do.

All bryozoans were analyzed together due to similarities in feeding and growth forms of orders found in the study area (**Table 10.3**). Polychaetes were analyzed together for the same reason. Barnacles (Class Cirripedia) and ascidians (Class Ascidiacea) were analyzed at the class level due to difficulty in identification at a lower level.

Table 10.3. Taxa found in the study area by site. Bold type indicates level of taxa used in the study. Presence within a study site is indicated with an "X."

Taxonomic Headings					Site			
Phyla	Class	Order	Family	Genus	1	4	5	9
Rhizopoda	Granulorcticulosea	Foraminifera			X	X	X	X
Porifera					X	X		
Cnidaria	Hydrozoa	Hydroida			X	X	X	X
	Anthozoa	Zoanthidea – zoanthids			X	X	X	X
		Actinaria – anemones			X	X	X	X
		Scleractinia – solitary disk corals			X	X	X	X
Ectoprocta (Bryozoa)	Stenolaemata							
		Cyclostomata			X	X	X	X
	Gymnolaemata							
		Ctenostomata			X	X	X	X
		Cheilostomata			X		X	X
Entoprocta					X	X	X	X
Mollusca	Bivalva	Pterioida						
			Pteriidae – winged oysters		X	X	X	X
			<i>Pteria</i>					
		Ostreoida						
			Pectinidae – scallops		X	X	X	X
			Dimyidae – small, oyster-like bivalves		X	X	X	X
			<i>Dimya</i>					
Annelida	Polychaeta				X	X	X	X
		Spionida						
			Spionidae					
		Sabellida						
			Sabellidae					
			Serpulidae					
			Spirorbidae					
Arthropoda	Cirripedia				X	X	X	X
Chordata	Asciacea				X	X	X	X

In addition to taxa identifications, presence or absence of stolon coverage, uncolonized area, and sediment coverage were recorded and analyzed. All of these categories are important to understand the ecological dynamics of the epibiont community. Stolon coverage refers to the area covered by stolons, or vine-like runners, of hydroid and bryozoan colonies. In many cases, there were no mature individuals within neighboring grid cells by which to identify the stolons as belonging to a hydroid colony or a bryozoan colony. In these cases, stolons were classified in their own category.

Uncolonized area refers to total area that was absent of any living organisms. Bivalve and polychaete valve pieces and tube fragments that were absent of epiphytes were categorized as uncolonized. Sediment coverage refers to any cell that contained sediment. Sediment levels may not have been high enough to interfere with feeding or other behaviors, but presence of sediment is important to note, both in terms of temporal variation and spatial differences. These three types of coverage will be referred to as 'categories' of coverage for the purposes of this study.

Temporal Study

Coverage

Percent cover of taxa and categories from the temporal study located 0 mab exhibited two patterns: those with greater than 10% total coverage (**Fig. 10.8**) and those with less than 10% total coverage (**Fig. 10.9**). Total area covered by organisms was greater than 96% at 5-month, 15-month, and 27-month exposure periods (**Figs. 10.10, 10.11, and 10.12**). Percent cover of many taxa and sediment increased significantly through time.

Experimental manipulation effects on coverage were not significant for any taxa or category. Ecological processes did not have a great effect on those taxa with greater than 10% total coverage (<15% change from net recruitment) (**Table 10.4**). Water-flow disruption (W) inhibited all organisms with greater than 10% total coverage with the exception of foraminiferans. Disturbance (D) had a more taxa-specific effect: hydroids and polychaetes were inhibited but coverage was enhanced for stolons, bryozoans, and foraminiferans.

Taxa and categories with less than 10% total coverage were affected to a greater extent but were still not significant (>28% change from net recruitment) (**Table 10.4**). Disturbance (D) and water-flow disruption (W) enhanced total coverage of plates as indicated by the reduction in uncolonized area. Ostreoida was enhanced by both disturbance (D) and water-flow disruption (W). Entoprocts were enhanced to a great extent (~400%) by both ecological processes. Ascidiaceans, anthozoans, and total sediment cover were all inhibited by both disturbance (D) and water-flow disruption (W).

Variance component analysis indicates that the majority of variance for coverage of all taxa is contained within the error component (**Table 10.5**). In other words, more variance is contained between the coverages of individual random samples than between components. However, several organisms with greater than 10% total coverage increased significantly over the 27 month study period (**Fig. 10.8**). Polychaetes increased throughout the study period. The difference in polychaete coverage between the 27-month exposure period and

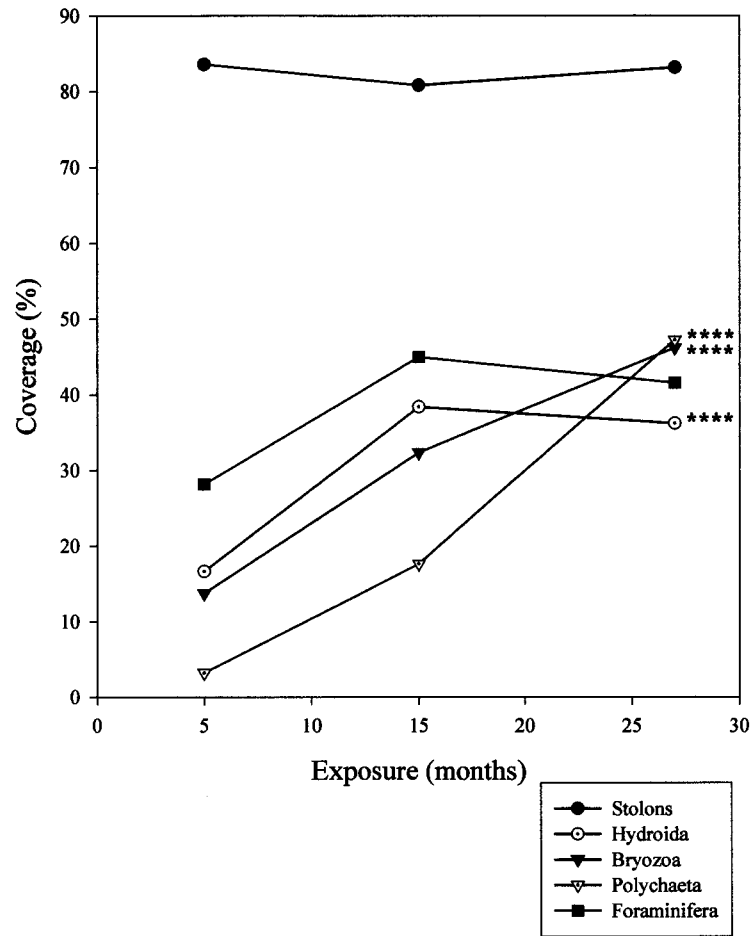


Fig. 10.8. Percent cover results for exposure period from temporal study by taxa with >10% total coverage. Depth of settlement plates was 0 meters above bottom. Significance levels from 2-way ANOVA are indicated with asterisks where **** = $p < 0.0001$, *** = $p < 0.001$, ** = $p < 0.01$, and * = $p < 0.05$.

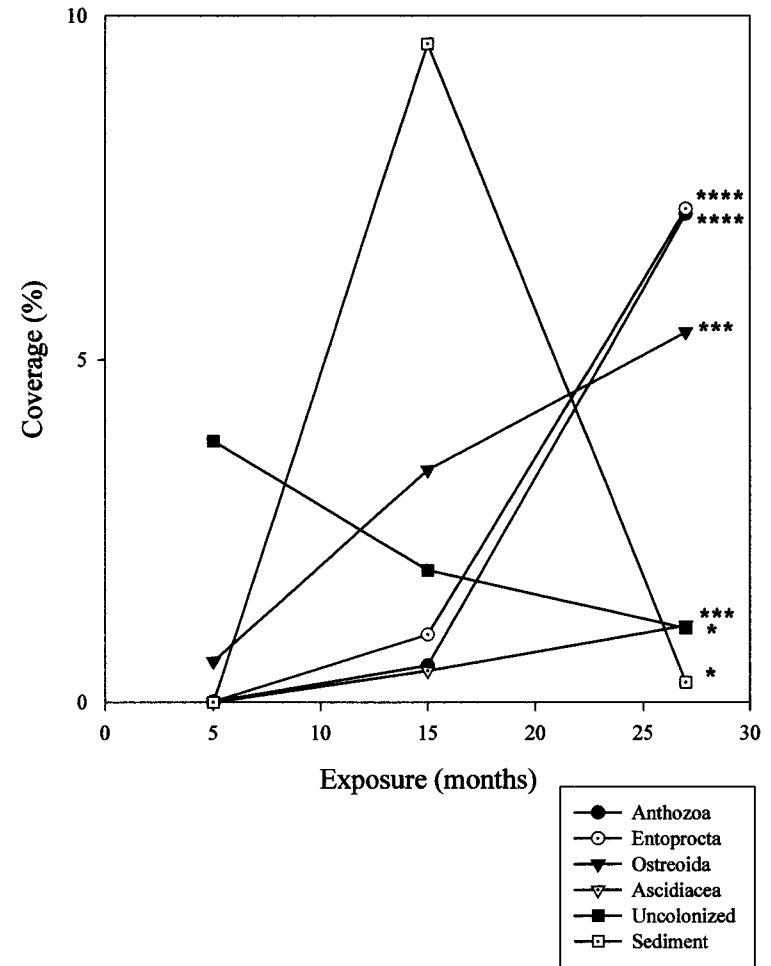


Fig. 10.9. Percent cover results for exposure period from temporal study by taxa and categories with <10% total coverage. Depth of settlement plates was 0 meters above bottom. Significance levels from 2-way ANOVA are indicated as in Fig. 10.8.

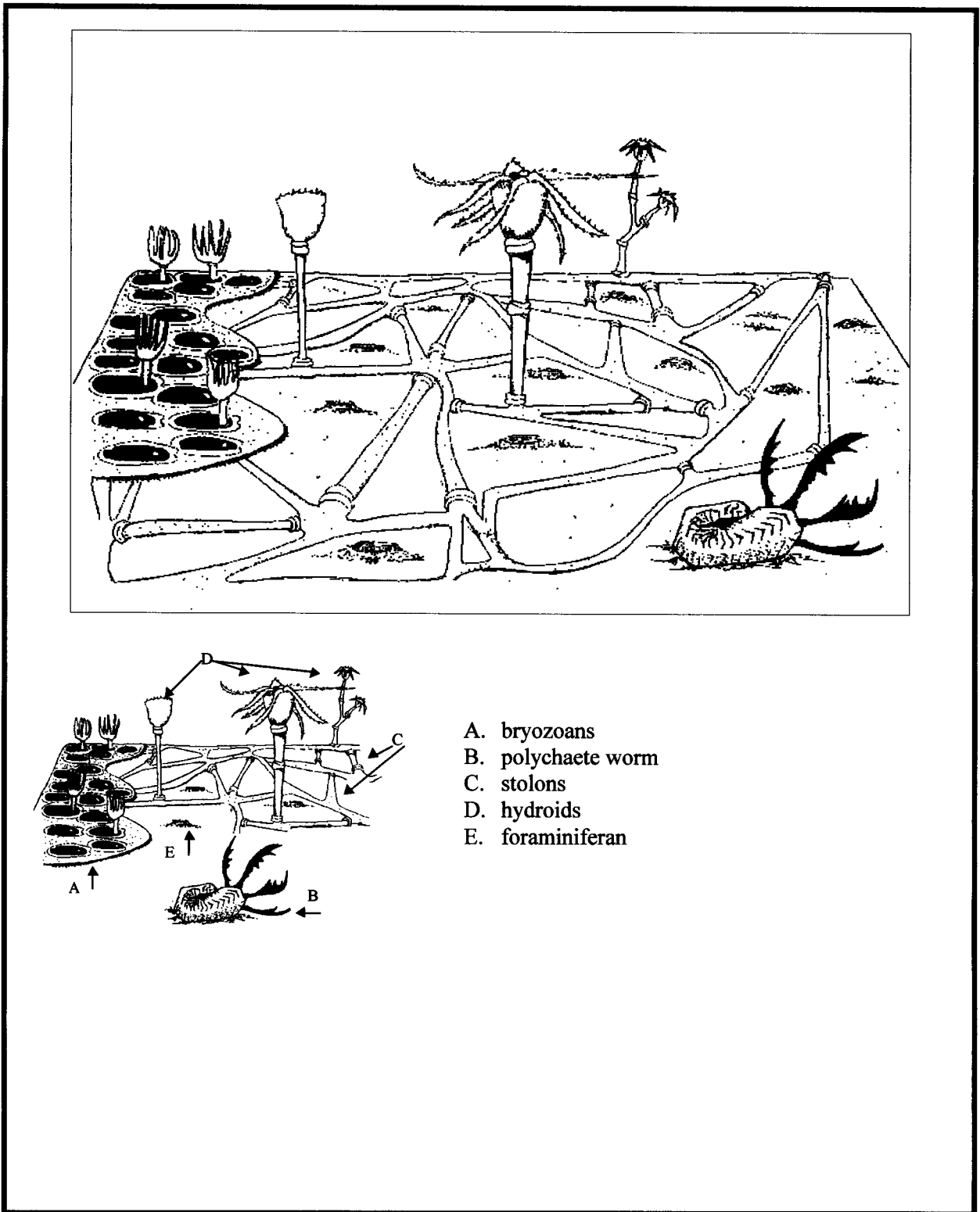
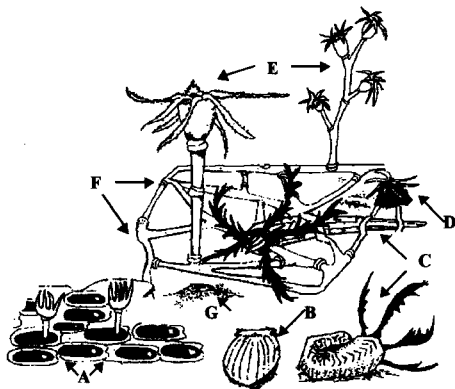
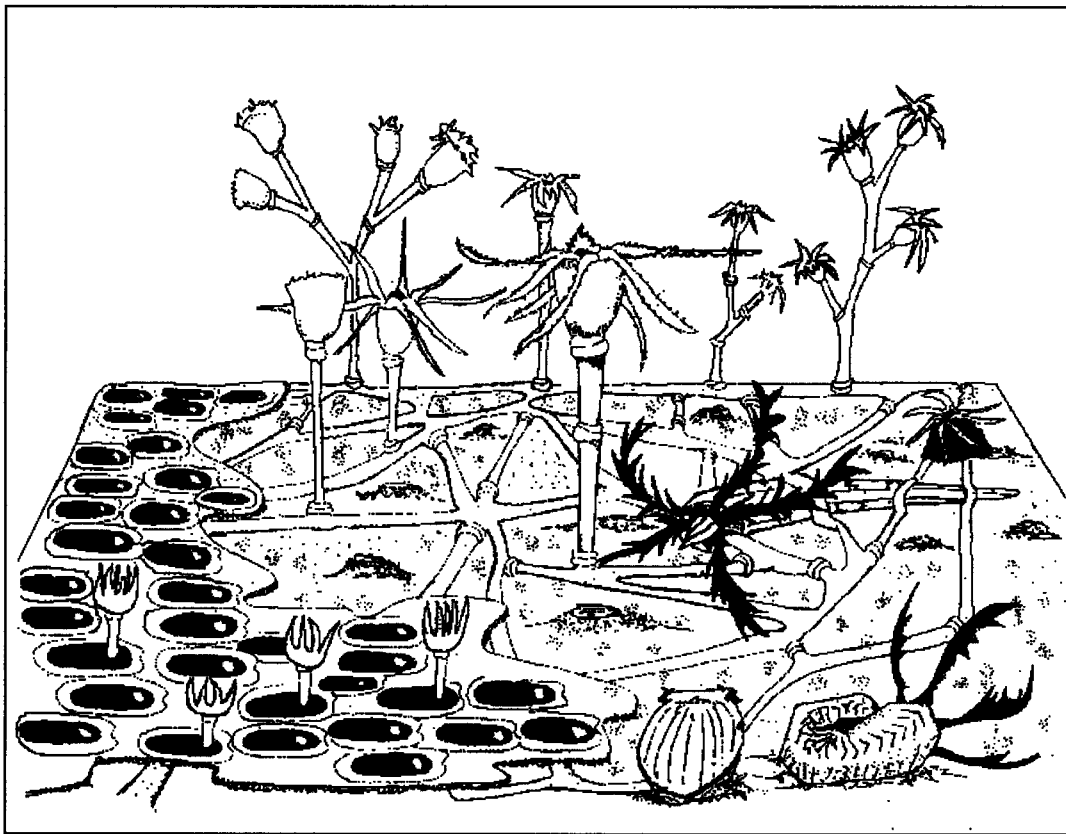
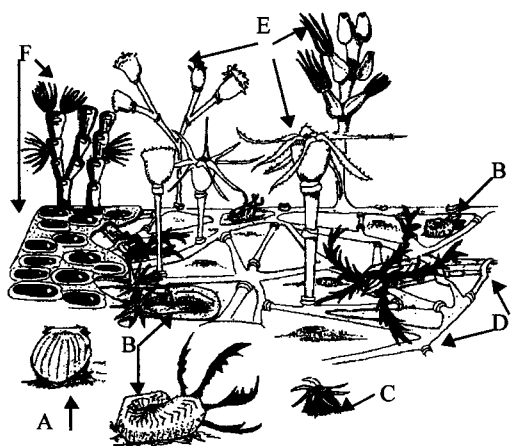
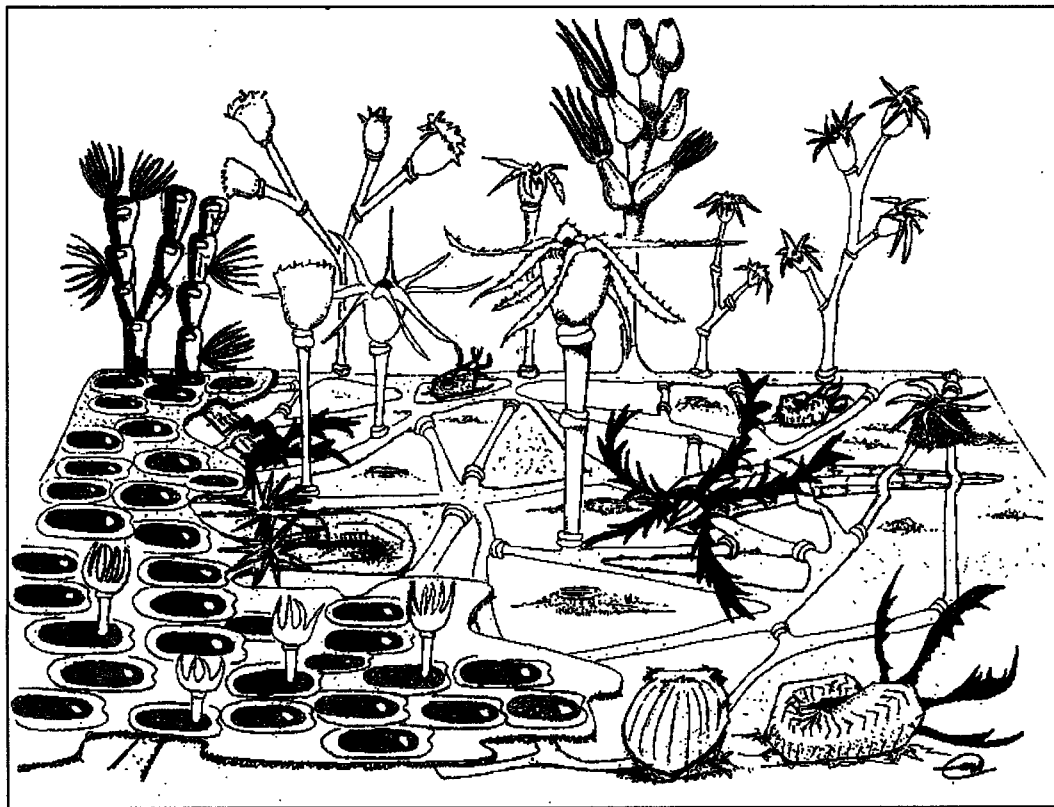


Fig. 10.10. Artistic interpretation of average epibenthic community structure at 0 m above bottom based on percent cover and abundance means after 5-month settling plate exposure period. Width of drawing represents ~10 cm, but organisms not to scale. Artwork by C. Halverson.



- A. bryozoans
- B. bivalve (Order Ostreoida)
- C. polychaete worms
- D. solitary anemone (Order Actinaria)
- E. hydroids
- F. stolons
- G. foraminiferan

Fig. 10.11. Artistic interpretation of average epibenthic community structure at 0 m above bottom based on percent cover and abundance means after 15-month settling plate exposure period. Width of drawing represents ~10 cm, but organisms not to scale. Artwork by C. Halverson.



- A. bivalve (Order Ostreoida)
- B. polychaete worms
- C. solitary anemones (Order Actinaria)
- D. stolons
- E. hydroids
- F. bryozoans

Fig. 10.12. Artistic interpretation of average epibenthic community structure at 0 m above bottom based on percent cover and abundance means after 27-month settling plate exposure period. Width of drawing represents ~10 cm, but organisms not to scale. Artwork by C. Halverson.

Table 10.4. Rates of change in taxa coverage (cm²) averaged over 27 months of exposure caused by ecological process in the temporal study. Positive rate values indicate coverage is enhanced by an ecological process. Negative values indicate ecological process inhibits coverage.

Taxa	Disturbance (D) (cm ² /27 months)	Water Flow Disruption (W) (cm ² /27 months)	Net Recruitment (S) (cm ² /27 months)
Stolons	0.09	-5.16	75.03
Hydroida	-1.73	-5.15	33.40
Bryozoa	4.02	-0.62	24.15
Entoprocta	1.22	1.58	-0.35
Anthozoa	-0.47	-0.18	1.70
Ostreoida	0.30	1.52	1.44
Polychaeta	-6.59	-0.51	21.22
Foraminifera	1.01	3.73	32.21
Asciacea	-0.04	-0.22	0.57
Uncolonized	-0.23	-0.73	2.61
Sediment	-8.96	-0.69	11.48

Table 10.5. Percent of variance for sources of variation from temporal study by taxa and category, calculated for percent cover by variance component analysis. Levels of variance by each source are indicated in percentages. Sources of variance include experimental manipulation (E.M.), exposure (E), their interaction (E.M. x E), and the total error (Error).

Source	Stolon	Hydroida	Bryozoa	Anthozoa	Entoprocta	Ostreoida
E.M.	0.85	0.00	0.00	0.00	2.44	3.36
E	0.00	22.25	21.83	44.17	24.82	13.93
E.M.x E	0.00	1.65	1.25	0.00	0.00	0.00
Error	99.15	76.10	76.92	55.83	72.75	82.71

Source	Polychaeta	Foraminifera	Asciacea	Uncolonized	Sediment
E.M.	0.26	0.00	0.00	0.10	0.00
E	22.24	6.50	16.20	5.76	8.65
E.M.x E	0.64	0.00	0.00	0.00	13.26
Error	76.86	93.50	83.80	94.14	78.09

the 5- and 15-month exposure periods is highly significant (2-way ANOVA, $p < 0.0001$; Tukey, Minimum Significant Difference (MSD) = 14.96%). Bryozoans exhibited a similar increasing trend. Bryozoan coverage at 15 and 27 months were significantly different from 5-month exposure periods (2-way ANOVA, $p < 0.0001$; Tukey, MSD = 14.51%). Both hydroids and foraminiferans increased from 5 to 15 months and decreased from 15 to 27 months. The trend for hydroids was significant where 27- and 15-month exposure periods had significantly higher percent cover than 5-month exposure periods (2-way ANOVA, $p < 0.0001$; Tukey, MSD = 16.15%). Stolons did not change significantly throughout the study period (2-way ANOVA, $p = 0.9811$).

All organisms with less than 10% total coverage increased throughout the study period (**Fig. 10.9**). Sediment increased significantly from 5 to 15 months and decreased significantly from 15 to 27 months (2-way ANOVA, $p = 0.0123$). Both anthozoans (primarily zoanths in the temporal study) and entoprocts increased significantly from 15 to 27 months (2-way ANOVA, $p < 0.0001$; Tukey, MSD = 1.87% and 2.87%, respectively). Percent cover of Ostreoida, the only bivalves present in the temporal study, was significantly different between 5 and 27 months (2-way ANOVA, $p = 0.0010$; Tukey, MSD = 2.98%). Ascidians increased significantly throughout the study period (2-way ANOVA, $p = 0.0002$). Ascidian coverage on plates from 5-month exposure periods was significantly less than coverage on plates at 27 months (Tukey, MSD = 0.72%). Uncolonized area decreased significantly between 5 and 27 months (2-way ANOVA, $p = 0.0444$; Tukey, MSD = 2.74%).

Abundance

Of the eight taxa found during the temporal study, three taxa were solitary (i.e., individual) organisms. Abundances of Ostreoida, polychaetes, and solitary disk corals (Scleractinia) all increased through time (**Fig. 10.13**). Experimental manipulation did not have a significant effect on abundances of any taxa. In general, disturbance had a greater overall affect on abundances (average 23% change from net recruitment) than did water-flow disruption (W) (average 3% difference from net recruitment) (**Table 10.6**). Polychaeta, the dominant solitary taxa, were inhibited by both ecological processes, while bivalves were enhanced by the ecological processes. Scleractinians were inhibited by disturbance, but were neutrally affected by water-flow disruption.

Variance component analysis shows that most of the variance for abundances of all taxa was contained within the error component (**Table 10.7**). Thus, there was more variance between individual samples than between other sources of variation in the experimental design.

Polychaetes increased logarithmically and significantly from 5 to 15 to 27 months (2-way ANOVA, $p < 0.0001$; Tukey, MSD = 0.94%). Ostreoida also increased logarithmically through time (**Fig. 10.13**). However, differences between exposure periods cannot be determined for Ostreoida because there was a significant interaction between exposure period and manipulation (**Fig. 10.14**; 2-way ANOVA, $p = 0.0122$). Solitary disk corals do not appear until after 15 months of exposure. However, significance of scleractinian abundance changes over time cannot be determined because of a significant interaction of exposure period and experimental manipulation (2-way ANOVA, $p < 0.0001$).

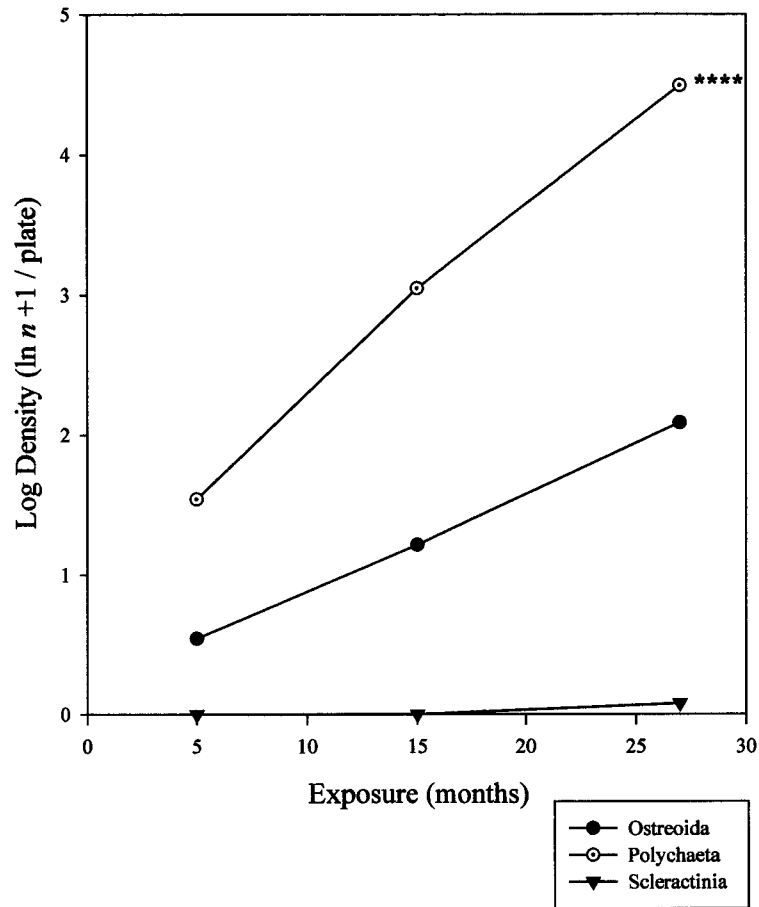


Fig. 10.13. Abundance of solitary taxa for exposure periods during the temporal study. Significance levels from 2-way ANOVA indicated as in Fig. 10.8. Abundances were log transformed ($\ln n + 1$) prior to analysis.

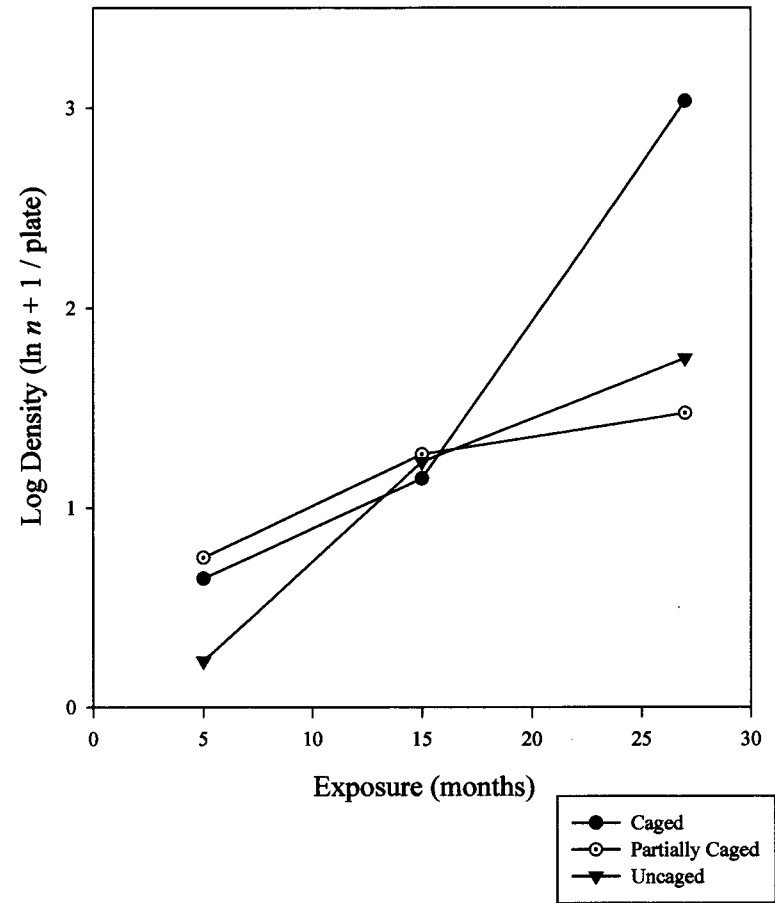


Fig. 10.14. Interaction for abundance ($\ln n + 1$) between exposure periods and experimental manipulations for Ostreoida.

Table 10.6. Rates of change in abundance ($\ln n + 1$ individuals) averaged over 27 months of exposure caused by ecological processes in temporal study. Positive values indicate abundances were enhanced by an ecological process. Negative values indicate an ecological process inhibited abundances.

Taxa	Disturbance (D) ($\ln n + 1/27$ months)	Water Flow Disruption (W) ($\ln n + 1/27$ months)	Net Recruitment (S) ($\ln n + 1/27$ months)
Bivalva	0.02	0.17	2.59
Polychaeta	-0.55	-0.05	1.97
Scleractinia	-0.04	0.00	0.10

Table 10.7. Percent of variance for taxa and categories in temporal study calculated for abundance ($\ln n + 1$) by variance component analysis. Levels of variance by each source are indicated in percentages. Sources of variance include experimental manipulation (E.M.), exposure (E), their interaction (E.M. x E), and the total error (Error).

Source	Ostreoida	Polychaeta	Scleractinia
E.M.	0.00	0.41	0.00
E	22.37	27.62	6.77
E.M. x E	1.80	0.45	6.30
Error	75.84	71.52	86.94

Elevated Spatial Study

All 12 taxa and three categories found during this entire project were found in the elevated spatial study. Stolons, hydroids, bivalves, foraminiferans, and zoanthids were the most abundant organisms in coverage, while bivalves were the most abundant solitary organisms. Sponges were found on only two samples, so were not statistically analyzed.

ANOVA – Coverage

Significant results from the 4-way ANOVA on percent cover were highly complex with interactions between main effects for most taxa and categories (**Table 10.8**). There were no consistent, overall patterns between sites (**Fig. 10.15**). Only entoprocts, scleractinian corals and uncolonized area had significant differences between sites. All other taxa and categories had significant site interactions. Scleractinians had significantly greater coverage at Site 4 than at Sites 1, 5, and 9 (4-way ANOVA, $p = 0.0003$; Tukey, MSD = 0.25%). Uncolonized area was significantly greater at Site 5 than at Sites 1, 4, and 9 (4-way ANOVA, $p < 0.0001$; Tukey, MSD = 1.42). Site 5 had the lowest overall coverage for stolons and hydroids and was never the site of greatest coverage except for solitary anemones (Order Actinaria) that were present only in Site 5.

Sediment coverage increases towards Site 9 (**Fig. 10.15**). Of the 12 taxa found, 5 had the greatest coverage at Site 4, including scleractinians, zoanthids, polychaetes, foraminiferans,

Table 10.8. Significance values for percent cover calculated by a 4-way ANOVA from elevated spatial study by taxa and category. Sources of variance, degrees of freedom (df), and significant p-values are listed for each taxa and category. Sources of variance include site (S), depth (D; i.e., height above bottom), experimental manipulation (E.M.), orientation (O), and their interactions.

Source	df	Taxa							
		Stolon	Hydroida	Bryozoa	Entoprocta	Zoanthidae	Actinaria	Scleractinia	Pterioida
S	3	<0.0001	<0.0001	ns	0.0013	<0.0001	<0.0001	<0.0001	0.0016
D	1	ns	ns	<0.0001	0.0058	ns	<0.0001	ns	ns
S × D	3	ns	ns	ns	ns	<0.0001	<0.0001	ns	ns
E.M.	2	ns	ns	0.0427	ns	ns	0.0229	ns	ns
S × E.M.	6	0.0398	0.0187	0.0109	ns	0.0021	0.0007	ns	ns
D × E.M.	2	ns	ns	ns	ns	ns	0.0205	ns	ns
S × D × E.M.	6	ns	ns	ns	ns	ns	0.0004	ns	ns
O	2	0.0251	ns	0.0312	ns	ns	ns	ns	ns
S × O	6	ns	ns	ns	ns	ns	ns	ns	0.0212
D × O	2	ns	ns	ns	ns	ns	ns	ns	ns
S × D × O	6	ns	ns	ns	ns	ns	ns	ns	ns
E.M. × O	4	ns	ns	ns	ns	ns	ns	ns	ns
S × E.M. × O	12	ns	ns	ns	ns	ns	ns	ns	ns
D × E.M. × O	4	ns	ns	ns	ns	ns	ns	ns	ns
S × D × E.M. × O	12	ns	ns	ns	ns	ns	ns	ns	ns

Source	df	Ostreoida	Polychaeta	Foraminifera	Ascidiacea	Cirripedia	Uncolonized	Sediment
S	3	<0.0001	ns	<0.0001	<0.0001	<0.0001	<0.0001	<0.0001
D	1	<0.0001	<0.0001	ns	<0.0001	<0.0001	0.0146	ns
S × D	3	ns	<0.0001	ns	0.0002	ns	ns	0.0083
E.M.	2	ns	<0.0001	ns	<0.0001	ns	0.0083	<0.0001
S × E.M.	6	ns	0.0008	<0.0001	<0.0001	0.0065	ns	<0.0001
D × E.M.	2	0.0134	0.0415	ns	ns	0.0290	ns	ns
S × D × E.M.	6	0.0171	ns	ns	ns	0.0037	ns	ns
O	2	<0.0001	0.0002	<0.0001	ns	<0.0001	ns	<0.0001
S × O	6	0.0027	ns	0.0009	ns	0.0014	ns	0.0048
D × O	2	0.0012	ns	0.0123	ns	ns	ns	ns
S × D × O	6	0.0011	0.0007	0.0117	ns	ns	ns	ns
E.M. × O	4	ns	ns	ns	ns	ns	ns	<0.0001
S × E.M. × O	12	0.0159	ns	<0.0001	ns	ns	ns	<0.0004
D × E.M. × O	4	ns	0.1998	0.0017	ns	ns	ns	ns
S × D × E.M. × O	12	0.0137	ns	ns	ns	ns	ns	ns

ns = not significant.

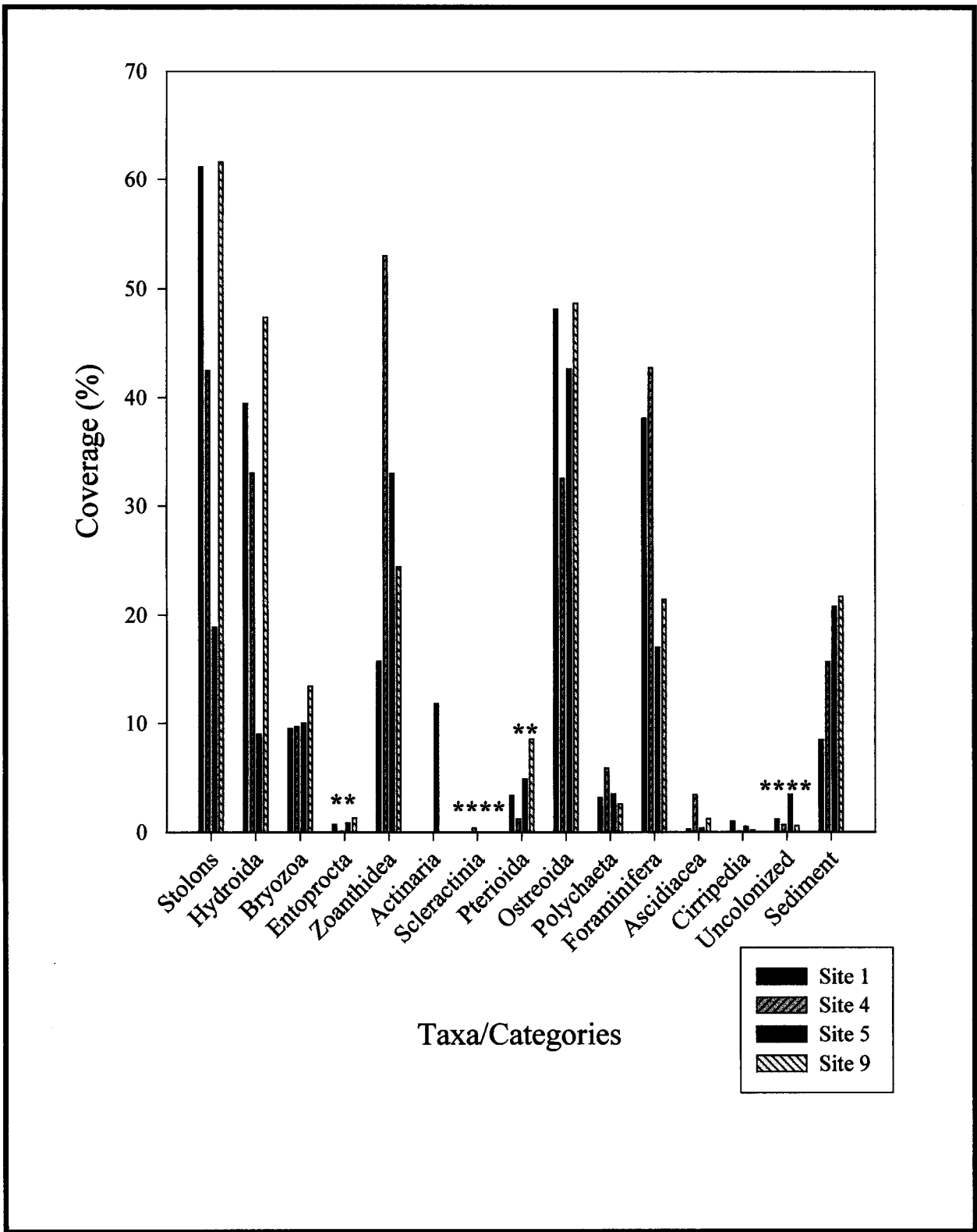


Fig. 10.15. Percent cover for taxa and categories by site from the elevated spatial study. Significance levels from 4-way ANOVA indicated as in Fig. 10.8.

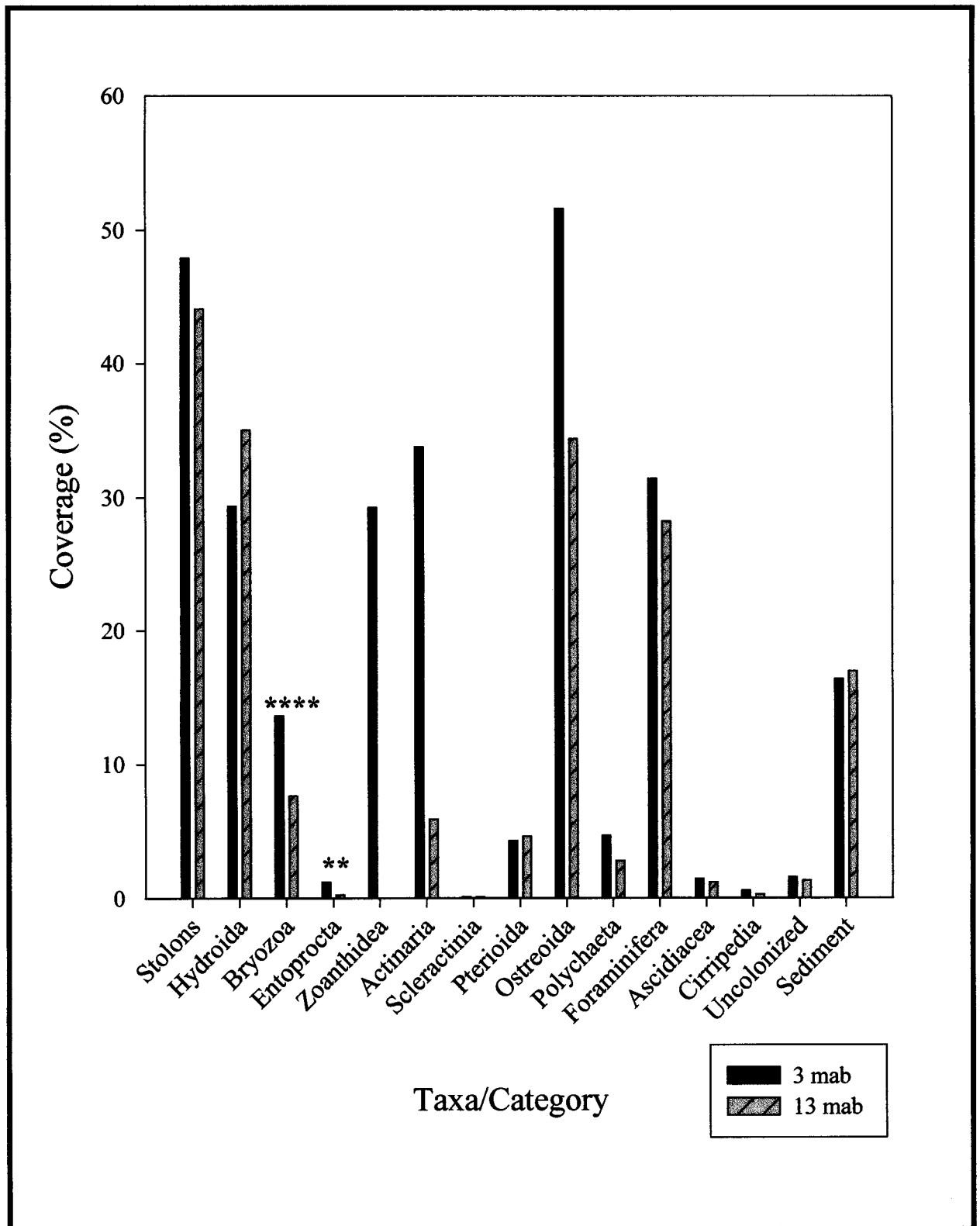


Fig. 10.16. Percent cover for taxa and categories for height (meters) above bottom (mab) from the elevated spatial study. Significance levels from 4-way ANOVA indicated as in Fig. 10.8.

and ascidians. Bivalves (Orders Pterioida and Ostreoida) had the greatest coverage at Site 9, and Site 1 had almost equal values for Ostreoida.

Most taxa and categories had greater coverage at 3 mab than at 13 mab (Table 10.8 and Fig. 10.16). Bryozoans had significantly greater coverage at 3 mab, as did entoprocts (4-way ANOVA, $p = <0.0001$ and 0.0058 , respectively; Tukey, MSD = 3.33% and 0.84% , respectively). Only Hydroida, Pterioida, and total sediment coverage were greater at 13 mab. Most taxa and categories were not significant due to significant height interactions with either site, orientation, or experimental manipulation (Table 10.8).

There were no general trends for taxa among experimental manipulations (Fig. 10.17). There were trends for taxa and categories when the data from the experimental manipulations were combined mathematically to indicate effects of ecological processes. In general, water-flow disruption (W) had much less of an effect on any taxa or category than did disturbance (D) (Table 10.9). Water-flow disruption enhanced coverage of actinarians by more than 156% as compared to overall net recruitment. Stolons, bryozoans, foraminiferans, and polychaetes were inhibited by both disturbance and water flow disruption. Hydroids, Pterioida, ascidians, barnacles, and total sediment cover were by enhanced by disturbance, but negatively affected by water flow disruption. Entoprocts were negatively affected by disturbance, while all anthozoans (including zoanthids, solitary anemones [Order Actinaria], and scleractinians) were greatly enhanced by both disturbance and water flow disruption (33%-235% increase in coverage as compared to net recruitment). Disturbance and small-scale water flow disruption both significantly enhanced total coverage by 50% and 28% from net recruitment, respectively (Table 10.9; Fig. 10.17; 4-way ANOVA, $p = 0.0083$; Tukey, MSD = 1.12).

Table 10.9. Rates of change in coverage (cm^2) caused by ecological process in the elevated spatial study over 19 months of exposure. Positive values indicate ecological processes enhance coverage. Negative values indicate ecological processes inhibit coverage.

Taxa/ Category	Disturbance (D) ($\text{cm}^2/19$ months)	Water Flow Disruption (W) ($\text{cm}^2/19$ months)	Net Recruitment (S) ($\text{cm}^2/19$ months)
Stolons	-2.93	-7.71	47.37
Hydroida	5.82	-2.38	25.89
Bryozoa	-4.16	-1.97	13.41
Entoprocta	-0.69	0.05	1.07
Zoanthidea	9.90	6.95	16.35
Actinaria	3.81	2.52	-1.62
Scleractinia	0.02	0.03	0.06
Pterioida	1.17	-0.15	3.25
Ostreoida	-2.85	0.91	38.91
Polychaeta	-2.56	-0.46	5.32
Foraminifera	-1.34	-3.97	29.63
Ascidacea	0.68	-0.46	1.01
Cirripedia	0.18	-0.05	0.29
Uncolonized	-1.30	-0.75	2.65
Sediment	10.37	-0.98	8.32

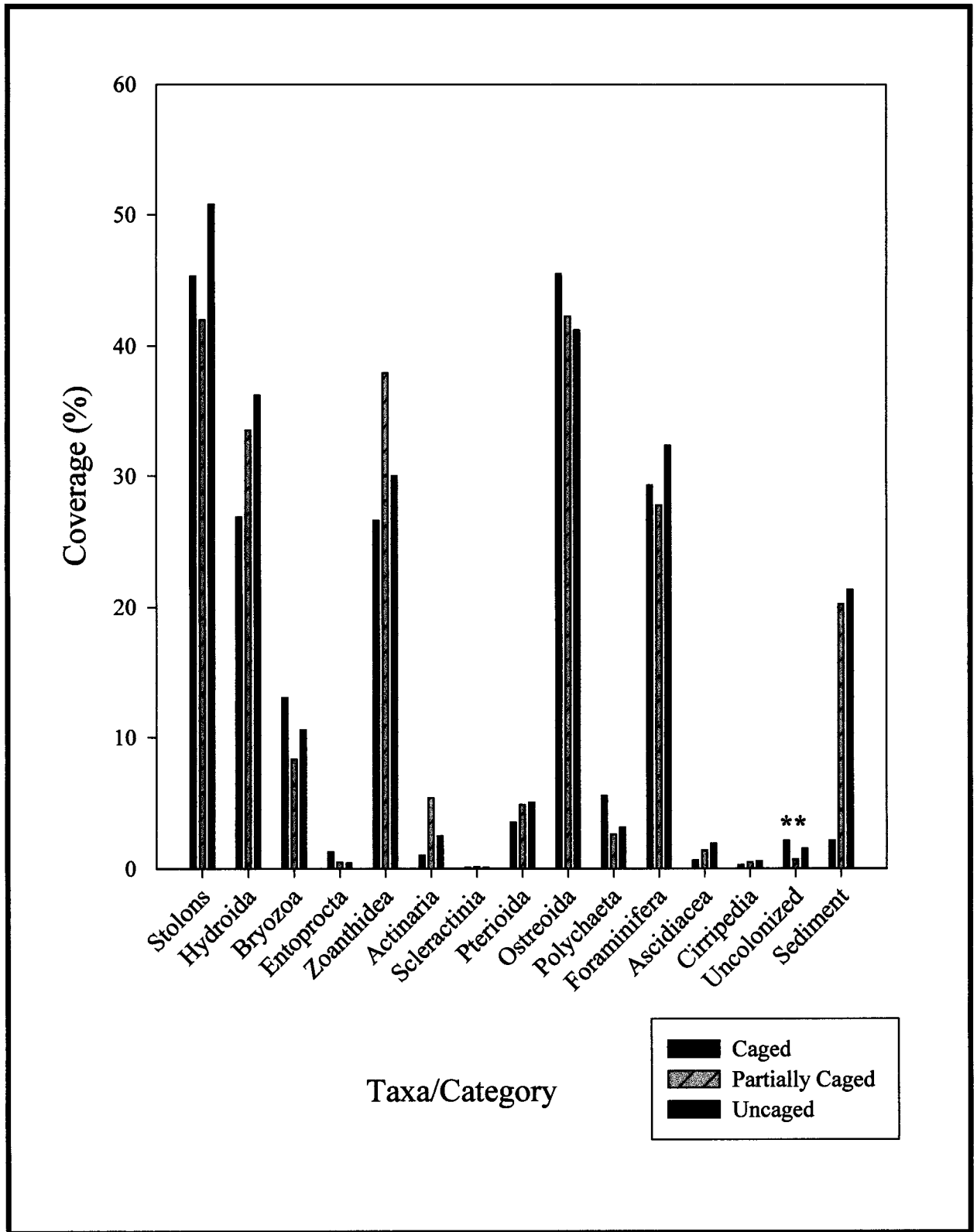


Fig. 10.17. Percent cover results for taxa and categories for experimental manipulations from the elevated spatial study. Significance levels from 4-way ANOVA indicated as in Fig. 10.8.

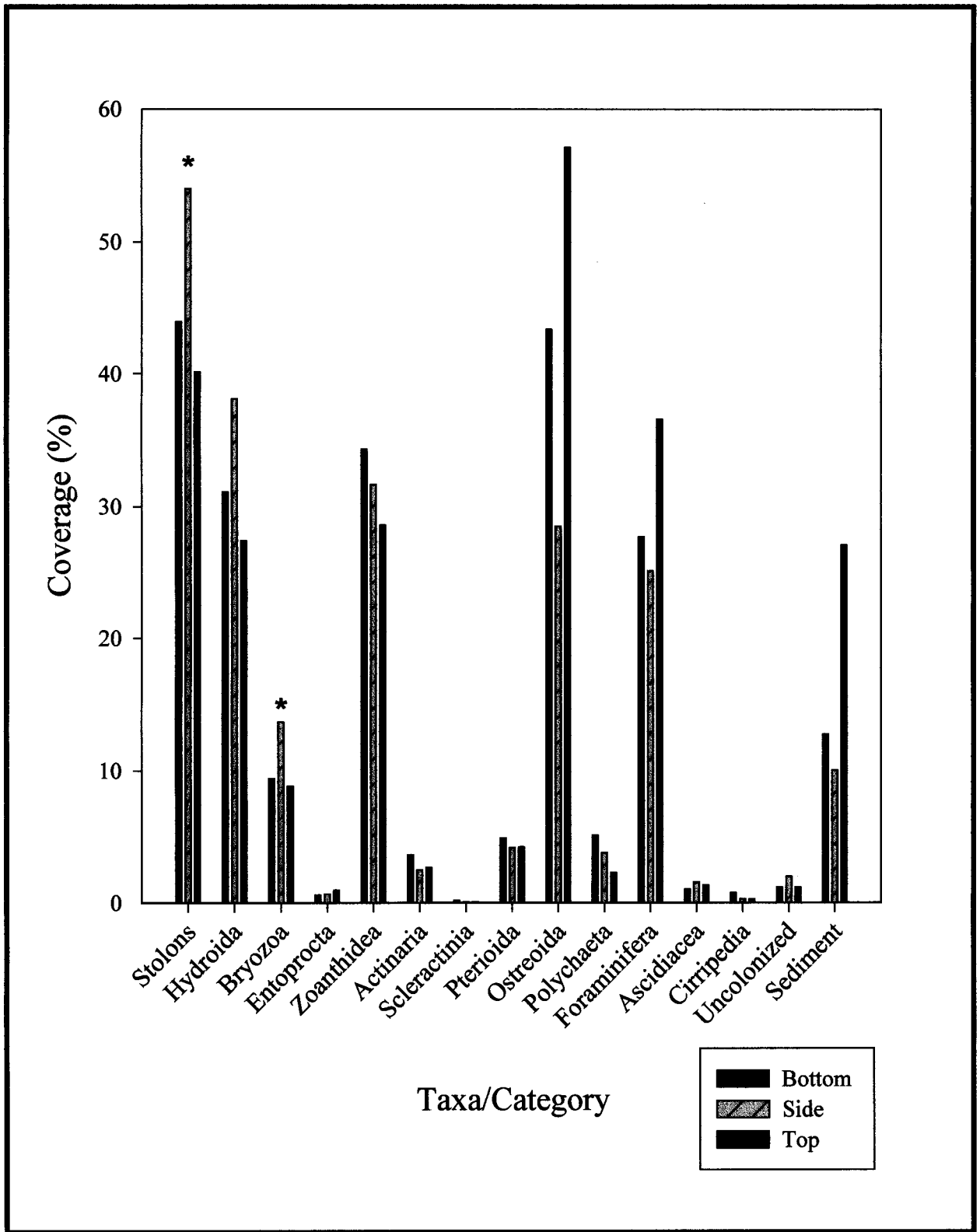


Fig. 10.18. Percent cover for orientation from the elevated spatial study by taxa and category. Significance levels from 4-way ANOVA indicated as in Fig. 10.8.

Orientation of settlement plates was not significant for most taxa and categories because of significant orientation interactions (**Table 10.8**). Orientation was significant for stolons and bryozoans (**Fig. 10.18**; 4-way ANOVA, $p = 0.0104$ and 0.0394 , respectively; Tukey, MSD = 10.07%, 10.11%, and 4.88%, respectively). Vertical orientation of settlement plates (i.e., sides) had significantly greater coverage for these two taxa than horizontally oriented plates (i.e., bottoms and tops). For most other taxa however, horizontal plates had more coverage than vertical plates, which is indicated by lower amounts of uncolonized area. Overall, sediment cover was greatest on the top plates as was coverage of Ostreoida and foraminiferans.

Variance components analysis for percent cover in the elevated spatial study indicates that for 13 of the 15 taxa and categories present, the majority of the variance lies between individual, random samples rather than between experimental sources of variation (**Table 10.10**). The majority of variance for anemones (Order Actinaria) is found in the interaction between site and experimental manipulation. The greatest variance in coverage of ascidians is between sites.

ANOVA – Abundance

Abundances of most taxa were not significantly different with respect to sampling site because of significant interactions with height above bottom or experimental manipulations (**Table 10.11**). As with percent cover, there were no consistent patterns for site in the abundance analysis (**Fig. 10.19**). Scleractinian corals were significantly more abundant at Site 4 than at any other site (4-way ANOVA, $p < 0.0001$; Tukey, MSD = 0.11/plate). Pterioidea was significantly more abundant at Site 9 than Sites 1 and 4 (4-way ANOVA, $p < 0.0001$; Tukey, MSD = 0.23/plate). Site 5 was not significantly different from the two groups (Site 9 and Sites 1 and 4). As in the percent cover analysis, individual anemones were greater at Site 5 than at any other site.

Of the six taxa analyzed for abundance differences between heights, five were more abundant at 3 mab (**Fig. 10.20**). Scleractinians were significantly more abundant at 3 mab (4-way ANOVA, $p = 0.0475$; Tukey, MSD = 0.06). Actinaria was the only solitary taxa found in greater abundance at 13 mab.

As with coverage, there were no overall trends among experimental manipulations for the six solitary taxa (**Fig. 10.21**). Manipulations were not significantly different for any taxa because of significant interactions with other main effects (**Table 10.11**). Actinarians were greatly enhanced by both disturbance and small-scale water flow disruption (218% and 254%, respectively), when compared to net recruitment (**Table 10.12**). Disturbance also enhanced abundances of barnacles (Order Cirripedia) and winged-oysters (Order Pterioidea). Water flow disruption, however, inhibited abundances of barnacles and winged-oysters. Solitary disk corals were negatively affected by disturbance, but were not affected by water flow disruption (**Table 10.12**). Disturbance and water flow disruption both negatively affected polychaete abundances.

Table 10.10. Percent of variance for each source of variation in the elevated spatial study, calculated for percent cover in a variance component analysis. Sources include site (S), depth (D; i.e., height above bottom), experimental manipulation (E.M.), orientation (O), interactions, and total error (Error).

Source	Taxa						
	Stolon	Hydroida	Bryozoa	Entoprocta	Zoanthida	Actinaria	Scleractinia
S	25.62	25.72	0.00	7.31	2.30	0.30	7.85
D	0.00	0.00	9.68	5.28	0.00	0.09	1.20
S x D	0.00	0.00	0.00	0.00	21.53	49.26	2.38
E.M.	0.00	0.00	0.00	1.37	0.00	0.07	0.52
S x E.M.	5.99	7.47	4.94	0.00	7.59	0.00	3.89
D x E.M.	3.88	4.34	1.89	0.55	1.22	0.00	0.00
S x D x E.M.	0.16	0.00	8.71	0.00	4.70	15.51	0.00
O	1.45	0.73	0.00	0.67	0.00	0.00	0.28
S x O	0.01	0.00	2.54	0.00	0.00	0.23	5.65
D x O	0.31	1.16	4.60	0.00	0.43	0.29	0.00
S x D x O	6.92	6.01	0.00	7.57	2.66	1.68	0.00
E.M. x O	0.77	0.84	2.22	0.00	0.00	0.08	0.00
S x E.M. x O	0.00	0.00	0.00	3.64	2.49	0.00	0.00
D x E.M. x O	0.00	0.00	0.00	2.53	0.58	0.00	3.81
S x D x E.M. x O	0.00	0.00	0.00	0.00	0.00	0.00	10.96
Error	54.89	53.72	65.42	71.08	56.50	32.49	63.45

Source	Taxa and Categories							
	Pterioida	Ostreioda	Polychaeta	Foraminifera	Ascidiacea	Cirripedia	Uncolonized	Sediment
S	3.28	5.80	0.00	20.87	34.56	15.46	14.53	0.00
D	0.00	14.89	3.51	0.94	4.77	7.95	1.25	0.00
S x D	0.00	0.00	13.78	0.00	7.19	0.00	1.81	2.32
E.M.	0.00	0.00	1.86	0.75	1.35	0.00	2.11	4.01
S x E.M.	2.62	0.00	6.99	4.53	10.83	0.62	0.30	26.45
D x E.M.	0.26	2.35	1.28	0.00	2.57	0.85	3.03	0.00
S x D x E.M.	1.97	1.73	2.73	3.10	0.00	11.10	3.52	2.63
O	0.00	17.36	5.78	4.81	0.00	4.26	1.02	11.90
S x O	7.41	0.00	0.00	0.00	1.43	7.07	0.00	0.00
D x O	0.00	3.57	0.00	0.00	1.64	0.00	0.04	0.00
S x D x O	1.14	6.59	16.63	7.18	0.00	1.82	2.81	2.73
E.M. x O	0.00	0.00	0.69	0.00	3.28	2.41	0.00	5.29
S x E.M. x O	1.55	0.00	0.00	15.03	0.00	0.00	8.06	11.94
D x E.M. x O	4.48	0.00	3.59	9.58	0.00	0.00	0.70	0.00
S x D x E.M. x O	0.00	13.78	0.00	0.00	3.14	2.92	0.00	0.00
Error	77.30	33.93	43.15	33.21	29.25	45.53	60.83	32.75

Table 10.11. Summary of 4-way ANOVA results for abundance ($\ln n + 1$) by taxa and category for the elevated spatial study. Sources of variance, degrees of freedom (df), and significant p -values are listed for each taxa and category. Sources of variance include site (S), depth (D), experimental manipulation (E.M.), orientation (O), and their interactions.

Source	df	Actinaria	Scleractinia	Pterioida	Ostreoida	Polychaeta	Cirripedia
S	3	<0.0001	<0.0001	<0.0001	<0.0001	ns	<0.0001
D	1	<0.0001	0.0475	ns	<0.0001	<0.0001	<0.0001
S×D	3	<0.0001	ns	ns	ns	<0.0001	ns
E.M.	2	ns	ns	ns	ns	0.0002	ns
S×E.M.	6	0.0009	ns	ns	ns	0.0004	0.0018
D×E.M.	2	0.0248	ns	ns	0.0019	0.0037	ns
S×D×E.M.	6	0.0025	ns	ns	ns	ns	0.0123
O	2	ns	ns	ns	<0.0001	0.0003	0.0005
S×O	6	ns	ns	ns	0.0120	ns	0.0180
D×O	2	ns	ns	ns	0.0010	ns	ns
S×D×O	6	ns	ns	ns	0.0014	0.0002	ns
E.M.×O	4	ns	ns	ns	0.0189	ns	ns
S×E.M.×O	12	ns	ns	ns	ns	ns	ns
D×E.M.×O	4	ns	ns	ns	ns	ns	ns
S×D×E.M.×O	12	ns	ns	ns	0.0407	ns	ns

ns = not significant.

Table 10.12. Rates of change in abundance ($\ln n + 1$ individuals) caused by ecological processes during the elevated spatial study over 19 months of exposure. Positive values indicate abundances are enhanced, and negative values indicate abundances are inhibited by ecological process.

Taxa	Disturbance (D) ($\ln n + 1/19$ months)	Water Flow Disruption (W) ($\ln n + 1/19$ months)	Net Recruitment (S) ($\ln n + 1/19$ months)
Actinaria	0.24	0.28	0.11
Scleractinia	-0.04	0.00	0.10
Pterioida	0.07	-0.05	0.21
Ostreoida	0.05	0.11	2.63
Polychaeta	-0.55	-0.05	1.97
Cirripedia	0.14	-0.03	0.48

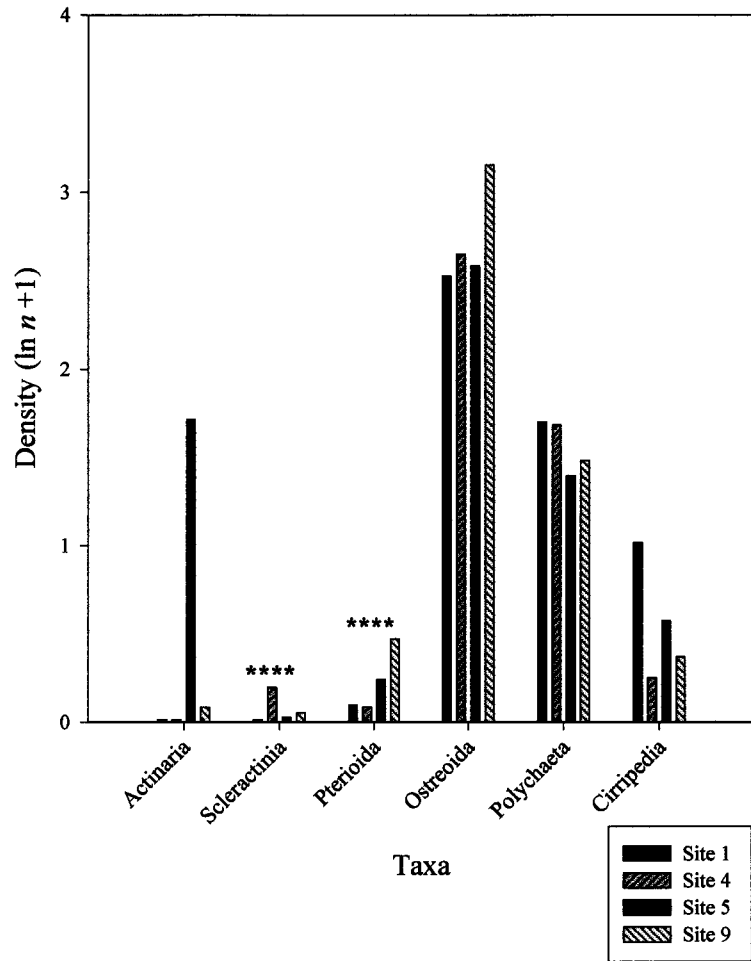


Fig. 10.19. Abundance ($\ln n + 1$) of solitary taxa for sites from the elevated spatial study. Significance levels from 4-way ANOVA indicated as in Fig.10.8.

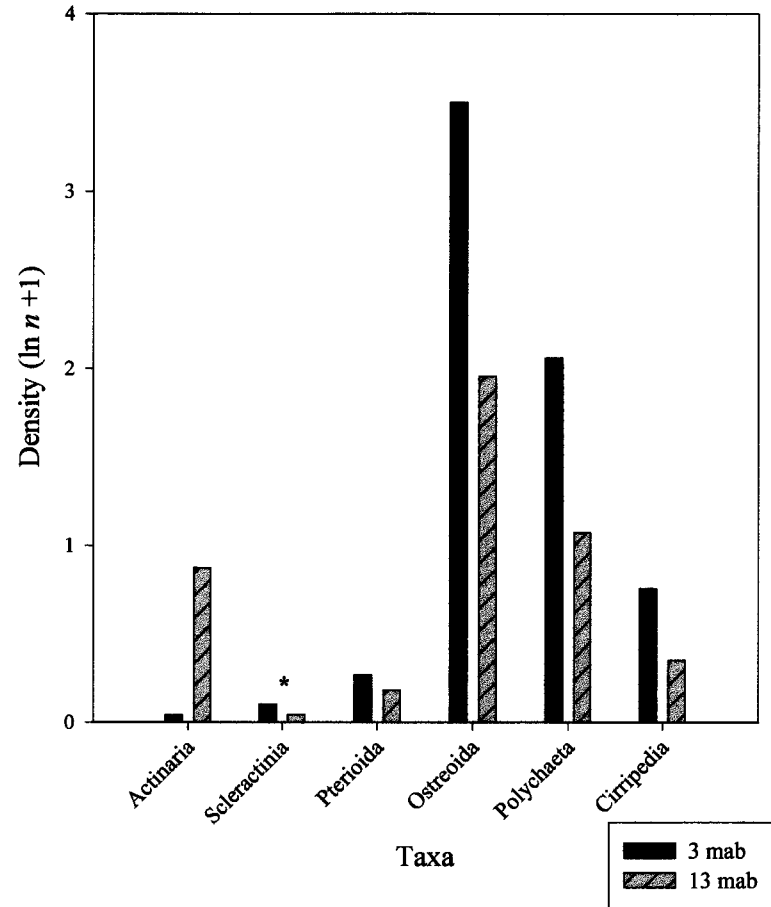


Fig. 10.20. Abundance ($\ln n + 1$) for solitary taxa by height (meters) above bottom (mab) during the elevated spatial study. Significance levels from 4-way ANOVA indicated as in Fig. 10.8.

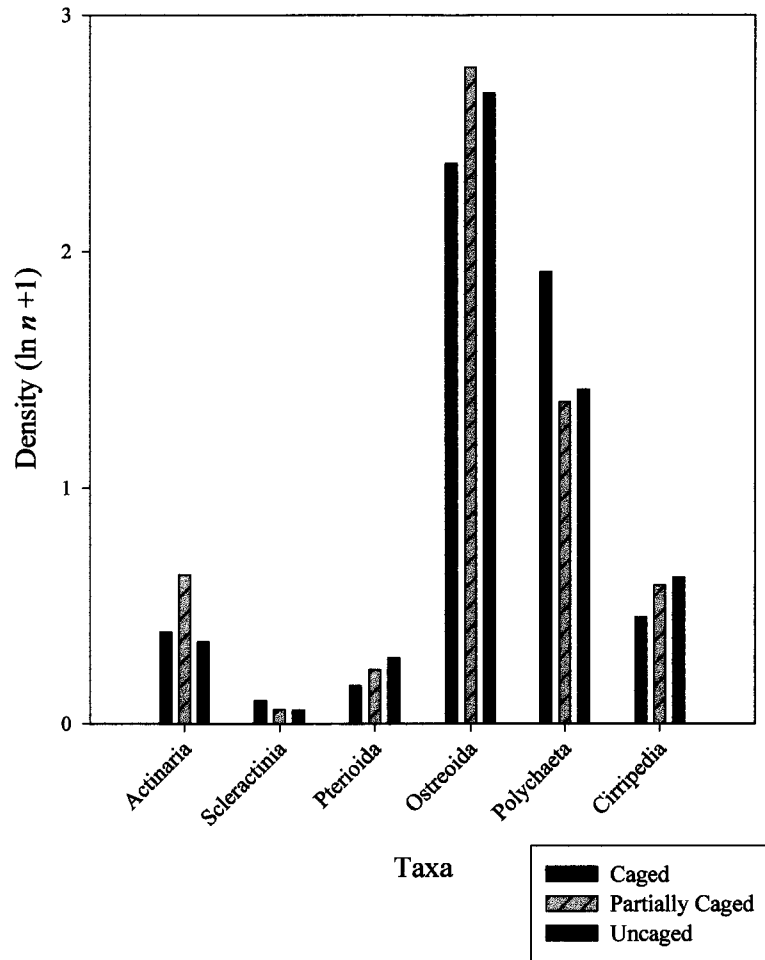


Fig. 10.21. Abundance ($\ln n + 1$) of solitary taxa by experimental manipulation during the elevated spatial study.

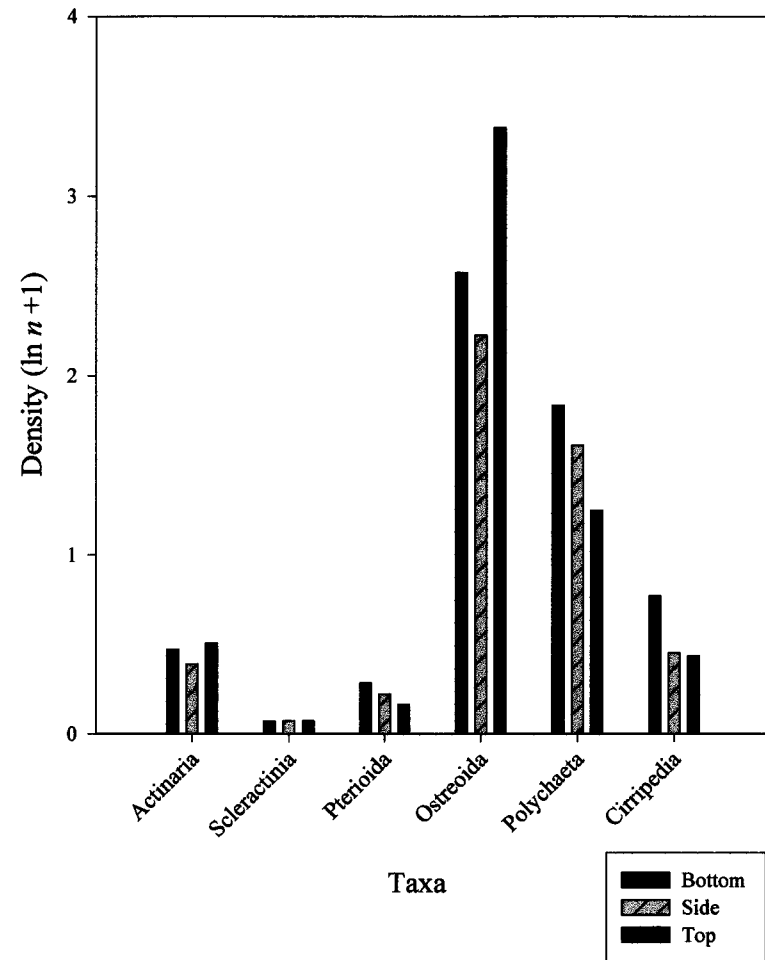


Fig. 10.22. Abundance ($\ln n + 1$) of solitary taxa by plate orientation during the elevated spatial study.

Abundances of solitary organisms were never greatest on vertical plates (**Fig. 10.22**). Horizontal plates had the highest abundances for all solitary taxa. No taxa were significantly affected by orientation of settlement plates, however, because of significant orientation interactions (**Table 10.11**).

The greatest source of variance in abundance for four of the six solitary taxa was for differences between individual samples (**Table 10.13**). Differences in abundances of Ostreoida were highest for changes in depth. Actinarians were affected most by the site and depth interaction.

Principal Component Analysis – Coverage

Settling plate coverage by taxa was analyzed by PCA to examine community structure changes relative to the study design. Percent cover of stolons, hydroids, and zoanthids were positively loaded on principal component 1 (PC1), while Ostreoida was positively loaded on PC2 (**Fig. 10.23**). Zoanthida were negatively loaded on both PC1 and PC2. However, when loading scores were plotted, no general trends were found for coverage by any source of variation in the study design (i.e., site, height above bottom, experimental manipulation, and orientation), so there are no obvious interpretations for what is causing taxa to correlate on either PC1 or PC2. One explanation for the pattern is that most stolons were hydroids, not bryozoans.

Principal Component Analysis – Abundance

For abundance, solitary anemones (Order Actinaria) and Ostreoida were inversely loaded on PC1, while polychaetes were positively loaded on PC2 (**Fig. 10.24**). Unlike coverage, however, loading scores for both site and height cluster on the bivariate loading axes (**Figs. 10.25** and **10.26**). Sites 1, 4, and 9 appear to cluster on negative values of PC1 (**Fig. 10.25**) as does 3 mab (“B”) for height (**Fig. 10.26**). Site 5 and the 13 mab height both have positive PC1 scores, therefore Actinaria are characteristic of Site 5 and higher distances from the sediment surface. Individual solitary anemones were rarely found at Sites 1, 4, and 9 and at 3 mab. Experimental manipulation and orientation do not exhibit clusters or groupings on the bivariate PC axes.

Bottom Spatial Study

Coverage

Of 15 taxa and categories found in the percent cover analysis of the elevated spatial study, 12 were found in the bottom (0 mab) spatial study (**Table 10.14**). In general, stoloniferous organisms (stolons, hydroids, bryozoans, and entoprocts) were significantly greater at Site 9 than Site 1 (**Fig. 10.27**; 2-way ANOVA, $p = 0.0003$, <0.0001 , 0.004 , and 0.0071 , respectively; Tukey, MSD = 13.97%, 16.55%, 16.05%, and 8.18%, respectively). Dominant solitary organisms (Ostreoida and Polychaeta), however, were often significantly greater at Site 1 than Sites 4 or 9 (**Fig. 10.27**; 2-way ANOVA, $p < 0.0001$ and 0.0288 , respectively; Tukey, MSD = 9.01% and 15.28%, respectively). Sediment coverage was greater at Site 4 than Sites 1 or 9, but was not significant (**Fig. 10.27**). Uncolonized area was significantly greater at Site 4 than Site 9 (2-way ANOVA, $p < 0.0001$; Tukey, MSD = 1.90%).

Table 10.13. Percent of variance from each component of the elevated spatial study. Variance components calculated on abundance ($\ln n + 1$). Main effects of the study included site (S), depth (D; i.e., height above bottom), experimental manipulation (E.M.), orientation (O), interactions, and total error (Error).

Source	Actinaria	Scleractinia	Pterioida	Ostreioda	Polychaeta	Cirripedia
S	0.00	9.26	8.41	3.79	0.00	12.51
D	0.00	0.47	1.25	52.55	17.19	11.79
S x D	57.34	3.02	0.00	0.00	15.06	0.00
E.M.	0.00	0.00	0.42	0.00	0.00	0.00
S x E.M.	1.08	3.27	0.66	0.43	7.12	3.45
D x E.M.	0.42	1.04	0.00	2.29	4.48	0.00
S x D x E.M.	10.01	0.00	5.01	0.00	0.10	6.70
O	0.00	0.00	1.11	14.33	3.81	4.05
S x O	0.33	5.44	2.46	0.00	0.00	3.33
D x O	0.80	0.47	0.00	1.37	0.00	0.00
S x D x O	0.49	0.00	1.06	3.48	14.79	1.28
E.M. x O	0.35	0.50	0.00	0.63	1.63	1.43
S x E.M. x O	0.00	0.00	3.55	0.00	0.00	0.00
D x E.M. x O	0.00	0.00	5.97	0.47	0.95	0.00
S x D x E.M. x O	0.00	8.18	0.00	4.71	0.00	8.56
Error	29.19	68.37	70.10	15.96	34.85	46.91

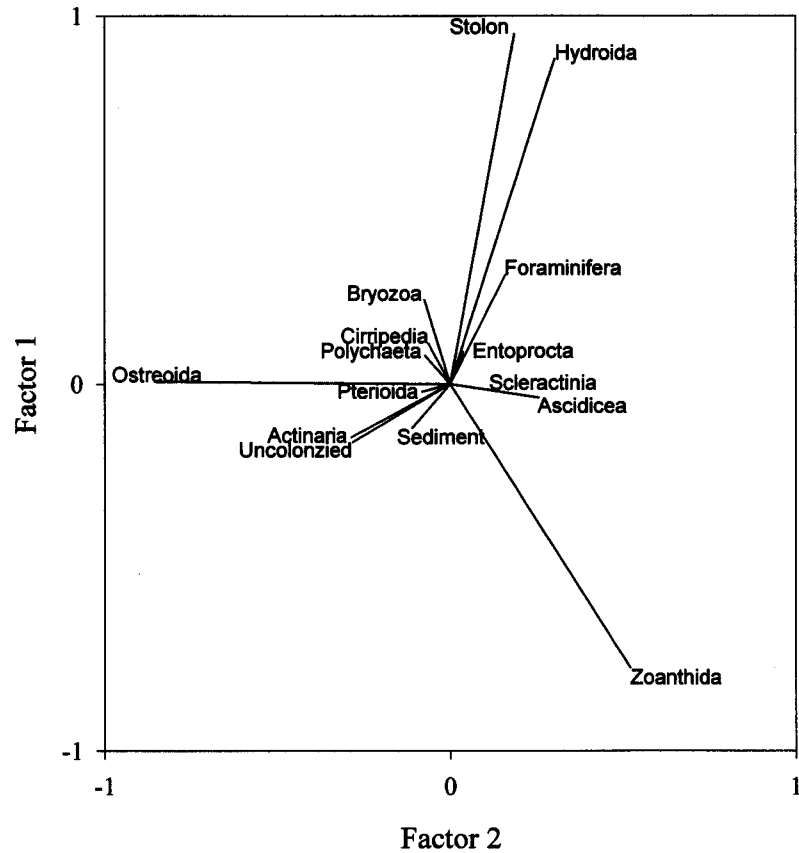


Fig. 10.23. Principal components analysis results of percent cover from the elevated spatial study for all taxa and categories.

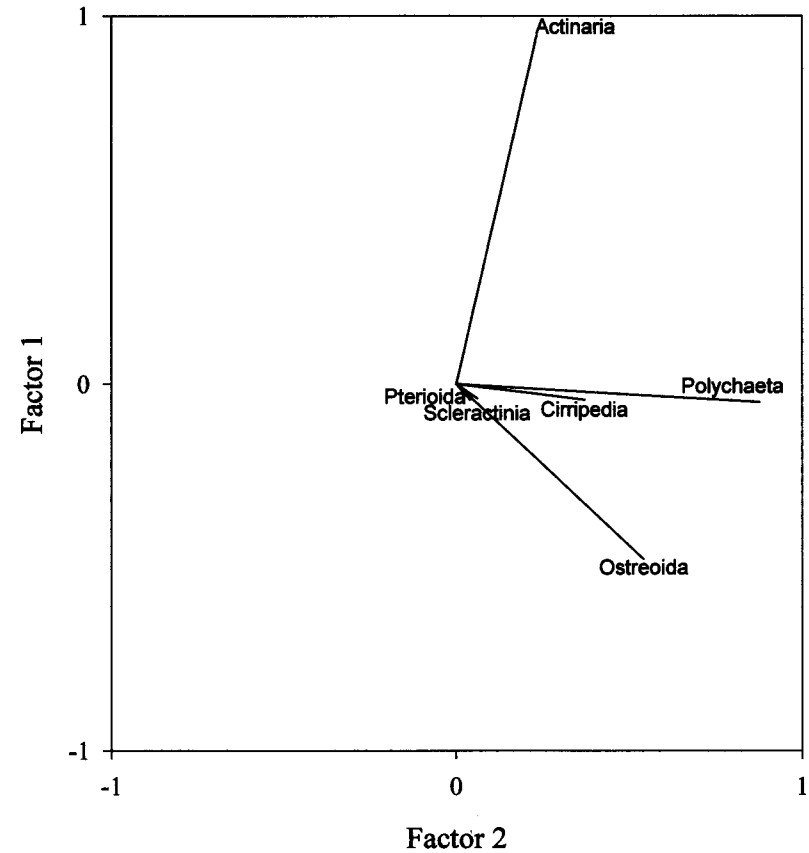


Fig. 10.24. Principal components analysis results of abundance from the elevated spatial study for all solitary taxa. Abundances were log transformed ($\ln n + 1$) prior to analysis.

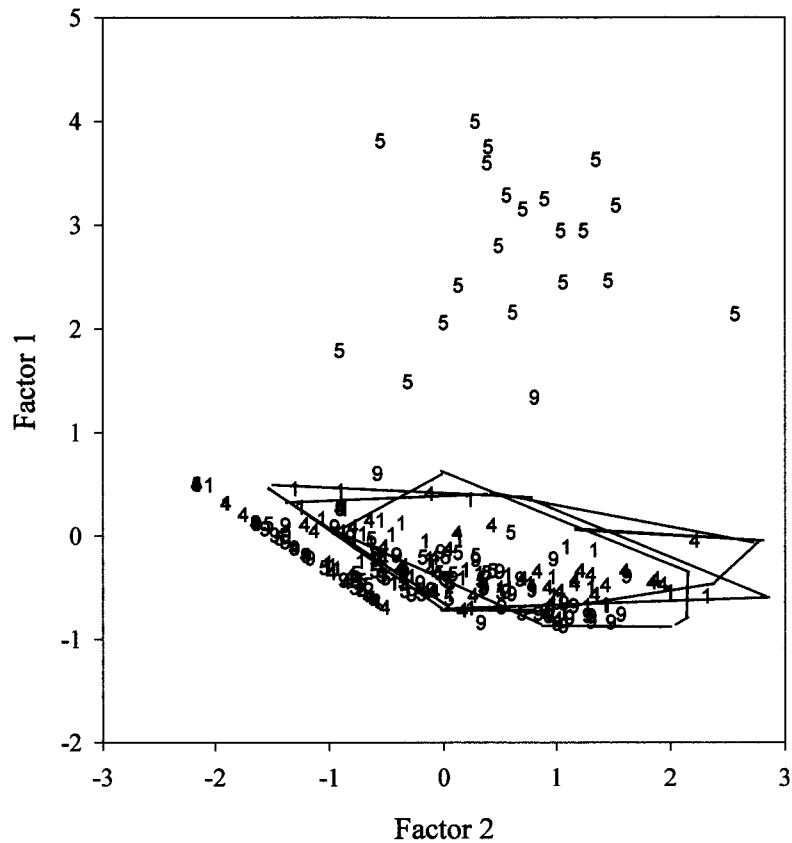


Fig. 10.25. Principal components analysis loading scores for abundances by site from the elevated spatial study. Lines indicate clusters of Sites 1, 4, and 9. Abundances were log transformed ($\ln n + 1$) prior to analysis.

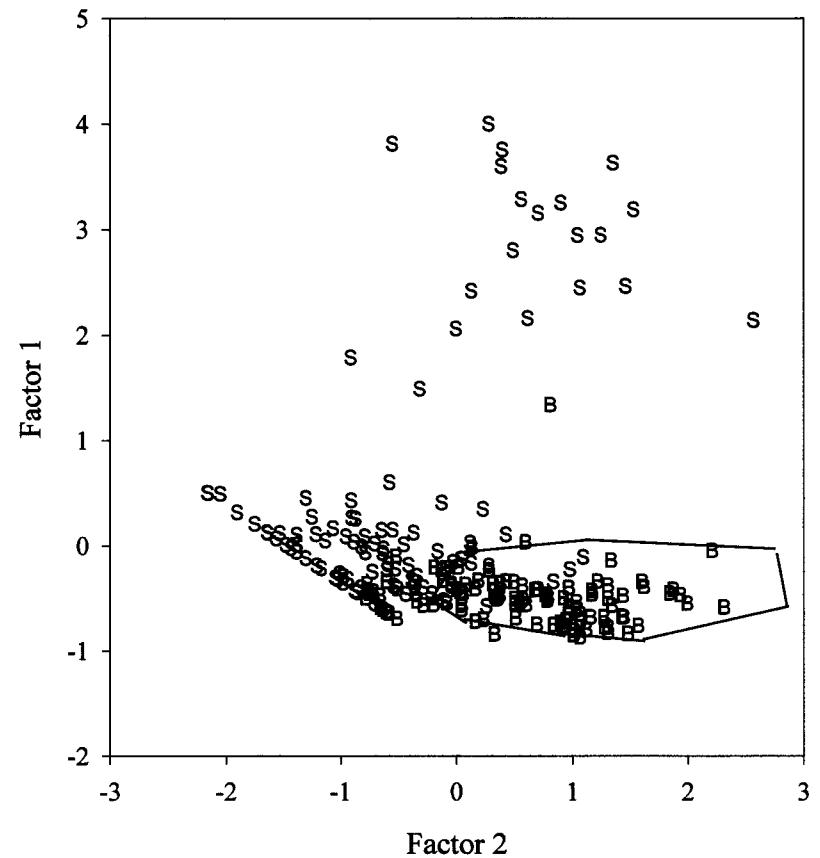


Fig. 10.26. Principal components analysis loading scores for abundance by height (meters) above bottom (mab) from the elevated spatial study. Lines indicate cluster of 3 mab (B) height. Height of 13 mab (S) is also indicated. Abundances were log transformed ($\ln n + 1$) prior to analysis.

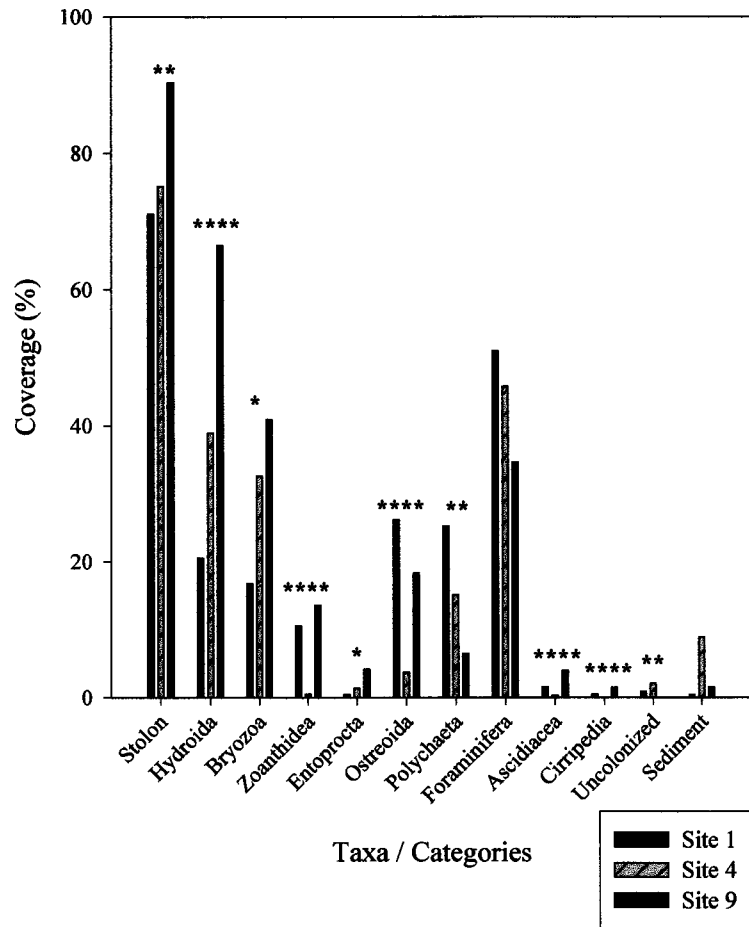


Fig. 10.27. Percent cover for taxa and categories by site during the bottom spatial study. Significance levels from 2-way ANOVA indicated as in Fig. 10.8.

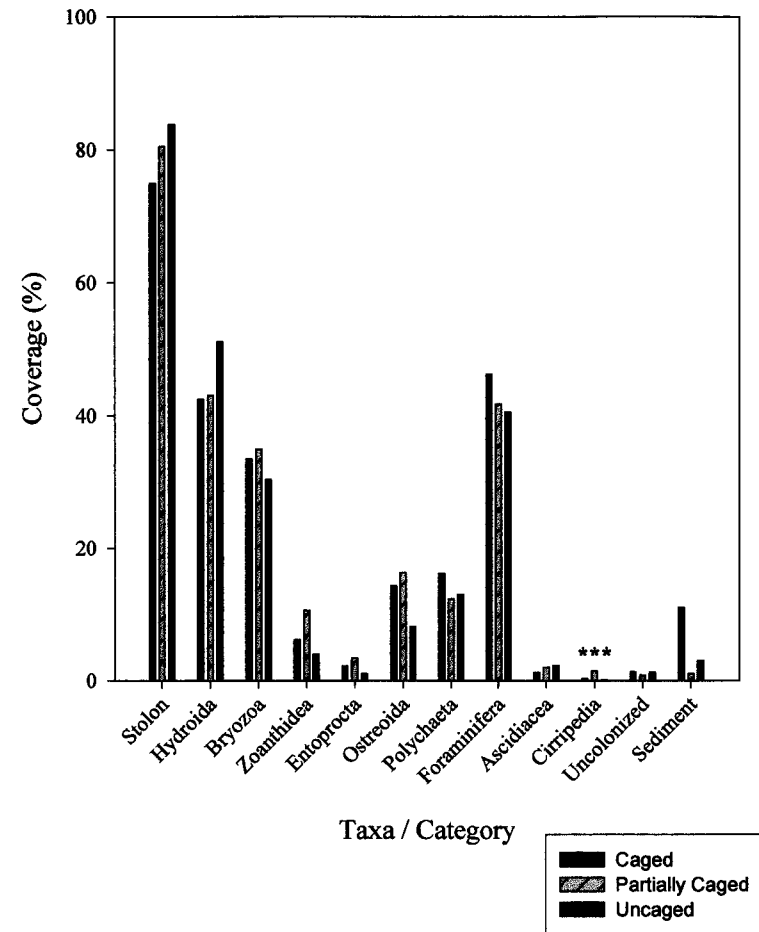


Fig. 10.28. Percent cover for taxa and categories by experimental manipulation during the bottom spatial study. Significance levels from 2-way ANOVA indicated as in Fig. 10.8.

Table 10.14. Results from 2-way ANOVA of percent cover by taxa and category for bottom spatial study. Sources of variance, degrees of freedom (df) and significant *p*-values are listed for each taxa and category. Sources of variance include site (S), experimental manipulation (E.M.), and the interaction (S x E.M.).

Source	df	Taxa					
		Stolon	Hydroida	Bryozoa	Zoanthidea	Entoprocta	Ostreoida
S	2	0.0003	<0.0001	0.004	<0.0001	0.0071	<0.0001
E.M.	2	ns	ns	ns	Ns	ns	0.0211
S x E.M.	4	ns	ns	ns	0.0191	ns	ns

Source	df	Taxa or Category					
		Polychaeta	Foraminifera	Ascidiacea	Cirripedia	Uncolonized	Sediment
S	2	0.0288	ns	<0.0001	<0.0001	<0.0001	ns
E.M.	2	ns	ns	ns	<0.0001	ns	ns
S x E.M.	4	ns	ns	ns	<0.0001	ns	ns

ns = not significant.

Experimental manipulations were significantly different for Ostreoida only (**Fig. 10.28**). For other taxa or categories, experimental manipulation was not or significant manipulation interactions existed (**Table 10.14**). Coverage of bryozoans, zoanthids, entoprocts, Ostreoida, and barnacles were enhanced by both disturbance (D) and water flow disruption (W) (**Table 10.15**). Zoanthids and entoprocts were enhanced by a factor of 750% to 1,600% over net recruitment by both ecological processes. Polychaetes and sediment cover were negatively affected by both disturbance (D) and water flow disruption (W) (**Table 10.15**). Water flow disruption (W) negatively affected stolons, hydroids, and ascidians, while disturbance (D) enhanced their total coverage. The opposite is true of Ostreoida and uncolonized area (**Table 10.15**). These organisms were negatively affected by disturbance, while small-scale water flow disruption enhanced coverage.

Table 10.15. Rate of change in coverage (cm²) over 15 months of exposure caused by ecological processes during the bottom spatial study. Positive values indicate abundances are enhanced and negative values indicate abundances are reduced by ecological processes.

Taxa and Categories	Disturbance (D) (cm ² /15 months)	Water Flow Disruption (W) (cm ² /15 months)	Net Recruitment (S) (cm ² /15 months)
Stolons	4.83	-2.90	68.51
Hydroida	0.53	-7.06	44.21
Bryozoa	1.33	4.02	25.23
Zoanthidea	3.87	5.76	-0.36
Entoprocta	1.06	2.07	-0.14
Polychaeta	-3.36	-0.59	14.75
Foraminifera	-3.91	1.07	39.36
Ostreoida	1.70	7.13	5.42
Ascidiacea	0.68	-0.19	1.27
Cirripedia	0.98	1.17	-0.90
Uncolonized	-0.40	-0.33	1.47
Sediment	-8.72	-1.71	11.33

Abundance

Three of six solitary taxa from the elevated spatial study were found in the bottom spatial study (**Table 10.16**). There were significant differences in abundances among sites only for Polychaeta (**Table 10.16** and **Fig. 10.29**). Polychaetes were significantly more abundant at Site 1 than Site 9 (2-way ANOVA, $p = 0.0009$; Tukey, MSD = 1.13/plate). Ostreoida and Cirripedia had significant site \times experimental manipulation interactions, thus site differences were not significant.

Barnacles and Ostreoida were enhanced by both disturbance and small-scale water flow disruption with barnacles increasing as much as 390% above net recruitment abundances (**Fig. 10.30**; **Table 10.17**). In contrast, polychaete abundance was negatively affected by both disturbance and small-scale water flow disruption.

Table 10.16. Results from 2-way ANOVA on taxa abundance ($\ln n + 1$) during the bottom spatial study. Sources of variance, degrees of freedom (df), and significant p -values are listed for each taxa and category. Sources of variance include site (S), experimental manipulation (E.M.), and interactions (S \times E.M.).

Source	df	Taxa		
		Polychaeta	Cirripedia	Ostreoida
S	2	0.0009	<0.0001	<0.0001
E.M.	2	Ns	<0.0001	ns
S \times E.M.	4	Ns	0.0009	0.0359

Table 10.17. Rate of change in abundance ($\ln n + 1$) over 15 months of exposure caused by ecological process in bottom spatial study. Positive values indicate abundances are enhanced, and negative values indicate abundances decreased by ecological processes.

Taxa	Ecological Process		
	Disturbance (D) ($\ln n + 1/15$ months)	Water Flow Disruption (W) ($\ln n + 1/15$ months)	Net Recruitment (S) ($\ln n + 1/15$ months)
Polychaeta	-0.33	-0.43	3.27
Cirripedia	0.51	0.83	-0.21
Ostreoida	0.42	0.64	1.76

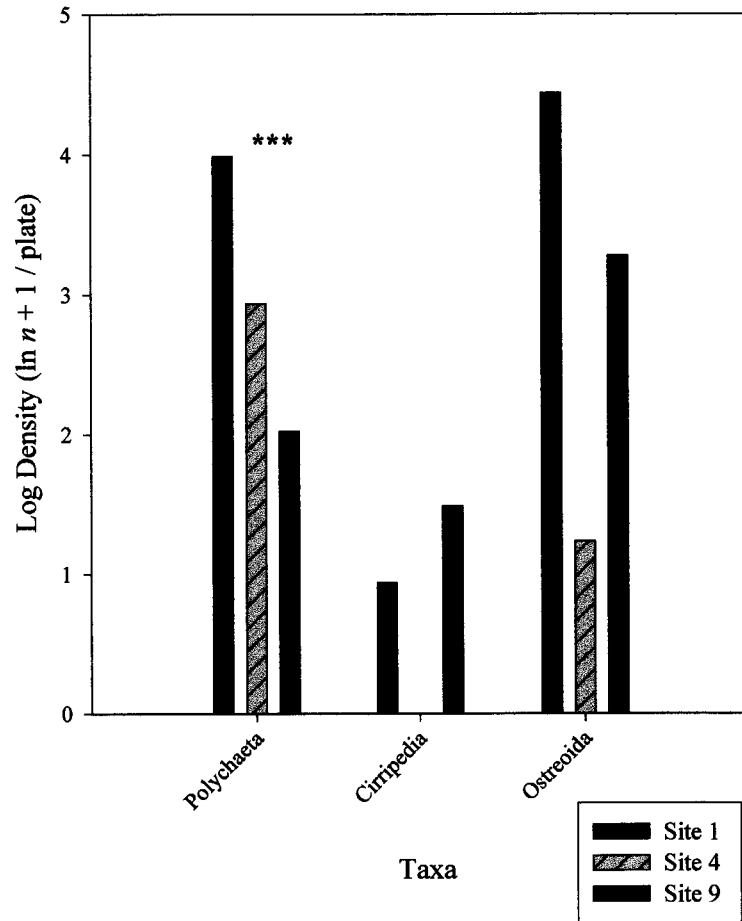


Fig. 10.29. Abundance ($\ln n + 1$) of solitary taxa by site during the bottom spatial study. Significance levels from 2-way ANOVA indicated as in Fig. 10.8.

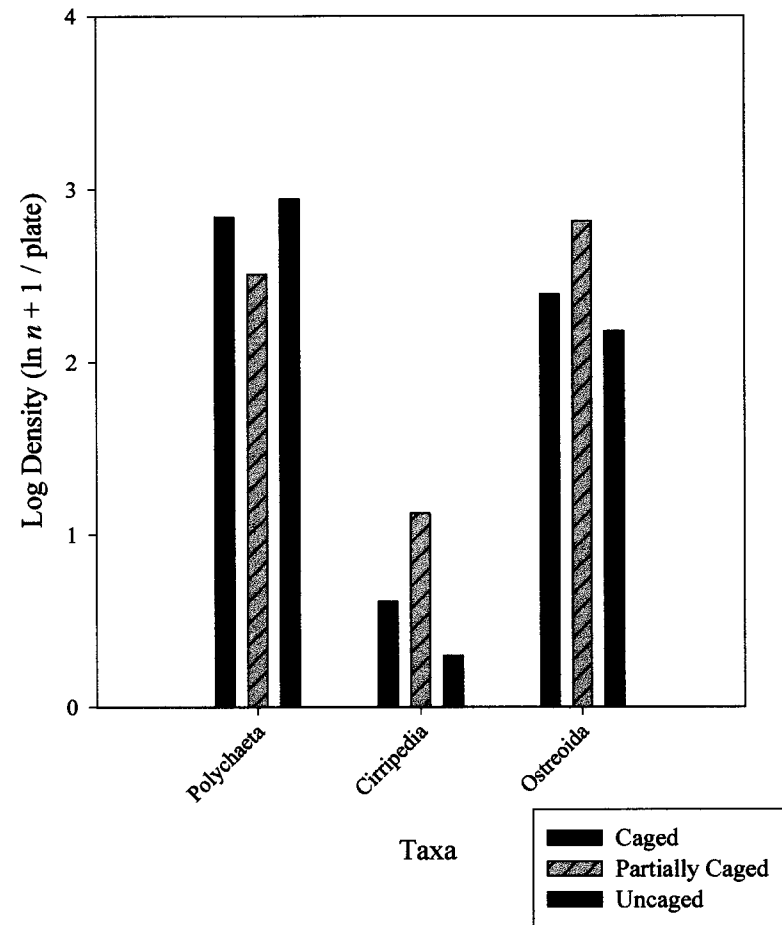


Fig. 10.30. Abundance of solitary taxa ($\ln n + 1$) by experimental manipulation during the bottom spatial study. Significance levels from 2-way ANOVA indicated as in Fig. 10.8.

Discussion

Bottom Temporal Study

There were significant temporal changes for most taxa and categories at near bottom depths. The first null hypothesis (H_1 : *epibiont coverage, abundance, and diversity do not change over time*) is therefore rejected. The *r*-selected, opportunistic epifauna were the earliest colonizers of new substrate patches (Type II) in the study area. Diversity was low after 5 and 15 months, but increased by 27 months of exposure. Specialized, *K*-selected species settled and grew in greater numbers throughout time. Community composition within phyla changed over time as well. For example, there was a shift in bryozoan communities from predominantly soft-bodied Ctenostomata to calcareous Cheilostomata and Cyclostomata. Overall, there was succession on the settling plates.

Just the earliest successional stages of community development were found on settling plates, because community structure was quite different from the surrounding, mature, hard bottom communities. The surrounding hard bottom communities were the likely source of recruits. *Rhizopsammia* sp., an ahermatypic solitary disk coral, is the most abundant organism in terms of coverage and abundance on the mounds (Chapter 7). Ahermatypic corals were very rare on settlement plates, even at different heights above bottom. The deep water community after 27 months, in terms of functional groups, is similar to early communities found in rocky intertidal and shallow subtidal regions. The early successional stage in both shallow and deep water is composed of *r*-selected species (e.g., bryozoans, hydroids, small bivalves, and polychaetes) that are better adapted to high sediment loading (Paine and Levin 1981; Connell and Keough 1985; Sousa 1985). In contrast to shallow regions, settlement and growth is slower, thus the time required for full community development in deep water is considerably longer.

The relative absence on settlement plates of dominant organisms from the surrounding hard bottoms may be caused by life history characteristics and dispersal patterns of those taxa. Many of the organisms on the mounds (e.g., octocorals, bryozoans, hydroids, entoprocts, some polychaetes, and some solitary disk corals) are brooding organisms that do not disperse larvae widely (Ruppert and Barnes 1994). Many of the organisms on the settlement plates, especially the early colonizers, disperse larvae over a wide area. Because the experiments emulate Type II patches, it would require a very long time before brooding organisms would be able to colonize the settlement plates (Sousa 1985).

Scale and resolution differences between the settling plate experiment and photo survey of the surrounding hard bottom community may also cause differences found between the two communities. The scale of photoquadrats was 100 times larger ($\sim 1 \text{ m}^2$) than the settlement plates ($\sim 100 \text{ cm}^2$). Scale and patch size differences have a great effect on differences in community structure (Dudgeon and Petraitis, in press; Hardin, pers. comm.). Resolution was 240 times greater examining plates under a microscope ($\sim 0.1 \text{ mm}^2$) than photographs on a monitor ($\sim 24 \text{ cm}^2$). It is likely the most abundant organisms found on settlement plates were present on the mounds, but the resolution of the photoquadrats was probably not fine enough to detect these small organisms (Hardin, pers. comm.).

Communities observed on settlement plates were not likely developed enough after 27 months to provide adequate substrates and cues for larval settlement of species characteristic of mature communities. Often, the presence of a single taxa or chemical is necessary to provide the chemosensory responses for settlement (Keough and Raimondi 1995). For example, the spat of several bivalve species settled 72% more often on collectors coated with chitin than a control (Harvey et al. 1997). Chitin is a polysaccharide found in the exoskeleton of many crustaceans and in the perisarc of hydroids. Like bivalves, polychaete and barnacle larvae also employ active testing of the substrate before settlement occurs (Crisp and Barnes 1954; Crisp 1974). Settlement behavior that incorporates chemoreception and physical contact with substrate to test substrate quality and suitability of a settlement site are likely to be employed by the later settling organisms (Crisp and Barnes 1954; Crisp 1974). It is likely that presence of early-stage successional species, such as hydroids and bryozoans, plays an important role in the settlement of later successional organisms. If sufficient levels of settlement cues were not present on plates, then dispersing larvae would not recognize the plates as open space for settlement and recruitment.

Bottom Spatial Study

There were significant differences in community structure and development among sites on near-bottom (0 mab) substrates. Settlement plates in the bottom spatial study were deployed and retrieved over a 15- or 27-month period. Site 4 was a polychaete-dominated community after 15 and 27 months exposure. Sites 1 and 9 were similar. Both sites were dominated by bivalves, but Site 1 had almost as many polychaetes as bivalves. Community differences among Sites 1, 4, and 9 at 0 mab were not reflected at 3 and 13 mab.

It is unclear if there was sufficient difference in physical variation among Sites 1, 4, and 9 to cause the difference in community structure and development. Sites 1 and 9, which were similar, were furthest apart and in different water depths. Sites 4 and 9 were at the same water depth. Sediment cover is less at Site 9 than at Site 4. Therefore, neither depth nor distance from the Mississippi Delta appear to be important in controlling settlement at the bottom. There may have been a stochastic event early in the exposure period that shaped the community development at Sites 1, 4, and 9. Total coverage is less at Site 4 than at Sites 1 or 9 even though Site 4 had the greatest sediment coverage (**Fig. 10.27**). Currents appear to be slightly stronger at Sites 9 than at Site 4 (Chapter 6), which could possibly enhance feeding and growth of organisms at the site. Larval supply from source communities and larval contact rates may differ among sites. Bulk sediment flux is greatest near the bottom and larvae may be caught within highly turbulent flows preventing active settlement by propagules and causing random settlement patterns at any given site.

Elevated Spatial Study

Sites

There were no consistent trends among sites for percent cover, abundance, or community structure. Therefore, the second null hypothesis (H_2 : *epibiont coverage, abundance, and diversity are not different between study sites*) is not rejected. The physical environment of the water column is relatively similar among the sites. All sites were near the shelf break, so Loop Current intrusions would most likely affect all sites equally (Kelly, pers. comm.).

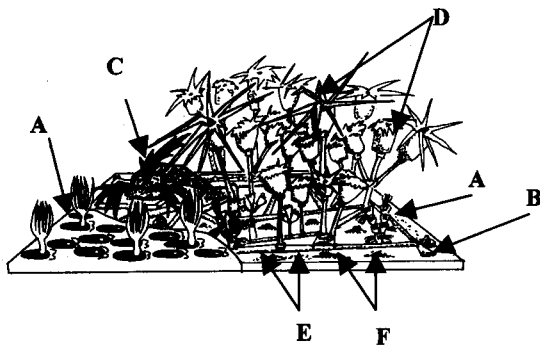
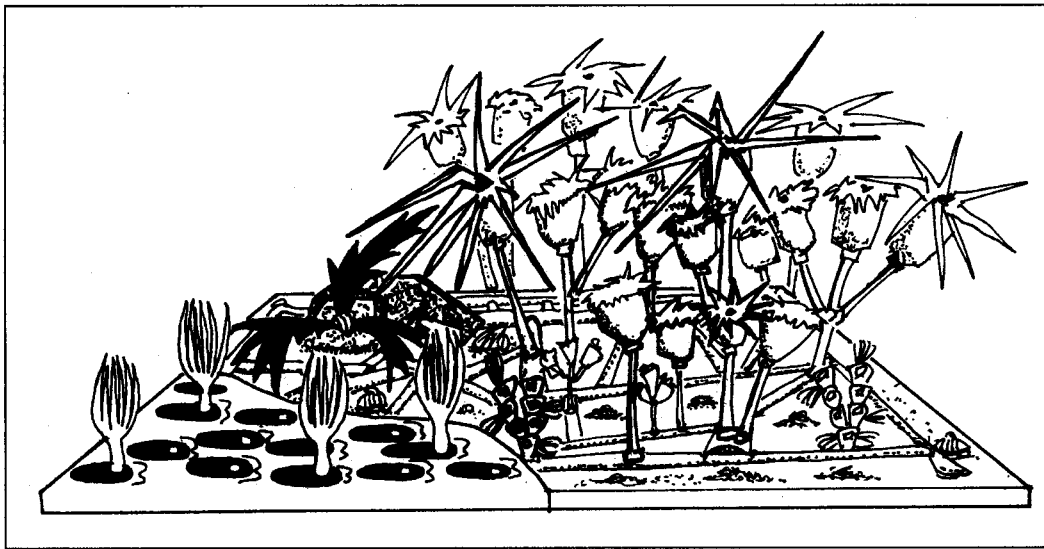
Sediment cover increased towards the Mississippi Delta, but total plate coverage didn't decrease towards the Delta (**Fig. 10.15**). Differences among sites were taxa-specific. Abundance of cover of functional groups, such as passive and active suspension feeders, were not different among sites. Taxa adapted to increased sediment loading, e.g., hydroids and bivalves, were slightly more abundant towards Site 9. This was not a statistically significant east-west trend. For example, Ostreoida coverage at Site 1 was similar to coverage at Site 9.

Larval supply could be responsible for spatial differences observed for specific taxa. Whether colonial or solitary, all organisms had to colonize settling plates with dispersing larvae, because settlement plates emulate Type II patches (Sousa 1985). Therefore, it is likely that adult source populations and physical phenomena are controlling colonization patterns. In the present study, community structure of the mature population did not vary with proximity to the Mississippi River Delta (see Chapter 7), contradicting findings from earlier studies (Gittings et al. 1992). The previous studies on the Mississippi-Alabama outer continental shelf were conducted closer to the Mississippi (<70 km from the Delta), however, and it is likely that much of the study area is beyond the Mississippi threshold for hard bottom habitat development (Gittings et al. 1992).

There was a strong competitive interaction between Zoanthidea and Ostreoida (**Fig. 10.15**). In sites where zoanthid colonies were established, Ostreoida had the lowest percent cover (Site 5). This was caused by either overgrowth of bivalves by zoanthids or by inhibition of further bivalve spat settlement. Abundances of bivalves were not affected by the presence of zoanthid colonies (**Fig. 10.19**). Thus, bivalves must have been established prior to zoanthid colonization and growth rates of Ostreoida were reduced. Resource competition is the likely mechanism, because surrounding zoanthid colonies could inhibit feeding by Ostreoida. Bivalves were often overgrown on the top valves by zoanthid colonies, which encroached from the valve hinge. Although the overgrown bivalves were still able to feed, it is possible that the presence of zoanthids would interfere with bivalve feeding currents.

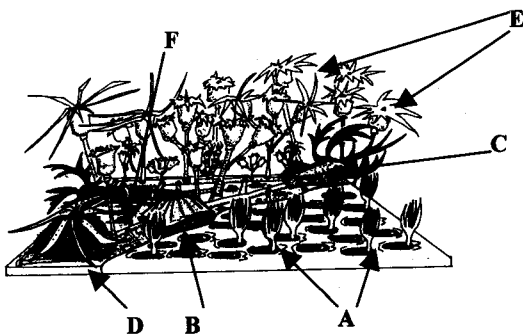
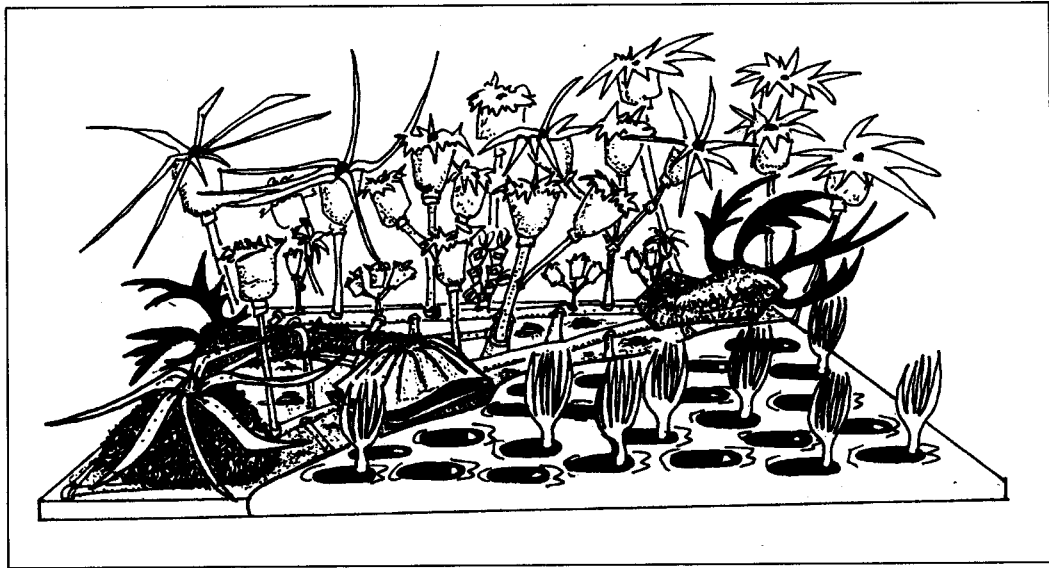
Height Above Bottom

Height of settlement plates above bottom had the greatest spatial effect on community abundance and structure (**Figs. 10.31, 10.32, and 10.33**). The third null hypothesis (H_3 : *epibiont coverage, abundance, and diversity do not change with increasing height above bottom*) is therefore rejected. This is concordant with observations of the surrounding



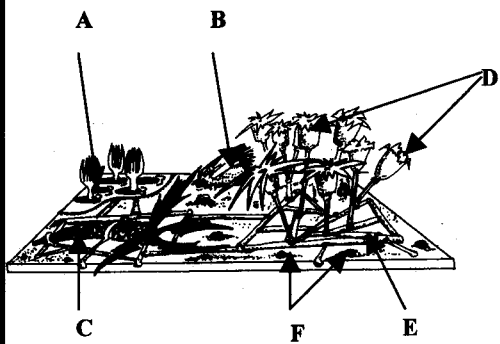
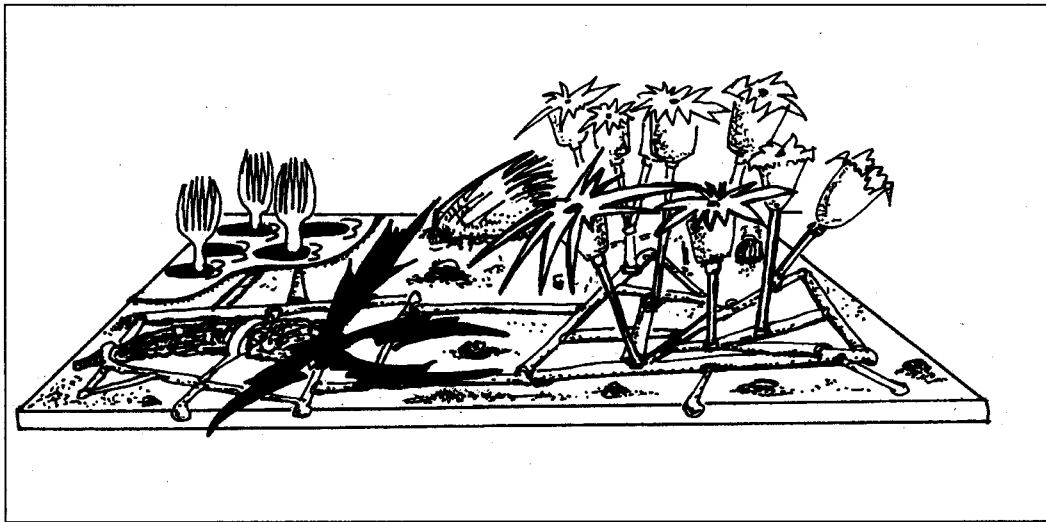
- A. bryozoans
- B. bivalve (Order Ostreoida)
- C. polychaete worms
- D. hydroids
- E. stolons
- F. foraminiferan

Fig. 10.31. Artistic interpretation of average epibenthic community structure at 0 m above bottom based on average percent cover and abundance after a 15-month settling plate exposure period. Width of drawing represents ~10 cm, but organisms are not to scale. Artwork by C. Halverson.



- A. bryozoans
- B. bivalve (Order Ostreoida)
- C. polychaete worms
- D. solitary anemone (Order Actinaria)
- E. hydroids
- F. foraminiferan

Fig. 10.32. Artistic interpretation of average epibenthic community structure at 3 m above bottom based on average percent cover and abundance after a 19-month settling plate exposure period. Width of drawing represents ~10 cm, but organisms are not to scale. Artwork by C. Halverson.



- A. bryozoans
- B. bivalve (Order Pterioida)
- C. polychaete worms
- D. hydroids
- E. stolons
- F. foraminiferan

Fig. 10.33. Artistic interpretation of average epibenthic community structure at 13 m above bottom based on average percent cover and abundance after a 19-month settling plate exposure period. Width of drawing represents ~10 cm, but organisms are not to scale. Artwork by C. Halverson.

community, which indicates vertical relief affects hard bottom communities to the greatest extent (Hardin, pers. comm.).

Percent cover and abundance were greatest at 3 mab compared to 0 and 13 mab when differences existed. However, this trend is different from previous studies in the northwestern Gulf of Mexico, which indicate increasing diversity, coverage, and abundance with the highest relief (Pequegnat 1964; Genin et al. 1986; Messing et al. 1990; Gittings et al. 1992; Hardin et al. 1994). Solitary anemones (Order Actinaria) were the exception in that their abundances were higher at 13 mab. This is similar to past findings.

Sediment cover and total percent cover were equal at 3 and 13 mab, even though bulk sediment flux is nine times greater at 3 mab than at 13 mab (see Chapter 5). Currents throughout the study area are much more variable in speed and direction at 3 mab than at 13 mab (Kelly, pers. comm.). Currents rather than flux appear to control sediment accumulation on plates. Variable current speeds and direction may prevent greater sediment loads from accumulating at 3 mab through constant resuspension of sediments.

The height differences in community structure may be caused by the physical dynamics in the region. Sediment flux and currents are highly variable and the majority of carbonate mounds are between 1 and 5 m in height. It is assumed the source communities are located in the study area and not at a distant location. Organisms evolve adaptations to cope with environmental conditions. It is axiomatic that the majority of organisms within the study area are best suited to survive in hydrographic conditions present at 1 to 5 mab and not those at higher relief, e.g., 13 mab, because these habitats are rare. This would explain the greater abundances and higher diversity of organisms on settlement plates 3 mab than on those at 13 mab. Currents also affect feeding. Many of these organisms are passive suspension feeders that rely on particle contact rates for feeding. Greater variability in speed and direction of currents may increase particle contact rates for these organisms by enhancing turbulence (Jokiel 1978; Dai and Lin 1993; Eckman and Duggins 1993).

Variability in physical conditions may be responsible for the increased diversity at 3 mab. Intermediate levels of disturbance can increase success of subordinate organisms in the presence of dominants and therefore increase diversity (Levin and Paine 1974; Levin 1976; Connell 1978; Connell and Slayter 1977; Quinn 1979; Hastings 1980; Sebens 1987). Currents and sediment flux at 13 mab are relatively homogeneous among all sites. Organisms that are dominant at this height are most likely inhibiting rare species through interference competition.

Mean current speeds may be responsible for the relative lack of passive suspension feeders at 13 mab. Currents at 13 mab are often greater than 20 cm s^{-1} , whereas currents at 3 mab rarely reach speeds greater than 15 cm s^{-1} (Chapter 6). Intermediate flow speeds ($4\text{--}7 \text{ cm s}^{-1}$) enhance growth of suspension feeders because of increased particle contact rates (Eckman and Duggins 1993). At speeds greater than 10 cm s^{-1} , however, feeding appendages of suspension feeders often become deformed and organisms are unable to feed completely or efficiently. Cnidarian metabolism may be regulated by ambient flow as well (Jokiel 1978). Increased flow increases respiration, but inhibition can occur at high rates of current speed

where respiration rates become excessive. Because mean current speeds at 3 mab ($5-10 \text{ cm s}^{-1}$) are within the optimal range for suspension feeders reported in laboratory studies ($4-8 \text{ cm s}^{-1}$), abundance, diversity, and cover should be greater at 3 mab than at 13 mab.

In September 1998, Hurricanes Earl and Georges passed directly over the study area. However, it is impossible to determine specific effects these hurricanes had on the recruitment study because of the long periods between retrievals. Current speeds during Hurricane Georges exceeded 100 cm s^{-1} , a speed at which all sizes of sediments, shell hash, and boulders are pushed along the bottom (Continental Shelf Associates, Inc. and Texas A&M University 1999; Walsh, pers. comm.). Erect organisms were likely scoured off substrate by the extreme shear forces created along the substrate and suspension feeders likely were unable to feed. Moving boulders, gravel, and shell hash should have the greatest impacts on epibiont communities by crushing and tearing organisms on the substrate. At current velocities reached during the peak of a hurricane, however, sediments continually sandblast substrates (Walsh, pers. comm.). The nepheloid layers during these events were pushed up to 40 meters above bottom by onshore flows. It is not known if substrates at 3 and 13 mab are affected similarly. While specific hurricane effects are not known, long-term average variation of physical factors at different heights above bottom is likely the major controlling process of community structure in this region.

Experimental Manipulation

There were no significant patterns for effects of ecological processes on community structure. The fourth and fifth null hypotheses (H_4 : *epibiont coverage, abundance, and diversity are not affected by disturbance*; and H_5 : *epibiont coverage, abundance, and diversity are not affected by differences in small-scale turbulence*) cannot be rejected. Differences between experimental manipulations for dominant organisms were not significantly different and were small in relation to the average total cover of organisms. Rare taxa, on the other hand, were enhanced or neutrally affected by disturbance. Small-scale water flow disruption often negatively affected rare taxa. Disturbance may enhance percent cover of rare organisms by preventing monopolization of substrate by one, or a few, dominant taxa (Sebens 1987). Turbulent water flows and eddies typically increase around and within caging structures. It was expected that water flow disruption would increase particle contact rates, and therefore growth, for some of the rare, passive suspension feeders. Small-scale turbulence may have had an additional unknown effect on some of these organisms, inhibiting their growth.

Assuming no differential mortality between partially-caged (P) and uncaged manipulations (U), water flow disruption and subsequent turbulence due to cages had no effect on abundances of bivalves, polychaetes, or barnacles. An initial theory was that turbulence would increase larval contact rates and that higher abundances would be found in the partially-caged (P) manipulations than in the uncaged (U) (Mullineaux 1989; Abelson and Denny 1997). However, caging effects have been found in other studies and it may be that predators may be attracted to caging structures (Connell 1997).

Orientation

Vertical plates were covered by significantly greater abundances of stoloniferous organisms, including bryozoans, while solitary or slow-growing colonial animals were less abundant on the sides when compared to the bottom-oriented, or often top-oriented, plates. Therefore, the sixth null hypothesis (H_6 : *epibiont coverage, abundance, and diversity are not affected by orientation of settling surface*) can be rejected. These are early colonizing species that tend to be reduced in late stage communities. This indicates that successional processes on vertical substrata may be slower than those of horizontal substrata. Similar results were found in the rocky intertidal where complete colonization of vertical plates took 18 months versus 5 months on horizontal plates (Menge 1976).

Location on vertically oriented substrata can affect community composition as well. Bluff bodies (e.g., pinnacles), or those with faces oriented normal to flow, force acceleration over the top and sides of the substrate (Leichter and Witman 1997). Bivalves have reduced competitive ability on vertical substrates (Menge 1976). This may be due to the reduced ability of dominant organisms to settle and colonize vertical substrates.

Sediment cover, typically attached by biofilm, was greatest on the top plates. Ostreoida and Foraminifera, the two taxa that seem best able to deal with high sediment loads, were found in greatest abundance and cover on the top plates. Passive, colonial, suspension feeders, such as hydroids and bryozoans, were less abundant and had less cover on top plates, so these organisms are more prone to sedimentation effects.

Cnidarians are also inhibited by increased sedimentation. These organisms must slough off tissue to remove sediment, and this is an energetically expensive process. These organisms were found most often on the bottom plates, where flow regimes were sufficient for feeding, but sedimentation is reduced.

Conclusions

The study area is an extremely dynamic and variable region. Current speeds, current direction, and sediment fluxes often vary to a greater extent within sites than among sites. There is also much variability in individual taxa and community structure across all scales. The variability of physical dynamics of the region indicates that community patterns may not be deterministic.

Data from this study and photographic surveys indicate that relief of the substrates in terms of height above bottom and microhabitat characteristics (e.g., orientation of substrata to mean flow) have the strongest effects on community structure and development. Variations in larval supply due to flow field variance and sediment flux may explain the site-to-site and height above bottom differences. Life histories and adaptations of source communities will have the greatest influence on vertical distribution of organisms.

Community development patterns indicate that communities within the study area are tolerant to the background physical variability of the region, but are likely to be sensitive to

strong, stochastic disturbance events. It may take decades for severely disturbed communities to fully recover because settlement and growth rates are slow. This is critical for management of oil and gas development on the outer shelf in this region. Organisms of the study area are likely sensitive to anchoring and dumping of highly contaminated sediments or drill cuttings because of slow development rates and inhibition of suspension feeders. All of these activities would likely result in patch formation. The frequency and severity of natural and anthropogenic patch formation, physical variability of current flows and sediment fluxes, and recruitment rates from surrounding source populations will determine the community's ability to retain and maintain diversity.

Future studies must employ longer exposure periods at multiple depths and more frequent retrievals to obtain better estimates of total recovery time and effects of specific stochastic events, such as hurricanes or anchor-dragging. The settling plate approach used in the current and past studies has relied on introducing vacant substrates to the environment. A different approach, experimentally clearing actual pinnacle habitat and following recolonization over time, would provide different data that would be relevant to managing disturbance of the habitat. Community development depends on two pre- and post-settlement processes. The current study focused exclusively on post-settlement processes, and this knowledge would be improved with habitat-clearing experiments. Pre-settlement processes, however, occur in the water column and depend on larval interactions with the environment. Larval ecology of the dominant or key species of concern must be studied. More complete studies in the future would include both planktonic and benthic components. In addition, more life history information is needed for the rare, and possibly endemic, epifauna. Knowledge of timing and mode of reproduction, in particular, are critical needs. For example, it is known that stochastic events in the study area advect enormous quantities of water out of the region. Timing of settlement in relation to other organisms has a great impact on the outcome of community development and succession due to competitive interactions (Osman 1977; Sutherland and Karlson 1977). If a storm were to occur during an annual mass spawning event, recruitment would most likely be zero for the year for these organisms, and the local community composition may be changed for an indefinite period of time.

Chapter 11: Synthesis

*Neal W. Phillips and David A. Gettleton
(with input from all chapter authors)*

The overall goal of this program was to characterize and monitor biological communities and environmental conditions at carbonate mounds along the Mississippi-Alabama OCS. Program objectives were as follows:

- To describe and monitor seasonal and interannual changes in community structure and zonation and relate these to changes in environmental conditions (i.e., dissolved oxygen, turbidity, temperature, salinity, etc.); and
- To characterize the geological, chemical, and physical environment of the mounds as an aid in understanding their origin, evolution, present-day dynamics, and long-term fate.

Previous chapters have summarized and synthesized the results of individual program components. Each component had specific objectives, many of which (in keeping with the program objectives stated above) involved either characterizing the environment or testing hypotheses about relationships between environmental variables and biological communities. This synthesis chapter (1) highlights relationships between hard bottom communities and environmental conditions, including temporal changes; (2) discusses the implications of study findings for resource management; (3) evaluates the program's success in addressing its goals.

Hard Bottom Communities and Environmental Conditions

The five megasites selected for geophysical reconnaissance and the nine sites selected for monitoring represent a range of mound occurrence and morphology, geographic location, water depth, and other environmental conditions. The program design explicitly focused on vertical relief, with three monitoring sites in each relief category (high, medium, and low); geographic location, with three sites in each category (western, central, and eastern); and time, with four monitoring cruises over two full years of field sampling.

Of particular interest from the standpoint of hard bottom community/environment relationships are the influences of (1) sediment flux and related variables; (2) substrate and microhabitat; (3) currents; and (4) recruitment.

Sediment Flux and Related Variables

Previous studies in the Gulf of Mexico, South Atlantic Bight, and off Southern California have shown that hard bottom community development varies with substrate relief (Marine Resources Research Institute 1984; Rezak et al. 1985; Continental Shelf Associates, Inc. 1987a; Phillips et al. 1990; Hardin et al. 1994). In the northern Gulf of

Mexico, the influence of vertical relief on hard bottom community development reflects the importance of two key environmental factors: sedimentation and light. A persistent benthic nepheloid layer characterizes the outer shelf environment in the central and western Gulf, and this layer negatively influences the distribution and abundance of attached invertebrates and fishes associated with hard banks (Rezak et al. 1985; Dennis and Bright 1988a). As substrate relief increases, chronic exposure to resuspended bottom sediments decreases. The detrimental effects of suspended sediments on hard bottom communities, especially corals, have been widely documented (Rice and Hunter 1992; Wesseling et al. 1999; Cox et al. 2000). Light levels *per se* are important mainly for communities on high relief features in clear, oceanic waters – e.g., the East and West Flower Garden Banks, which have sufficient vertical relief so that their crests can support reef-building corals (Rezak et al. 1985).

Previous visual observations in and near the present study area have suggested that community development varies with substrate relief and proximity to the Mississippi River. Gittings et al. (1992) noted that “the effects of resuspended bottom sediments may be the principal environmental control over hard-bottom epibenthic community development in the study area.” They hypothesized that long-term water quality becomes suboptimal for hard bottom community development within about 70 km from the Mississippi River delta. East of this “Mississippi Threshold,” factors other than those influenced by the Mississippi were considered likely to predominate. The potential influence of the Mississippi River was the principal reason for stratifying monitoring sites by longitude in the present study.

Our study sites were initially categorized as high, medium, or low relief. However, high relief sites were generally located (in part) on top of large mounds where there were extensive areas of relatively flat hard bottom. At other sites, the presence of multiple smaller mounds created a variety of hard bottom relief and orientation that was not captured by the single relief designation of a whole site. Despite the oversimplification, the three relief categories generally did correspond to the range of depths sampled photographically at each site (**Fig. 11.1**). The range of photograph depths was greatest at the three high relief sites (1, 5, and 7) and lowest at the three low relief sites (3, 6, and 9). All three of the high relief sites included areas on top of flat-top mounds rising 15 to 20 m above the surrounding seafloor.

Transmissometry data (Walsh, Chapter 5) indicate that a benthic nepheloid layer was present at all four of the mooring sites (1, 4, 5, and 9) during all casts, though with a wide range in concentrations. The benthic nepheloid layer was found to be associated with lower bottom water temperatures, indicating that intrusions of slope water were commonly accompanied by bed shear stresses exceeding the sediment resuspension threshold. The benthic nepheloid layer extended up to 15 to 20 m above the bottom. As indicated on Fig. 11.1, such a nepheloid layer probably would encompass all but the tops of the highest relief mounds (e.g., Sites 1 and 7).

The benthic nepheloid layer was particularly persistent and intense at Site 5 (central) and Site 9 (western), and less so at Site 1 (eastern) and Site 4 (central) (**Fig. 11.2**). Since

Vertical Relief (Range of Photo Depths within Site)

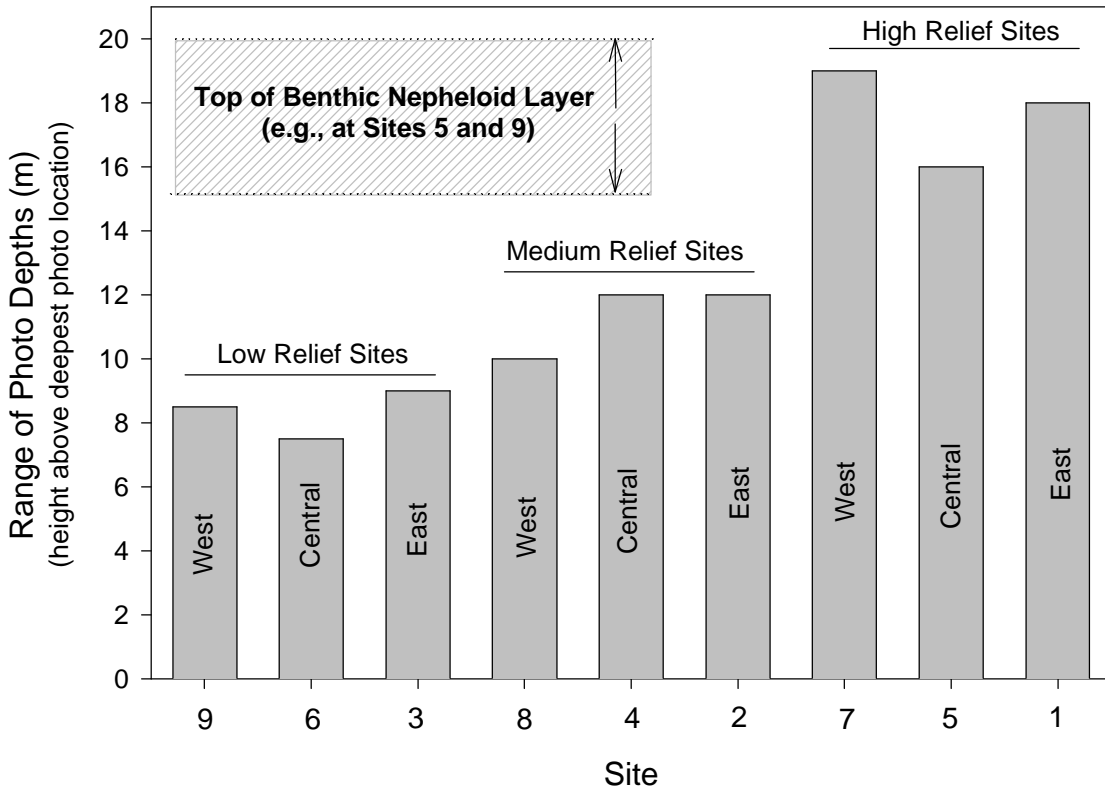


Fig. 11.1. Vertical relief (range of photographic station depths) at each site.

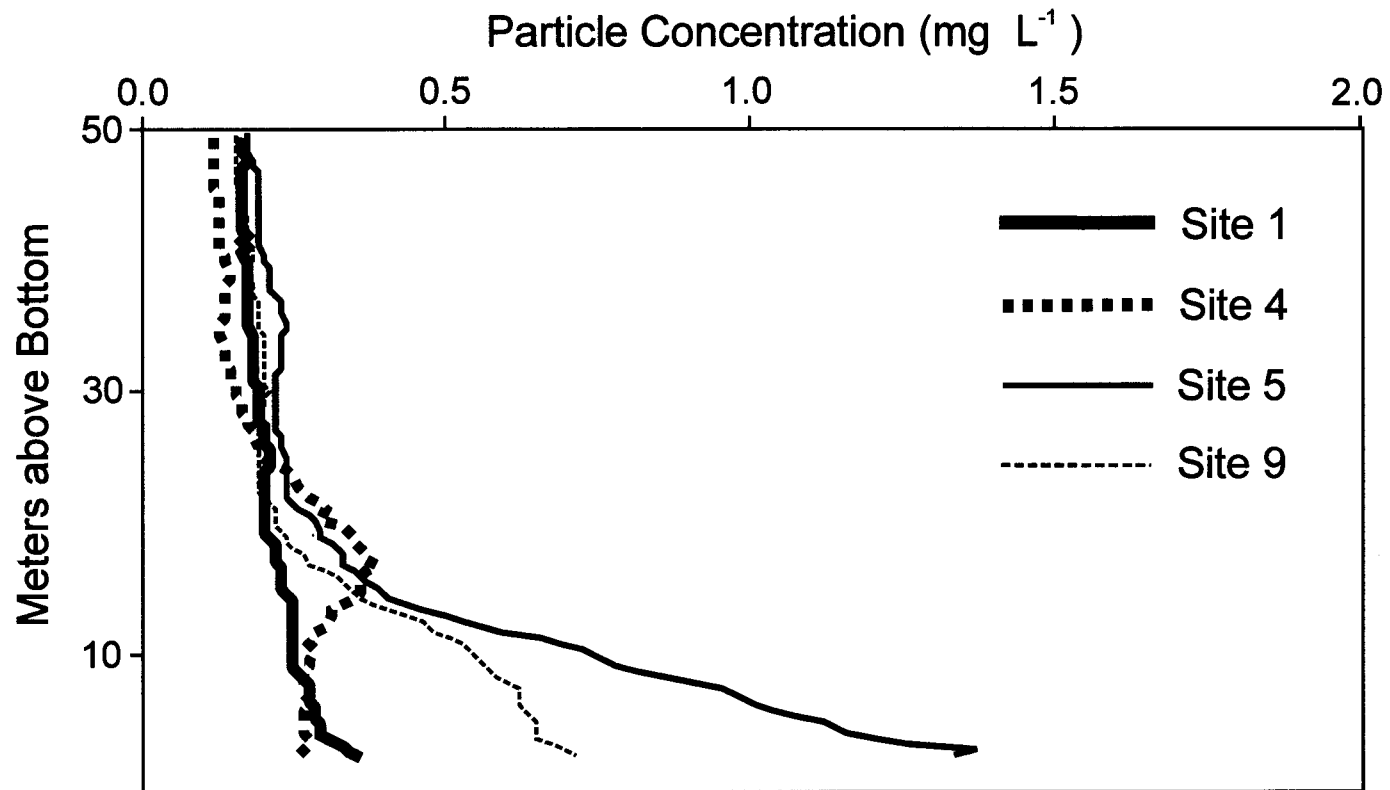


Fig. 11.2. Mean particle concentration profiles presented on a common height above bottom scale (From Walsh, Chapter 5).

Sites 5 and 9 represent nearly the full range of water depths studied, it is difficult to discern obvious bathymetric trends. However, there were bathymetric differences among the sites in terms of the particle distribution in the bottom water. Site 4, which was deeper than Site 9, often had an intermediate nepheloid layer with higher concentrations than in the benthic nepheloid layer, reflecting advection of a detached benthic nepheloid layer from shallower depths (Walsh, personal communication). While Sites 1 and 4 encompassed the full range of water depths studied and had similar mean particle concentrations in the benthic nepheloid layer, Site 1 showed a mean that increased toward the bottom (generally indicative of active resuspension), while Site 4 did not.

There is also some indication of an east-west trend. This can be illustrated further with the vertical sediment flux data (from sediment traps). **Fig. 11.3** shows plots of sediment fluxes (averaged over all non-hurricane periods) vs. distance from the Mississippi River. There is a slight overall decline in fluxes with increasing distance from the Mississippi. In addition, fluxes at the easternmost sites (1 and 4) vary less with height above bottom. Finally, the near-bottom fluxes at Sites 5 and 9 are quite high, consistent with the presence of a robust nepheloid layer at those sites. Site 5 and Site 1 arrays were at about the same water depth, but had quite different sediment fluxes (**Fig. 11.3**). It should be noted that these differences among sites are small compared with the temporal variations caused by the passage of hurricanes (Walsh, Chapter 5).

Near-bottom sediment fluxes are attributable mainly to local resuspension of sediments (Walsh, Chapter 5). An east-west trend in vertical sediment fluxes, or in near-bottom particle concentrations, does not mean that Mississippi River particulates are being transported through the water column and then deposited directly on the study sites. More likely, western sites are closer to areas of Mississippi-derived silts and clays, which are more easily resuspended than sand or gravel. The limited sediment sampling conducted around each site provides only a slight indication of this (e.g., data presented by Kennicutt in Chapter 4 showed a slight trend of decreasing carbonate content and increasing metal concentrations [associated with finer sediments] toward the west). The overall trend of increasing fine sediments toward the Mississippi River is well known from previous data for the region (Brooks 1991).

The density, diversity, and species composition of hard bottom communities vary among and between sites, and may be affected by numerous subtle factors (Chapters 7 and 9). Interpretation of environmental influences is confounded by the large number of intercorrelated variables. Nonetheless, some possible relationships between community development, vertical relief, and distance from the Mississippi River are evident. **Fig. 11.4** shows that generally, biotic cover and number of epifaunal taxa increased with vertical relief (as measured by the range of photographic station depths at each site). Similarly, the number of fish taxa appears to be positively related to relief. However, as noted by Snyder in Chapter 8, high numbers of fish taxa at Site 1 (one of the shallowest sites) include numerous shelf species not found at the other sites; thus, it is not simply a matter of high relief at this site. Two high relief sites (1 and 5) had low numbers of epibiotal and/or fish taxa.

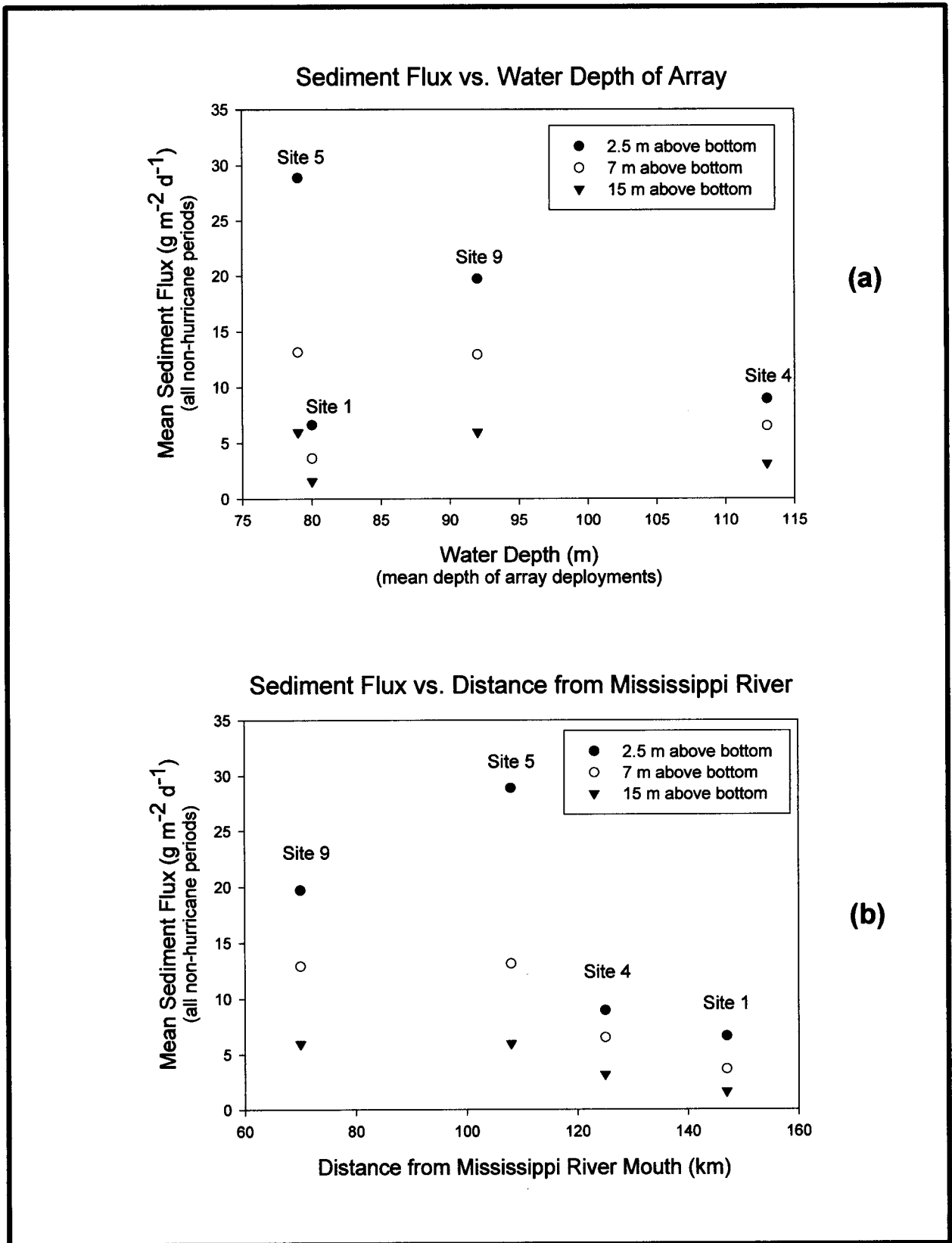


Fig. 11.3. Sediment flux (mean over all non-hurricane periods) vs. (a) water depth and (b) distance from Mississippi River mouth.

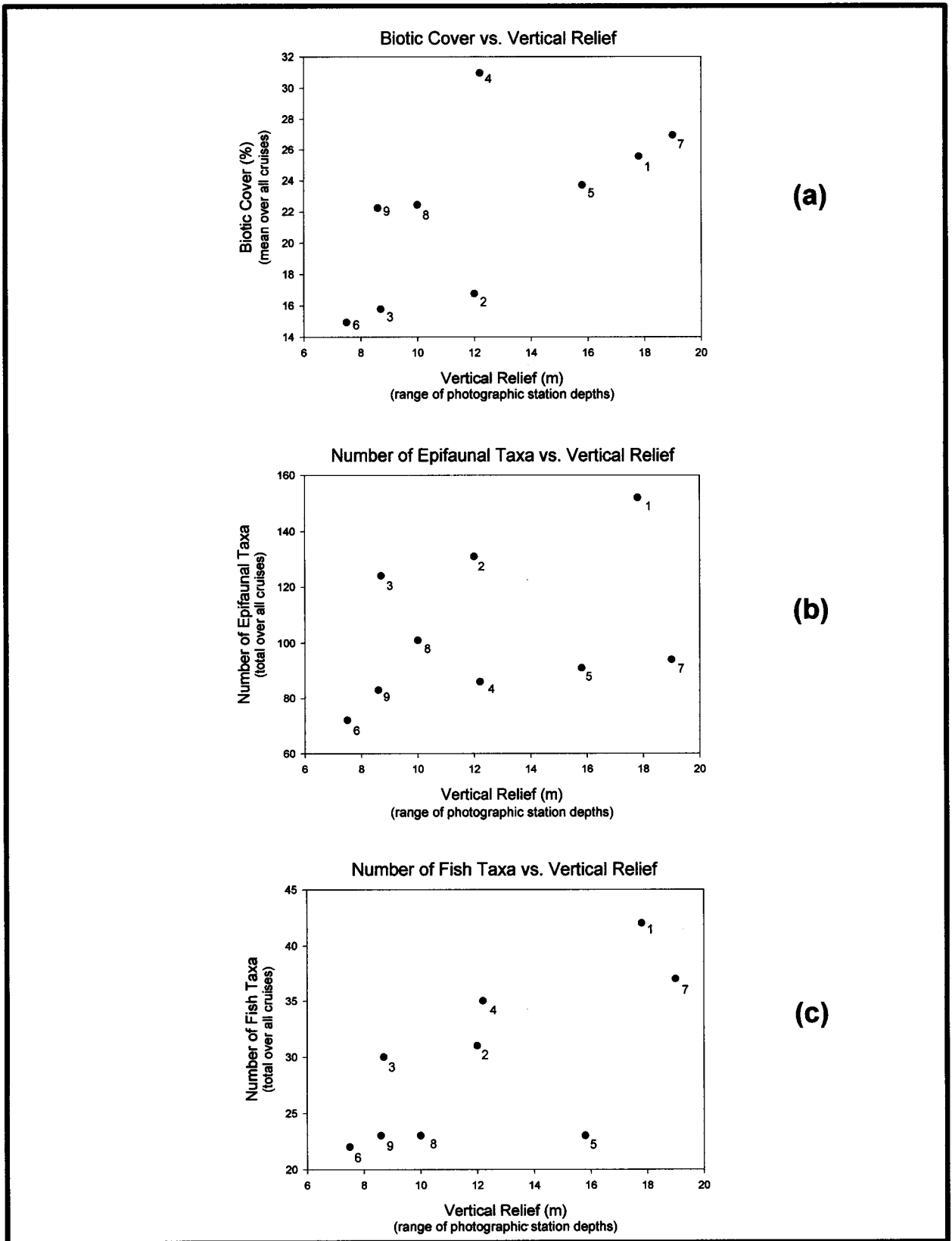


Fig. 11.4. Overall relationships between hard bottom communities and substrate vertical relief. (a) biotic cover; (b) number of epifaunal taxa; and (c) number of fish taxa. Numerals next to data points are site numbers.

To investigate the influence of sedimentation more directly, vertical sediment fluxes were estimated for each monitoring site. Sediment trap data are available only for the four mooring sites (1, 4, 5, and 9). In Chapter 7, Hardin et al. developed a multiple regression equation to predict vertical sediment flux at photoquadrats within each site, as a function of height above “bottom” and distance from the Mississippi River. A slightly different approach is taken here. Data from the four mooring sites (for non-hurricane periods) are used to estimate fluxes for nearby sites, as follows:

<u>To predict flux at:</u>	<u>Used data from the following site:</u>	<u>Used the following trap height:</u>
Site 1	Site 1	15 mab
Site 2	Site 1	7 mab
Site 3	Site 1	2.5 mab
Site 4	Site 4	7 mab
Site 5	Site 5	15 mab
Site 6	Site 5	2.5 mab
Site 7	Site 9	15 mab
Site 8	Site 9	7 mab
Site 9	Site 9	2.5 mab

High-relief sites were represented by data from the 15 mab trap; medium-relief sites were represented by the 7 mab trap; and low-relief sites were represented by the 2.5 mab trap. The results suggest a negative relationship between biotic cover and sediment flux, but there is a lot of variability (**Fig. 11.5[a]**). For example, Sites 2 and 3 had low biotic cover even though estimated sediment flux was low. The low percentage of emergent hard bottom at those sites may be a factor (discussed below). A more consistent negative relationship is apparent between sediment flux and total number of epibiotal taxa (**Fig. 11.5[b]**).

Further analysis of the influence of relief, sediment flux, and sediment veneer is presented by Hardin et al. in Chapter 7. The analysis includes relationships with individual taxa not considered here. For example, many taxa were found in higher abundances toward the east. Conversely, some taxa increased toward the west. Several analyses indicated an important effect of sediment veneer, especially for medium-high relief taxa. Microhabitat analyses by MacDonald and Peccini (Chapter 9) also showed that sediment veneer was a significant influence on gorgonian and antipatharian abundance.

In conclusion, this study found that hard bottom community development is generally greater on higher relief features, as expected, and this result is likely due in part to the negative effects of resuspended sediments on hard bottom epibiota. Also, even though all of our sites are at or east of the 70 km “Mississippi Threshold” hypothesized by Gittings et al. (1992), it appears that there are some east-west patterns in hard bottom communities in the study area. Whether these patterns reflect a direct or indirect influence of the Mississippi River or some other factor (e.g., frequency of mesoscale intrusions impinging on the shelf edge) is not known. It should also be noted that repetitive observations of

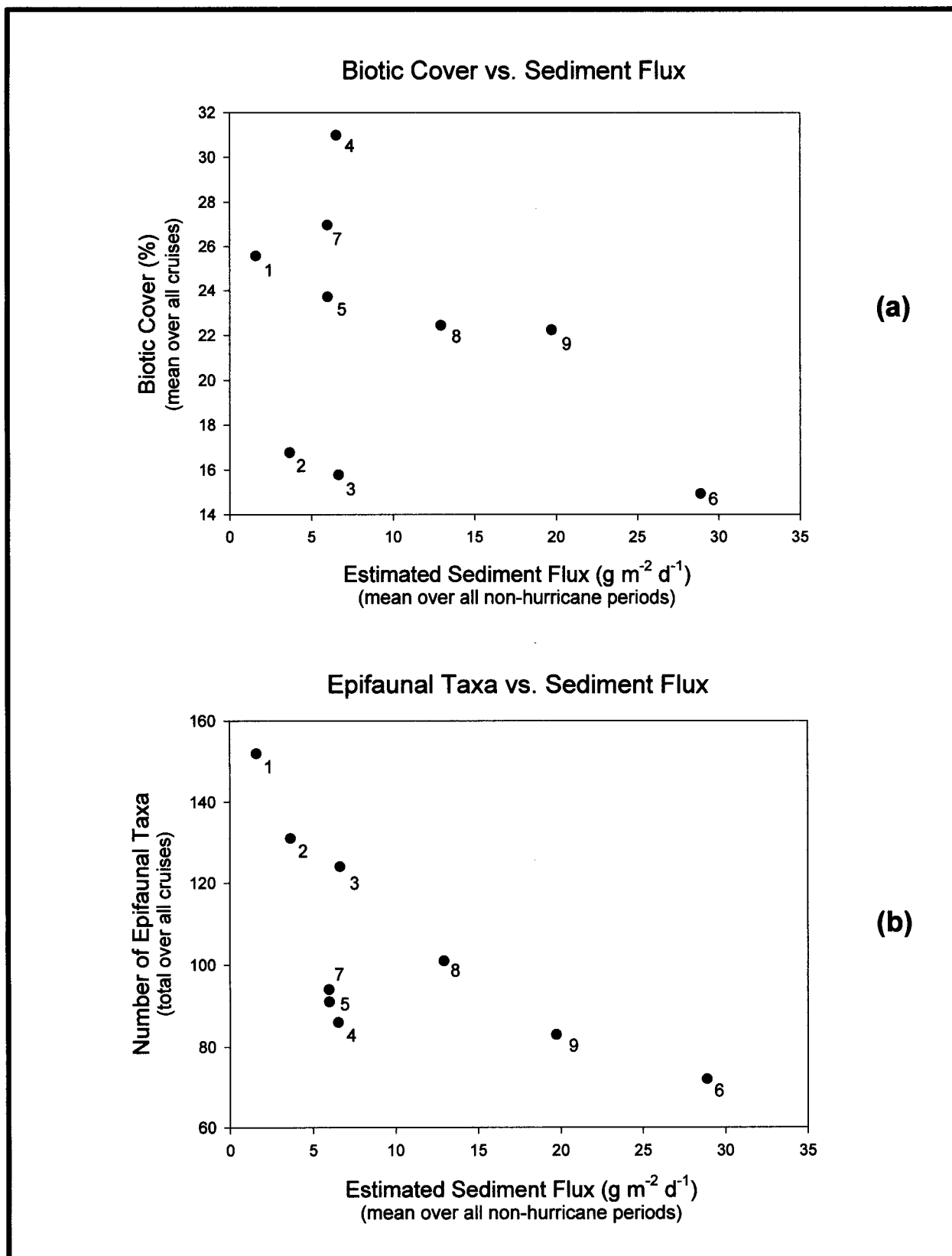


Fig. 11.5. Overall relationships between hard bottom communities and sediment flux: (a) biotic cover; and (b) number of epibiotal taxa at each site. Numerals next to data points are site numbers. Sediment flux was estimated for each site as described in the text.

fixed quadrats (Hardin et al., Chapter 7) suggest that many sessile organisms become buried and may remain that way for extended periods, while other taxa thrive in an environment characterized by frequent sediment movement. Results also suggest that other factors, including substrate variables (discussed below) and stochastic or unexamined processes, contribute substantially to distribution patterns of hard bottom communities.

Substrate and Microhabitat

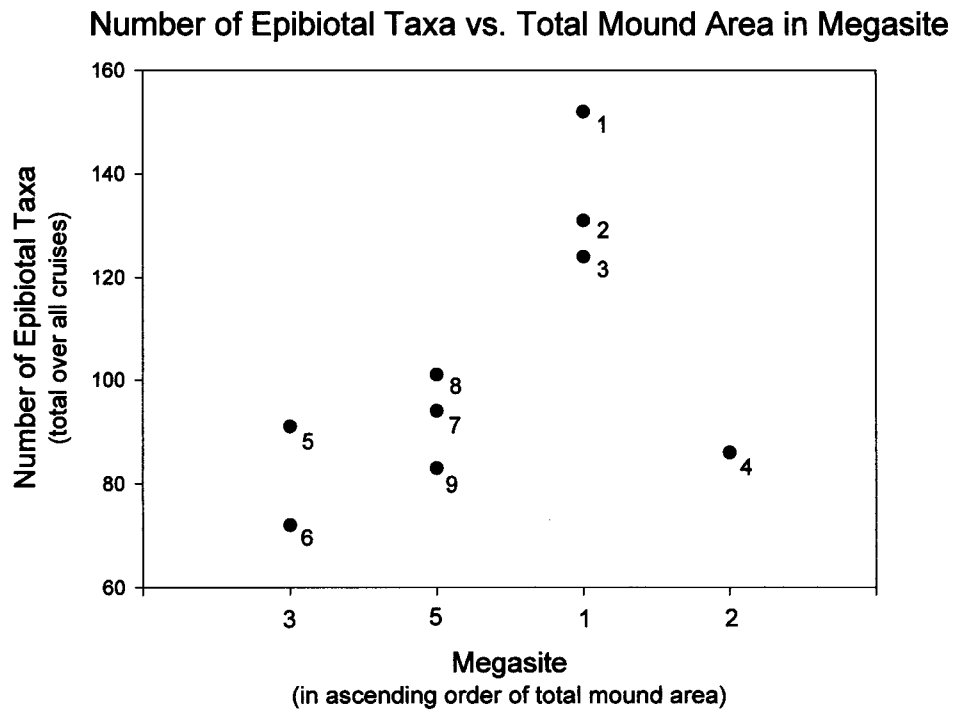
Substrate characteristics exert a profound influence on the distribution and abundance of hard bottom epibiota. This influence was evident at several scales examined in this program.

At the regional scale, the distribution of hard bottom communities is obviously related to the distribution of mounds. These features are essentially “islands” of hard bottom in a surrounding “sea” of soft bottom sediments. The overall distribution of mounds in the study area was documented during the previous MAMES and MASPTHMS reconnaissance studies. Thousands of mounds ranging from less than a few meters in diameter to nearly a kilometer were found arrayed mostly in two isobath-parallel bands (Sager et al. 1992). Mound distribution within megasites 1, 2, 3, and 5 has now been mapped in much greater detail in this program (Sager and Schroeder, Chapter 3).

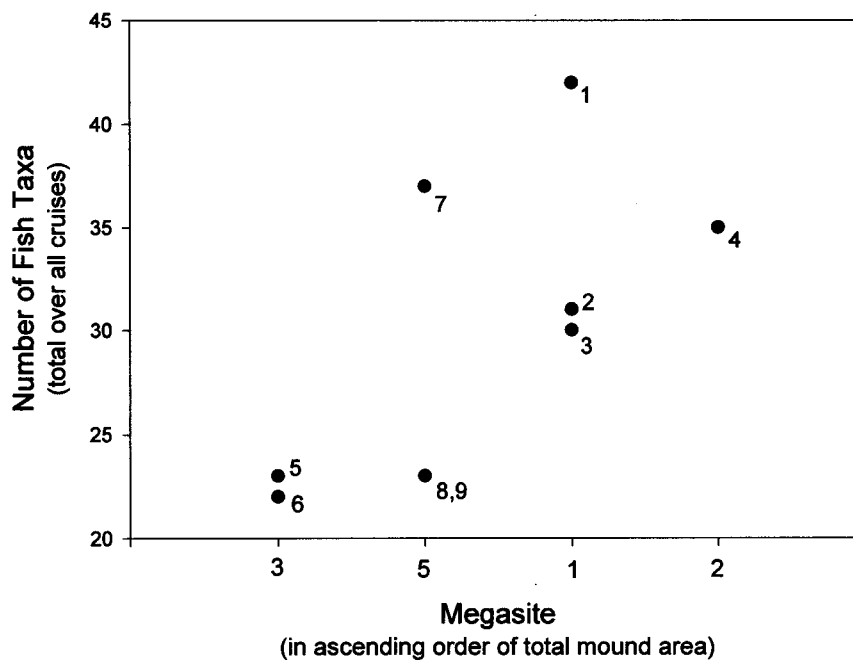
From the standpoint of “island” biogeography, one may expect to find more well developed communities on larger features than on smaller ones. Gittings et al. (1992) reported such an observation in the pinnacle trend area. It would be difficult to make this generalization for the present study, due to the small number of sites visited (nine) and the fact that larger features also tend to have greater relief. Among the only three “high relief” sites, Site 7 was on the largest feature, followed by Site 1 and Site 5. While mean biotic cover followed the same rank order (26.96%, 25.57%, and 23.72%, respectively), the total number of epibiotical taxa did not (94, 152, and 91, respectively).

One can also speculate that total numbers of hard bottom taxa might be related to the total area of hard bottom features in a megasite. **Fig. 11.6** shows a plot of total number of epifaunal taxa and fish taxa for sites in each megasite, with megasites arranged in order of increasing total mound area. Both plots suggest a positive relationship, but also much variability that must be due to other factors. Comparisons among megasites are also confounded by geography, since the megasites are arranged along an east-west gradient. Also, megasite 2 is represented by only one site in this analysis, further limiting the conclusions that can be drawn.

For the geology and microhabitat analyses, substrates maps of each site were prepared, as shown by Sager and Schroeder in Chapter 3. The major categories were continuous hard bottom, monoliths, mounds, flats with rubble, and sediment flats. The substrate composition of monitoring sites is summarized in “pie chart” form in **Fig. 11.7**. For this presentation, flats with rubble and sediment flats were combined as sediment flats. The other categories represent different forms of emergent hard bottom.



(a)



(b)

Fig. 11.6. Overall relationships between numbers of taxa at each site and total area of mounds in each megasite: (a) number of epibiotal taxa and (b) number of fish taxa . Numerals next to data points are site numbers. Relative areas of mounds are from Sager and Schroeder (Chapter 3).

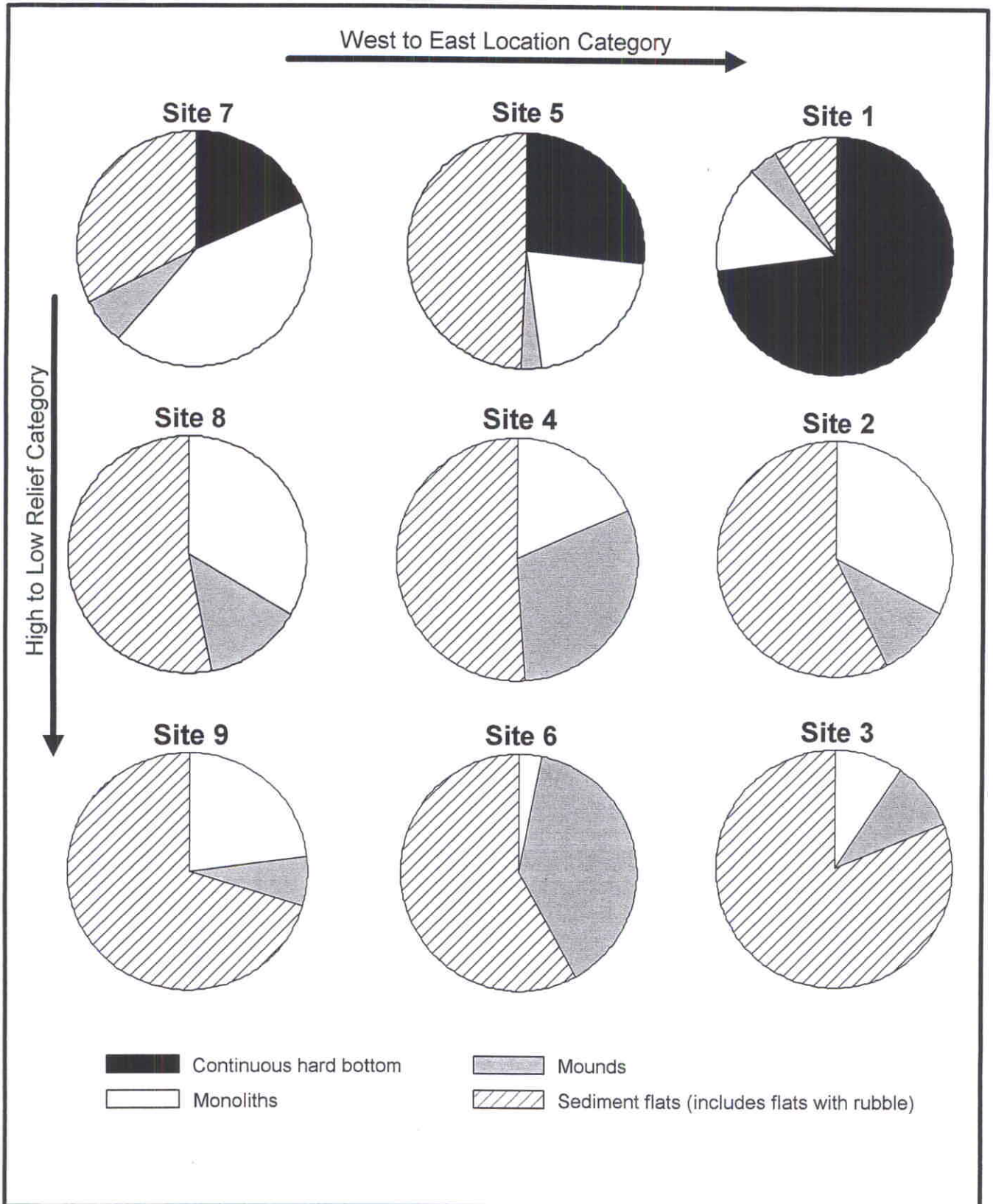


Fig. 11.7. Percentages of substrate types making up each of the nine monitoring sites.

Site 1, located mostly on top of a flat-top mound, had the largest percentage of continuous hard bottom (73%). Not surprisingly, this site had the highest number epibiotal and fish taxa, although not the highest mean biotic cover. The community at Site 1 emerged as distinct from the other sites in ordination analyses performed for the hard bottom community and fish chapters. This was also the shallowest monitoring site (though similar to Site 5 in mean depth).

To illustrate the relationship between substrate types and hard bottom community development, biotic cover and numbers of taxa were plotted against the total percentage of emergent hard bottom within a site (**Fig. 11.8**). This includes continuous hard bottom, mounds, and monoliths. Generally, there is a positive relationship for all three variables (biotic cover, epibiotal taxa, and fish taxa). However, there is also much variability that is not evidently explained by the hard bottom percentage.

At a finer scale, many relationships between microhabitat factors and distributions of hard bottom taxa have been documented in this program. Hardin et al. (Chapter 7) documented significant effects of small- and medium-scale roughness on the distribution of individual hard bottom taxa. MacDonald and Peccini (Chapter 9) showed that microhabitat factors including small- and medium-scale roughness, slope, and location on feature significantly affected the abundance of selected antipatharians and gorgonians. Snyder (Chapter 8) documented habitat use by fishes at different scales within sites, including associations with microhabitat features such as crevices, holes of different sizes, and specific epibiota such as sponges, crinoids, and soft corals.

Currents

Across the entire study area there was substantial similarity in the observed flow at 16 meters above bottom, which is the mesoscale flow just above the mounds (Kelly et al., Chapter 6). Principal axis analysis showed a slight east-west trend in the orientation of the major axes, i.e., 66.2° at Site 1 to 75.5° at Site 9, which probably is related to the large-scale trend of the bathymetry, rather than the mesoscale-scale topography near each site.

Closer to the seafloor, the current regime is more likely to be affected by the presence of large mounds nearby. This was most evident at Site 1, where mooring 1A was within one mound diameter northeast of the feature. The near-bottom data for Site 1 had a lower mean speed and a larger percentage of near-bottom current speeds in the 0–5 cm/s range than did Sites 4, 5, or 9. At Site 1, currents were also less strongly directional, and the counterclockwise rotation of the principal axis at 4 mab (relative to that at 16 mab) was greater than at Sites 4, 5, or 9. The literature review of flow over generalized mounds (Kelly et al., Chapter 6) provides a possible explanation for the observed flow effects at mooring 1A. There were also some inconclusive indications of possible flow perturbation at Site 5, where the moorings were near a smaller, high relief mound.

Storm-related bottom currents may be responsible for some of the patterns of sediment distribution around mounds (Sager and Schroeder, Chapter 3). When Hurricanes Earl and Georges passed through the study area in September 1998, they created strong

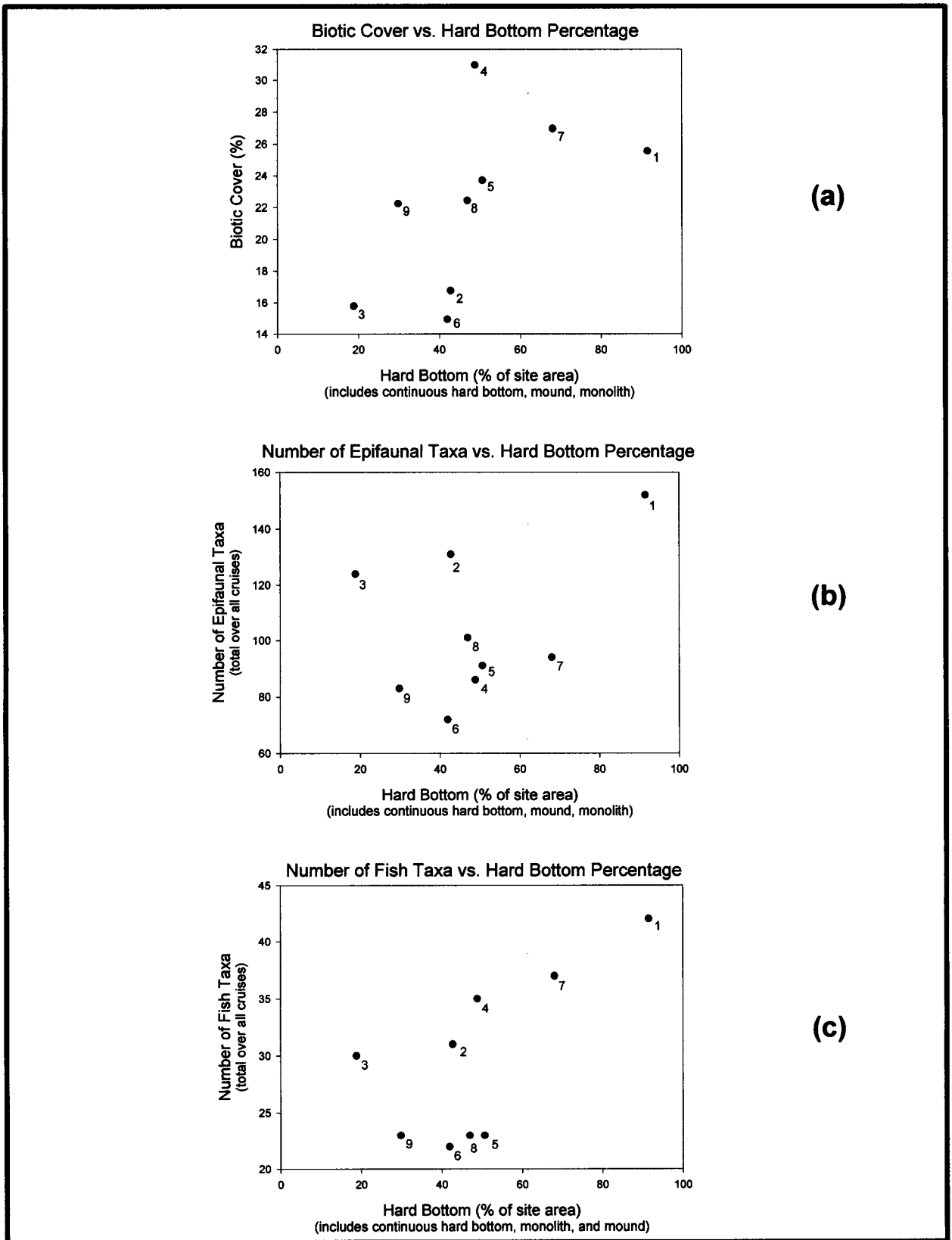


Fig. 11.8. Overall relationships between hard bottom communities and areal percentage of hard bottom within sites (including continuous hard bottom, mound, and monolith substrate types): (a) biotic cover; (b) number of epifaunal taxa; and (c) number of fish taxa. Numerals next to data points are site numbers.

currents toward the southwest in approximately the same direction as the linear scour marks observed in side-scan sonar records. These large storms created currents in the right direction to cause the scour marks and, based on sediment trap data (Walsh, Chapter 5), had the power to move the sediments. Sager and Schroeder hypothesize that eddies created when storm currents impinge on the mounds are responsible for this current scour. Strong currents during storms may also explain the observation that sediments are piled up against the north sides of many mounds. Finally, storm-related resuspension may also explain the mixture of sand and clay observed in grab samples (Sager and Schroeder, Chapter 3).

Hardin et al. (Chapter 7) showed that distribution patterns of some epibiota (e.g., bearing relative to the center of a feature) may be related to current direction. The analysis focused on two derived variables, "kinetic energy" and "food flux." Kinetic energy, which suspends sediments and may bend or break tall, upright organisms, is proportional to the square of the current speed. The flux of food particles available to suspension feeding organisms is proportional to the current speed. These two indicators of current effects have slightly different percent distributions among different headings (i.e., the directions toward which the currents flow) and each is slightly different from the directional distribution of currents. Combined abundances of *Madracis/Oculina* sp., crinoids, and total antipatharians varied spatially (bearing relative to the center of the hard bottom feature) in a way that was significantly correlated with the spatial distribution of both kinetic energy and food flux. None of the other organism distribution patterns examined was related to current parameters.

MacDonald and Peccini (Chapter 9) examined orientations of gorgonian and antipatharian sea fans in relation to current directions. Sea fans display characteristic orientations that can be readily determined from video imaging (the angle perpendicular to the major axis of the fans was used for the analysis). The analysis found that these mean orientations appear to be strongly influenced by the mean direction of water flow. Octocoral orientations at Sites 1, 3, 5, 7, and 9 generally agreed with the mean vector of the water flow data from the nearest current meter(s). Deviations from the current meter readings probably indicate local topographic steering. That is, local topography may be acting to steer water flow over the mounds in ways that are not captured by the current meter data. The analysis of flow structure over generalized mounds in Chapter 6 (Kelly et al.) indicates that such influences depend on the relief and horizontal extent of the feature, as well as current speed. The available current meter data and knowledge of flow over generalized mounds are insufficient to predict the current exposure of organisms at various locations on specific features studied. The orientation of sea fans provide a better indication of their current exposure than can be modeled with the present current meter data.

The overall picture emerging from the current meter data is a regional flow regime with local variations dependent on topography, rather than a strong east-west or onshore-offshore gradient. Clearly, current direction is an important influence on the orientation of filter-feeding sea fans. The distribution of other epifauna on hard bottom features may also be affected by current directions. Further, existing knowledge of flow

over bottom features suggests that different mounds, and different areas within a mound or mound complex, could experience different flow regimes that could affect the exposure of epibiota to sedimentation, erosion, and food flux. Finally, effects of storm currents on sediment distribution around mounds is evident in the geological data, though effects on hard bottom community distribution have not been investigated.

Epibiont Recruitment

The distribution of hard bottom communities is affected by biotic processes as well as the physical processes discussed above. The biotic processes occur in two phases: the pre-settlement ecological process in the water column (e.g., larval supply and interactions), and post-settlement ecological processes in the benthos (e.g., settlement, growth, competition for space, and predation). In contrast to rocky intertidal or shallow subtidal ecosystems, little is known about mechanisms controlling settlement, growth, and community development of deepwater epibiont communities. The recruitment component of the present study focused on the early post-settlement process (Holmberg and Montagna, Chapter 10). There was little difference in epibiont development among the four sites studied (1, 4, 5, 9). A likely explanation is that recruitment is a small scale process, and the source populations are much the same across the region. Relief (i.e., height above bottom) and microhabitat characteristics (i.e., orientation of substrata to mean flow) had the strongest effects on community development. Variations in larval supply with respect to depth, selection cues, and sediment flux may explain these microspatial differences. Physical effects were more important in regulating epibiont development than potential ecological interactions. Thus, the adult communities present were likely structured by larger scale physical processes examined in other study components. Life histories and adaptations of source populations likely have the greatest influence on vertical distribution of organisms on the mounds.

Management Implications

Oil and Gas Activities

Ultimately, information from this program may be used by the MMS to aid in leasing decisions and to develop and evaluate protective lease stipulations. For example, a series of studies during the 1970's and 1980's resulted in a biological community-based classification scheme for the Flower Garden Banks and northern Gulf hard banks (Rezak et al. 1985). These studies also documented the extent and importance of the nepheloid layer in controlling the composition of hard bottom communities. Biological, geological, and oceanographic data from these studies were used to develop lease stipulations, including shunting requirements and no-discharge zones near certain banks, which have been used successfully for many years in the northern Gulf of Mexico.

Fig. 11.9 shows the locations of petroleum platforms near the study area. Although no platforms are located next to study sites, there are several in the vicinity and over a dozen within 25 km of one or more megasites. Sediment barium concentrations around the study sites are close to background levels, showing little or no evidence of drilling

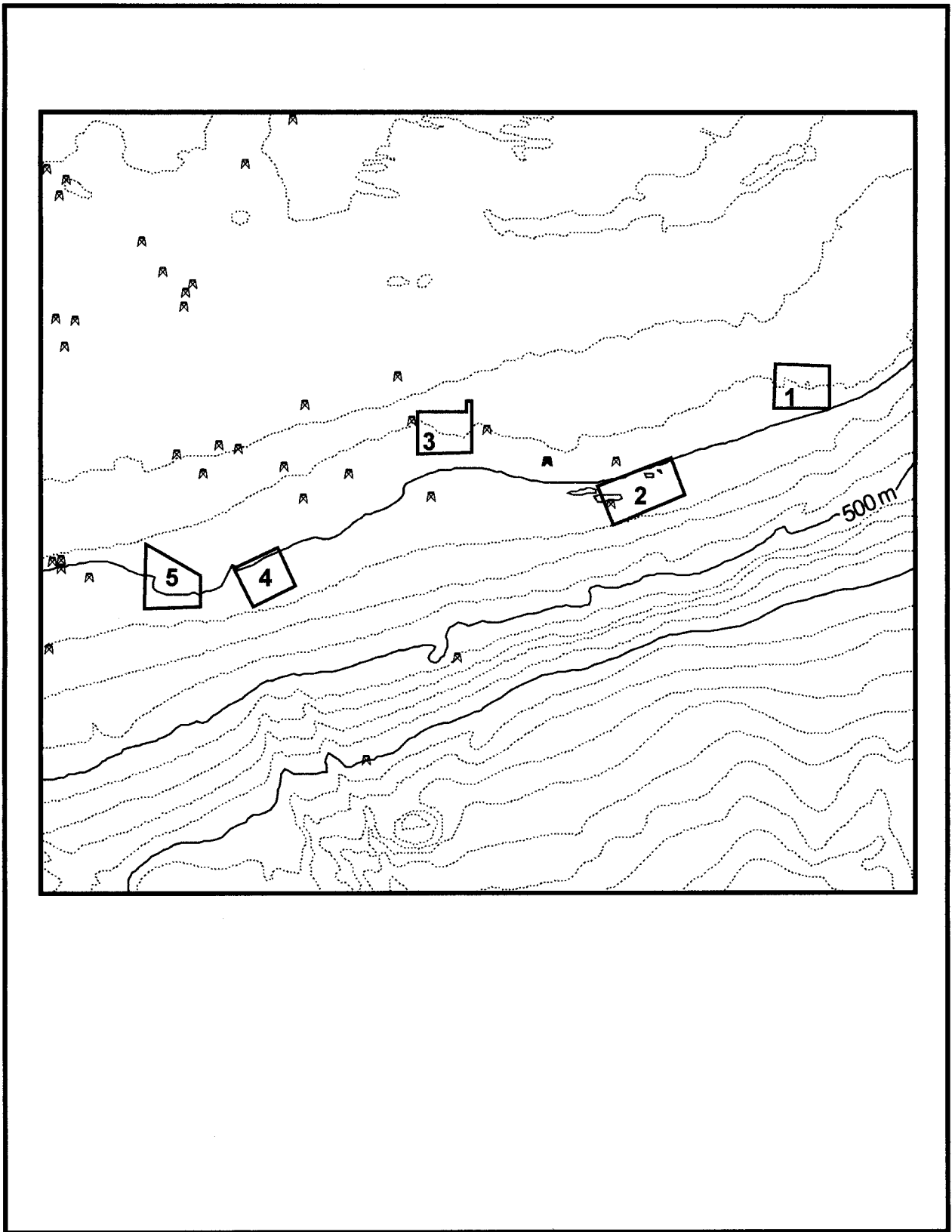


Fig. 11.9. Locations of oil and gas platforms near the five megasites.

discharges (Chapter 4). This is not surprising, given that drilling discharges are most likely to affect sediment composition within a few hundred meters to about 1 km of a drillsite (National Research Council 1983; Neff 1987).

Currently, 70 lease blocks in the Central Planning Area include a Live Bottom (Pinnacle Trend) stipulation (MMS 2000). The stipulation requires lessees to conduct a bathymetric survey prior to drilling, anchoring, or placing structures (rigs, platforms, or pipelines) on the bottom. If pinnacles are present, the MMS generally requires the operator to relocate activities to avoid mechanical damage from anchoring and placement of structures.

“By identifying the individual pinnacles present at the activity site, the lessee would be directed to avoid placement of the drilling rig and anchors on the sensitive areas. Thus, mechanical damage to the pinnacles is eliminated when measures required by the stipulation are imposed. The stipulation does not address the discharge of effluents near the pinnacles because the pinnacle trend is subjected to heavy natural sedimentation and is at considerable depths. The rapid dilution of drill cuttings and muds will minimize the potential of significant concentration of effluents on the pinnacles.”

The emphasis on mechanical damage rather than sedimentation due to drilling discharges seems appropriate, given that the communities are already exposed to significant natural sedimentation. Observations of fixed quadrats by Hardin et al. (Chapter 7) suggest that many sessile organisms become buried and may remain that way for extended periods, while other taxa thrive in an environment characterized by frequent sediment movement. While low-growing ahermatypic coral *Rhizopsammia manuelensis* were being buried in a fixed quadrat, taller antipatharians were growing. None of the prominent colonies of *R. manuelensis* showed evidence of tissue loss or disease, despite their apparently chronic inundation with fine sediments. The authors also observed that massive spherical or amorphous sponges seemed to be capable of removing loose sediment from their surfaces.

Although many hard bottom epibiota presumably tolerate sedimentation, the overall relationships discussed previously among community development, relief, and sediment flux suggest that it would be more detrimental to discharge drilling muds and cuttings on top of large, flat top mounds than to discharge them in low relief areas. Because the stipulation specifies avoidance of features during rig placement, it seems unlikely that drilling discharges would occur on or near large, high relief mounds.

Pipeline placement is another activity that could affect hard bottom features in the region. In water depths greater than 61 m, burial (trenching) of pipelines is not required. Therefore, the main concern is mechanical damage due to anchoring and placement of pipelines *per se*. The Live Bottom (Pinnacle Trend) stipulation includes the same limitations on placing structures (pipelines) near sensitive areas that apply to drilling rigs. Because high, medium, and many low relief mounds are detectable through bathymetric surveys, this stipulation should be effective in avoiding most impacts to pinnacle trend

communities. Some live bottom areas with little or no relief, or those where the hard substrate is partly or intermittently covered by a thin sediment veneer, may not be detected through bathymetric or geophysical surveys.

This study does not suggest any simple classification scheme for mound communities for management purposes. Although the study began with designation of study sites simply as high, medium, or low relief, the study area consists of an enormous number of mounds of varying sizes and shapes. In Chapter 3, Sager and Schroeder classified mounds into several different forms: (1) small, "unit" mounds, (2) composite mounds, (3) irregular mounds, (4) smooth-top mounds, and (5) carbonate hard bottoms. These classifications were useful for purposes of the geological discussion, but the distribution of biological communities does not correspond to these categories. Rather, it appears likely that suites of organisms are associated with substrate categories such as continuous hard bottom, monoliths, flats with rubble, or sediment flats, which are found in varying percentages in most sites regardless of the overall configuration. In addition, many subtle microhabitat variables influence the distribution of individual taxa (Hardin et al., Chapter 7; MacDonald and Peccini, Chapter 9).

The present study also confirms that drilling discharge restrictions (e.g., shunting) near carbonate mounds would not be effective in preventing exposure of hard bottom communities to drilling effluents. MMS oceanographic studies in the northwestern Gulf provided the basis for modeling the flow regime associated with topographic features (Rezak et al. 1985). As a result, lease stipulations were developed that require shunting of all drilling discharges to within 10 m of the bottom within certain areas near topographic features in the northwestern Gulf. However, the same considerations do not apply in the present study area. To model flow over and around features, one must first determine the general type of flow regime that is applicable. For the carbonate mounds studied here, the physics of non-rotating stratified flow applies, whereas for the Flower Garden Banks, rotating stratified flow physics applies (Kelly, personal communication). Rezak et al. (1985, pp. 110-112) discuss the latter case in detail. The principal differences between the two cases are the widths and heights above bottom of the features. While the Flower Garden Banks have diameters of several kilometers and occupy about 80% of the water depth, the mounds in our study area have diameters of hundreds of meters and heights that are 20% or less of the water depth. Based on order of magnitude estimates, theory and laboratory studies, near-bottom water upstream from a mound would indeed flow over it much of the time, and our study observations are consistent with this model. Therefore, if drilling discharges were shunted into near-bottom waters, the effluents could be transported onto mound communities.

Two sets of data collected during this program suggest that recovery of hard bottom communities following a disturbance would be slow. First, the repetitive quadrats analyzed in the hard bottom community study (Hardin et al., Chapter 7) showed a dynamic sedimentary environment but relatively little net growth or mortality of epibiota. Second, the epibiont recruitment study (Holmberg and Montagna, Chapter 10) showed relatively slow development of a fouling community on recruitment plates. Basically, only the earliest successional stages were observed by the end of the study (27 months of

exposure), and the epibiota typically associated with nearby hard bottom features were rare on the plates. It is not known whether the results would have differed if the substrate had consisted of exposed patches of natural hard bottom. Analysis of larger substrates (artificial reefs exposed for months to several years) also indicates slow community development (Marine Resources Research Institute 1984).

Fishing

Another human activity potentially affecting mound communities is fishing. Fishing gear, anchors, and other debris commonly observed in the video footage of the study sites indicate regular use of the area by fishers. It is likely that populations of groupers have been subjected to heavy fishing pressure from commercial and recreational fishers operating in the region. As noted by Snyder in Chapter 8, landings of warsaw grouper, other groupers, red snapper, and amberjack have all declined since the early 1970's. Catches of the smaller vermilion snapper have increased during the latter part of the same time period (**Fig. 11.10**). Collectively these trends resemble a situation called "fishing down the food web" (Pauly et al. 1998). This phenomenon occurs in areas where overfishing depletes more desirable species (usually top predators) forcing the fishery to target smaller, lower trophic level species in order to meet demands and generate revenue. These observations are intriguing, but a much more detailed analysis would be required to support this assertion for the study area.

Evaluation of Program Objectives

Information collected during MAMES, MASPTHMS, and earlier reconnaissance efforts in the study area consisted mainly of descriptive observations. These studies characterized major habitat types and identified some representative species. In addition, they generated some initial hypotheses about environmental relationships (Gittings et al. 1991, 1992).

The present study provided much more detailed information about the distribution of carbonate mounds in the study area (Chapter 3). In addition, it documented the characteristics of hard bottom communities at greater resolution and in greater detail than was previously possible (Chapters 7 and 9). It provided an opportunity to study relationships between hard bottom communities and environmental variables, and to monitor the dynamics of biological and physical variables over time. The information gathered has been analyzed in this report and will continue to be disseminated through peer-reviewed publications in the scientific literature.

Of the two program goals stated at the outset, the second ("characterize the geological, chemical, and physical environment of the mounds as an aid in understanding their origin, evolution, present-day dynamics, and long-term fate") was clearly met. An enormous amount of environmental data has been collected and interpreted to characterize the environment of the mounds. The data provide a basis for speculating on the origin and evolution of the mounds, though coring would be required to provide definitive information.

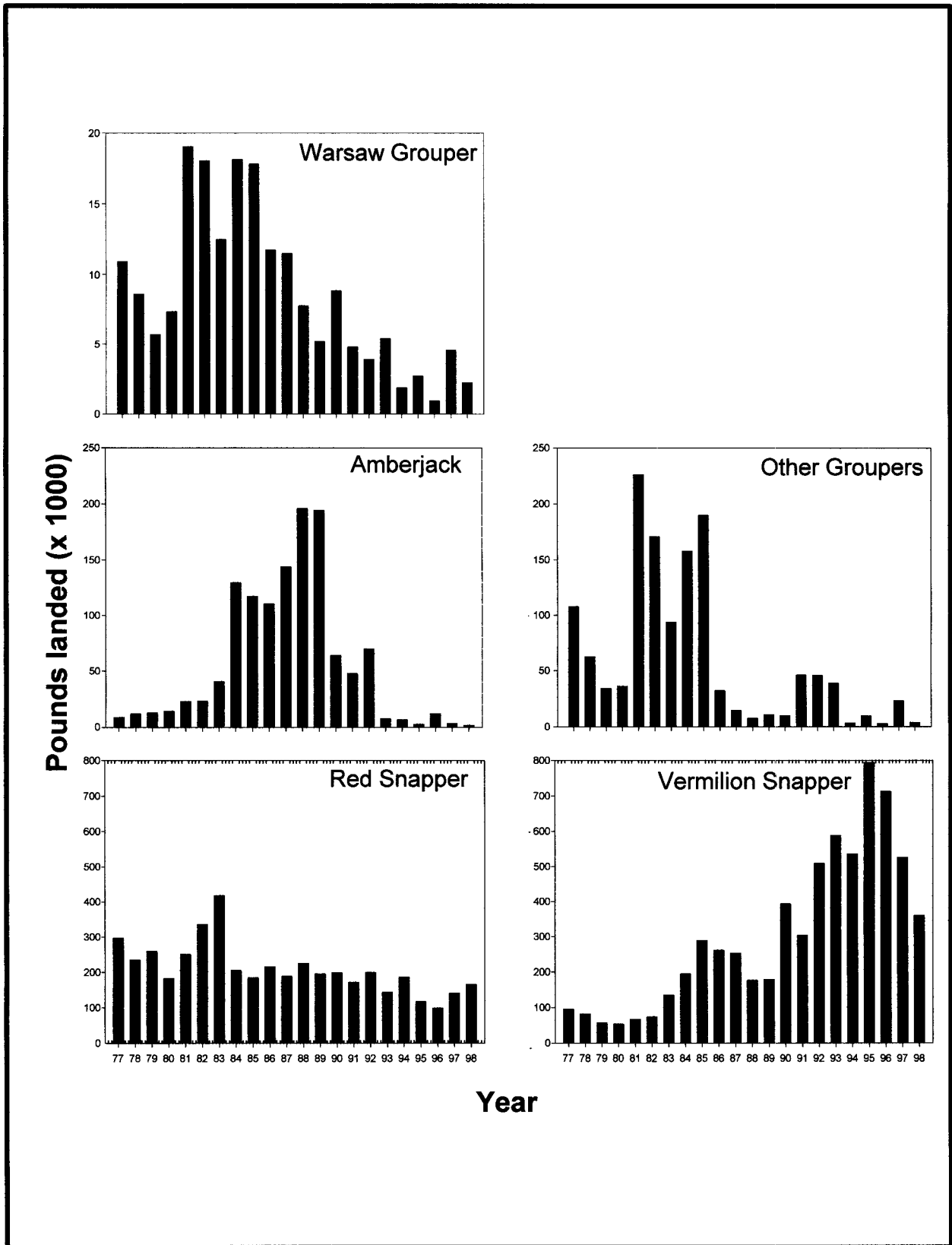


Fig. 11.10. Snapper-grouper landing trends for NMFS statistical grid 10, which includes the study area, for 1977 to 1998 (From: NMFS 2000). Note the declining trends of most larger species/groups and the increase in landings of vermilion snapper, a smaller, lower trophic level species.

Addressing the other program goal (“describe and monitor seasonal and interannual changes in community structure and zonation and relate these to changes in environmental conditions”) was more problematic, for several reasons. First, the number and timing of sampling cruises (four in a two-year period) does not provide sufficient basis for identifying either seasonal or interannual patterns. Second, the enormous spatial heterogeneity within sites makes it difficult to detect changes by random sampling within sites. A limited number of repetitive quadrats were sampled, providing some information about temporal changes. Third, because many of the organisms making up the mound communities are slow-growing and long-lived, one would not expect to see dramatic changes in communities between cruises. While the program has provided some information about temporal changes, the four monitoring cruises essentially provided a chance to accumulate spatial detail and increase the sample size for baseline characterization of each site.

Chapter 12: Literature Cited

- Abelson, A. and M. Denny. 1997. Settlement of marine organisms in flow. *Annu. Rev. Ecol. Syst.* 28:317-339.
- Babcock, R. and P. Davies. 1991. Effects of sedimentation on settlement of *Acropora millepora*. *Coral Reefs* 9(4):205-208.
- Baines, P.G. 1995. *Topographic Effects in Stratified Flows*. Cambridge Monographs on Mechanics and Applied Mathematics. Cambridge University Press, New York. 482 pp.
- Baker, E.T. and J.W. Lavelle. 1984. The effect of particle size on the light attenuation coefficient of natural suspensions. *J. Geophys. Res.* 89:8,197-8,203.
- Barham, E.G. and I.E. Davies. 1968. Gorgonians and water motion studies in Gulf of California. *Underwater Naturalist* 5(3):24-28.
- Barnes, R.D. 1980. *Invertebrate Zoology*. Saunders, Tokyo. 1,098 pp.
- Bartz, R., H. Pak, and J.R.V. Zaneveld. 1978. A transmissometer for profiling and moored observations in water. *Proc. Soc. Photo-Opt. Instr. Engineers, Ocean Optics V*, 160:102-108.
- Batschelet, E. 1981. *Circular Statistics in Biology*. Academic Press, New York. 371 pp.
- Boehm, P.D. and A.G. Requejo. 1986. Overview of the recent sediment hydrocarbon geochemistry of Atlantic and Gulf Coast over continental shelf environments. *Est. Coast. Shelf. Sci.* 23:29-58.
- Boesch, D.F. and N.N. Rabalais. 1987. *Long-term environmental effects of offshore oil and gas development*. Elsevier Applied Science Publishers Ltd., England. 708 pp.
- Bohnsack, J.A. 1976. An investigation of a photographic method for sampling hard-bottom benthic communities. M.S. Thesis, University of Miami. 188 pp.
- Bohnsack, J.A. 1979. Photographic quantitative sampling of hard-bottom communities. *Bull. Mar. Sci.* 29(2):242-252.
- Bohnsack, J.A., D.E. Harper, D.B. McClellan, D.L. Sutherland, and M.W. White. 1987. Resource survey of fishes within Looe Key National Marine Sanctuary. NOAA Tech. Mem. 5. 108 pp.
- Boland, G.S., B.J. Gallaway, J.S. Baker, and G.S. Lewbel. 1983. *Ecological effects of energy development on reef fish of the Flower Garden banks*. Final Report to National Marine Fisheries Service, Galveston Laboratory by LGL Ecological Research Associates. 466 pp.
- Boothe, P.N. and W.D. James. 1985. Neutron activation analysis of barium in marine sediments from the north central Gulf of Mexico. *J. Trace and Microprobe Techniques* 3:377-399.
- Boothe, P.N. and B.J. Presley. 1987. The effects of exploratory petroleum drilling in the northwest Gulf of Mexico on trace metal concentrations in near rig sediments and organisms. *Environ. Geol. Water Sci.* 9:173-182.
- Brassell, S.C., G. Eglinton, J.R. Maxwell, and R.P. Philip. 1978. Natural background of alkanes in the aquatic environment, pp. 69-86. In: O. Huntzinger, L.H. van Lelyveld, and B.C.J. Zoetman (eds.), *Aquatic Pollutants, Transformations and Biological Effects*. Pergamon Press, Oxford.
- Bright, T.J. and L.H. Pequegnat (eds). 1974. *Biota of the West Flower Garden Bank*. Gulf Publishing Company, Houston, TX. 435 pp.

- Brooks, J. M., ed. 1991. Mississippi-Alabama Continental Shelf Ecosystem Study: Data Summary and Synthesis, Volume I: Executive Summary, Volume II: Technical Narrative, Volume III: Appendices, Part 1 (Appendices A-D), Volume III: Part 2, (Appendix E), OCS Study MMS 91-0062 (I), 91-0063 (II), 91-0064 (III). U.S. Department of the Interior. Minerals Mgmt. Service, Gulf of Mexico OCS Regional Office, New Orleans, LA., 43 pp.(I), 862 pp.(II), 1001 pp. (III-1), and 1001 pp. (III-2).
- Carney, D., J.S. Oliver and C. Armstrong. 1999. Sedimentation and composition of wall communities in Alaskan fjords. *Polar Biology* 22(1):38-49.
- Carricart-Ganivet, J.P., G. Horta-Puga, M.A. Ruiz-Zarate, and E. Ruiz-Zarate. 1994. Retrospective determination of growth in the hermatypic coral *Monastrea annularis* (Scleractinia: Faviidae) in reefs of the Gulf of Mexico. *Revista de Biologia Tropical* 42(3):515-521.
- Cashman, C.W. 1973. Contributions to the ichthyofauna of the West Flower Garden reefs and other reef sites in the Gulf of Mexico and western Caribbean. Ph.D. Dissertation, Texas A&M Univ., College Station, TX. 247 pp.
- Chow, T.J. and C.B. Snyder. 1981. Barium in marine environment: a potential indicator of drilling contamination, pp. 691-722. In: Proceedings on Research on Environmental Fate and Effects of Drilling Fluids and Cuttings Symposia. Lake Buena Vista, Florida, 21-23 January 1980.
- Cleveland, W.S. 1985. The Elements of Graphing Data. Wadsworth Advanced Books and Software. Monterey, CA.
- Colin, P.L. 1974. Observation and collection of deep-reef fishes off the coasts of Jamaica and British Honduras (Belize). *Mar. Biol.* 24:29-38.
- Colin, P.L. 1976. Observations of deep-reef fishes in the Tongue-of-the-Ocean, Bahamas. *Bull. Mar. Sci.* 26(4):603-604.
- Connell, J.H. 1978. Diversity in tropical rain forests and coral reefs. *Science* 199:1,302-1,309.
- Connell, J.H. and M.J. Keough. 1985. Disturbance and patch dynamics of subtidal marine animals on hard substrata, pp. 125-151. In: S.T.A. Pickett and P.S. White (eds.), *The Ecology of Natural Disturbance and Patch Dynamics*. Academic Press, New York, NY.
- Connell, J.H. and R.O. Slayter. 1977. Mechanisms of succession in natural communities and their role in community stability and organization. *Am. Nat.* 111:1,119-1,144.
- Connell, S.D. 1997. Exclusion of predatory fish on a coral reef: the anticipation, pre-emption and evaluation of some caging artifacts. *J. Exp. Mar. Biol. Ecol.* 213:181-198.
- Continental Shelf Associates, Inc. 1983. Environmental monitoring program for Exploratory Well No. 3, Lease OCS-G 3316, Block A-384, High Island Area, South Extension near the West Flower Garden Bank. Draft Final Report to Union Oil Company. 2 vol.
- Continental Shelf Associates, Inc. 1985. Live-bottom survey of drillsite locations in Destin Dome Area Block 617. Report to Chevron U.S.A., Inc. 40 pp. + app.
- Continental Shelf Associates, Inc. 1987a. Southwest Florida Shelf Regional Biological Communities Survey, Year 3 Final Report. A report for the U.S. Department of the Interior, Minerals Management Service. Contract No. 14-12-0001-29036. Three volumes.
- Continental Shelf Associates, Inc. 1987b. Live bottom survey for Destin Dome Area Lease Block 57. A final report prepared for Conoco, Inc.
- Continental Shelf Associates, Inc. 1989. Fate and effects of drilling fluid and cutting discharges in shallow nearshore waters. Prepared for the American Petroleum Institute. 129 pp.

- Continental Shelf Associates, Inc. 1992. Mississippi-Alabama Shelf Pinnacle Trend Habitat Mapping Study. OCS Study MMS 92-0026. U.S. Department of the Interior, Minerals Management Service, Gulf of Mexico OCS Region, New Orleans, LA. 75 pp. + app.
- Continental Shelf Associates, Inc. and Texas A&M University, Geochemical and Environmental Research Group. 1998a. Northeastern Gulf of Mexico Coastal and Marine Ecosystem Program: Ecosystem Monitoring, Mississippi/Alabama Shelf; First Annual Interim Report. U.S. Department of the Interior, U.S. Geological Survey, Biological Resources Division, USGS/BRD/CR-1997-0008 and Minerals Management Service, Gulf of Mexico OCS Region, New Orleans, LA. OCS Study MMS 97-0037. 133 pp.
- Continental Shelf Associates, Inc. and Texas A&M University, Geochemical and Environmental Research Group. 1998b. Northeastern Gulf of Mexico Coastal and Marine Ecosystem Program: Ecosystem Monitoring, Mississippi/Alabama Shelf; Second Annual Interim Report. U.S. Department of the Interior, U.S. Geological Survey, Biological Resources Division, USGS/BRD/CR-1998-0002 and Minerals Management Service, Gulf of Mexico OCS Region, New Orleans, LA. OCS Study MMS 98-0044. 198 pp.
- Continental Shelf Associates, Inc. and Texas A&M University, Geochemical and Environmental Research Group. 1999. Northeastern Gulf of Mexico Coastal and Marine Ecosystem Program: Ecosystem Monitoring, Mississippi/Alabama Shelf; Third Annual Interim Report. U.S. Department of the Interior, U.S. Geological Survey, Biological Resources Division, USGS/BRD/CR-1999-0005 and Minerals Management Service, Gulf of Mexico OCS Region, New Orleans, LA, OCS Study MMS 99-0055. 211 pp.
- Cox, R., R.K. Atkinson, B.R. Bear, M.E. Brandriss, C.B. Chokel, J.B. Comstock, E.D. Gutmann, L.B. Interest, T.F. Schildgen, S.J. Teplitzky and M.P. Willis. 2000. Changes in a fringing reef complex over a thirty-year period: Coral loss and lagoon infilling at Mary Creek, St. John, U.S. Virgin Islands. *Bull. Mar. Sci.* 66(1):269-277.
- Crisp, D.J. 1974. Factors influencing the settlement of marine invertebrate larvae, pp. 177-265. In: P.T. Grant, and A.M. Mackie (eds.), *Chemoreception in Marine Organisms*. Academic Press, New York.
- Crisp, D.J. and H. Barnes. 1954. The orientation and distribution of barnacles at settlement with particular reference to surface contour. *J. Anim. Ecol.* 23:142-162.
- Dahlgren, E.J. 1989. Gorgonian community structure and reef zonation patterns on Yucatan coral reefs. *Bull. Mar. Sci.* 45:678-696.
- Dai, C.F. and M.C. Lin. 1993. The effects of flow on feeding of three gorgonians from southern Taiwan. *J. Exper. Mar. Biol. Ecol.* 173:57-69.
- Darnell, R. 1991. Summary and synthesis, pp. 15-1 to 15-144. In: J.M. Brooks (ed.), *Mississippi-Alabama Continental shelf ecosystem study: Data Summary and Synthesis*. Vol. II: Technical Narrative. OCS Study MMS 91-0063. U.S. Department of the Interior, Minerals Management Service, Gulf of Mexico OCS Region, New Orleans, LA. 862 pp.
- Dennis, G.D. and T.J. Bright. 1988a. Reef fish assemblages on hard banks in the northwestern Gulf of Mexico. *Bull. Mar. Sci.* 43(2):280-307.
- Dennis, G.D. and T.J. Bright. 1988b. New records of fishes in the northern Gulf of Mexico, with notes on some rare species. *N.E. Gulf Sci.* 10(1):1-18.
- Dudgeon, S.R. and P.S. Petraitis. In press. Scale dependent recruitment and divergence of intertidal communities. *Ecology*.
- Eckman, J.E. and D.O. Duggins. 1993. Effects of flow speed on growth of benthic suspension feeders. *Biol. Bull.* 185:28-41.
- Felley, J.M. and M. Vecchione. 1995. Assessing habitat use by nekton on the continental slope using archived videotapes from submersibles. *Fish. Bull.* 93(2):262-273.

- Felley, J.M., M. Vecchione, G.R. Gaston, and S.M. Felley. 1989. Habitat selection by demersal nekton: Analysis of videotape. *N.E. Gulf Sci.* 10(2):69-84.
- Folk, R.L. 1974. Petrology of sedimentary rocks. Hemphill Publishing Co., Austin, TX. 184 pp.
- Foster, M.S., C. Harrold, and D.D. Hardin. 1991. Point vs. photo quadrat estimates of the cover of sessile marine organisms. *J. Exp. Mar. Biol. Ecol.* 146:193-203.
- Gardner, W.D. and I.D. Walsh. 1990. The role of aggregates in horizontal and vertical flux across a continental margin. *Deep-Sea Res.* 37:401-412.
- Gardner, W.D., M.J. Richardson, K.R. Hinga, and P.E. Biscaye. 1983. Resuspension measured with sediment traps in a high-energy environment. *Earth Planet. Sci. Lett.* 66:262-278.
- Gardner, W.D., P.E. Biscaye, J.R.V. Zaneveld, and M.J. Richardson. 1985. Calibration and comparison of the LDGO nephelometer and the OSU transmissometer on the Nova Scotian Rise. *Mar. Geol.* 66:323-344.
- Gardner, W.D., S.P. Chung, M.J. Richardson, and I.D. Walsh. 1995. The oceanic-mixed layer pump. *Deep-Sea Res. pt. II* 42:757-776.
- Gauch, H.G. 1982. *Multivariate Analysis in Community Ecology*. Cambridge University Press, New York, NY. 298 pp.
- Genin, A., P.K. Dayton, P.F. Lonsdale, and F.N. Spiess. 1986. Corals on seamount peaks provide evidence of current acceleration over deep-sea topography. *Nature* 322:59-61.
- Genin, A., C.K. Paull, and W.P. Dillon. 1992. Anomalous abundances of deep-sea fauna on a rocky bottom exposed to strong currents. *Deep-Sea Res.* 39(2):293-302.
- Gili, J.M., J. Murillo, and J. Ros. 1989. The distribution of benthic cnidarians in the Western Mediterranean. *Scientia Marina* 53(1):19-35.
- Gilmore, R.G., C.J. Donahoe, and D.W. Cooke. 1987. Fishes of the Indian River Lagoon and adjacent waters, Florida. Harbor Branch Foundation Tech. Rep. 41. 68 pp.
- Gittings, S., T. Bright, and W. Schroeder. 1991. Topographic features characterization - biological, pp. 13-1 to 13-117. In: J.M. Brooks (ed.), *Mississippi-Alabama Continental Shelf Ecosystem Study: Data Summary and Synthesis. Volume II: Technical Narrative*. OCS Study MMS 91-0063. U.S. Department of the Interior, Minerals Management Service, Gulf of Mexico OCS Region, New Orleans, LA.
- Gittings, S.R., T.J. Bright, and E.N. Powell. 1984. Hard-bottom macrofauna of the East Flower Garden Brine Seep: Impact of a long-term, sulfurous brine discharge. *Contrib. Mar. Sci.* 27:102-125.
- Gittings, S.R., T.J. Bright, W.W. Schroeder, W.W. Sager, J.S. Laswell, and R. Rezak. 1992. Invertebrate assemblages and ecological controls on topographic features in the northeast Gulf of Mexico. *Bull. Mar. Sci.* 50:435-455.
- Gordon, H.R., R.C. Smith, and J.R.V. Zaneveld. 1984. Introduction to ocean optics, *SPIE Ocean Optics* 489:2-41.
- Gotelli, N.J. 1988. Determinants of recruitment, juvenile growth, and spatial distribution of a shallow-water gorgonian. *Ecology* 69:157-166.
- Green, R.H. 1979. *Sampling Design and Statistical Methods for Environmental Biologists*. Wiley-Interscience, NY. 257 pp.
- Grigg, R.W. 1972. Orientation and growth form of sea fans. *Limnol. Oceanogr.* 17(2):185-192.
- Hardin, D.D., E. Imamura, D.A. Coats, and J.F. Campbell. 1993. A Survey of Prominent Anchor Scars and the Level of Disturbance to Hard-Substrate Communities in the Point Arguello Region. Report to Chevron U.S.A Production Company, Ventura CA. 58 pp.

- Hardin, D.D., J. Toal, T. Parr, P. Wilde, and K. Dorsey. 1994. Spatial variation in hard bottom epifauna in the Santa Maria Basin, California: The importance of physical factors. *Mar. Environ. Res.* 37:165-193.
- Harvey, M., E. Bourget, and N. Gagné. 1997. Spat settlement of the giant scallop, *Placopecten magellanicus* (Gmelin, 1791), and other bivalve species on artificial filamentous collectors coated with chitinous material. *Aquaculture* 148:277-298.
- Hastings, A. 1980. Disturbance, coexistence, history, and competition for space. *Theor. Popul. Bio.* 18:363-373.
- Heezen, B.C. and C.D. Hollister. 1971. *The Face of the Deep*. Oxford Univ. Press, New York. 659 pp.
- Helmuth, B. and K. Sebens. 1993. The influence of colony morphology and orientation to flow on particle capture by the scleractinian coral *Agaricia agaricites* (Linnaeus). *J. Exper. Mar. Biol. Ecol.* 165:251-278.
- Hill, M.O. and H.G. Gauch. 1980. Detrended correspondence analysis an improved ordination technique. *Vegetatio*. 42:47-58.
- Hitchcock, G.L., W.J. Wiseman Jr., W.C. Boicourt, A.J. Mariano, N. Walker, T.A. Nelsen and E. Ryan. 1997. 27th International Leige Colloquium on Ocean Hydrodynamics, Liege Belgium, 8-12 May 1995 12(1-4):109-126.
- Hogg, N.G. 1973. On the stratified Taylor column. *J. Fluid Mech.* 58:517-537.
- Houghton, J.P., D.L. Beyer, and E.D. Thielk. 1981. Effects of oil well drilling fluids on several important Alaskan marine organisms, pp. 1,017-1,043. In: *Proceedings on Research on Environmental Fate and Effects of Drilling Fluids and Cuttings Symposia*. Lake Buena Vista, Florida, 21-23 January 1980.
- Hunt, J.C.R. and W.H. Snyder. 1980. Experiments on stably and neutrally stratified flow over a model three-dimensional hill. *J. Fluid. Mech.* 96:671-704.
- Hyland, J., D. Hardin, D. Coats, R. Green, M. Steinhauer, and J. Neff. 1994. Impacts of offshore oil and gas development on the benthic environment of the Santa Maria Basin. *Mar. Environ. Research* 37:195-229.
- Ibarra, G. and D.J. Stewart. 1989. Longitudinal zonation of sandy beach fishes in the Napo River Basin, eastern Ecuador. *Copeia* 2:364-381.
- Jerlov, N.G. 1976. *Marine Optics*. Elsevier Applied Science Publishers Ltd., New York.
- Jochens A.E. and W.D. Nowlin, Jr. (eds.). 2000. *Northeastern Gulf of Mexico Chemical Oceanography and Hydrography Study, Annual Report: Year 3*. OCS Study MMS 2000-078. U.S. Department of the Interior, Minerals Management Service, Gulf of Mexico OCS Region, New Orleans, LA. 89 pp.
- Johnson, H.P. and M. Helferty. 1990. The geological interpretation of side-scan sonar. *Rev. Geophys.* 28:357-380.
- Jokiel, P.L. 1978. Effects of water motion on reef corals. *Biol. Bull.* 35:87-97.
- Kelly, F.J. 1991. Physical oceanography/water mass characterization, pp. 10-1 to 10-151. In: *Mississippi-Alabama Continental Shelf Ecosystem Study: Data Summaries and Synthesis. Volume II: Technical Narrative*. OCS Study MMS 91-0063. U.S. Department of the Interior, Minerals Management Service, Gulf of Mexico OCS Region, New Orleans, LA.
- Kendall, J.J. 1990. Detection of effects at long-term production sites, pp. 23-28. In: R.S. Carney (ed.), *Northern Gulf of Mexico Environmental Studies Planning Workshop. Proceedings of a workshop held in New Orleans, Louisiana, 15-17 August 1989*. Prepared by Geo-Marine, Inc. OCS Study MMS 90-0018. U.S. Department of the Interior, Minerals Management Service, Gulf of Mexico OCS Region, New Orleans, LA. 156 pp.

- Kennicutt, M.C., II (ed.). 1995. Gulf of Mexico offshore operations monitoring experiment, Phase I: Sublethal responses to contaminant exposure. Final Report. OCS Study MMS 95-0045. U.S. Department of the Interior, Minerals Management Service, Gulf of Mexico OCS Region, New Orleans, LA. 739 pp.
- Kennicutt, M.C. II and P. Comet. 1992. Resolution of sediment hydrocarbon sources: Multiparameter approaches, pp. 308-337. In: J.K. Whelan and J.W. Farrington (eds.), Organic productivity, accumulation, and preservation in recent and ancient sediments. Columbia University Press.
- Kennicutt, M.C. II, P.N. Boothe, T.L. Wade, S.T. Sweet, R. Rezak, F.J. Kelly, J.M. Brooks, B.J. Presley, and D.A. Wiesenburg. 1996. Geochemical patterns in sediments near offshore production platforms. *Can. J. Fish. Aquat. Sci.* 53:2,254-2,566.
- Keough, M.J. and P.T. Raimondi. 1995. Responses of settling invertebrate larvae to bioorganic films: Effects of different types of films. *J. Exp. Mar. Biol. Ecol.* 185:235-253.
- Kindinger, J. L. 1988. Seismic stratigraphy of the Mississippi-Alabama shelf and upper continental slope. *Mar. Geol.* 83: 79-94.
- Kindinger, J. L. 1989. Depositional history of the Lagniappe Delta, Northern Gulf of Mexico. *Geo-Mar. Lett.* 9:59-66.
- Kingsford, M. and C. Battershill. 1998. Studying temperate marine environments. Canterbury Press, Christchurch, New Zealand. 335 pp.
- Lake Buena Vista Symposium. 1981. Research on environmental fate and effects of drilling fluids and cuttings: Volumes 1 and 2. Lake Buena Vista, Florida, 21-24 January 1980. 1,122 pp.
- Laswell, J.S., W.W. Sager, W.W. Schroeder, K.S. Davis, and R. Rezak. 1992. High-resolution geophysical mapping of the Mississippi-Alabama outer continental shelf, pp. 155-192. In: R. Geyer (ed.), Geophysical Exploration at Sea. CRC Press, Boca Raton, FL.
- Lauenstein, G.G., A.Y. Cantillow, and S.S. Dolvin. 1993. Benthic surveillance and mussel watch projects analytical protocols 1984-1992, pp. III-151 to III-185. In: NOAA Technical Memorandum NPS ORCA. NOAA, Silver Spring, MD.
- Leichter, J.J. and J.D. Witman. 1997. Water flow over subtidal rock walls: Relation to distributions and growth rates of sessile suspension feeders in the Gulf of Maine. *J. Exp. Mar. Biol. Ecol.* 209:293-307.
- Leversee, G.J. 1976. Flow and feeding in fan-shaped colonies of the gorgonian coral, *Leptogorgia*. *Biol. Bull.* 151:344-356.
- Levin, S.A. 1976. Population dynamics in heterogeneous environments. *Annu. Rev. Ecol. Syst.* 7:287-310.
- Levin, S.A. and R.T. Paine. 1974. Disturbance, patch formation, and community structure. *Proc. Natl. Acad. Sci. U.S.A.* 71:2,744-2,747.
- Lohrenz, S.E., G.L. Fahnensteil, D.G. Redalje, G.A. Lang, X. Chen and M.J. Dagg. 1997. Variations in primary production of northern Gulf of Mexico continental shelf waters linked to nutrient inputs from the Mississippi River. *Mar. Ecol. Prog. Ser.* 155:45-54.
- Ludwick, J.C. and W.R. Walton. 1957. Shelf-edge, calcareous prominences in the northeastern Gulf of Mexico. *Amer. Assoc. Petrol. Geol. Bull.* 41(9):2054-2101.
- MacDonald, I.R., W.W. Schroeder, F.J. Kelly, and N.L. Guinasso Jr. In review. Biological current meters: a study of near-bottom circulation on the Gulf of Mexico continental slope. *Deep-Sea Research*.
- Marine Resources Research Institute. 1984. South Atlantic OCS Area Living Marine Resources Study, Phase III. A report for the U.S. Department of the Interior, Minerals Management Service, Washington, DC. Contract No. 14-12-0001-29185.

- Mathsoft. 1999. S-Plus 2000 Guide to Statistics. Data Analysis Products Division, Mathsoft, Inc., Seattle, WA. 638 pp.
- Menge, B.A. 1976. Organization of the New England rocky intertidal community: Role of predation, competition, and environmental heterogeneity. *Ecol. Monogr.* 46:355-393.
- Menge, B.A. and A.M. Olson. 1991. Role of scale and environmental factors in regulation of community structure. *Trends Ecol. & Evol.* 5(2): 52-57
- Messing, C.G., A.C. Neumann, and J.C. Lang. 1990. Biozonation of deep-water lithoherms and associated hardgrounds in the northeast Straits of Florida. *Palaios* 5:15-33.
- Middleditch, B.S. 1981. Environmental effects of offshore production. *The Buccaneer Gas and Oil Field Study*. Plenum Press, NY. 446 pp.
- Miller, G.C. and W.J. Richards. 1980. Reef fish habitat, faunal assemblages, and factors determining distributions in the South Atlantic Bight, pp. 114-130. In: *Proc. Gulf. Carib. Fish. Inst., 32nd Annual Meeting*.
- Minerals Management Service. 2000. Live bottom (pinnacle trend) stipulation. Information provided on MMS Gulf of Mexico Region website. <http://www.gomr.mms.gov>.
- Minnery, G.A. 1990. Crustose coralline algae from the Flower Garden Banks, northwestern Gulf of Mexico: Controls on distribution and growth morphology. *J. Sedimentary Petrology* 60(6):992-1,007.
- Mitchum, R.M. Jr. and P.R. Vail. 1977. Seismic stratigraphy and global changes of sea level, part 7: seismic stratigraphic interpretation procedure, pp. 135-143. In: C.E. Payton (ed.), *Seismic Stratigraphy – Applications to Hydrocarbon Exploration*, Memoir 26. Amer. Assoc. Petrol. Geol., Tulsa, OK.
- Moody, J.A., B. Butman, and M.H. Bothner. 1986. Estimates of near-bottom suspended-matter concentration during storms. *Cont. Shelf Res.* 7:609-628.
- Morel, A. 1974. Optical properties of pure water and pure sea water, In: *Optical Aspects of Oceanography*, N. Jerlov and E. Steeman Nielsen (eds.), Academic Press, New York, pp. 1-24.
- Mortensen, P.B. and H.T. Rapp. 1998. Oxygen and carbon isotope ratios related to growth line patterns in skeletons of *Lophelia pertusa* (L) (Anthozoa, Scleractinia): Implications for determination of linear extension rates. *Sarsia* 83(5):433-446.
- Mullineaux, L.S. 1989. Vertical distributions of the epifauna on manganese nodules: Implications for settlement and feeding. *Limnol. Oceanogr.* 34(7):1,247-1,262.
- National Marine Fisheries Service. 2000. General canvass landings for statistical grid 10, Southeast Fisheries Science Center, Miami, FL.
- National Research Council. 1983. *Drilling Discharges in the Marine Environment*. National Academy Press, Washington, DC. 180 pp.
- Neff, J.M. 1987. Biological effects of drilling fluids, drill cuttings and produced waters, pp. 469-538. In: D.F. Boesch and N.N. Rabalais (eds.), *Long-Term Effects of Offshore Oil and Gas Development*. Elsevier Applied Science Publishers, London.
- Nowlin, W.D., Jr., A.E. Jochens, R.O. Reid, and S.F. DiMarco. 1998. Texas-Louisiana Shelf Circulation and Transport Processes Study – Synthesis Report. Vol. I: Technical Report. OCS Study MMS-98-0035. U.S. Department of the Interior, Minerals Management Service, Gulf of Mexico OCS Region, New Orleans, LA. 502 pp.
- Osman, R.W. 1977. The establishment and development of a marine epifaunal community. *Ecol. Monogr.* 47:37-63.
- Ou, H.W. 1991. Some effects of a seamount on oceanic flows. *J. Phys. Oceanogr.* 21:1835-1845.

- Paine, R.T. and S.A. Levin. 1981. Intertidal landscapes: Disturbance and the dynamics of pattern. *Ecol. Monogr.* 51:145-178.
- Pak, H., D.A. Kiefer, and J.C. Kitchen. 1988. Meridional variations in the concentration of chlorophyll and microparticles in the North Pacific Ocean. *Deep-Sea Res.* 35:1,151-1,171.
- Palmer, M.W. 1993. Putting things in even better order: the advantages of canonical correspondence analysis. *Ecology* 74:2,215-2,230.
- Parker, N.R., P.V. Mladenov, and K.R. Grange. 1997. Reproductive biology of the antipatharian black coral *Antipathes fiordensis* in Doubtful Sound, Fiordland, New Zealand. *Mar. Biol.* 130(1):11-22.
- Parker, R.O. and R.W. Mays. 1998. Southeastern United States deepwater reef fish assemblages, habitat characteristics, catches, and life history summaries. NOAA Tech. Rep. 138. 41 pp.
- Parker, R.O. and S.W. Ross. 1986. Observing reef fishes from submersibles off North Carolina. *N.E. Gulf Sci.* 8(1):31-50.
- Pauly, D., V. Christensen, J. Dalsgaard, R. Froese, and F. Torres, Jr. 1998. Fishing down the marine food webs. *Science* 279:860-863.
- Pequegnat, W.E. 1964. The epifauna of a California siltstone reef. *Ecology* 45:272-283.
- Petrie, C.D. and E.O. Keith. 2000. Building a better settling plate: A comparison of settling rates on cured plates and plates containing a chemical morphogen. Presented at the Benthic Ecology Meeting 2000, Wilmington, NC.
- Phillips, N.W., D.A. Gettleton, and K.D. Spring. 1990. Benthic biological studies of the southwest Florida shelf. *Amer. Zool.* 30:65-75.
- Philp, R.P. 1985. Fossil fuel biomarkers: Application and spectra. *Methods in geochemistry and geophysics.* Elsevier, NY. 294 pp.
- Pickett, S.T.A. and P.S. White. 1985. Patch dynamics: a synthesis, pp. 371-384. In: S.T.A. Pickett and P.S. White (eds.), *The Ecology of Natural Disturbance and Patch Dynamics.* Academic Press, New York, NY.
- Quinn, J.F. 1979. Disturbance, Predation, and Diversity in the Rocky Intertidal Zone. Ph.D. dissertation, University of Washington, Seattle, WA.
- Rabalais, N.N., W.J. Wiseman Jr., R.E. Turner, D. Justic, B.K. Sen Gupta and Q. Dortch. 1996. Nutrient changes in the Mississippi River and system responses on the adjacent continental shelf. *Estuaries* 19(2B):386-407.
- Randall, J.E. 1967. Food habits of reef fishes of the West Indies. *Studies in Tropical Oceanography* 5:665-847.
- Rezak, R., T.J. Bright, and D.W. McGrail. 1985. *Reefs and Banks of the Northern Gulf of Mexico: Their Geological, Biological, and Physical Dynamics.* John Wiley and Sons, New York. 259 pp.
- Rezak, R., S.R. Gittings and T.J. Bright. 1990. Biotic assemblages and ecological controls on reefs and banks of the northwest Gulf of Mexico. *Amer. Zool.* 30:23-35.
- Rice, S.A. and C.L. Hunter. 1992. Effects of suspended sediment and burial on scleractinian corals from west central Florida patch reefs. *Bull. Mar. Sci.* 51(3):429-442.
- Riggs, S.R., S.W. Snyder, A.C. Hine, and D.L. Mearns. 1996. Hardbottom morphology and relationship to the geologic framework: Mid-Atlantic continental shelf. *J. Sediment. Res.* 66:830-846.
- Robins, C.R. 1971. Distributional patterns of fishes from coastal and shelf waters of the tropical western Atlantic, pp. 249-254. In: *Symposium on investigations and resources of the Caribbean and adjacent regions.* Papers on fisheries resources, FAO, Rome.

- Roden, G. I. 1991. Mesoscale flow and thermohaline structure around Fieberling Seamount. *Jour. Geophys. Res.* 96:16653-16672.
- Rogers, A.D. 1994. The biology of seamounts. *Adv. Mar. Bio.* 30:305-350.
- Rosenfeld, M, V. Bresler and A. Abelson. 1999. Sediment as a possible source of food for corals. *Ecology Letters* 2(6):345-348.
- Rowe, G.T. and R.J. Menzies. 1968. Orientation in two bathy, benthic decapods, *Munida valida* Smith and *Parapagurus pilosimanus* Smith. *Limnol. Oceanogr.* 13(3):549-552.
- Rubinstein, N.I., R. Rigby, and C.N. D'Asaro. 1981. Acute and sublethal effects of whole used drilling fluids on representative estuarine organism, pp. 828-846. In: *Proceedings on Research on Environmental Fate and Effects of Drilling Fluids and Cuttings Symposia*. Lake Buena Vista, Florida, 21-23 January 1980.
- Ruppert, E.F. and R.D. Barnes. 1994. *Invertebrate Zoology*, 6th edition. Saunders College Publishers, Fort Worth, TX.
- Sager, W.W., W.W. Schroeder, J.S. Laswell, K.S. Davis, R. Rezak, and S.R. Gittings. 1992. Topographic features of the Mississippi-Alabama outer continental shelf and their implications for sea level fluctuations during the Late Pleistocene-Holocene transgression. *Geo-Mar.Lett.* 12:41-48.
- Sager, W.W., W.W. Schroeder, K.S. Davis, and R. Rezak. 1999. A tale of two deltas: seismic mapping of near surface sediments on the Mississippi-Alabama outer shelf and implications for recent sea level fluctuations. *Mar. Geol.* 160:119-136.
- Sale, P.F. 1991. Reef fish communities: Open nonequilibrium systems, pp. 564-598. In: P.F. Sale. (ed.), *The ecology of Fishes on Coral Reefs*. Academic Press. 754 pp.
- Sale, P.F. and W.A. Douglas. 1984. Temporal variability in the community structure of fish on coral patch reefs and the relation of community structure to reef structure. *Ecology* 65(2):409-422.
- Sale, P.F. J.A. Guy, and W.J. Steel. 1994. Ecological structure of assemblages of coral reef fishes on isolated patch reefs. *Oecologia* 98:83-99.
- SAS Institute, Inc. 1989. *SAS/STAT User's Guide*, Version 6, Fourth edition. Volumes 1 and 2. SAS Institute Inc., Cary, NC.
- Schroeder, W.W., M.R. Dardeau, J.J. Dindo, P. Fleisher, K.L. Heck, Jr., and A.W. Shultz. 1989a. Geophysical and biological aspects of hardbottom environments on the L'MAFLA shelf, northern Gulf of Mexico, pp. 17-21. In: *Proceeding Oceans '88 Conference*.
- Schroeder, W.W., A.W. Shultz, and J.J. Dindo. 1989b. Inner-shelf hardbottom areas northeastern Gulf of Mexico. *Trans. Gulf Coast Assoc. Geol. Soc.* 38:535-541.
- Sebens, K.P. 1987. Competition for space: Effects of disturbance and intermediate competitive success. *Theor. Popul. Biol.* 32:430-441.
- Shipp, R.L. and T.S. Hopkins. 1978. Physical and biological observations of the northern rim of the De Soto Canyon made from a research submersible. *Northeast Gulf Sci.* 2(2):113-121.
- Smith, G.B. 1976. The ecology and distribution of the eastern Gulf of Mexico reef fishes. *FL Dept. Nat. Res. Mar. Res. Pub.* 19:1-78.
- Smith, G.B., H.M. Austin, S.A. Bortone, R.W. Hastings, and L.H. Ogren. 1975. Fishes of the Florida Middle Ground with comments on ecology and zoogeography. *FL Dept. Nat. Res. Mar. Res. Pub.* 9:1-14.
- Sokal, R.R. and F.J. Rohlf. 1998. *Biometry*. W.H. Freeman and Co., New York. 887 pp.
- Sonnier, F., H.D. Hoese, and J. Teerling. 1976. Observations on the offshore reef and platform fish fauna of Louisiana. *Copeia* (1):105-111.

- Sousa, W.P. 1985. Disturbance and patch dynamics on rocky intertidal shores, pp. 101-124. In: S.T.A. Pickett and P.S. White (eds.), *The Ecology of Natural Disturbance and Patch Dynamics*. Academic Press, New York.
- Southwest Research Institute. 1978. Ecological investigations of petroleum production platforms in the Central Gulf of Mexico. Report prepared for the U.S. Department of Commerce.
- Spinrad, R.W., J.R.V. Zaneveld, and J.C. Kitchen. 1983. A study of the optical characteristics of the suspended particles in the benthic boundary layer of the Scotian Rise. *J. Geophys. Res.* 88:7,641-7,645.
- Sutherland, J.P. and R.H. Karlson. 1977. Development and stability of the fouling community at Beaufort, North Carolina. *Ecol. Monogr.* 47:425-446.
- Sydow, J. and H.H. Roberts. 1994. Stratigraphic framework of a late Pleistocene shelf-edge delta, northeast Gulf of Mexico. *Amer. Assoc. Petrol. Geol. Bull.* 78:1,276-1,312.
- Syms, C. 1995. Multi-scale analysis of habitat association in a guild of blennioid fishes. *Mar. Ecol. Prog. Ser.* 125:31-43.
- Taylor, B.J. and B.J. Presley. 1998. TERL trace element quantification techniques, pp. 32-73. In: *Sampling and Analytical Methods of the National Status and Trends Program, Mussel Watch Project: 1993-1996 update*. NOAA Technical Memorandum NOS ORCA 130.
- ter Braak, C.J.F. 1986. Canonical correspondence analysis: A new eigenvector technique for multivariate direct gradient analysis. *Ecology* 67(5):1,167-1,179.
- ter Braak, C.J.F. and P. Smilauer. 1998. CANOCO reference manual and user's guide to Canoco for windows: software for canonical community ordination (Vers. 4.0). Microcomputer Power, Ithaca, NY. 352 pp.
- Tornberg, L.D., E.D. Thielk, R.E. Nakatani, R.C. Miller, and S.O. Hillman. 1981. Toxicity of drilling fluids to marine organisms in the Beaufort Sea, Alaska, pp. 997-1,016. In: *Proceedings on Research on Environmental Fate and Effects of Drilling Fluids and Cuttings Symposia*. Lake Buena Vista, Florida, 21-23 January 1980.
- Underwood, A.J. and E.J. Denley. 1984. Paradigms, explanations, and generalizations in models for the structure of intertidal communities on rocky shores, pp. 151-180. In: D.R. Strong, Jr., D. Simberloff, L.G. Abele, and A.B. Thistle (eds.), *Ecological Communities: Conceptual Issues and the Evidence*. Princeton University Press, Princeton, NJ.
- Van Katwijk, M.M., N.F. Meier, R. Van Loon, E.M. Van Hove, W.B.J.T. Giesen, G. Van der Velde and C. Den Hartog. 1993. Sabaki River sediment load and coral stress: Correlation between sediments and condition of the Malindi-Watamu Reefs in Kenya (Indian Ocean). *Mar. Biol.* 117(4):675-683.
- Velimirov, B. 1983. Orientation in the sea fan *Eunicella cavolinii* related to water movement. *Helgoländer wiss. Merresunter.* 24:163-173.
- Wade, T.L., E.L. Atlas, J.M. Brooks, M.C. Kennicutt II, R.G. Fox, J. Sericano, B. Garcia-Romero, and D. DeFreitas. 1988. NOAA Gulf of Mexico status and trends program: Trace organic contaminant distribution in sediments and oysters. *Estuaries* 11:171-179.
- Wainwright, S.A. and J.R. Dillon. 1969. On the orientation of sea fans (Genus *Gorgonia*). *Biological Bulletin*, pp. 130-139.
- Walker, N.D. and L.J. Rouse. 1993. Satellite assessment of Mississippi River discharge plume variability. Louisiana Universities Marine Consortium Rept. No. OCSMMS930044, Baton Rouge, LA USA. 59 pp.
- Walsh, I.D. 1990. Project CATSTIX: Camera, Transmissometer, and Sediment Trap Integration Experiment. Ph.D. Dissertation, Texas A&M University, College Station, TX.

- Walsh, I.D., S.P. Chung, M.J. Richardson, and W.D. Gardner. 1995. The Diel Cycle in the integrated particle load in the equatorial Pacific: A comparison with primary production. *Deep-Sea Res.* pt. II 42:465-478.
- Walsh, I.D., K. Fischer, D. Murray, and J. Dymond. 1988. Evidence for resuspension of rebound particles from near-bottom sediment traps. *Deep-Sea Res.* 35:59-70.
- Weaver, D.C. and K.J. Sulak. 2000. Food subsidies in the twilight zone: Food web structure of the Mississippi-Alabama outer continental shelf, pp. 204-207. In: M. McKay and J. Nides, Proceedings: Eighteenth annual Gulf of Mexico information transfer meeting, December 1998. U.S. Department of the Interior, Minerals Management Service, Gulf of Mexico OCS Region, New Orleans, LA. OCS Study MMS 2000-030. 538 pp.
- Wessel, P. and W.H.F. Smith. 1995. New version of the Generic Mapping Tools released. *EOS, Trans. AGU* 76:329.
- Wesseling, I., A.J. Uychiaoco, P.M. Alino, T. Aurin, and J.E. Vermaat. 1999. Damage and recovery of four Philippine corals from short-term sediment burial. *Mar. Ecol. Prog. Ser.* 176:11-15.
- Woodward-Clyde Consultants. 1979. Eastern Gulf of Mexico marine habitat mapping study. Report to U.S. Department of the Interior, Bureau of Land Management, OCS Office, New Orleans, LA. Contract No. AA551-CT8-22.
- Zar, J.H. 1999. *Biostatistical Analysis*. Simon and Schuster, Upper Saddle River, NJ. 663 pp.
- Zhang, Y. 1997. Sedimentation and resuspension across the central Louisiana inner shelf. Ph.D. Dissertation, Texas A&M University, College Station, TX. 171 pp.

Appendices

Appendix A: Cruise Summaries

Appendix A: Cruise Summaries

With the exception of Cruise 1A as noted below, all cruises were staged out of Ocean Springs, MS aboard the R/V TOMMY MUNRO. A Magnavox MX300 differential global positioning system (GPS) was used for navigation.

The remotely operated vehicle (ROV) used during monitoring cruises was the Benthos Openframe SeaROVER with a Python multifunction manipulator arm. Video, photographic, and ancillary equipment included a Sony high-resolution videocamera, DeepSea Power & Light Micro-SeaCam 2000 color videocamera, Photosea 1000 still camera and strobe, DeepSea Power & Light lasers, and a Simrad MS900 color imaging sonar.

Phase 1

Phase 1 included three cruises. Cruise 1A was a geophysical reconnaissance of five megasites containing potential monitoring sites. Cruise 1B was a visual reconnaissance to check out a few potential sites that had no previous video or photographic data. The cruise also served to field test the ROV and monitoring techniques. Finally, Cruise 1C was the first of four monitoring cruises at the nine selected sites. Activities during this first monitoring cruise included setting up fixed stations, collecting samples and data, and deploying oceanographic and biological moorings.

Cruise 1A - Geophysical Reconnaissance

Cruise 1A was conducted from 6-22 November 1996. The survey vessel was the M/V OCEAN SURVEYOR. The cruise was staged out of Pascagoula, MS.

The purpose of the cruise was to collect high-resolution digital side-scan sonar and subbottom profiler data within five megasites believed to contain potential monitoring sites. Equipment used included the TAMU² side-scan sonar and an X-STAR 2-12 kHz chirp sonar subbottom profiler. Navigation was accomplished with *Skyfix*, a type of differential GPS navigation which provides an accuracy of 3-5 m. The position of the sonar towfish relative to the ship was determined using an ultra-short baseline acoustic ranging system.

The main problem during the cruise was poor weather. Gale conditions forced a return to port on 8-9 November and again on 14-18 November.

Cruise 1B - Visual Reconnaissance

Cruise 1B was conducted from 21-24 March 1997. The objectives of the cruise were (1) to collect information from potential sites to aid in site selection; (2) to test ROV maneuverability and the various camera, light, and laser configurations; and (3) to check sampling techniques to be used during subsequent monitoring cruises. Four low and medium relief features within Megasites 1, 3, and 5 were visited.

Problems encountered during the cruise included additional mobilization time to integrate extra cameras and lasers with the ROV system, minor flooding of the ROV during one dive, and the loss of several ship anchors during anchor recovery operations.

Cruise 1C - Baseline Characterization and Monitoring

Cruise 1C was conducted from 7-18 May 1997. Each of the nine final sites was sampled during the cruise. Subbottom profiling was conducted to geophysically characterize each site in more detail than was possible with the broad-scale geophysical reconnaissance cruise. Grab samples were collected for geological and geochemical analyses. Hydrographic profiling was also conducted at each station, including conductivity/temperature/depth (CTD), dissolved oxygen (DO), and transmissivity/optical backscatter.

Hard bottom and fish community monitoring was conducted at each site using the ROV. Monitoring included random video/photographic transects and stations and establishment of fixed video/photoquadrats. Voucher specimens were also collected at some sites to aid in species identification.

Six physical oceanographic/sediment dynamics moorings were installed during the cruise. Three moorings were installed at Site 1, and one each at Sites 4, 5, and 9. Two of the moorings at Site 1 were "rotating" moorings which were subsequently redeployed for an interval at Sites 4, 5, and 9.

Eleven biological moorings were also deployed for the epibiont recruitment study. Eight biological moorings were deployed at Site 4 and one mooring each at Sites 1, 5, and 9. The moorings at Sites 1, 5, and 9 were to be recovered after one year (Cruise M3) and redeployed for another year. The biological moorings at Site 4 were for a "temporal study," with moorings to be retrieved at different times over the course of the program.

Problems encountered during the cruise included ROV cable connectors breaking, the loss of two ROV thruster motors due to use of the ROV in high currents, the stripping of gears in the manipulator arm on two occasions, high currents at Site 4 during the first site visit, high turbidity at Site 9 preventing the initial establishment of fixed video/photoquadrats, and the presence of fishing boats on Site 7 preventing the collection of additional subbottom profile data.

Phase 2

Phase 2 included two monitoring cruises, M2 (October 1997) and M3 (April-May 1998). (Cruise M3 began in April but was shut down due to weather delays; it was completed in August 1998). In addition, mooring service cruises were conducted in July 1997 (S1), January 1998 (S2), and July 1998 (S3).

Cruise S1

The first mooring service cruise, conducted from 27 to 31 July 1997, successfully serviced the oceanographic moorings and collected 11 CTD casts. A problem was encountered with the scheduled recovery of the first biomoooring at Site 4, as the acoustic release would not work. An attempt was made to release several of the other identical biomoorings at the site in order to recover one biomoooring, but these also would not release. It was decided to attempt to recover two biomoorings during Cruise M2 by cutting the moorings from their anchors using the ROV.

Cruise M2 and Follow-Up Meeting

Cruise M2 was conducted as several legs from 30 September to 31 October 1997. Approximately 21 days of weather downtime were incurred. All samples and data were obtained other than the biomoorings, as explained below.

Each of the nine monitoring sites was sampled during the cruise. Grab samples were collected for geological and geochemical analyses. Hydrographic profiling was also conducted at each station; a total of 29 CTD casts were collected during the cruise. Hard bottom and fish community monitoring was conducted at each site using the ROV.

All six physical oceanographic/sediment dynamics moorings were retrieved and redeployed during Cruise M2. The moorings at Sites 1 and 5 were serviced during the 30 September through 6 October leg. The remaining moorings, including the one at Site 4, were serviced during the 28 to 31 October leg.

As noted above, during Cruise S1, a problem was encountered with the scheduled recovery of the first biomoooring at Site 4, as the acoustic release would not work. An attempt was made to release several of the other identical biomoorings at the site in order to recover one biomoooring, but these would also not release. It was decided to attempt to recover two biomoorings during Cruise M2 by cutting the moorings from their anchors using the ROV. However, during Cruise M2, only one of the Site 4 biomoorings was retrieved and another was found to be damaged (due to shackle failure, the biomoooring was resting on the bottom).

Following the cruise, a meeting was held on 20 November 1997 between the MMS Contract Officer's Technical Representative, Contract Inspector, and CSA management. The participants discussed problems in retrieving the biomoorings and damage to the unrecovered biomoooring. A new plan was developed and later approved to deploy four new biomoorings on the January 1998 service cruise (S2) and to recover the biomoorings with the assistance of the ROV on Cruises M3 (April-May 1998) and M4 (April 1999).

Cruise S2

The next service cruise was conducted during 29 to 30 January 1998. All six oceanographic moorings were successfully serviced and 12 CTD casts were made. Four new biomoorings were deployed--one each at Sites 1, 4, 5, and 9.

Cruise M3

The first part of Cruise M3 was conducted between 21 April and 2 May 1998. Poor weather delayed departure for two days (21 to 23 May) and interrupted the cruise for about three-and-one-half days on 26 to 28 May. The cruise was shut down by mutual agreement and was continued in August 1998.

Despite the weather problems, all of the hydrographic profiling was done, and all six of the oceanographic moorings were serviced. The two re-locatable moorings at Site 1 were moved to Site 5. However, ROV sampling of only one hard bottom site was completed (Site 1). Grab samples were collected only at Sites 1, 2, 3, and 4.

Phase 3

Phase 3 included one monitoring cruise, M4, which was conducted in two legs. During the first part (April 1999), oceanographic moorings were retrieved and hydrographic profiling was conducted at the four mooring stations. During the second leg (July-August 1999), video and grab sampling were conducted and the remaining biomoorings were retrieved. In addition, mooring service cruises were conducted in October 1998 (S4) and January-February 1999 (S5).

Cruise S4

Mooring Service Cruise S4 was conducted during 13 to 14 October 1998. All six oceanographic moorings were successfully serviced (retrieved and redeployed) and 12 CTD casts were made.

Cruise S5

Mooring Service Cruise S5 began on 24 to 25 January 1999, but the generator on the TOMMY MUNRO broke less than six hours after departure and the ship had to return to the dock. The cruise was completed during 9 to 10 February 1999. Five of the six oceanographic moorings were successfully serviced and 12 CTD casts were made. Mooring C5C7 would not surface and a replacement mooring was deployed in its place. The flotation and top (Aanderaa) current meter were found by a charter fishing boat off Destin, Florida in late May and returned to the principal investigators. The data set was good through about the beginning of February 1999. The ROV attempted to locate and recover the bottom instruments and acoustic release on the second leg of Cruise M4 (July-August 1999), but they were not found.

Cruise M4

The first part of Cruise M4 was conducted from 13 to 14 April 1999. All six of the oceanographic moorings were retrieved and six CTD profiles were made at the mooring sites. During the second part of Cruise M4 (July-August 1999), ROV and grab sampling and CTD profiling were conducted at all nine monitoring sites. All remaining biomoorings were retrieved at Sites 1, 4, 5, and 9.

Appendix B: Data Management

Appendix B: Data Management

A data management program was established to monitor, control, and facilitate data flow and ensure the integrity of the data through each phase of the program. As part of this process, a program data management plan was developed which consisted of four interrelated elements: (1) data administration; (2) data control; (3) data utilization; and (4) data archiving submission.

The purpose of data administration was to ensure continuous tracking and custody of samples and data. Evidence of data possession, comparison, and security with signatures, dates, times, and location of data were noted. This element also ensured proper formatting and reporting of all data and distribution of data as required among the principal investigators.

Data control consists of monitoring the progress of data flow to identify data gaps and to facilitate further processing. The data control procedures adopted for the data management plan document data availability, data reduction, and data analysis.

Data utilization includes processing and validating data as they are submitted. The processed data are then made available to all study participants.

Available data have been routinely archived to ensure permanency.

Data types, formats, and procedures have been established to insure reliable and accurate data receipt and distribution. Sample inventories from the cruises have been developed, and a master inventory of samples received and analyses required is being maintained. A sample inventory for all project components has been finalized. This includes cruise dates with standardized cruise, site, and station nomenclature for all work elements, ensuring the smooth acquisition of data into the project database.

An inventory of the program data has been developed to ensure appropriate data processing and availability. Data that have been submitted to data management are presented in **Table B.1**.

Table B.1. Data submitted to data management.

Data Description	Cruise and Date	Media
Detailed Mosaics for Sites 1 and 2	Cruise 1A (Nov 96)	Tape
Bathymetric Observations	Cruise 1C (May 97)	Electronic
Bathymetric Observations	Cruise M2 (Oct 97)	Electronic
Bathymetric Observations	Cruise M3 (Apr/Aug 98)	Electronic
Bathymetric Observations	Cruise M4 (Jul 99)	Electronic
Survey Videotapes	Cruise 1C (May 97)	Videotape
Survey Videotapes	Cruise M2 (Oct 97)	Videotape
Survey Videotapes	Cruise M3 (Apr/Aug 98)	Videotape
Survey Videotapes	Cruise M4 (Jul 99)	Videotape
Random Photo Locations	Cruise 1C (May 97)	Electronic
Random Photo Locations	Cruise M2 (Oct 97)	Electronic
Random Photo Locations	Cruise M3 (Apr/Aug 98)	Electronic
Random Photo Locations	Cruise M4 (Jul 99)	Electronic
Random Photos	Cruise 1C (May 97)	CD ROM
Random Photos	Cruise M2 (Oct 97)	CD ROM
Random Photos	Cruise M3 (Apr/Aug 98)	CD ROM
Random Photos	Cruise M4 (Jul 99)	CD ROM
Still Photo Logs	Cruise 1C (May 97)	Electronic
Still Photo Logs	Cruise M2 (Oct 97)	Electronic
Still Photo Logs	Cruise M3 (Apr/Aug 98)	Electronic
Still Photo Logs	Cruise M4 (Jul 99)	Electronic
Random Photo Percent Cover Data	Cruise 1C (May 97)	Electronic
Random Photo Percent Cover Data	Cruise M2 (Oct 97)	Electronic
Random Photo Percent Cover Data	Cruise M3 (Apr/Aug 98)	Electronic
Random Photo Percent Cover Data	Cruise M4 (Jul 99)	Electronic
Random Photo Occurrence Data	Cruise 1C (May 97)	Electronic
Random Photo Occurrence Data	Cruise M2 (Oct 97)	Electronic
Random Photo Occurrence Data	Cruise M3 (Apr/Aug 98)	Electronic
Random Photo Occurrence Data	Cruise M4 (Jul 99)	Electronic
Sediment Grab Locations	Cruise 1C (May 97)	Electronic
Sediment Grab Locations	Cruise M2 (Oct 97)	Electronic
Sediment Grab Locations	Cruise M3 (Apr/Aug 98)	Electronic
Sediment Grab Locations	Cruise M4 (Jul 99)	Electronic
Sediment Grain Size	Cruise 1C (May 97)	Electronic
Sediment Trace Metals	Cruise 1C (May 97)	Electronic
Sediment PAHs	Cruise 1C (May 97)	Electronic
Sediment TPH, EOM, TOC, and TIC	Cruise 1C (May 97)	Electronic
Sediment TOC and TIC	Cruise M2 (Oct 97)	Electronic
Sediment TOC and TIC	Cruise M3 (Apr/Aug 98)	Electronic
Sediment TOC and TIC	Cruise M4 (Jul 99)	Electronic
Sediment Trap Trace Metals	Cruise 1C (May 97)	Electronic
Sediment Trap Trace Metals	Cruise M2 (Oct 97)	Electronic
Sediment Trap Trace Metals	Cruise M3 (Apr/Aug 98)	Electronic
Sediment Trap Trace Metals	Cruise M4 (Jul 99)	Electronic
Sediment Trap TOC	Cruise 1C (May 97)	Electronic
Sediment Trap TOC	Cruise M2 (Oct 97)	Electronic
Sediment Trap TOC	Cruise M3 (Apr/Aug 98)	Electronic
Sediment Trap TOC	Cruise M4 (Jul 99)	Electronic

Abbreviations: EOM = extractable organic matter; TIC = total inorganic carbon; TOC = total organic carbon; TPH = total petroleum hydrocarbons; PAH = polycyclic aromatic hydrocarbons.

**Appendix C: Grab and Box Core Locations and
Sediment Grain Size Data**

Table C.1. Grab (G) and box core (BC) locations (page 1 of 3).

	Cruise 1C				Cruise M2				Cruise M3				Cruise M4			
	X (m)	Y(m)	Lat.	Lon.	X (m)	Y(m)	Lat.	Lon.	X (m)	Y(m)	Lat.	Lon.	X (m)	Y(m)	Lat.	Lon.
Site 1																
G4	444327	3256626	29.43938	-87.57401												
G5	444340	3256633	29.43944	-87.57388												
G6	444383	3256634	29.43946	-87.57343	444448	3256567	29.43885	-87.57276	444418	3256584	29.43900	-87.57307	444507	3256592	29.43908	-87.57217
G7a	444683	3257043	29.44315	-87.57036	444686	3257071	29.44341	-87.57034	444722	3257115	29.44381	-87.56997	444808	3257137	29.44402	-87.56908
G7b	444665	3257125	29.44390	-87.57055												
G8	444069	3256361	29.43698	-87.57666	444039	3256359	29.43695	-87.57697	443959	3256338	29.43676	-87.57779	443980	3256360	29.43697	-87.57758
G10	443808	3256515	29.43835	-87.57935	443770	3256549	29.43866	-87.57975	443718	3256548	29.43864	-87.58028	443790	3256537	29.43855	-87.57955
G11	443782	3256503	29.43825	-87.57963												
G12	444430	3256347	29.43687	-87.57293												
G13	443909	3256238	29.43586	-87.57830	443867	3256224	29.43573	-87.57873	443794	3256222	29.43571	-87.57949	443903	3256231	29.43580	-87.57837
G14	443866	3255436	29.42861	-87.57870												
G15	444537	3256520	29.43843	-87.57184												
BC1	444499	3256875	29.44163	-87.57225												
BC2	444915	3257109	29.44377	-87.56797												
BC3	445000	3256477	29.43806	-87.56707												
BC4	445417	3257041	29.44318	-87.56279												
BC5	445420	3257057	29.44332	-87.56277												
BC6	445359	3257053	29.44328	-87.56339												
BC7	445112	3256230	29.43584	-87.56589												
BC8	443891	3256184	29.43537	-87.57849												
BC9	444074	3255905	29.43286	-87.57659												
Site 2																
G1	441234	3257219	29.44459	-87.60594	441257	3257180	29.44424	-87.60570	441220	3257182	29.44425	-87.60607	441213	3257137	29.44385	-87.60615
G2	441267	3256983	29.44246	-87.60558	441235	3256944	29.44211	-87.60590	441175	3256957	29.44222	-87.60652	441183	3256964	29.44228	-87.60645
G3	441250	3256661	29.43956	-87.60573												
G4	440981	3257274	29.44508	-87.60854	440988	3257289	29.44521	-87.60848	440945	3257302	29.44532	-87.60892	441028	3257291	29.44523	-87.60807
G5	441068	3257223	29.44462	-87.60764	441009	3257213	29.44453	-87.60825	440962	3257187	29.44429	-87.60873	441003	3257140	29.44387	-87.60832
G6	441083	3257140	29.44387	-87.60748	441089	3257188	29.44430	-87.60743	441005	3257167	29.44411	-87.60829	441039	3257184	29.44427	-87.60795
G7	440686	3257265	29.44498	-87.61159												
G8	440677	3256968	29.44229	-87.61166												
G9	441000	3256953	29.44218	-87.60833												
G10	440690	3256685	29.43975	-87.61151												
G11	440995	3256658	29.43951	-87.60837												
Site 2																
BC1	441059	3256957	29.44222	-87.60772												
BC2	440811	3256649	29.43943	-87.61027												
BC3	441244	3254924	29.42388	-87.60571												
BC4	442674	3254665	29.42161	-87.59095												

Table C.1. Grab (G) and box core (BC) locations (page 2 of 3).

	Cruise 1C				Cruise M2				Cruise M3				Cruise M4			
	X (m)	Y(m)	Lat.	Lon.	X (m)	Y(m)	Lat.	Lon.	X (m)	Y(m)	Lat.	Lon.	X (m)	Y(m)	Lat.	Lon.
Site 3																
G1	444786	3256405	29.43740	-87.56927												
G2	444654	3256417	29.43750	-87.57063	444620	3256383	29.43720	-87.57098	444588	3256297	29.43643	-87.57131	444582	3256334	29.43676	-87.57137
G3	444581	3256395	29.43731	-87.57138												
G4	444643	3256496	29.43822	-87.57075												
G5	444689	3256309	29.43653	-87.57026												
G6	444677	3256422	29.43755	-87.57039												
G7	444730	3256570	29.43889	-87.56986	444743	3256588	29.43905	-87.56971	444743	3256530	29.43853	-87.56971	444825	3256504	29.43830	-87.56888
G8	444830	3256414	29.43749	-87.56881	444807	3256458	29.43788	-87.56906	444778	3256461	29.43791	-87.56935	444766	3256475	29.43803	-87.56948
G9	444689	3256272	29.43620	-87.57026	444698	3256280	29.43627	-87.57017	444666	3256295	29.43640	-87.57050	444657	3256326	29.43668	-87.57060
G10	444485	3256401	29.43735	-87.57237	444405	3256347	29.43687	-87.57319	444357	3256321	29.43663	-87.57368	444301	3256259	29.43607	-87.57427
Site 4																
G1	425990	3244678	29.33060	-87.76225												
G2	426027	3244584	29.32975	-87.76187												
G3	425969	3244416	29.32823	-87.76246												
G4	425773	3244546	29.32855	-87.76244												
G5	425962	3244308	29.32726	-87.76252	425966	3244300	29.32719	-87.76248	425940	3244314	29.32731	-87.76276	425986	3244309	29.32727	-87.76228
G6	425804	3244433	29.32838	-87.76416												
G7	425789	3244524	29.32920	-87.76432												
G8	425666	3244482	29.32881	-87.76559	425660	3244390	29.32798	-87.76563	425700	3244368	29.32778	-87.76522	425823	3244361	29.32773	-87.76397
G9	425462	3244354	29.32765	-87.76768	425440	3244334	29.32747	-87.76791	425443	3244338	29.32750	-87.76787	425525	3244382	29.32790	-87.76703
G10	425785	3244078	29.32517	-87.76433	425791	3244100	29.32537	-87.76427	425832	3244070	29.32511	-87.76384	425838	3244101	29.32538	-87.76380
G11	425488	3243885	29.32341	-87.76737	425510	3243926	29.32379	-87.76715	425545	3243920	29.32374	-87.76679	425627	3244058	29.32498	-87.76597
Site 5																
G1	404689	3251639	29.39198	-87.98223												
G2	405037	3251804	29.39350	-87.97865												
G3	404963	3251808	29.39354	-87.97942	404951	3251799	29.39345	-87.97954	404967	3251841	29.39383	-87.97938	405050	3251833	29.39377	-87.97853
G4	404788	3251706	29.39259	-87.98121	404768	3251703	29.39257	-87.98142	404903	3251651	29.39211	-87.98002	404908	3251633	29.39195	-87.97998
G5	404757	3251748	29.39298	-87.98154												
G6	404585	3251757	29.39304	-87.98331	404562	3251810	29.39352	-87.98356	404746	3251837	29.39377	-87.98166	404758	3251886	29.39422	-87.98155
G7	404796	3251527	29.39098	-87.98112	404819	3251506	29.39080	-87.98087	404965	3251513	29.39087	-87.97937	404955	3251544	29.39115	-87.97948
G8	404596	3251406	29.38988	-87.98317												
G9	404759	3251448	29.39027	-87.98149												
G10	404860	3251899	29.39435	-87.98048	404890	3251836	29.39377	-87.98017	404926	3251820	29.39363	-87.97980	405016	3251858	29.39398	-87.97888
Site 6																
G1	405109	3252933	29.40370	-87.97801	405113	3252957	29.40391	-87.97798	405153	3252963	29.40397	-87.97757	405231	3252990	29.40422	-87.97677
G2	405113	3252597	29.40066	-87.97794												
G3	405077	3252473	29.39954	-87.97830	405054	3252489	29.39969	-87.97854	405057	3252519	29.39995	-87.97851	405088	3252502	29.39980	-87.97820
G4	405256	3252407	29.39896	-87.97645												
G5	405068	3252300	29.39798	-87.97838	405026	3252318	29.39814	-87.97881	405037	3252310	29.39807	-87.97870	404989	3252251	29.39753	-87.97920
G6	405169	3252219	29.39726	-87.97733												
G7	405230	3252224	29.39731	-87.97670	405230	3252216	29.39723	-87.97671	405264	3252225	29.39731	-87.97635	405284	3252173	29.39685	-87.97615
G8	405063	3252077	29.39597	-87.97841	405067	3252118	29.39634	-87.97838	405096	3252130	29.39645	-87.97807	405341	3252213	29.39722	-87.97557
G9	405326	3252107	29.39626	-87.97570												
G10	405108	3251999	29.39526	-87.97794												

C4

Table C.1. Grab (G) and box core (BC) locations (page 3 of 3).

	Cruise 1C				Cruise M2				Cruise M3				Cruise M4			
	X (m)	Y(m)	Lat.	Lon.	X (m)	Y(m)	Lat.	Lon.	X (m)	Y(m)	Lat.	Lon.	X (m)	Y(m)	Lat.	Lon.
Site 7																
G1	370017	3237317	29.25964	-88.33779	369884	3237347	29.25990	-88.33916	369914	3237308	29.25955	-88.33885	369825	3237405	29.26042	-88.33978
G2	369571	3236981	29.25656	-88.34233	369550	3236978	29.25653	-88.34255	369552	3236936	29.25615	-88.34253	369670	3236892	29.25577	-88.34132
G3	370183	3236976	29.25658	-88.33604	370199	3237005	29.25685	-88.33587	370166	3237002	29.25681	-88.33622	370128	3236986	29.25667	-88.33662
G4	370116	3236802	29.25500	-88.33670												
G5	370170	3236691	29.25401	-88.33614	370220	3236694	29.25404	-88.33562	370217	3236710	29.25418	-88.33565	370293	3236840	29.25537	-88.33490
G6	369649	3236730	29.25431	-88.34150												
G7	369798	3236370	29.25107	-88.33993	369817	3236352	29.25091	-88.33973	370250	3236107	29.24875	-88.33525	370342	3236156	29.24920	-88.33432
G8	370380	3236388	29.25130	-88.33395												
G9	370156	3236025	29.24799	-88.33620												
G10	369548	3236313	29.25053	-88.34249												
Site 8																
G1	372274	3234519	29.23463	-88.31424	372250	3234496	29.23442	-88.31448	372229	3234520	29.23463	-88.31470	372286	3234477	29.23425	-88.31412
G2	371985	3234253	29.23220	-88.31718	371969	3234226	29.23195	-88.31735	371988	3234221	29.23191	-88.31714	371948	3234221	29.23190	-88.31757
G3	371967	3234026	29.23015	-88.31734												
G4	371920	3233990	29.22982	-88.31782												
G5	371862	3233762	29.22775	-88.31839	371854	3233735	29.22751	-88.31847	371854	3233710	29.22728	-88.31847	371851	3233808	29.22817	-88.31852
G6	371928	3233886	29.22887	-88.31772												
G7	371955	3234012	29.23002	-88.31746	371963	3233984	29.22977	-88.31738	371970	3233980	29.22973	-88.31731	371982	3234026	29.23015	-88.31720
G8	372051	3234150	29.23128	-88.31649												
G9	371904	3234217	29.23186	-88.31801	371887	3234210	29.23180	-88.31818	371907	3234240	29.23207	-88.31798	371945	3234223	29.23192	-88.31760
G10	372222	3234419	29.23371	-88.31477												
G11	374104	3232556	29.21710	-88.29519												
Site 9																
G1	371618	3235244	29.24110	-88.32107	371627	3235249	29.24114	-88.32098	371667	3235220	29.24089	-88.32056	371771	3235189	29.24062	-88.31950
G2	371353	3235110	29.23986	-88.32378												
G3	371180	3234971	29.23859	-88.32555												
G4	371104	3234946	29.23836	-88.32632	371113	3234922	29.23814	-88.32623	371102	3234893	29.23788	-88.32634	371200	3234813	29.23717	-88.32533
G5	370983	3234785	29.23690	-88.32756												
G6	370787	3234651	29.23567	-88.32955	370752	3234642	29.23558	-88.32990	370806	3234626	29.23544	-88.32936	370841	3234645	29.23562	-88.32900
G7	371171	3235008			371199	3235019	29.23902	-88.32536	371238	3235070	29.23949	-88.32496	371348	3235046	29.23928	-88.32383
G8	371146	3234899	29.23794	-88.32588												
G9	371298	3235066	29.23946	-88.32434												
G10	371273	3234895	29.23792	-88.32458	371202	3234913	29.23800	-88.32531	371184	3234879	29.23776	-88.32549	371230	3234919	29.23813	-88.32504

C-5

Table C.2. Sediment grain size data (page 1 of 6)

Cruise	Grab	% Gravel	% Sand	% Silt	% Clay	Mean Phi	Sorting	Skewness	Kurtosis
Site 1									
1C	1G4	32.01	56.73	0.75	10.51	0.67	3.41	2.30	6.77
1C	1G5	22.88	71.71	1.45	3.96	0.44	2.32	2.95	12.48
1C	1G6	4.32	93.01	0.65	2.01	2.04	1.65	2.01	14.11
1C	1G7	0.38	89.60	1.85	8.17	2.45	2.38	2.62	8.76
1C	1G8	15.73	74.20	1.30	1.14	0.23	1.54	3.63	22.07
1C	1G10	1.65	65.06	4.48	28.81	4.56	4.04	1.67	3.22
1C	1G11	13.60	81.41	0.55	4.42	0.80	2.38	2.77	11.52
1C	1G12	5.58	83.32	1.99	9.10	2.14	2.88	1.94	6.31
1C	1G13	13.62	68.00	2.28	16.10	1.92	3.79	1.50	3.76
1C	1G14	0.30	85.58	1.33	12.79	3.21	2.87	1.88	5.30
1C	1G15	0.50	89.95	1.66	7.88	2.96	2.20	2.99	10.62
Site 2									
1C	2G1	13.17	74.33	2.05	10.46	1.87	3.12	1.84	5.76
1C	2G2	2.23	91.02	0.99	5.75	2.47	2.20	2.24	9.38
1C	2G3	0.07	88.25	2.77	8.91	2.96	2.45	2.44	7.89
1C	2G4	0.32	93.69	0.80	5.19	2.67	1.91	3.28	13.86
1C	2G5	25.94	46.41	7.35	20.30	2.82	3.96	0.85	2.40
1C	2G6	12.92	72.91	0.87	13.30	2.15	3.48	1.04	3.35
1C	2G7	0.07	92.56	0.89	6.49	2.93	2.08	3.31	12.60
1C	2G8	0.04	86.71	3.18	10.07	3.10	2.40	2.59	7.81
1C	2G9	4.56	86.42	0.64	8.38	2.25	2.24	1.82	6.45
1C	2G10	7.20	80.63	0.96	11.21	3.21	2.65	2.49	7.25
1C	2G11	4.79	83.94	1.88	9.40	9.02	6.36	1.19	1.45
Site 3									
1C	3G1	1.71	91.54	0.36	6.38	2.67	2.14	2.58	10.74
1C	3G2	11.51	76.64	0.49	11.36	2.05	3.12	1.22	4.13
1C	3G3	4.00	83.55	1.79	10.66	3.02	2.64	2.51	7.61
1C	3-G4	0.37	95.06	0.31	4.27	2.65	1.74	3.55	16.64
1C	3-G5	1.02	94.24	0.84	3.89	2.25	1.84	2.31	11.62
1C	3-G6	4.22	74.62	2.34	18.81	3.14	3.59	1.65	3.83
1C	3-G7	0.89	89.84	0.62	8.64	2.84	2.42	2.61	8.87
1C	3-G8	7.55	76.17	3.55	12.74	2.57	3.00	1.32	4.41
1C	3-G9	0.58	92.90	0.74	5.78	2.55	2.08	2.61	10.62
1C	3-G10	10.19	70.48	4.35	14.98	2.73	3.22	1.28	3.71
Site 4									
1C	4-G1	12.14	62.01	5.76	20.09	2.67	3.76	0.94	2.53
1C	4-G2	10.97	50.27	5.23	33.53	3.79	4.59	1.09	2.03
1C	4-G3	18.23	55.23	4.54	22.00	2.71	4.25	0.94	2.31
1C	4-G4	17.39	72.88	0.53	9.20	0.99	3.57	0.32	2.36
1C	4-G5	6.35	59.98	6.00	27.68	3.56	4.43	1.21	2.40
1C	4-G6	16.49	64.57	5.10	13.84	1.65	3.71	0.49	2.17
1C	4-G7	13.50	59.55	5.01	21.93	2.32	3.47	0.84	2.30
1C	4-G8	6.93	67.57	4.97	20.53	2.71	3.88	1.04	2.52
1C	4-G9	5.10	70.47	3.28	21.16	2.47	4.03	1.01	2.49
1C	4-G10	25.84	30.12	13.16	30.88	3.82	4.74	0.98	1.96
1C	4-G11	14.93	60.36	5.25	19.47	2.43	4.01	0.90	2.45

Table C.2. Sediment grain size data (page 2 of 6)

Cruise	Grab	% Gravel	% Sand	% Silt	% Clay	Mean Phi	Sorting	Skewness	Kurtosis
Site 5									
1C	5-G1	26.37	39.51	8.24	25.88	3.08	4.54	0.91	2.08
1C	5-G2	0.31	85.86	4.07	9.76	3.12	2.63	2.38	7.23
1C	5-G3	32.30	48.40	5.16	14.15	1.77	3.96	0.57	2.29
1C	5-G4	14.17	72.52	3.49	9.82	1.88	3.30	0.83	3.35
1C	5-G5	35.13	52.64	0.89	11.40	1.25	3.77	0.33	2.26
1C	5-G6	2.65	72.28	4.45	20.62	3.22	3.79	1.47	3.28
1C	5-G7	7.07	78.62	2.82	11.49	1.93	3.30	0.98	3.39
1C	5-G8	10.99	60.34	5.34	23.33	2.87	4.30	1.06	2.38
1C	5-G9	11.35	71.09	2.82	14.74	1.99	3.75	0.90	2.78
1C	5-G10	5.67	86.50	1.50	6.32	1.72	2.70	0.86	4.43
Site 6									
1C	6-G1	3.95	74.00	6.37	15.68	3.38	3.39	1.65	4.15
1C	6-G2	10.84	59.41	7.24	22.51	3.20	4.09	1.18	2.65
1C	6-G3	7.75	69.26	6.48	16.52	2.83	3.66	1.24	3.22
1C	6-G4	6.39	70.35	6.42	16.85	3.22	3.55	1.47	3.66
1C	6-G5	8.87	59.51	6.65	24.27	3.47	4.25	1.23	2.58
1C	6-G6	2.15	89.18	1.79	6.89	2.17	2.49	1.47	5.92
1C	6-G7	4.34	74.49	2.88	18.28	3.45	3.53	1.69	4.01
1C	6-G8	4.45	80.55	2.52	12.48	2.52	3.22	1.42	4.18
1C	6-G9	0.13	67.71	13.48	18.67	4.32	3.51	1.95	4.21
1C	6-G10	1.92	80.79	3.03	14.27	3.20	3.16	1.79	4.75
Site 7									
1C	7-G1	1.65	81.97	1.66	14.72	3.19	3.12	1.98	5.18
1C	7-G2	15.16	52.26	4.88	27.71	3.00	4.67	0.95	2.01
1C	7-G3	0.42	67.25	5.34	27.00	4.77	4.11	1.78	3.34
1C	7-G4	1.65	65.06	4.48	28.81	4.56	4.04	1.67	3.22
1C	7-G5	1.13	79.06	3.15	16.66	3.69	3.27	2.01	4.89
1C	7-G6	22.73	50.41	3.86	23.00	2.73	4.38	0.91	2.22
1C	7-G7	25.67	39.70	5.96	28.67	3.20	4.68	0.91	1.98
1C	7-G8	0.66	80.80	2.45	16.10	3.62	3.14	2.21	5.46
1C	7-G9	4.04	81.36	0.16	14.45	3.10	3.14	1.89	5.07
1C	7-G10	17.17	49.86	3.48	29.49	3.28	4.69	1.02	2.07
Site 8									
1C	8-G1	0.24	84.19	2.32	13.26	3.31	2.87	2.38	6.44
1C	8-G2	0.99	86.64	1.06	11.30	2.71	2.82	2.05	6.04
1C	8-G3	0.81	88.71	1.67	8.80	2.65	2.61	2.08	6.85
1C	8-G4	1.97	88.61	0.41	9.00	2.42	2.68	1.89	6.31
1C	8-G5	1.15	91.99	0.35	6.50	2.08	2.44	1.78	6.91
1C	8-G6	0.68	93.04	0.30	5.98	2.31	2.24	2.11	8.49
1C	8-G7	0.56	91.58	0.94	6.91	2.45	2.31	2.24	8.30
1C	8-G8	1.86	87.17	2.34	8.63	2.44	2.66	1.86	6.18
1C	8-G9	27.10	39.37	11.57	21.96	3.11	4.15	0.89	2.32
1C	8-G10	1.09	80.07	2.10	16.74	3.45	3.01	2.10	5.19
1C	8-G11	0.30	56.84	5.72	37.13	5.10	4.51	1.59	2.67

Table C.2. Sediment grain size data (page 3 of 6)

Cruise	Grab	% Gravel	% Sand	% Silt	% Clay	Mean Phi	Sorting	Skewness	Kurtosis
Site 9									
1C	9-G1	11.98	39.27	8.87	39.89	4.98	5.00	1.21	1.99
1C	9-G2	6.32	42.31	6.26	45.11	5.31	5.36	1.20	1.81
1C	9-G3	7.42	60.79	3.68	28.10	3.59	4.44	1.24	2.44
1C	9-G4	20.70	47.41	5.31	26.59	3.24	4.45	1.03	2.26
1C	9-G5	6.12	66.90	3.21	23.77	3.50	3.99	1.39	3.02
1C	9-G6	2.57	83.40	1.50	12.54	2.81	3.02	1.84	5.26
1C	9-G7	13.01	53.25	3.60	30.14	3.54	4.63	1.11	2.19
1C	9-G8	8.79	71.74	2.98	16.48	2.50	3.68	1.15	3.14
1C	9-G9	16.44	51.33	3.39	28.84	3.30	4.36	1.02	2.17
1C	9-G10	7.09	57.36	5.47	30.07	3.78	4.48	1.24	2.40
Site 1									
M2	1G6	12.18	72.60	0.53	14.10	2.13	3.64	1.00	3.14
M2	1G7A	12.67	76.14	0.43	10.76	1.88	3.45	0.89	3.31
M2	1G8	11.89	71.43	2.30	14.38	2.24	3.62	1.00	3.11
M2	1G10	11.54	80.61	2.72	5.13	1.38	2.78	0.11	3.08
M2	1G13	8.71	83.28	1.99	6.03	0.89	3.13	0.02	2.29
Site 2									
M2	2G1	1.21	93.88	1.64	3.27	1.97	1.87	1.20	7.78
M2	2G2	0.55	91.21	2.10	6.15	2.69	1.97	2.54	10.20
M2	2G4	12.70	76.30	0.30	10.71	1.83	3.39	0.84	3.30
M2	2G5	2.87	89.89	0.99	6.25	1.86	2.46	1.16	5.43
M2	2G6	6.16	79.19	4.18	10.47	1.52	2.67	0.65	4.23
Site 3									
M2	3G2	0.73	75.39	0.56	23.33	4.04	3.86	1.88	3.85
M2	3G7	0.53	79.23	1.20	19.04	3.81	3.43	2.11	4.83
M2	3G8	0.50	75.38	1.69	22.43	4.11	3.71	1.96	4.12
M2	3G9	0.50	78.88	0.76	19.86	3.76	3.50	2.05	4.59
M2	3G10	11.52	69.20	2.53	16.75	2.43	3.71	1.03	2.96
Site 4									
M2	4G5	13.73	44.59	5.02	36.67	4.35	5.07	1.15	1.97
M2	4G8	10.73	58.82	4.92	25.53	3.10	4.49	1.09	2.30
M2	4G9	5.94	56.92	7.82	29.32	3.89	4.75	1.22	2.20
M2	4G10	5.47	48.94	3.87	41.72	4.57	5.27	1.19	1.87
M2	4G11	21.06	36.57	9.13	33.23	4.02	4.97	1.06	1.95
Site 5									
M2	5G3	0.56	82.00	4.19	13.24	3.33	2.77	2.10	5.78
M2	5G4	12.14	78.52	1.84	7.50	1.34	3.06	0.38	2.93
M2	5G6	3.58	86.04	1.94	8.45	2.24	2.58	1.25	4.94
M2	5G7	13.36	76.51	1.54	8.59	1.27	3.34	0.47	2.75
M2	5G10	1.60	90.30	2.85	5.25	2.64	2.07	1.94	8.69
Site 6									
M2	6G1	0.17	75.55	4.69	19.05	4.05	3.50	1.97	4.43
M2	6G3	10.19	57.11	7.20	25.50	3.60	4.33	1.24	2.56
M2	6G5	0.84	43.78	12.19	43.19	5.98	4.99	1.39	2.11
M2	6G7	1.28	76.80	3.80	18.11	3.60	3.51	1.85	4.27
M2	6G8	2.75	78.82	1.78	16.65	2.80	3.56	1.53	3.76

Table C.2. Sediment grain size data (page 4 of 6)

Cruise	Grab	% Gravel	% Sand	% Silt	% Clay	Mean Phi	Sorting	Skewness	Kurtosis
Site 7									
M2	7G1	4.08	75.84	1.37	18.71	2.49	3.69	1.30	3.31
M2	7G2	19.35	46.96	2.49	31.20	3.41	4.91	1.03	1.99
M2	7G3	0.23	70.04	5.00	24.72	4.51	3.80	1.90	3.81
M2	7G5	0.34	71.09	4.81	23.76	4.43	3.79	1.90	3.87
M2	7G7	27.94	45.45	2.84	23.77	2.44	4.56	0.79	1.99
Site 8									
M2	8G1	0.17	66.05	1.74	32.04	4.72	4.16	1.73	3.14
M2	8G2	1.15	73.55	1.04	24.25	4.48	4.28	1.55	2.83
M2	8G5	0.69	72.50	1.62	25.19	3.76	3.90	1.69	3.40
M2	8G7	0.40	75.18	1.33	23.10	3.88	3.85	1.82	3.76
M2	8G9	16.35	47.95	3.10	32.60	2.53	4.37	1.06	2.43
Site 9									
M2	9G1	9.58	50.97	4.33	35.12	4.02	4.77	1.25	2.25
M2	9G4	7.00	56.41	4.86	31.73	4.00	4.53	1.28	2.37
M2	9G6	0.90	77.65	0.71	20.74	3.58	3.73	1.83	3.96
M2	9G7	10.59	48.98	3.01	37.42	2.50	4.06	1.26	2.93
M2	9G10	3.92	51.83	5.04	39.20	4.82	4.86	1.33	2.18
Site 1									
M3	1-G6	1.83	93.85	0.53	3.80	2.13	0.95	-0.33	1.57
M3	1-G7a	0.11	95.11	0.76	4.01	2.42	0.62	0.10	1.35
M3	1-G8	22.18	75.04	0.36	2.42	-0.01	1.25	0.08	1.14
M3	1-G10	13.05	81.98	0.75	4.22	0.70	1.64	0.19	1.03
M3	1-G13	21.78	73.59	0.58	4.05	0.20	1.55	0.20	1.07
Site 2									
M3	2-G1	7.41	87.92	0.76	3.91	1.44	1.34	-0.23	1.16
M3	2-G2	0.21	92.94	1.64	5.21	2.44	1.29	0.19	4.38
M3	2-G4	0.21	94.51	0.82	4.46	2.44	0.73	0.02	2.50
M3	2-G5	0.28	75.45	5.94	18.32	4.32	3.21	0.72	2.09
M3	2-G6	11.13	71.16	3.99	13.72	2.26	3.13	0.26	1.71
Site 3									
M3	3-G2	0.41	92.80	0.90	5.88	2.44	1.76	0.51	4.68
M3	3-G7	1.03	92.24	0.72	6.02	2.39	1.66	0.27	5.18
M3	3-G8	0.31	90.47	1.53	7.68	2.44	1.68	0.35	4.59
M3	3-G9	1.28	89.56	1.25	7.91	2.18	1.80	0.29	4.17
M3	3-G10	16.35	72.42	1.04	10.19	0.86	2.72	0.29	1.85
Site 4									
M3	4-G5	7.71	36.84	7.12	48.33	5.40	4.31	-0.27	0.50
M3	4-G8	9.14	65.62	4.58	20.65	3.50	4.32	0.62	1.09
M3	4-G9	8.24	57.64	3.99	30.13	3.60	4.36	0.64	0.51
M3	4-G10	27.96	50.66	4.25	17.12	2.52	4.25	0.58	1.31
M3	4-G11	14.59	72.69	2.70	10.02	0.70	2.65	0.51	2.40
Site 5									
M3	5-G3	1.20	78.09	5.55	15.17	3.50	2.90	0.46	2.28
M3	5-G4	2.54	86.28	2.48	8.71	1.86	2.33	0.31	1.98
M3	5-G6	23.90	62.32	2.68	11.10	1.31	3.06	0.16	1.26
M3	5-G7	2.44	85.48	3.25	8.83	2.04	2.37	0.27	1.98
M3	5-G10	2.41	90.69	0.99	5.90	2.04	2.14	0.15	2.31

Table C.2. Sediment grain size data (page 5 of 6)

Cruise	Grab	% Gravel	% Sand	% Silt	% Clay	Mean Phi	Sorting	Skewness	Kurtosis
Site 6									
M3	6-G1	0.39	79.41	6.38	13.82	3.67	2.53	0.46	2.51
M3	6-G3	6.28	71.79	6.23	15.70	3.27	3.72	0.49	1.53
M3	6-G5	19.90	64.08	3.76	12.26	1.23	3.14	0.43	1.62
M3	6-G7	2.01	72.50	6.76	18.74	4.19	3.48	0.47	1.52
M3	6-G8	1.54	88.70	2.86	6.91	1.92	2.16	0.44	2.33
Site 7									
M3	7-G1	2.17	88.39	1.68	7.76	1.78	2.23	0.31	2.88
M3	7-G2	34.06	58.08	1.16	6.70	-0.09	2.58	0.42	2.33
M3	7-G3	0.49	80.35	4.86	14.30	3.45	2.45	0.58	2.48
M3	7-G5	0.69	79.20	4.93	15.17	3.52	2.49	0.60	2.47
M3	7-G7	0.72	94.44	0.62	4.23	1.89	0.99	0.13	1.46
Site 8									
M3	8-G1	0.30	83.50	3.02	13.18	2.86	2.05	0.64	3.86
M3	8-G2	1.32	94.10	0.29	4.29	1.73	0.85	0.02	1.64
M3	8-G5	1.60	88.04	1.27	9.09	1.78	2.01	0.36	4.03
M3	8-G7	0.72	94.44	0.62	4.23	1.89	0.99	0.13	1.46
M3	8-G9	12.18	77.79	1.03	9.00	0.74	2.42	0.23	2.62
Site 9									
M3	9-G1	2.50	75.94	3.70	17.86	3.94	3.32	0.67	2.31
M3	9-G4	8.49	76.13	2.16	13.22	1.68	2.75	0.29	1.96
M3	9-G6	0.44	88.71	1.61	9.24	2.10	1.91	0.42	4.63
M3	9-G7	14.55	64.02	3.27	18.17	2.92	4.13	0.56	1.50
M3	9-G10	11.16	71.27	2.70	14.88	2.26	3.45	0.49	1.94
Site 1									
M4	1-G6	0.39	94.14	0.80	4.67	2.43	0.77	0.04	3.53
M4	1-G7a	0.17	96.77	0.27	2.79	2.00	0.51	-0.03	1.27
M4	1-G8	17.11	78.56	0.57	3.76	1.30	1.28	0.21	0.84
M4	1-G10	11.06	81.35	1.38	6.21	1.23	2.38	0.08	1.40
M4	1-G13	7.07	88.33	0.44	4.16	0.47	1.11	0.20	1.26
Site 2									
M4	2-G1	1.85	90.66	1.18	6.31	2.08	1.87	0.11	5.85
M4	2-G2	0.11	95.27	0.36	4.26	2.37	0.61	-0.28	1.79
M4	2-G4	0.10	95.98	0.46	3.47	2.30	0.57	-0.07	1.43
M4	2-G5	1.65	89.53	1.72	7.10	2.15	1.93	0.21	4.23
M4	2-G6	44.71	39.27	3.95	12.08	0.87	2.93	0.83	1.40
Site 3									
M4	3-G2	0.74	94.18	1.07	4.01	2.33	0.69	-0.05	2.38
M4	3-G7	0.90	94.40	0.94	3.76	2.23	0.72	-0.19	1.21
M4	3-G8	0.71	94.97	1.00	3.32	2.30	0.69	-0.26	1.58
M4	3-G9	2.67	91.26	1.17	4.90	1.97	1.47	0.02	2.39
M4	3-G10	31.82	69.20	2.53	16.75	-0.02	0.98	0.40	0.69
Site 4									
M4	4-G5	12.76	57.89	5.18	24.17	3.57	4.17	0.61	0.70
M4	4-G8	16.85	74.68	1.70	6.77	0.33	2.28	0.46	2.30
M4	4-G9	13.64	71.92	2.79	11.65	1.05	2.78	0.53	2.07
M4	4-G10	10.18	77.74	2.27	9.81	0.43	2.29	0.46	4.10
M4	4-G11	15.81	72.98	1.83	9.38	0.27	2.32	0.43	2.65

Table C.2. Sediment grain size data (page 6 of 6)

Cruise	Grab	% Gravel	% Sand	% Silt	% Clay	Mean Phi	Sorting	Skewness	Kurtosis
Site 5									
M4	5-G3	0.88	89.14	3.22	6.76	2.25	1.92	0.29	2.22
M4	5-G4	2.96	83.14	4.01	9.90	1.95	2.48	0.33	1.75
M4	5-G6	5.77	85.66	1.99	6.58	1.17	2.23	0.33	4.14
M4	5-G7	0.78	84.06	5.22	9.94	2.40	2.33	0.26	2.07
M4	5-G10	1.24	85.64	4.24	8.88	2.33	2.19	0.30	2.34
Site 6									
M4	6-G1	0.24	81.57	6.34	11.84	3.03	2.19	0.28	2.39
M4	6-G3	8.34	77.99	3.60	10.06	8.34	77.99	3.60	10.06
M4	6-G5	5.21	55.83	13.16	25.80	4.42	4.04	0.34	0.78
M4	6-G7	0.74	66.16	10.72	22.39	4.57	3.48	0.48	1.15
M4	6-G8	0.28	71.89	9.56	18.27	4.50	3.11	0.52	1.95
Site 7									
M4	7-G1	14.30	71.72	2.33	11.65	1.20	2.78	0.39	2.22
M4	7-G2	19.57	65.77	1.69	12.97	0.75	2.68	0.57	2.22
M4	7-G3	1.75	78.08	5.36	14.81	3.43	2.70	0.46	2.61
M4	7-G5	0.44	80.13	6.09	13.34	3.27	2.22	0.52	2.43
M4	7-G7	0.31	80.93	4.39	14.38	3.07	2.38	0.69	2.33
Site 8									
M4	8-G1	0.45	85.09	2.58	11.87	2.55	1.89	0.55	2.52
M4	8-G2	14.02	71.02	3.06	11.90	0.57	2.86	1.08	1.49
M4	8-G5	0.88	96.33	0.25	2.54	1.48	0.79	-0.05	1.43
M4	8-G7	1.20	92.97	0.73	5.10	1.97	1.45	0.30	1.89
M4	8-G9	34.82	54.78	1.69	8.72	0.57	2.54	0.55	1.67
Site 9									
M4	9-G1	0.29	82.47	3.67	13.57	2.93	2.23	0.69	2.49
M4	9-G4	12.36	71.98	2.50	13.16	1.80	2.74	0.31	1.86
M4	9-G6	2.37	91.20	0.79	5.63	1.70	1.84	0.16	3.57
M4	9-G7	8.48	66.83	4.50	20.19	3.43	4.05	0.54	1.28
M4	9-G10	5.10	72.92	4.17	17.81	3.43	3.71	0.55	2.07

Appendix D:
Synopses of Hydrographic and Collateral Data for Cruises

Appendix D: Synopses of Hydrographic and Collateral Data for Cruises

Cruise 1C (21–24 May 1997)

Setting: The TOPEX/ERS-1 analysis shows a 10–15 cm/s, up-shelf geostrophic flow. The AVHRR (from JHU APL, Ocean Remote Sensing Group) 3-day composite for 21 May shows a surface temperature of ~26°C in the study area, but 28°C water closer on-shore. The AVHRR 3-day composite for 24 May, three days later than the previous composite, shows ~28°C water in the study area. There is also indication in the composite of a warm 31°C plume emanating from the South Pass of the Mississippi delta that is headed to the south of the study area. For the period of the cruise, the NDBC 42040 3-m discuss buoy recorded an average hourly wind speed of 2.76 m/s, an average significant wave height of 0.28 m, and an average water temperature of 26.0°C. Vertical mixing would not be expected to be significant under these conditions. Wind direction recorded by NDBC 42040 indicates winds out of 167 degrees over the previous several days. These winds are capable of transporting water in the surface layer from the warm plume located to the south of the study region. The combined river discharge over the past month was 573,788 cfs, 39% greater than the yearly average of 413,164 cfs.

Hydrography: The vertical profiles taken at Sites 5, 6, 7, 8, and 9 indicate a shallow, 5-m thick surface layer of warm (>27°C), low salinity (~30) water. The corresponding transmissivity profiles show a surface layer of low optical transparency, while the deeper layer remains clear. The high temperature, low salinity, and high beam attenuation are indications of a river source for the surface layer in the western part of the study region. The vertical profiles taken in the eastern part at Sites 1, 2, 3, and 4 show a colder surface temperature of ~25°C, a much higher surface salinity (33.5 to 34.0) and a deeper mixed layer to 25–30 m with a sharp thermocline at ~30 m. The transmissivity profiles at all four sites show high optical transparency throughout the water column. The signature of river influenced surface water is not seen at the eastern sites. The results suggest that winds and geostrophic currents are directing Mississippi River plume water into the western part of the study region.

In the vertical profiles of salinity, the bottom 16 m at all sites ranged from 36.4 to 36.5. The bottom salinity at all four sites never exceeded 36.3. The salinities in the middle of the water column were all greater than 36.5. Typically, salinity above 36.5 suggests possible Loop Current intrusions; these values do not indicate the presence of a Loop Current related water.

The density profiles correlate very well within each megasite. At Megasite 5, the density profiles at Sites 7, 8, and 9 are very similar, but show variations in the bottom 16 m. At Megasite 3, the Sites 5 and 6 density profiles are very similar, but uniquely different from the profiles taken at the other megasites. The profiles show that between 40 and 50-m depth the density profiles are virtually identical and nearly constant with depth. At Megasite 1, Sites 1 and 2 are very similar.

Because more than one profile was taken at each mooring site, we are able to subjectively examine the variability in the slope of the density profiles taken near the bottom and compare that variability to the average seen for all the cruises. The variability was moderate at Sites 1 and 5 compared to the study average,. At Sites 4 and 9 the variability was large.

Cruise S1 (28–29 July 1997)

Setting: Hurricane Danny passed through the study area on 18 July. The Tropical Prediction Center estimate it dropped ~1 m of precipitation. The NDBC 42040 buoy recorded a maximum

hourly surface wind of 16.32 m/s and a maximum significant wave height of 3.34 m. This is sufficient to cause noticeable vertical mixing in the water column, but given the right conditions, ten days is also adequate for the surface layer to restratify. The TOPEX/ERS-1 satellite altimetry for 1 August suggests very weak down-shelf geostrophic flow being driven by an off-slope cyclonic circulation feature. The AVHRR 3-day composite for 28 July is suspect because of intermittent cloud cover, due in part to the passage of Hurricane Danny. However, it does provide hints that the surface temperature is very high. For the period of the cruise, the NDBC 42040 3-m discus buoy recorded an average hourly wind speed of 2.74 m/s and an average significant wave height of 0.3 m. Vertical mixing would not be expected to be significant under these conditions. Wind direction recorded by NDBC 42040 indicates winds out of 210 degrees over the previous several days. These winds are capable of transporting water in the surface layer from the vicinity of the Mississippi delta. During the period of the cruise, the NDBC buoy recorded an average water temperature of 29.7°C. The combined river discharge over the past month was 373,974 cfs, ~9% less than the yearly average of 413,164 cfs.

Hydrography: The vertical profiles taken at mooring Sites 1, 4, 5, and 9 indicate a shallow, 5-m thick, well mixed surface layer with a surface temperature greater than 30.0°C and a surface salinity less than 30. This is suggestive of river water origin, but there are no transmissivity profiles available to confirm if the surface layer is carrying sediment from river runoff. However, it is probably a very good assumption the favorable winds, in spite of the weak down-shelf geostrophic currents, are directing Mississippi River plume water into the all of the study region.

The bottom salinity at all four sites never exceeded 36.4. The salinities in the middle of the water column were all greater than 36.5, which suggests the presence of a Loop Current related intrusion.

Density profiles taken at Site 1 and Site 4 are similar, despite the greater depth at Site 4. The density profiles taken at Site 5 and Site 9 are similar, but different from the other two sites. At Site 1, compared to the study average, the variability between casts in the slope of the density profiles was large. At Sites 4 and 9 the slope variability was small, and at Site 5 it was average.

Cruise M2 (29 September to 5 October and 31 October 1997)

Setting: *First half of the cruise: 29 September to 5 October.* On-shelf geostrophic flow of ~20 cm/s is seen in the TOPEX/ERS-1 satellite image of 1 October. The on-shelf flow appears to be bringing water from an eddy located to the southwest of the study region that could account for the subsurface warm feature seen in the hydrography. The AVHRR 3-day composite satellite image for 3 October shows ~29°C water in the study area, but no clear indication of a Mississippi river plume. The 42040 NDBC data suggests a strong atmospheric event accompanied by high winds occurred in the study area on 2 October at 0500 UTC and lasted for approximately sixteen hours. The average hourly surface wind peaked at 10 m/s. The average significant wave height recorded by the 42040 NDBC buoy during the period from 29 September to 5 October was 0.62 m and the average hourly wind speed was 4.11 m/s. The buoy recorded an average water temperature of 27.8°C measured 0.6 m below the sea surface. Wind direction recorded by NDBC 42040 indicates winds out of 286 degrees over the previous several days. The combined river discharge over the past month was 195,602cfs, ~53% less than the yearly average of 413,164 cfs. This is the lowest freshwater flow of any cruise.

Setting: *Second half of the cruise: 31 October.* The TOPEX/ERS-1 satellite image of 1 November still shows an on-shelf geostrophic flow of ~25 cm/s. The flow is still apparently from the eddy mentioned above. The AVHRR 3-day composite satellite image for 3 November shows clouds obscuring the coastal regions out to ~30 nmi from shore. In the study area the surface temperature is approximately ~25°C. There is an indication of a warmer, 26.5°C,

filament being pulled from the Gulf eddy. The average significant wave height recorded by the 42040 NDBC buoy for 31 October was 0.95 m and the average hourly wind speed was 4.78 m/s. The buoy recorded an average water temperature of 23.2°C measured 0.6 m below the sea surface. There is considerable evidence that the surface layer has cooled 4–5°C from the beginning of the month to the end of the month. Wind direction recorded by NDBC 42040 indicates winds out of 92 degrees over the previous several days.

Hydrography: *First half of the cruise:* The vertical profiles near Sites 1, 2, 5, and 6 were taken between 29 September and 5 October. The profiles show a well-mixed surface layer down to 20 m, with a temperature of 28°C and a salinity of 33–34. There is no indication of Mississippi River plume water in the surface layer seen in the transmissivity profiles. Beneath the surface layer is a warmer (~29°C) subsurface layer approximately 10-m thick. The bottom salinity at all four sites is very close to 36.4.

The density profiles at Sites 5 and 6 are very similar. The density profiles in the bottom half of the water column at Sites 1 and 2 are similar to Sites 5 and 6.

Second half of the cruise: The vertical profiles taken at Sites 4, 7, 8, and 9 were all taken on 31 October. The profiles at Site 4, locations 4A, 4B, and 4C, show a well mixed surface layer (temperature of 24°C) down to 35 m, but do not show the warm subsurface layer seen in the first half of the cruise. The vertical profiles taken at Sites 7, 8, and 9 show a well mixed surface layer (temperature of 24°C, salinity of 34.5) down to 20 m, and a warm layer (temperature of 26°C) below the surface layer that is approximately 30-m thick. These temperatures are considerably cooler than those at the beginning of the month. There is no indication of Mississippi River plume water in the surface layer seen in the transmissivity profiles. The bottom salinity at all four sites is very close to 36.4.

The density profiles at Sites 7, 8, and 9 are very similar, but different from the profile taken at Site 4. At Site 4, the well-mixed layer results in a nearly constant density surface layer, followed by a sharp pycnocline. At Site 1 and 4, compared to the study average, the variability in the slope of the density profile was large. At Site 5 it was average, and at Site 9 it was small.

Cruise S2 (29–30 January 1998)

Setting: The TOPEX/ERS-1 satellite image of 29 January shows weak up-shelf and then off-shelf geostrophic flow driven by an off-slope anti-cyclonic circulation feature. The AVHRR 3-day composite for 30 January shows significant spatial variation in the surface temperature (18–21°C) throughout the Mississippi-Alabama shelf. It also clearly shows a filament of colder (temperature of 18°C) shelf water being pulled across the shelf break to the east of the study area, i.e., Site 1. This coincides with the off-shelf geostrophic flow seen in the satellite altimetry. There are also clear indications of a plume, emanating from the North Pass of the Mississippi River, that passes to the north of the study area. The average significant wave height recorded by the 42040 NDBC buoy during this period was 0.27 m and the average hourly wind speed was 3.36 m/s. These conditions are not conducive to vertical mixing in the surface layer. Wind direction recorded by NDBC 42040 indicates winds out of 315 degrees over the previous several days. The NDBC 42040 buoy recorded an average water temperature of 17.2°C measured 0.6 m below the sea surface. The average composite river discharge over the past month was 656,664 cfs, ~60% greater than the yearly average of 413,164 cfs. This is the highest freshwater flow just before any of the cruises.

Hydrography: Typically one would expect the water column to be well mixed during the winter; this was not seen for this cruise. Each of the vertical profiles taken at Site 1 shows a considerable amount of temporal variability. The first profile taken at Site 1A (1614 UTC on 29 January)

shows a vertically well-mixed water column (temperature of 18°C, salinity of 35) down to 70 m. Three hours later at 1922 UTC, the second profile at Site 1A reveals the presence of a thin, warm, saline intrusion 50 m below the surface. The profile at Site 1B, taken at 2033 UTC, shows that the vertical extent of the warm, saline intrusion is more pronounced. Two hours later at 2255 UTC, the second profile at Site 1B shows that the warm intrusion has grown to a subsurface layer that extends from 25 to 60 m below the surface and has a T of 20°C and a salinity of 36. This profile is subsequently seen at site 1C(1729 UTC and 2015 UTC), site 4A, site 5A, and site 9; a vertically well-mixed surface layer (temperature of ~ 17°C) that overlays a warm, saline subsurface layer. The one exception to this pattern is the second profile taken at site 5A. Taken five hours after the first profile, it shows a vertically well-mixed water column with the exception of a thin warm saline intrusion 50 m below the surface. The profile is surprisingly similar to the second profile taken at Site 1A. The profiles at Site 9 were taken more than two hours later, yet show the presence of a warm saline subsurface layer that extends from 25 to 60 m below the surface.

The density profiles at each of the four sites indicates the presence of a unique water mass associated with the warm saline subsurface layer seen in the temperature and salinity profiles. The density profiles show a surprising amount of temporal variability

The bottom salinity at all four sites never exceeded 36.2. The salinities in the middle of the water column never exceeded 36.1.

Cruise M3 (24 April to 3 May 1998)

(Sites 1 and 2 were sampled on 24 April, Site 4 was sampled on 26 April, and Sites 5, 6, 7, 8, and 9 were sampled on 1 May).

Setting: *First half of the cruise: 24-26 April.* The AVHRR 3-day composite for 24 April shows ~ 22°C water in the study area. There is evidence ~ 25°C water proceeding to the northeast from the North Pass. The average significant wave height recorded by the 42040 NDBC buoy during this cruise period was 0.69 m and the average hourly wind speed was 4.82 m/s. These conditions are conducive to vertical mixing in the surface layer. Wind direction recorded by NDBC 42040 indicates winds out of 310 degrees over the previous several days. The NDBC 42040 buoy recorded an average water temperature of 21.1°C measured 0.6 m below the sea surface. The combined river discharge over the past month was 608,669 cfs, ~ 47% greater than the yearly average of 413,164 cfs.

Second half of the cruise: May 1. The TOPEX/ERS-1 satellite image of 1 May shows ~ 25 cm/s on-shelf geostrophic flow. The AVHRR 7-day composite for 2 May shows a warm core eddy filament wrapping up toward the study area, but being folded back to the southwest well before it approaches the shelf. The average significant wave height recorded by the 42040 NDBC buoy during this cruise period was 0.85 m and the average hourly wind speed was 4.5 m/s. These conditions are conducive to vertical mixing in the surface layer. Wind direction recorded by NDBC 42040 over the previous day is unavailable. The NDBC 42040 buoy recorded an average water temperature of 21.9°C measured 0.6 m below the sea surface.

Hydrography: *First half of the cruise.* The vertical profiles taken at Sites 1, 2, and 4 indicate a shallow, 10-m thick surface layer with a temperature of 21°C and a salinity of 33 – 34. The transmissivity profiles at all three sites show high optical transparency throughout the water column. The signature of river influenced surface water is not seen at the eastern sites. The density profiles for Sites 1 and 2 show a surprising amount of variation in the surface layer, but they are nearly identical from 40 m on down. The density profile for Site 4 has the same general shape, but shows the density throughout the water column is lower.

Second half of the cruise. The vertical profiles taken at Sites 5 and 6 indicate a shallow, 10-m thick surface layer with a temperature of 21°C and a salinity of 32. The vertical profiles taken at Sites 7, 8, and 9 indicate a shallow, 10-m thick surface layer with a temperature of 22°C and a salinity of 34.8. The transmissivity profiles at all five sites show high optical transparency throughout the water column. The signature of river influenced surface water is not seen at the western sites. The density profiles for Sites 5 and 6 are nearly identical from the surface to the bottom. They are different from the density profiles at Sites 7, 8, and 9. The shape of the density profiles at Sites 7, 8, and 9 are similar and show noticeable variation in the bottom 16 m. The salinity profiles for Site 7 is a good example of the minimum amount of temporal and spatial variation that can be seen. All three casts were completed within 33 minutes. The bottom salinity at all four sites never exceeded 36.2. The salinities in the middle of the water column never exceeded 36.3. At Site 1, compared to the study average, the variability in the slope of the density profile was very large. At Site 4 it was large, at Site 5 it was average, and at Site 9 it was small.

Cruise S3 (20–22 July 1998)

Setting: The TOPEX/ERS-1 satellite image of 15 July shows ~50 cm/s up-shelf geostrophic flow. The TOPEX/ERS-1 satellite image of 1 August shows continuing up-shelf geostrophic flow on the order of 25 cm/s. The AVHRR 3-day composite for 21 July shows a 32°C feature in the study area that apparently has its source in the Mississippi delta. The average significant wave height recorded by the 42040 NDBC buoy during this cruise period was 0.52 m and the average hourly wind speed was 3.85 m/s. These conditions are not conducive to causing vertical mixing in the surface layer. Wind direction recorded by NDBC 42040 was out of 210 degrees over the previous two days. These winds are capable of transporting water in the surface layer from the vicinity of the Mississippi delta. The NDBC 42040 buoy recorded an average water temperature of 30.3°C measured 0.6 m below the sea surface. The average composite river discharge over the past month 390,617 cfs, is ~ 5 % less than the yearly average of 413,164 cfs.

Hydrography: The surface temperature at all four sites was in the range of 30.5–30.9°C. The surface salinity was ~ 28. The transmissivity profile at all four sites shows a surface layer of high beam attenuation, while the deeper layer remains clear. The high temperature, low salinity, and high beam attenuation are clear indications of sediment from river runoff being carried in the surface layer. The results suggest that the combination of favorable winds and strong up-shelf geostrophic currents are directing Mississippi River plume water into the study region. The bottom salinity at all four sites ranged from 36.0 to 36.3. The salinities in the middle of the water column never exceeded 36.3. Density profiles taken at Site 1 and Site 4 are similar in shape, despite the greater depth at Site 4. The density profiles taken at Site 5 and Site 9 are similar to each other, but different from the other two sites. Density profile slopes were small at Site 1, compared to the study average, and average at Sites 4, 5, and 9.

Cruise S4 (13–14 October 1998)

Setting: Two hurricanes and a tropical storm occurred during the preceding month of September. It is believed that the entire water column in the study area was vertically well mixed by the end of September. The TOPEX/ERS-1 satellite image of 15 October shows weak up-shelf geostrophic flow being driven by an off-shelf anticyclonic circulation feature. The AVHRR 3-day composite for 21 July shows ~ 26°C surface water in the study area. There is 24°C water emanating from the North Pass of the Mississippi River delta. The average significant wave height recorded by the 42040 NDBC buoy during this cruise period was 0.84 m and the average hourly wind speed was 5.67 m/s. The buoy recorded a maximum significant wave height of 1.19 m. These conditions are conducive to vertical mixing in the surface layer. Wind direction

recorded by NDBC 42040 was out of 40 degrees over the two days prior to the start of the cruise. The NDBC 42040 buoy recorded an average water temperature of 26.1°C measured 0.6 m below the sea surface. The temperature remained at or above 25.8°C until 1 November. The combined river discharge over the past 30 days was 220,956 cfs, ~ 47 % less than the yearly average of 413,164 cfs

Hydrography: Vertical profiles taken at all four sites show the upper 35 to 40 m of the water column to be a well-mixed layer with a temperature of 26.4°C and a salinity of 35. The transmissivity profiles at all four sites show high optical transparency throughout the water column, except near the bottom. The signature of river influenced surface water is not seen in the study region. A strong thermocline is seen below the surface layer. The bottom salinity at all four sites was ~ 36.5. However, the salinities in the middle of the water column never exceeded 36.0. At Sites 1, 4, and 9, compared to the study average, the variability in density slope was small. At Site 5 it was average.

Cruise S5 (9–10 February 1999)

Setting: The TOPEX/ERS-1 satellite image of 15 February shows weak easterly geostrophic flow being driven by an off-shelf anticyclonic circulation feature. The AVHRR 3-day composite for 11 February shows that the study area lies in or somewhat to the south of the right limb of a classic hammerhead. The surface temperature is 23 to 24°C. To the east of the study area, it appears that cold (21C) water is being pulled off the shelf. The average significant wave height recorded by the 42040 NDBC buoy during this cruise period was 0.55 m and the average hourly wind speed was 4.46 m/s. These are conditions conducive to vertical mixing in the surface layer. Wind direction recorded by NDBC 42040 was out of 225 degrees over the two days prior to the start of the cruise. These winds are capable of transporting water in the surface layer from the nearby hammerhead. Over the three days prior to the start of the cruise, the NDBC 42040 buoy recorded a water temperature of 19.0 to 20.0°C measured 0.6 m below the sea surface. Beginning about 1600 UTC on 9 February and continuing until 2100 UTC on 10 February, the temperature rose from 19.7°C, typical for wintertime conditions, to 25.6°C. The air temperatures rose as well, but the dewpoint remained fairly constant at about 20.0°C. The average composite river discharge over the past month 575,514 cfs, ~ 39 % greater than the yearly average of 413,164 cfs.

Hydrography: Vertical profiles taken at all four sites show the surface temperature to range from 19.2 to 21.1°C and a salinity of 33.4 - 35.7. The transmissivity profiles at all four sites show high optical transparency throughout the water column. The signature of river influenced surface water is not seen in the study region. Sites 1 and 9 are nearly uniformly mixed throughout the water column, whereas Sites 5 and 9 are stratified continuously. The temperature profile at Site 9 clearly shows the intrusion of a warm subsurface layer, almost identical to that seen in the previous year's winter cruise (S2). The bottom salinity at all four sites never exceeded 36.1 . The salinities in the middle of the water column never exceeded 36.2.

Cruise M4, Leg 1 (14–15 April 1999)

Setting: The TOPEX/ERS-1 satellite image of 15 April shows weak easterly geostrophic flow being driven by an anticyclonic circulation feature off the Mississippi River delta. The AVHRR 3-day composite for 15 April shows ~ 26°C surface water in the study area. The average significant wave height recorded by the 42040 NDBC buoy during this cruise period was 1.29 m and the average hourly wind speed was 7.85 m/s. Both the wind speed and the wave height continuously increased during the cruise. Wind direction recorded by NDBC 42040 was out of the north, on average, over the two days prior to the start of the cruise. For the period of the cruise, the NDBC 42040 buoy recorded an average water temperature of 23.3°C measured 0.6 m

below the sea surface. The combined river discharge over the past month 517,267 cfs, ~25 % greater than the yearly average of 413,164 cfs.

Hydrography:. The vertical profiles taken at Sites 1, 4, 5, and 9 indicate a shallow, 10-m thick surface layer of warm (22 - 23°C) water. The surface salinity at sites 1, 4, and 5 was ~ 34.5, whereas the salinity at site 9 is 30.5. The corresponding transmissivity profile for site 9 shows a surface layer of low optical transparency, while the deeper layer remains clear. The transmissivity profile for the other three sites shows high optical transparency throughout the water column. The high temperature, low salinity, and high beam attenuation are indications of a river source for the surface layer in the western part of the study region at site 9. The signature of river influenced surface water is not seen at the eastern sites. The results suggest that winds and weak easterly geostrophic currents are responsible for directing Mississippi River plume water into the western part of the study region. In the vertical profiles of salinity, the bottom 16 m at all sites was ~ 36.1. The salinities in the middle of the water column never exceeded 36.2.

Cruise M4, Leg 2 (29 July to 6 August 1999)

Setting: The TOPEX/ERS-1 satellite image of 1 August shows 25-cm/s up-shelf geostrophic flow. The AVHRR 7-day composite for 5 August 1999 shows ~ 32°C surface water remained in the study area over the cruise period. The average significant wave height recorded by the 42040 NDBC buoy during this cruise period was 0.71 m and the average hourly wind speed was 4.20 m/s. Wind direction recorded by NDBC 42040 was out of 225 degrees over the two days prior to the start of the cruise. For the period of the cruise, the NDBC 42040 buoy recorded an average water temperature of 30.6°C measured 0.6 m below the sea surface. The combined river discharge over the past month 345,826 cfs, ~ 16 % less than the yearly average of 413,164 cfs.

Hydrography. All eight sites were sampled over an eight-day period. Sites 1 and 2 were sampled on 29 July, Site 4 on 30 July, Sites 5 and 6 on 1 August, Sites 7 and 8 on 2 August and Sites 8 and 9 on 6 August. Generally, the surface temperatures ranged from 30 to 31°C at all the sites. The surface salinity at Sites 1, 2, 4, 5, and 6 ranged from 30.6 to 33.0, and the surface salinity at Sites 7, 8, and 9 ranged from 26.2 to 28.0. The transmissivity profiles for all eight sites show low optical transparency in the surface layer, while the deeper layer remains clear. The high temperature, low salinity, and high beam attenuation are clear indications of Mississippi River plume water in the surface layer. The results suggest that the combination of favorable winds and up-shelf geostrophic currents are directing the Mississippi River plume water into the study region over at least an eight-day period. The bottom salinity at all sites never exceeded 36.4 . The salinities in the middle of the water column never exceeded 36.2.



The Department of the Interior Mission

As the Nation's principal conservation agency, the Department of the Interior has responsibility for most of our nationally owned public lands and natural resources. This includes fostering sound use of our land and water resources; protecting our fish, wildlife, and biological diversity; preserving the environmental and cultural values of our national parks and historical places; and providing for the enjoyment of life through outdoor recreation. The Department assesses our energy and mineral resources and works to ensure that their development is in the best interests of all our people by encouraging stewardship and citizen participation in their care. The Department also has a major responsibility for American Indian reservation communities and for people who live in island territories under U.S. administration.



The Minerals Management Service Mission

As a bureau of the Department of the Interior, the Minerals Management Service's (MMS) primary responsibilities are to manage the mineral resources located on the Nation's Outer Continental Shelf (OCS), collect revenue from the Federal OCS and onshore Federal and Indian lands, and distribute those revenues.

Moreover, in working to meet its responsibilities, the **Offshore Minerals Management Program** administers the OCS competitive leasing program and oversees the safe and environmentally sound exploration and production of our Nation's offshore natural gas, oil and other mineral resources. The **MMS Royalty Management Program** meets its responsibilities by ensuring the efficient, timely and accurate collection and disbursement of revenue from mineral leasing and production due to Indian tribes and allottees, States and the U.S. Treasury.

The MMS strives to fulfill its responsibilities through the general guiding principles of: (1) being responsive to the public's concerns and interests by maintaining a dialogue with all potentially affected parties and (2) carrying out its programs with an emphasis on working to enhance the quality of life for all Americans by lending MMS assistance and expertise to economic development and environmental protection.



The U.S. Geological Survey Mission

The U.S. Geological Survey (USGS) is a world leader in the natural sciences through our scientific excellence and responsiveness to society's needs. The USGS serves the Nation by providing reliable scientific information to 1) describe and understand the Earth; 2) minimize loss of life and property from natural disasters; 3) manage water, biological, energy, and mineral resources; and 4) enhance and protect our quality of life.